Exploring the Reactivity of Novel Diazo-Enones in the Construction of Heterocyclic Compounds

by
© Sima Alavi

School of Graduate Studies
in partial fulfillment of the requirements
for the degree of Doctor of Philosophy
Department of Chemistry
Memorial University
2023

St. John's, Newfoundland

Dedicated To:

My Dear Mother♥

My Forever Motivation and Light in Life

Abstract

This thesis delves into the multifaceted world of diazo compounds, exploring their synthetic potential, mechanistic intricacies, and innovative applications. Chapter 1 of the thesis discusses the nucleophilic reactivity of the in situ generated malonic ester product from *α*-diazocarbonyls, followed by a tandem C−H functionalization/Conia-ene cyclization of *N*-propargyl tethered indoles. This double functionalization of diazodicarbonyls generates a range of pyrrolo[1,2-*a*]-, pyrido[1,2-*a*]-, and azepino[1,2-*a*]indole products with good synthetic efficiency.

Chapter 2 introduces the chemistry of *α,β*-unsaturated diazoketones or "diazo-enones. Diazo-enones are a structurally interesting class of *α*-diazocarbonyl compounds which have been steadily gaining interest from the synthetic community over the last decade. Characteristically, these multifunctional synthons possess three distinct reactive sites, a diazo-functional group, a ketone, and a C=C double bond.

Chapter 3 describes a novel intramolecular rearranged cyclization by using a copper catalyst from indolyl *α*-diazocarbonyls starting from substituted indoles and diazo-enones. Activation of the diazo functional group under metal catalysis generates a spiro-cyclic indolenine-type intermediate, which rearranges to provide two distinct carbazoles upon oxidation. The study investigates the effects of the catalyst as well as the substituents on the migratory group involved in controlling the selectivity of the rearrangement.

Chapter 4 develops a novel total synthesis of naphthofuranone containing natural products via a Hauser-Kraus annulation/O–H insertion process. By utilizing substituted phthalides via two tandem C–C bond formations in a one-pot process a class of fused furane ring systems have been formed. Several influential factors were identified in the formation of naphthofuranone derivatives; first, optimization studies showed the importance of the type of nucleophilic phthalide and secondly the choice of the base was revealed as the most effective factor alongside the work-up method. Chapter 5 provides a comprehensive overview of the research conducted in this thesis and outlines potential directions for future investigations.

Acknowledgements

First, I would like to express my deepest gratitude to my supervisor Dr. Huck Grover, for his invaluable guidance, unwavering support, and constant encouragement through my PhD journey. His influence on my academic life is immeasurable, and I am forever grateful for the profound impact he has had on my development as an organic chemist.
I would like to thank all the researchers in the Grover lab, both present and former, for their support and collaboration in different stages of my PhD program.
I express my gratitude to other members of my supervisory committee, Dr. Graham Bodwell and Dr. Michael Katz for providing me their valuable suggestions and helpful comments over the years. I would also like to appreciate Dr. Graham Bodwell for his fruitful guidance during the past "Grover–Bodwell" group meetings.
I would like to thank all the Memorial University C-CART members; Dr. Celine Schneider for help and training with NMR spectroscopy, Nick Ryan for training on the IR instrument, Dr. Jian-Bin Lin for the XRD characterizations, and Dr. Stefana Egli for assistance with mass spectroscopic analysis.
Finally, I would like to deeply appreciate my dear husband for his constant encouragement and belief in me during all the research years. I am deeply grateful to my father and brother for their endless encouragement, support, and inspiration. Their belief in my abilities has been a driving force behind my achievements, and I am truly fortunate to have them in my life.

List of Figures

List of Schemes

List of Tables

List of Abbreviations and Symbols

Å	Angstroms
Ac	acetyl
acac	acetylacetonate
APPI	atmospheric pressure photoionization
Bn	benzyl
°C	degrees centigrade
calcd	calculated
cm	centimeter(s)
^{13}C NMR	carbon nuclear magnetic resonance spectroscopy
DABCO	1,4-diazabicyclo[2.2.2]octane
DBN	1,5-diazabicyclo[4.3.0]non-5-ene
DBU	1,8-diazabicyclo[5.4.0]undec-7-ene
DCE	1,2-dichloroethane
DCM	dichloromethane
DDQ	2,3-dichloro-5,6-dicyano-1,4-benzoquinone
$(DHQ)_2PHAL$	dihydroquinine 1,4-phthalazinediyl diether
$(DHQD)_2PHAL$	dihydroquinidine 1,4-phthalazinediyl diether
DIPEA	*N,N*-diisopropylethylamine
DMF	*N,N*-dimethylformamide
DMSO	dimethyl sulfoxide
EDA	ethyl diazoacetate
EDG	electron donating group
Et	ethyl
EtOAc	ethylacetate
equiv	equivalent(s)
EWG	electron withdrawing group
FT-IR	Fourier transform infrared
g	gram(s)
hfacac	hexafluoroacetylacetonate
^{1}H NMR	proton nuclear magnetic resonance

HRMS	high resolution mass spectrometry
Hz	Hertz
hv	light
^{i}Pr	isopropyl
IR	Infrared
J	*coupling constant (Hz) (in NMR)*
K	degrees Kelvin
L	ligand
LDA	lithium diisopropylamine
LiHMDS	lithium hexamethyldisilazide
M	metal
m	multiplet
m-	*meta*
mg	milligram(s)
mL	milliliter(s)
min	minute(s)
mmol	millimole
mol	mole(s)
mp	melting point
Me	methyl
MHz	megahertz
Ms	mesyl
m/z	mass to charge ratio
NMR	nuclear magnetic resonance
p-	*para*
p-ABSA	4-acetamidobenzenesulfonyl azide
pfb	perfluorobutyrate
Ph	phenyl
ppm	parts per million
py	pyridine
rt	room temperature
q	quartet

R_f	retention factor
s	singlet
TBAF	tetrabutylammonium fluoride
TBS	*tert*-butyldimethylsilyl
t-Bu	*tert*-butyl
Tf	trifluoromethanesulfonyl
TFAA	trifluoroacetic anhydride
TFEA	trifluoroethyl trifluoroacetate
THF	tetrahydrofuran
TLC	thin-layer chromatography
TMEDA	*N,N,N′,N′*-tetramethylethylenediamine
TMS	trimethylsilyl
TOF	time of flight
Ts	4-toluenesulfonyl or tosyl
UV	ultraviolet
δ	chemical shift
ν	wavenumber (cm^{-1})
Δ	heat

Chapter 1: Tandem Carbenoid C−H Functionalization/Conia-ene Cyclization for the Synthesis of Pyrroloindoles

1.1 Introduction

The synthesis, study, and utilization of unique/reactive organic reagents in bond-forming reactions is one of the essential goals in modern organic chemistry. This thesis focuses on improving chemical efficiency by exploring novel reagents and reaction pathways in processes that generate multiple new covalent bonds in as little as one step. As such, the thesis has been organized as follows: Chapter 1 discusses the use of a compound with amphiphilic reactivity as a one carbon synthon in formal [4+1], [5+1] and [6+1] annulation reactions, processes in which two new bonds are formed to one central carbon atom. Chapters 2-4 (the bulk of this thesis work), explore a new reagent with multiple sites of reactivity, which can be leveraged to form multiple new bonds to different carbon atoms in one step. The overall theme connecting this thesis work is the functional moiety known as α-diazocarbonyls.

Over the past several decades diazo compounds have emerged as easily accessible, versatile starting materials in organic synthesis and have been employed in many different organic transformations. Structurally, the diazo functional group is a net neutral terminal dinitrogen moiety connected to a carbon atom, herein referred to as the diazo carbon, as represented by the two resonance contributors shown in Scheme 1.1A.[1] From a reactivity standpoint, this functional group class has gathered synthetic attention as carbene (**2**) and metal carbenoid (**3**) precursors due to the mild conditions required (thermal, photochemical, or transition metal catalysis) to promote the loss of dinitrogen (Scheme 1.1B).

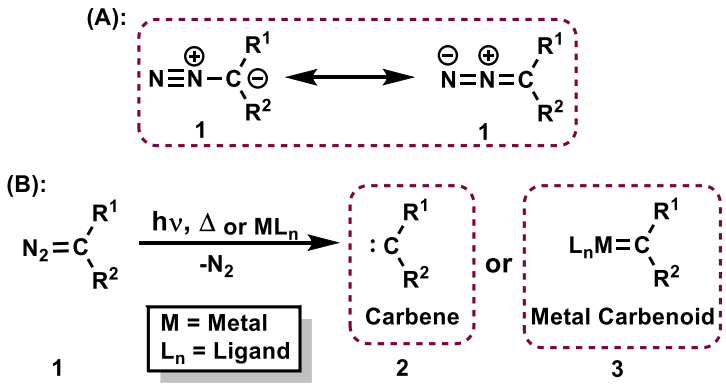

Scheme 1.1: **(A)** Structure of a diazo compound. **(B)** Free carbene and metal carbene precursor structures.

The stability of diazo compounds, and the carbenes/metal carbenoids generated from them, is strongly influenced by the electronic character of the substituents at the diazo carbon atom. For example, the incorporation of electron withdrawing groups (EWGs) onto the diazo carbon helps stabilize the resulting carbene or metal carbenoid, thus increasing the electrophilicity of these compounds when compared to diazo compounds substituted with electron donating groups (EDGs). Accordingly, diazo compounds are classified based on the substituents on the diazo carbon and grouped into three major categories, "acceptor" (one EWG group bound to the diazo carbon), "acceptor/acceptor" (two EWG groups bound to the diazo carbon), and "acceptor/donor" (one EWG group and one EDG group bound to the diazo carbon) (Figure 1.1). It is worth mentioning that the "donor/donor" (two EDG groups bound to the diazo carbon) diazo category of compounds has been known for years; however, the electron rich character of the diazo carbon makes their isolation problematic, and due to their fast dimerization, the applicability of this emerging category of a diazo compound has been limited in the literature.[2]

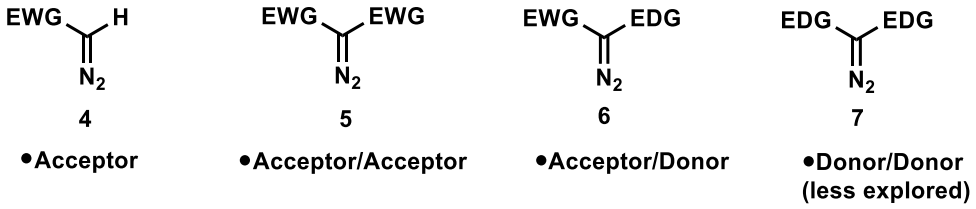

Figure 1.1: Different categories of diazo compounds.

Among the great structural diversity that can be embedded into this class of compounds by varying the substituents about the diazo carbon, the most common structural motif is the carbonyl group. In fact, α-diazocarbonyl compounds (**8**), in which the diazo functionality is located at the α-position to a carbonyl group, as the EWG (Figure 1.2), have found countless uses in organic chemistry and have been the focal point of many popular review articles on diazo compounds.[3] Owing to their ease of synthesis, bench stability, and many activation methods, this class of diazo compounds is generally the starting point in any exploration into reactivity.

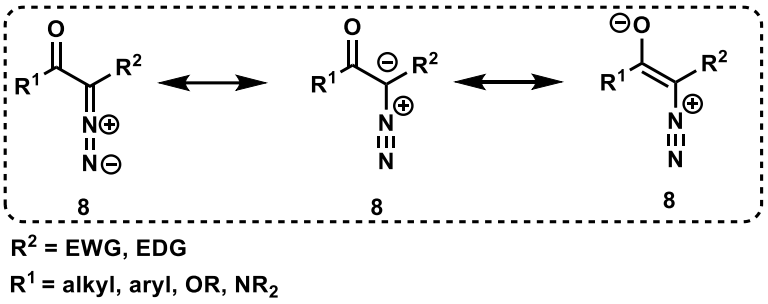

Figure 1.2: Structure of *α*-diazocarbonyls compounds.

1.2 Synthesis of Diazo Compounds

1.2.1 Primary Synthesis of Diazo Compounds

The chemistry of carbenes and metal carbenoids, generated from a diazo compound, can give rise to a wide array of organic transformations. However, the successful employment of diazo compounds in organic reactions depends on the availability of reliable and accessible synthetic methods to prepare these compounds.[4] Furthermore, because of the broad applications of this class of compounds, there remains a long-standing interest in the synthesis of diazo compounds.

In 1883, Curtius[5a] described one of the first synthetic method for preparation of diazo compounds. In this study diazotization of ethyl glycinate (**9**) took place in the presence of sodium nitrite to obtain ethyl diazoacetate (**10**) (Scheme 1.2A). Nearly a decade later, in 1894, Pechmann discovered a method to produce the simplest diazo compound, diazomethane **12**, which is an extremely sensitive explosive yellow gas, through the reaction of *N*-methyl-*N*-oxomethoxy carbohydrazide **11** and sodium hydroxide (Scheme 1.2B).[5b] Notably, variations of this historically important synthetic method are still used today for the preparation of diazomethane.[6]

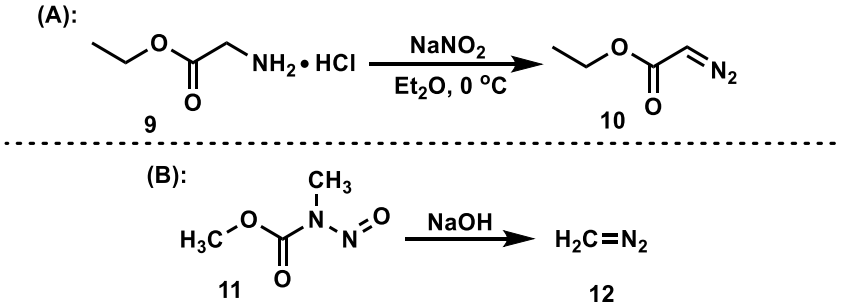

Scheme 1.2: (A) Curtius method for synthesis of the first known diazo compound. **(B)** Synthesis of diazo methane by Pechmann.

1.2.2 Modern Synthetic Methods for Diazo Compounds

Since the discovery of diazo compounds, several modern methods have been developed for synthesis of all categories of diazo compound (acceptor, acceptor/acceptor, donor/acceptor). Scientists have developed modern methods to synthesize diazo compounds with focus on reducing safety hazards associated with their thermal sensitivity and chemical reactivity. These novel approaches have been specifically designed to address safety concerns during the synthesis of diazo compounds.[7] Many of these major routes are shown in Scheme 1.3 including: A) diazo transfer group to activated methylene compounds,[8] B) dehydrogenation of hydrazones,[9] C) diazotisation of primary amines,[10] D) cross-coupling at the diazo carbon,[11] E) substituent modification of an existing diazo substrate,[12] and F) fragmentation of triazenes.[13]

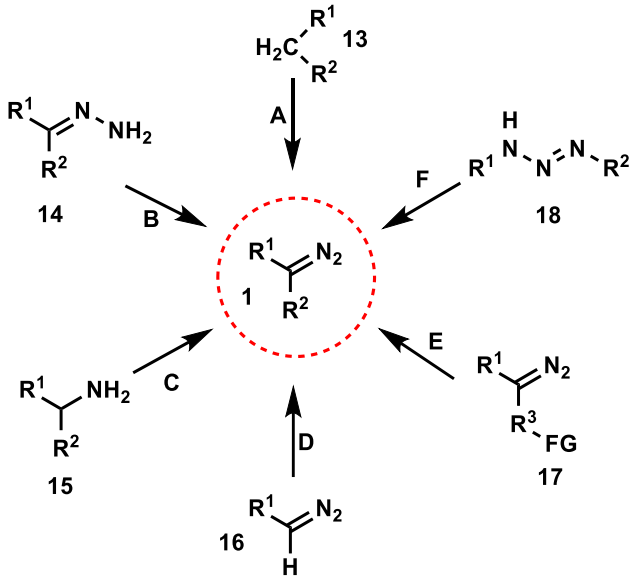

Scheme 1.3: Major synthetic routes to diazo compounds.

1.3 Reactivity of *α*-Diazocarbonyl Compounds

Although the thermal or photochemical activation of *α*-diazocarbonyl compounds has already found diverse applications in synthesizing complex organic structures,[14] reactions of diazo reagents involving transition metal catalysts have gained significant attention in modern organic synthesis. In the presence of various transition metal catalysts and ligands, the diazo carbon can undergo a dinitrogen

extrusion to form a metal carbenoid intermediate **19** (Scheme 1.4). Upon generation, the reactive metal carbenoid species can participate in a range of bond-forming transformations. Among the various types of reactions these intermediates are known to participate in, the most common are C–H insertion reactions leading to **21**,[15] Wolff rearrangements to provide ketone **22**,[16] and cyclopropanation [17] reactions to give **24** (Scheme 1.4).

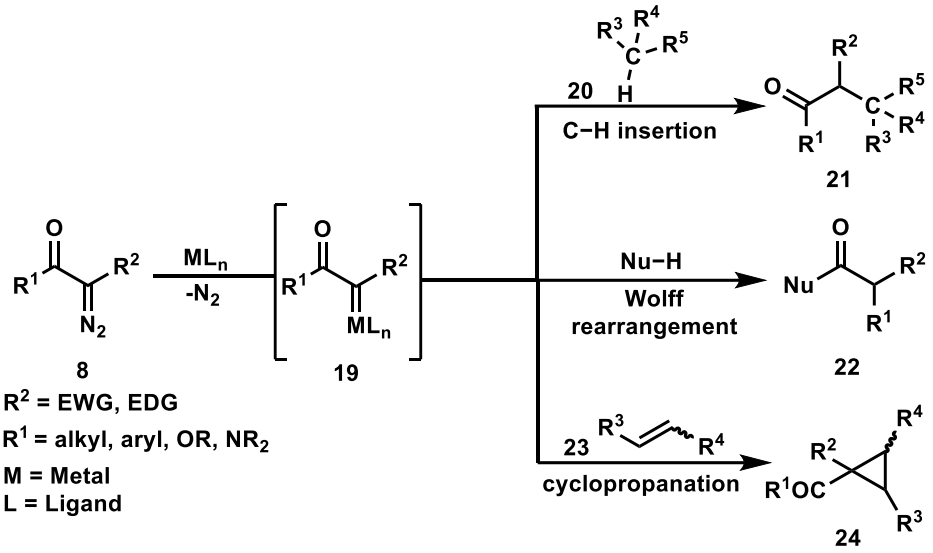

Scheme 1.4: Common reactions of diazocarbonyl compounds by activation with metal catalysts.

1.3.1 *α*-Diazocarbonyl Compounds in C–H Functionalization Chemistry

Of importance to this thesis work, C−H functionalization reactions involving diazo compounds is among the essential subjects. Overall, the net transformation in this area of research are the formal insertion of a diazo carbon into a C–H bond of an organic molecule (**8** → **21**, Scheme 1.4). Various reaction manifolds have been developed to promote and control the net C–H insertion reactions of diazo compounds, including concerted C–H insertion pathways (Scheme 1.5A)[18a] and metal catalyzed C–H activation, metal carbenoid formation, followed by migratory insertion pathways (Scheme 1.5B).[18b] However, the pathways that proceed via electrophilic aromatic type substitution with electron-rich arenes (Scheme 1.5C) are paramount in the work described herein. The coupling reaction of electron rich aromatic compounds with *α*-diazocarbonyl compounds in the presence of metal catalyst have become a reliable

method for the C–H functionalization of arene compounds over the last several decades.[18c]

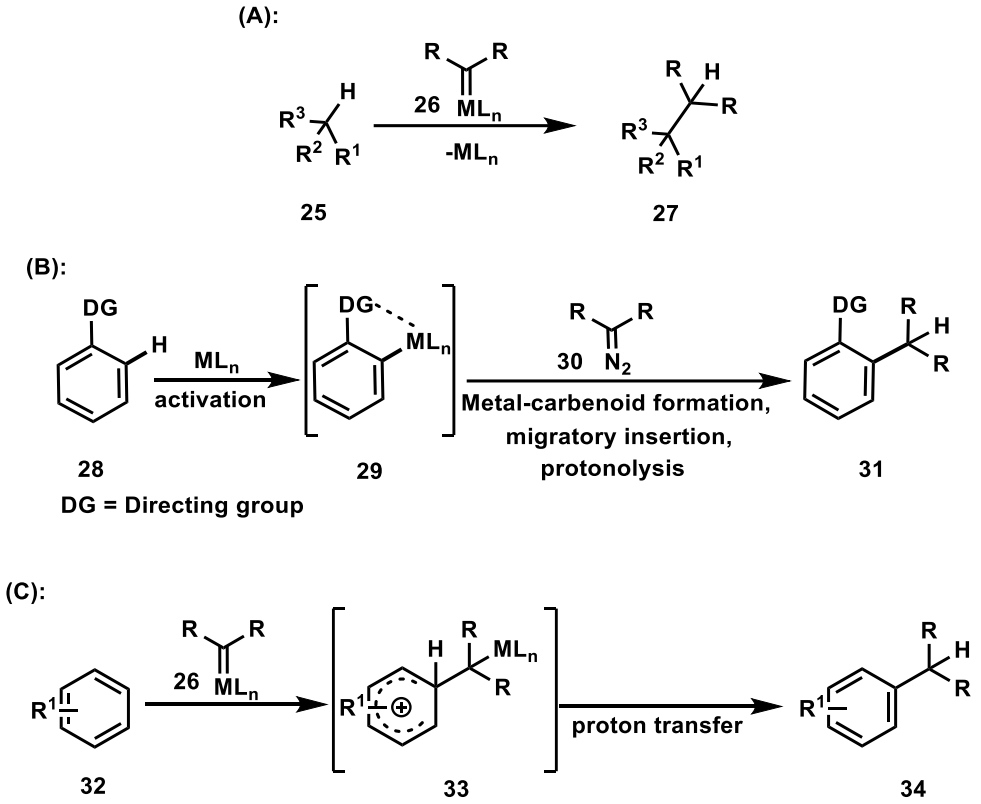

Scheme 1.5: (A) Direct C(sp^3)–H insertion with metal carbenoids. **(B)** Metal catalyzed C–H activation followed by diazo coupling. **(C)** Electrophilic aromatic substitution reaction via carbenoid metals.

For example, Zhang and co-workers developed a gold catalyzed method for the aromatic functionalization of unprotected substituted phenols (Scheme 1.6).[19] By subjecting *α*-aryl-*α*-diazoacetates (**35**) to a reaction with substituted phenols (**36**) in the presence of a tris(2,4-di-*t*-butylphenyl)phosphite derived gold complex a series of *para*-substituted phenols were obtained (**37**). The corresponding C−H functionalization products (**37**) are delivered, rather than O–H insertion, in a chemo- and regioselective manner. The authors also discovered when *meta*-methylphenol and *meta*-methoxyphenol were employed, *ortho* C−H functionalization products **38** and **39** could be also isolated along with the *para* C−H functionalization products **40** and **41**, indicating that the methyl and methyoxy groups could also act as the directing groups.

A preliminary mechanistic study showed that the reaction may proceed via electrophilic addition of the gold-carbene followed by rapid loss of proton.

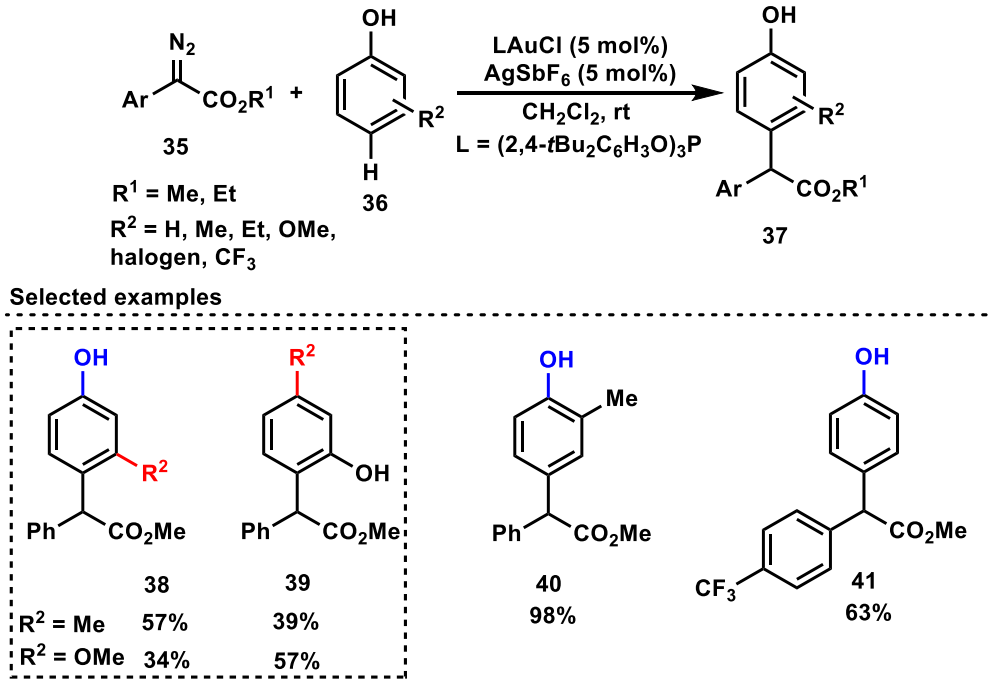

Scheme 1.6: Selective C–H functionalization of phenols with diazo compounds.

In the same year, Hu and colleagues reported a rhodium-carbene-induced, aromatic C–H functionalization for synthesis of *α,α*-diaryl benzylic quaternary stereocenters (Scheme 1.7).[20] The reaction involves three components: *N,N*-disubstituted anilines (**42**), diazo compounds (**43**), and imines (**44**) in the presence of Rh(II)/chiral phosphoric acid cocatalysts. Mechanistically, this reaction is proposed to proceed via the generation of zwitterionic intermediates (**47** and **48**) by electrophilic addition of the metal carbene (**46**) to the aromatic ring (Scheme 1.7). In the absence of any additional electrophiles, a subsequent proton transfer of intermediate **47** and **48** can proceed to deliver the net C–H insertion product **50** (Scheme 1.7, path a). Interestingly however, in the presence of the imine electrophile **44**, the zwitterionic intermediates can be intercepted prior to the 1,2-proton transfer (Scheme 1.7, path b) leading to **45** upon rearomatization; a net process that forms two new non-hydrogen bonds to the diazo carbon. This method highlights the application of diazo reagents not only in C–H functionalization chemistry, but also in their utility to form multiple new C–C bonds in a single step.

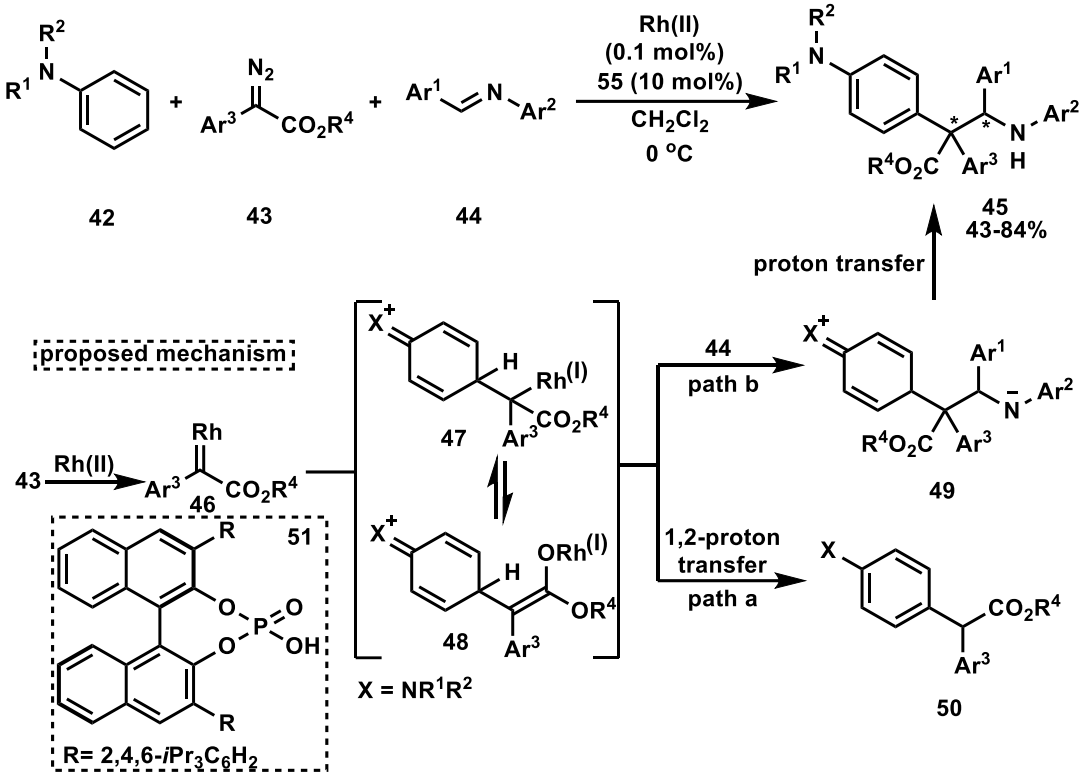

Scheme 1.7: Catalytic asymmetric aromatic C−H functionalization by trapping of a metal-carbene-induced intermediate with an electrophile.

1.4 Chemistry of Indole

Since the discovery of indole in 1866 from the natural indigo dye,[21] this heterocyclic aromatic scaffold has been assigned as a valuable compound in numerous research areas such as pharmaceuticals, fragrances, agrochemicals, pigments, and materials science.[22] Indole is a bicyclic structure, consisting of a benzene ring fused to a pyrrole ring (Scheme 1.8). Due to the electron rich nature of the pyrrole ring, this heterocycle undergoes electrophilic aromatic substitution reactions with an array of electrophiles to furnish both C3 or C2 functionalized indole products.[23] The most reactive position of unsubstituted indole for electrophilic aromatic substitution is C3 rather than the C2-position, due to the greater stability of intermediate **52** vs. **54** (Scheme 1.8).

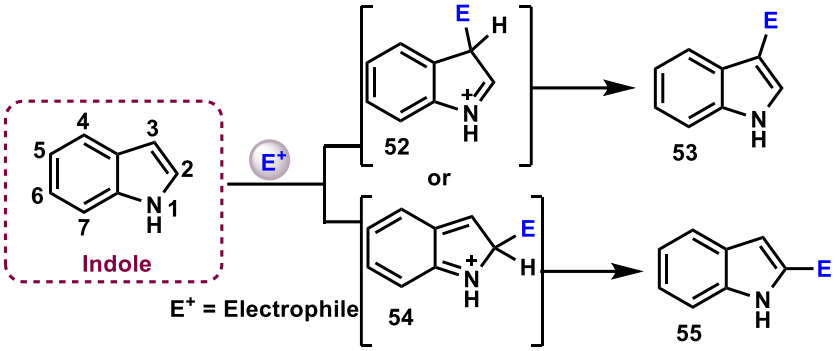

Scheme 1.8: Reactive sites for electrophilic substitution reactions of indole.

1.4.1 Reaction of Indoles with Diazo Compounds

Functionalization of indole derivatives appears to be an efficient and versatile method for accessing multifunctional indole-containing scaffolds. Importantly, the reaction of indoles, as electron rich aromatic systems, and metal carbenoid species (generated from a diazo compound) represents a powerful route in constructing complex structures (Scheme **1.9**).[24] One mechanistic proposal for this net C–H insertion reaction, that parallels the pathways described with other electron rich arenes (see section 1.3.1), is highlighted in Scheme 1.9. Nucleophilic attack by indole, at C3-position, to the metal carbenoid forms the new C−C bond and generates intermediate **58**. Subsequent proton transfer (R = H) of **58** would provide functionalized C3 indole **60**. Alternatively, collapse of zwitterionic intermediate **58** to generate cyclopropane intermediate **59** could provide both C3-functionalized product **60** (R = H) and C2-functionalized indole **61** (R ≠ H) upon ring-opening and proton transfer.

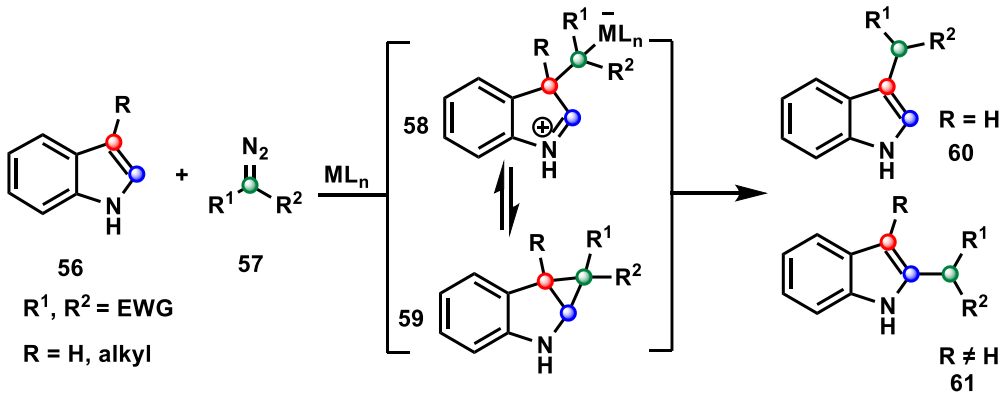

Scheme 1.9: C–H functionalization of indole with diazo compounds.

An excellent application of this type of functionalization is highlighted in the 2003 work by the Kerr group who developed a rhodium-catalyzed method for installation of a malonate moiety into the C3-position of indoles (Scheme 1.10).[25] To achieve this, a variety of indole substrates (**62**) were subjected to a reaction with dimethyldiazo malonate (**63**) under the influence of catalytic rhodium acetate. When the nitrogen atom of indole was substituted with an alkyl group, such as methyl group, higher yields were obtained compared to the non-substituted indole (**66** and **67** respectively), whereas the C2-position substituted indole substrates resulted in reduced yields (**65** vs. **66**). Through the investigations of the electronic effects of the benzenoid ring, it was discovered that a substitution on the benzenoid portion, like methoxy and bromo groups, also delivered high yields 86% and 91%, respectively. It is observed when the C3-substituted indole substrates, such as 1,3-dimethyl indole, were subjected to the reaction with **63**, substitution took place at the C2-position (**68**). However, the yield of the desired product was found to be lower compared to the reaction with 1,2-dimethyl indole (**66**). It is worth noting that low temperature NMR studies have provided certain indications of a possible cyclopropylindoline intermediate. This observation lends support to the hypothesis that **64** may be formed through the initial formation of a cyclopropane ring, followed by ring opening. In a follow-up to this seminal work, the Kerr group enhanced the efficiency of the reaction by replacing the Rh(II) catalyst with a more cost-effective Cu(II) catalyst, which also provided C3 or C2 functionalized products in higher yields in most cases when compared to the rhodium examples.[26]

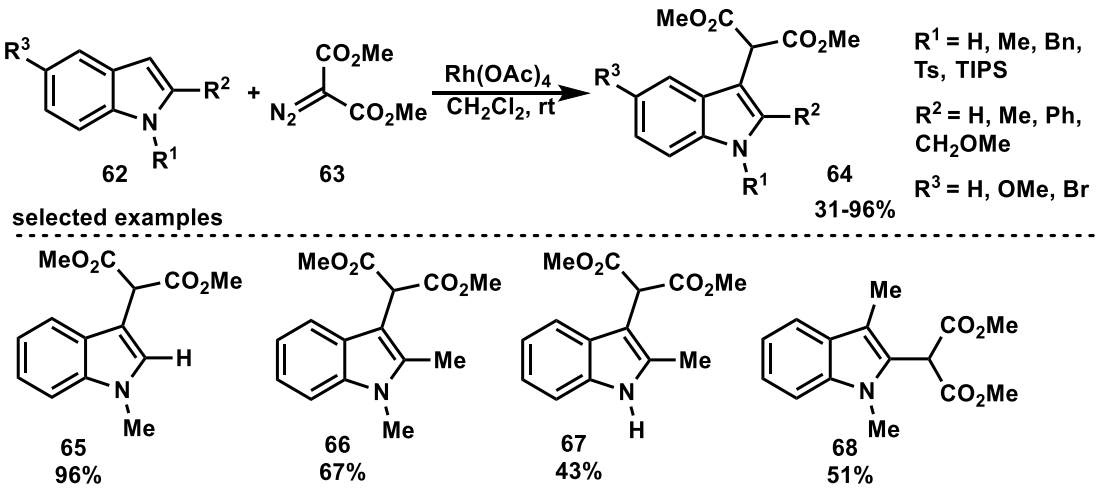

Scheme 1.10: Preparation of indolyl malonates via carbenoid insertion.

1.5 Conia-ene Reactions

An interesting area of research within organic synthesis is the field devoted to the construction of functionalized ring systems (carbocycles and heterocycles), a prevalent structural motif found in natural products, pharmaceuticals, and material molecules.[27] The Conia-ene reaction is a synthetically useful tool that holds significant value in this area. In general, the Conia-ene reaction involves a C−C bond formation through an intramolecular, preferably *exo* cyclization of an enolizable carbonyl (enol and enolate **69′**forms) with either an alkyne or an alkene (Scheme 1.11). The discovery of this reaction dates to 1975 by the report of Conia and Perchec[28] and traditionally this transformation was preformed using high temperatures or strong Brønsted acids. However, modern advances in this area of research have led to milder activation conditions, typically through the use of Lewis acids or transition metal catalysts.[29]

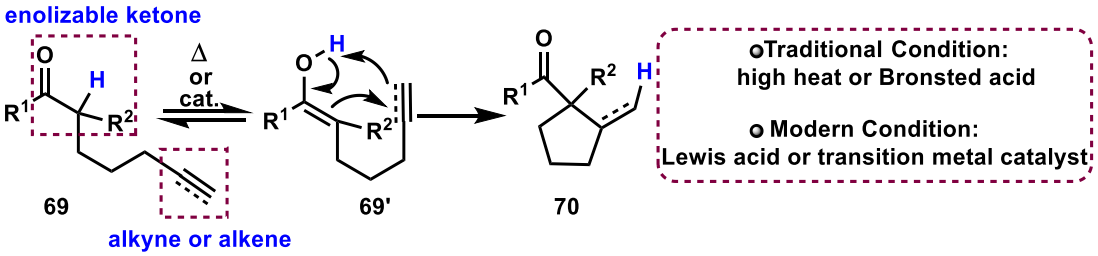

Scheme 1.11: The Conia-ene reaction.

1.5.1 Tandem Conia-ene Reaction Involving Diazocarbonyls

A notable advancement of the Conia-ene reaction is through its utilization in tandem reaction processes. Tandem reactions are reactions, in which a minimum of two sequential transformations occur without isolation of any intermediates or adding additional reagents, which have become popular practices in synthetic chemistry due to their efficiency, selectivity, and atom economy.[30] In this context, transformations that generate an enolate in one step could be coupled with a Conia-ene cyclization in a second step as a one-pot approach to the synthesis of complex multifunctional cyclized materials. An example of this type of tandem reaction process can be seen through the heteroatom–H bond insertion of diazo compounds, which can generate a metal enolate intermediate that can undergo a cyclization with an alkene or alkyne. In 2014, Hatakeyama showed [4 + 1]-cycloaddition of readily available homopropargyl alcohols

71 with diazo *α*-dicarbonyl compounds **72** to construct substituted tetrahydrofurans (Scheme **1.12**, **74)**. The methodology utilizes cooperative Rh(II)/Zn(II) catalysis and involves a tandem O−H insertion/Conia-ene cyclization.[31]

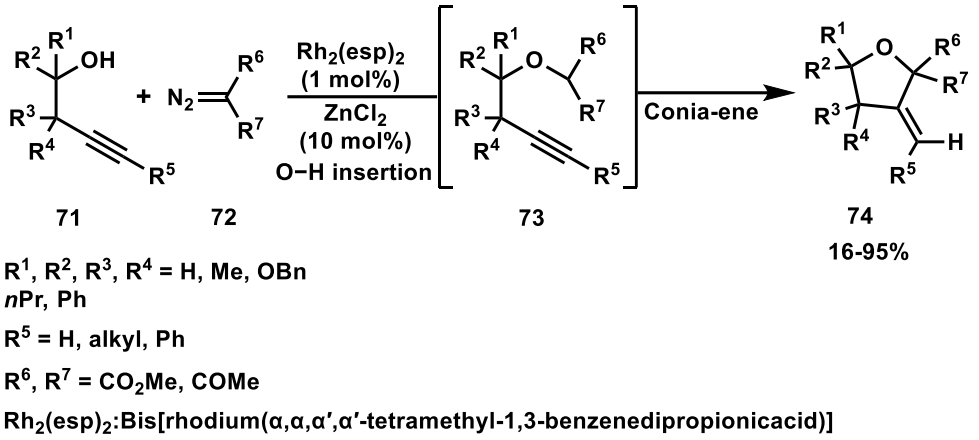

Scheme 1.12: Tetrahydrofuran synthesis via a tandem O−H insertion/conia-ene cyclization.

1.6 Project Objectives

Given the known and predictable C–H functionalization reaction of indoles with diazo compounds and inspired by the work of Hatakeyama,[31] we envisioned that it would be feasible to construct multi-functionalized bicyclic indole compounds by developing a tandem diazo C–H insertion/Conia-ene protocol (Scheme 1.13). From the onset, we believed that the most facile entry point in developing this tandem reaction would be to employ functionalized indole substrates where the alkyne electrophile, required for the Conia-ene step of the reaction (**77** → **78**), was connected to the indole nitrogen (**75**). These substrates were chosen as starting materials due to the ease of installing the electrophile through standard basic *N*-alkylation chemistry, ultimately allowing us to start our project with simple indole building blocks. Based on the location of alkyne electrophile, the initial C–C bond forming step of our tandem reaction, the diazo C–H insertion (**75** → **77**), would need to occur at the C2 position of the indole. To help control the regioselectivity of this C–H functionalization, appropriate functional groups would be required at the C3 position of the indole starting materials. If successful, the development of this unique tandem reaction would provide an efficient way to obtain substituted 1,2-pyrroloindoles **78**.

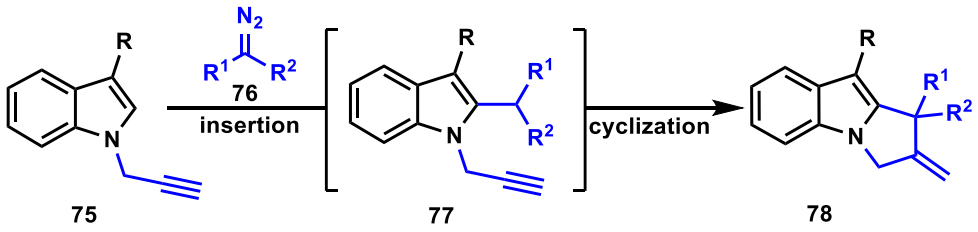

Scheme 1.13: Proposed route for the tandem insertion/conia-ene reaction.

1.7 Results and Discussion

1.7.1 Preparation of Starting Materials

To investigate the effect of different substituents on the tandem insertion/cyclization reaction, we required a diverse library of easily accessible C3 functionalized indoles. Since various functional groups needed to be installed on C3-position of the indole, divergent synthetic strategies were employed to functionalize the indole scaffolds involving multiple synthetic steps. The final step toward synthesizing the indole substrates was subjecting the C3-substituted indoles to a reaction with propargyl bromide. For example, compound **82** was synthesized via a sequential three-step process initiated by the reduction of 3-indolepropionic acid (**79**) with $LiAlH_4$ (Scheme 1.14A). The primary alcohol produced from this reduction was then protected as the TBS ether **81** using *t*-butyldimethyl silyl chloride (**80**, TBSCl) and imidazole. The final step involved propargylation of the nitrogen atom of the indole yielding 55% of the desired product **81**. While many other functionalized indoles were obtained from similar sequential functional group interconversion and protection strategies, starting from commercially available starting material (e.g., tryptamine and tryptophan), C3-aryl indoles could be obtained via a direct C–H arylation reaction with indole. For example, the synthesis of 3-(4-methoxyphenyl)-1*H*-indole (**86**) was conducted by the cross-coupling reaction of 1*H*-indole with 4-bromoanisole (**84**), facilitated by palladium acetate, $Pd(OAc)_2$ (Scheme 1.14B). The subsequent propargylation step resulted in the formation of compound **86** with a yield of 70%.

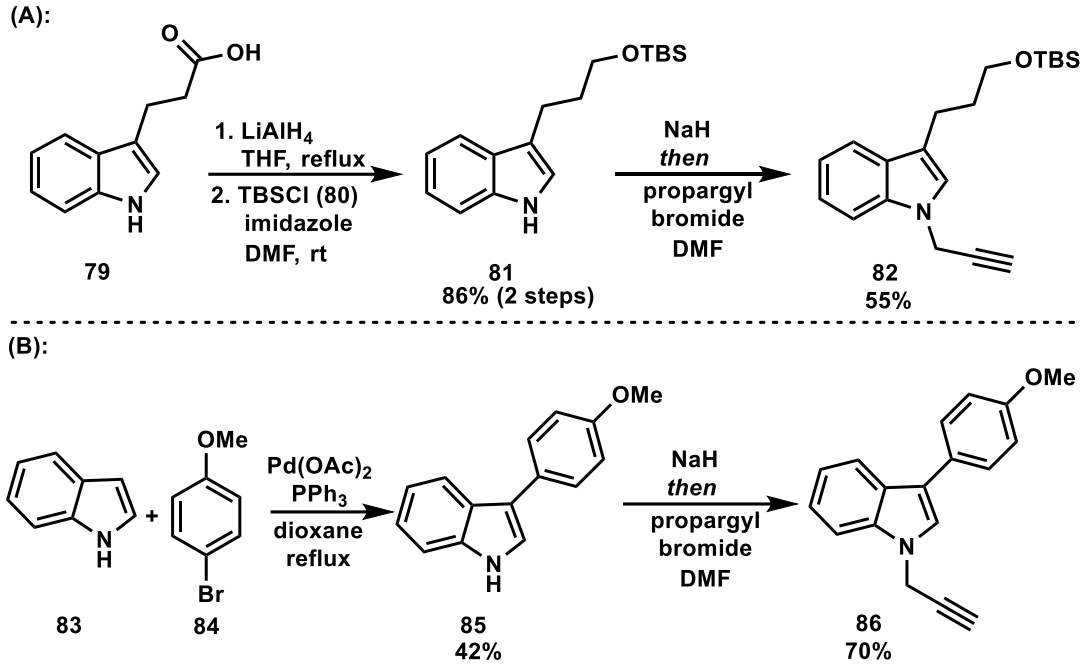

Scheme 1.14: Selected procedures for the preparation of C3-substituted indole substrates.

By using these general strategies, a diverse collection of *N*-propargylindole substrates was prepared, which are displayed in Table 1.1; for simplicity only the propargylation step has been showcased in this table. In most cases, the propargylation step was performed by treating the indole with sodium hydride followed by adding propargyl bromide to the reaction vial at 0 °C (**90-95**, conditions A). However, in some cases, certain indole substrates produced various side products under these conditions, a problem which could be addressed by adding the propargyl bromide to the reaction at – 10 °C (**96-99**, conditions B).

Table 1.1: C3-Substituted *N*-Propargyl Indole Substrates

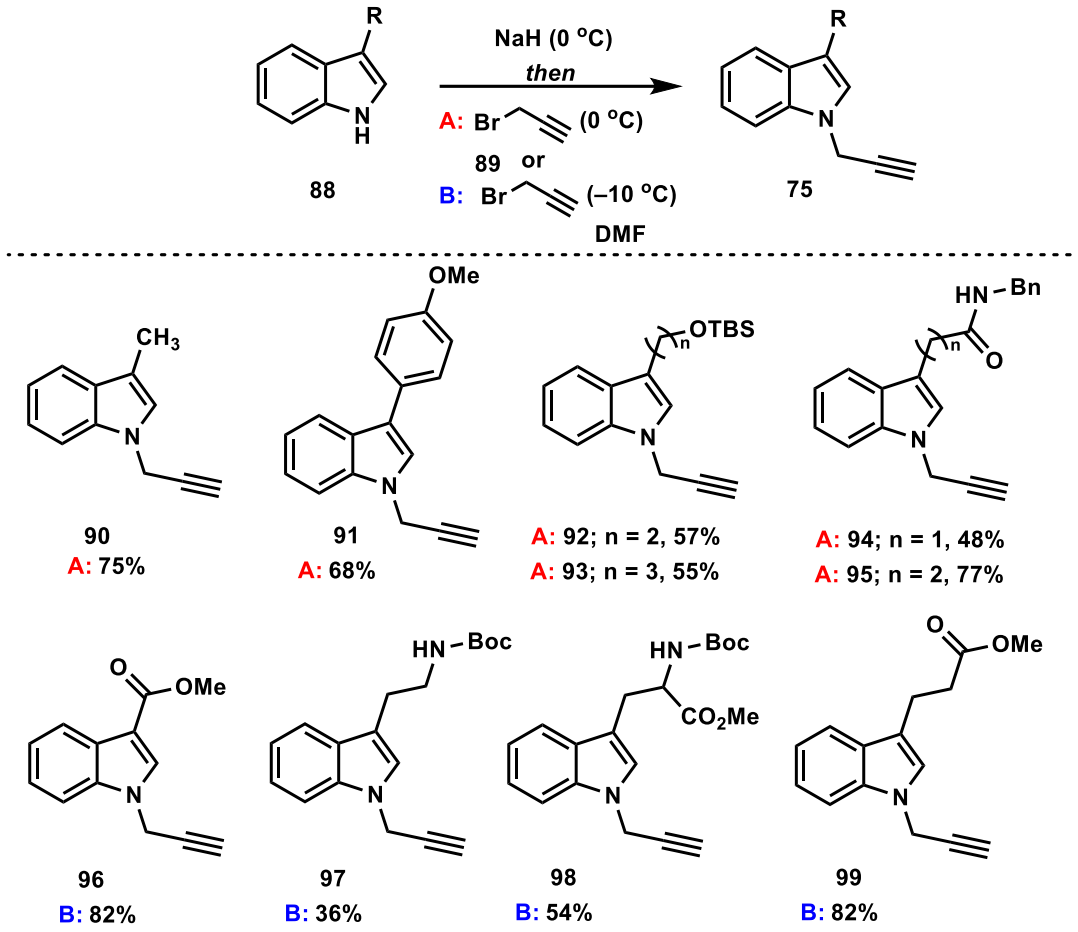

1.7.2 Preliminary Optimization of the Tandem Reaction and Preliminary Substrate Scope

With access to indole starting materials and diazomalonates (from a diazo transfer reaction)[32] we next focused our efforts on discovering a catalyst system capable of promoting both the formal C–H insertion and Conia-ene processes in a tandem fashion. Indole **90** and diazomalonate **101** were chosen for these optimization experiments (Table 1.2). Initial reactions between **90** and **101** were conducted with copper-based catalysts due to their known reactivity towards *α*-diazodicarbonyl compounds[33] and their use in the Conia-ene reaction.[34] Despite the literature precedent, the use of copper catalyst (e.g., Table 2.1, entry 1) failed to produce the desired cyclized product **102** and only provided the C–H insertion product **103** in modest yields. Interestingly, switching from copper to the rhodium(II) acetate dimer catalyst yielded **103** in 38% yield along with 7% of the desired product **102** (entry 2). To increase the

solubility of the rhodium catalyst, reactions were heated at reflux dichloromethane (CH_2Cl_2), resulting in a higher yield of **102** (12%) (while formation of **103** decreased to 34%), and reduced reaction time (entry 3). With the aim of promoting the cyclization step of the tandem sequence, the focus was on the development of a dual catalyst system capable of promoting both the C2 functionalization and Conia-ene cyclization (entries 4−6). In combination with $Rh_2(OAc)_4$, Lewis acid catalysts recognized for their ability to facilitate the cyclization process (Cu, Zn)[35] were examined. Both of these additional catalysts yielded **102** as the major isolable product, with $ZnBr_2$ providing a 47% yield and complete consumption of the limiting reagent **101** (entry 6).

Table 1.2: Primary Optimization of the Tandem C−H Insertion/ Conia-ene Cyclization

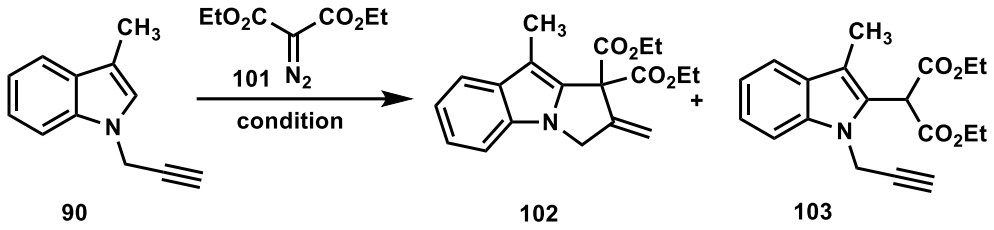

Entry	Catalyst (mol%)	Solvent (temp °C)	time (h)	result[b]
1	$Cu(acac)_2$ (10%)	C_6H_6 (reflux)	24	**103**: 35%
2	$Rh_2(OAc)_4$ (2%)	C_6H_6 (reflux)	24	**103**: 38%, **102**: 7%
3	$Rh_2(OAc)_4$ (2%)	CH_2Cl_2 (reflux)	2	**103**: 34%, **102**: 12%
4	$Rh_2(OAc)_4$ (2%) $Cu(acac)_2$ (10%)	CH_2Cl_2 (reflux)	2	**103**: 24%, **102**: 28%
5	$Rh_2(OAc)_4$ (2%) $Zn(OTf)_2$ (10%)	CH_2Cl_2 (reflux)	2	**103**: 10%, **102**: 30%
6	$Rh_2(OAc)_4$ (2%) $ZnBr_2$ (10%)	CH_2Cl_2 (reflux)	2	**102**: 47%

[a] Reaction conditions: **100** (1.2 equiv), **101** (1.0 equiv), cat. (as per table), solvent (0.2 M). [b] Isolated yields.

Following these findings, the objective was to explore the possibility of achieving enhanced yields by varying the substituent on C3 of indole substrates. Utilizing the prepared library of C3-substituted *N*-propargylindoles **91**-**99**, we performed a series of reactions under the Rh/Zn reaction conditions (Scheme 1.15). Unfortunately, although each reaction consumed the diazo starting material **101** all the

reactions explored resulted in complex intractable mixtures of products. The ^{1}H NMR analysis of the crude mixtures indicated the presence of both the indole and diazo components. However, the crude material, which proved difficult to purify by chromatography, contained various compounds, making it challenging to identify the structure connectivity of any individual product in the mixture.

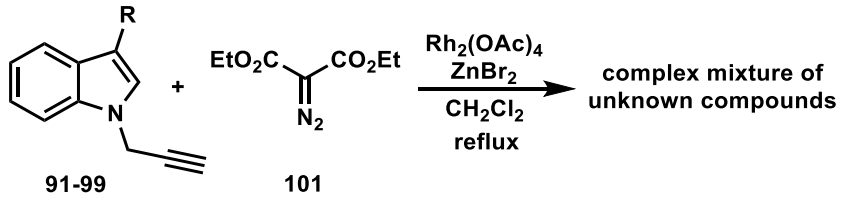

Scheme 1.15: Rh/Zn catalyzed of C3-substituted *N*-propargylindoles.

Having observed the formation of multiple unknown side-products in the initial substrate screen (Scheme 1.15), it was hypothesized that these side products could have formed from undesired reactions of the diazo compound with the indole substrate at a position other than the C2 site (Scheme 1.16). For example, reaction of the diazo compound with the alkyne moiety could generate the cyclopropene **104**.[36] Alternatively, C–H functionalization on the benzenoid ring[37] of the indole with the diazo reagent, would lead to a functionalized indole product (**105**) incapable of undergoing the subsequent annulation step.

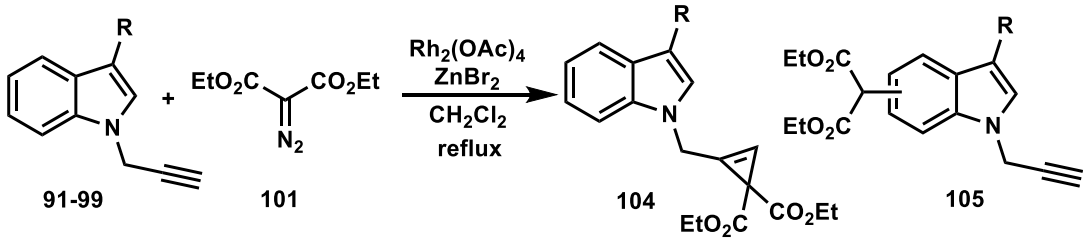

Scheme 1.16: Potential products in the unknown mixture.

To avoid some of the side reactions, it was considered to explore an intramolecular version of the tandem process in hopes of increasing the site selective indole C2–H functionalization step. In order to accomplish this goal, first the C3-diazosubstituted *N*-propargylindole was synthesized (**108**) through a scandium-catalyzed Michael addition reaction of *N*-propargylindole and diazo-enone **107**, following a known literature procedure (Scheme 1.17).[38] The intramolecular

cyclization of the **108** in the presence of the dual catalyst system ($Rh_2(OAc)_4/ZnBr_2$) unfortunately did not deliver the desired compound and again formed a complex mixture of unknown products (this section will be discussed in detail in Chapter 3).

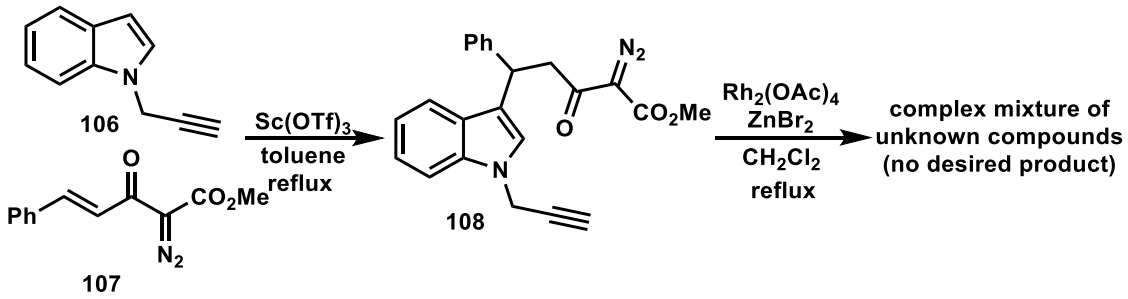

Scheme 1.17: Intramolecular reaction of **108** catalyzed by Rh/Zn

1.7.3 Identification of Reaction Side-Product and Final Optimization of Tandem Reaction

Continuing our exploration into identifying the side-products, upon employing the less reactive diazo-bis(2,2,2-trifluoroethyl) malonate **109** under the given conditions, a yield of 57% for **110** was obtained (Table 1.3, entry 1). This change in reagent not only resulted in an increase in yield but also enabled the detection of four competing side products, **111** (8%) and **112** (3%), wherein functionalization takes place either on C5 or C6 benzenoid ring, and **113** and **114** where two positions are functionalized in trace amount. It should be noted that further optimizations studies, varying solvents and reaction temperatures, were conducted by my colleague and ultimately resulted in a 64% yield of the desired pyrroloindole **110**, as well as a combined yield of 15% for the benzenoid-substituted indoles **111** and **112** (entry 2). (For full details on the reaction optimization refer to reference 39)

Table 1.3: Optimization of the Tandem C−H Insertion/ Conia-ene Cyclization

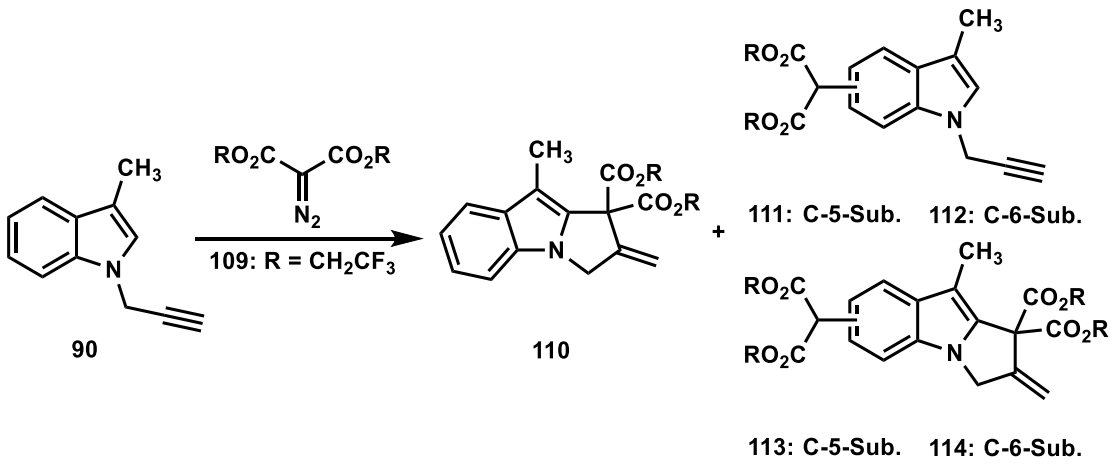

Entry	Catalyst (mol%)	Solvent (temp °C)	time (h)	result[b]
1	$Rh_2(OAc)_4$ (2%) $ZnBr_2$ (10%)	CH_2Cl_2 (reflux)	2	**110**: 57%, **111**: 8%, **112**: 3%
2	$Rh_2(OAc)_4$ (2%) $ZnBr_2$ (10%)	$CF_3C_6H_5$ (90 °C)	2	**110**: 64%, **111**: 9%, **112**: 6%

[a] Reaction conditions: **100** (1.2 equiv), **109** (1.0 equiv), cat. (as per table), solvent (0.2 M). [b] Isolated yields. [c]**113** and **114** are isolated in very small quantities (less than 3%)

To address the issue related to the side-product resulting from benzenoid insertion, it was hypothesized that installing a blocking group on the benzenoid ring could be a potential solution, due to the steric effect of the substitution at C5. To probe this theory, the 5-methoxy-*N*-propargylskatole (**118**) was synthesized and subjected to a reaction with **109** under optimized conditions, allowing a direct comparison with the results obtained from substrate **90** (Scheme 1.18). As anticipated, the pyrroloindole **116** was successfully obtained in an increased yield (76%) with methoxy substituent at C5-position of the indole, compared to the unsubstituted product **110** (64%). Notably, in this experiment there was no indication by ^{1}H NMR of any competitive benzenoid C–H insertion products.

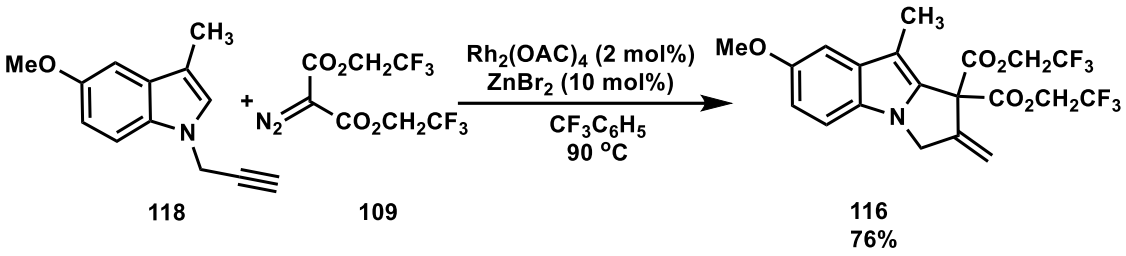

Scheme 1.18: Control experiment of 5-methoxy substituted substrate **118**.

Given the success of this blocking group strategy, a library of C3-substituted indole substates in which a methoxy group was installed at C5 of the indole where then prepared. Each C3-substituted indole starting material (**117**) was prepared through similar multi-step processes as described in Scheme 1.14, utilizing an appropriate C5-methoxy indole building block. Subsequent propargylation of the nitrogen yielded the desired *N*-propargylindoles in **44**% to **71**% yields (Table 1.4).

Table 1.4: 5-Methoxy-*N*-Propargyl Indole Substrates

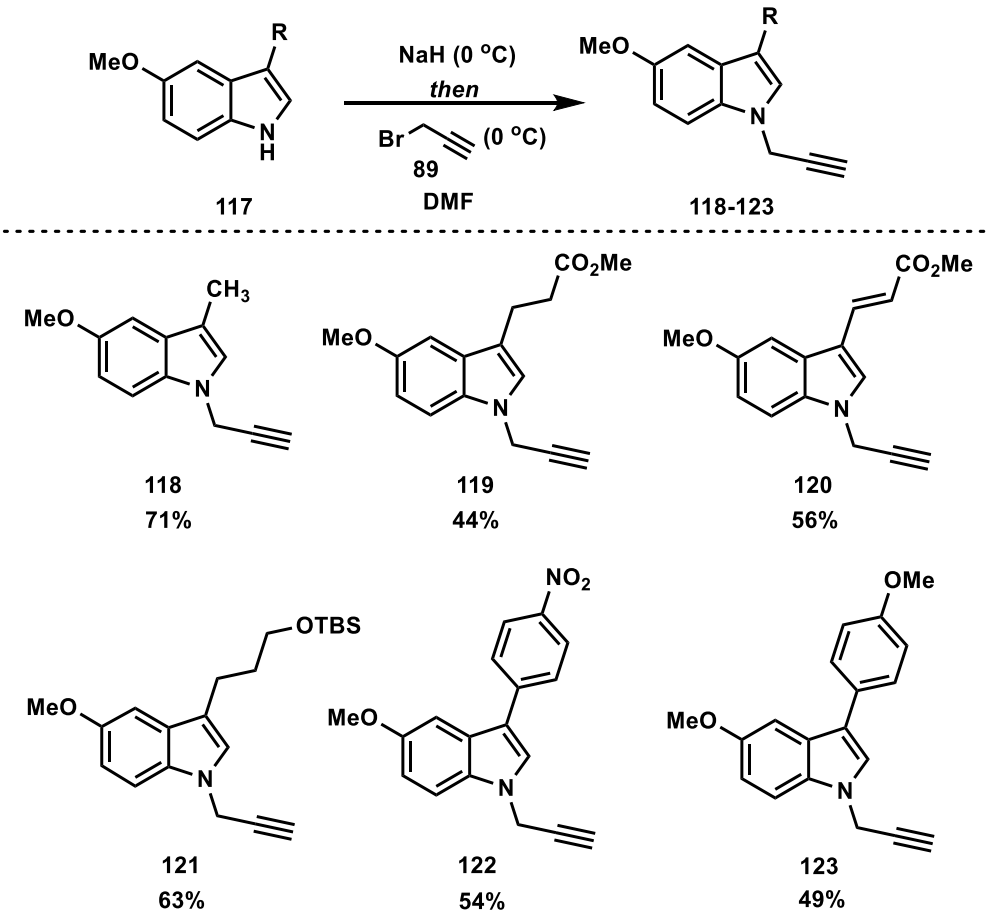

1.7.4 Synthesis of Pyrroloindoles via Tandem C−H Functionalization/Conia-ene Reaction

Utilizing the optimized reaction conditions (entry 2, Table 1.3), with diazo **109**, next the tolerance of the tandem C−H functionalization/Conia-ene cyclization protocol was evaluated on varying substituents on the indole starting material **124** (Table 1.5). It is worth noting that apart from the methoxy group, other substitutions were incorporated into C5 or C6 position to expand the substrate scope and explore how different substituents affect the efficiency of the reaction*.[39] As expected, based on the optimization studies, the incorporation of substituents at the C5 and C6 positions of the indole starting material resulted in higher yields of the desired pyrroloindoles (**126**-**132**) compared to using unsubstituted indole starting materials (**110**) (Table 1.5). The enhanced yields obtained by incorporating substituents at the C5 and C6 positions of the indole starting materials can be attributed to a reduction in the formation of undesired benzenoid C−H functionalization side-products. Both electron-donating and alkyl substituents were tolerated under the optimal reaction conditions providing pyrroloindoles **116** (5-OMe), **129** (6-OMe), and **130** (6-Me) in moderate yields, while substrates substituted with halogen substituents gave the highest yields (**126**, **127**, and **131**). Conversely, when a strongly electron-withdrawing group was substituted to indole, its reactivity sharply decreased, resulting in a low yield of only 21% for pyrroloindole **128**. This outcome is not surprising since deactivating effect of nitro groups (and other electron-withdrawing groups) at the C5 position of indole is well-known.[40] Such groups can influence the nucleophilic nature of the indole, thereby reducing the ability to undergo functionalization with electrophilic metal carbenoids. Next, we investigated the influence of different substituents at the C3 position. It was discovered that replacing the C3 methyl group on the indole starting material with longer alkyl chains led to a noticeable decrease in the isolated yields of the desired product. For instance, pyrroloindoles **133** and **135** with longer alkyl substitutions were obtained only in 38% and 30% yields compared to the C3 methyl product **110** which was isolated in a 64% yield. Potentially, when there is an increase in steric hindrance

* These experiments were conducted by my colleague (A. Bhat), and a few of these have been included in Table 1.5; for more details, refer to reference 39.

adjacent to C2, it leads to a higher possibility of benzenoid substitution, which by could be solved by placing substitution on benzenoid ring (**134** and **136**). Although this approach shows promise, its effectiveness is restricted to specific types of C-3 substituents. We observed that when the electronic properties or size of the substituent group is changed, the overall yield decreases (e.g., **137** and **138**).

Table 1.5: Synthesis of Pyrroloindoles, Substrate Scope

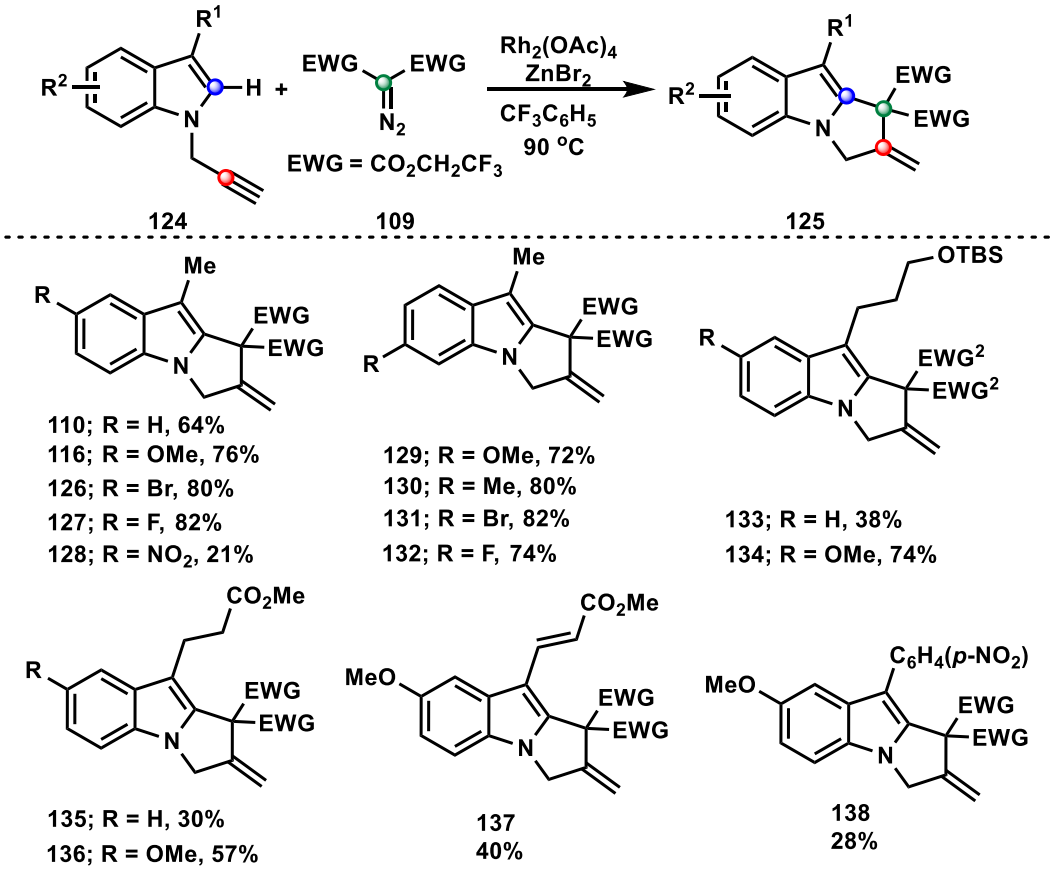

In addition to the experiments discussed in Table 1.5, my colleague has extensively investigated the impact of various functional groups on the indole starting materials and substitution on the diazo reagent. Notably, the findings have proven useful in synthesizing larger ring systems such as pyridoindoles and azepinoindoles by starting with a longer alkyne chain tethered to nitrogen. (For more detailed information, please refer to reference 39).

1.8 Conclusion

In conclusion, a variety of pyrroloindole scaffolds have been successfully

synthesized employing a tandem C–H functionalization/Conia-ene cyclization approach. The first step toward this goal was preparing a library of C3-substituted-*N*-propargylated indole substrates. Next, through an applicable dual catalyst system (Rh/Zn), a series of diversely substituted pyrroloindoles were synthesized in a one-pot process. Concerning other methodologies, this strategy offers several noteworthy advantages, including (i) being tolerant of various EWG and EDG groups on the benzenoid ring of indole starting material and various alkyl groups on the C3 of indole; (ii) delivering moderate to high yields of the desirable pyrroloindole products; and (iii) being effective in the construction of larger ring systems, such as pyridoindoles and azepinoindoles in good overall yield.

1.9 Experimental

1.9.1 General Procedure

Unless stated otherwise, all reactions were performed in flame-dried glassware under an atmosphere of dry nitrogen. Dry trifluorotoluene ($PhCF_3$) and *N,N*-dimethylformamide (DMF) were obtained from Sigma Aldrich Sure/Seal™ bottles. Dry methyl *t*-butyl ether (MTBE) was obtained from Alfa Aesar™. All other reagents were used as received from commercial sources, unless stated otherwise. When indicated, solvents or reagents were degassed by sparging with argon for 10 min in an ultrasound bath at 25 °C. For reactions the were conducted above room temperature, oil bath heating was used as the heat source. Reactions were monitored by thin layer chromatography (TLC) on Silicycle Siliaplate™ glass-backed TLC plates (250 μm thickness, 60 Å porosity, F-254 indicator) and visualized by UV irradiation or development with an anisaldehyde. Volatile solvents were removed under reduced pressure with a rotary evaporator. All flash column chromatography was performed using Silicycle SiliaFlash® F60, 230-400 mesh silica gel (40-63 μm). ^{1}H NMR and ^{13}C NMR spectra were recorded with Bruker AV, spectrometers operating at 300 or 500 MHz for ^{1}H NMR (75, and 125 MHz for ^{13}C) in $CDCl_3$ or acetone-D_6. Except when noted otherwise, chemical shifts are reported relative to the residual solvent signal (^{1}H NMR: $\delta = 7.26$ ($CDCl_3$), $\delta = 2.05$ (acetone-D_6); ^{13}C NMR: $\delta = 77.16$ ($CDCl_3$)). NMR data are reported as follows: chemical shift (multiplicity, coupling constants where applicable, number of hydrogens). Splitting is reported with the

following symbols: s = singlet, br. s = broad singlet, d = doublet, t = triplet, app t = apparent triplet, dd = doublet of doublets, ddd = doublet of doublet of doublets, dddd = doublet of doublet of doublet of doublets, m = multiplet. Infrared (IR) spectra were recorded using neat samples on a Bruker Alpha spectrometer. High resolution mass spectrometry (HRMS) data were obtained using an Agilent 6200 series instrument, employing a TOF mass analyzer. Melting points (M.P.) were obtained on an OptiMelt instrument (a digital apparatus) produced by Stanford Research Systems by scanning temperature ranges from 40-150 °C at a rate of 3 °C/s.

1.9.2 Synthesis and Characterization of Substituted Indole Starting Materials

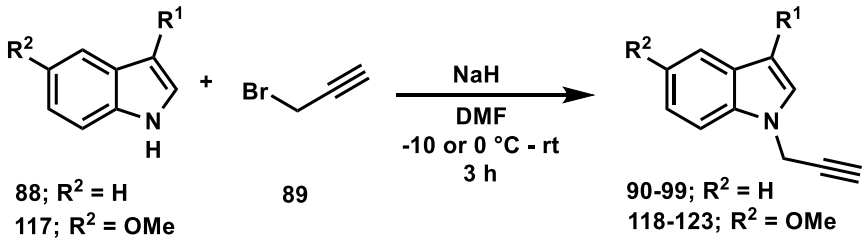

General Experimental Procedure A:

Substituted indole **88** or **117** (1 equiv) was added to a round bottom flask equipped with a magnetic stir bar and dissolved in DMF (2.5 mL/mmol of indole) under a N_2 atmosphere. The solution was cooled to –10/0 °C and NaH (60 % dispersion in mineral oil, 2.0 equiv) was added. The resulting slurry was stirred for 1 h at 0 °C, followed by the dropwise addition of propargyl bromide (80 wt. % solution in toluene, 2.0 equiv). The reaction mixture was then warmed to room temperature and stirred for 2 hrs. When the reaction was considered complete as determined by TLC analysis, the mixture was slowly quenched with H_2O, extracted three times with ethyl acetate, washed twice with H_2O, washed once with brine, dried over anhydrous Na_2SO_4, and concentrated in vacuo. The resulting residue was purified by silica gel flash column chromatography using a hexanes/EtOAc gradient to yield the substituted *N*-propargyl indoles (**90-99**) and (**118-123**).

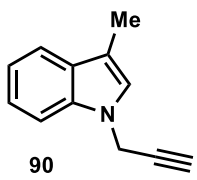

90

N-Propargylindole **90** was prepared using General Experimental Procedure **A**. Reagents employed: skatole (3.00 g, 22.9 mmol), propargyl bromide (4.33 mL, 45.7 mmol), NaH (1.82 g, 45.7 mmol). **90** (2.90 g, 17.1 mmol, 75%) was obtained as thick light brown oil:

***R*f** = 0.32, 20% EtOAc in hexanes;
M.P. = 124-127 ºC
^{1}H NMR (300 MHz, $CDCl_3$) δ = 7.55 (app dt, *J* = 7.8, 0.8 Hz, 1H), 7.30 (app dt, *J* = 8.2, 1.0 Hz, 1H), 7.25 – 7.17 (m, 1H), 7.11 (ddd, *J* = 8.0, 7.0, 1.1 Hz, 1H), 6.90 (q, *J* = 1.1 Hz, 1H), 4.71 (d, *J* = 2.5 Hz, 2H), 2.33-2.26 (m, 4H).
^{13}C NMR (75 MHz, $CDCl_3$) δ = 136.3, 129.3, 124.9, 121.9, 119.3, 111.5, 109.3, 78.3, 73.2, 35.5, 9.7. (one carbon missing due to overlap at 119.3).
IR (neat): ν_{max} = 3285, 2885, 1480, 1328, 924, 735 cm^{-1}.
HRMS (APPI+): calc'd for $C_{12}H_{11}N$ $[M+H]^+$ 170.0964, found 170.0960.

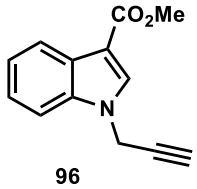

96

N-Propargylindole **96** was prepared using General Experimental Procedure A. Reagents employed: indole starting material (0.1 g, 0.57 mmol), propargyl bromide (0.11 mL, 1.14 mmol), NaH (0.046 g, 1.14 mmol). **96** (0.10 g, 0.47 mmol, 82%) was obtained as cream solid. **Note a change in the general procedure**: propargyl bromide was added to a solution of NaH and indole starting material at –10 °C instead of 0 °C.

***R*f** = 0.35, 20% EtOAc in hexanes;
^{1}H NMR (300 MHz, $CDCl_3$): δ 8.22 – 8.16 (m, 1H), 7.97 (s, 1H), 7.46 – 7.40 (m, 1H), 7.35 – 7.29 (m, 2H), 4.91 (d, *J* = 2.6 Hz, 2H), 3.92 (s, 3H), 2.50 (t, *J* = 2.6 Hz, 1H).
^{13}C NMR (75 MHz, $CDCl_3$): δ 165.4, 136.3, 133.7, 127.0, 123.2, 122.4, 122.1, 109.90, 108.0, 77.6, 75.1, 51.2, 36.6.

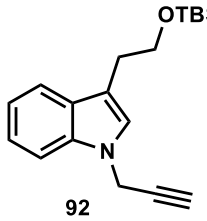

92

N-Propargylindole **92** was prepared using General Experimental Procedure A. Reagents employed: indole starting material (0.21 g, 0.76 mmol), propargyl bromide (0.15 mL, 1.52 mmol), NaH (0.061 g, 1.52 mmol). **92** (0.135 g, 0.43 mmol, 57%) was obtained as white solid:

***R*f** = 0.45, 20% EtOAc in hexanes;
^{1}H NMR (300 MHz, $CDCl_3$): δ 7.57 (app dt, *J* = 7.8, 1.0 Hz, 1H), 7.33 (app dt, *J* = 8.2, 0.9 Hz, 1H), 7.24 – 7.16 (m, 1H), 7.10 (ddd, *J* = 8.0, 7.0, 1.1 Hz, 1H), 7.01 (s, 1H), 4.79 (d, *J* = 2.5 Hz, 2H), 3.84 (t, *J* = 7.4 Hz, 2H), 2.95 (t, *J* = 7.7 Hz, 2H), 2.34 (t, *J* = 2.5 Hz, 1H), 0.87 (s, 9H), 0.00 (s, 6H).
^{13}C NMR (75 MHz, $CDCl_3$): δ 136.1, 128.8, 125.4, 122.0, 119.4, 119.4, 112.9, 109.4, 78.1, 73.4, 64.0, 35.7, 29.1, 26.2, 18.5, -5.1.

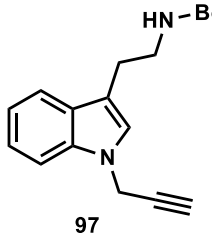

97

N-Propargylindole **97** was prepared using General Experimental Procedure A. Reagents employed: indole indole starting material (0.374 g, 1.44 mmol), propargyl bromide (0.281 mL, 2.88 mmol), NaH (0.115 g, 2.88 mmol). **97** (0.155 g, 0.52 mmol, 36%) was obtained as white solid: **Note a change in the general procedure**: propargyl bromide was added to a solution of NaH and indole starting material at –10 °C instead of 0 °C.

***R*f** = 0.40, 20% EtOAc in hexanes;
^{1}H NMR (300 MHz, $CDCl_3$): δ 7.60 (app dt, *J* = 7.9, 1.0 Hz, 1H), 7.38 (app dt, *J* = 8.2, 0.9 Hz, 1H),7.30 – 7.21 (m, 1H), 7.14 (ddd, *J* = 8.0, 7.0, 1.1 Hz, 1H), 7.04 (s, 1H),

4.84 (d, J = 2.6 Hz, 2H), 4.60 (br. s, 1H), 3.45 (app q, J = 6.0 Hz, 2H), 2.95 (t, J = 6.9 Hz, 2H), 2.39 (t, J = 2.5 Hz, 1H), 1.44 (s, 6H).
^{13}C NMR (75 MHz, $CDCl_3$): δ 156.1, 136.4, 128.5, 125.3, 122.2, 119.7, 119.3, 113.0, 109.5, 79.2, 77.9, 73.6, 41.0, 35.8, 28.6, 25.9.

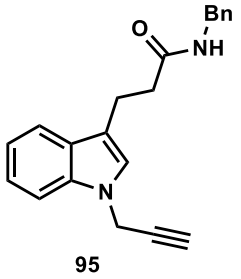

95

N-Propargylindole **95** was prepared using General Experimental Procedure A. Reagents employed: indole starting material (0.098 g, 0.35 mmol), propargyl bromide (0.069 mL, 0.7 mmol), NaH (0.028 g, 0.7 mmol). **95** (0.086 g, 0.27 mmol, 77%) was obtained as white solid:

***R*$_f$** = 0.27, 20% EtOAc in hexanes;
^{1}H NMR (300 MHz, $CDCl_3$): δ 7.60 (app dt, J = 7.9, 1.0 Hz, 1H), 7.38 (app dt, J = 8.2, 0.9 Hz, 1H), 7.28 – 7.22 (m, 4H), 7.16 – 7.09 (m, 3H), 6.99 (br. s, 1H), 5.57 (br. s, 1H), 4.79 (d, J = 2.5 Hz, 2H), 4.38 (d, J = 5.7 Hz, 2H), 3.15 (t, J = 7.3 Hz, 2H), 2.60 (t, J = 7.3 Hz, 2H), 2.36 (t, J = 2.5 Hz, 1H).
^{13}C NMR (75 MHz, $CDCl_3$): δ 172.5, 138.4, 136.3, 128.8, 128.2, 127.9, 127.5, 125.1, 122.2, 119.6, 119.2, 114.7, 109.6, 73.5, 43.7, 37.6, 35.8, 25.1, 21.4.

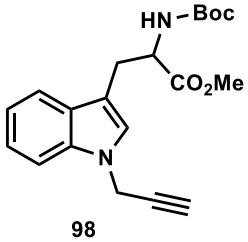

98

N-Propargylindole **98** was prepared using General Experimental Procedure A. Reagents employed: indole starting material (0.315 g, 0.99 mmol), propargyl bromide (0.195 mL, 1.98 mmol), NaH (0.080 g, 1.98 mmol). **98** (0.188 g, 0.53 mmol, 54%) was obtained as thick clear oil: **Note a change in the general procedure**: propargyl bromide was added to a solution of NaH and indole starting material at –10 °C instead of 0 °C.

***R*$_f$** = 0.30, 20% EtOAc in hexanes;
^{1}H NMR (300 MHz, $CDCl_3$): δ 7.55 (app dt, J = 7.8, 1.0 Hz, 1H), 7.36 (app dt, J = 8.2, 1.0 Hz, 1H), 7.28 – 7.21 (m, 1H), 7.14 (ddd, J = 8.1, 7.0, 1.1 Hz, 1H), 7.02 (s, 1H), 5.06 (d, J = 8.0 Hz, 1H), 4.83 (d, J = 2.5 Hz, 2H), 4.69 – 4.60 (m, 1H), 3.68 (s, 3H), 3.28 (d, J = 4.8 Hz, 2H), 2.39 (t, J = 2.5 Hz, 1H), 1.43 (s, 9H).
^{13}C NMR (75 MHz, $CDCl_3$): δ 172.8, 155.3, 136.2, 128.8, 125.9, 122.3, 119.9, 119.3, 110.0, 109.5, 77.8, 75.5, 73.7, 54.3, 52.8, 52.4, 35.8, 28.5.

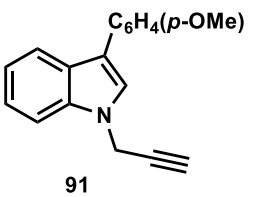

91

N-Propargylindole **91** was prepared using General Experimental Procedure A. Reagents employed: indole starting material (0.062 g, 028 mmol), propargyl bromide (0.055 mL, 0.56 mmol), NaH (0.022 g, 0.56 mmol). **91** (0.050 g, 0.19 mmol, 68%) was obtained as cream solid:

***R*$_f$** = 0.48, 20% EtOAc in hexanes;
^{1}H NMR (300 MHz, $CDCl_3$): δ 7.89 (app dt, J = 7.9, 1.0 Hz, 1H), 7.61 – 7.54 (m, 2H), 7.43 (app dt, J = 8.2, 1.0 Hz, 1H) 7.33 – 7.26 (m, 2H), 7.20 (ddd, J = 8.1, 7.0, 1.1 Hz, 1H), 7.03 – 6.97 (m, 2H), 4.91 (d, J = 2.5 Hz, 2H), 3.86 (s, 3H), 2.42 (t, J = 2.5 Hz, 1H).

^{13}C NMR (75 MHz, $CDCl_3$): δ 158.3, 136.6, 128.7, 128.0, 127.0, 124.4, 122.4, 120.4, 120.3, 117.7, 114.4, 109.7, 73.9, 55.5, 36.0.

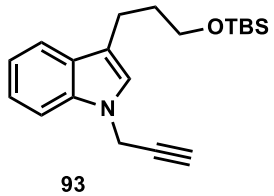

93

N-Propargylindole **93** was prepared using General Experimental Procedure A. Reagents employed: 3-(3-((*t*-butyldimethylsilyl) oxy)propyl)-1*H*-indole (1.00 g, 3.46 mmol), propargyl bromide (0.650 mL, 6.92 mmol), NaH (0.206 g, 5.19 mmol). **93** (0.605 g, 1.85 mmol, 53%) was obtained as pale yellow oil: **Note a change in the general procedure**: propargyl bromide was added to a solution of NaH and indole starting material at –10 °C instead of 0 °C.

***R*f** = 0.74, 20% EtOAc in hexanes;

^{1}H NMR (300 MHz, $CDCl_3$): δ 7.54 (app dt, *J* = 7.9, 1.1 Hz, 1H), 7.29 (app dt, *J* = 8.3, 1.0 Hz, 1H), 7.28 – 7.17 (m, 1H), 7.05 (ddd, *J* = 8.0, 7.0, 1.1 Hz 1H), 6.98 (s, 1H), 4.82 (d, *J* = 2.5 Hz, 2H), 3.69 (t, *J* = 6.3 Hz, 2H), 2.87 – 2.70 (m, 2H), 2.37 (t, *J* = 2.5 Hz, 1H), 1.99 – 1.76 (m, 2H), 0.92 (s, 9H), 0.06 (s, 6H).

^{13}C NMR (75 MHz, $CDCl_3$): δ 136.3, 128.7, 124.5, 122.0, 119.5, 119.3, 116.3, 109.3, 78.2, 73.3, 62.8, 35.7, 33.3, 26.1, 21.4, 18.5, -5.1.

IR (neat): ν_{max} = 3309, 2951, 2855, 1465, 1252, 1094, 833, 773 cm^{-1}.

HRMS (APPI+): calc'd for $C_{20}H_{29}NOSi$ $[M+H]^+$ 328.2097, found 328.2092.

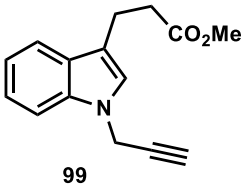

99

N-Propargylindole **99** was prepared using General Experimental Procedure A. Reagents employed: methyl-3-(1*H*-indol-3-yl)propanoate (0.203 g, 1.00 mmol), propargyl bromide (0.189 mL, 2.00 mmol), NaH (0.060 g, 1.5 mmol). **99** (0.194 g, 0.804 mmol, 80%) was obtained as thick clear oil: **Note a change in the general procedure**: propargyl bromide was added to a solution of NaH and indole starting material at –10 °C instead of 0 °C.

***R*f** = 0.6, 20% EtOAc in hexanes;

^{1}H NMR (300 MHz, $CDCl_3$): δ 7.59 (app dt, *J* = 7.9, 1.1 Hz, 1H), 7.35 (app dt, *J* = 8.3, 1.0 Hz, 1H), 7.28 – 7.20 (m, 1H), 7.13 (ddd, *J* = 8.0, 7.1, 1.1 Hz, 1H), 7.00 (t, *J* = 1.0, 1H), 4.82 (d, *J* = 2.5 Hz, 2H), 3.68 (s, 3H), 3.15 – 3.01 (m, 2H), 2.74 – 2.69 (m, 2H), 2.37 (t, *J* = 2.5 Hz, 1H).

^{13}C NMR (75 MHz, $CDCl_3$): δ 173.9, 136.3, 128.3, 124.7, 122.2, 119.6, 119.2, 114.8, 109.5, 78.0, 73.5, 51.7, 35.7, 34.9, 20.7.

IR (neat): ν_{max} = 3281, 3053, 2950, 1728, 1465, 1435, 1331, 1161, 778, 425 cm^{-1}.

HRMS (APPI+) calc'd for $C_{15}H_{15}NO_2$ $[M+H]^+$ 242.1176, found 242.1165.

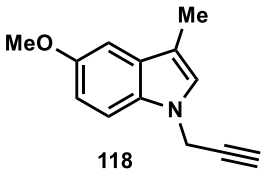

118

N-Propargylindole **118** was prepared using General Experimental Procedure A. Reagents employed: indole starting material (0.550 g, 3.41 mmol), propargyl bromide (0.646 ml, 6.82 mmol), NaH (0.272 g, 6.83 mmol). **118** (0.480 g, 2.41 mmol, 71%) was obtained as light brown solid:

***R*f** = 0.25, 10% EtOAc in hexanes;

M.P. = 85.0-91.0 ºC

^{1}H NMR (300 MHz, $CDCl_3$): δ 7.24 (d, *J* = 8.8 Hz, 1H), 7.00 (d, *J* = 2.3 Hz, 1H), 6.93 (q, *J* = 0.7 Hz, 1H), 6.89 (dd, *J* = 8.8, 2.5 Hz, 1H), 4.76 (d, *J* = 2.5 Hz, 2H), 3.86 (s, 3H), 2.34 (t, *J* = 2.5 Hz, 1H), 2.28 (d, *J* = 1.0 Hz, 3H).

^{13}C NMR (75 MHz, $CDCl_3$): δ 154.2, 131.6, 129.7, 125.7, 112.1, 111.1, 110.1, 101.4, 78.3, 73.2, 56.1, 35.8, 9.8.
IR (neat): ν_{max} = 3257, 2918, 1490, 1227, 1045, 786 cm^{-1}.
HRMS (APPI+): calc'd for $C_{13}H_{13}NO$ $[M+H]^+$ 200.1070, found 200.1061.

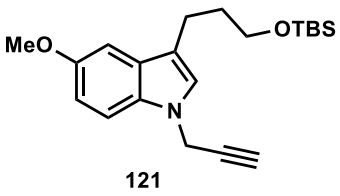

121

N-Propargylindole **121** was prepared using General Experimental Procedure A. Reagents employed: indole starting material (373 mg, 1.17 mmol), propargyl bromide (218 μL, 2.33 mmol), NaH (0.070 g, 1.8 mmol). **121** (0.264 g, 0.738 mmol, 63%) was obtained as thick brown oil: **Note a change in the general procedure**: propargyl bromide was added to a solution of NaH and indole starting material at –10 °C instead of 0 °C.

R_f = 0.66, 20% EtOAc in hexanes;
^{1}H NMR (300 MHz, $CDCl_3$): δ 7.25 (d, *J* = 8.8 Hz, 1H), 7.04 (d, *J* = 2.4 Hz, 1H), 6.95 (s, 1H), 6.89 (dd, *J* = 8.8, 2.4 Hz, 1H), 4.79 (d, *J* = 2.5 Hz, 2H), 3.86 (s, 3H), 3.70 (t, *J* = 6.3 Hz, 2H), 2.82 – 2.69 (m, 2H), 2.36 (t, *J* = 2.5 Hz, 1H), 1.98 – 1.83 (m, 2H), 0.92 (s, 9H), 0.07 (s, 6H).
^{13}C NMR (75 MHz, $CDCl_3$): δ 154.1, 131.7, 129.0, 125.3, 115.8, 112.0, 110.1, 101.5, 78.3, 73.3, 62.9, 56.1, 35.9, 33.3, 26.1, 21.4, 18.5, -5.1.
IR (neat): ν_{max} = 3287, 2928, 2855, 1485, 1253, 1228, 1094, 832, 773 cm^{-1}.
HRMS (APPI+): calc'd for $C_{21}H_{31}NO_2Si$ [M] 357.2124, found 357.2131.

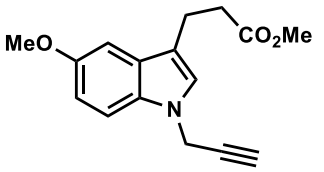

119

N-Propargylindole **119** was prepared using General Experimental Procedure A. Reagents employed: indole starting material (0.350 g, 1.50 mmol), propargyl bromide (0.350 mL, 6.83 mmol), NaH (0.120 g, 3.00 mmol). **119** (0.181 g, 0.667 mmol, 44%) was obtained as yellow oil: **Note a change in the general procedure**: propargyl bromide was added to a solution of NaH and indole starting material at –10 °C instead of 0 °C.

R_f = 0.33, 20% EtOAc in hexanes;
^{1}H NMR (300 MHz, $CDCl_3$): δ 7.26 (d, *J* = 8.8 Hz, 1H), 7.02 (d, *J* = 2.3 Hz, 1H), 6.98 (s, 1H), 6.90 (dd, *J* = 8.8, 2.4 Hz, 1H), 4.78 (d, *J* = 2.5 Hz, 2H), 3.87 (s, 3H), 3.69 (s, 3H), 3.10 – 3.03 (m, 2H), 2.78 – 2.68 (m, 2H), 2.37 (t, *J* = 2.5 Hz, 1H).
^{13}C NMR (75 MHz, $CDCl_3$): δ 173.9, 154.2, 131.6, 128.6, 125.4, 114.2, 112.3, 110.3, 101.1, 78.1, 73.4, 56.1, 51.7, 35.9, 34.8, 20.7.
IR (neat): ν_{max} = 3277, 2994, 2835, 1728, 1485, 1217, 1170, 1038, 791, 640 cm^{-1}.
HRMS (APPI+): calc'd for $C_{16}H_{17}NO_3$ $[M+H]^+$ 272.1208, found 272.1211.

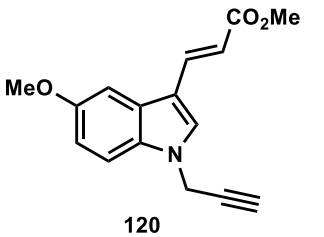

120

N-Propargylindole **120** was prepared using General Experimental Procedure A. Reagents employed: indole starting material (0.400 g, 1.73 mmol), propargyl bromide (0.325 mL, 3.46 mmol), NaH (0.103 g, 2.59 mmol). **120** (0.263 g, 0.977 mmol, 56%) was obtained as light brown solid: **Note a change in the general procedure**: propargyl bromide was added to a solution of NaH and indole starting material at –10 °C instead of 0 °C.

R_f = 0.23, 20% EtOAc in hexanes;

M.P. = 110.7-111.5 °C
^{1}H NMR (300 MHz, $CDCl_3$): δ 7.89 (d, *J* = 16.0 Hz, 1H), 7.50 (s, 1H), 7.32 (d, *J* = 8.6 Hz, 1H), 7.32 (d, *J* = 2.6 Hz, 1H), 6.97 (dd, *J* = 9.0, 2.3 Hz, 1H), 6.35 (d, *J* = 16.0 Hz, 1H), 4.85 (d, *J* = 2.6 Hz, 2H), 3.90 (s, 3H), 3.81 (s, 3H), 2.47 (t, *J* = 2.6 Hz, 1H).
^{13}C NMR (75 MHz, $CDCl_3$): δ 168.8, 155.9, 138.2, 132.2, 131.6, 127.2, 113.3, 112.6, 112.4, 111.0, 102.9, 77.4, 74.8, 56.1, 51.6, 36.5.
IR (neat): ν_{max} = 3254, 3110, 2835, 1704, 1622, 1485, 1281, 1158, 1046, 797, 632 cm^{-1}.
HRMS (APPI+): calc'd for $C_{16}H_{15}NO_3$ $[M+H]^+$ 270.1130, found 270.1127.

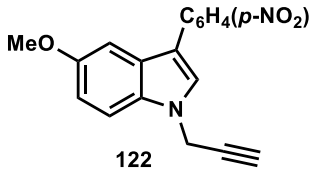

122

N-Propargylindole **122** was prepared using General Experimental Procedure A. Reagents employed: indole starting material (0.416 g, 1.55 mmol), propargyl bromide (0.276 mL, 1.86 mmol), NaH (0.124 g, 3.10 mmol). **122** (0.255 g, 0.832 mmol, 54 %) was obtained as yellow solid:

***R*$_f$** = 0.38, 20% EtOAc in hexanes;
M.P. = 111.0-112.0 °C
^{1}H NMR (300 MHz, $CDCl_3$): δ 8.35 – 8.19 (m, 2H), 7.85 – 7.72 (m, 2H), 7.53 (s, 1H), 7.38 (d, *J* = 8.6 Hz, 1H), 7.38 (d, *J* = 2.6 Hz, 1H),7.01 (dd, *J* = 9.0, 2.3 Hz, 1H), 4.93 (d, *J* = 2.6 Hz, 2H), 3.90 (s, 3H), 2.49 (t, *J* = 2.6 Hz, 1H).
^{13}C NMR (75 MHz, $CDCl_3$): δ 155.7, 145.5, 142.8, 132.1, 127.3, 126.9, 126.7, 124.5, 115.4, 113.1, 111.0, 102.1, 77.4, 74.6, 56.2, 36.5.
IR (neat): ν_{max} = 3280, 3108, 2920, 1591, 1503, 1334, 1217, 1191, 845, 788, 657 cm^{-1}.
HRMS (APPI+): calc'd for $C_{18}H_{14}N_2O_3$ [M] 306.1004, found 306.1015.

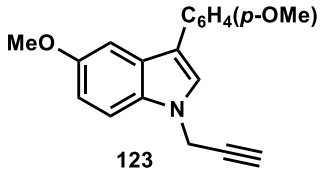

123

N-Propargylindole **123** was prepared using General Experimental Procedure A. Reagents employed: indole starting material (0.340 g, 1.34 mmol), propargyl bromide (0.264 mL, 2.68 mmol), NaH (0.107 g, 2.68 mmol). **123** (0.190 g, 0.650 mmol, 49 %) was obtained as yellow solid:

***R*$_f$** = 0.45, 20% EtOAc in hexanes;
^{1}H NMR (300 MHz, $CDCl_3$): δ 7.61 – 7.51 (m, 2H), 7.37 – 7.31 (m, 2H), 7.27 (s, 1H), 7.03 – 6.98 (m, 2H), 6.95 (dd, *J* = 9.0, 2.4 Hz, 1H), 4.88 (d, *J* = 2.6 Hz, 2H), 3.86 (s, 6H), 2.42 (t, *J* = 2.5 Hz, 1H).
^{13}C NMR (75 MHz, $CDCl_3$): δ 158.2, 154.9, 131.9, 128.6, 128.1, 127.4, 125.1, 117.2, 114.4, 112.5, 110.5, 102.1, 77.8, 73.8, 56.1, 55.5, 36.2.

Synthesis and Characterization of Substituted Pyrroloindole Compounds

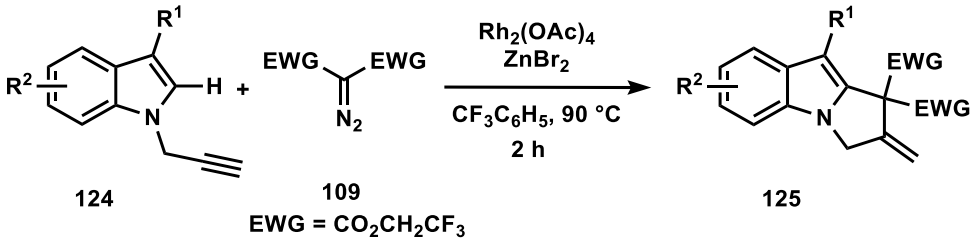

124 109 125

EWG = $CO_2CH_2CF_3$

General Experimental Procedure B:

Substituted indole **124** (1.2 equiv) was added to a reaction vessel equipped with a stir bar and the vessel was then evacuated and backfilled with N_2. This cycle was repeated two additional times followed by the addition of trifluorotoluene (5 mL/mmol of indole) under a N_2 atmosphere. $Rh_2(OAc)_4$ (2 mol %) and $ZnBr_2$ (10 mol %) were then added to the reaction vessel and again the vessel was evacuated (quickly) and backfilled with N_2. Diazo reagent **109** (1 equiv) was added to a separate reaction vessel and the vessel was then evacuated and backfilled with N_2. This cycle was repeated two additional times. The diazo reagent was then dissolved in trifluorotoluene (3 mL/mmol of diazo) under a N_2 atmosphere and transferred dropwise by syringe to the solution of indole starting material. Two sequential rinses and transfers using small quantities of trifluorotoluene were then conducted to ensure complete transfer of the diazo reagent. The reaction mixture was then heated to 90 °C and stirred at this temperature for 2 h. The reaction progress was monitored by TLC analysis and considered complete upon consumption of diazo reagent. Upon completion, the reaction mixture was directly loaded and purified by silica gel flash column chromatography (hexanes/EtOAc gradient) to yield the substituted pyrroloindole **125.**

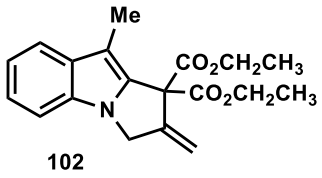

102

Pyrroloindole **102** was prepared using General Experimental Procedure B. Reagents employed: Diethyl-2-diazomalonate **101** (0.100 g, 0.540 mmol), *N*-propargyl indole **90** (110 mg, 0.64 mmol), rhodium(II) acetate (4.7 mg, 0.011 mmol), zinc(II) bromide (12 mg, 0.054 mmol). **102** (0.0830 g, 0.254 mmol, 47%) was obtained as a thick greenish yellow oil.

R_f = 0.30, 30% Et_2O in hexanes;

^{1}H NMR (300 MHz, $CDCl_3$): δ 7.59 (app dt, J = 7.8, 1.1 Hz, 1H), 7.24 – 7.21 (m, 1H), 7.21 – 7.14 (m, 1H), 7.14 – 7.08 (m, 1H), 5.74 (td, J = 2.3, 0.9 Hz, 1H), 5.57 (td, J = 2.0, 1.0 Hz, 1H), 4.80 (t, J = 2.2 Hz, 2H), 4.32 – 4.16 (m, 4H), 2.33 (s, 3H), 1.27 (t, J = 7.1 Hz, 6H).

^{13}C NMR (75 MHz, $CDCl_3$): δ 167.8, 144.9, 135.1, 132.6, 132.4, 121.8, 119.5, 119.2, 114.1, 109.7, 106.0, 63.2, 62.4, 48.3, 14.1, 9.1.

IR (neat): ν_{max} = 2918, 1732, 1456, 1227, 1250, 1095, 738, cm^{-1}.

HRMS (APPI+): calc'd for $C_{19}H_{21}NO_4$ $[M+H]^+$ 328.1543, found 328.1524.

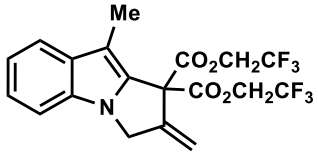

110

Pyrroloindole **110** was prepared using General Experimental Procedure D. Reagents employed: **109** (0.100 g, 0.340 mmol), *N*-propargylindole **90** (69 mg, 0.40 mmol), rhodium(II) acetate (3.0 mg, 0.0068 mmol), zinc(II) bromide (7.6 mg, 0.034 mmol). **110** (0.0950 g, 0.218 mmol, 64%) was obtained as a greenish yellow thick oil. Minor products **111** (0.0130 g, 0.030 mmol, 9%) and **112** (0.0090 g, 0.020 mmol, 6%) were obtained as thick yellowish green oils:

R_f = 0.25, 20% acetone in hexanes;

^{1}H NMR (300 MHz, $CDCl_3$): δ 7.60 (app dt, *J* = 7.9, 1.0 Hz, 1H), 7.24 – 7.21 (m, 2H), 7.17 – 7.11 (m, 1H), 5.75 (dd, *J* = 4.0, 2.4 Hz, 1H), 5.67 (dd, *J* = 2.0, 4.0 Hz, 1H), 4.83 (t, *J* = 2.2 Hz, 2H), 4.69 – 4.43 (m, 4H), 2.30 (s, 3H).

^{13}C NMR (75 MHz, $CDCl_3$): δ 165.8, 143.8, 132.7, 132.6, 132.5, 122.6 (q, *J* = 277.4 Hz), 122.5, 119.9, 119.6, 115.6, 109.8, 107.3, 62.1, 61.8 (q, *J* = 37.3 Hz) 48.1, 8.6.

IR (neat): ν_{max} = 2927, 1756, 1587, 1424, 1250, 1166, 1093, 646 cm^{-1}.

HRMS (APPI+): calc'd for $C_{19}H_{15}F_6NO_4$ $[M+H]^+$ 436.0978, found 436.0963.

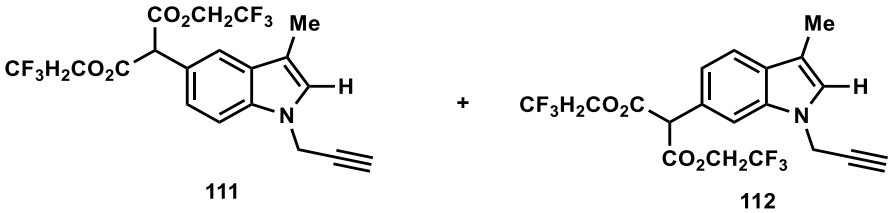

111 112

Compound **111**:

R_f = 0.20, 20% acetone in hexanes;

^{1}H NMR (300 MHz, $CDCl_3$): δ 7.58 (d, *J* = 1.6 Hz, 1H), 7.37 (d, *J* = 8.5 Hz, 1H), 7.25 (dd, *J* = 8.5, 1.8 Hz, 1H), 7.00 (d, *J* = 0.9 Hz, 1H), 4.93 (s, 1H), 4.81 (d, *J* = 2.5 Hz, 2H), 4.64 – 4.43 (m, 4H), 2.37 (t, *J* = 2.5 Hz, 1H), 2.31 (d, *J* = 1.0 Hz, 3H).

^{13}C NMR (75 MHz, $CDCl_3$): δ 166.7, 136.3, 129.6, 126.1, 122.8 (d, *J* = 277.3 Hz), 122.7, 121.6, 120.4, 112.0, 109.9, 77.9, 73.5, 61.4 (q, *J* = 277.3 Hz), 57.0, 35.8, 9.6.

IR (neat): ν_{max} = 3290, 2921, 1753, 1277, 1159, 1124, 800, 763, 647 cm^{-1}.

HRMS (APPI+): calc'd for $C_{19}H_{15}F_6NO_4$ [M] 435.0905, found 435.0908.

Compound **112**:

R_f = 0.20, 20% acetone in hexanes;

^{1}H NMR (300 MHz, $CDCl_3$): δ 7.57 (d, *J* = 8.2 Hz, 1H), 7.40 (d, *J* = 1.3 Hz, 1H), 7.12 (dd, *J* = 8.2, 1.6 Hz, 1H), 7.03 (d, *J* = 1.0 Hz, 1H), 4.94 (s, 1H), 4.82 (d, *J* = 2.5 Hz, 2H), 4.69 – 4.41 (m, 4H), 2.38 (t, *J* = 2.5 Hz, 1H), 2.33 – 2.29 (m, 3H).

^{13}C NMR (75 MHz, $CDCl_3$): δ 166.5, 136.2, 129.8, 126.3, 124.2, 122.7 (d, *J* = 277.3 Hz), 120.4, 119.9, 111.7, 110.1, 77.8, 73.7, 61.4 (q, *J* = 37.2 Hz), 66.0, 57.1, 9.6.

IR (neat): ν_{max} = 3290, 2923, 1753, 1275, 1158, 1125, 1056, 979, 647 cm^{-1}.

HRMS (APPI+): calc'd for $C_{19}H_{15}F_6NO_4$ [M] 435.0905, found 435.0903

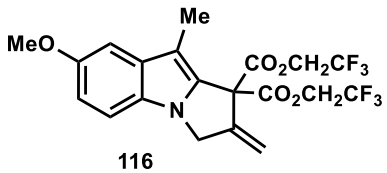

116

Pyrroloindole **116** was prepared using General Experimental Procedure D. Reagents employed: **109** (0.100 g, 0.340 mmol), *N*-propargylindole **118** (81 mg, 0.40 mmol), rhodium(II) acetate (3.0 mg, 0.0068 mmol), zinc(II) bromide (7.6 mg, 0.034 mmol).

116 (120 mg, 0.26 mmol, 76%) was obtained as thick brown oil:
R_f = 0.25, 25% EtOAc in hexanes;
^{1}H NMR (300 MHz, $CDCl_3$): δ 7.13 (d, *J* = 8.8 Hz, 1H), 7.02 (d, *J* = 2.3 Hz, 1H), 6.89 (dd, *J* = 8.8, 2.4 Hz, 1H), 5.74 (dd, *J* = 3.9, 2.3 Hz, 1H), 5.66 (dd, *J* = 3.6, 2.0 Hz, 1H), 4.81 (t, *J* = 2.2 Hz, 2H), 4.70 – 4.36 (m, 4H), 3.87 (s, 3H), 2.27 (s, 3H).
^{13}C NMR (75 MHz, $CDCl_3$) δ 165.8, 154.4, 143.8, 133.2, 132.8, 128.1, 122.6 (d, *J* = 277.4 Hz), 115.5, 113.1, 110.6, 106.8, 101.5, 62.3, 61.8 (q, *J* = 37.3 Hz), 56.1, 48.3, 8.7.
IR (neat): ν_{max} = 2924, 1755, 1440, 1281, 1156, 1053, 962, 648 cm^{-1}.
HRMS (APPI+): calc'd for $C_{20}H_{17}F_6NO_5$ $[M+H]^+$ 466.1084, found 466.1071.

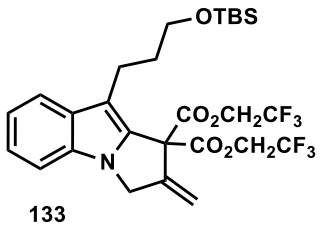

133

Pyrroloindole **133** was prepared using General Experimental Procedure D. Reagents employed: **109** (0.100 g, 0.340 mmol), *N*-propargylindole **93** (98 mg, 0.32 mmol), rhodium(II) acetate (3.0 mg, 0.0068 mmol), zinc(II) bromide (7.6 mg, 0.034 mmol). **133** (77 mg, 0.13 mmol, 38%) was obtained as colorless oil:

R_f = 0.35, 25% acetone in hexanes;
^{1}H NMR (300 MHz, $CDCl_3$): δ 7.67 (app dt, *J* = 8.1, 1.1 Hz, 1H), 7.25 – 7.24 (m, 1H), 7.23 (dd, *J* = 2.7, 0.9 Hz, 1H), 7.17 – 7.09 (m, 1H), 5.73 (dd, *J* = 4.0, 2.3 Hz, 1H), 5.66 (q, *J* = 3.7, 2.0 Hz, 1H), 4.85 (t, *J* = 2.1 Hz, 2H), 4.67 – 4.47 (m, 4H), 3.70 (t, *J* = 6.2 Hz, 2H), 2.86 – 2.74 (m, 2H), 1.94 – 1.74 (m, 2H), 0.93 (s, 9H), 0.08 (s, 6H).
^{13}C NMR (75 MHz, $CDCl_3$): δ 165.8, 144.0, 132.9, 132.5, 131.8, 122.5 (d, *J* = 277.5 Hz), 120.5, 119.6, 115.4, 111.9, 109.9, 63.3, 62.8 (q, *J* = 37.3 Hz), 62.3, 48.1, 33.4, 26.1, 21.0, 18.5, -5.2.
IR (neat): ν_{max} = 2956, 2857, 1754, 1280, 1158, 962, 810, 736, 661 cm^{-1}.
HRMS (APPI+): calc'd for $C_{27}H_{33}F_6NO_5Si$ $[M+H]^+$ 594.2105, found 594.2082.

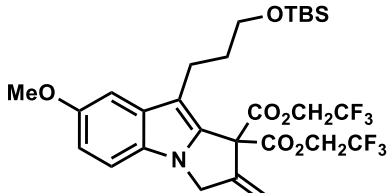

134

Pyrroloindole **134** was prepared using General Experimental Procedure D. Reagents employed: **109** (0.0800 g, 0.272 mmol), *N*-propargylindole **121** (117 mg, 0.320 mmol), rhodium(II) acetate (2.4 mg, 0.0054 mmol), zinc(II) bromide (6.0 mg, 0.027 mmol). **134** (126 mg, 0.202 mmol, 74%) was obtained as brown oil:

R_f = 0.40, 20% acetone in hexanes;
^{1}H NMR (300 MHz, $CDCl_3$): δ 7.18 (d, *J* = 8.8 Hz, 1H), 7.12 (d, *J* = 2.3 Hz, 1H), 6.93 (dd, *J* = 8.8, 2.4 Hz, 1H), 5.72 (dd, *J* = 3.8, 2.1 Hz 1H), 5.65 (dd, *J* = 3.9, 2.3 Hz, 1H), 4.85 (t, *J* = 2.0 Hz, 2H), 4.68 – 4.54 (m, 4H), 3.89 (s, 3H), 3.74 (dd, *J* = 7.9, 4.5 Hz, 2H), 2.81 (dt, *J* = 12.4, 4.8 Hz, 2H), 1.90 – 1.82 (m, 2H), 0.97 (s, 9H), 0.08 (s, 6H).
^{13}C NMR (75 MHz, $CDCl_3$): δ 165.9, 154.3, 144.0, 133.1, 132.1, 128.3, 122.6 (d, *J* = 277.6 Hz), 115.4, 113.1, 111.4, 110.8, 102.0, 63.3, 62.5, 61.8 (q, *J* = 37.4 Hz), 56.1, 48.3, 33.3, 26.1, 21.0, 18.5, -5.2.
IR (neat): ν_{max} = 2954, 2858, 1758,1481, 1282, 1163, 1072, 834, 775, 660 cm^{-1}.

HRMS (APPI+): calc'd for $C_{28}H_{35}F_6NO_6Si$ $[M+H]^+$ 624.2211, found 624.2191.

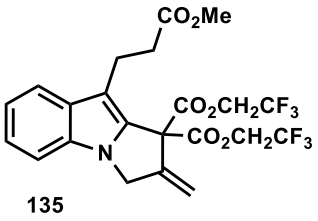

135

Pyrroloindole **135** was prepared using General Experimental Procedure D. Reagents employed: **109** (92 mg, 0.31 mmol), *N*-propargylindole **99** (90 mg, 0.4 mmol), rhodium(II) acetate (2.7 mg, 0.0062 mmol), zinc(II) bromide (7 mg, 0.03 mmol). **135** (47 mg, 0.093 mmol, 30%) was obtained as thick yellow oil:

R_f = 0.25, 20% acetone in hexanes;
^{1}H NMR (300 MHz, $CDCl_3$): δ 7.63 (app dt, *J* = 7.9, 0.9 Hz, 1H), 7.26 – 7.23 (m, 2H), 7.19 – 7.09 (m, 1H), 5.77 (dd, *J* = 4.1, 2.3 Hz, 1H), 5.68 (dd, *J* = 3.8, 2.0 Hz, 1H), 4.85 (t, *J* = 2.2 Hz, 2H), 4.70 – 4.50 (m, 4H), 3.67 (s, 3H), 3.20 – 3.05 (m, 2H), 2.73 – 2.56 (m, 2H).
^{13}C NMR (75 MHz, $CDCl_3$): δ 173.7, 165.7, 143.6, 133.0, 132.9, 131.3, 122.7, 122.6 (q, *J* = 277.4 Hz), 120.1, 120.0, 115.8, 110.1, 110.0, 62.3, 61.9 (q, *J* = 37.3 Hz), 51.7, 48.2, 34.4, 20.1.
IR (neat): ν_{max} = 2955, 1754, 1281, 1280, 1157, 1072, 741 cm^{-1}.
HRMS (APPI+): calc'd for $C_{22}H_{19}F_6NO_6$ $[M+H]^+$ 508.1189, found 508.1189.

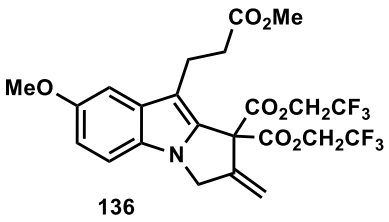

136

Pyrroloindole **136** was prepared using General Experimental Procedure D. Reagents employed: **109** (0.100 g, 0.340 mmol), *N*-propargylindole **119** (109 mg, 0.40 mmol), rhodium(II) acetate (3.0 mg, 0.0068 mmol), zinc(II) bromide (7.6 mg, 0.034 mmol). **136** (105 mg, 0.195 mmol, 57%) was obtained as a greenish oil:

R_f = 0.20, 25% Et_2O in hexanes;
^{1}H NMR (300 MHz, $CDCl_3$): δ 7.15 (dd, *J* = 8.8, 0.6 Hz, 1H), 7.05 (d, *J* = 2.2 Hz, 1H), 6.90 (dd, *J* = 8.8, 2.4 Hz, 1H), 5.75 (dd, *J* = 4.0, 2.3 Hz, 1H), 5.67 (dd, *J* = 3.7, 2.0 Hz, 1H), 4.82 (t, *J* = 2.2 Hz, 2H), 4.72 – 4.45 (m, 4H), 3.86 (s, 3H), 3.68 (s, 3H), 3.14 – 3.01 (m, 2H), 2.69 – 2.55 (m, 2H) .
^{13}C NMR (75 MHz, $CDCl_3$): δ 173.9, 165.8, 154.5, 143.6, 133.5, 131.7, 128.3, 122.5 (d, *J* = 277.5 Hz), 115.7, 113.2, 110.9, 109.5, 101.8, 62.7, 62.1 (q, *J* = 37.4 Hz), 56.2, 51.7, 48.4, 34.2, 20.1.
IR (neat): ν_{max} = 2955, 1754, 1735, 1411, 1281, 1158, 1072, 970, 741, 650 cm^{-1}.
HRMS (APPI+): calc'd for $C_{23}H_{21}F_6NO_7$ $[M+H]^+$ 538.1295, found 538.1301.

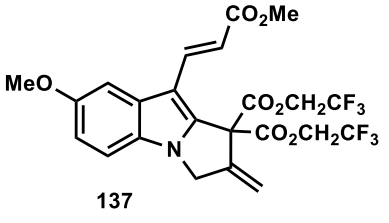

137

Pyrroloindole **137** was prepared using General Experimental Procedure D. Reagents employed: **109** (53 mg, 0.18 mmol), *N*-propargylindole **120** (58 mg, 0.21 mmol), rhodium(II) acetate (1.6 mg, 0.0036 mmol), zinc(II) bromide (4.0 mg, 0.018 mmol). **137** (39 mg, 0.073 mmol, 40%) was obtained as yellow oil:

R_f = 0.25, 25% EtOAc in hexanes;
^{1}H NMR (300 MHz, $CDCl_3$): δ 7.91 (d, *J* = 16.1 Hz, 1H), 7.36 (d, *J* = 2.3 Hz, 1H), 7.20 (d, *J* = 8.9 Hz, 1H), 6.97 (dd, *J* = 8.9, 2.3 Hz, 1H), 6.37 (d, *J* = 16.1 Hz, 1H), 5.82 (dd, *J* = 4.3, 2.3 Hz, 1H), 5.73 (dd, *J* = 3.9, 2.0 Hz, 1H), 4.89(t, *J* = 2.3 Hz, 2H), 4.74 – 4.48 (m, 4H), 3.90 (s, 3H), 3.80 (s, 3H).

^{13}C NMR (75 MHz, $CDCl_3$): δ 168.3, 165.0, 156.2, 142.2, 138.8, 136.5, 130.2, 128.5, 122.5 (d, J = 277.7 Hz), 116.5, 114.5, 114.0, 111.4, 107.7, 103.8, 63.3, 62.1 (q, J = 37.6 Hz), 56.2, 51.5, 48.9.
IR (neat): ν_{max} = 2921, 2851, 1761, 1715, 1618, 1247, 1158, 1026, 788 cm^{-1}.
HRMS (APPI+): calc'd for $C_{23}H_{19}F_6NO_7$ $[M+H]^+$ 536.1138, found 536.1121.

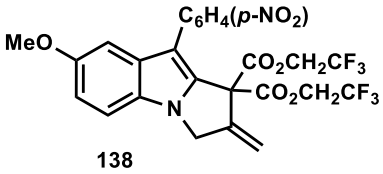

138

Pyrroloindole **138** was prepared using General Experimental Procedure D. Reagents employed: **109** (0.050 g, 0.17 mmol), *N*-propargylindole **122** (62 mg, 0.20 mmol), rhodium(II) acetate (1.5 mg, 0.0034 mmol), zinc(II) bromide (3.8 mg, 0.017 mmol). **138** (27 mg, 0.047 mmol, 28%) was obtained as a thick yellow oil:
$\boldsymbol{R_f}$ = 0.30, 20% acetone in hexanes;
^{1}H NMR (300 MHz, $CDCl_3$): δ 8.32 – 8.23 (m, 2H), 7.66 – 7.56 (m, 2H), 7.26 (d, J = 8.6 Hz, 1H), 7.08 (d, J = 2.2 Hz, 1H), 7.26 (dd, J = 8.8, 2.4 Hz, 1H), 5.73 (dq, J = 7.7, 2.1 Hz, 2H), 4.94 (t, J = 2.2 Hz, 2H), 4.65 – 4.25 (m, 4H), 3.82 (s, 3H).
^{13}C NMR (75 MHz, $CDCl_3$): δ 165.5, 155.8, 146.3, 143.4, 141.6, 134.3, 131.1, 129.8, 128.3, 123.9, 122.3 (q, J = 277.7 Hz) 116.1, 114.3, 111.32, 111.25, 101.9, 63.1, 61.8 (q, J = 37.4 Hz), 56.1, 48.6.
IR (neat): ν_{max} = 2925, 1753, 1597, 1513, 1342, 1279, 1151, 1070, 847 cm^{-1}.
HRMS (APPI+): calc'd for $C_{25}H_{18}F_6N_2Oz_7$ $[M+H]^+$ 573.1096, found 573.1103.

1.10 References

1. Clusius, K.; Lüthi, U. *Helv. Chim. Acta*, **1957**, *40*, 445-456.
2. a) Soldi, C.; Lamb, K. N.; Squitieri, R. A.; González-López, M.; Di Maso, M. J.; Shaw, J. T. *J. Am. Chem. Soc.* **2014**, *136*, 15142-15145. b) Morton, D.; Blakey, S. B. *ChemCatChem* **2015**, *7*, 577-578.
3. a) Kirmse, W. Eur. *J. Org. Chem.* **2002**, 193-2256. b) Ye, T.; McKervey, M. A. *Chem. Rev.* **1994**, *94*, 1091-1160. c) Zhangab, Y.; Wang, J. *Chem. Commun*. **2009**, 5350-5361.
4. Regitz, M.; Maas, G. Diazo Compounds, Properties and Synthesis, Academic Press, Orlando, **1986**.
5. a) Curtius, T. *Ber. Dtsch. Chem. Ges.* **1883**, *16*, 2230-2231. b) Pechmann, H. V. *Ber. Dtsch. Chem. Ges.* **1894**, *27*, 1888-1891.
6. Arndt, F. *Org. Synth*, **1935**, *15*, 1-3.
7. Maas, G. *Angew. Chem. Int. Ed.* **2009**, *48*, 8186-8195.
8. a) Regitz, M. *Angew. Chem., Int. Ed.* **1967**, *6*, 733-749. b) Heydt, H. *Science of Synthesis*, Vol. *27*, Thieme, Stuttgart, 2004, pp. 843-915.
9. a) Holton, T. L.; Schechter, H. *J. Org. Chem.* **1995**, *60*, 4725-4729. b) Tanbouza, N.; Caron, L.; Khoshoei, A.; Ollevier, T. *Org. Lett.* **2022**, *24*, 2675-2678.
10. a) Friedman, L.; Bayless, H. *J. Am. Chem. Soc.* **1969**, *91*, 1790-1794. b) Audubert, C.; Lebel, H. *Org. Lett.* **2017**, *19*, 4407-4410.
11. a) Likhar, P. R.; Roy, S.; Roy, M.; Subhas, M. S.; Kantam M. L. *Synlett* **2008**, 1283-1286. b) Li, P.; Majireck, M. M.; Korboukh, I.; Weinreb, S. M. *Tetrahedron Lett*. **2008**, *49*, 3162-3164. c) Saraireh, I. A. M. *Tetrahedron Lett*. **2012**, *53*, 2023-2025.
12. Pinho, V. D.; Burtoloso, A. C. B. *J. Org. Chem.* **2011**, *76*, 289-292.
13. Myers, E. L.; Raines, R. T. *Angew. Chem. Int. Ed*. **2009**, *48*, 2359-2363.
14. a) Galkina, O. S.; Rodina, L. L. *Russ. Chem. Rev.* **2016**, *85*, 537-555. b) Bogdanova, A.; Popik**,** V. V. *J. Am. Chem. Soc.* 2004, *126*, 11293-11302.
15. a) Bonge, T.; Hansen, T. *Eur. J. Org. Chem.* **2010**, *23*, 4355-4359. B) Zhao, X.; Zhang, Y.; Wang, J. *Chem. Commun*. **2012**, *48*, 10162-10173.
16. Wolff, L. *Justus Liebigs Ann. Chem.* **1902**, *325*, 129-195.
17. Roy, A.; Goswami, S. P.; Sarkar, A. *Synth. Commun.* **2018**, *48*, 2003-2036.

18. a) Davies, H. M. L.; Manning, J. R. Nature **2008**, *451*, 417-424. **b)** Yang, Y.; Wang, X.; Li, Y.; Zhou, B. *Angew. Chem. Int. Ed.* **2015**, *127*, 15620-15624. **c)** Ford, A.; Miel, H.; Ring, A.; Slattery, C. N.; Maguire, A. R.; McKervey, M. A. *Chem. Rev.* **2015**, *115*, 9981-10080.
19. Yu, Z.; Ma, B.; Chen, M.; Wu, H. H.; Liu, L.; Zhang, J. *J. Am. Chem. Soc.* **2014**, *136*, 19, 6904-6907.
20. Jia, S.; Xing, D.; Zhang, D.; Hu, W. *Angew. Chem. Int. Ed.* **2014**, *126*, 13314-13317.
21. Baeyer, A. *Justus Liebigs Ann. Chem.* **1866**, *140*, 295- 313.
22. a) Sundberg, R. J. The Chemistry of Indoles; Academic Press: New York, **1970**, 129-135. b) Bandini, M.; Eichholzer, A. *Angew. Chem. Int. Ed.* **2009**, *48*, 9608-9644.
23. Sundberg, R.J. in Heterocyclic Scaffolds II: Reactions and Applications of Indoles, **2010**, 47.
24. Davies, H. M. L.; Hedley, S. *J. Chem. Soc. Rev.* **2007**, *36*, 1109-1119.
25. Gibe, R.; Kerr, M. A. *J. Org. Chem.* **2002**, *67*, 6247-6249.
26. Johansen, M. B.; Kerr, M. A. *Org. Lett.,* **2010**, *12*, 4956-4959.
27. Lin, E. Z.; Xu, Y.; Ji, K.; Ye, L. W. *Chin. Chem. Lett.* **2012**, *32*, 954-962.
28. Conia, J. M.; Le Perchec, P. *Synthesis* **1975**, *01*, 1-19.
29. Hack, D.; Blümel, M.; Chauhan, P.; Philipps, A. R.; Enders, D. *Chem. Soc. Rev.*, **2015**, *44*, 6059-6093.
30. Hayashi, Y. *Chem. Sci.* **2016**, *7*, 866-880.
31. Urabe, F.; Miyamoto, S.; Takahashi, K.; Ishihara, J.; Hatakeyama, S. *Org. Lett.* **2014**, *16*, 1004-1007.
32. Regitz, M.; Menz, F.; Liedhegener, A. *Liebigs Ann. Chem.* **1970**, *739*, 174-184.
33. Zhao, X.; Zhang, Y.; Wang, *Chem. Commun.* **2012**, *48*, 10162-10173.
34. a) Beltran, F.; Fabre, I.; Ciofini, I.; Miesch, L. *Org. Lett.* **2017**, *19*, 5042-5045. b) Tashima, S.; Sawada, T.; Saito, K.; Yamada, T. *Chem. Lett.* **2016**, *45*, 649-651. c) Chen, Y. J.; Chuang, C. P. *Synthesis* **2016**, *48*, 3603-3617.
35. a) Hack, D.; Blumel, M.; Chauhan, P.; Philipps, A. R.; Enders, D. *Chem. Soc. Rev.* **2015**, *44*, 6059-6093. b) Clarke, M. L.; France, M. B. *Tetrahedron* **2008**, *64*, 9003-9031. c)Fang, G.; Zheng, C.; Cao, D.; Pan, Lu.; Hong, H.; Wang, H.; Zhao, G. *Tetrahedron* **2019**, *75*, 2706-2716.

36. Mass, G. *Chem. Soc. Rev.,* **2004**, ***33***, 183-190.
37. Prabagar, B.; Yang, Y.; Shi, Z. *Chem. Soc. Rev.*, **2021**, *50*, 11249-11269.
38. Shanahan, C. S.; Truong, P.; Mason, S. M.; Leszczynski, J. S.; Doyle, M. P. *Org. Lett.* **2013**, *15*, 3642-3645.
39. Bhat. A. H.; Alavi, S.; Grover, H. K. *Org. Lett.* 2020, *22*, 224-229.
40. Ziarani, M. G.; Moradi, R.; Ahmadi, T.; Lashgari, *RSC Adv*. **2018**, *8*, 12069-12103.

1.11 Selected ^{1}H and ^{13}C NMR spectral data

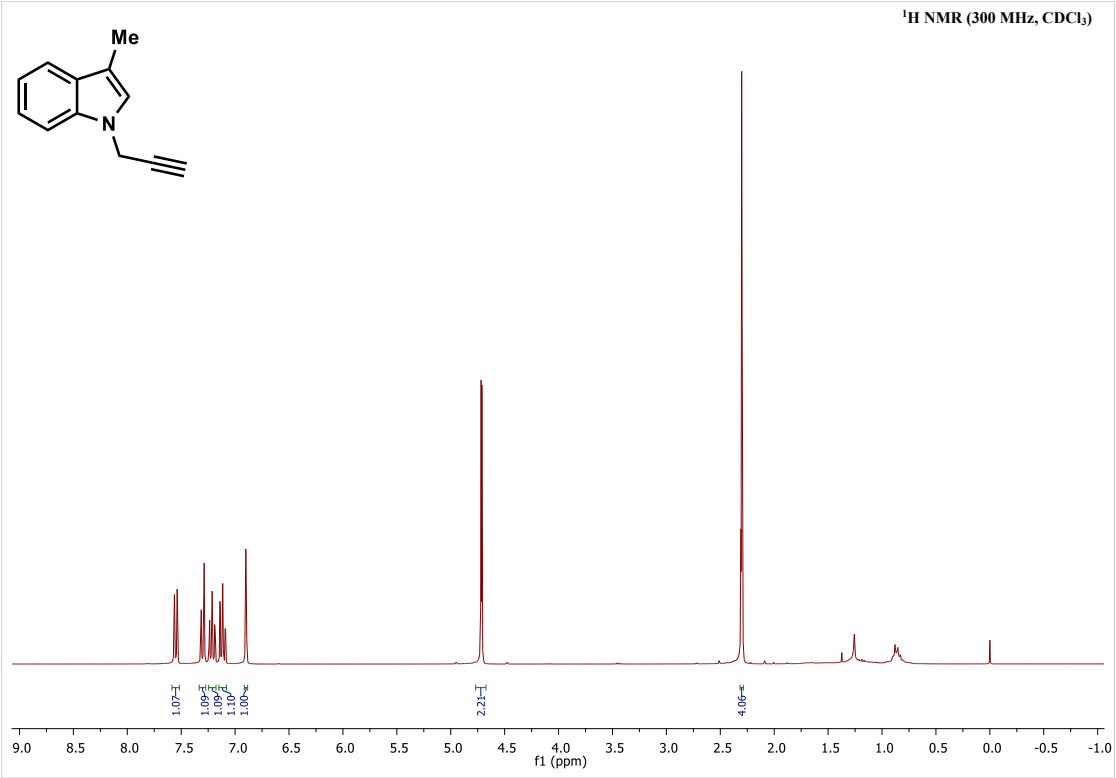

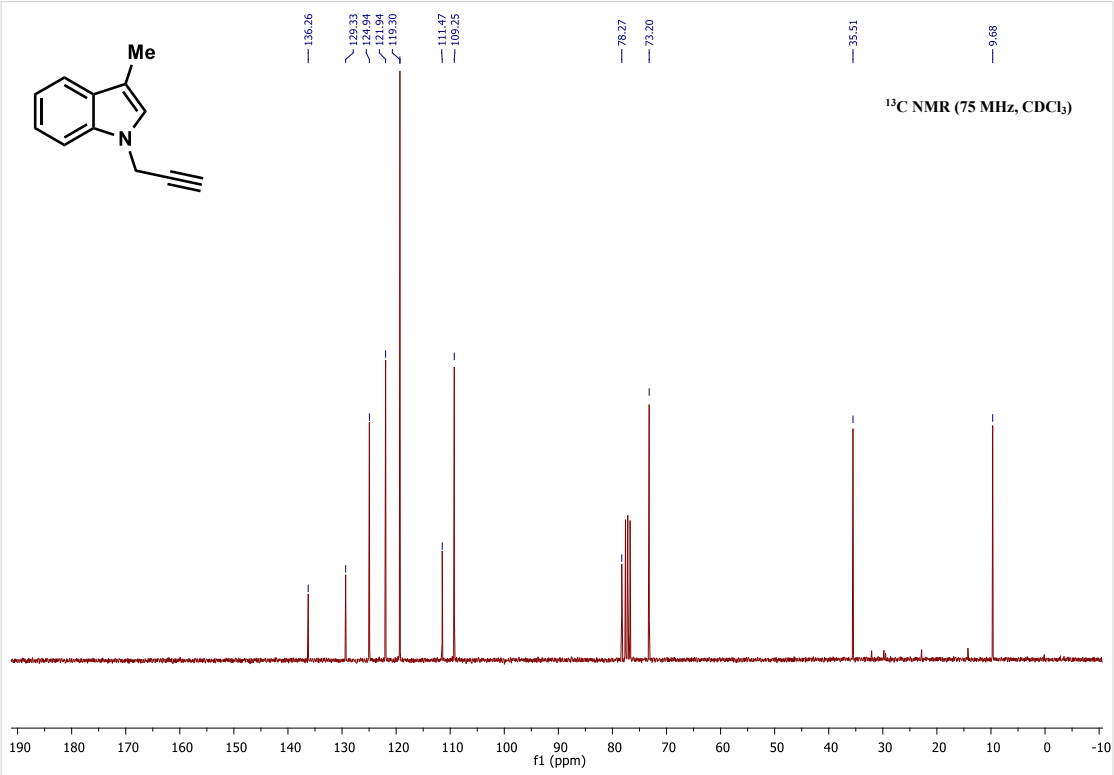

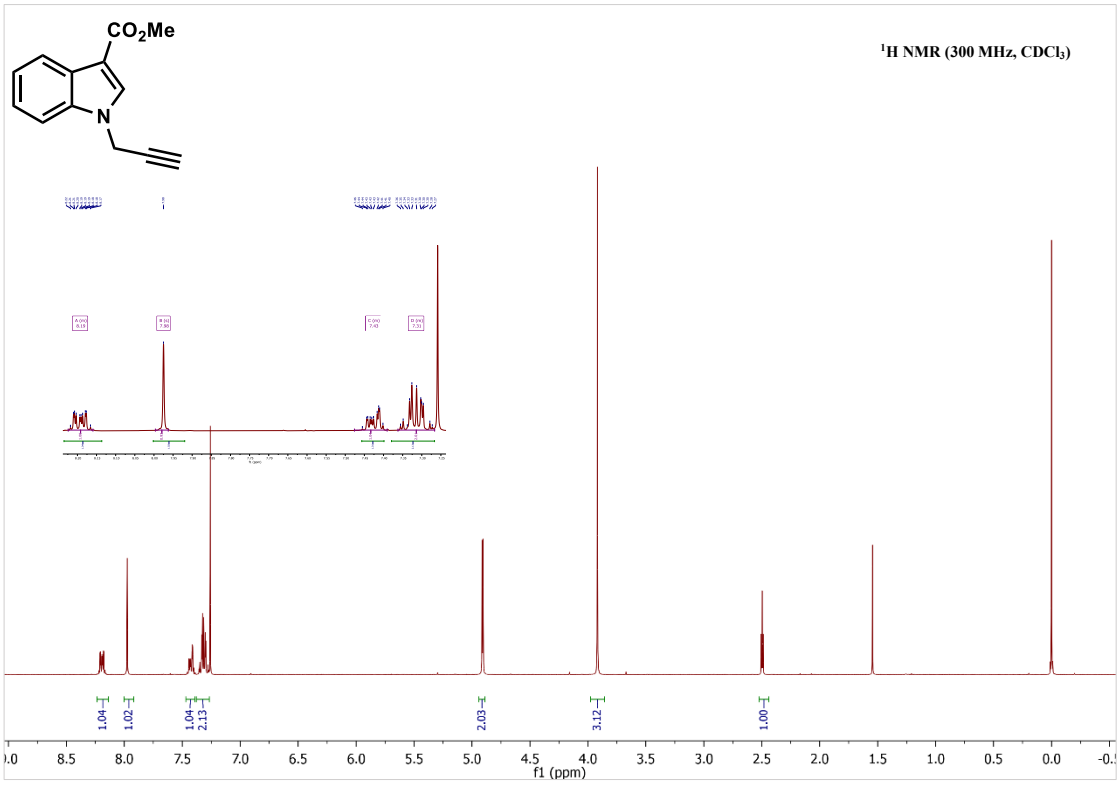
CO2Me
N
1H NMR (300 MHz, CDCl3)
1.04
1.02
1.04
2.13
2.03
3.12
1.00
f1 (ppm)

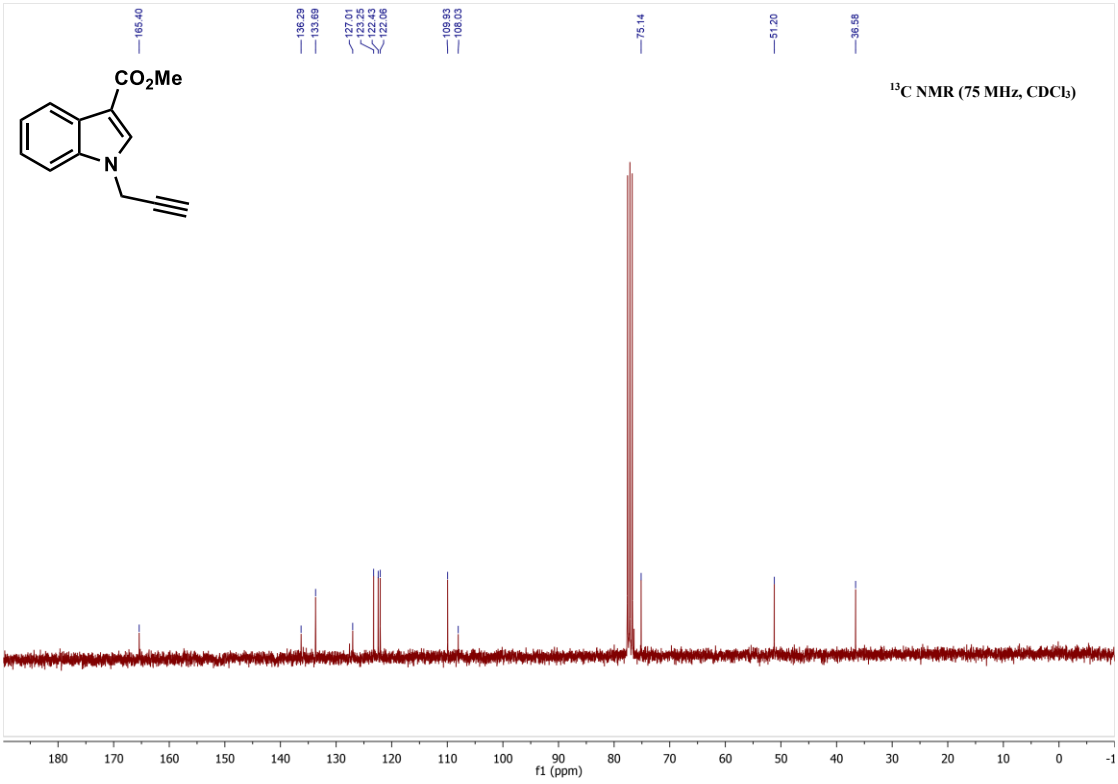
165.40
136.29
133.69
127.01
125.35
122.43
122.06
109.93
108.03
75.14
51.20
36.58
CO2Me
N
13C NMR (75 MHz, CDCl3)
f1 (ppm)

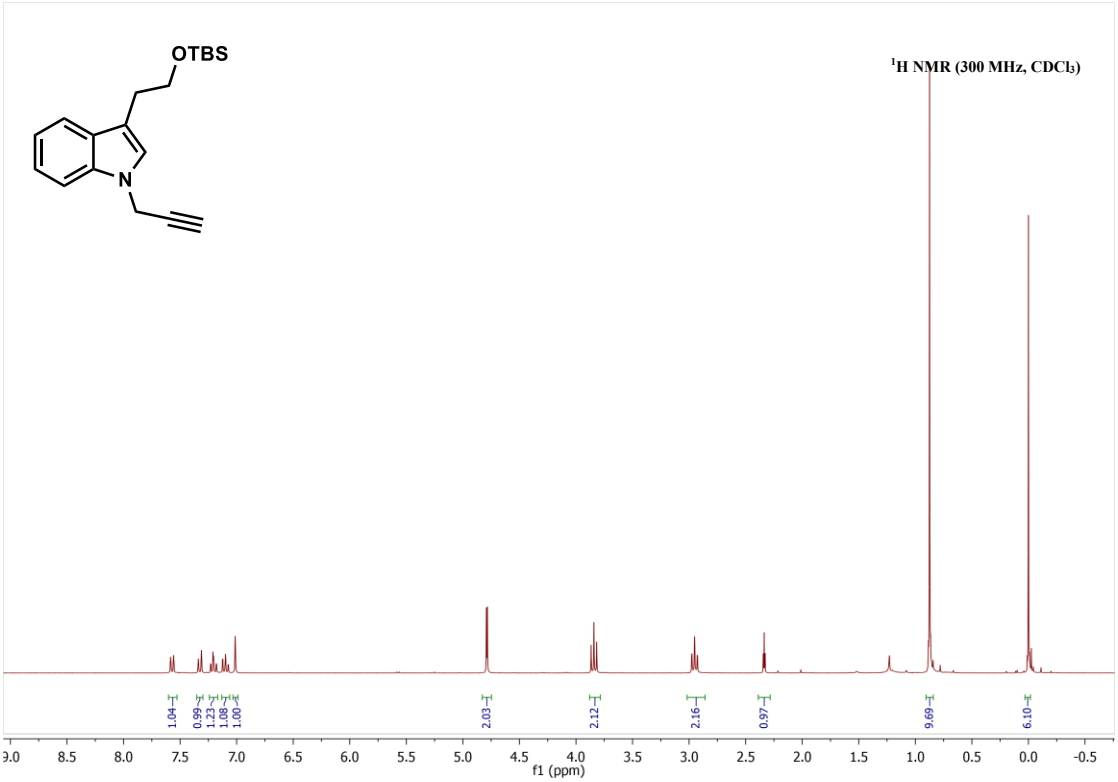
OTBS
N
^{1}H NMR (300 MHz, CDCl$_3$)
1.04
0.99
1.23
1.08
1.00
2.03
2.12
2.16
0.97
9.69
6.10
f1 (ppm)

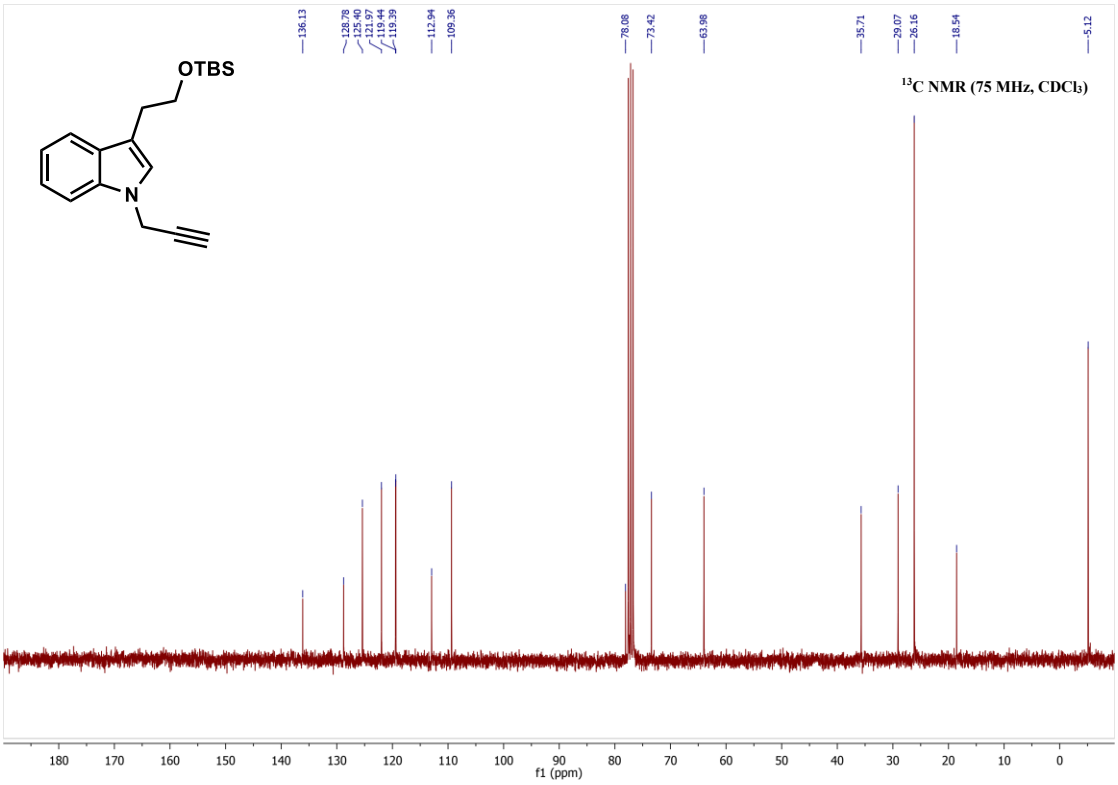
OTBS
N
^{13}C NMR (75 MHz, CDCl$_3$)
136.13
128.78
125.40
121.97
119.44
119.39
112.94
109.36
78.08
73.42
63.98
35.71
29.07
26.16
18.54
5.12
f1 (ppm)

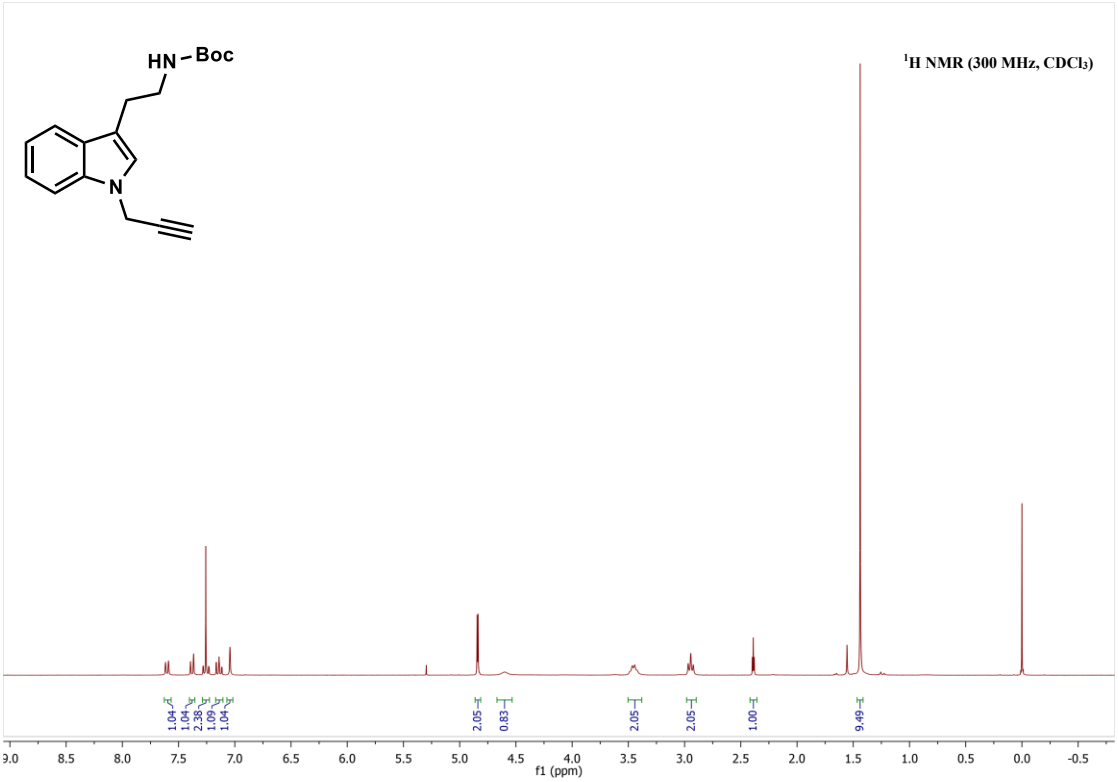
HN
Boc
N
^{1}H NMR (300 MHz, CDCl$_3$)
1.04
1.04
2.38
1.09
1.04
2.05
0.83
2.05
2.05
1.00
9.49
f1 (ppm)

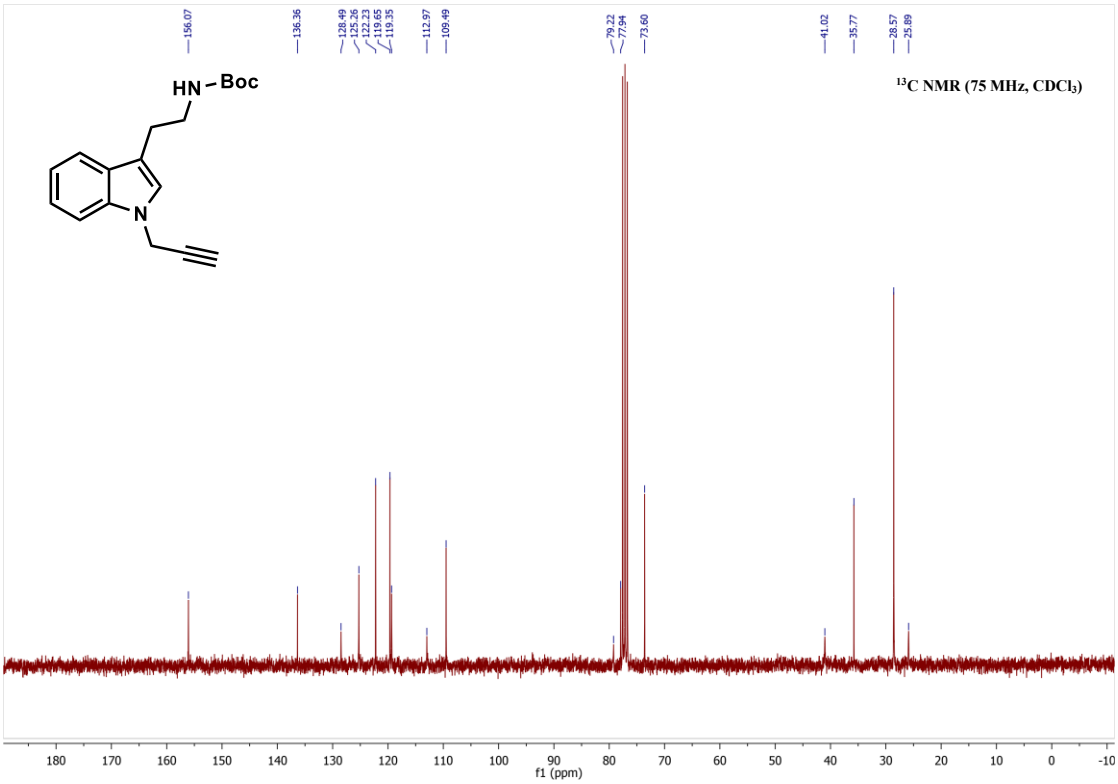
156.07
136.36
128.49
125.26
122.23
119.65
119.35
112.97
109.49
79.22
77.94
73.60
41.02
35.77
28.57
25.89
HN
Boc
N
^{13}C NMR (75 MHz, CDCl$_3$)
f1 (ppm)

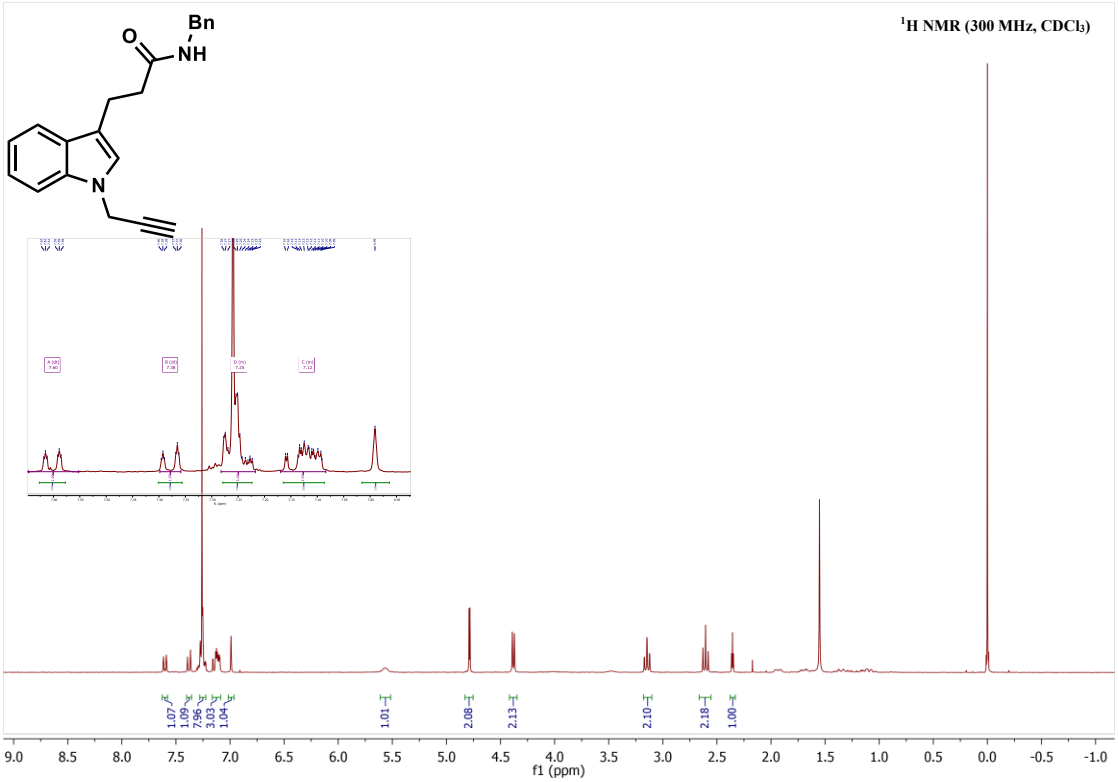
Bn
O
NH
N
^{1}H NMR (300 MHz, CDCl$_3$)
1.07
1.09
7.96
3.03
1.04
1.01
2.08
2.13
2.10
2.18
1.00
9.0 8.5 8.0 7.5 7.0 6.5 6.0 5.5 5.0 4.5 4.0 3.5 3.0 2.5 2.0 1.5 1.0 0.5 0.0 -0.5 -1.0
f1 (ppm)

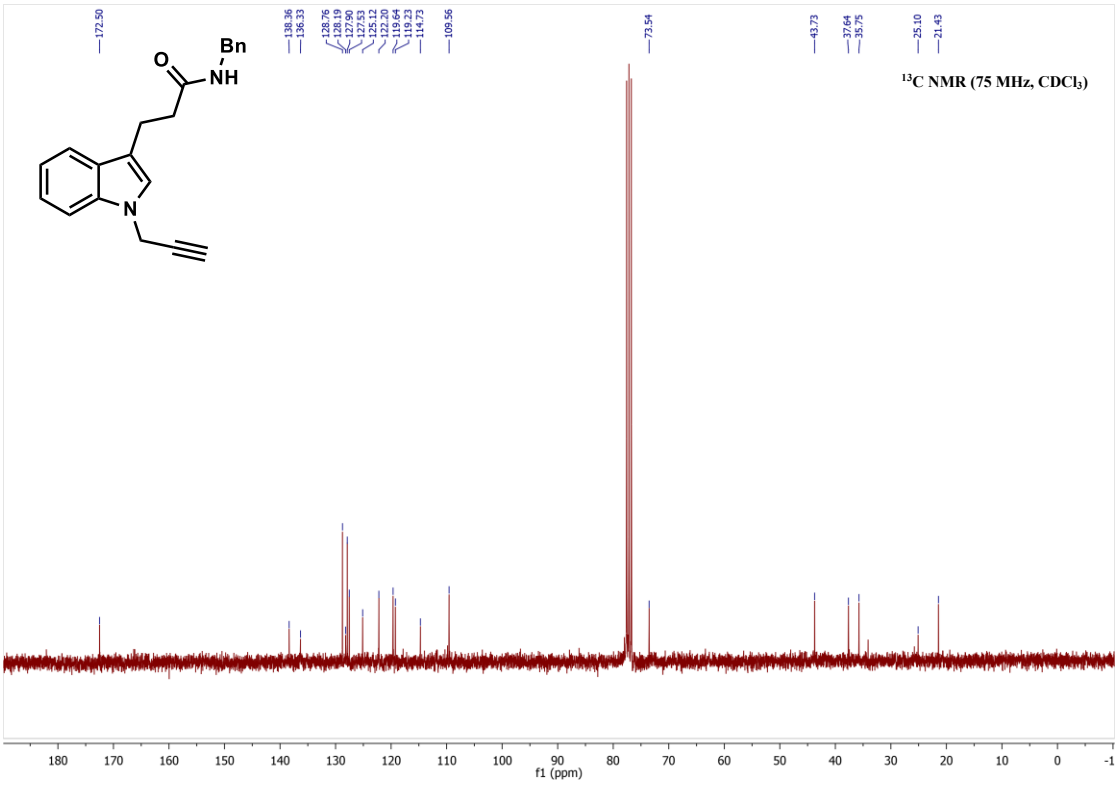
172.50
138.36
136.33
128.76
128.19
127.90
127.53
125.12
122.20
119.64
119.23
114.73
109.56
73.54
43.73
37.64
35.75
25.10
21.43
Bn
O
NH
N
^{13}C NMR (75 MHz, CDCl$_3$)
180 170 160 150 140 130 120 110 100 90 80 70 60 50 40 30 20 10 0 -1
f1 (ppm)

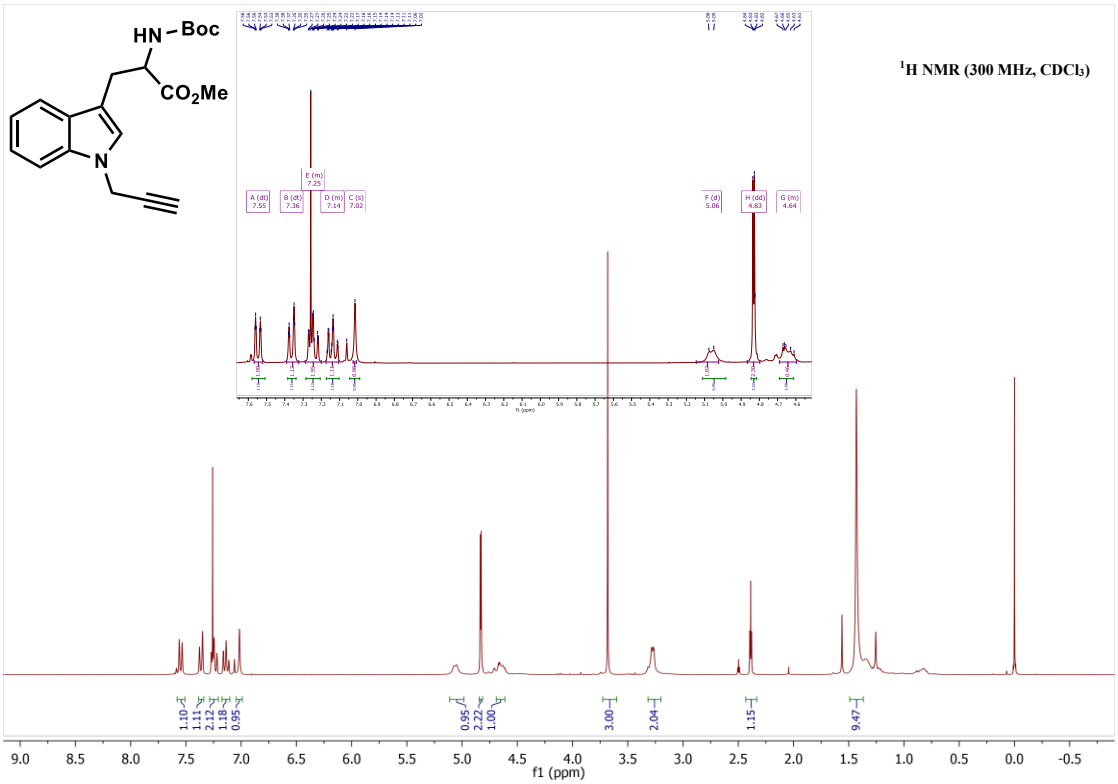
HN – Boc
CO2Me
N
1H NMR (300 MHz, CDCl3)
f1 (ppm)

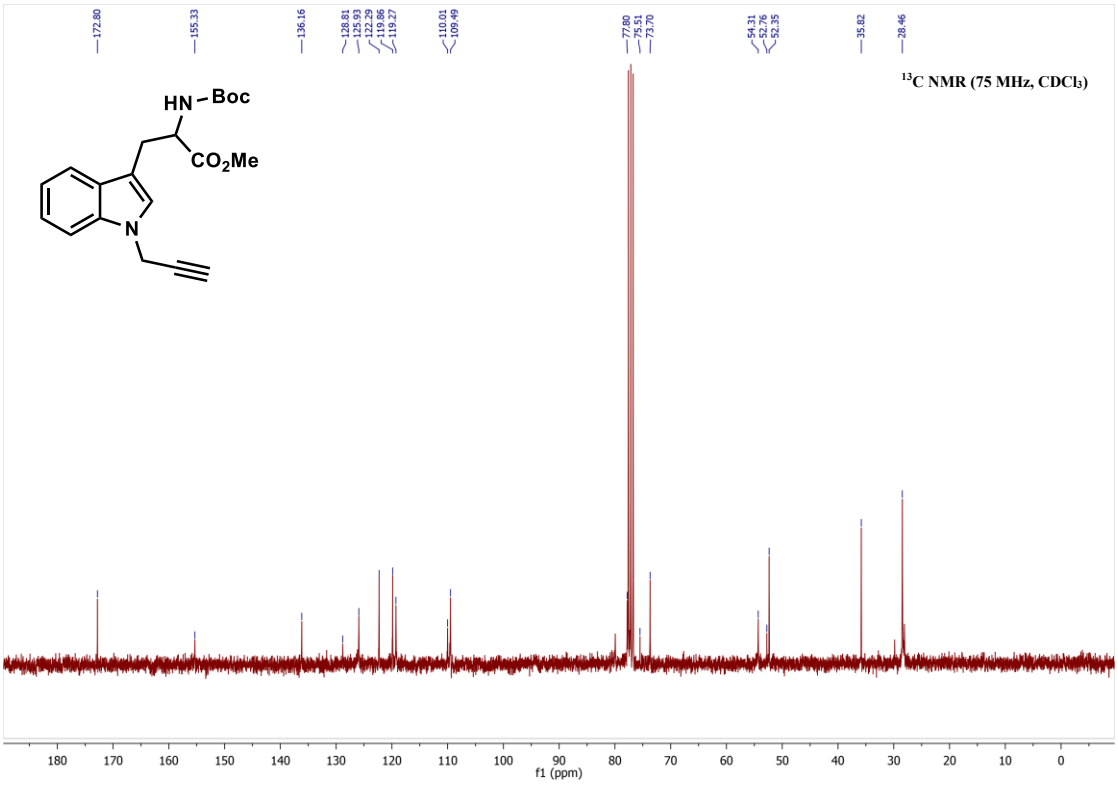
HN – Boc
CO2Me
N
13C NMR (75 MHz, CDCl3)
f1 (ppm)

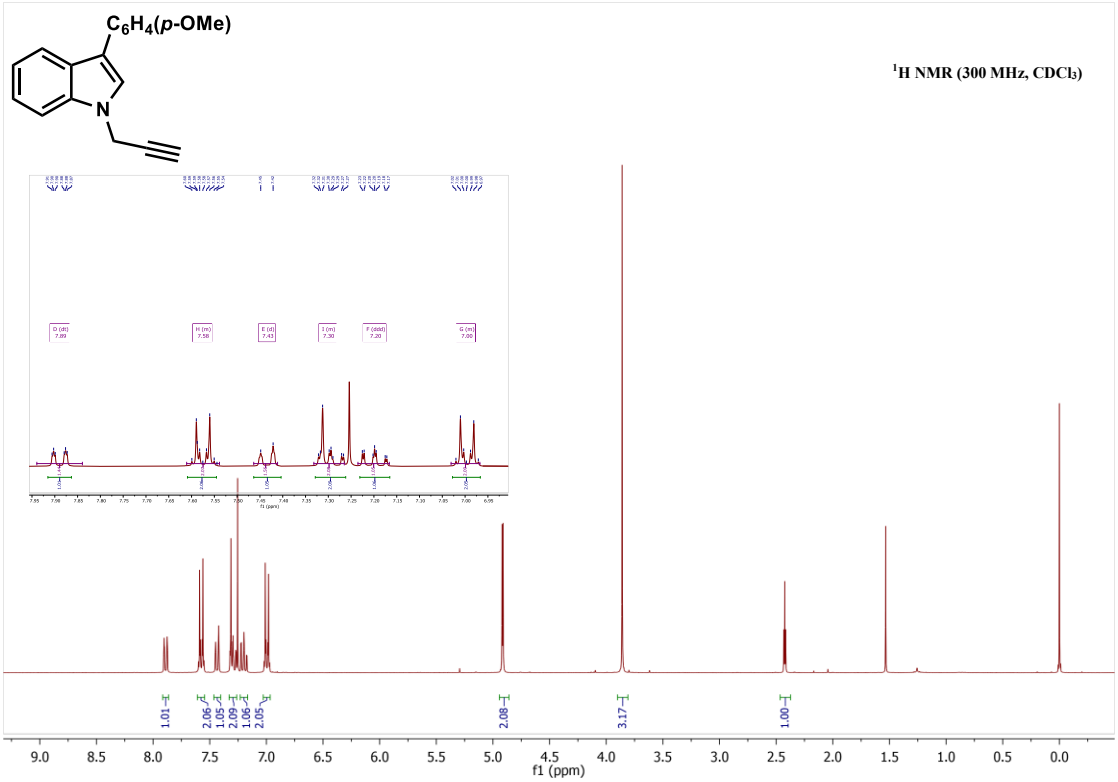
C6H4(p-OMe)
N
1H NMR (300 MHz, CDCl3)
1.01
2.06
1.05
2.08
1.06
2.05
2.08
3.17
1.00
9.0 8.5 8.0 7.5 7.0 6.5 6.0 5.5 5.0 4.5 4.0 3.5 3.0 2.5 2.0 1.5 1.0 0.5 0.0
f1 (ppm)

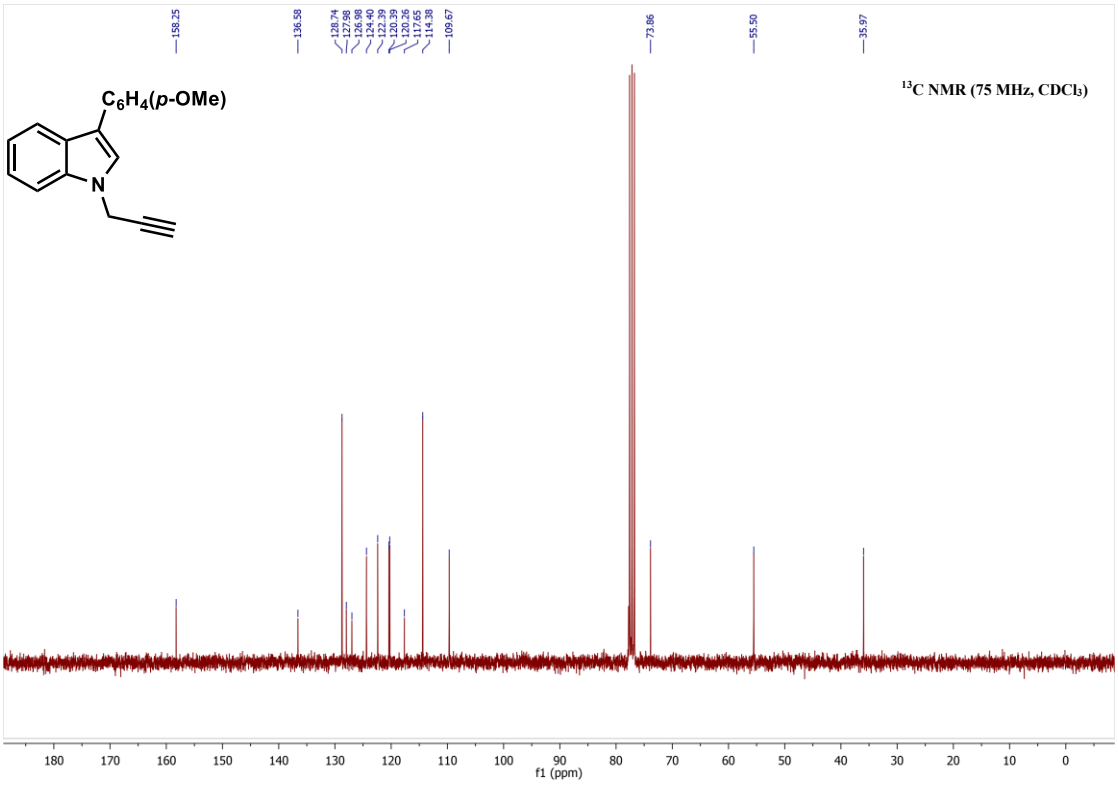
158.25
136.58
129.74
127.98
126.88
124.40
122.39
120.39
120.26
117.65
114.38
109.67
73.86
55.50
35.97
C6H4(p-OMe)
N
13C NMR (75 MHz, CDCl3)
180 170 160 150 140 130 120 110 100 90 80 70 60 50 40 30 20 10 0
f1 (ppm)

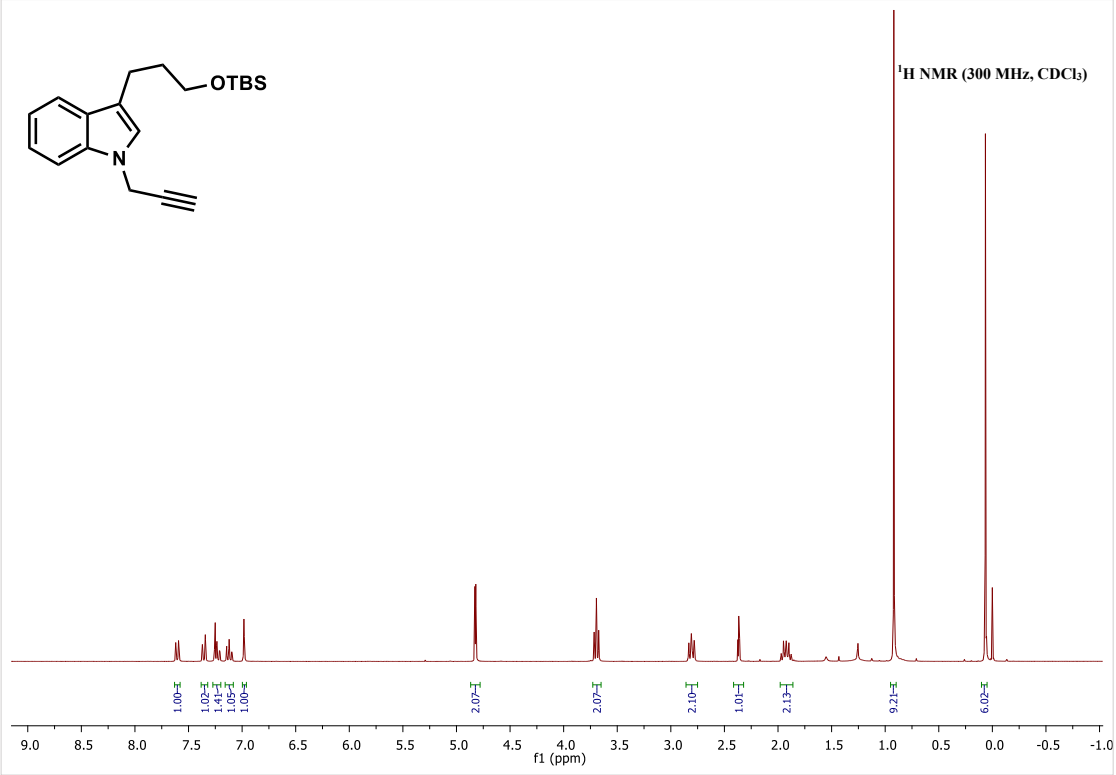
OTBS
N
^{1}H NMR (300 MHz, CDCl$_3$)
1.00
1.02
1.41
1.05
1.00
2.07
2.07
2.10
1.01
2.13
9.21
6.02
9.0 8.5 8.0 7.5 7.0 6.5 6.0 5.5 5.0 4.5 4.0 3.5 3.0 2.5 2.0 1.5 1.0 0.5 0.0 -0.5 -1.0
f1 (ppm)

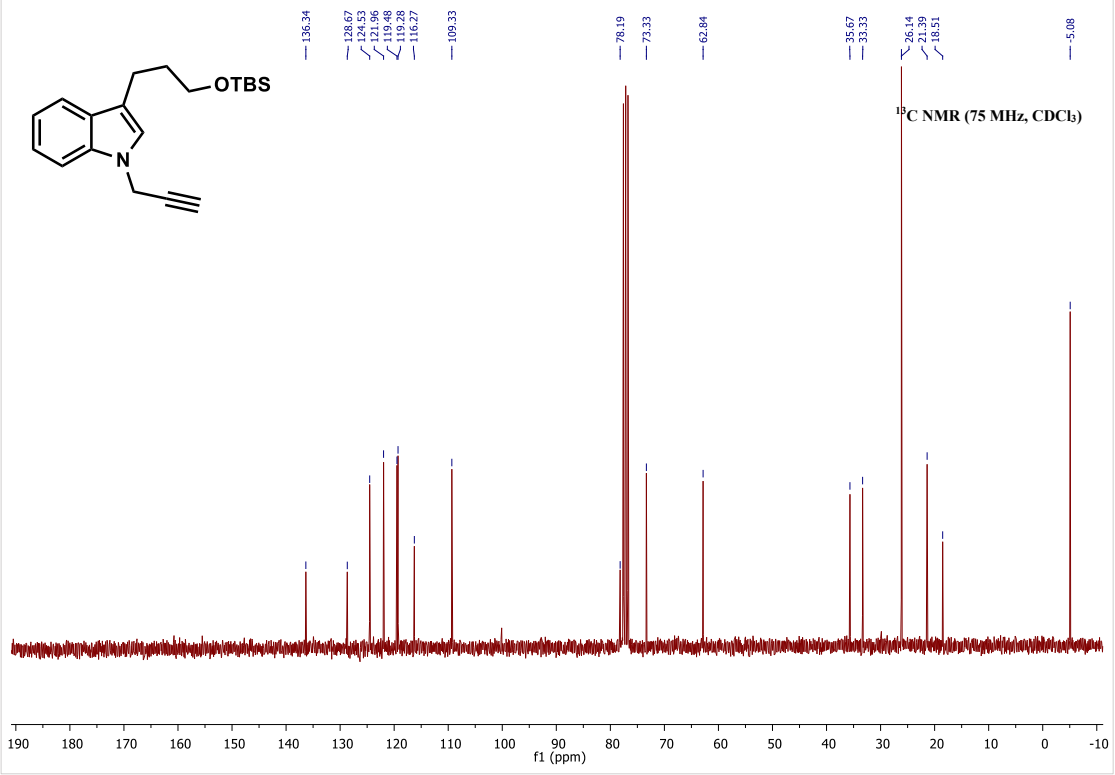
OTBS
N
^{13}C NMR (75 MHz, CDCl$_3$)
136.34
128.67
124.53
121.96
119.48
119.28
116.27
109.33
78.19
73.33
62.84
35.67
33.33
26.14
21.39
18.51
-5.08
190 180 170 160 150 140 130 120 110 100 90 80 70 60 50 40 30 20 10 0 -10
f1 (ppm)

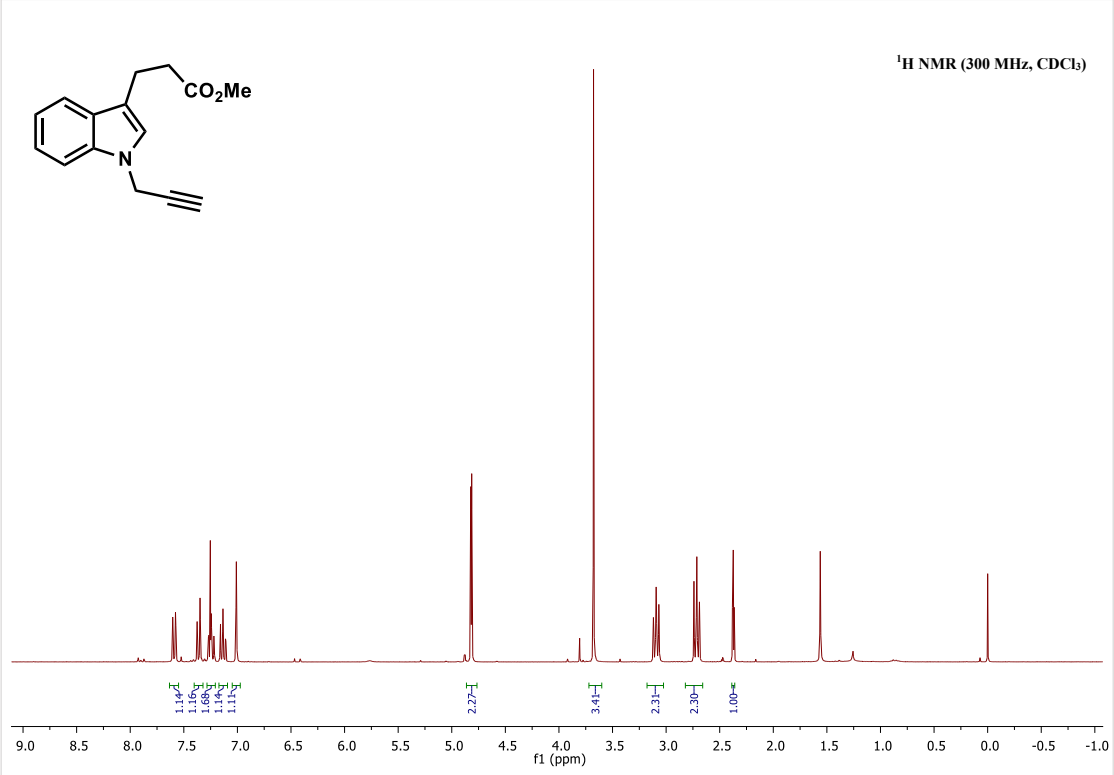
^{1}H NMR (300 MHz, CDCl$_3$)
CO2Me
N
1.14
1.16
1.68
1.14
1.11
2.27
3.41
2.31
2.30
1.00
9.0 8.5 8.0 7.5 7.0 6.5 6.0 5.5 5.0 4.5 4.0 3.5 3.0 2.5 2.0 1.5 1.0 0.5 0.0 -0.5 -1.0
f1 (ppm)

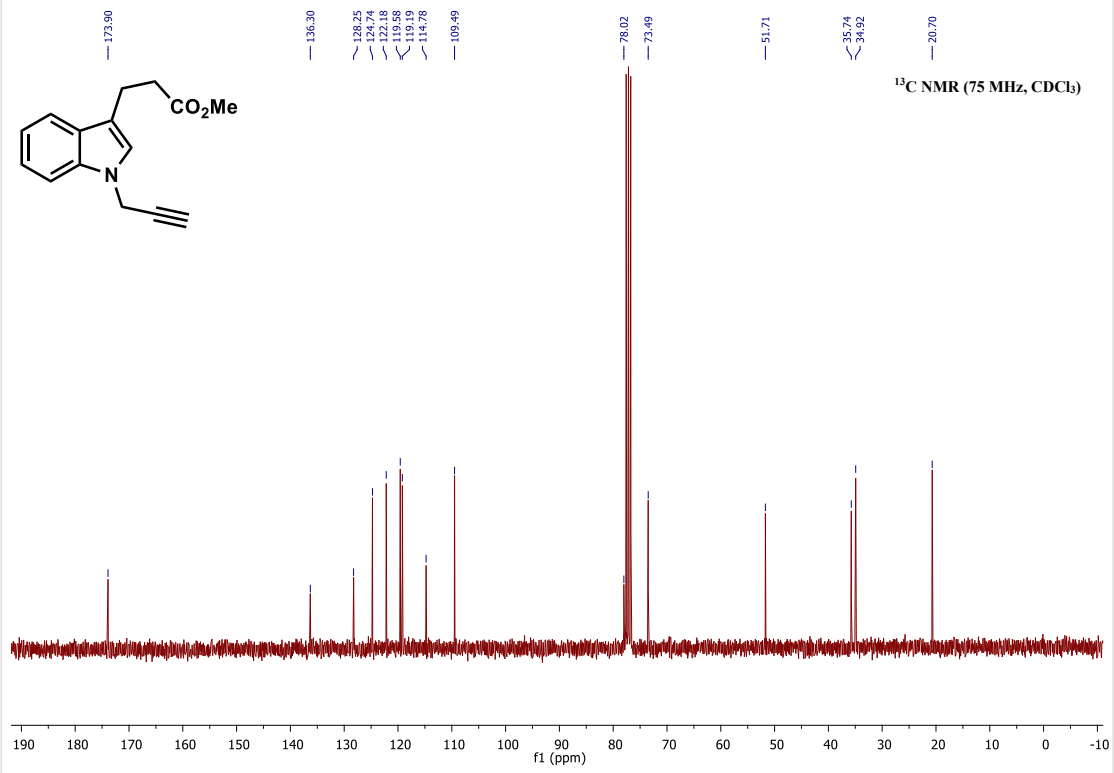
173.90
136.30
128.25
124.74
122.18
119.58
119.19
114.78
109.49
78.02
73.49
51.71
35.74
34.92
20.70
^{13}C NMR (75 MHz, CDCl$_3$)
CO2Me
N
190 180 170 160 150 140 130 120 110 100 90 80 70 60 50 40 30 20 10 0 -10
f1 (ppm)

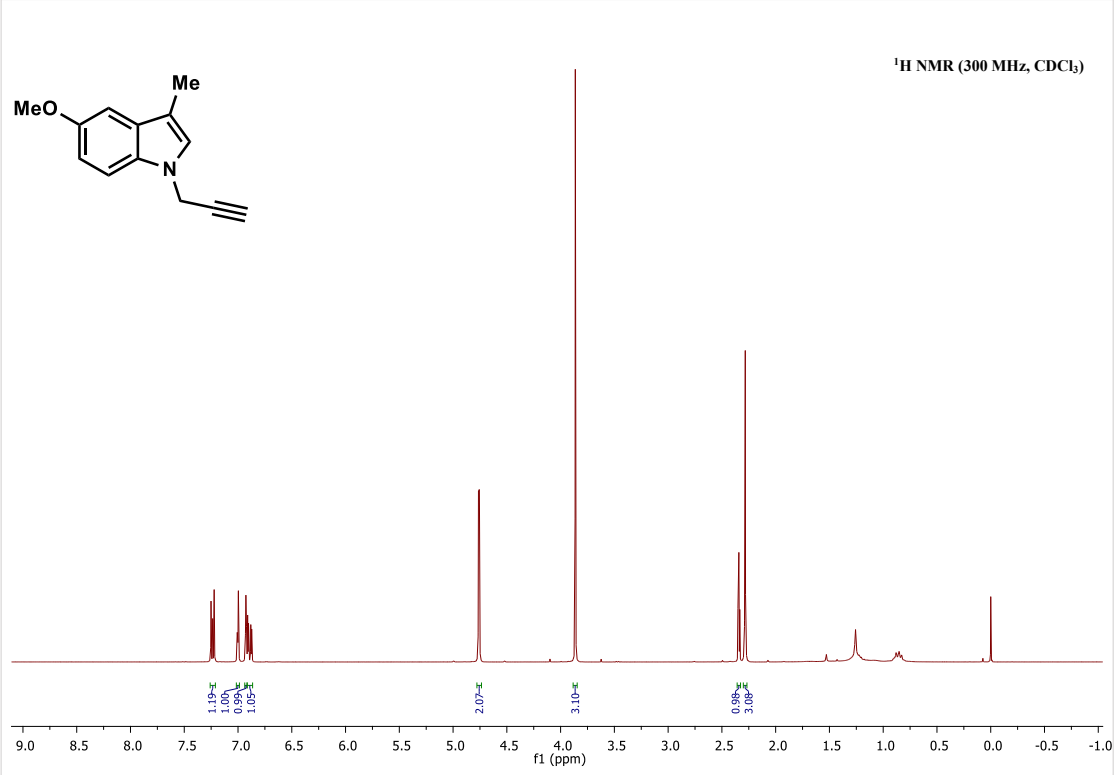
^{1}H NMR (300 MHz, CDCl$_3$)
Me
MeO
N
1.19
1.00
0.99
1.05
2.07
3.10
0.98
3.08
9.0 8.5 8.0 7.5 7.0 6.5 6.0 5.5 5.0 4.5 4.0 3.5 3.0 2.5 2.0 1.5 1.0 0.5 0.0 -0.5 -1.0
f1 (ppm)

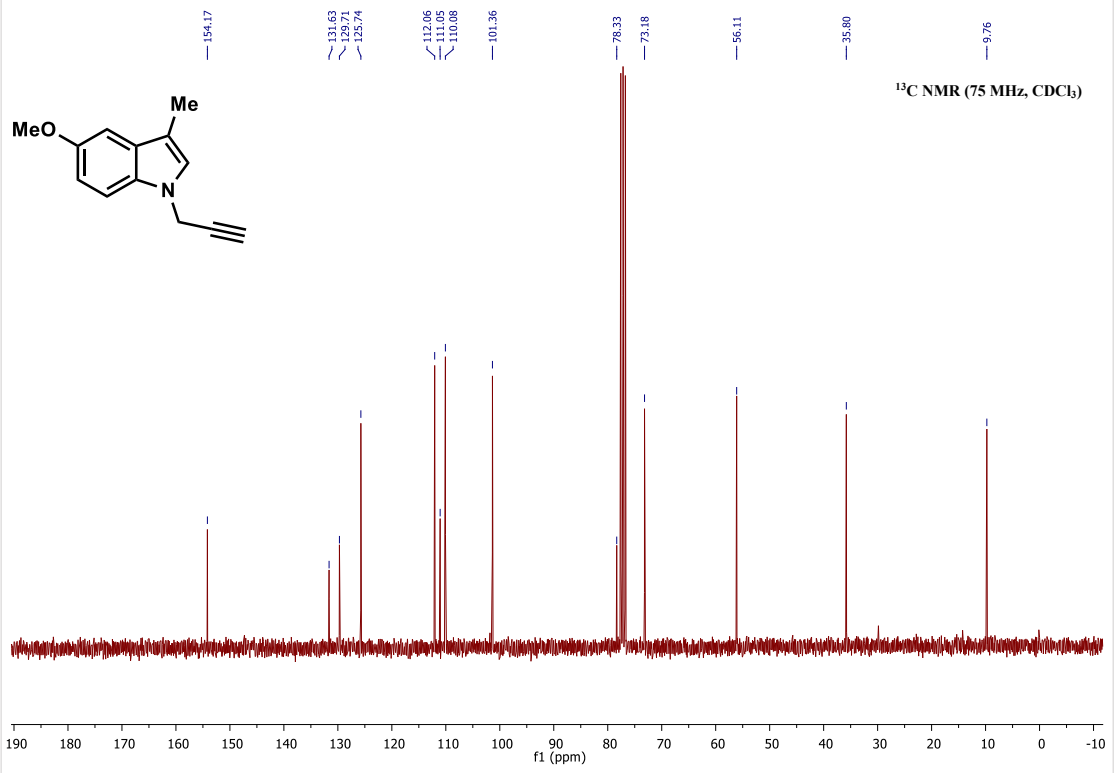
154.17
131.63
129.71
125.74
112.06
111.05
110.08
101.36
78.33
73.18
56.11
35.80
9.76
^{13}C NMR (75 MHz, CDCl$_3$)
Me
MeO
N
190 180 170 160 150 140 130 120 110 100 90 80 70 60 50 40 30 20 10 0 -10
f1 (ppm)

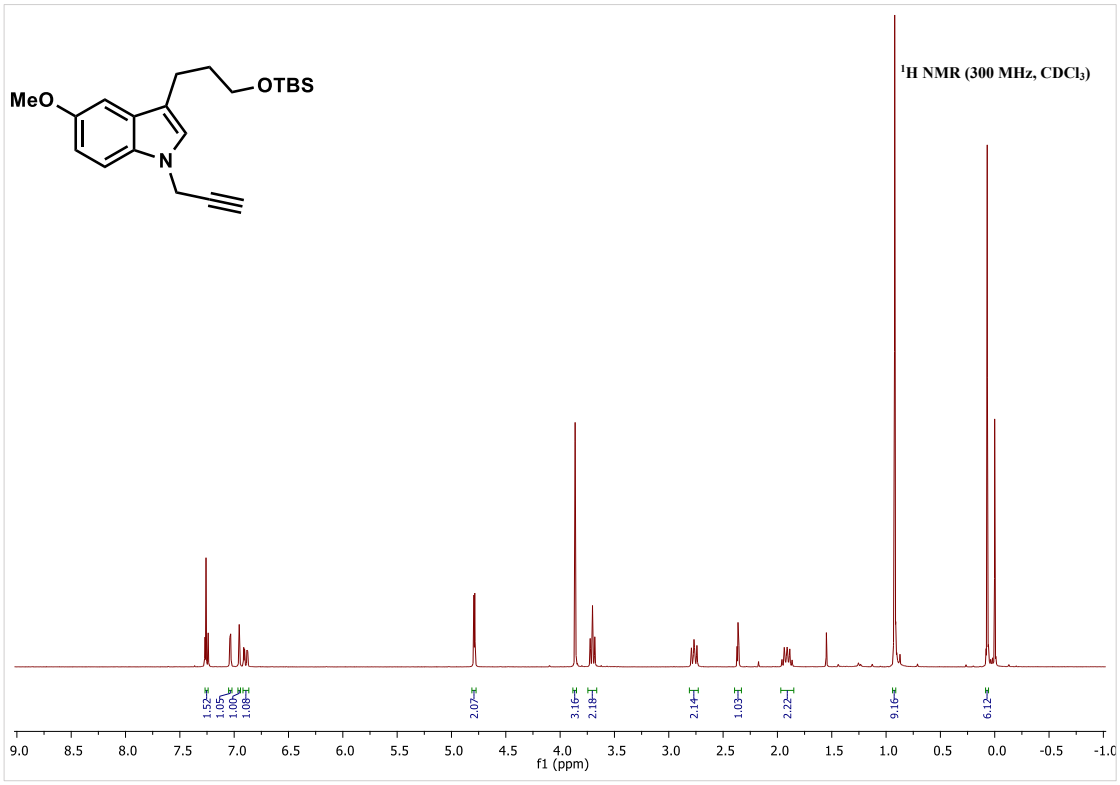
MeO
OTBS
N
^{1}H NMR (300 MHz, CDCl$_3$)
1.52
1.05
1.00
1.08
2.07
3.16
2.18
2.14
1.03
2.22
9.16
6.12
f1 (ppm)

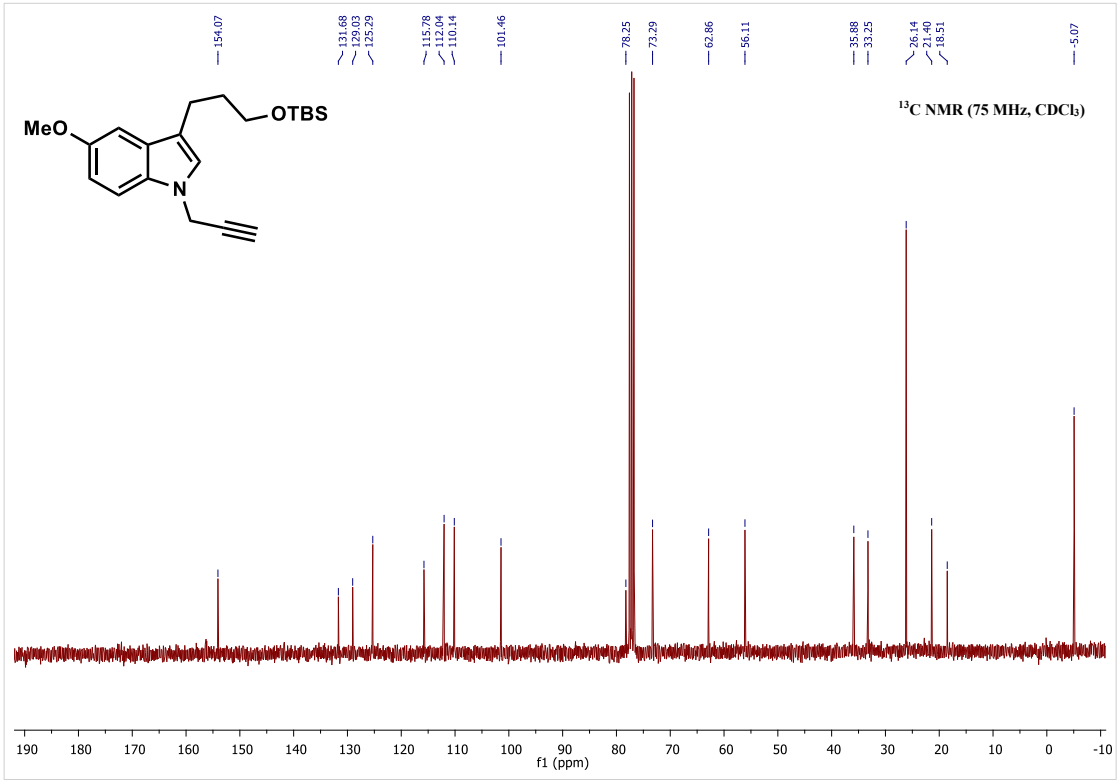
MeO
OTBS
N
^{13}C NMR (75 MHz, CDCl$_3$)
154.07
131.68
129.03
125.29
115.78
112.04
110.14
101.46
78.25
73.29
62.86
56.11
35.88
33.25
26.14
21.40
18.51
-5.07
f1 (ppm)

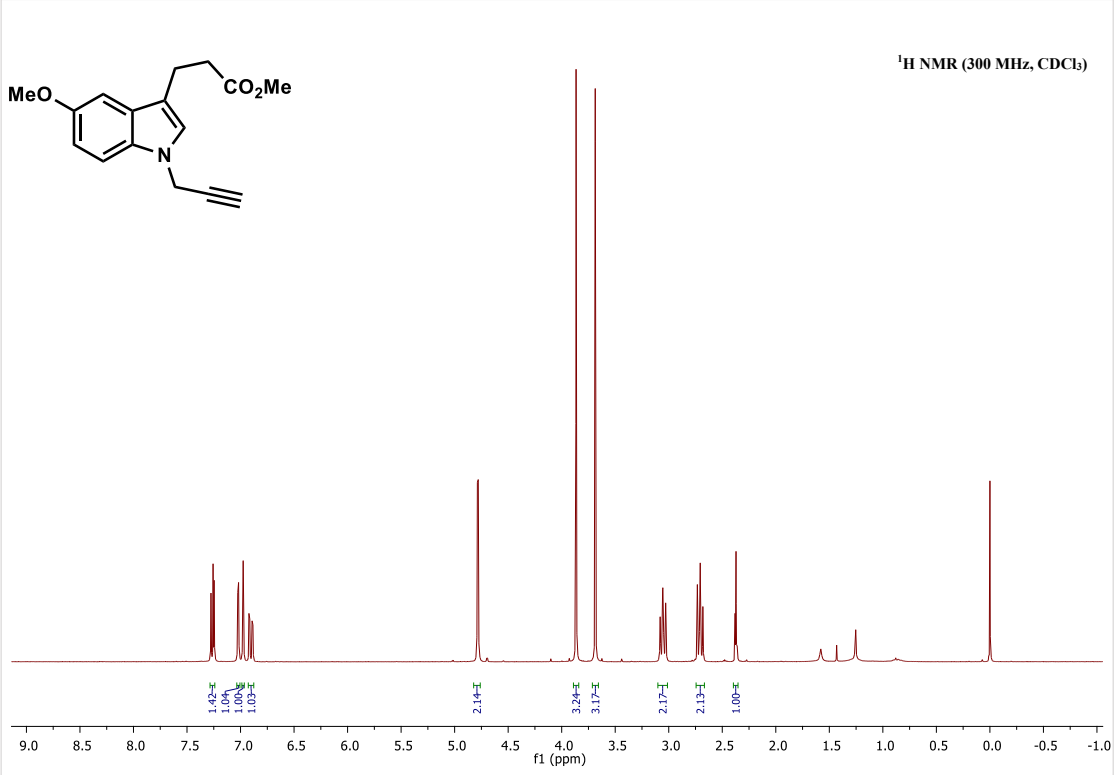
MeO
CO2Me
N
1H NMR (300 MHz, CDCl3)
1.42
1.04
1.00
1.03
2.14
3.24
3.17
2.17
2.13
1.00
9.0 8.5 8.0 7.5 7.0 6.5 6.0 5.5 5.0 4.5 4.0 3.5 3.0 2.5 2.0 1.5 1.0 0.5 0.0 -0.5 -1.0
f1 (ppm)

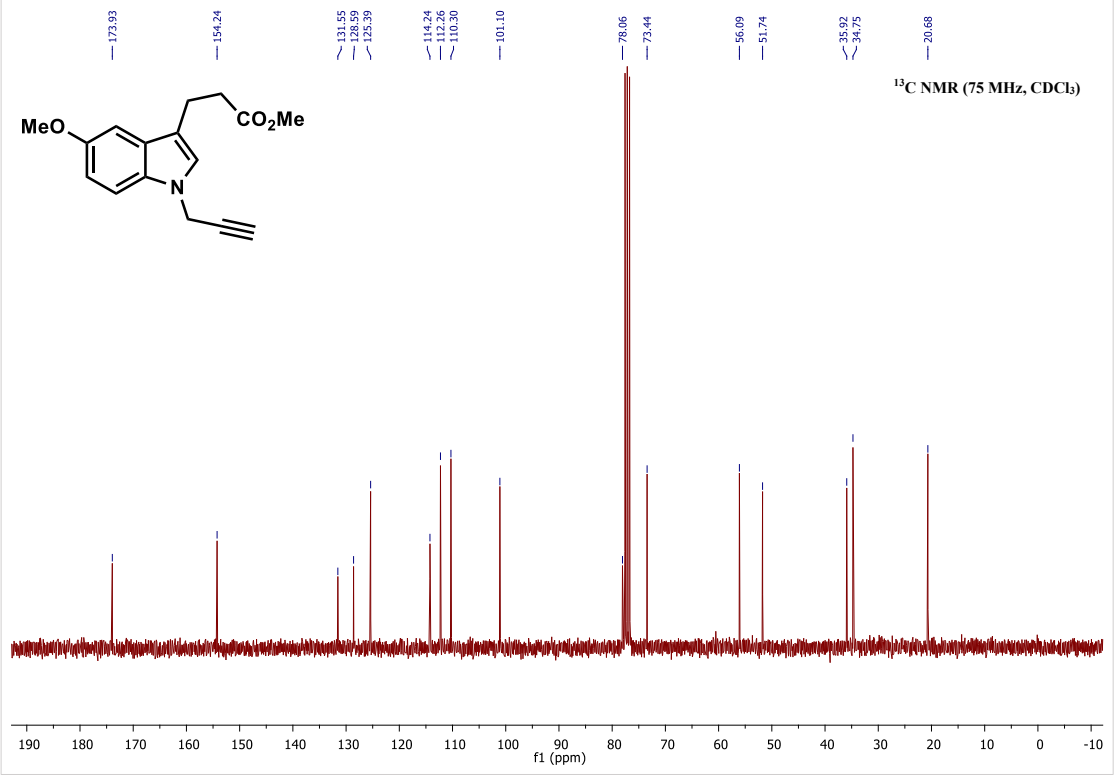
173.93
154.24
131.55
128.59
125.39
114.24
112.26
110.30
101.10
78.06
73.44
56.09
51.74
35.92
34.75
20.68
MeO
CO2Me
N
13C NMR (75 MHz, CDCl3)
190 180 170 160 150 140 130 120 110 100 90 80 70 60 50 40 30 20 10 0 -10
f1 (ppm)

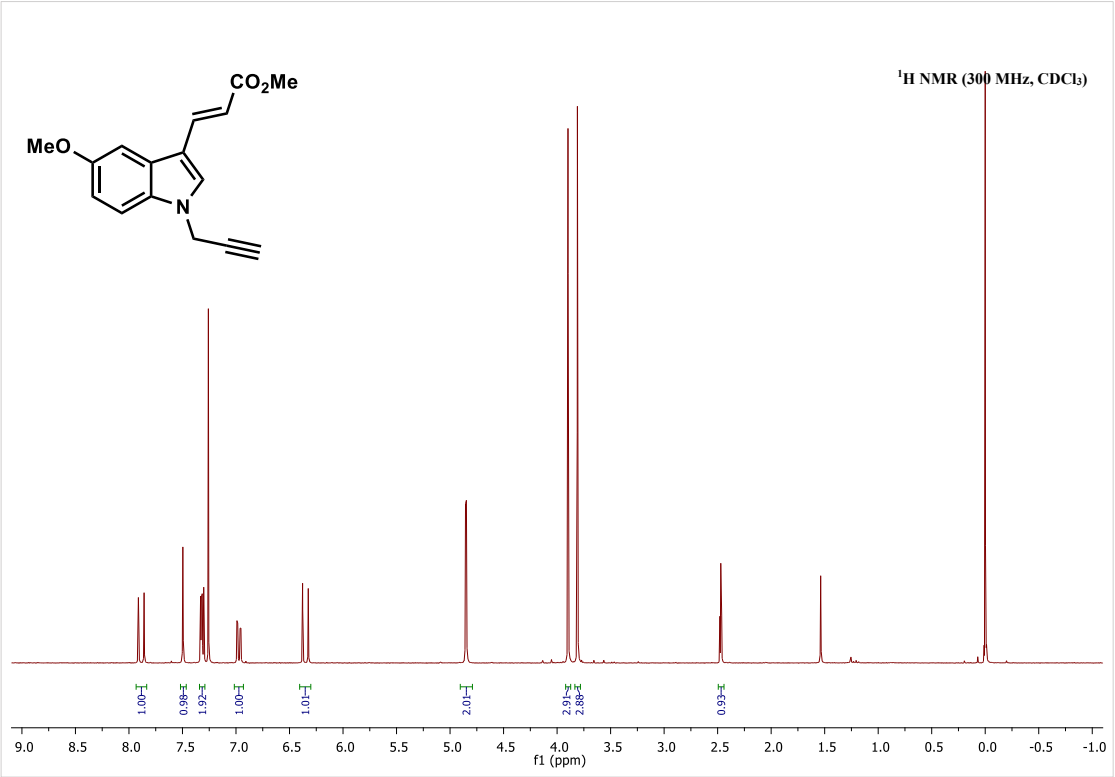
CO2Me
MeO
N
1H NMR (300 MHz, CDCl3)
1.00
0.98
1.92
1.00
1.01
2.01
2.91
2.88
0.93
9.0 8.5 8.0 7.5 7.0 6.5 6.0 5.5 5.0 4.5 4.0 3.5 3.0 2.5 2.0 1.5 1.0 0.5 0.0 -0.5 -1.0
f1 (ppm)

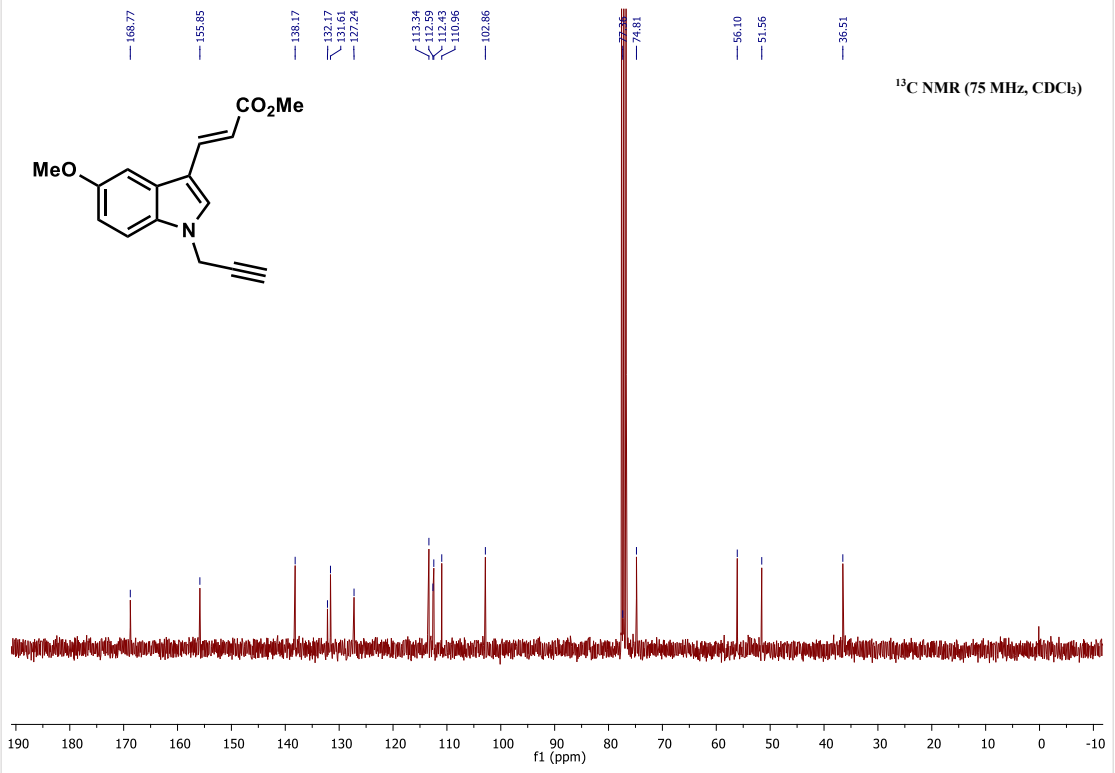
168.77
155.85
138.17
132.17
131.61
127.24
113.34
112.59
112.43
110.96
102.86
77.36
74.81
56.10
51.56
36.51
CO2Me
MeO
N
13C NMR (75 MHz, CDCl3)
190 180 170 160 150 140 130 120 110 100 90 80 70 60 50 40 30 20 10 0 -10
f1 (ppm)

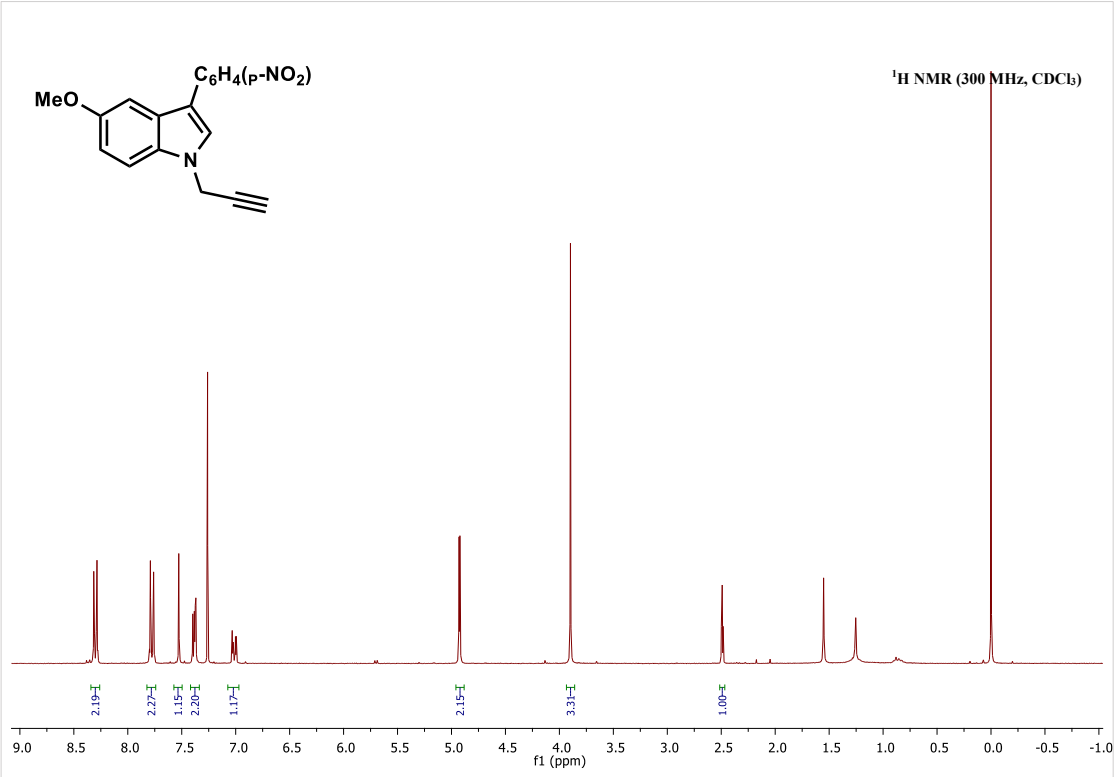
MeO
C6H4(P-NO2)
N
1H NMR (300 MHz, CDCl3)
2.19
2.27
1.15
2.20
1.17
2.15
3.31
1.00
9.0 8.5 8.0 7.5 7.0 6.5 6.0 5.5 5.0 4.5 4.0 3.5 3.0 2.5 2.0 1.5 1.0 0.5 0.0 -0.5 -1.0
f1 (ppm)

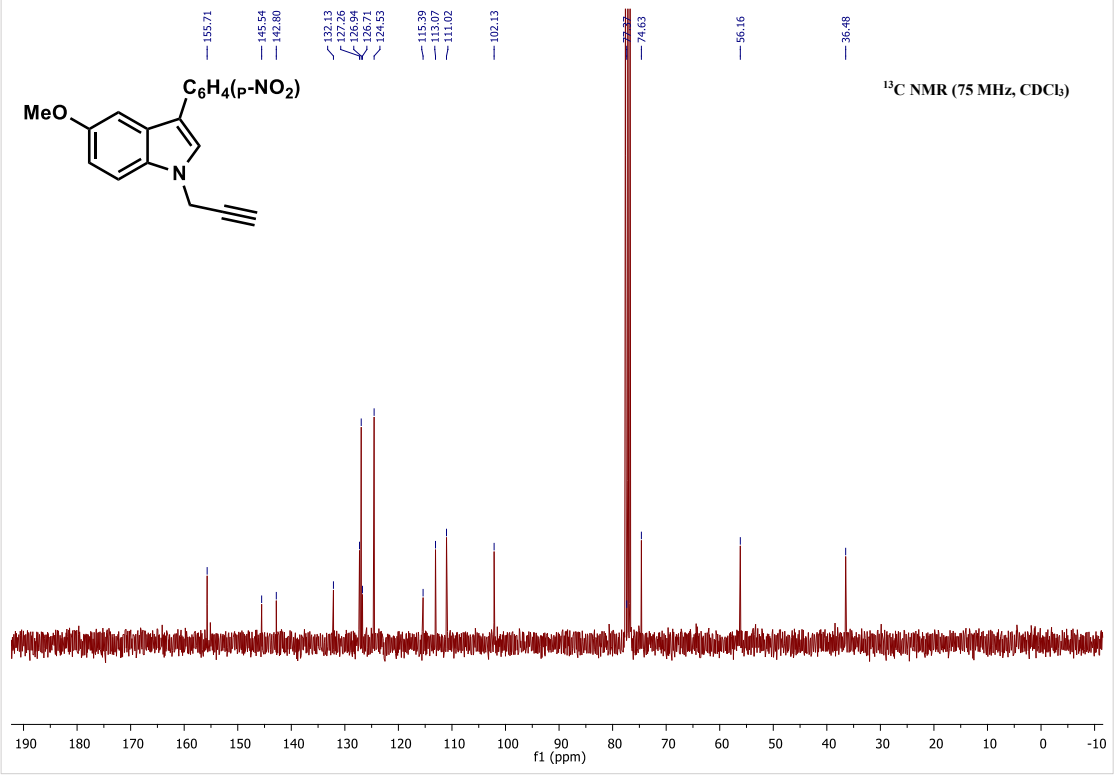
155.71
145.54
142.80
132.13
127.26
125.94
126.71
124.53
115.39
113.07
111.02
102.13
77.32
74.63
56.16
36.48
MeO
C6H4(P-NO2)
N
13C NMR (75 MHz, CDCl3)
190 180 170 160 150 140 130 120 110 100 90 80 70 60 50 40 30 20 10 0 -10
f1 (ppm)

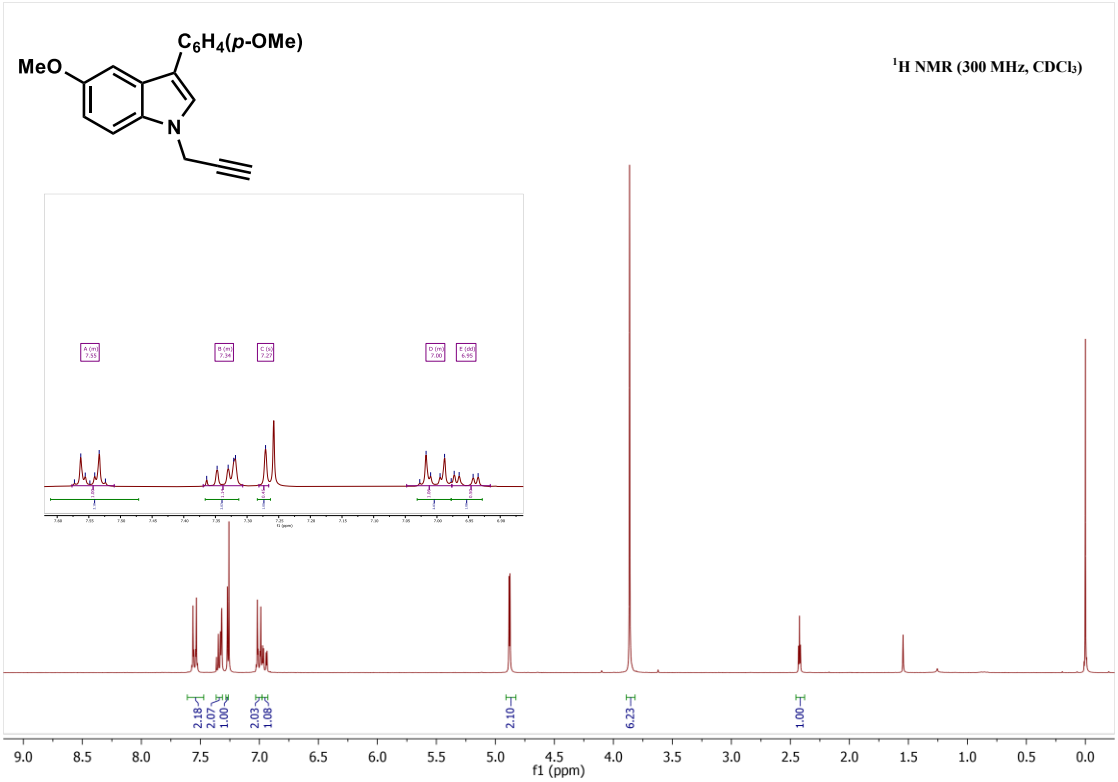
C6H4(p-OMe)
MeO
N
1H NMR (300 MHz, CDCl3)
2.18
2.07
1.00
2.03
1.08
2.10
6.23
1.00
f1 (ppm)

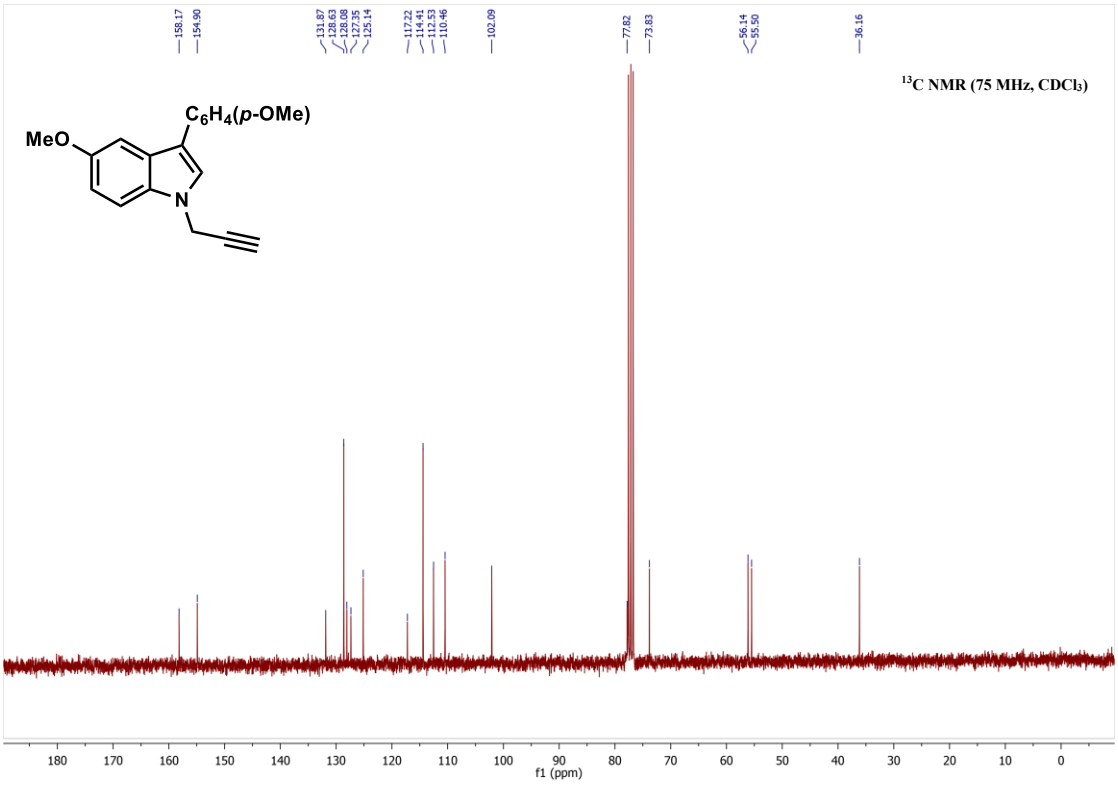
158.17
154.90
131.87
128.63
128.08
127.35
125.14
117.22
114.41
112.53
110.46
102.09
77.82
73.83
56.14
55.50
36.16
C6H4(p-OMe)
MeO
N
13C NMR (75 MHz, CDCl3)
f1 (ppm)

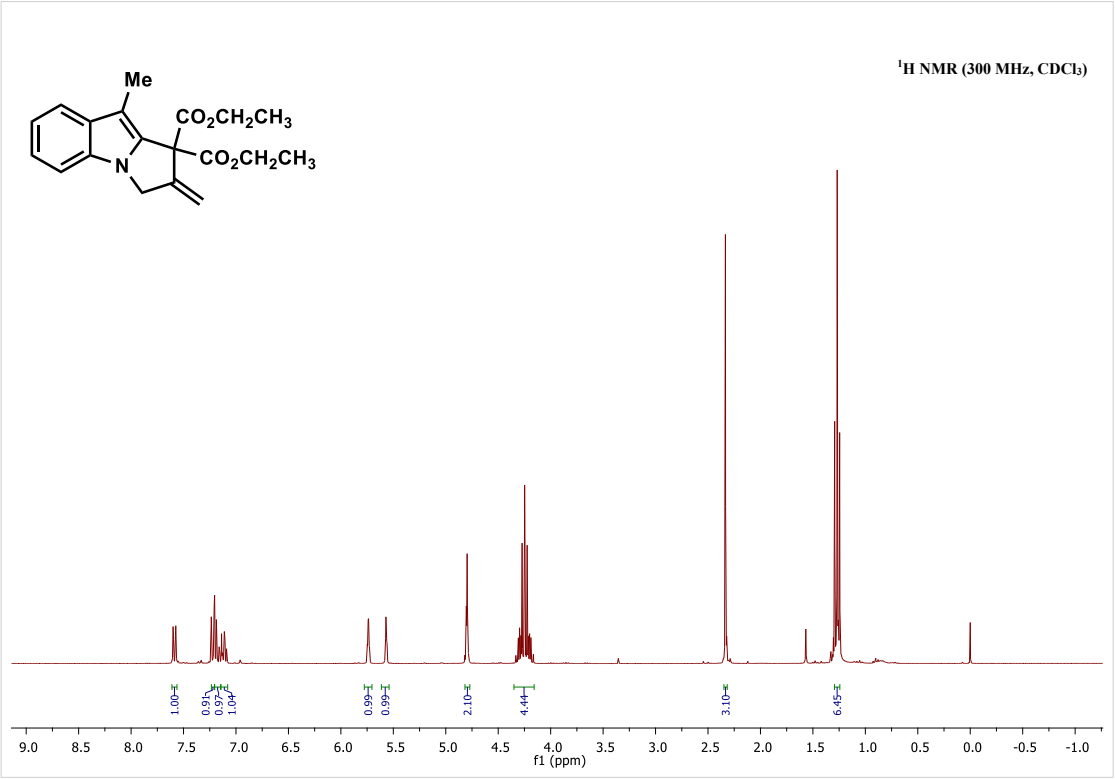
Me
CO2CH2CH3
CO2CH2CH3
N
1H NMR (300 MHz, CDCl3)
1.00
0.91
0.97
1.04
0.99
0.99
2.10
4.44
3.10
6.45
9.0 8.5 8.0 7.5 7.0 6.5 6.0 5.5 5.0 4.5 4.0 3.5 3.0 2.5 2.0 1.5 1.0 0.5 0.0 -0.5 -1.0
f1 (ppm)

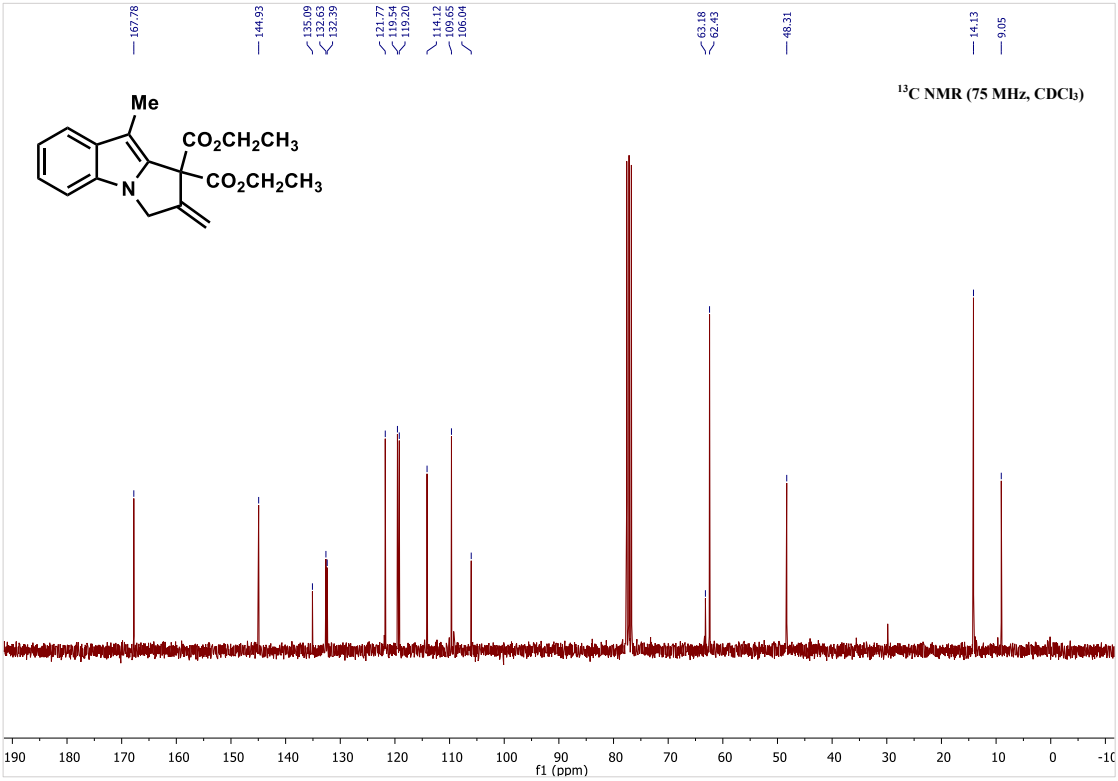
167.78
144.93
135.09
132.63
132.39
121.77
119.54
119.20
114.12
109.65
106.04
63.18
62.43
48.31
14.13
9.05
Me
CO2CH2CH3
CO2CH2CH3
N
13C NMR (75 MHz, CDCl3)
190 180 170 160 150 140 130 120 110 100 90 80 70 60 50 40 30 20 10 0
f1 (ppm)

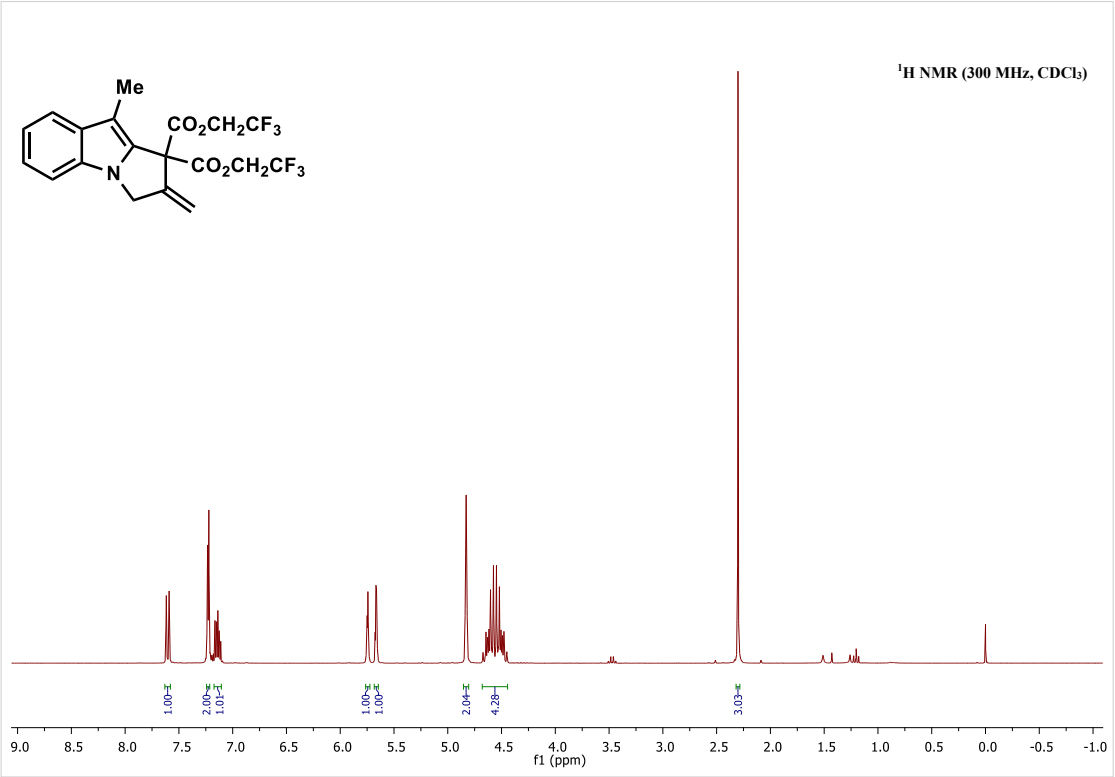
Me
CO2CH2CF3
CO2CH2CF3
N
1H NMR (300 MHz, CDCl3)
1.00
2.00
1.01
1.00
1.00
2.04
4.28
3.03
9.0 8.5 8.0 7.5 7.0 6.5 6.0 5.5 5.0 4.5 4.0 3.5 3.0 2.5 2.0 1.5 1.0 0.5 0.0 -0.5 -1.0
f1 (ppm)

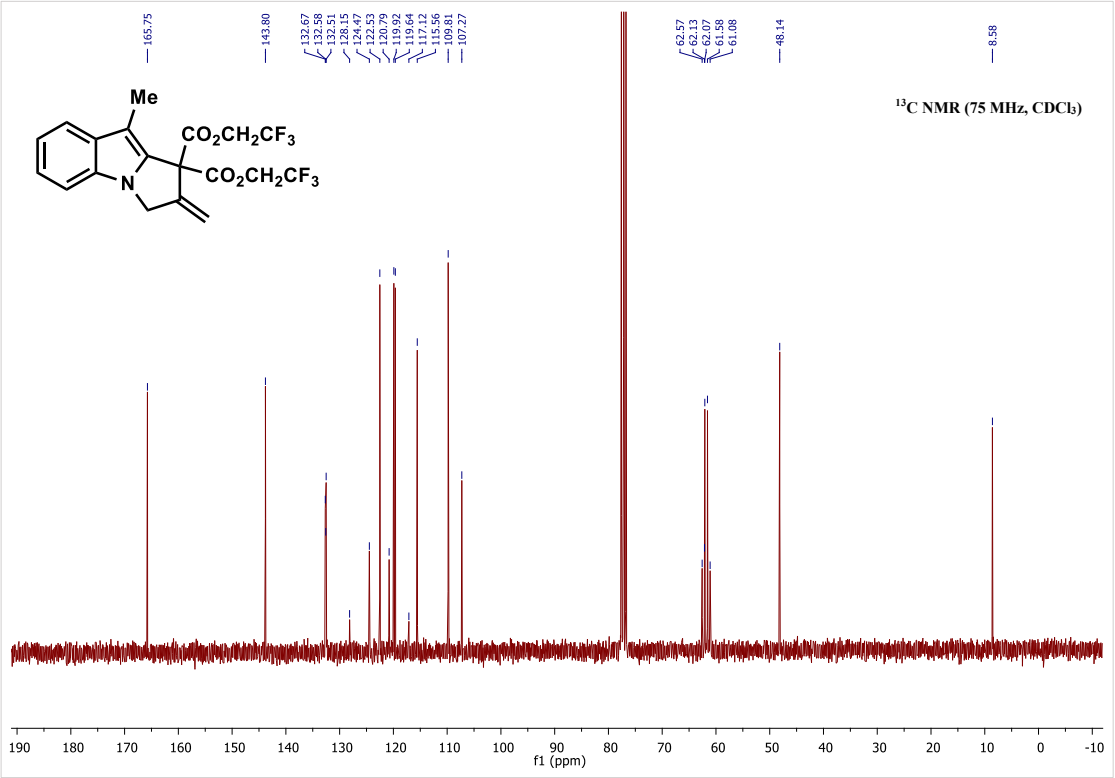
165.75
143.80
132.67
132.58
132.51
128.15
124.47
122.53
120.79
119.92
119.64
117.12
115.56
109.81
107.27
62.57
62.13
62.07
61.58
61.08
48.14
8.58
Me
CO2CH2CF3
CO2CH2CF3
N
13C NMR (75 MHz, CDCl3)
190 180 170 160 150 140 130 120 110 100 90 80 70 60 50 40 30 20 10 0 -10
f1 (ppm)

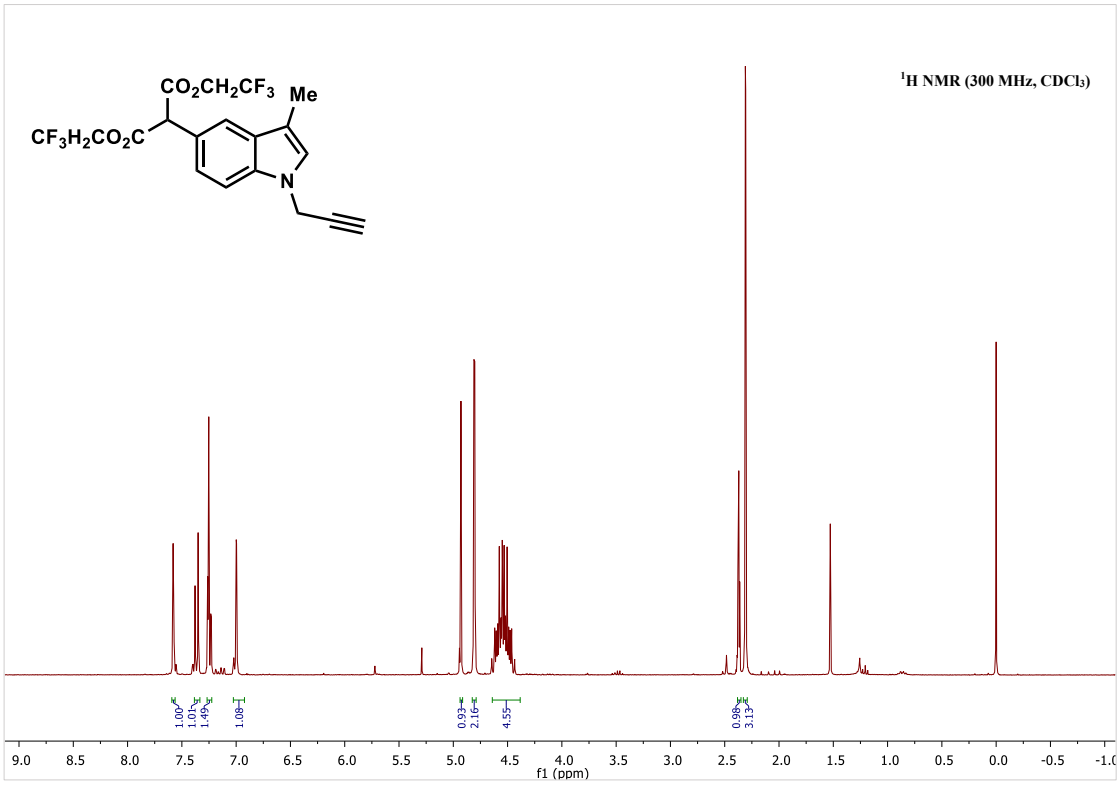
^{1}H NMR (300 MHz, CDCl$_3$)
CO2CH2CF3
Me
CF3H2CO2C
N
1.00
1.01
1.49
1.08
0.93
2.16
4.55
0.98
3.13
9.0 8.5 8.0 7.5 7.0 6.5 6.0 5.5 5.0 4.5 4.0 3.5 3.0 2.5 2.0 1.5 1.0 0.5 0.0 -0.5
f1 (ppm)

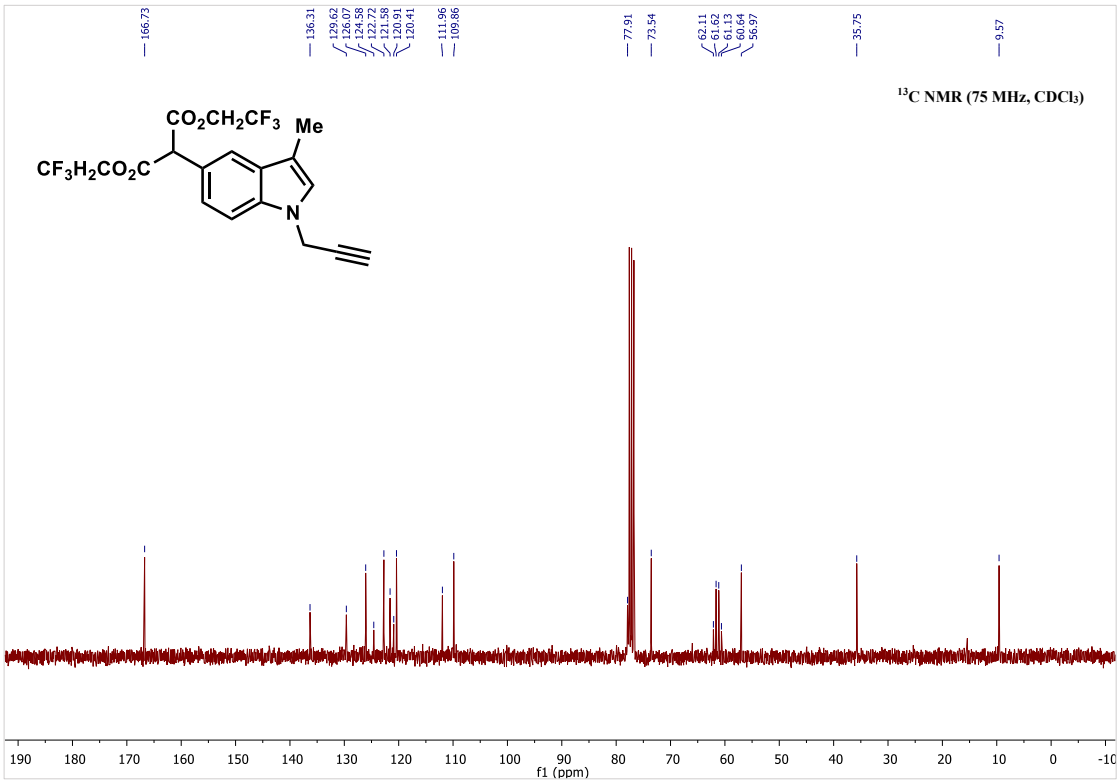
166.73
136.31
129.62
126.07
124.58
122.72
121.58
120.91
120.41
111.96
109.86
77.91
73.54
62.11
61.62
61.13
60.64
56.97
35.75
9.57
^{13}C NMR (75 MHz, CDCl$_3$)
CO2CH2CF3
Me
CF3H2CO2C
N
190 180 170 160 150 140 130 120 110 100 90 80 70 60 50 40 30 20 10 0 -10
f1 (ppm)

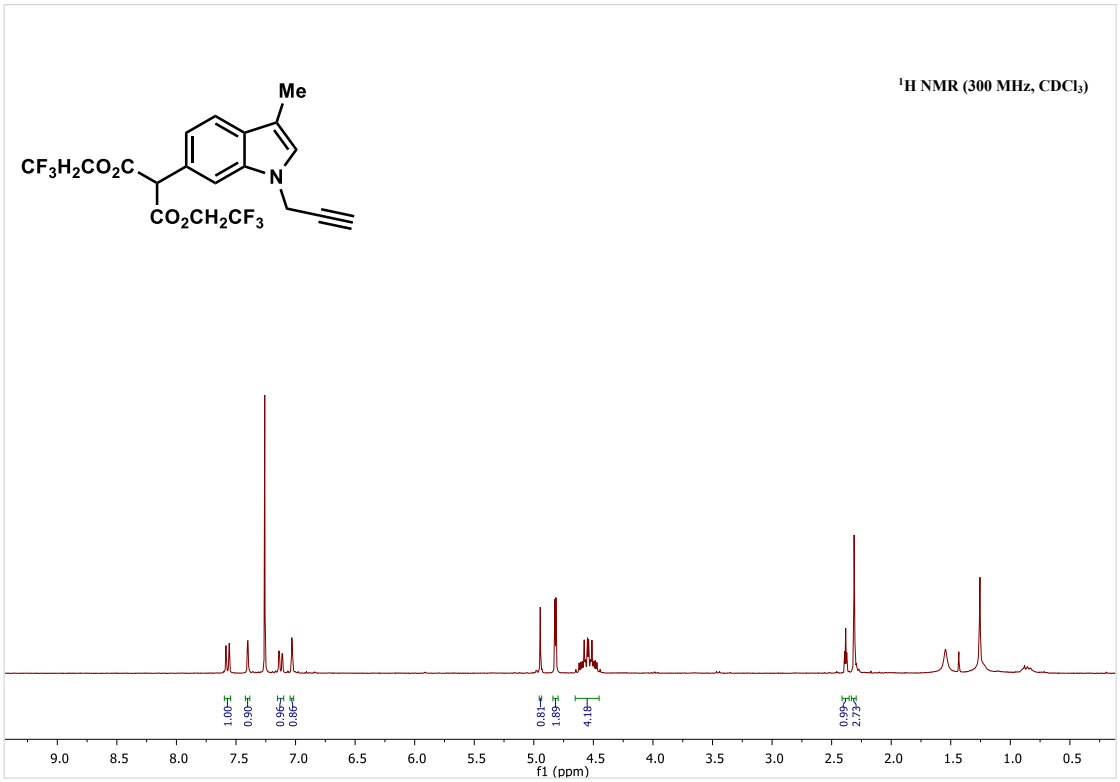
Me
CF3H2CO2C
N
CO2CH2CF3
1H NMR (300 MHz, CDCl3)
1.00
0.90
0.96
0.86
0.81
1.89
4.18
0.99
2.73
9.0 8.5 8.0 7.5 7.0 6.5 6.0 5.5 5.0 4.5 4.0 3.5 3.0 2.5 2.0 1.5 1.0 0.5
f1 (ppm)

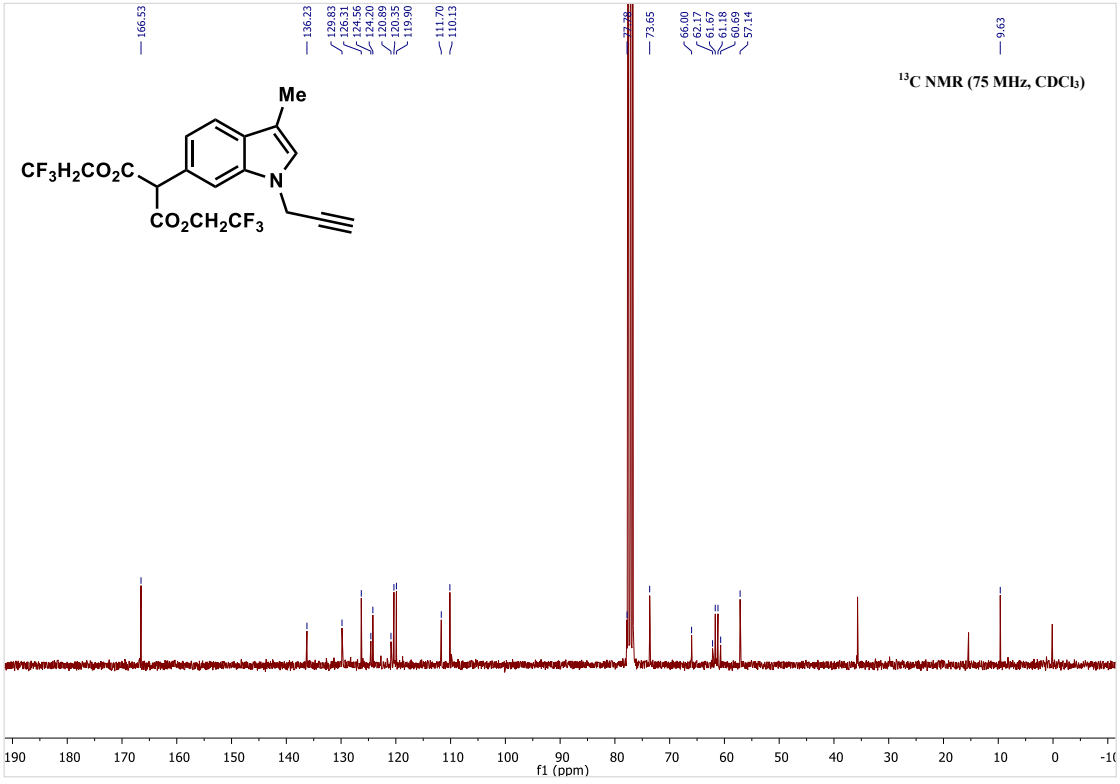
166.53
136.23
129.83
126.31
124.55
124.20
120.89
120.35
119.90
111.70
110.13
77.28
73.65
66.00
62.17
61.67
61.18
60.69
57.14
9.63
Me
CF3H2CO2C
N
CO2CH2CF3
13C NMR (75 MHz, CDCl3)
190 180 170 160 150 140 130 120 110 100 90 80 70 60 50 40 30 20 10 0
f1 (ppm)

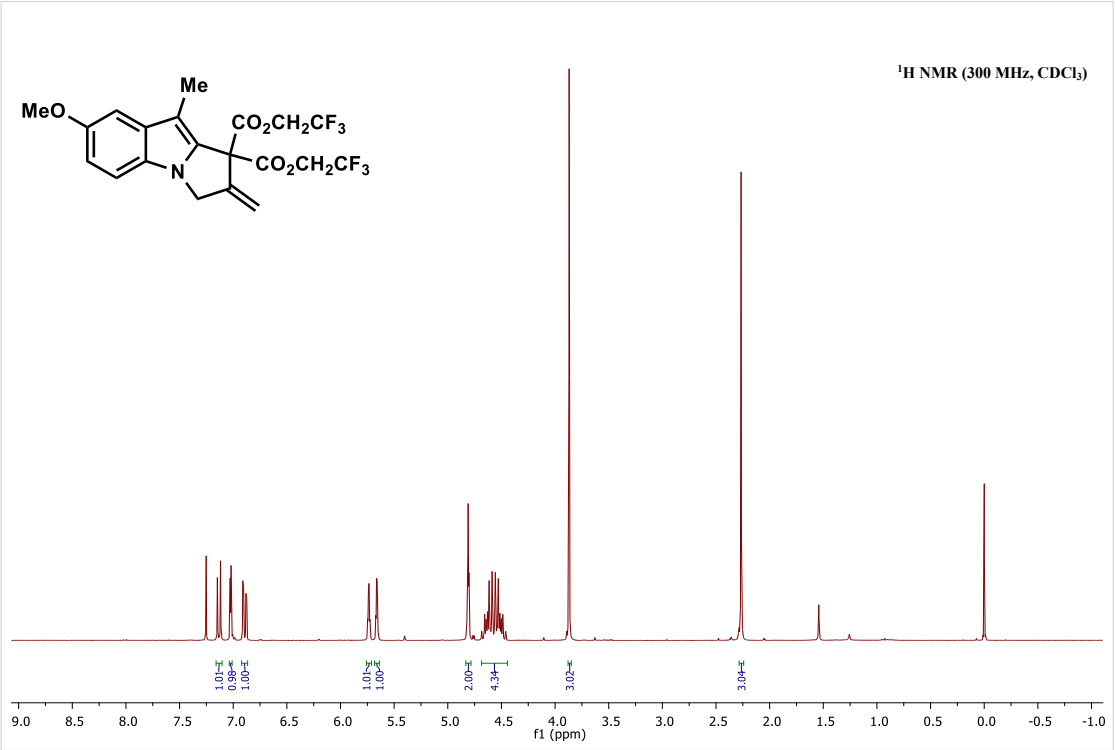
^{1}H NMR (300 MHz, CDCl$_3$)
Me
MeO
$CO_2CH_2CF_3$
$CO_2CH_2CF_3$
N
1.01
0.98
1.00
1.01
1.00
2.00
4.34
3.02
3.04
9.0 8.5 8.0 7.5 7.0 6.5 6.0 5.5 5.0 4.5 4.0 3.5 3.0 2.5 2.0 1.5 1.0 0.5 0.0 -0.5 -1.0
f1 (ppm)

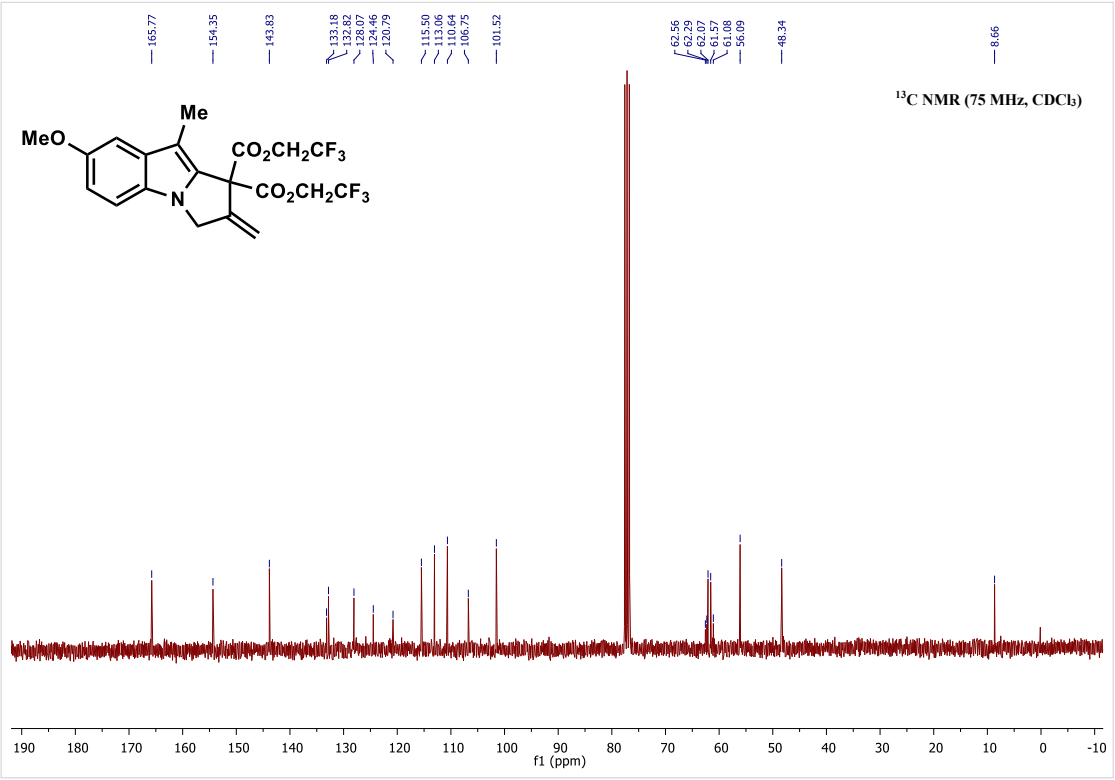
165.77
154.35
143.83
133.18
132.82
128.07
124.46
120.79
115.50
113.06
110.64
106.75
101.52
62.56
62.29
62.07
61.57
61.08
56.09
48.34
8.66
^{13}C NMR (75 MHz, CDCl$_3$)
Me
MeO
$CO_2CH_2CF_3$
$CO_2CH_2CF_3$
N
190 180 170 160 150 140 130 120 110 100 90 80 70 60 50 40 30 20 10 0 -10
f1 (ppm)

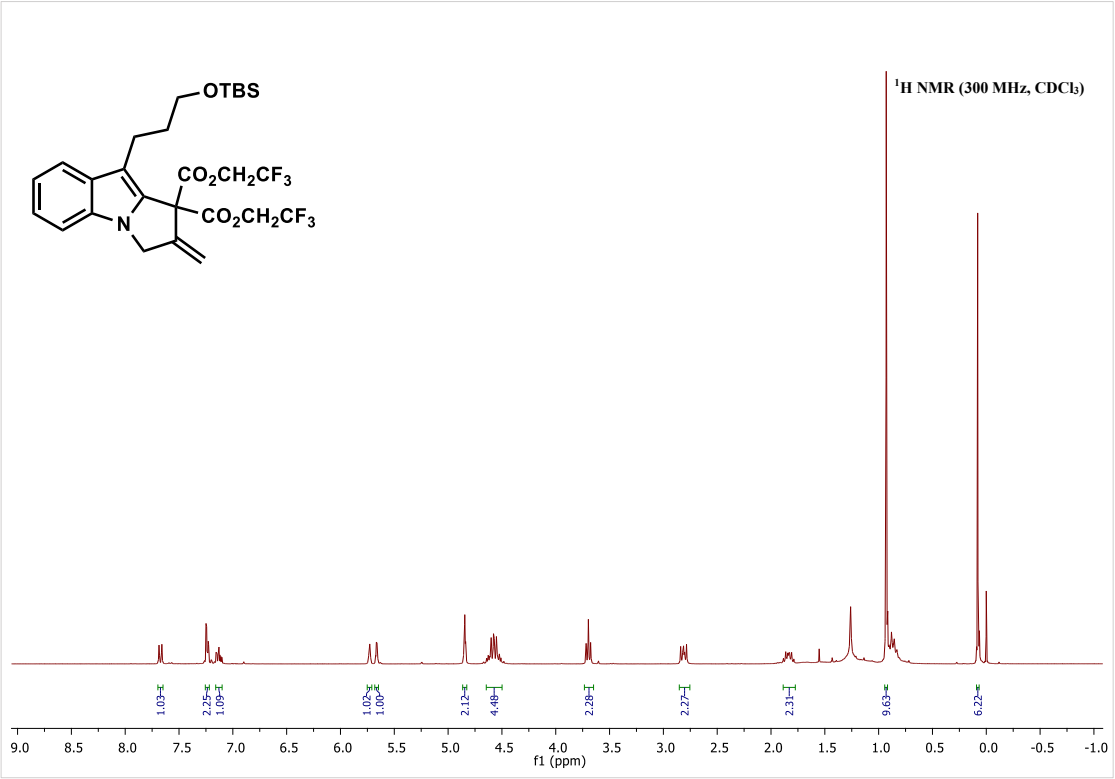
OTBS
CO2CH2CF3
CO2CH2CF3
N
1H NMR (300 MHz, CDCl3)
1.03
2.25
1.09
1.02
1.00
2.12
4.48
2.28
2.27
2.31
9.63
6.22
9.0 8.5 8.0 7.5 7.0 6.5 6.0 5.5 5.0 4.5 4.0 3.5 3.0 2.5 2.0 1.5 1.0 0.5 0.0 -0.5 -1.0
f1 (ppm)

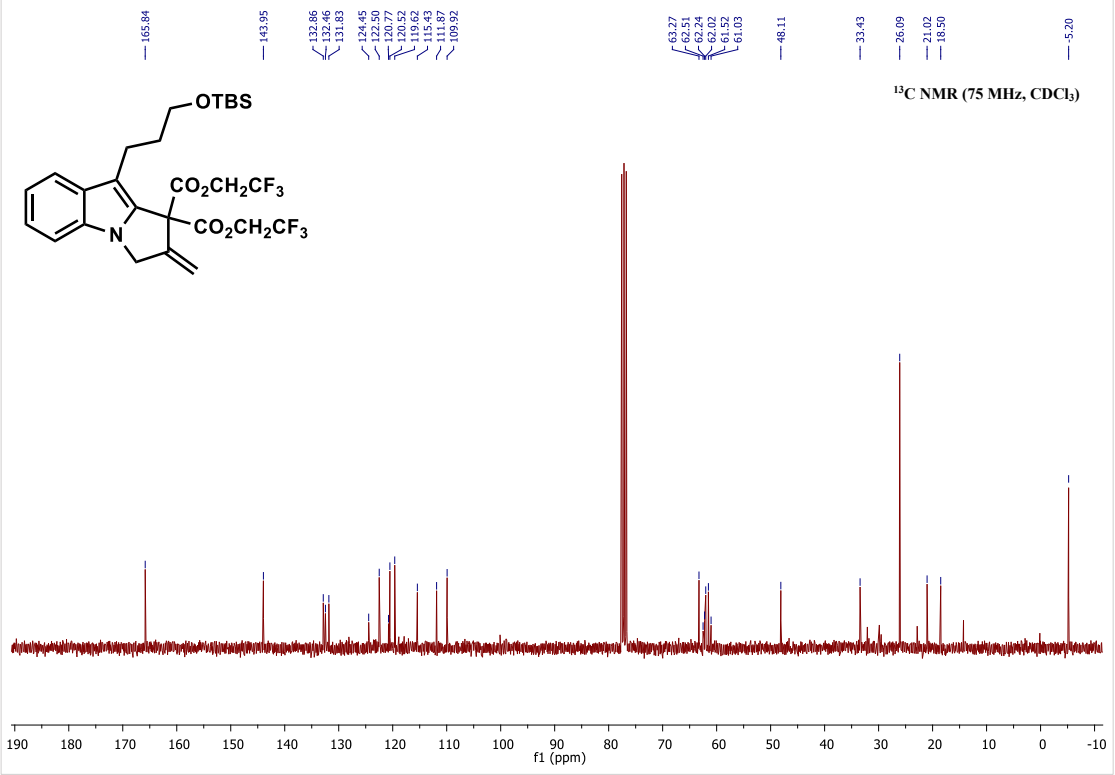
165.84
143.95
132.86
132.46
131.83
124.45
122.50
120.77
120.52
119.62
115.43
111.87
109.92
63.27
62.51
62.24
62.02
61.52
61.03
48.11
33.43
26.09
21.02
18.50
5.20
OTBS
CO2CH2CF3
CO2CH2CF3
N
13C NMR (75 MHz, CDCl3)
190 180 170 160 150 140 130 120 110 100 90 80 70 60 50 40 30 20 10 0 -10
f1 (ppm)

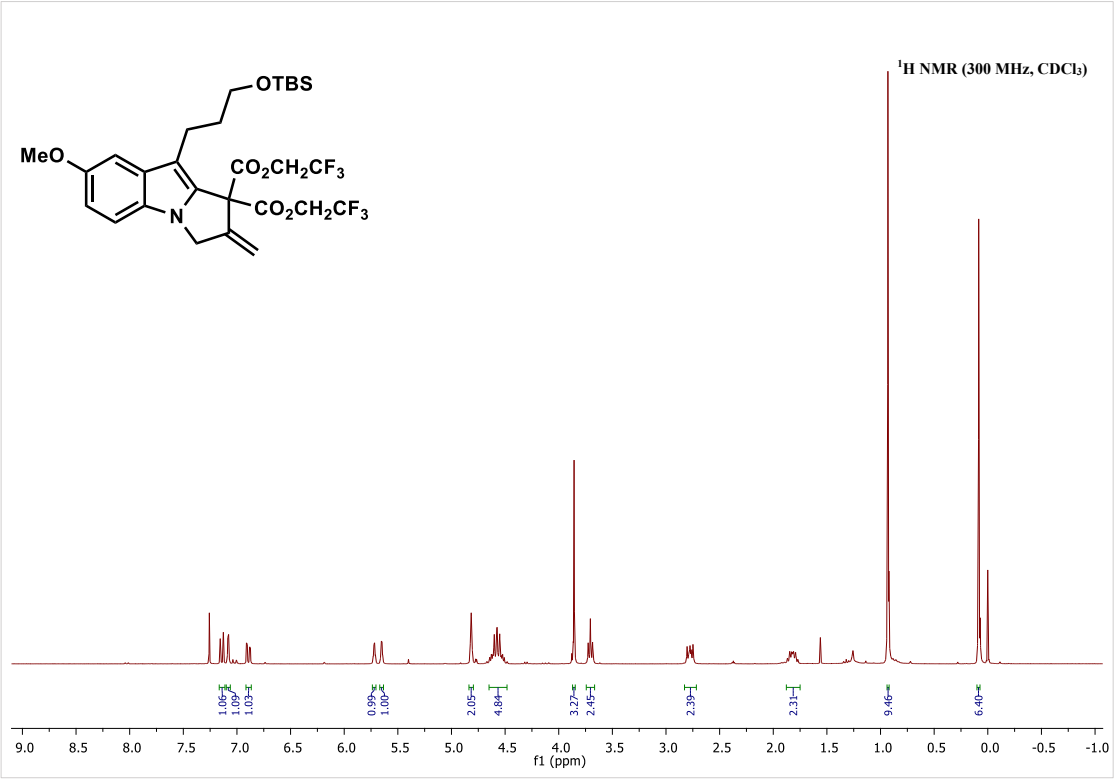
^{1}H NMR (300 MHz, CDCl$_3$)
OTBS
MeO
$CO_2CH_2CF_3$
$CO_2CH_2CF_3$
N
1.06
1.09
1.03
0.99
1.00
2.05
4.84
3.27
2.45
2.39
2.31
9.46
6.40
9.0 8.5 8.0 7.5 7.0 6.5 6.0 5.5 5.0 4.5 4.0 3.5 3.0 2.5 2.0 1.5 1.0 0.5 0.0 -0.5 -1.0
f1 (ppm)

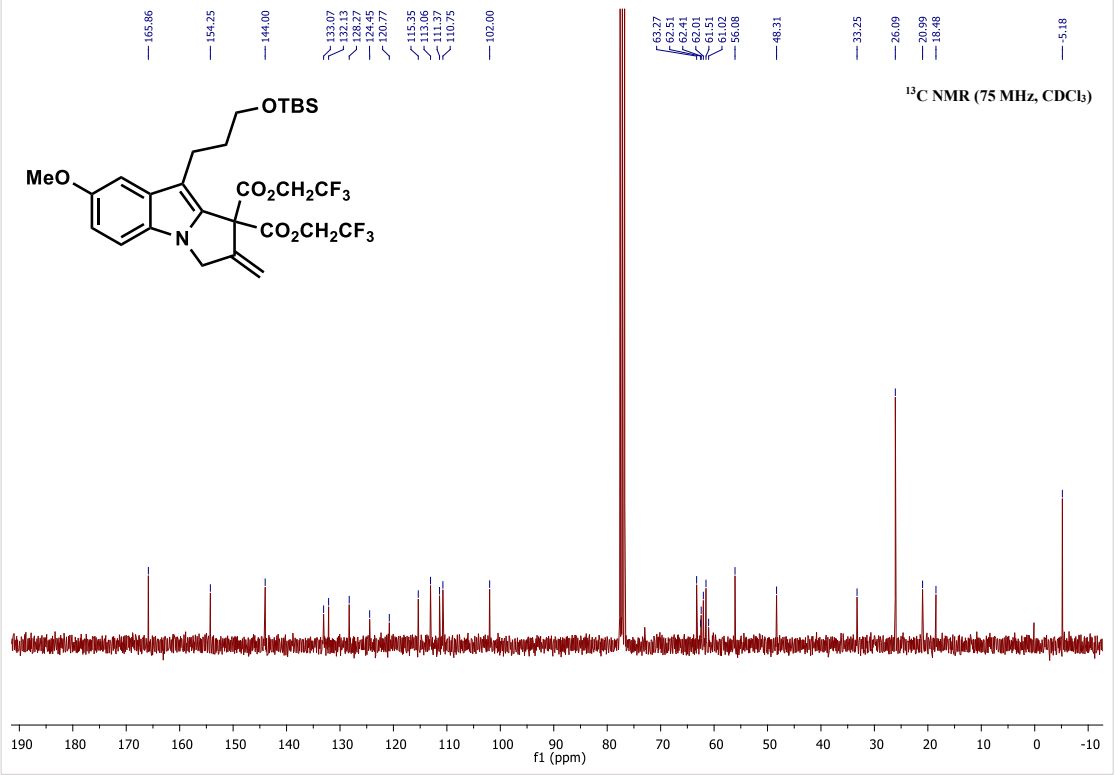
165.86
154.25
144.00
133.07
132.13
128.27
124.45
120.77
115.35
113.96
111.77
110.75
102.00
63.27
62.51
62.41
62.01
61.51
61.02
56.08
48.31
33.25
26.09
20.99
18.48
-5.18
^{13}C NMR (75 MHz, CDCl$_3$)
OTBS
MeO
$CO_2CH_2CF_3$
$CO_2CH_2CF_3$
N
190 180 170 160 150 140 130 120 110 100 90 80 70 60 50 40 30 20 10 0 -10
f1 (ppm)

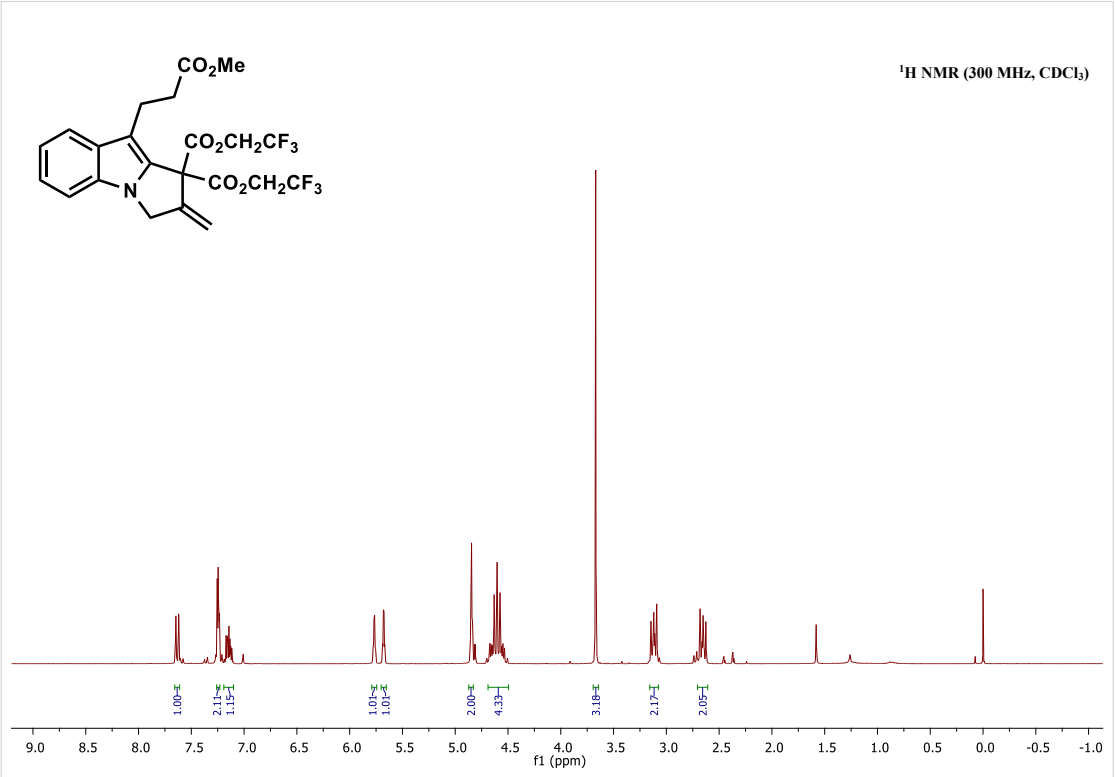
CO2Me
CO2CH2CF3
CO2CH2CF3
N
1H NMR (300 MHz, CDCl3)
1.00
2.11
1.15
1.01
1.01
2.00
4.33
3.18
2.17
2.05
9.0 8.5 8.0 7.5 7.0 6.5 6.0 5.5 5.0 4.5 4.0 3.5 3.0 2.5 2.0 1.5 1.0 0.5 0.0 -0.5 -1.0
f1 (ppm)

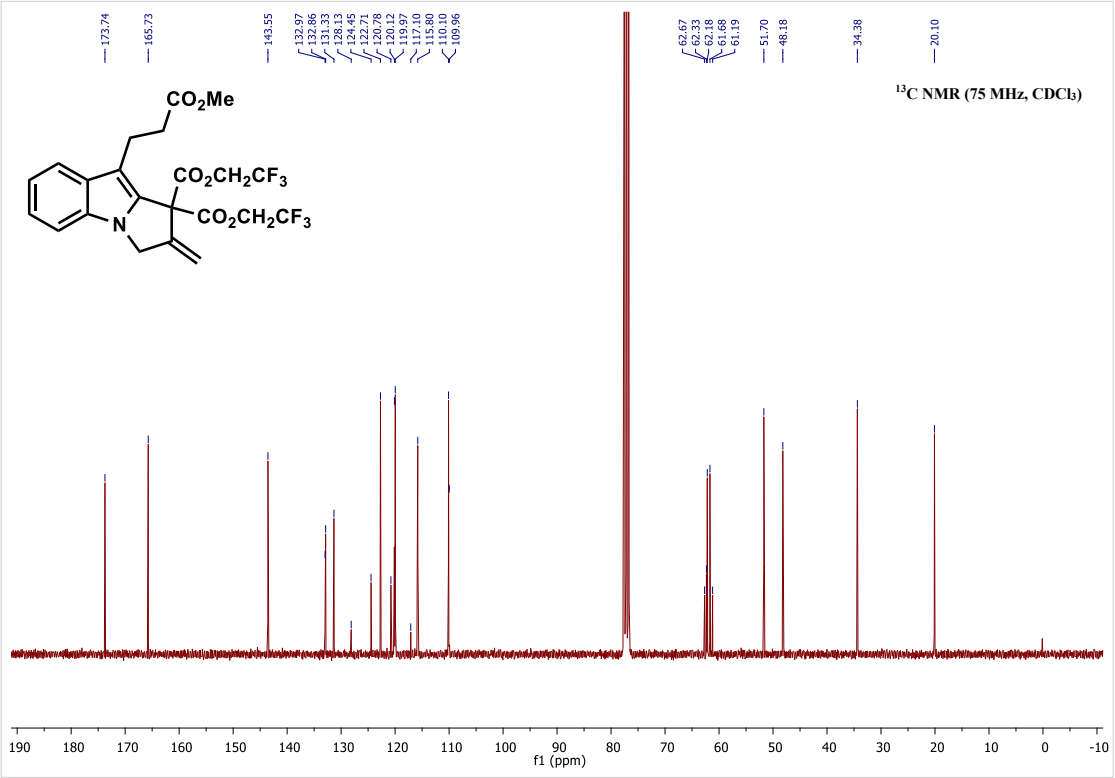
173.74
165.73
143.55
132.97
132.86
131.33
128.13
124.45
122.71
120.78
120.12
119.97
117.10
115.80
110.10
109.96
62.67
62.33
62.18
61.68
61.19
51.70
48.18
34.38
20.10
CO2Me
CO2CH2CF3
CO2CH2CF3
N
13C NMR (75 MHz, CDCl3)
190 180 170 160 150 140 130 120 110 100 90 80 70 60 50 40 30 20 10 0 -10
f1 (ppm)

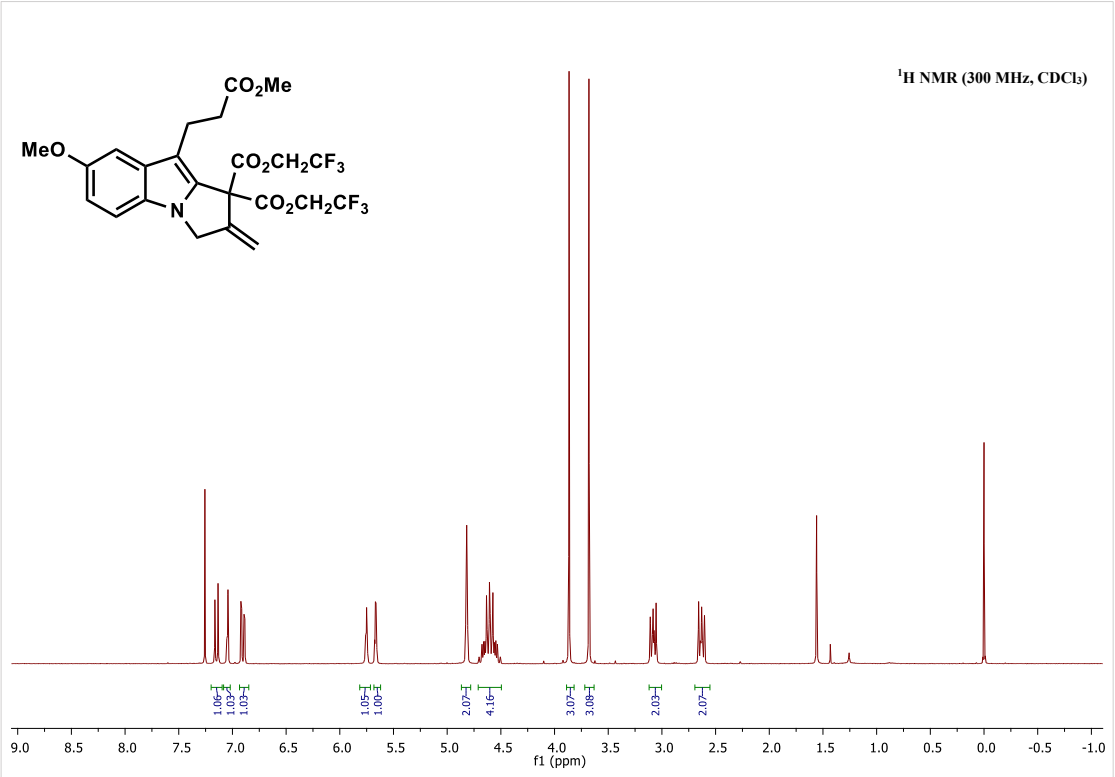
^{1}H NMR (300 MHz, CDCl$_3$)
CO2Me
MeO
CO2CH2CF3
CO2CH2CF3
N
1.06
1.03
1.03
1.05
1.00
2.07
4.16
3.07
3.08
2.03
2.07
9.0 8.5 8.0 7.5 7.0 6.5 6.0 5.5 5.0 4.5 4.0 3.5 3.0 2.5 2.0 1.5 1.0 0.5 0.0 -0.5 -1.0
f1 (ppm)

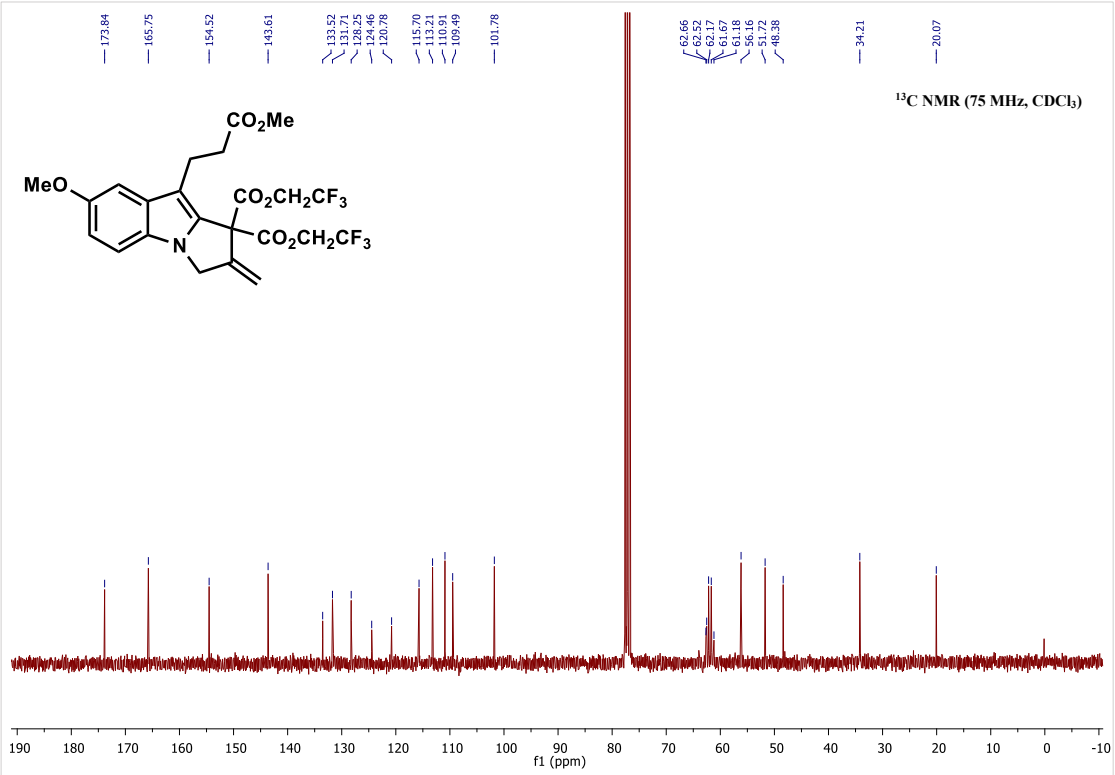
173.84
165.75
154.52
143.61
133.52
131.71
128.25
124.46
120.78
115.70
113.21
110.91
109.49
101.78
62.66
62.52
62.17
61.67
61.18
56.16
51.72
48.38
34.21
20.07
^{13}C NMR (75 MHz, CDCl$_3$)
CO2Me
MeO
CO2CH2CF3
CO2CH2CF3
N
190 180 170 160 150 140 130 120 110 100 90 80 70 60 50 40 30 20 10 0 -10
f1 (ppm)

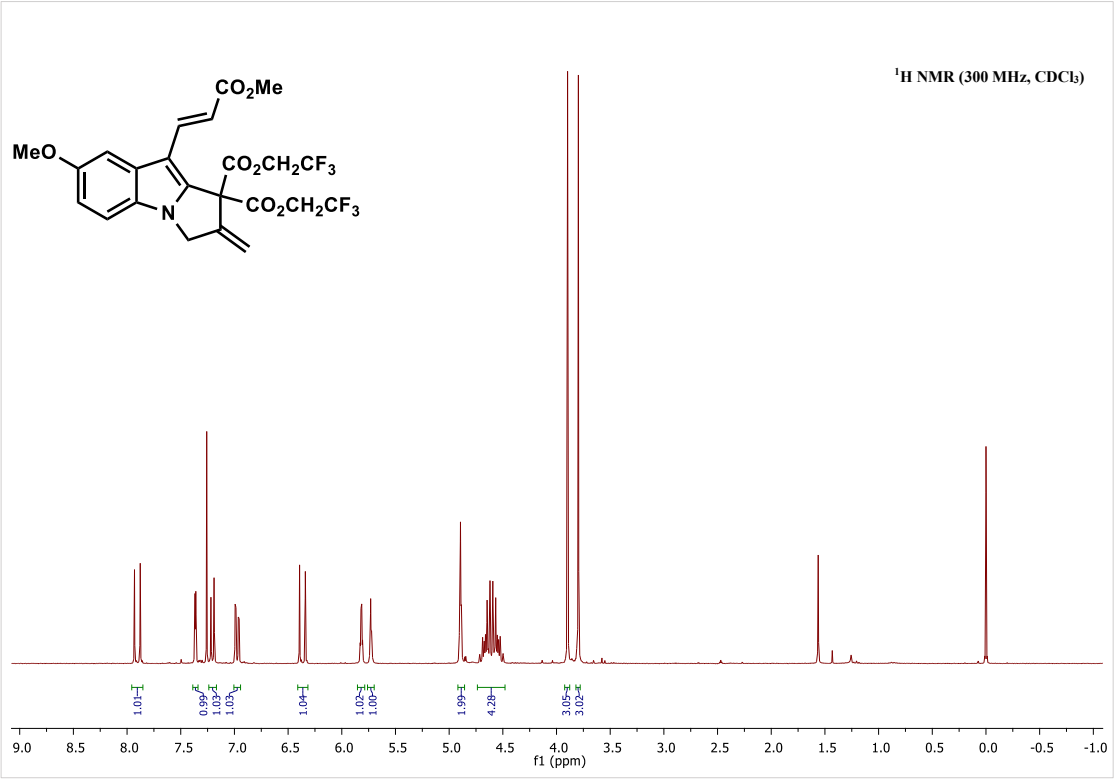
^{1}H NMR (300 MHz, CDCl$_3$)
CO$_2$Me
MeO
CO$_2$CH$_2$CF$_3$
CO$_2$CH$_2$CF$_3$
N
1.01
0.99
1.03
1.03
1.04
1.02
1.00
1.99
4.28
3.05
3.02
9.0 8.5 8.0 7.5 7.0 6.5 6.0 5.5 5.0 4.5 4.0 3.5 3.0 2.5 2.0 1.5 1.0 0.5 0.0 -0.5 -1.0
f1 (ppm)

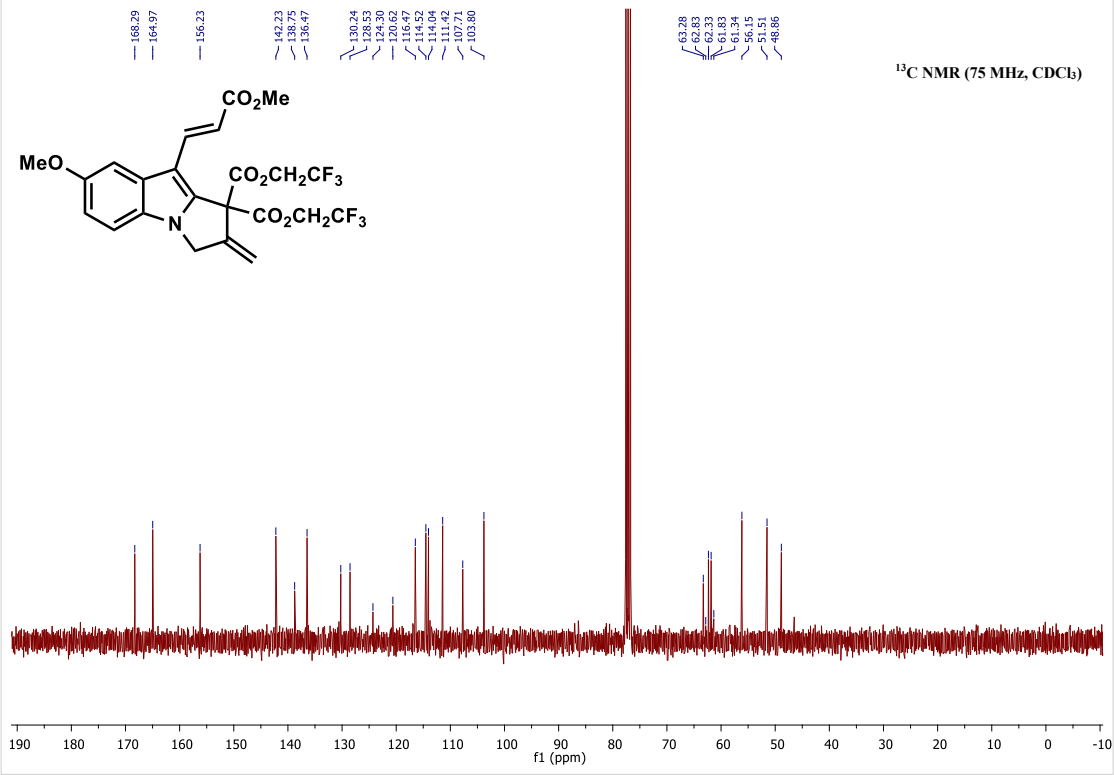
168.29
164.97
156.23
142.23
138.75
136.47
130.24
128.53
124.30
120.62
116.47
114.52
114.04
111.42
107.71
103.80
63.28
62.83
62.33
61.83
61.34
56.15
51.51
48.86
^{13}C NMR (75 MHz, CDCl$_3$)
CO$_2$Me
MeO
CO$_2$CH$_2$CF$_3$
CO$_2$CH$_2$CF$_3$
N
190 180 170 160 150 140 130 120 110 100 90 80 70 60 50 40 30 20 10 0 -10
f1 (ppm)

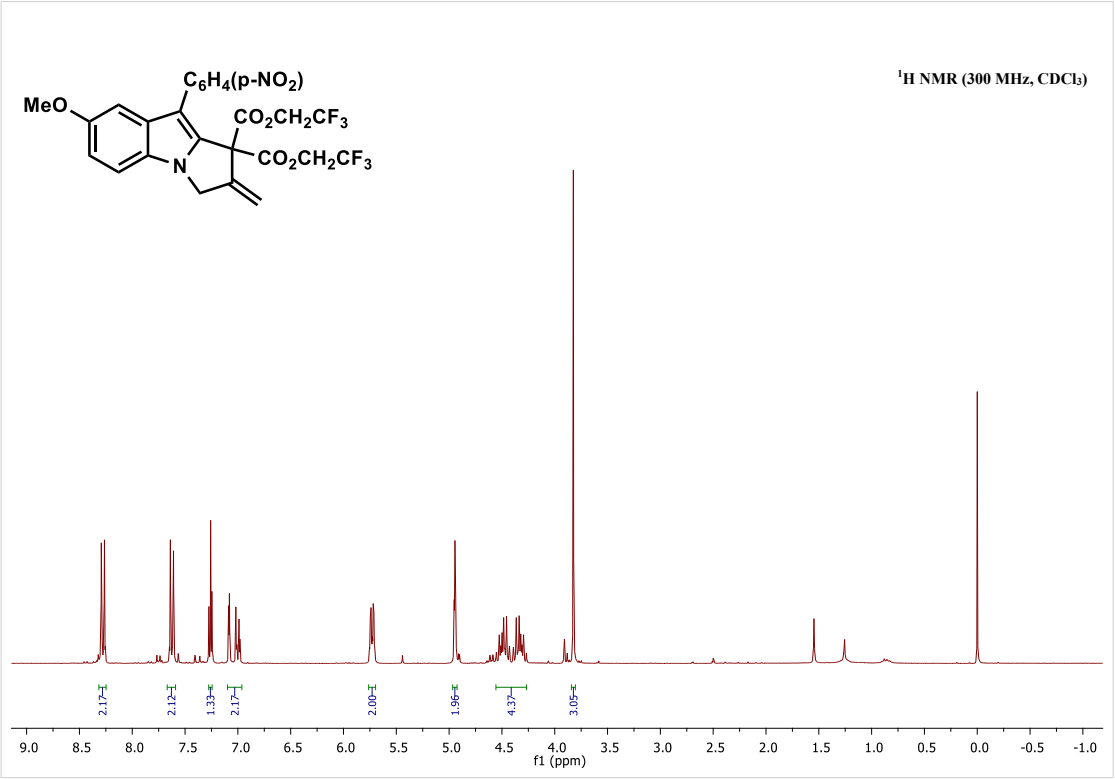
^{1}H NMR (300 MHz, CDCl$_3$)
MeO
C$_6$H$_4$(p-NO$_2$)
CO$_2$CH$_2$CF$_3$
CO$_2$CH$_2$CF$_3$
N
2.17
2.12
1.33
2.17
2.00
1.96
4.37
3.05
f1 (ppm)

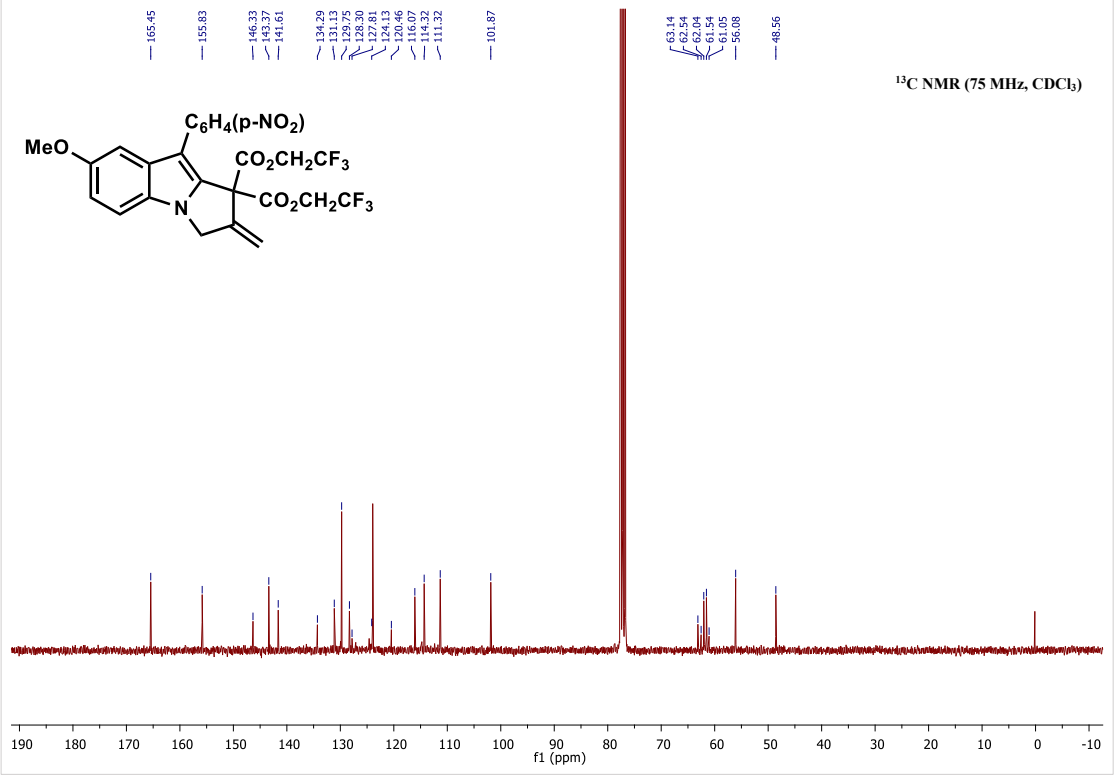
165.45
155.83
146.33
143.37
141.61
134.29
131.13
129.75
128.30
127.81
124.13
120.46
116.07
114.32
111.32
101.87
63.14
62.54
62.04
61.54
61.05
56.08
48.56
^{13}C NMR (75 MHz, CDCl$_3$)
MeO
C$_6$H$_4$(p-NO$_2$)
CO$_2$CH$_2$CF$_3$
CO$_2$CH$_2$CF$_3$
N
f1 (ppm)

Chapter 2: Chemistry of Diazo-Enones

2.1 Introduction

The development of more synthetically efficient methods for the construction of carbon–carbon (C–C) bonds has continually presented itself as a primary goal in modern synthetic organic chemistry.[1] Among the myriad of methods available to achieve such a goal, the process of directly functionalizing a C–H bond through the use of a diazocarbonyl compound, by way of a metal carbenoid intermediate, has emerged as a promising approach (Scheme 2.1).[2] While numerous advances in this area of research have been attained to control the site selectivity of the C–H functionalization (see Chapter 1), the use of diazocarbonyl compounds in this reaction manifold has traditionally focused on the generation of only one new C–C bond.

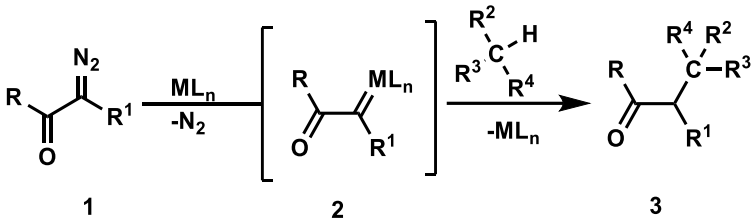

Scheme 2.1: C–H functionalizing reaction through metal carbenoid intermediate.

Efforts to improve synthetic efficiency in the construction of complex organic frameworks have inspired several new innovative applications of α-diazocarbonyl compounds. For example, leveraging the dual reactivity of diazo reagents (**4**) could be used to form two new C–C bonds in a single transformation (**7**) (Scheme 2.2A), the details of which have been highlighted in Chapter 1.[3] Alternatively, there has been a recent interest in the pursuit of designer diazocarbonyl compounds that contain multiple sites of reactivity, in addition to the diazo functional group.[4] In principle, these types of diazo reagents (**8**) could be used to construct multiple new sigma bonds (**9**) in as little as one step and thus, provide a platform to generate molecular complexity in an efficient fashion (**10**) (Scheme 2.2B).[3,5]

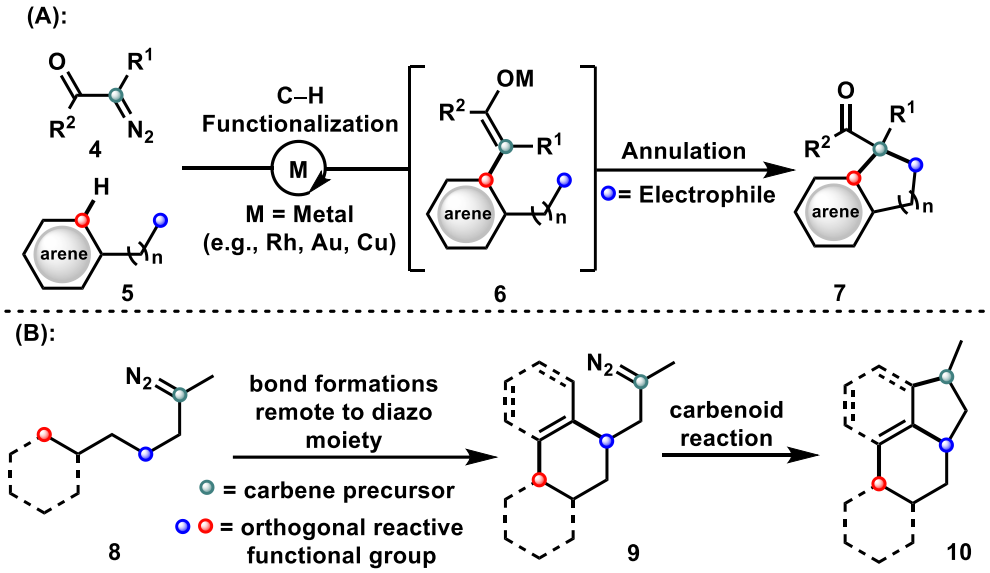

Scheme 2.2: (A) Tandem C–H functionalization/annulation reaction manifold. **(B)** Potential utility of diazo compounds with multiple sites of reactivity.

2.2 *α,β*-Unsaturated Diazoketones

"*α,β*-Unsaturated diazoketones" commonly referred to as "diazo-enones", represent one class of promising multi-functionalized diazo compounds (Figure 2.1). Characteristically, these multifunctional synthons possess three distinct reactive sites, a diazo-functional group, a ketone, and a C=C double bond. As reviewed in Chapter 1, upon proper activation of the diazo group, loss of dinitrogen can generate a carbene that can then participate in a variety of interesting transformations, including Wolff rearrangements, cyclizations, cyclopropanations, and sigma bond insertion reactions.[6] The ketone moiety in compound **11** (Figure 2.1) plays a dual role; firstly, due to the electron withdrawing nature of carbonyl, it leads to the stabilization of the diazo compound. Secondly, it performs as a primary site for chemical reactions by acting as an electrophilic center. The conjugated vinyl site of **11** can serve as an electrophile in Michael-addition type reactions or as a reactive dienophile in cycloaddition reactions such as a Diels-Alder reaction.

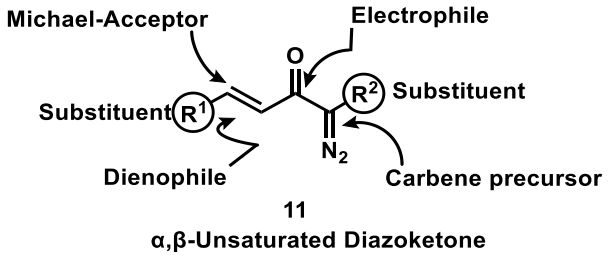

Figure 2.1: Active sites of *α, β*-unsaturated diazoketone substrate.

Diazo-enones are classified into three categories as ″acceptor‟, ″acceptor/acceptor‟, and ″acceptor/donor‟, depending on the nature of the non-enone substituent on the α-position of the diazo carbon. The result and efficiency of a reaction involving a diazo compound depend on the nature of the functional groups (acceptors or donors) (Figure 2.2) on both the vinyl site and the diazo carbon of the substrate. Acceptor diazo-enones (**12**) are the widely known class of unsaturated diazo carbonyl compounds, while the acceptor/acceptor class is moderately known (**13**).[22] The electron-withdrawing substituents of **13** enhance the electrophilicity of a diazo compound, which leads to an increase in the stability of these building blocks. The third class, acceptor/donor diazo-enones (**14**), is the least explored despite the capacity of their donor substituents to stabilize carbenoid intermediates through resonance. The functional groups substituted at the β-position of the enone (R, Figure 2.2) can be utilized to enhance the reactivity of the electron deficient alkene or the diazo carbon.

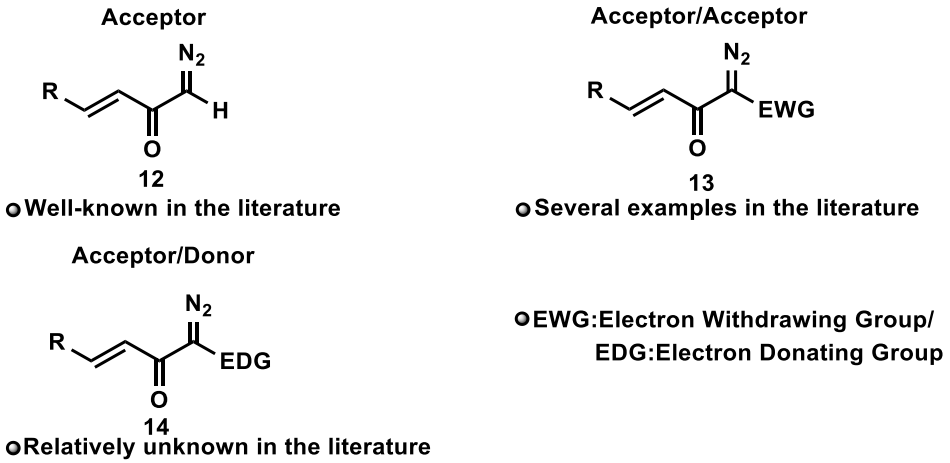

Figure 2.2: Different classes of diazo-enones.

2.3 Notable Synthetic Approaches to *α,β*-Unsaturated Diazoketones

2.3.1 Primary Reported Methods for Acceptor Diazo-enone Synthesis

One of the first attempts to synthesize an *α,β*-unsaturated diazoketone was reported in 1936 by Grundmann.[7] In the preliminary report, Grundmann treated unsaturated acid chloride **15** with diazomethane (**16**) in an attempt to install the diazo functionality in a similar fashion as conducted by Arndt-Eistert in the synthesis of other types of *α*-diazoketones (Scheme 2.3).[8] However, the expected product **17** was not isolated from these experiments, and instead compound **18**, which is the result of a two-step diazo formation and intermolecular cycloaddition process, was formed. It is unclear whether the 1,3-dipolar cycloaddition of the diazomethane and the alkene group of **15** occurs first or if the addition of diazo to the acyl group serves as the initial step.

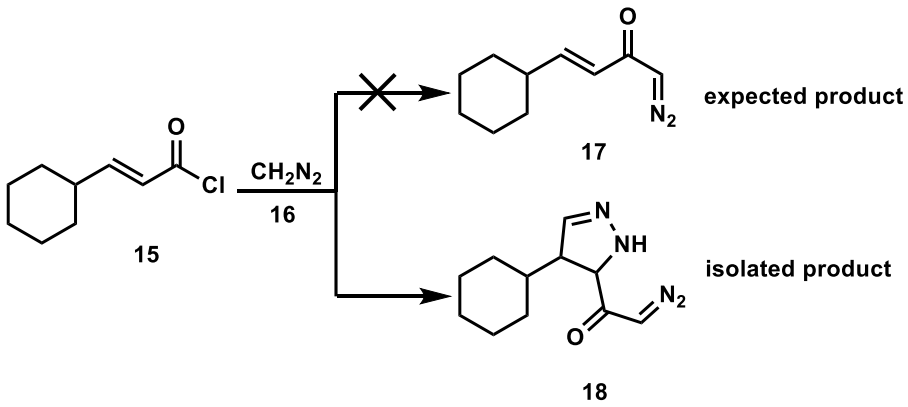

Scheme 2.3: Formation of pyrazoline ring via Arndt-Eistert type reaction.

Several years later, in 1954, Wotiz and Buco[9] studied the same transformation with similar unsaturated acid chloride **19** (Scheme 2.4). In their work it was noted that although the pyrazoline ring **20** was formed as the major product, via the cycloaddition reaction with diazomethane, they also isolated a small quantity of the desired l-diazo-4-phenyl-3-butenone diazoketone **21** (Scheme 2.4). It was mentioned that slightly higher yields of the **21** could be obtained by increasing the dilution of the reaction in ether, however in all cases, the **21** was isolated as a minor product compared to **20**. In the following year, Moore[10] showed it was possible to isolate diazo-enones in appreciable yields by placing a substituent on the alpha position of the acid chloride **19** (R = CH_3). By making this small structural change, the authors could successfully isolate the diazo-enone substrate **22** in 67% yield, through a slow addition of a solution of α-substituted enone **19** to diazomethane in ether at 10 °C (Scheme 2.4). Subsequently,

they showed that diazomethyl α-methylstyryl ketone **22** could be converted to the pyrazoline **23** in 55% yield upon prolonged treatment with diazomethane. This result potentially indicates that acyl addition occurs first and is followed by a cycloaddition reaction in the production of the pyrazoline isolated in the previous experiments. While this approach was moderately successful with acid chloride **19**, the scope of the reaction was limited.

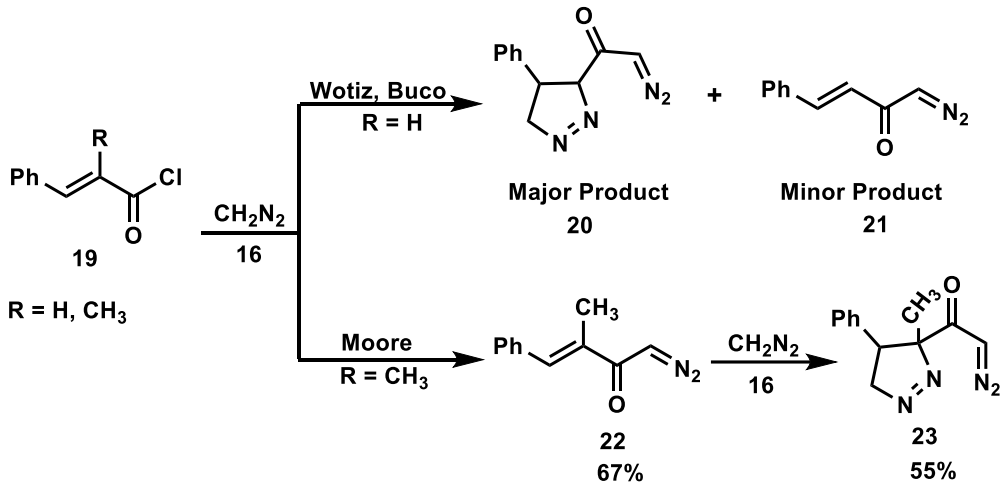

Scheme 2.4: Synthesis of α,β-unsaturated diazoketone by Wotiz and Moore.

To combat the undesirable reaction between the enone and diazomethane when synthesizing α,β-unsaturated diazoketone for the corresponding acid chloride, Chapman and Rosenquist[11] developed a method in which the double bond is installed after the formation of diazoketone (Scheme 2.5). In a two-step process bromo acid **24** was converted to alpha diazoketone **25** by first generation of the acid chloride followed by treatment with diazomethane. Subsequent elimination reaction of **25** provided diazo enones **26** and **27** in 32% and 77% respectively. Notably this method showcases the stability of diazomethyl ketones (**25**) to the basic conditions required to generate the double bond.

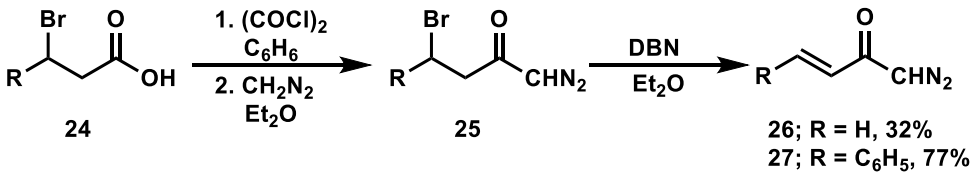

Scheme 2.5: Synthesis of α,β-unsaturated diazoketone by Chapman.

A significant advancement in the efficient construction of *α,β*-unsaturated diazocarbonlys was achieved after Regitz published a novel diazo transfer method between 1,3-dicarbonyl compounds and sulfonyl azides.[12] In 1970, Regitz expanded this method to synthesize unsaturated diazoketones starting from *α,β*-unsaturated methyl ketone **28** and converting it into the corresponding 1,3-dicarbonyl compound **29** before the diazo transfer step (Scheme 2.**6**). Treatment of **29** with *p*-toluenesulfonyl azide (TsN_3) readily formed a triazine intermediate (**30**), which underwent loss of *p*-toluenesulfonylamide followed by concomitant deformylation of **31** to provide **32** in low yield. A few years later, Gupta[13] improved this transformation by employing diethyl oxalate $(CO_2C_2H_5)_2$ in the place of ethyl formate, which afforded the unsaturated diazoketone **32** with improved yield from 13% in the Regitz method to 75%.

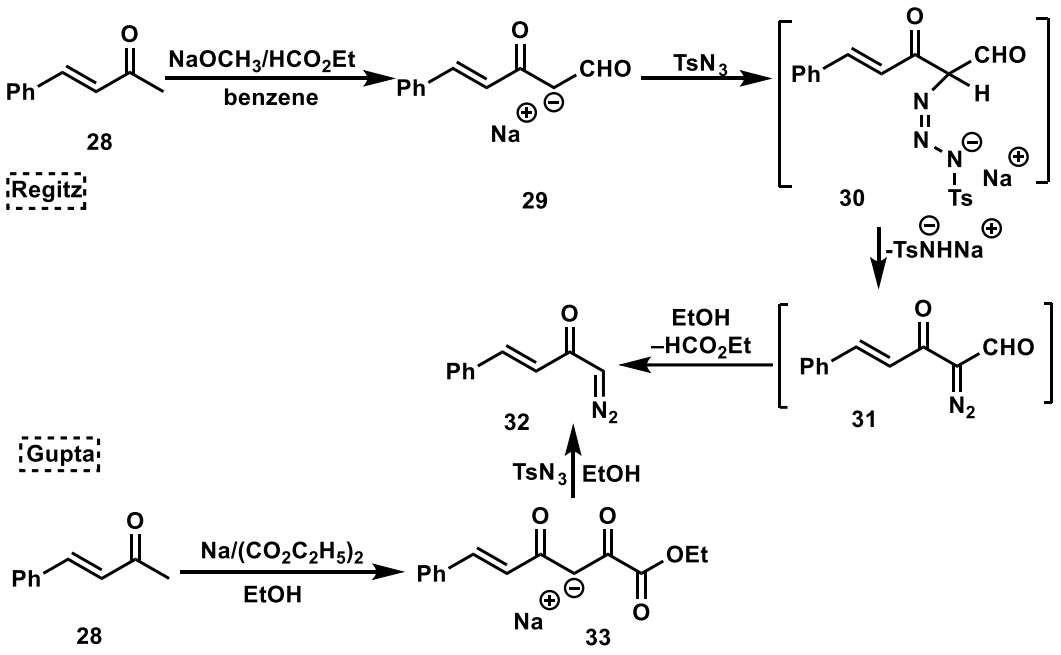

Scheme 2.6: Regitz's and Gupta's methodologies for diazo transfer procedure.

2.3.2 Recent Synthetic Strategies in Construction of Acceptor Diazo-Enones

Building on the precedent set by Regitz and Gupta, in 1990 Danheiser[14] developed a general and successful method to convert methyl ketones, including *α,β*-unsaturated methyl ketones, to the corresponding *α*-diazocarbonly compounds by first treating the lithium enolate of **34** with trifluoroethyl trifluoroacetate (TFEA) (Scheme 2.7). The resulting *α*-trifluoroacetyl ketone **35** was then converted directly to

the corresponding diazo product **36** upon reaction with methanesulfonyl azide. This protocol effectively constructs various diazo ketones, including the formation of fourteen unsaturated diazoketones derivatives in modest to high overall yields.

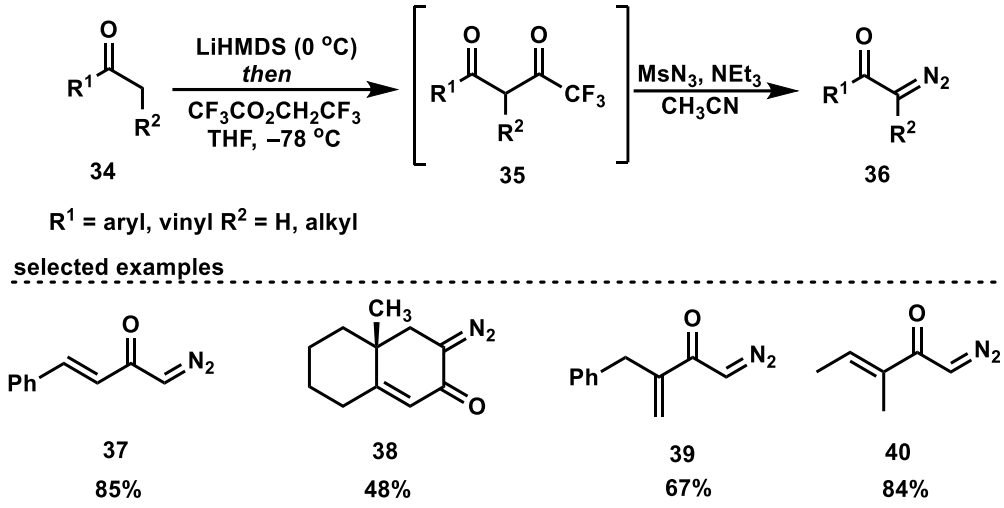

Scheme 2.7: Danheiser methodology for the synthesis of unsaturated diazoketones.

In 2000, Aller[15] showed that acyl chlorides could be utilized as effective starting materials for the construction of diazo-enones by replacing diazomethane with *N*-isocyanotriphenyliminophosphorane **41** (Scheme 2.8). This change of reagent not only avoided the unwanted cycloaddition products observed in previous research (Schemes 2.3 and 2.4) but also provided a general method to access various *α*-diazocarbonyl compounds from acyl chlorides through a process that avoids the limitation associated with diazomethane (e.g., toxicity and operational inconvenience that requires specially designed apparatus). The two-step process is initiated by acylation of **41** with an acid chloride (**42**) followed by hydrolysis to provide the *α*-ketohydrazidoyl chloride intermediate **43**. The intermediate **43** is then treated with triethylamine and *p*-toluenesulfonyl chloride at room temperature to deliver the corresponding *α*-diazocarbonyl **44** through an *N*-tosyl-*α*-ketohydrazidoyl chloride intermediate. Direct conversion of acyl chlorides **42** into *α*-diazoketones **44** can be achieved in similar yields by a one-flask reaction process without the isolation of the intermediate *α*-ketochlorides **43**.

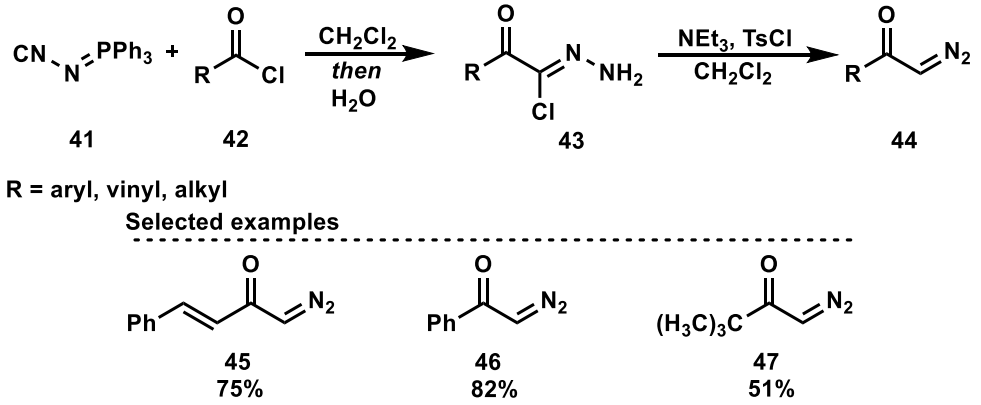

Scheme 2.8: Conversion of acyl chlorides into α-diazoketones with **41**.

Between 2010-2013, the Burtoloso[16,17] research group reported the synthesis of the various *α,β*-unsaturated diazoketones based on a Horner-Wadsworth-Emmons olefination[18] strategy utilizing novel diazophosphonate reagents **51** and **52** (Scheme 2.9). Both diazophosphonates were prepared from the respective phosphorylacetic acids **49** and **50**, via first conversion to the corresponding acid chlorides, followed by treatment with diazomethane. Although only modest yields of **51** and **52** were observed by this route, the authors have indicated that substantial quantities of both reagents (>1 mmol) can be prepared and the regents themselves are bench stable.

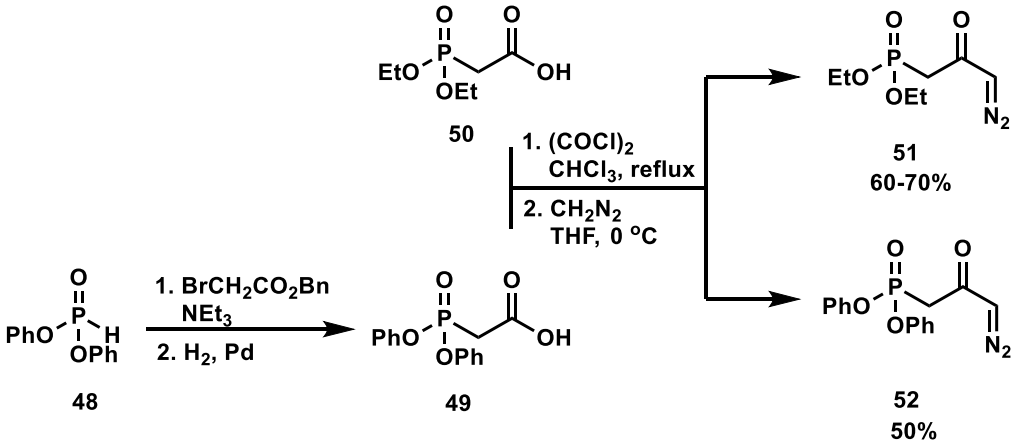

Scheme 2.9: Preparation of diazo-substituted Horner-Wadsworth-Emmons reagents.

Depending on the class of phosphonate reagent employed (**51** vs **52**) the authors showed that the stereochemistry of the olefination could be controlled providing access to a series of diazo-enones with *E*- and *Z*- olefin geometries (Scheme 2.10). Treating **51**

with sodium hydride, followed by addition of aldehyde, led to diazo-enones with complete selectivity for the formation of the *E* isomer. In contrast, when **52** is utilized under similar conditions, with potassium *t*-butoxide, the *Z* alkene isomers are furnished as the major stereoisomers in good yields and modest selectivity. While complete stereocontrol in the formation of the *Z* isomers has yet to be achieved, this approach marks one of the only methods currently available to generate these diazo-enone isomers.[19]

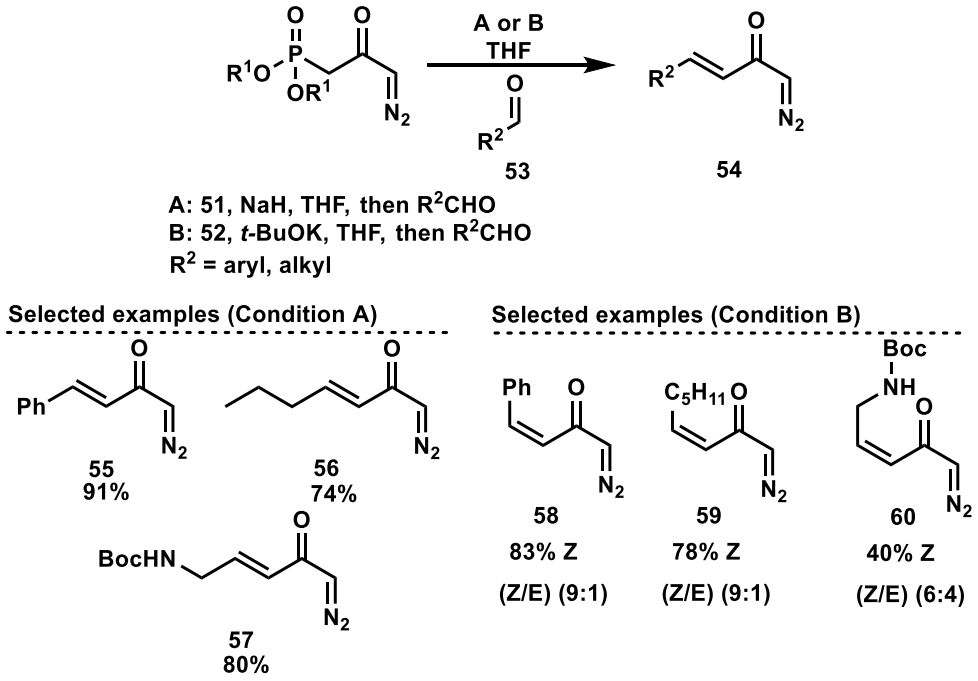

Scheme 2.10: Synthesis of *E*- and *Z*-diazoketones by Horner-Wadsworth-Emmons methodology.

2.3.3. Reported Methodologies for Acceptor/Acceptor Diazo-enone Synthesis

Diazo-enones bearing an additional electron withdrawing group on the diazo carbon (acceptor/acceptor) were less investigated by the pioneers of diazo chemistry. In 1983 Taylor successfully synthesized a series of novel diazo-enones (**66**) by utilization a dipotassium salt of *γ*,*δ*-unsaturated-*β*-ketoesters **62** in a condensation reaction with benzophenones **63** (Scheme 2.11).[20] Conversion of the unsaturated-*β*-ketoesters to diazoacetoacetate enones (DAAE) was fulfilled by treatment with *p*-(*n*-dodecyl)benzenesulfonyl azide **65** in 67-94% yield.

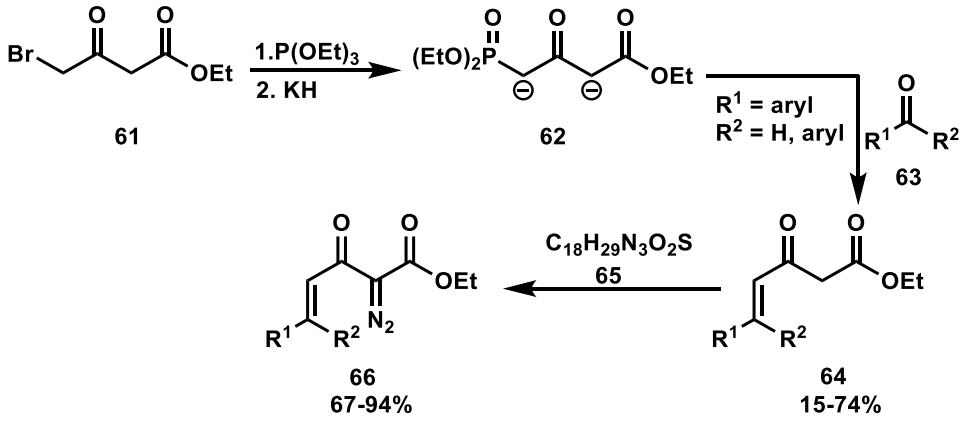

Scheme 2.11: Synthesis of acceptor/acceptor **66** via Horner-Wadsworth-Emmons.

In 1990 Wenkert [21] illustrated the formation of an acceptor/acceptor type of diazo-enone reagent (**69**), by commencing from carboxylic acid **67** (Scheme 2.12). Treatment of the sodium salt of acid **67** with oxalyl chloride resulted in acid chloride **68** (Scheme 2.12). Then the acyl chloride **68** was subjected to a reaction with ethyl diazoacetate (EDA), which produced the desired diazo-enone, **69**, in 46% yield. While this transformation is suitable with **68**, the extension of this sequence to a broad substrate scope is limited to the known reaction of unsaturated acyl chloride and diazomethane to produce acceptor type diazo-enones.

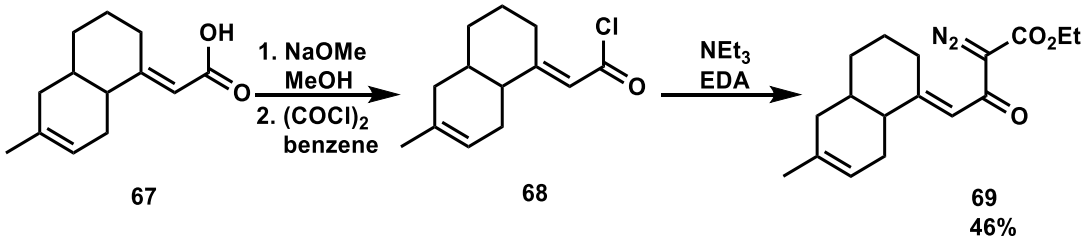

Scheme 2.12: *α,β*-unsaturated diazoketone construction from carboxylic acids.

One of the most recent methods to synthesize diazoacetoacetate enones (DAAEs) in an efficient one-pot protocol was reported by Doyle in 2013. By this methodology, the authors have described an olefination reaction between aromatic aldehydes and Wittig reagent **70** to provide the requisite enones. The in-situ generation of enone **72** is followed by a diazo transfer step by employing *p*-acetamidobenzenesulfonyl azide (*p*-ABSA) to afford DAAE **73** as mixtures (1:1 to 3:1) of (*E*) and (*Z*)-isomers. To increase the selectivity of the olefination it was noted

that isomerization of the in-situ generated *Z*-enones to the more thermodynamically favored *E*-enones could be promoted by the addition of DABCO in catalytic amounts which ultimately delivered (*E*)-diazoacetoacetate enones **73** as single isomers in 64-75% yield (Scheme 2.13).[22]

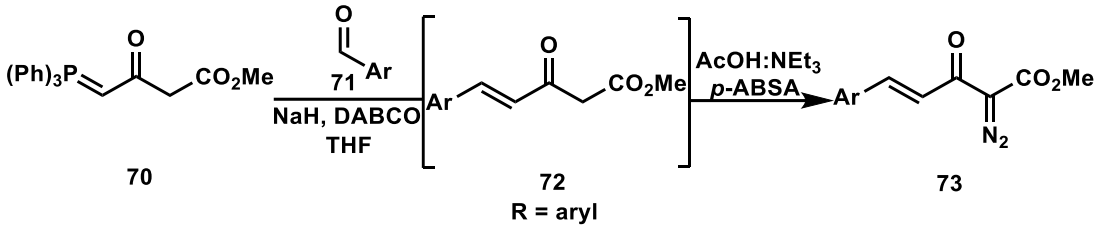

Scheme 2.13: Doyle's methodology in the synthesis of diazoacetoacetate enones.

2.4 Synthetic application of *α,β*-unsaturated diazoketones

2.4.1 General applications

As described above, several methodologies have been explored for the synthesis of the multifunctional diazo-enones (presence of a diazo group, a carbonyl function, and a double bond in the same molecule) in the past decades. Diazo-enones are interesting synthetic building blocks, in which reactions can take place selectively at the *α,β*-unsaturated double bond or the diazo moiety (or both) to generate new sigma bonds. The synthetic community gained interest in these types of diazo compounds over the last few decades because the multiple sites of reactivity contained within these molecules can be leveraged to form dense structural complexity in a single transformation.

2.4.2 Preliminary Utilizations of *a,β*-Unsaturated Diazoketones in Organic Synthesis

In 1981 Regitz[23] studied one of the first synthetic applications of *a,β*-unsaturated diazoketones in a cycloaddition reaction with 1,2,4-triazolindinones. In this seminal work, the authors reported the use of novel conjugated diazo-enone **74**, which selectively acts as the diene, to provide bicyclic heterocycles **76** in good yield (Scheme 2.14). This study presented only one example (**76**) however it displays a chemoselective process in which a reaction occurs at the conjugated double bond position of **74**, without loss of the diazo moiety.

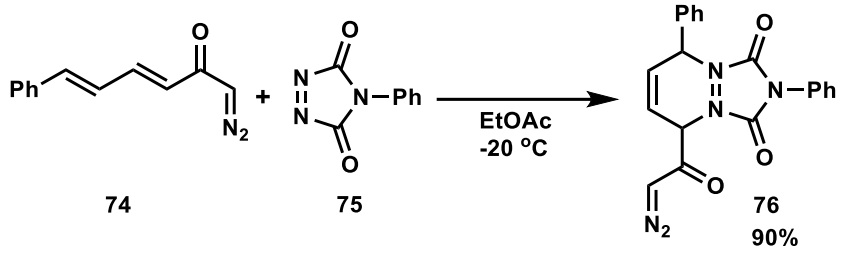

Scheme 2.14: First synthetic application of *α*,*β*-unsaturated diazoketones.

In contrast to Regitz's work, which explored the double bond reactivity of these compounds, Wenkert and co-workers studied the utility of the diazo moiety. They illustrated the synthesis of cyclic compounds by studying the decomposition behavior of diazoketones derived from *α*,*β*-unsaturated acids (Scheme 2.15).[21] The authors described a Rh(II)-catalyzed intramolecular C–H insertion reaction of *β*,*β*-dialkylated *α*,*β*-unsaturated diazoketones **78**, compounds that could be prepared from *α*,*β*-unsaturated acids **77**. The cyclopentenones **79** are furnished in a range of 47-65% yield. These two pioneering projects demonstrated that chemoselectivity in the reaction of diazo enones was attainable, thereby igniting further advancements and future research in this field.

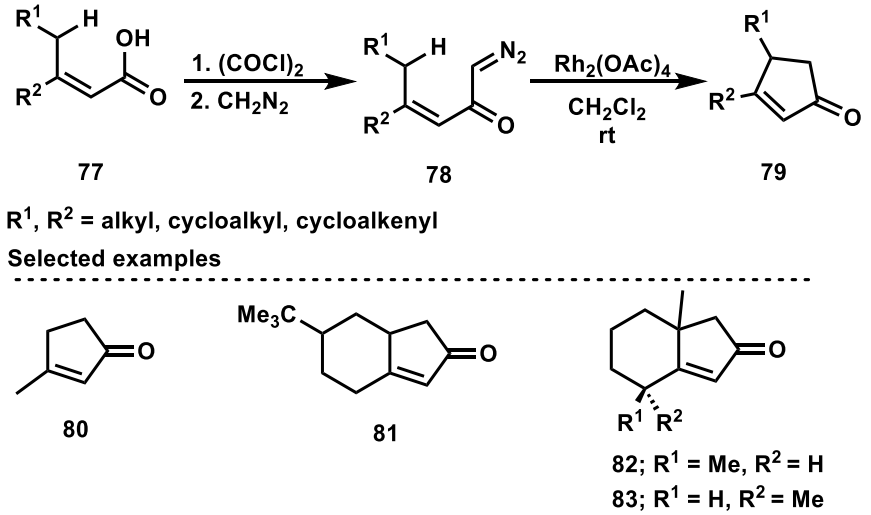

Scheme 2.15: Cyclopentenone synthesis via palladium-catalyzed C–H insertion reaction.

2.5 Reactions Initiated at the Diazo Moiety of the Diazo-Enones as a Driving Force in Organic Transformations

In a significant progression in the field of the diazo-enones chemistry Danheiser and co-workers developed a strategy for the synthesis of highly substituted polycyclic aromatic and heteroaromatic compounds through a direct benzannulation reaction in 1990.[24] A variety of both vinyl and aryl α-diazo ketones **84** have been employed in this reaction along with several activated (heterosubstituted) or non-activated acetylenes (Scheme 2.16). Mechanistically, the reaction is initiated by decomposition of the diazo group under photo-irradiation conditions (low-pressure mercury lamp), which induces a Wolff rearrangement to produce a vinylketene **86**. The vinylketene can then be intercepted with acetylene **85** in a [2 + 2] cycloaddition to provide cyclobutenone **87**. Upon an electrocyclic cleavage, the dienylketene **88** formed, undergoes 6π-electrocyclization to afford a 2,4-cyclohexadienone, which following tautomerization furnishes the aromatic product **89** in 31-95% yield.

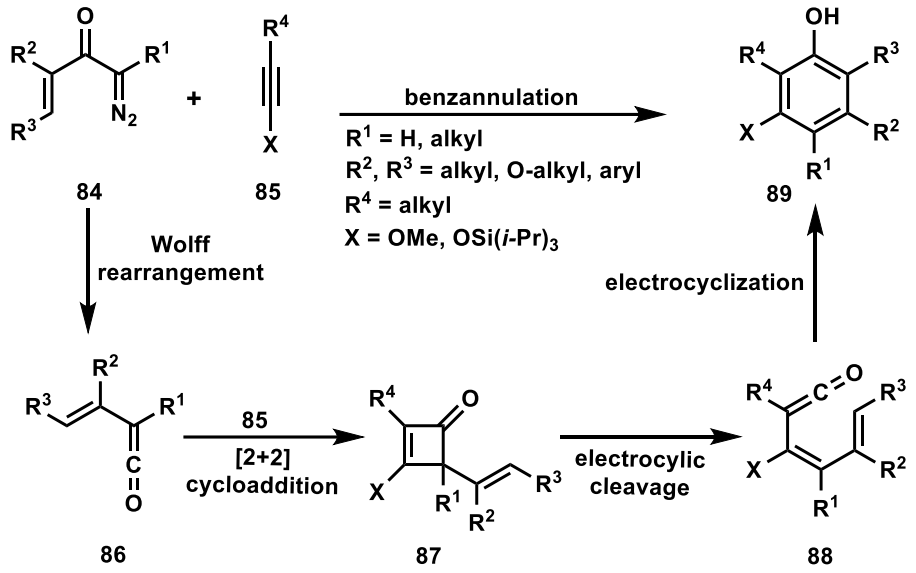

Scheme 2.16: Benzannulation reaction through a Wolff rearrangement intermediate.

A few years later, the Brückner group used a silver benzoate-induced Wolff rearrangement strategy to synthesize β,γ-unsaturated methyl esters from diazo-enone **91** (Scheme 2.17).[25] By exploiting α,β-unsaturated acid bromides rather than the chloride analogous, the α,β-dialkyl α,β-unsaturated are generated successfully (avoiding pyrazoline formation through a 1,3-dipolar cycloaddition). Upon a subsequent Wolff

rearrangement employing AgOBz and NEt_3 in MeOH, the *α,β*-unsaturated diazoketones **91** were converted into the desired *β,γ*-unsaturated methyl esters **92**. The *β,γ*-unsaturated methyl esters were then utilized as intermediates for preparation of substituted *γ*-butyrolactones (**94-95)** via Sharpless asymmetric dihydroxylation[26] and spontaneous cyclization.

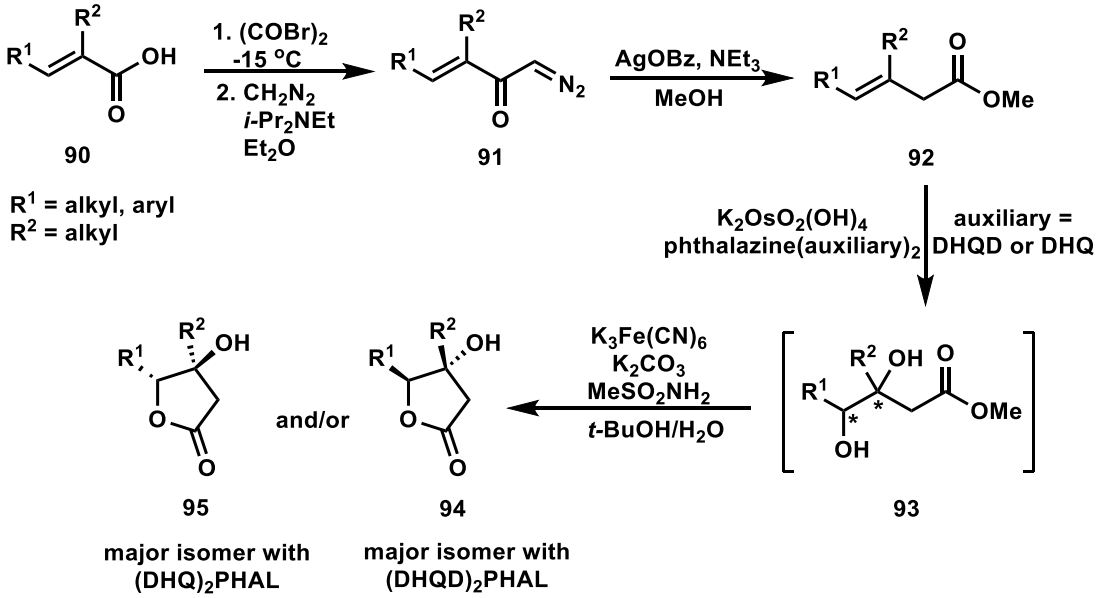

Scheme 2.17: Lactonization reaction of disubstituted *α,β*-unsaturated ketones.

Further expansions of the chemoselective reactivity of diazo-enones in Wolff-type rearrangements were described by Burtoloso in 2012 in the construction of nitrogen-heterocycles. The investigation involved the utilization of unsaturated diazoketone **98** for the total synthesis of indolizidine alkaloids.[27] *N*-Cbz-prolinal (Cbz: carbobenzyloxy) (**97**) was treated with 3-diazo-2-oxopropylphosphonate **96** to provide diazo enone **98** (Scheme 2.18). *β,γ*-unsaturated ester **99** was furnished from diazoketone **98** through a photochemical Wolff rearrangement in 97% yield. The sequence was followed by one-pot removal of Cbz group in the presence of H_2/Pd and NEt_3, which upon alkene reduction and lactamization, afforded the requisite **100** in a 92% yield. The addition of propylmagnesium bromide to lactam **100**, followed by AcOH/$NaBH_4$, delivered indolizidine (–)-167B as a single diastereomer **102** in a 42% yield. They have also shown that intermediate **100** could serve as a precursor for

synthesis of the natural alkaloid coniceine **103** through reduction of **100**,[28] and (–)-indolizidine 209D (**104**)[29] through reductive alkylation of **100**.

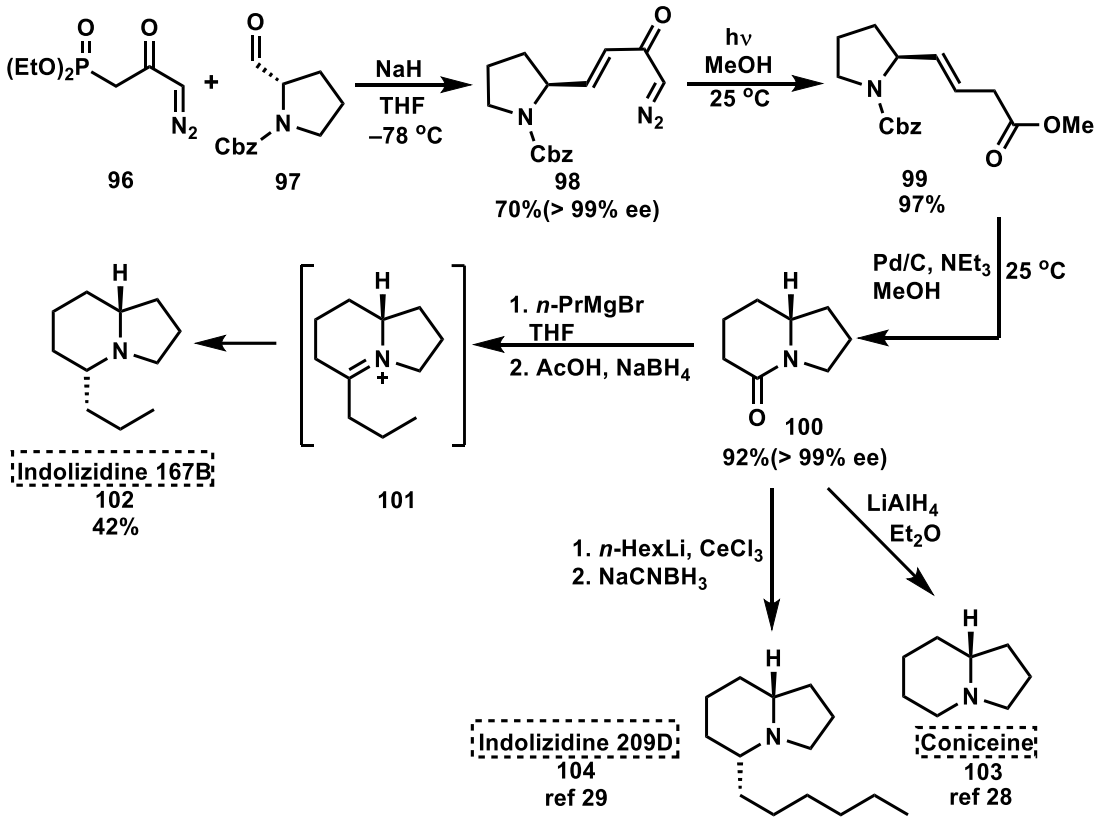

Scheme 2.18: Total synthesis of indolizidine scaffolds via Wolff rearrangement.

Another extension of the Wolff rearrangement strategy with diazo-enones was reported by Burtoloso in 2014 in the synthesis of bioprotective agent JP4-039 (**111**) from *α,β*-unsaturated enone **106** (Scheme 2.19B).[30] JP4-039 is a mitochondria-target nitroxide which has been demonstrated to be a potent small-molecule radiation mitigator in X-ray tests, and is safe over a wide dose range.[31] Exploiting the ability to generate *β,γ*-unsaturated esters in the presence of alcohols via a Wolff rearrangement, the Burtoloso group expanded this method to the direct synthesis of *β,γ*-unsaturated amides **107** (Scheme 2.19A). Using this strategy, they have submitted aliphatic, aryl, acyclic-amino, and cyclicamino diazoketones to the photochemical Wolff rearrangement in the presence of different amines by utilizing an Osram 150 Xenon arc lamp to furnish a series of *β,γ*-unsaturated amides. By employing *N*-Boc-L-leucinal **108** as the aldehyde and subjecting it to their Horner−Wadsworth−Emmons olefination reaction condition, the *α,β*-unsaturated diazoketone **109** was afforded in 83% yield. UV

irradiation of diazoketone **109** in the presence of 4-amino-TEMPO **110** in CH_3CN delivered JP4-039 (**111**) in 65% yield (Scheme 2.19B).

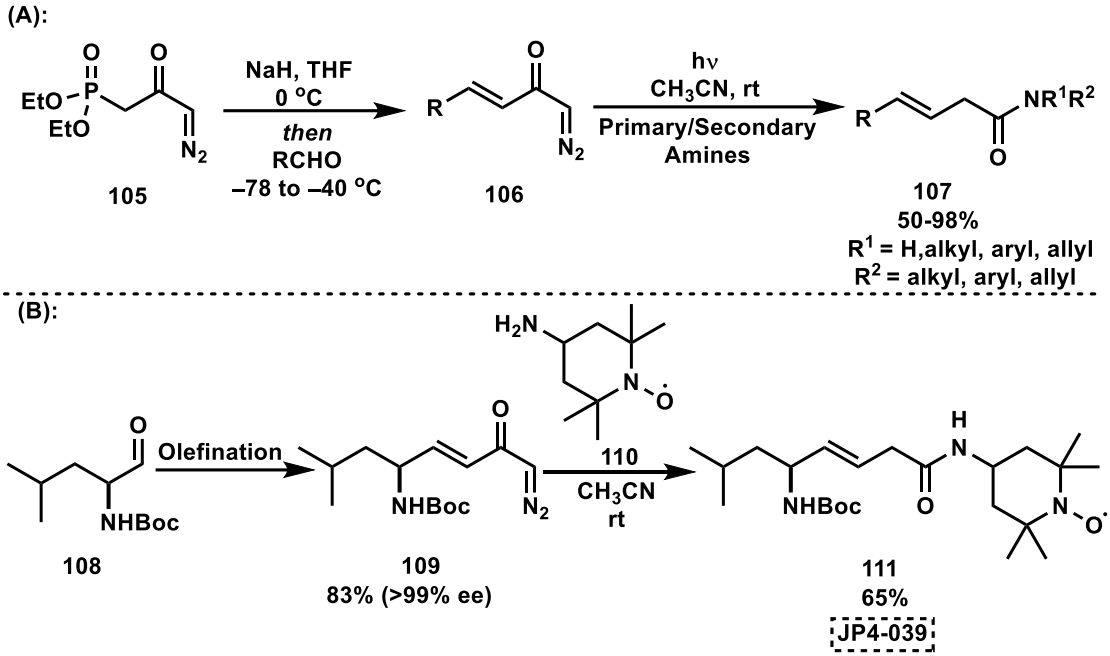

Scheme 2.19: (A) Two-step synthesis of several *β*,*γ* -unsaturated amides from aldehydes. **(B)** Synthesis of JP4-039 from *N*-Boc-L-leucinal.

2.6 Reactions Initiated at the Enone Moiety of the Diazo Enones as a Driving Force in Organic Transformations

In 1989 Danishefsky described a selective Michael addition reaction between secondary thiolactams **113** as the nucleophile and diazomethylvinylketone **112** as the Michael acceptor (Scheme 2.20).[32] Notably, both **112** and **114**, containing reactive diazo functionality, proved to be stable under the basic reaction conditions required to promote the Michael addition. **114** was then treated with a Rh(II) catalyst to promote an annulation type process followed by a reduction to form dihydro-*γ*-pyridones **115**. This approach has been applied to the synthesis of iso-A58365A (**116**), the *γ*-pyridone analog of the angiotensin converting enzyme (ACE) inhibitor, in a 35% overall yield by commencing from dihydro-*γ*-pyridones **115** through an eight-step synthetic sequence.

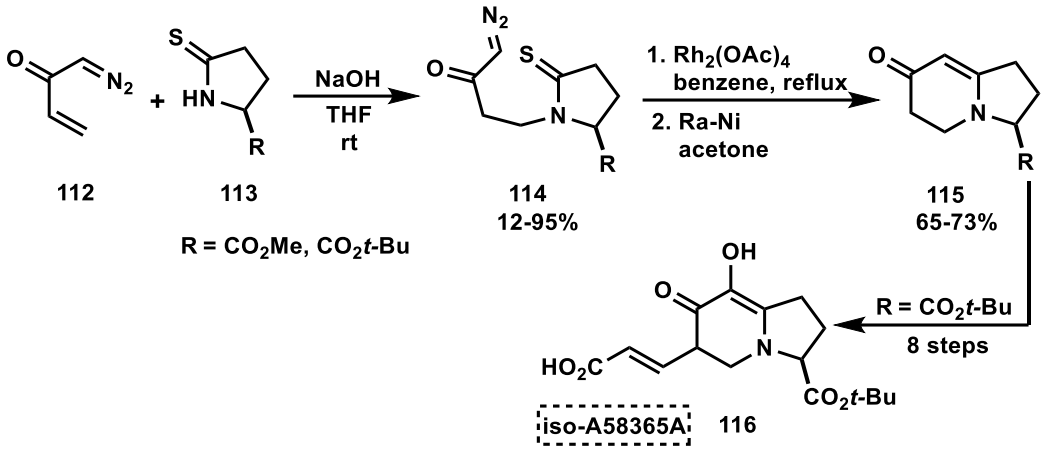

Scheme 2.20: Aza-Robinson annulation of thiolactams followed by synthesis of Iso-A58365A.

Afterwards, other researchers developed methods for the construction of cyclic amines, by employing unsaturated diazoketones as Michael acceptors with amine nucleophiles.[33] Notably, in 2011, the Burtoloso group[16] described the two-step conversion of *α,β*-unsaturated diazo-enone **117** to the substituted pyrrolidine **119**. The synthetic route has been shown in Scheme 2.21 and illustrates the Michael addition reaction between benzyl amine and the diazo-enone **117**, which followed by a rhodium catalyzed N–H insertion, resulted in cyclized products. By this method, a vast library of pyrrolidines can be synthesized by varying the amine and the enone starting materials.

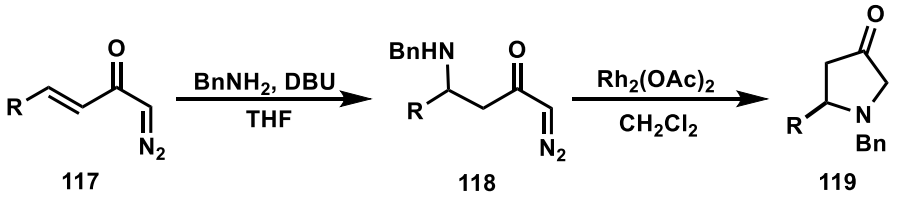

Scheme 2.21: Construction of pyrrolidinones via N–H insertion of *γ*-amino diazoketones.

A few years later, in 2018, Burtoloso described an intramolecular Michael addition pathway from *N*-terminal unsaturated diazo-ketones (**122**) to afford *N*-heterocycle cores including indolizidines and pyrrolizidines in a one-pot transformation (Scheme 2.22).[34] Compound **122** was prepared from different *N*-protected amino-alcohols (**120**), following oxidation of the hydroxyl group to the aldehyde and finally by a Horner-Wadsworth-Emmons olefination (Scheme 2.22A).

With **122** in hand a unique one-pot transformation involving three sequential steps, an *N*-deprotection, an intramolecular aza-Michael reaction, followed by a photochemical Wolff rearrangement in the presence of K_2CO_3, was developed to access a series of substituted bicyclic alkaloids (**125-127**, Scheme 2.22B). The best results were achieved for the formation of indolizidine (n = 2, **126**) and pyrrolizidine (n = 1, **125**) cores. This is in accordance with the difficulty in the formation of four and seven membered rings ((n-1) and n = 3, **127**), 0 and 15%, respectively.

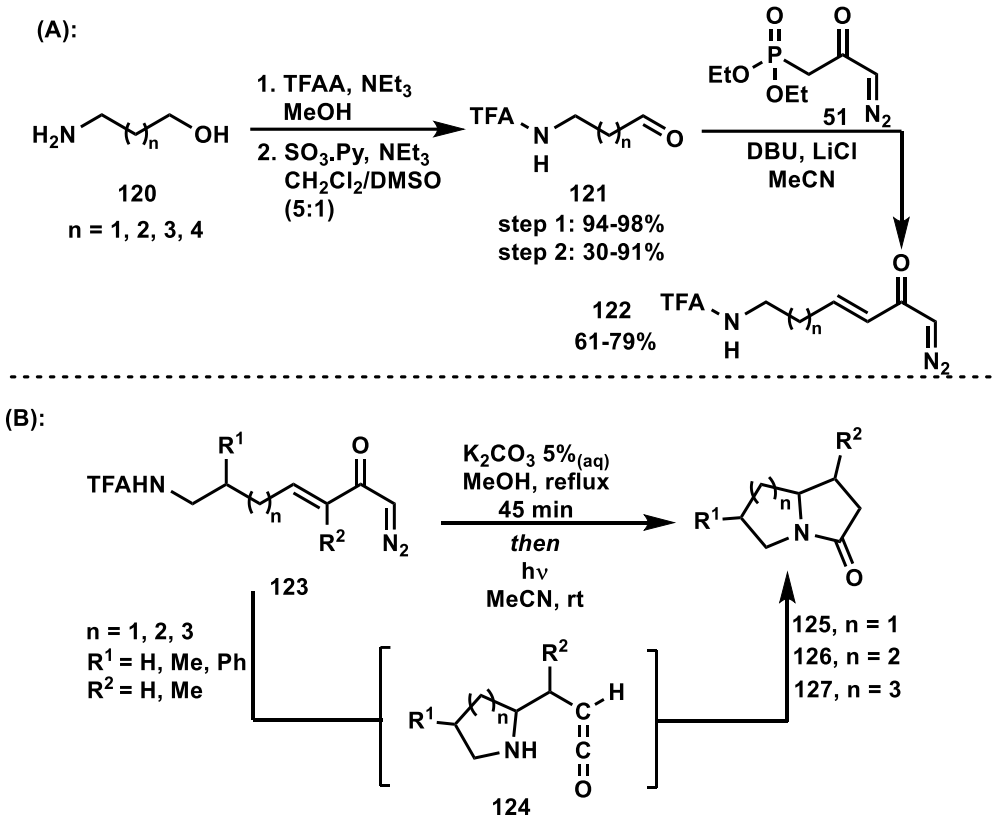

Scheme 2.22: (A) Synthesis of *N*-terminal *α,β*-unsaturated diazoketones.
(B) Synthesis of substituted bicyclic *N*-heterocycles.

Recently, in 2022, a stereoselective sulfa-Michael addition to *α,β*-unsaturated diazocarbonyl **129** has been reported by Burtoloso group using alkyl and aryl thiols (Scheme 2.23).[35] They have employed a quinine-derived squaramide catalyst **131** to promote C–S bond formation to the alkene moiety of the diazo **129** to access enantioenriched diazo compounds **130**. Results have revealed that strong electron withdrawing (NO_2) and electron donating (NH_2) groups in the para position of the

thiophenol decreased the enantioselectivity of the reaction (**132-134**). However, the electron donor or electron withdrawing groups substituted in the para position of the benzyl thiols did not affect the level of enantiocontrol (**135-137**).

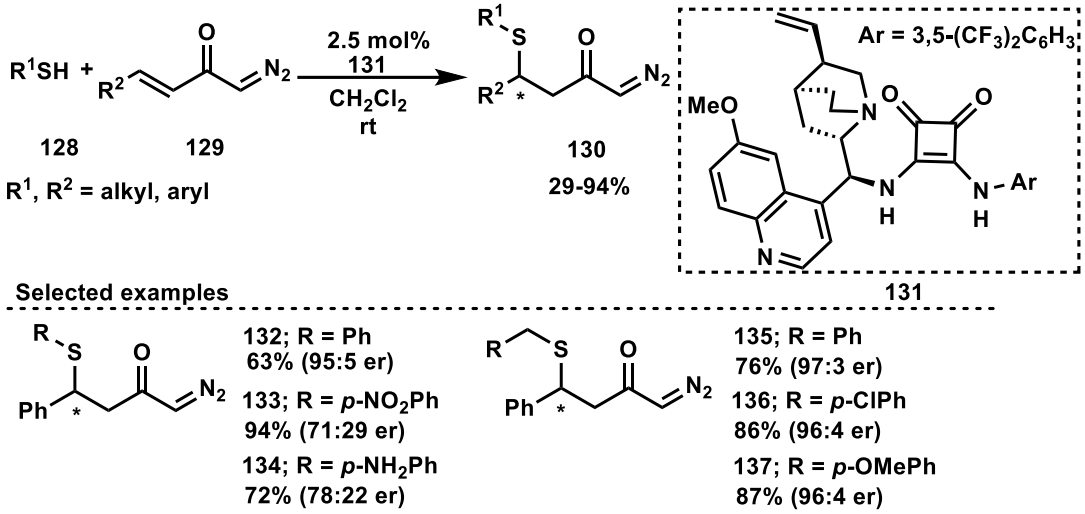

Scheme 2.23: Stereoselective sulfa-Michael reaction.

As mentioned previously, in 2013, Doyle developed a new route to the acceptor/acceptor diazo-enones class of reagent via a Wittig olefination/diazo transfer sequence.[22] These diazoacetoacetate enones, as novel Michael acceptors, have been employed in the construction of carbo- and heterocyclic ring systems in the presence of π-nucleophiles (Scheme 2.24). The silyl ketene acetal **139** was first chosen to test the proposed electrophilic behavior of the enones, which provided the diazo derivatives **140** in excellent yields under mild Lewis acid catalyst conditions with various Michael acceptors (**138**, Scheme 2.24A). The Michael adducts (**140** or **141**) were then studied in a catalytic dinitrogen extrusion reaction using dirhodium(II) catalysis. After treatment of the Michael adducts with a catalytic amount of $Rh_2(pfb)_4$, an intermediate metal carbene was formed, which upon a C–H insertion, provided *β*-tetralones (**142** or **143**) (Scheme 2.24B). They expanded the scope of this reaction to include other nucleophiles which after the Michael addition and C–H insertion provided a series of carbocyclic and heterocyclic ring systems such as dihydroindoles (from pyrrole), dihydrocarbazoles (from indole), *β*-tetralones (from silyl enol ethers), and pyrrolidinones (from amines) (**144-146**). These novel synthetic strategies offer advantages over traditional synthetic techniques to prepare similar natural product-like ring systems.

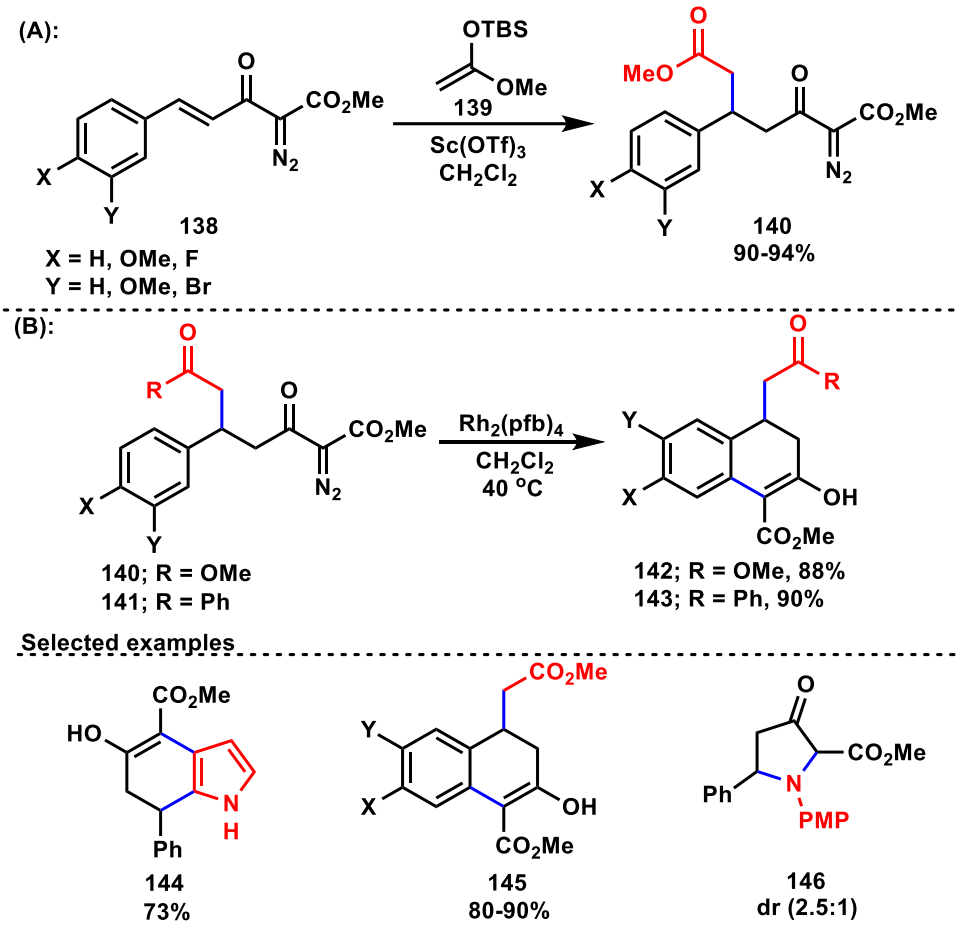

Scheme 2.24: (A) Nucleophilic additions of diazoacetoacetate enones. **(B)** Synthesis of natural product-like heterocycles by Doyle.

2.7 Conclusion

In conclusion, this chapter highlighted the importance of diazo-enones as unique and multi-functional synthetic building blocks. The multifunctionality of *α,β*-unsaturated diazoketones make them valuable tools in modern organic chemistry for synthesizing complex structures. There are many unexplored areas and untapped potential within the realm of these serviceable compounds. Looking ahead, in the upcoming Chapters (3 and 4), novel synthetic methods in the construction of fused-ring systems by utilization of diazo-enones have been explored in reaction with different substrates.

2.8 References

1. a) Chaturvedi, D.; Barua, N. C. *Curr. Org. Synth.* **2012**, *9*, 17-30. b) Shinokubo. H.; Oshima, K. *Eur. J. Org. Chem*. **2004**, 2081-2091. c) Kakiuchi, F.; Kochi, T. *Synthesis* **2008**, 3013–3039. d) Fagnou, K.; Lautens, M. *Chem. Rev.* **2003**, *103*, 169-196.
2. a) Doyle, M. P. *Chem. Rev.* **1986**, *86*, 919-939. b) Padwa, A.; Weingarten, M. D. *Chem. Rev.* **1996**, *96*, 223-269. c) Gurmessa, G. T.; Singh, G. S. *Res. Chem. Intermed.* **2017**, *43*, 6447-6504.
3. Bhat, A. H.; Alavi, S.; Grover, H. K. *Org. Lett.* 2020, *22*, 224-229.
4. Ford, A.; Miel, H.; Ring, A.; Slattery, C. N.; Maguire, A. R.; McKervey, M. A. *Chem. Rev.* **2015**, *115*, 9981-10080.
5. a) Marshall, J. A.; Audia, J. E.; Grote, J. *J. Org. Chem.* **1986**, *51*, 1157-1158. b) Padwa, A.; Cheng, B.; Zou, Y. *Aust. J. Chem.* **2014**, *67*, 343-353.
6. Ford, A.; Miel, H.; Ring, A.; Slattery, C. N.; Maguire, A. R.; McKervey, M. A. *Chem. Rev.* **2015**, *115*, 9981−10080.
7. Grundmann, C. *Liebigs Ann. Chem.* **1936**, *524*, 31-48.
8. Arndt, F. *Org. Synth*. **1935**, *15*, 1-3.
9. Wotiz, J. H.; Buco, S. N. The Arnt-Eistert Synthesis of Unsaturated Acids. *J. Org. Chem.* **1955**, *20*, 210-214.
10. Moore, J. A. *J. Org. Chem.*, **1955**, *20*, 1607-1612.
11. Rosenquist, N. R.; Chapman, O. L. A. *J. Org. Chem.* **1976**, *41*, 3326-3327.
12. Regitz, M.; Menz, F.; Liedhegener, A. *Justus Liebigs Ann. Chem.* **1970**, *739*, 174-184.
13. Harmon, R. E.; Sood, V. K.; Gupta, S. K. *Synthesis* **1974**, *1974*, 577-578.
14. Danheiser, R. L.; Miller, R. F.; Brisbois, R. G.; Park, S. Z. *J. Org. Chem.* **1990**, *55*, 1959-1964.
15. Aller, E.; Molina, P.; Lorenzo, A. *Synlett* **2000**, 526-528.
16. Pinho, V. D.; Burtoloso, A. C. B. *J. Org. Chem*. **2011**, *76*, 289-292.
17. Rosset, I. G.; Bertolo, A. C. B. *J. Org. Chem.* **2013**, *78*, 9464-9470.
18. Horner, L.; Hoffmann, H.; Wippel, H. G. *Chem. Ber.* **1958**, *91*, 61-63.
19. Pinho, V. D.; Burtoloso, A. C. B. *Tetrahedron Lett.* **2012**, *53*, 876-878.

20. a) Bolaski, R.; Pietrusiewicz, K.M.; Monkiewicz, J.; Koszuk, J. *Tetrahedron Lett*. **1980**, *12*, 3621-3624. b) Taylor, E. C.; Davies, H. M. L. *Tetrahedron Lett.* **1983**, *24*, 5453-5456.
21. Ceccherelli, P.; Curini, M.; Marcotullio, M. C.; Rosati, O.; Wenkert, E. *J. Org. Chem.* **1990**, *55*, 311-315.
22. Shanahan, C. S.; Truong, P.; Mason, S. M.; Leszczynski, J. S.; Doyle, M. P. *Org. Lett.* **2013**, *15*, 3642-3645.
23. Bethluser, W.; Regitz, M.; Theis, W. *Tetrahedron Lett.* **1981**, *22*, 2535-2538.
24. Danheiser, R. L.; Brisbois, R. G.; Kowalczyk, J. J.; Miller, R. F. *J. Am. Chem. Soc.* **1990**, *112*, 3093-3100.
25. Kapferer, T.; Brückner, R. *Eur. J. Org. Chem.* **2006**, 2119-2133.
26. Jacobsen, E. N.; Marko, I.; Mungall, W. S.; Schroeder, G.; Sharpless, K. B. *J. Am. Chem. Soc.* 1988, *110*, 1968-1970.
27. Pinho, V. D.; Burtoloso, A. C. B. *Tetrahedron Lett*. **2012**, *53*, 876-878.
28. Nukui, S.; Sodeoha, M.; Shibasaki, M. *Tetrahedron Lett*. **1993**, *34*, 4965-4968.
29. Nukui, S.; Sodeoha, M.; Sasai, H.; Shibasaki, M. *J. Org. Chem.* **1995**, *60*, 398-404.
30. Bernardim, B.; Burtoloso, A. C. B. *Tetrahedron* **2014**, *70*, 3291-3296.
31. Kagan, V. E.; Wipf, P.; Stoyanovsky, D.; Greenberger, J. S.; Borisenko, G.; Beli1kova, N. A.; Yanamala, N.; Samhan Arias, A. K.; Tungekar, M. A.; Jiang, J.; Tyurina, Y. Y.; Ji, J.; Klein-Seetharaman, J.; Pitt, B. R.; Shvedova, A. A.; Bayir, H. Adv. *Drug Delivery Rev*. **2009**, *61*, 1375-1385.
32. Fang, F. G.; Frato,M.; Kim, G.; Danishefsky, S. J. *Tetrahedron Lett.* **1989**, *30*, 3625-3628.
33. a) Chelucci, G.; Saba, A.; Valentia, R.; Bacchi, A. *Tetrahedron: Asymmetry* **2000**, *11*, 3449-3453. b) J. Clark, S.; Hodgson, P. B.; Goldsmith, M. D.; Stree, L. J. *J. Chem. Soc., Perkin Trans.* **2001**, 3312-3324.
34. Santiago, J. V.; Burtoloso, A. C. B. *Eur. J. Org. Chem.* **2018**, 2822-2830.
35. Momo, P. B.; Mizobuchi, E. F.; Echemendía, R.; Baddeley, I.; Grayson, M. N.; Burtoloso, A. C. B. *J. Org. Chem.* **2022**, *87*, 3482-3490.

Chapter 3: Indolyl α-Diazocarbonyl Annulation: Rearranged Carbazole Formation

3.1 Michael Addition Reactions of Indoles

As reviewed in Chapter 1, in most cases the C3-position of indole is the most reactive site in which electrophilic aromatic substitution reactions, such as protonation, halogenation, alkylation, and acylation, occur. In addition to these simple functionalization reactions, it is well-known that indole behaves as an enamine upon reaction with electron deficient alkene electrophiles. One of the first reported applications of this type of reactivity was the synthesis of tryptophan analog **3** by utilizing *α*-acetamidoacrylic acid **2** and indole **1** in a dioxane solution containing acetic acid (Scheme 3.1).[1] Another early attempt was a two-step construction of tryptamine **5** in a reaction of nitroethylene **4** and **1** in benzene, followed by reduction (Scheme 3.1).[2]

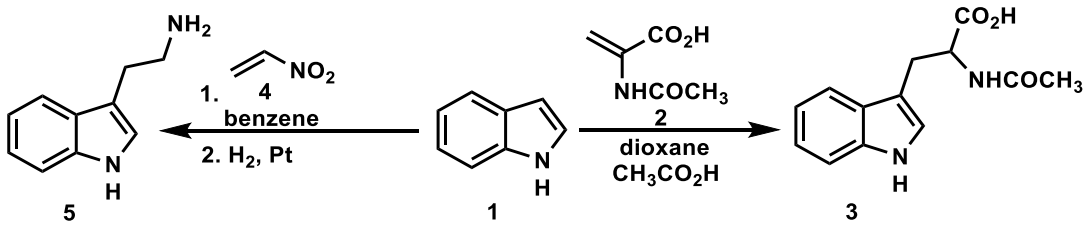

Scheme 3.1: Primary reported applications of C3 functionalization.

3.1.1 Lewis Acid Catalyzed Conjugate Addition Reactions of Indoles

Several decades after these initial protic acid catalyzed reports, in 1996, investigations addressing the catalytic 1,4-addition of indoles to enones featuring the use of $BF_3 \cdot OEt_2$ as a Lewis acid catalyst were disclosed.[3] Unfortunately, the scope of substrates was relatively narrow and mainly confined to methyl vinyl ketone. Another primary investigation on the Lewis acid catalyzed Micheal addition reaction of indole to a series of enones was reported by Kerr in 1996 (Scheme 3.2).[4] Treatment of indole, in the present of ytterbium triflate ($Yb(OTf)_3$) and electron deficient olefins delivered 3-alkylated indoles **8** in low to moderate yields. It should be noted that many Michael acceptors, including phenyl vinyl sulphone, ethyl cinnamate, methyl acrylate, acrylonitrile and several *α,β*-unsaturated aldehydes failed to react under the described conditions. In general, highly activated Michael acceptors such as *α,β*-unsaturated ketones seem to worked efficiently. Over the last 20 years a wide range of Lewis

catalysts including $InCl_3$,[5a] $InBr_3$,[5b] $CuBr_2$,[5c] $GaCl_3$,[5d] and $Bi(OTf)_3$[5e] have been utilized to activate α,β-unsaturated carbonyl compounds in indole alkylation reactions.

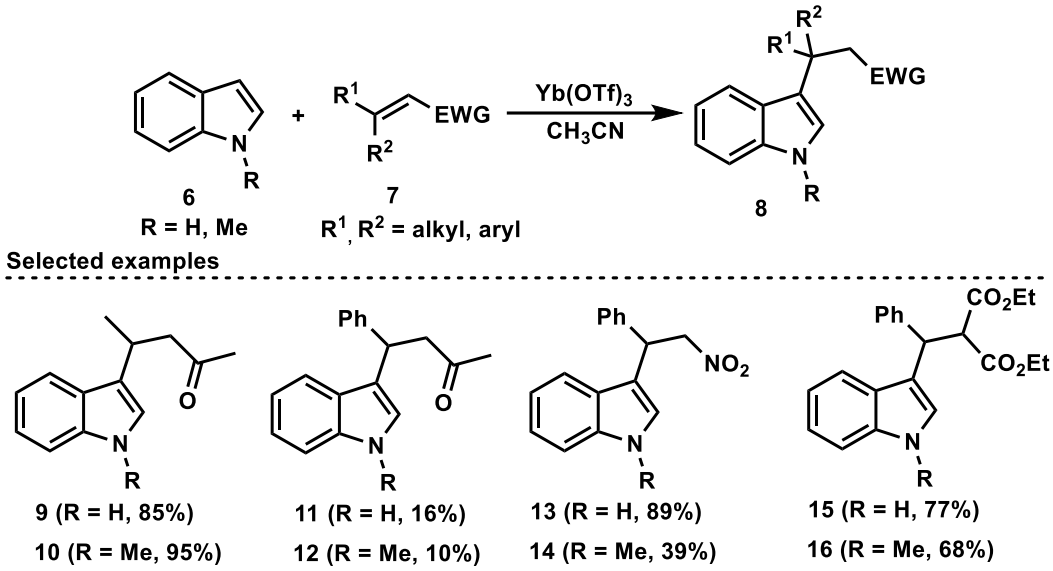

Scheme 3.2: $Yb(OTf)_3$ catalyzed alkylation of indoles.

3.2 Annulation of Indoles to Construct 2,3-Ring Fused Indoles

The term annulation, which originates from the Latin word 'anellus', refers to a synthetic process in which fusion of a ring to a molecule through the formation of two bonds occurs. Among the various relevant methods for generating a ring system are the powerful intramolecular electrophilic aromatic substitution transformations. As a subset of these transformations, annulations on indole motifs to construct 2,3-ring fused derivatives are important synthetic strategies due to the existence of these ring fused scaffolds in various natural products, drugs, and biologically active compounds.[6] The construction of 2,3-ring fused indoles can be achieved through many different synthetic approaches, however, the methods that are important, with regards to this thesis, are the reactions in which an appropriately C3-substituted indoles undergoes an annulation reaction to forge a new C–C bond at the C2 position.

In 1968, Smith and Jackson described a cyclization of a 3-indolylbutanol **19** in the construction of tetrahydrocarbazoles **22** and **24** by utilizing boron trifluoride etherate ($BF_3.Et_2O$) (Scheme 3.3B).[7] The authors proposed that upon activation of the primary alcohol with the Lewis acid, the ensuing annulation could proceed via several different

mechanistic pathways. The new bond to the C2-position of the indole could possibly occur through direct C2-functionalization leading to carbocation intermediate **21**, which following the loss of a proton, would deliver **22**. Alternatively, this new bond could be installed via a stepwise approach in which first nucleophilic attack of indole C3-position to the electrophile could form a spirocyclic intermediate **20**. This intermediate could then undergo a 1,2-shift (path a or b) to form the new C–C bond at the C2-position of the indole and ultimately lead to **22** and **24** upon the loss of a proton. To help shed light on the mechanism, the authors constructed an isotopically labelled derivative of the 3-indolylbutanol **19**, in a three-step process (Scheme 3.3A) and subjected this starting material to the annulation conditions. The outcome of this reaction provided an equal mixture of isomers **22** and **24**, a result which lends support to the formation of these products via a spirocyclic intermediate/1,2-shift pathway.

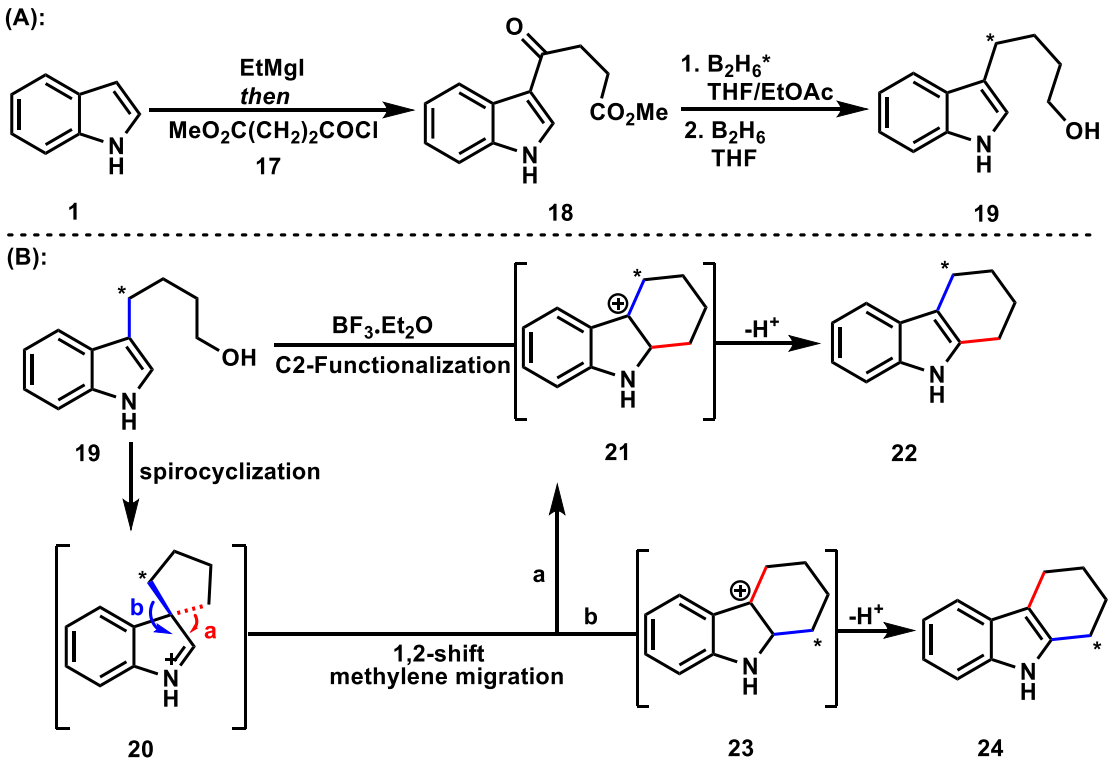

Scheme 3.3: (A) Synthesis of indolylbutanol substrate. **(B)** Tetrahydrocarbzaole via annulation of C3-substituted indoles.

3.2.1 Recent Developments in Construction of 2,3-Ring Fused Indoles

Among the various supports for the formation of the spriocyclic intermediate proposed by Smith and Jackson is a set of recent publications by Taylor and

Unsworth.[8-9] This collection of works focused on annulation reactions of indolyl ynone substrates **27**, a starting material that could be easily prepared from an alkynylation reaction of the relevant amide **26** (Scheme 3.4A). Their initial[8] study showed that subjecting C3-substituted indoles (**27**) to a reaction with silver triflate (AgOTf) catalyst, promoted a C3 annulation process leading to spirocyclic enones **28** in good to excellent overall yields. Importantly, in a subsequent study, the authors developed a method that could convert ynone **29** directly into a 2,3-ring fused indole product **33**, presumably through a spirocyclic intermediate (Scheme 3.4B).[9] Subjecting the C3-substituted indole substrate **27** to an Au(I) catalyzed ($Ph_3PAuNTf_2$) reaction delivered substituted carbazole **33** in a high 94% yield. Mechanistically the process involved the generation of a spirocyclic intermediate **30**, which was followed by an intramolecular cyclopropanation leading to **31**. Either upon C–C bond cleavage and ring expansion of **31** or through a direct 1,2-type shift of **30**, the carbocation intermediate **32** is formed. The final step entailed deprotonation and aromatization of **32** to attain a hydroxycarbazole **33**.

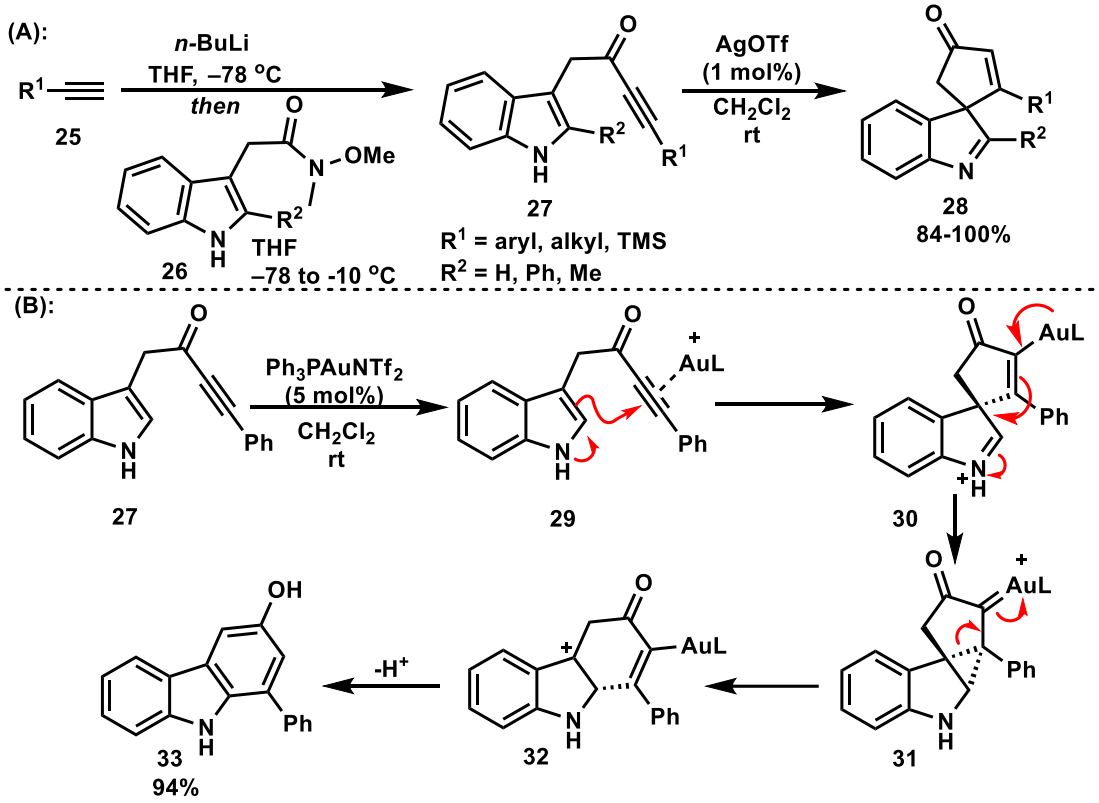

Scheme 3.4: (A) Synthesis of indolyl ynone starting materials followed by silver-catalyzed spirocyclization. **(B)** Gold-catalyzed construction of substituted carbazoles from indolyl ynones.

Furthermore, as part of this study, when the authors took the same spirocyclic substrates (**34**) obtained from their AgOTf catalyzed reaction (Scheme 3.4A) and subjected these compounds to a reaction with $AlCl_3 \cdot 6H_2O$, a unique quinolone product **38** was formed via a novel rearrangement process (Scheme 3.5). It is thought that the Al(III) catalyst could promote the formation of enolate **35**, and subsequent cyclopropanation could deliver intermediate **36**. Upon a ring expansion, tricyclic **37** was formed, and rearomatization furnished quinoline **38** in 88% yield. Through this approach, the authors successfully generated a library of quinolines with yields ranging from 71% to 92% (**39-41**). The overall importance of the investigations conducted by Taylor and Unsworth lies on appropriately substituted C3 functionalized indoles (i.e., the indolyl ynone substrates) by producing a spirocyclic intermediate, which in turn provides access to a variety of annulated products (**28** and **33**) in a controlled fashion by varying catalyst and reaction conditions.

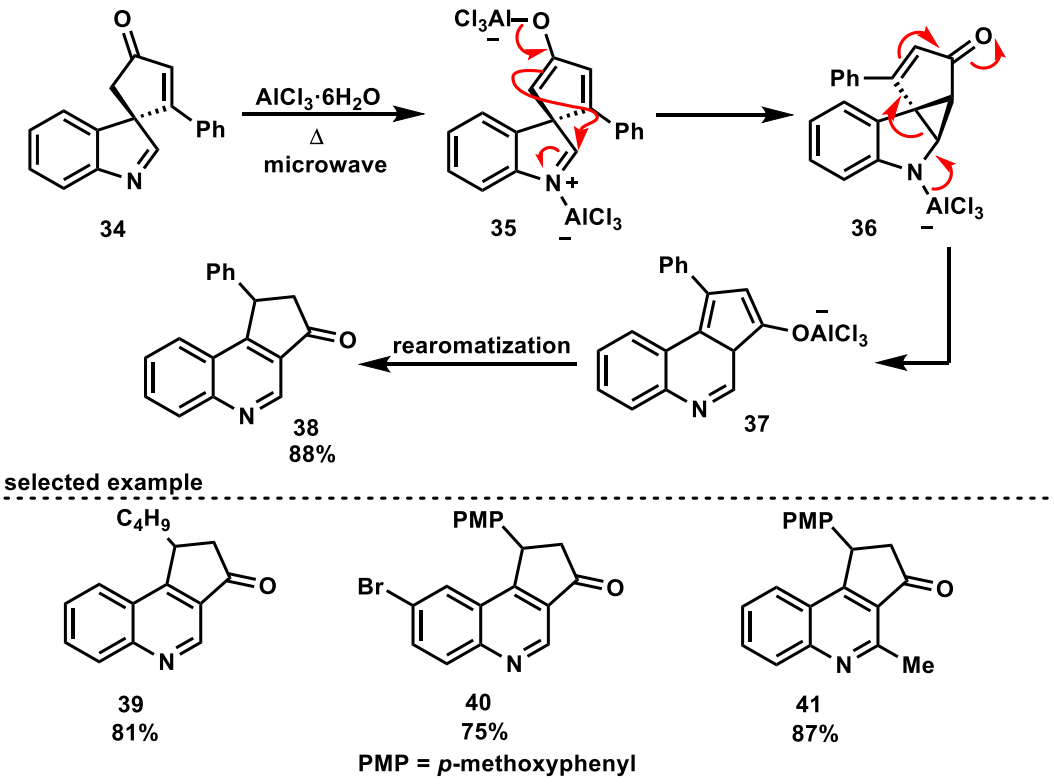

Scheme 3.5: Quinoline synthesis via rearrangement pathway.

3.2.2 Constructing of 2,3-Ring Fused Indoles by a Skeletal Rearrangement Process

In recent years, studies have explored the construction of 2,3-ring fused indole variants, which undergo rearrangement compared to the connectivity of the corresponding starting material. This investigation aimed to access synthetically valuable indole fused cascades. Several studies have focused on rearrangements that preserve the pyrrole ring of the indole, resulting in a valuable class of fused indole products. A recent example of this type of annulation that involves a skeletal rearrangement is showcased by You et al. in their 2013 report on the enantioselective synthesis of 2,3-fused indoles by treating functionalized indole **42** with an iridium catalyst system (Scheme 3.6).[10] The proposed plausible mechanism for this transformation is initiated by oxidative addition of **42** to generate an Ir(III)−π-allyl complex. Next, nucleophilic attack by the indole C3 position forms the spiroindolenine intermediate **44**, an intermediate structure that was supported by IR spectroscopic evidence. A 1,2-migration of spiroindolenine **44** resulted in shifting the substituent from the C3 to the C2 position of indole to deliver intermediate **45**. The intermediate **45** has undergone a structural rearrangement in comparison to the connectivity of the indole starting material. The product **46** is delivered upon a proton transfer and rearomatization of **45** in 80% yield, without loss of the enantiomeric purity. Utilizing this catalyst system, the rearranged products were selectively delivered as the sole isomer with yields ranging from 63% to 93% and exhibiting high enantioselectivity (ee: 88-96%).

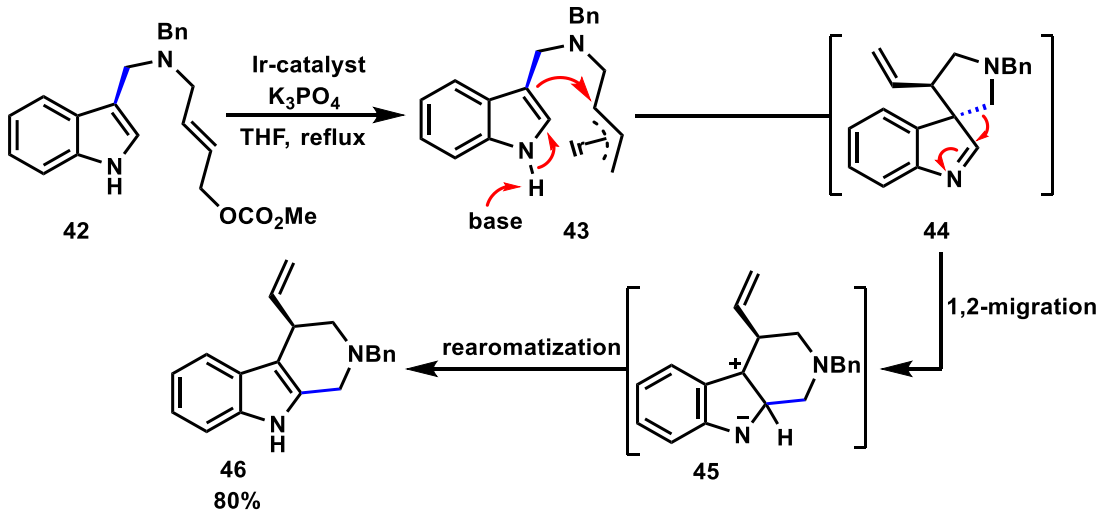

Scheme 3.6: Synthesis of 2,3-ring fused indoles via a controlled 1,2-migration.

3.3 Carbazoles

Carbazole and its derivatives are a predominant class of nitrogen-containing π-excessive aromatic heterocycles. Historically, 9*H*-carbazole **47** was isolated for the first time from coal tar by Graebe and Glazer in 1872 (Figure 3.1).[11] Since the initial isolation of the parent heterocycle (**47**), derivatives of this scaffold have become well-known in a wide range of natural products, marketed drugs, functional and photoelectrical materials, dyes etc. (Figure 3.1).[12] Due to important biological and pharmaceutical activities displayed by many carbazoles compounds (e.g., antibiotic properties of murrayanine **48**) the syntheses of carbazole derivatives have been extensively investigated. Traditionally, several methodologies such as Fischer indolization,[13a] Borsche-Drechsel,[13b] Graebe-Ullmann synthesis,[13c] and transition-metal-catalyzed intramolecular cyclization[13d] have been employed for the synthesis of carbazoles.

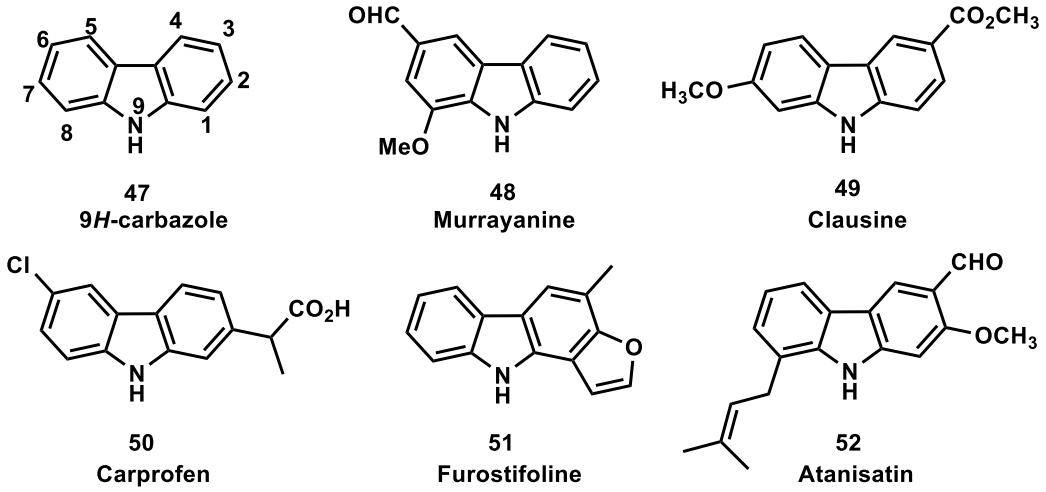

Figure 3.1: Representative carbazole-based natural products.

3.3.1 Carbazole synthesis from Diazo Compounds

As a valuable resource in modern organic synthesis, diazo compounds have also been utilized as starting materials for the construction of carbazoles. In 2016, the Unsworth group showed that a series of diverse indole derived products could be obtained from one starting material by reacting indolyl α-diazocarbonyls **53** with various catalysts (Scheme 3.7).[14] Among other results, the authors showed that the C3 substituted indole substrates (**53**) could efficiently undergo cyclization to the 2,3-ring fused indole in the presence of either palladium or copper catalysts. Exploiting $Cu(OTf)_2$, in the presence of an oxygen atmosphere led to fully aromatized carbazole **55**, while treating **53** with $Pd(MeCN)_4(BF_4)_2$ delivered tetrahydrocarbazole **54**. Mechanistically, it has been proposed that these reactions can proceed through two potential pathways. The first involves a direct C–H bond insertion of the activated diazo compound at the C2-position of the indole. The second pathway commences with an initial C3 attack, leading to a spirocyclic intermediate, followed by a 1,2-migration, which would deliver the 2,3-ring fused indole product.

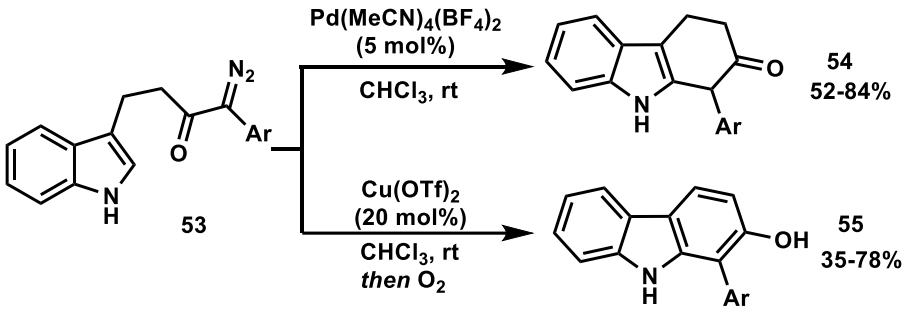

Scheme 3.7: Selective formation of **54** and **55**.

In a study conducted two years later, Balamurugan investigated a synthetic approach that involved the simultaneous tandem catalysis of $Sc(OTf)_3$ and $Rh_2(OAc)_4$ (Scheme 3.8).[15] They described formation of tetrahydrocarbazole **58** derivatives by utilization of indoles **56** and α,β-unsaturated diazoketones **57**. The reaction was initiated through an intermolecular Michael addition, facilitated by the presence of $Sc(OTf)_3$. This was subsequently followed by an intramolecular cyclization, mediated by the catalyst $Rh_2(OAc)_4$, resulting in the formation of the desired tetrahydrocarbazole compounds. Although these reaction conditions resulted in the formation of tetrahydrocarbazoles **58**, they were able to access the fully aromatized carbazoles (**59**) by treating these intermediates with trimethylamine (NMe_3) open to an air atmosphere. In fact, the annulation and aromatization can be carried out in a one-pot reaction by adding 2 equivalents of trimethylamine to the reaction flask after the completion of the Michael and annulation reactions.

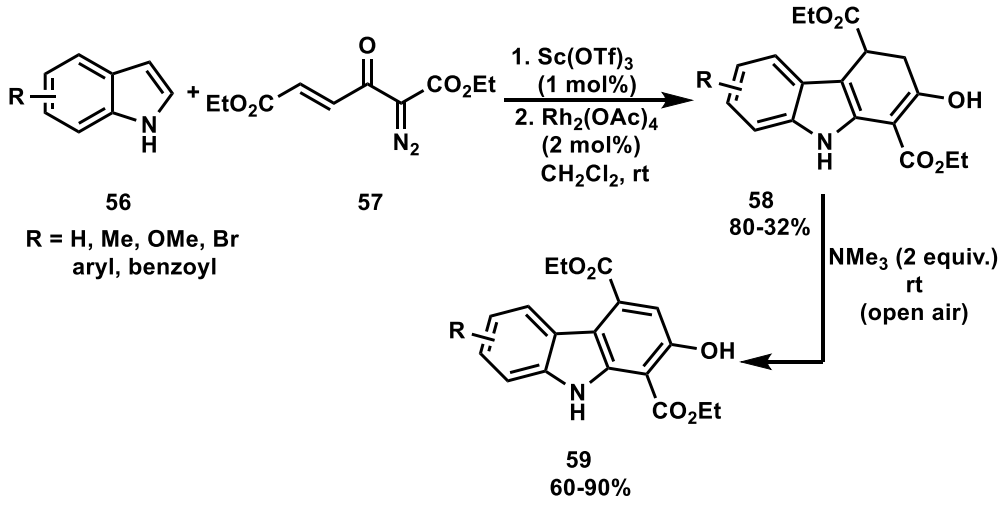

Scheme 3.8: Direct benzannulation of indole to carbazole.

3.4 Result and Discussion

3.4.1 Preliminary Research Findings

While exploring the reaction of *N*-propargyl indoles and *α*-diazocarbonyl compounds in a tandem C–H insertion/Conia-ene sequence (Chapter 1), a unique intramolecular reaction of *N*-propargyl indolyl *α*-diazocarbonyl **60** was attempted (Scheme 3.9A). While the outcome of this reaction, as discussed in Chapter 1, was unsuccessful in the formation of the desired pyrroloindole, an interesting observation was made when synthesizing **60** (Scheme 3.9B). Upon treatment of *N*-propargyl indole **61**, and diazo-enone **62** with scandium triflate, under modified Michael addition conditions developed by Doyle and co-workers,[16] **60** was isolated in 49% yield along with a small amount (less than 5%) of an unknown set of side products.

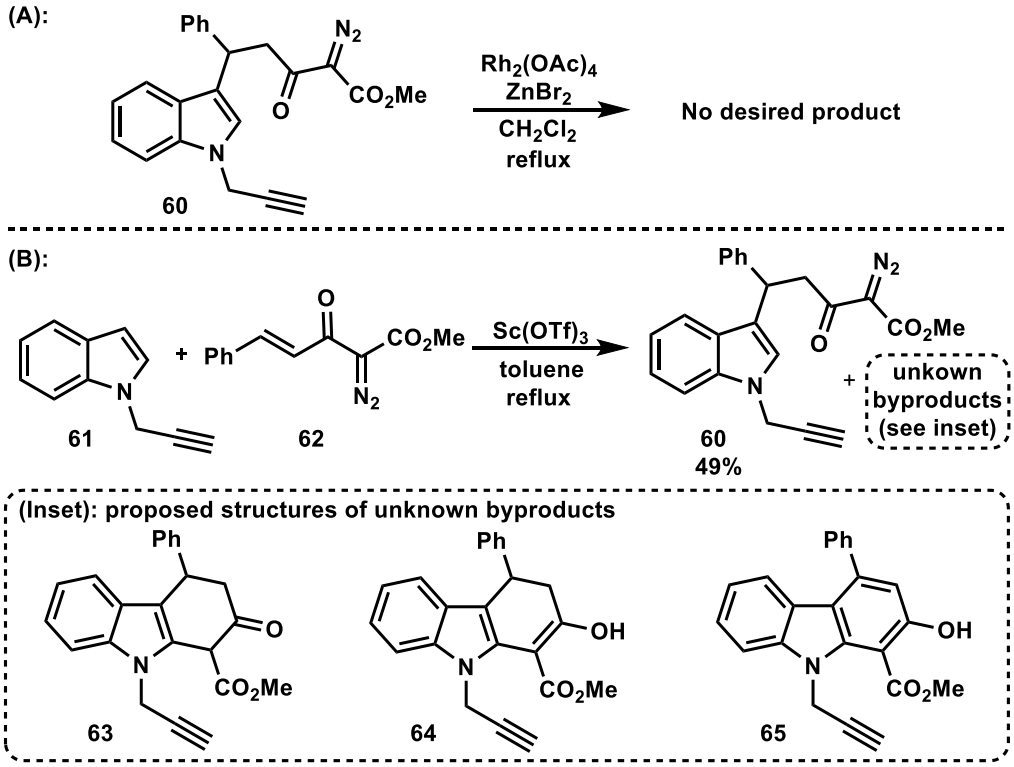

Scheme 3.9: (A) Unsuccessful C–H insertion/Conia-ene reaction of **60**. **(B)** Synthesis of **60**. **(Inset)** tentative proposed structures of side-products.

Although attempts to separate the unknown mixture of side products were unsuccessful, ^{1}H NMR analysis of the mixture showed the presence of both coupling fragments. Additionally, this analysis indicated that the *N*-propargyl indole components

in this mixture no longer contained protons on the C2 or C3 positions. Unable to determine the definitive structure of these compounds, it was hypothesized that these compounds could be a mixture of carbazole products (Scheme 3.9, inset); an interesting result which would arise from of a tandem Michael addition/annulation event involving the diazo moiety. These hypothesized structures were also supported by the independent work of Doyle[16] and Balamurugan[15] who reported a similar annulation of indole **66** that could be achieved in high yields utilizing different Rh(II) catalysis (Scheme 3.10). The dihydrocarbazole products (**67**/**68**) obtained from these reactions are a result of a net C–C bond formation between the indole C2 position and the diazo carbon.

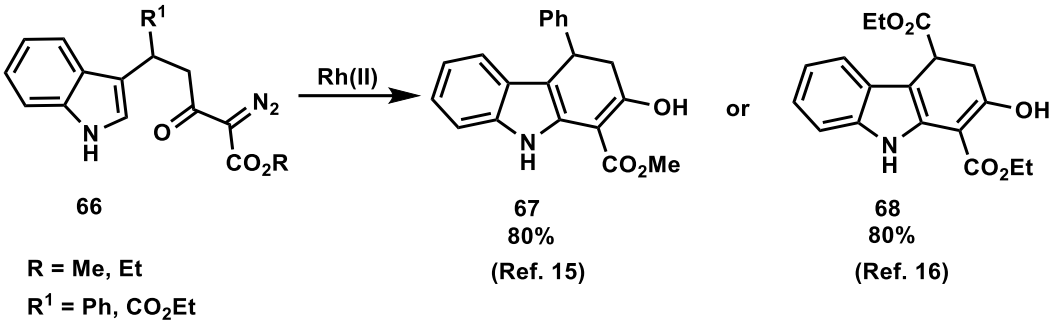

Scheme **3.10:** Annulation indolyl *α*-diazocarbonyls via rhodium Catalysis.

To further shed light on the identity of the minor side products from the scandium triflate catalyzed Michael addition reaction (Scheme 3.9), it was decided to change the structure of the indole starting material in the reaction. This decision was made to (i) simplify the NMR analysis of the products from the reaction and (ii) to be able to directly compare the tentative annulation products of the reaction to the known dihydrocarbazole **67** characterized by Doyle and co-workers.[16] Consequently, the reaction of indole (**1**) and diazo-enone **62** was conducted using scandium triflate in toluene at reflux (Scheme 3.11A). This reaction not only led to the formation of Michael addition product **69** in 61% yield but also resulted in two fully aromatized carbazole compounds, **70** (major isomer) and **71** (minor isomer). The structure of the major carbazole isomer **70** was determined by converting the Michael addition product **69** into the known dihydrocarbazole **72**, first prepared by Doyle, by treatment with $Rh_2(OAc)_4$ (Scheme 3.10). Further oxidation of **72** with 2,3-dichloro-5,6-dicyano-1,4-benzoquinone (DDQ) resulted in the formation carbazole **70**. The ^{1}H NMR spectrum of **70**, synthesized in two steps from **69** (Scheme 3.11B)

matched that of the major carbazole isomer produced from the one-step reaction (Scheme 3.11A), thus confirming the identity of one of the carbazole isomers.

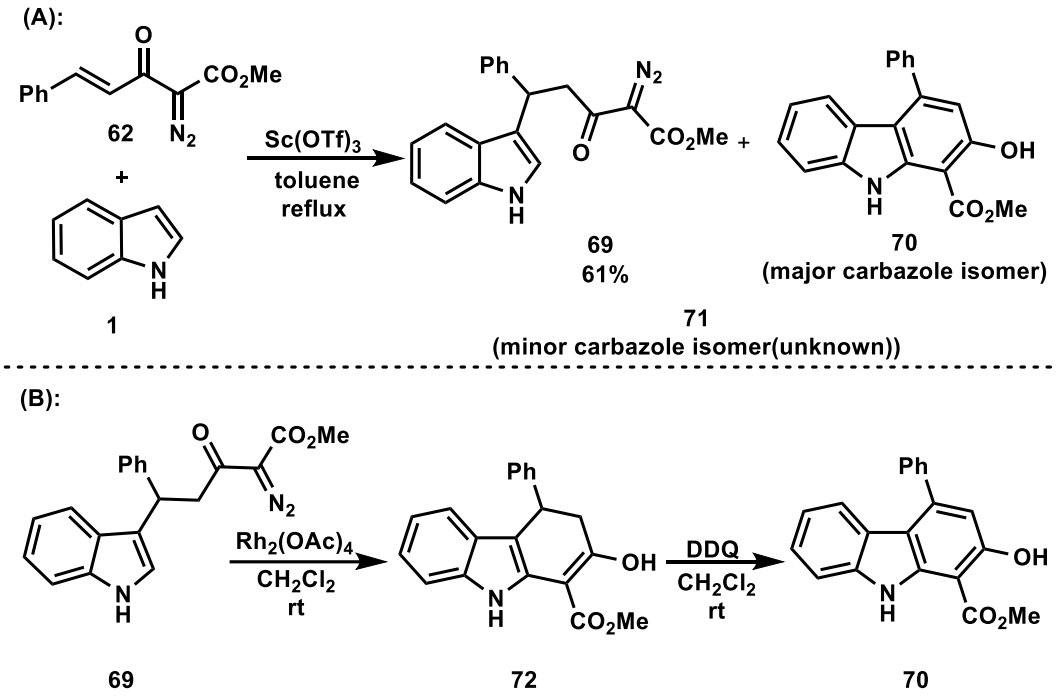

Scheme 3.11: (A) Scandium catalyzed reaction of indole and diazo-enone **62**.
(B) Structural confirmation of **70** via known dihydrocarbazole **72**.

The structure of the minor carbazole isomer **71**, was first tentatively assigned by comparing the ^{1}H NMR spectra of **70** and **71** (Figure 3.2). The ^{1}H NMR analysis of the two spectra revealed a big difference between the chemical shifts of the proton on the indole nitrogen, H(b) and H(b'), at 8.31 and 9.39 ppm, respectively. The proton of carbazole **70** (H(b')) was more downfield shifted, probably due to hydrogen bonding with the ester group on C1, which arise from electron density redistribution. While the proton H(b) of unknown carbazole **71** was notably shielded and suggested that it experiences a more electron rich environment at C1 compared to H(b'). Another distinguishing difference between the two spectra was related to the proton at the C5-position. C5-H(a) of the minor carbazole shows up at 8.48 ppm, where in contrast the corresponding proton H(a') of the carbazole **70** was observed at 7.43 ppm. The H(a') was more upfield shifted according to the negative inductive effect of the phenyl ring on C4 of carbazole **70**.

In addition to the NMR comparisons, the identity of the minor isomer **71** was confirmed through the single crystal X-ray structure elucidation of an analogous isomer constructed from *N*-methyl indole **73** (Scheme 3.12).[17] The crystal structure analysis of carbazole **126** provided explanations for the variations observed in the chemical shifts of the apparently identical protons. The chemical shift of H(b) at 8.31 ppm could be attributed to the phenyl ring attached to the C1 position of carbazole **71**, indicating a comparatively electron rich environment in contrast to H(b'), which was influenced by the ester group. Subsequently, the electron density of the phenyl ring at compound **70** (H(a')) resulted in a higher field chemical shift of proton at C5 of this isomer, while the ^{1}H NMR analysis showed the (H(a)) as a doublet peak at 8.48 ppm, compared to H(a') at 7.43 ppm (Figure 3.2). Lastly, the hydrogen bonding could explain the sharp peak of the OH group at C3 of the rearranged carbazole (**71**), which was observed at 11.16 ppm. This OH group was more downfield shifted compared to the OH group of carbazole **70** which was revealed at 11.02 ppm as a broad singlet peak.

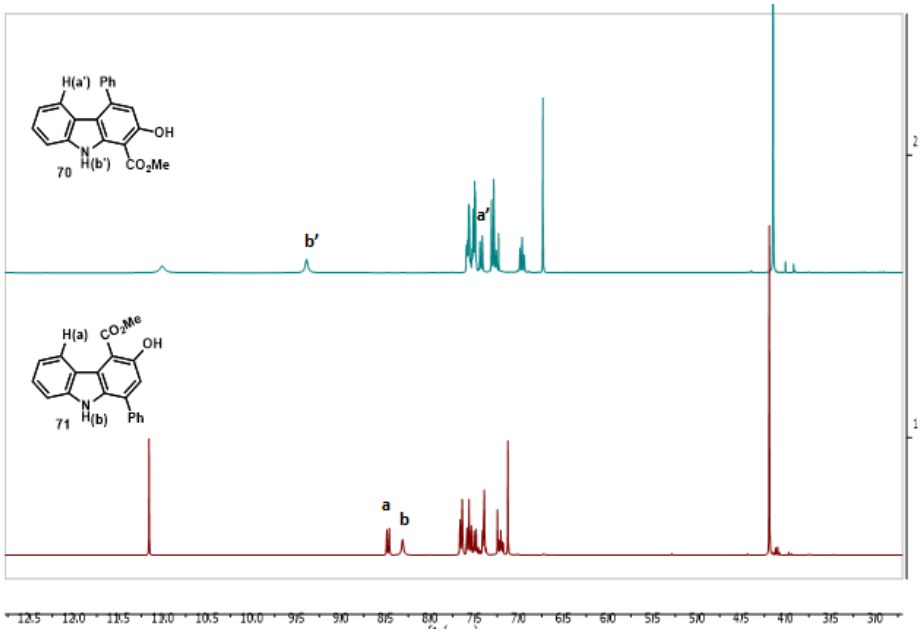

Figure 3.2: Partial ^{1}H NMR spectra of **70** and **71**.

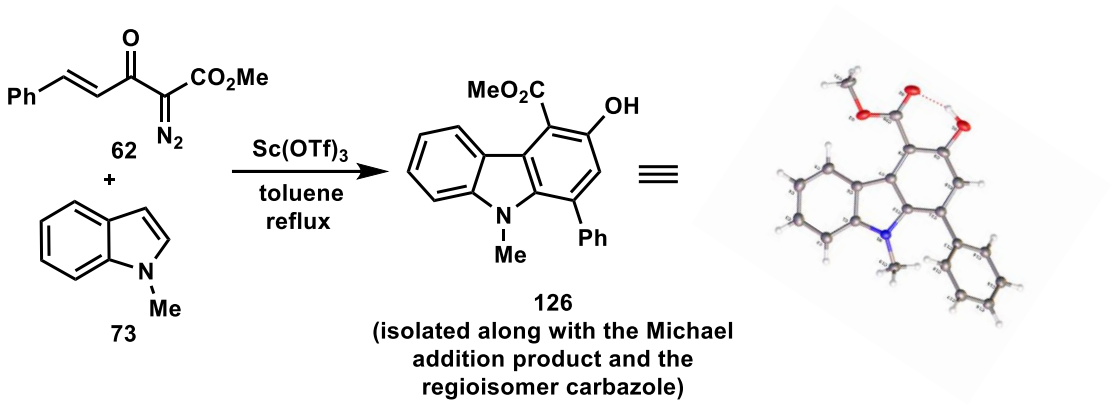

Scheme 3.12: Crystal structure of *N*-Methyl carbazole derivative **126**.

Having confirmed the identity of both carbazole isomers, we hypothesized that the formation of the minor carbazole **71** could be produced through a Wagner-Meervein like rearrangement/annulation pathway.[18] A plausible mechanism for the formation of both carbazole products is shown in Scheme 3.13. Activation of the diazo moiety of **69** by the Lewis acid followed by intramolecular nucleophilic addition of the indole, could lead to the five-membered spiro cyclic indolenine intermediate **74**. A Wagner-Meerwein type 1,2-shift of **74** could then occur through path (a) to construct carbocation **75**, which following oxidation, would deliver the rearranged carbazole **71**. In contrast to a 1,2-shift, the iminium intermediate **74** could also provide cyclopropane intermediate **76** (path b), which after ring opening and subsequent oxidation, would form carbazole **70**. Alternatively, the construction of dihydrocarbazole **77** could occur directly from a 1,2-shift of spiro cyclic intermediate **74** (path c).

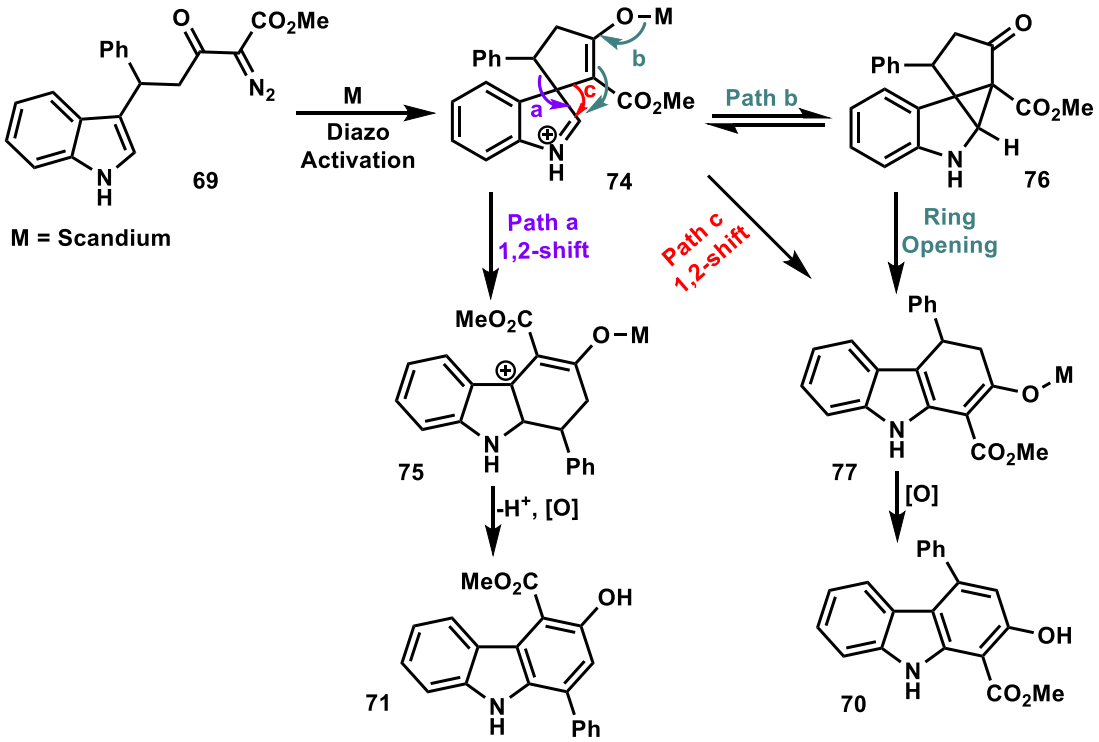

Scheme 3.13: Plausible mechanism of formation carbazole **70** and **71**.

3.4.2 Research Objectives

The formation of carbazoles through a unique rearranged-annulation pathway commencing from indolyl α-diazocarbonyls, similar to pathway (a) in Scheme 3.13, is not known in the literature. Therefore, our main research objective became identifying conditions that would afford this rearranged carbazole (**71**) as the major product. To help expedite our efforts we envisioned optimizing a method to achieve the highly functionalized rearranged carbazole as the major isomer from the indolyl α-diazocarbonyls **79** starting materials (Scheme 3.14). In this regard, to access the indolyl α-diazocarbonyls, we needed a series of substituted indoles **80** and diazo-enones **81** starting materials.

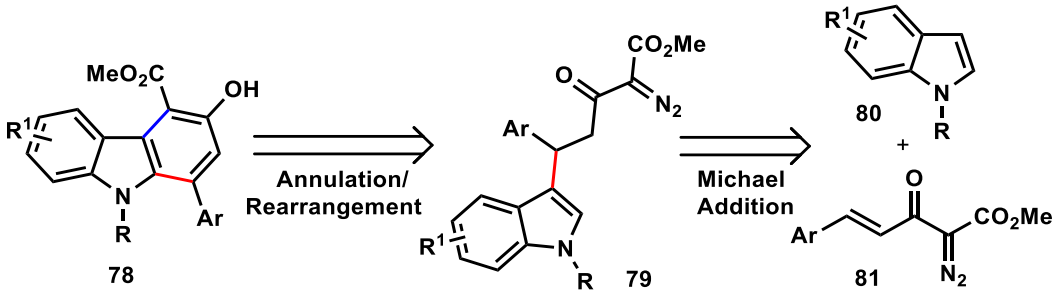

Scheme 3.14: Two-Step synthetic pathway to the rearranged carbazoles.

3.5 Synthesis of Starting Materials

To obtain the required diazoacetoacetate enones (DAAE) (**81**), we applied a modifed one-pot, two-step reaction sequence developed by Doyle and co-workers.[16] A Wittig-type olefination between aromatic aldehydes **82** and methyl 4-(triphenylphosphoranylidene) acetoacetate **83**, as the Wittig ylide, was conducted in the presence of sodium hydride (NaH) and 1,4-diazabicyclo[2.2.2]octane (DABCO), to provide intermediate **84** (Scheme 3.15). Without isolation, **84** was subjected to a Regitz diazo transfer reaction with tosyl azide (TsN_3) to furnish the crude diazoacetoacetates **81**. [19] Unfortunately, column chromatography purification of these diazo compounds proved problematic, resulting in low isolated yields presumably due to the polar byproducts (triphenylphosphine oxide (Ph_3PO) and *p*-toluenesulfonamide ($TsNH_2$)), which perpetually co-eluted with the products. To circumvent this problem, a method to purify the crude material by recrystallization was developed. First the crude material was dissolved in hot dichloromethane followed by cooling (ice/water bath) and the slow addition of hexanes to precipitate the majority of the Ph_3PO. Upon filtration and concentration, this material was then subjected to crystallization in a minimal amount of hot ethanol. This stage of the purification removed the $TsNH_2$ and any remaining Ph_3PO (soluble in ethanol) resulting in analytically pure DAAE products **81**. By employing this synthetic procedure and purification method, a series of DAAE compounds could be prepared reproducibly, in serviceable yields, on multigram scales, without the need for column chromatography purification.

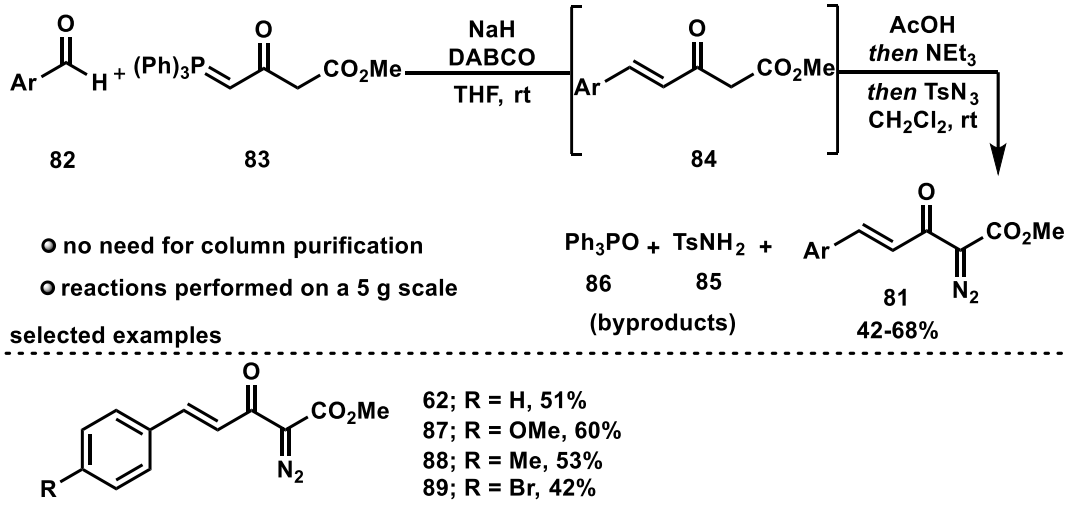

Scheme 3.15: Preparation of diazoacetoacetate enones **62** and **87-89**.

With access to the required diazo-enones, we next focused on synthesizing the Michael addition products. Although the Lewis acid catalyzed Michael addition reactions of indoles are known in the literature,[16] our aim was to optimize the reaction conditions by exploring various Lewis acids and solvents to improve the overall yield. Initially, we conducted a series of parallel small-scale experiments (qualitatively analyzed by TLC only) whereby indole and diazo-enone **62** were subjected to varying solvents and different Lewis acid catalysts. Next, we focused on carrying out reactions on a larger scale, utilizing the conditions that delivered the most promising results in the preliminary investigations (results are summarized in Table 3.1). The aim was to determine conditions that would induce the highest overall yield for the reaction. The initial findings, from room temperature to 50 °C, revealed that the consumption of starting materials in the presence of the promising Lewis acids required the reaction to be heated at higher temperatures. Through subjecting the starting materials to a reaction with $La(OTf)_3$ and refluxing in toluene, there was no observed increase in the yield of products compared to lower temperatures (Table 3.1, entry 1). Although employing $Cu(acac)_2$ resulted in full consumption of starting materials, a complex mixture of unknown compounds was achieved, which did not include the desired product (entry 2). Next, the reaction was heated to reflux in toluene in the presence of $Cu(OTf)_2$ and delivered a trace amount of **69** (entry 3). Upon refluxing **1** and **62** in acetonitrile with $Cu(OTf)_2$, conversion to the desired product **69** increased. However, when the starting materials (**1** and **62**) were not entirely consumed, carbazoles **70** and **71** formed in the reaction alongside the Michael adduct **69**; consequently, the yield of the desired product was low (entry 4). By replacing the catalyst with $Sc(OTf)_3$ and heating the reaction in toluene, the TLC analysis showed the complete consumption of the starting materials; however, the Michael addition product was unstable to these high temperatures and started converting to a mixture of fully aromatized carbazole **70** and **71** (entry 5). Finally, utilization of $Sc(OTf)_3$ and refluxing in CH_3CN not only consumed the indole and diazo-enone substrates but also delivered the desired product as the major component in 64% yield in reduced reaction time (entry 6). By using *N*-methylindole **73** instead of indole in a reaction with diazo-enone **62** in the presence of $Sc(OTf)_3$, the corresponding Michael adduct **111** was formed in higher yield, 67%, and shorter reaction time (3 h).

Table 3.1: Optimization of Lewis Acid Catalyzed Michael-Addition Reaction

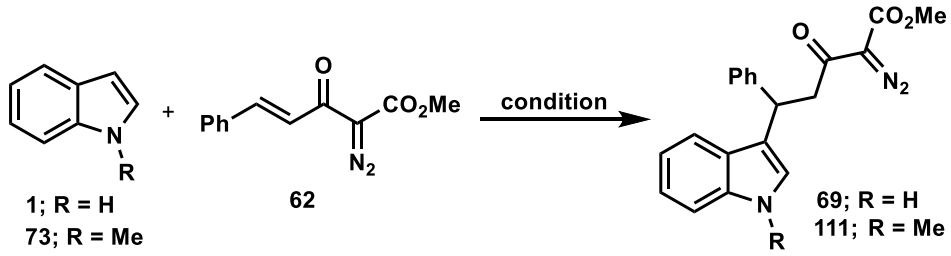

Entry	Catalyst[a]	Solvent	Temp (time)	Result
1	$La(OTf)_3$	toluene	reflux (24 h)	Low conversion[b]
2	$Cu(acac)_2$	toluene	reflux (18 h)	No Product[c]
3	$Cu(OTf)_2$	toluene	reflux (18 h)	Trace Product[d]
4	$Cu(OTf)_2$	CH_3CN	reflux (24 h)	Low Yield[e]
5	$Sc(OTf)_3$	toluene	reflux (18 h)	61%
6	$Sc(OTf)_3$	CH_3CN	reflux (5 h)	64%
7[f]	$Sc(OTf)_3$	CH_3CN	reflux (3 h)	67%

[a] Reactions carried out with 10 mol% catalyst, **1**/**73** (1.2 equiv.), enone **62** (1 equiv.). [b] No isolated yield, consumption of starting materials followed by crude ^{1}H NMR. [c] Intractable mixture of compounds. [d] Trace amount of Michael-addition product in a complex mixture of compounds. [e] Low yield based on ^{1}H NMR analysis of the mixture of crude. [f] Reaction was done utilizing indole **73**, entries 1-6 were carried out by indole **1**.

Utilizing the optimized conditions that worked in a satisfactory 67% yield for *N*-methylindole (1.1 equivalent), we proceeded to employ these conditions with other substrates (Scheme 3.16). Our investigations commenced by exploring the impact of substitution on the indole nucleophile. Various substituted *N*-methylindoles were subject to the $Sc(OTf)_3$ reaction conditions with diazo-enone **62** (Scheme 3.16). Indole starting materials substituted with an electron donating methoxy group on the benzenoid ring (**90** and **91**) underwent smooth conversion to the corresponding Michael addition products (**96** and **97**) in modest to excellent yields (40% and 76% respectively) with complete consumption of the limiting reagent (**62**). Notably, the decreased yield in the formation of **90** is not the result of an ineffective conjugate addition but rather a rapid cyclization, with loss of N_2, of the product upon formation (this will be discussed in the following sections). In contrast to indoles substituted with EDGs, starting materials

containing electron withdrawing groups on the benzenoid ring (**92**-**95**) were much more resistant towards the Michael addition under the current conditions. In these reactions, increasing indole and catalyst loadings, as well as extended reaction times (up to 12 h) were required to produce low to moderate yields of the products **98**, **99**, and **101**, with indole **94** failing to undergo addition with **62** even with prolonged reaction times (48 h). Presumably, in these experiments, the electron-withdrawing groups reduce the electron density of the indole moiety originating from the pyrrole core rendering them weaker nucleophiles.

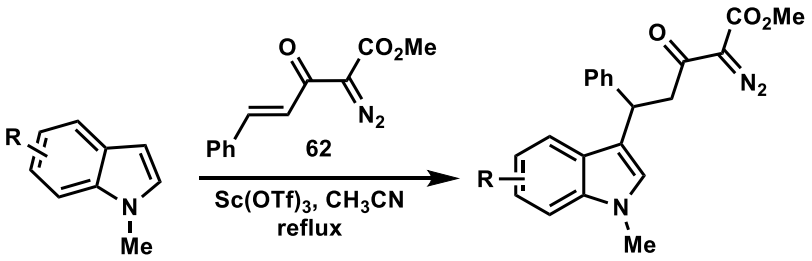

90; R = C5-OMe (1.1 equiv, 10% cat)
91; R = C6-OMe (1.1 equiv, 10% cat)
92; R = C5-Br (2.0 equiv, 15% cat)
93; R = C6-Br (1.1 equiv, 10% cat)
94; R = C5-NO_2 (2.0 equiv, 20% cat)
95; R = C6-NO_2 (2.0 equiv, 15% cat)

96; R = C5-OMe, 40%
97; R = C6-OMe, 76%
98; R = C5-Br, 60%
99; R = C6-Br, 43%
100; R = C5-NO_2, 0%
101; R = C6-NO_2, 23%

Scheme 3.16: Effect of *N*-methylindoles substitution in the Michael reaction.

Next, we investigated the effects of substitution on the α-diazocarbonyl substrates in the Michael addition reaction. A series of diazo-enones containing electron donating and electron withdrawing groups at the *para*-position of the phenyl ring (**87**-**89,** and **102**) were reacted with *N*-methylindole under the optimized reaction conditions (Scheme 3.17). The most favorable yields were obtained when the phenyl group was substituted at the *para*-position with EWGs. For instance, the presence of NO_2 and Br groups resulted in yields of 89% (**106**) and 62% (**105**), respectively, when 10% catalyst was employed. Alternatively, diazo-enones containing EDGs at this position (**87** and **88**) were much less effective in this reaction, requiring increased loadings of **73** and the catalyst to provide the desired addition products. Potentially, the incorporation of an electron withdrawing group on the phenyl ring of the diazo-enone, polarizes the enone double bond making the β-carbon a better electrophile in

comparison to an enone with an electron donating group,[21] which can account for the stark difference in yields between these types of substituted starting materials.

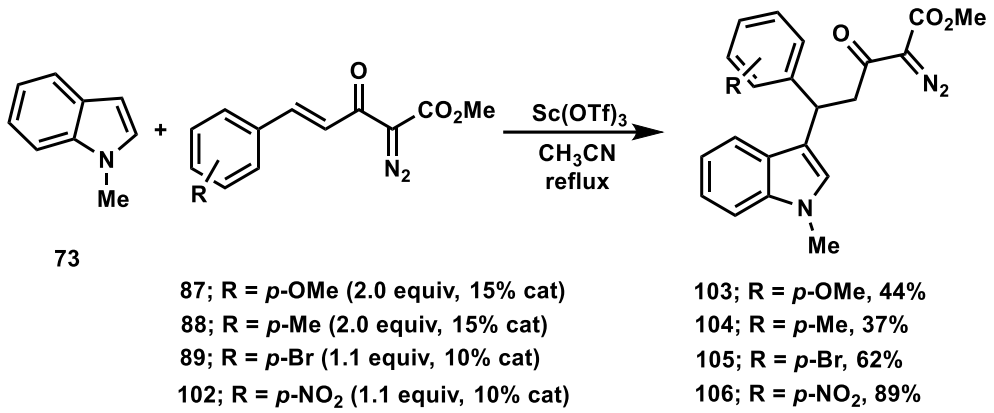

Scheme 3.17: Effects of substitution on the diazo-enones in the Michael addition reaction.

Finally, a series of indolyl α-diazocarbonyl compounds containing different substitutions on the indole nitrogen were prepared from diazo-enone **62** (Scheme 3.18A). The use of *N*-benzylindole as the nucleophile in the Michael addition reaction was effective under the standard reaction conditions, resulting in a 78% yield of **112**. By utilizing 1*H*-indole in a reaction with **62**, the yield was slightly reduced to 64% (**69**). A further decrease in yield was noted when *N*-phenylindole **110** was reacted with **62** providing **111** in a 46% yield; a result that could potentially be attributed to the inductive withdrawing effect of the aromatic ring on the indole nitrogen thus decrease the nucleophilicity of this starting material. In fact, attempts to promote the Michael addition with indole starting materials that contained a strong electron withdrawing group on the indole nitrogen, such as a *p*-toluenesulfonyl (Ts) group or a *t*-butyloxycarbonyl (Boc) group, resulted solely in recovery of starting materials. To overcome this limitation, an indolyl α-diazocarbonyl compound containing an electron withdrawing group on the indole nitrogen was prepared by the reaction of indolyl α-diazocarbonyl **69** with di-*t*-butyl dicarbonate (Boc_2O) and catalytic 4-dimethylaminopyridine (DMAP) to deliver **114** in a high yield (92%) (Scheme 3.18B). Unfortunately, attempts to make the *N*-Ts and *N*-acyl analog via similar transformations of **114** proved ineffective.

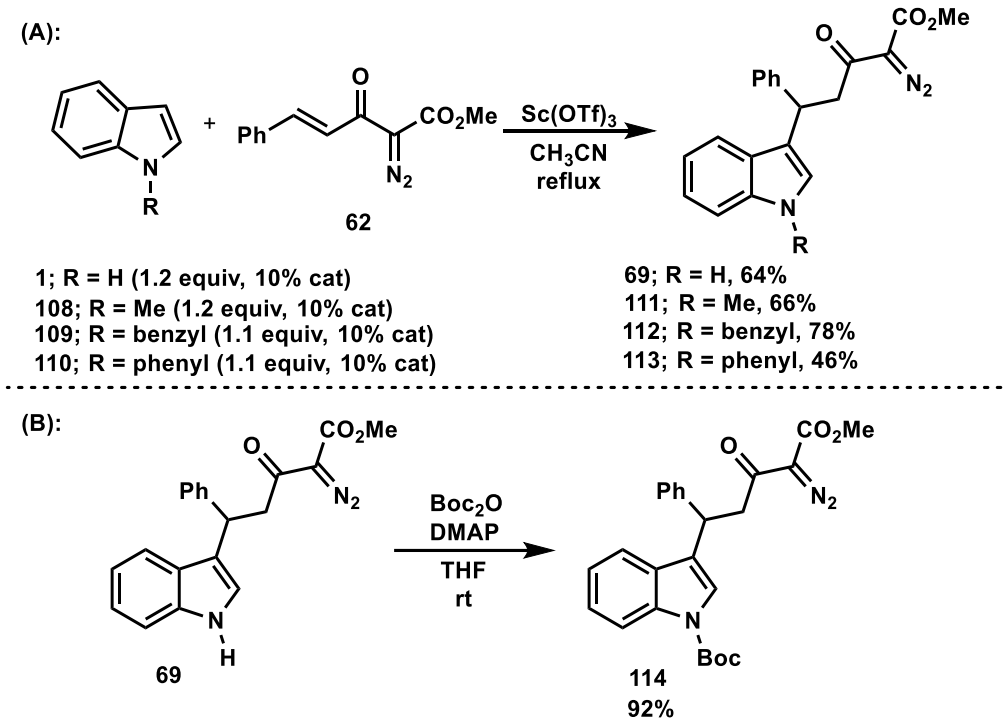

Scheme 3.18: (A) Electronic effect of nitrogen substitution on Michael addition Reaction. **(B)** Synthesizing *N*-Boc substituted diazo-enone **114**.

Guided by the initial experiments on the influence of indole and diazo-enone substitution on the outcome of Michael addition reaction, a library of indolyl *α*-diazocarbonyl compounds was prepared by reacting a range of substituted *N*-methylindoles with *α*-diazocarbonyls that contained various substituents on the *para*, *ortho*, and *meta* position of the phenyl ring (Table 3.2). In general, when the indoles were substituted with EDG or the diazo-enone contained an EWG on the phenyl ring, conditions 'A' (see Table 3.2) were utilized. When the indoles were substituted with an EWG or the diazo-enone contained an EDG on the phenyl ring, conditions 'B' were utilized. By varying these methods and substrates, multi-substituted indolyl *α*-diazocarbonyl compounds **115-125** were obtained in 17-89% yields.

Table 3.2: Scandium Catalyzed Michael-Addition of Indoles and Diazo-Enones

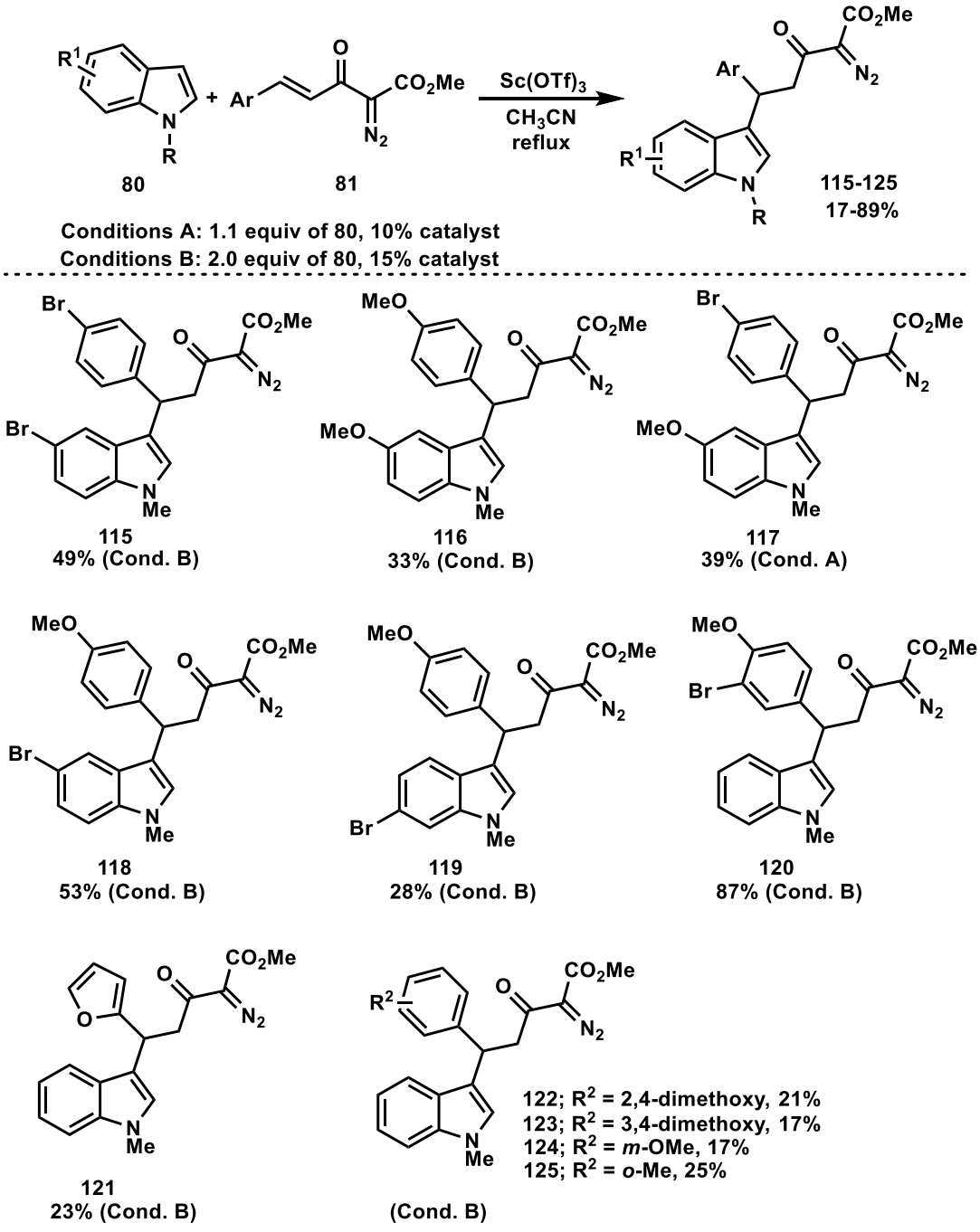

3.6 Synthesis of Carbazoles

As previously stated, the primary goal of our project was to synthesize the rearranged carbazole isomers (**78**, Scheme 3.14) using the indolyl α-diazocarbonyl substrates. To accomplish this goal, indolyl α-diazocarbonyl substrate **111** was selected

to conduct our optimization studies (Table 3.3). The initial investigations (see Scheme 3.11A) demonstrated the effectiveness of $Sc(OTf)_3$ in the reaction of **1** and **62** when refluxing in toluene. Hence, we commenced this study by treating the indole substrate **111** with 15 mol% $Sc(OTf)_3$, which provided a 2:1 mixture of carbazole **126** and **127**, in an overall 30% yield (entry 1). Inspired by these results, we then screened several other Lewis acids in hopes of improving both the yield and selectivity.

We proceeded by subjecting **111** to various Lewis acid catalysts in toluene and open to the air (Table 3.3). The reactions were performed on small scale, and ^{1}H NMR analysis was used to determine the ratio of the products (**126** vs **127**). The experimental protocol involved subjecting each reaction to a gradual temperature increase commencing at 50 °C, and subsequently to 80 °C, while monitoring by TLC for the consumption of the starting material. In some cases, the initial indole substrate remained unreacted at both 50 °C and 80 °C (entries 2 and 3). The use of $Zn(OTf)_2$ as a catalyst at 50 °C led to the decomposition of **111** and produced an intractable mixture of unknown side-products (entry 4). The use of $In(OTf)_3$ at 50 °C was promising, indicating trace formation of **126** and **127** (by TLC analysis), however, at this temperature a significant amount of starting material remained. As such, this reaction was then heated at 80 °C, which led to the complete consumption of the indole substrate, resulting in the formation of a mixture of carbazoles in a 1:1 ratio, along with formation of unknown side-products (entry 6).

Table 3.3: Primary Catalyst Screen for Carbazole Formation

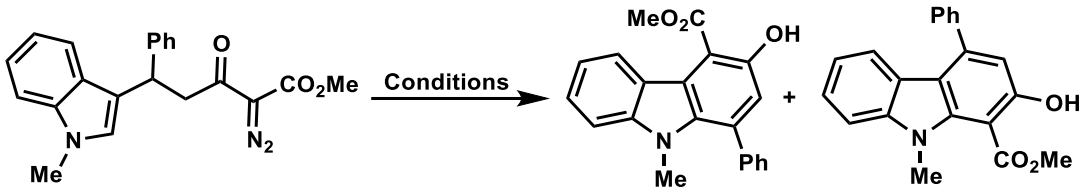

111 126 127

Entry	Catalyst[a]	Additive	Temperature	Time	126:127 (yield)[b]
1	$Sc(OTf)_3$[c]	air	reflux	12 h	2.0:1.0[d]
2	$Co(OAc)_2$[c]	air	50-80 °C	12 h[e]	No Reaction
3	$Cu(acac)_2$[c]	air	50-80 °C	12 h[e]	No Reaction
4	$Zn(OTf)_2$[c]	air	50-80 °C	12 h[e]	No Product[f]
5	$Cu(OAc)_2$	air	50-80 °C	12 h[e]	Low conversion
6	$In(OTf)_3$[c]	air	50-80 °C	12 h[e]	1.0:1.0[d]
7	$Cu(OTf)_2$	air	80 °C	4 h	1.0:1.2 (91%)
8	$Cu(OTf)_2$	N_2[h]	80 °C	4 h	Trace Product[g]
9	$Cu(OTf)_2$	N_2[h] *then* O_2	80 °C	4 h *then* 45 min	1.2:1.0[d]
10	$Cu(OTf)_2$	O_2[h]	80 °C	1.25 h	1.1:1.0 (66%)

All the reaction performed in toluene, [a] 20 mol% catalyst. [b] isolated yield of separable isomers. [c] 15 mol% catalyst. [d] ratio determined by ^{1}H NMR of crude reaction mixture. [e] 4 hours at 50 °C, then 8 h at 80 °C. [f] Intractable mixture of compounds. [g] Trace amount of **126**/**127**, among an intractable mixture of non-oxidized annulation product. [h] 1 atm.

Treatment of indole substrate **111** with $Cu(OTf)_2$ in toluene initially showed low conversion at 50 °C. However, when this reaction was heated to 80 °C, **111** was completely consumed and a mixture of carbazole **126** and **127** was obtained in a ratio of 1:1.2, respectively (entry 7). Although the $Cu(OTf)_2$ catalyst delivered the favorable carbazole **126** in a lower ratio than the scandium reaction, when the reaction was performed in the presence of copper on a larger scale, a substantial yield of 91% combined yield of carbazoles was obtained (entry 7).

Presumably, the copper-catalyst served a dual purpose in the transformation, first by activating the diazocarbonyl moiety and then by aiding the oxidation of the incipient dihydrocarbazole intermediate when in the presence of adventitious oxygen

from the atmosphere. The utilization of air as an oxidant source in these initial experiments was shown to be essential to obtain high yields of the carbazoles. Primarily when the reactions were performed under an N_2 atmosphere (entry 8), nonoxidized products were obtained, whereas reactions under oxygen (entry 10) suffered from significantly decreased yields to 66% in a ratio of 1.1:1 of **126** and **127**, probably due to oxidative decomposition of the products. In addition to oxidant sources, we also evaluated several solvents, including $CHCl_3$, CF_3CH_2OH, and $CF_3C_6H_5$ (not included in the table); however, all led to lower yields and comparable selectivity in delivering the carbazole **126**.

With the goal of improving selectivity, other copper catalysts were investigated; $Cu(ClO_4)_2 \cdot 6H_2O$ emerged as a highly promising catalyst yielding a 3:1 mixture of **126**:**127** with an acceptable 74% overall yield (Table 3.4). In fact, on a small scale, NMR analysis of the crude reaction mixture revealed an impressive selectivity ratio of up to 10:1 favoring **126**, when employing higher copper loadings (50%), however, reproducibility of these results on larger scale proved difficult. A significant limitation that impeded the utilization of this catalyst in the project was solubility. The $Cu(ClO_4)_2 \cdot 6H_2O$ catalyst was not soluble in toluene, and thus a polar solvent mixture, with ethyl acetate proving to be the most effective, was required for the reaction to proceed. Unfortunately, the isomer **126** appears to be unstable under these conditions, indicated by entry 2. We hypothesized that the observed decrease in yield and selectivity in this reaction could be attributed to the facile decomposition of **126**. To overcome limitations associated with $Cu(ClO_4)_2 \cdot 6H_2O$, we proposed generating the copper(II) perchlorate in situ from the anhydrous copper(II) triflate with a perchlorate salt additive. The addition of perchloric acid ($HClO_4$), sodium perchlorate ($NaClO_4$), and magnesium perchlorate ($Mg(ClO_4)_2$) as additives (1 equivalent per reaction) had little impact on the selectivity of the reaction, all resulting in an equal mixture of **126** and **127** (entries 3-5). The lack of selectivity involving $NaClO_4$ and $Mg(ClO_4)_2$ can be attributed to the low solubility of these salts in toluene. A convenient solution was found to address the low solubility issue by switching to the more soluble tetrabutylammonium perchlorate ($Bu_4N(ClO_4)$) salt under N_2 atmosphere. This change achieved a remarkable outcome, resulting in a high yield and selectivity. The overall yield was an impressive 90%, with **126** being predominantly formed as the major product in a notable 2.5:1 ratio (entry 6).

Interestingly, the perchlorate additive not only impacts the selectivity of the annulation reaction but also serves as an efficient oxidant, facilitating the generation of carbazole products within 3 hours under an inert atmosphere. Further efforts to optimize the reaction by employing higher perchlorate salt loadings or conducting reactions open to air conditions led to slightly diminished yields (entry 7).

Table 3.4: Copper Catalyzed Reaction Optimization

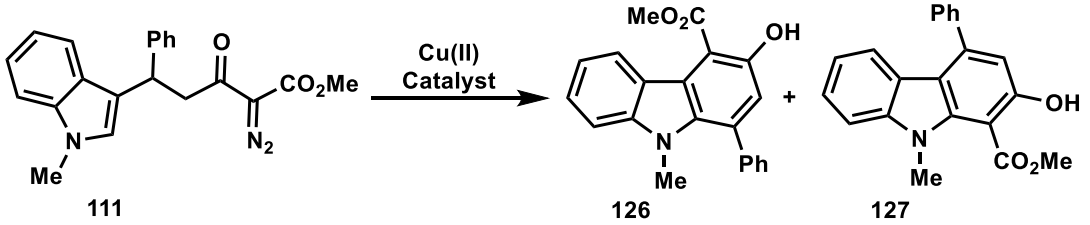

111 126 127

Entry	Catalyst[a]	Additive	Solvent	Temp (time)	126:127 (yield)[b]
1	$Cu(ClO_4)_2 \cdot 6H_2O$	air	toluene /EtOAc	80 °C (1 h)	3.0:1.0 (74%)
2	$Cu(ClO_4)_2 \cdot 6H_2O$	air	EtOAc	reflux (3 h)	1.7:1.0 (56%)
3	$Cu(OTf)_2$	$HClO_4/N_2$[c]	toluene /EtOAc	80 °C (6 h)	1.0:1.0[d]
4	$Cu(OTf)_2$	$NaClO_4/N_2$[c]	toluene	80 °C (6 h)	1.0:1.0[d]
5	$Cu(OTf)_2$	$Mg(ClO_4)_2/N_2$[c]	toluene	80 °C (6 h)	1.0:1.0[d]
6	$Cu(OTf)_2$	$Bu_4N(ClO_4)/N_2$[c]	toluene	80 °C (3 h)	2.5:1.0 (90%)
7	$Cu(OTf)_2$	$Bu_4N(ClO_4)$/air	toluene	80 °C (1.5 h)	2.6:1.0 (78%)

[a] 20 mol% catalyst. [b] Combined yield of **126**/**127**. [c] 1 atm. [d] Ratio determined by ^1H NMR analysis.

Satisfied with the copper(II) triflate/tetrabutylammonium perchlorate reaction conditions, we sought to evaluate the influence of substitution on both the migratory group and the indole (Scheme 3.19). To evaluate the compatibility of the Michael adducts in optimized reaction conditions, we first assessed the effect of substitution on the *para*-position of the aryl migratory group (Scheme 3.19A). The results indicate a relationship between the electronic property of the substituent and the selectivity in the annulation process. For instance, the (*p*-OMe)-phenylindole analog **103** exhibits complete selectivity in annulation, yielding carbazole isomer **128** with a 75% yield. While when a strong electron withdrawing group (EWG) like NO_2 (**106**) is present in

the starting material, the annulation produces **134** in a slight excess compared to **133**, with a ratio of 1.6:1.0. These findings highlight the significance of the migratory group in determining the selectivity of the annulation process, which probably is attributed to the enhanced stabilization of the spiro cyclic indolenine intermediate (**74**, Scheme 3.13). A migratory group with higher electron density promotes the occurrence of C–C cleavage through the 1,2-migratory shift (path a, Scheme 3.13).

Next, we examined the impact of substitution on the benzenoid ring of the indole (C5 or C6) (Scheme 3.19B), which revealed a decrease in formation of the desired carbazole. Although the outcome showed the substitution had little impact on the yield of the annulation process (ranging from 75% to 87%), it displayed a moderate influence on the selectivity of the reaction (Scheme 3.19B, **135**-**144**) with the exception of C6-NO_2 substituted substrate (**101**). It is known in the literature that benzenoid substitution on indole can display some influence in diazo-insertion reactions, however, the exact cause for the observed decrease in selectivity remains uncertain.[22]

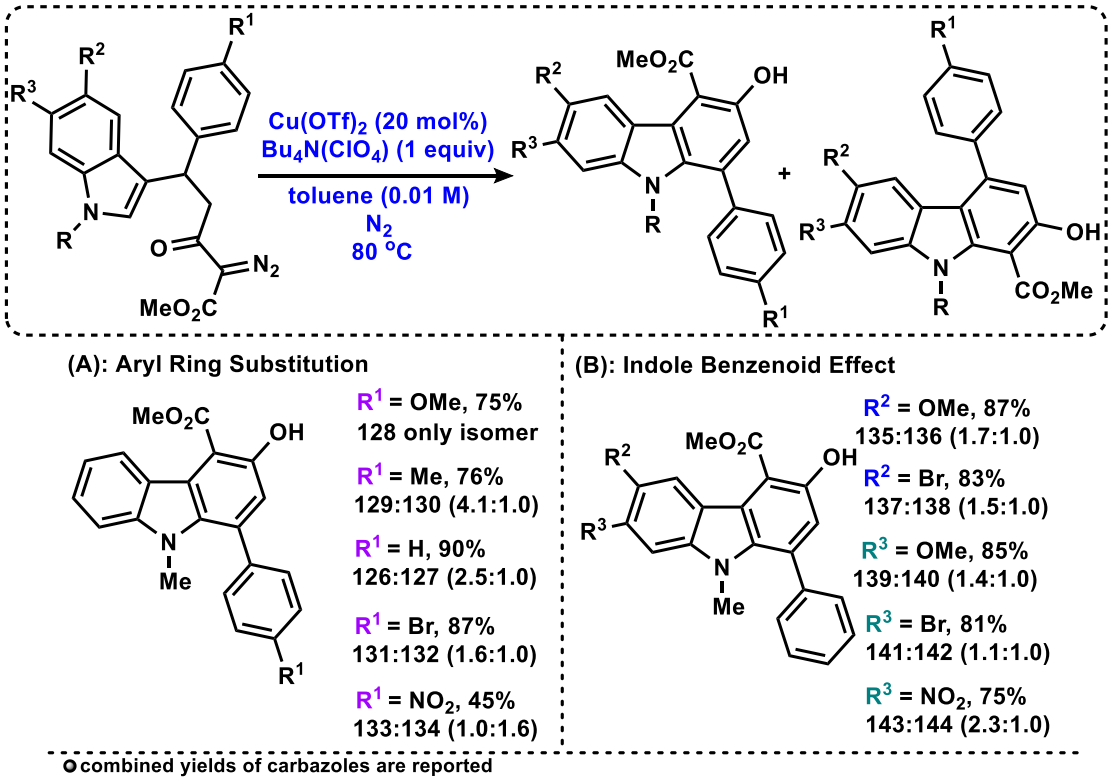

Scheme 3.19: The effect of substitution on the annulation.

Among the notable factors influencing the selectivity of annulation observed in our study, one of the most significant was the substitution on the nitrogen atom of indole (Scheme 3.20). The *N*-alkylated indoles demonstrated a remarkable preference for annulation, particularly when *N*-benzyl substitution was present, resulting in the highest selectivity (4.4:1.0, **145**:**70**). In contrast, when a weak withdrawing aryl group was substituted on the indole nitrogen, a complete reversal of annulation selectivity was observed (1.0:1.7, **146:147**). Under optimized conditions, the reaction of **114** underwent loss of the Boc group, resulting in a mixture of **71** and **70** with a ratio of 1.0:2.0. Surprisingly, the absence of substituent on the indole substrate resulted in inversion of annulation selectivity and provided carbazoles **71** and **70** in a 1.0:2.8 ratio.

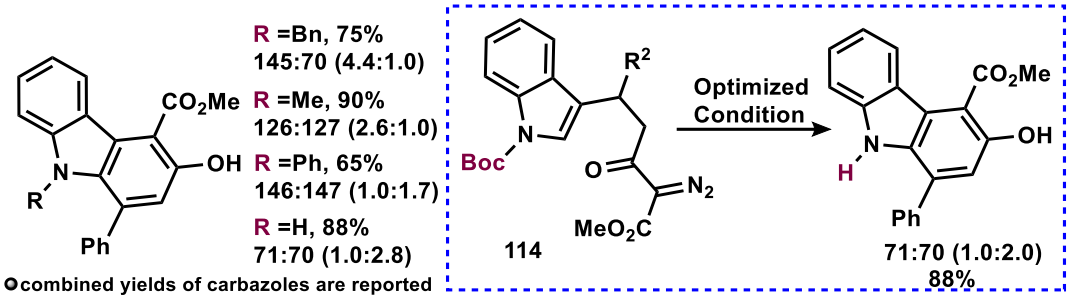

Scheme 3.20: The effect of nitrogen substitution on the annulation.

Since the selectivity of this annulation is influenced by the reaction condition, it is important to note that the rhodium catalysis studies of the Doyle group revealed that the reaction of substrate **69** delivered only the dihydrocarbazole of isomer **70**, a result that highlights the importance of the copper catalyst in the selectivity of the reaction (Scheme 3.21A). Another experiment which also affirms the selectivity of cyclization is critically influenced by the choice of ligand is shown in Scheme 3.21B. Employing indole substrate **69** and utilization of $Cu(OTf)_2$ resulted in formation of **70** in a higher ratio compared to the rearranged carbazole (1.0:4.5, **71:70**). While exploiting the perchlorate additive in the optimized condition reduced the formation of **70** and resulted in the construction of **71** (1.0:2.8, **71:70**) compared to $Cu(OTf)_2$ experiment (Scheme 3.20).

Regarding the importance of catalyst in the selectivity of the annulation process, we carried out an additional control experiment in small scales to further support our findings (Scheme 3.21C). The experiment initiated by employing the substrate **103**

under the annulation conditions established by Doyle,[16] which, upon oxidation, yielded a mixture consisting of **128** and **128′** in a ratio of 5:1. This outcome indicates a significant decrease in selectivity compared to our optimized condition, since in the presence of $Cu(OTf)_2$/perchlorate the **128′** is not formed. Although the sequence cannot directly be compared to the copper conditions due to variations in solvents and temperatures, the results show that while the migratory group's nature plays a vital role, the choice of catalyst also exerts a substantial influence on controlling selectivity.

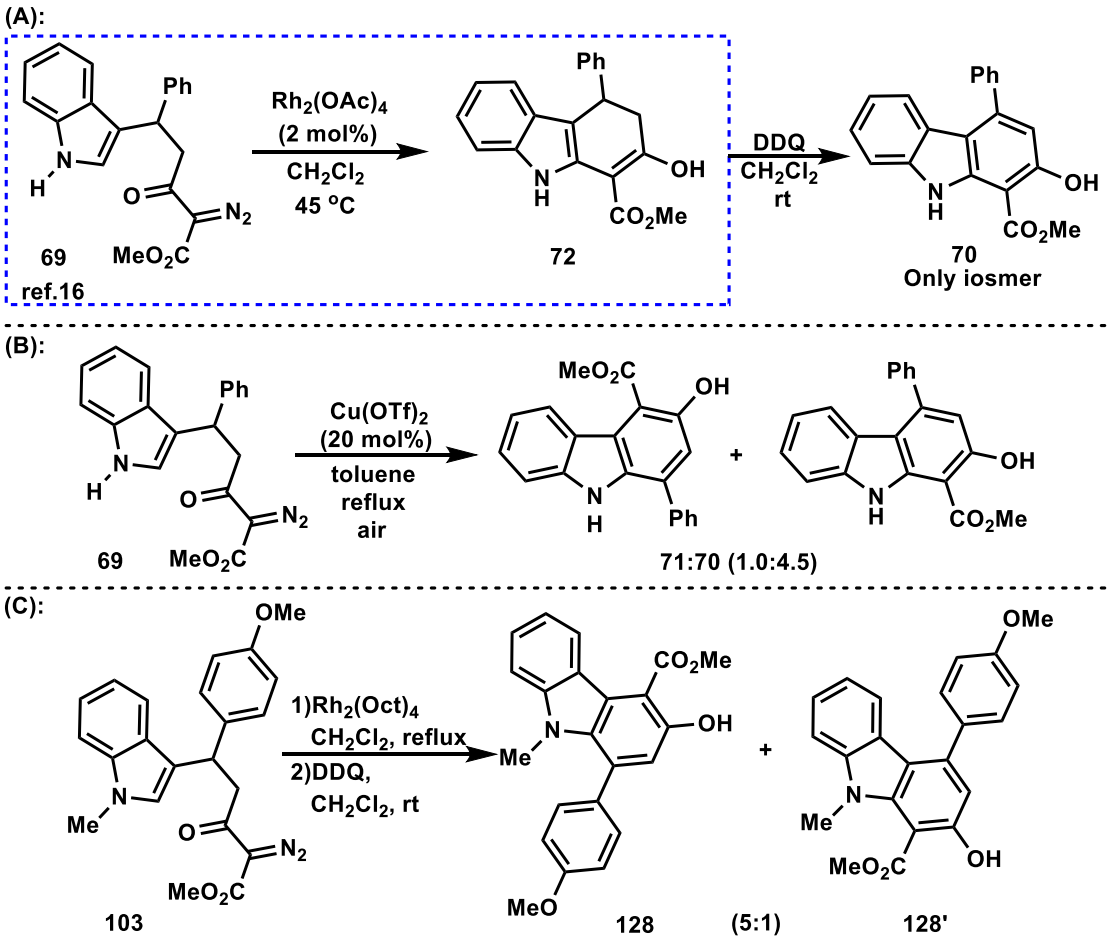

Scheme 3.21: Effect of catalyst in annulation selectivity.

Another experiment which revealed the influence of substitution on nitrogen indole was when we performed a reaction by subjecting indole substrate **148** in the optimized condition. Unlike the reaction with **103**, which yielded the rearranged carbazole **128** as the only isomer (Scheme 3.19), employing the substrate **148** resulted in an 85% yield of a mixture of carbazoles **149** and **150**. Although the major isolated compound remained the rearranged isomer (**149**), a significant decrease in selectivity

was observed, with a ratio of 1.6:1.0, compared to the **103** substrate (Scheme 3.22). This outcome emphasized the significance of *N*-substitution in the selectivity of the annulation process.

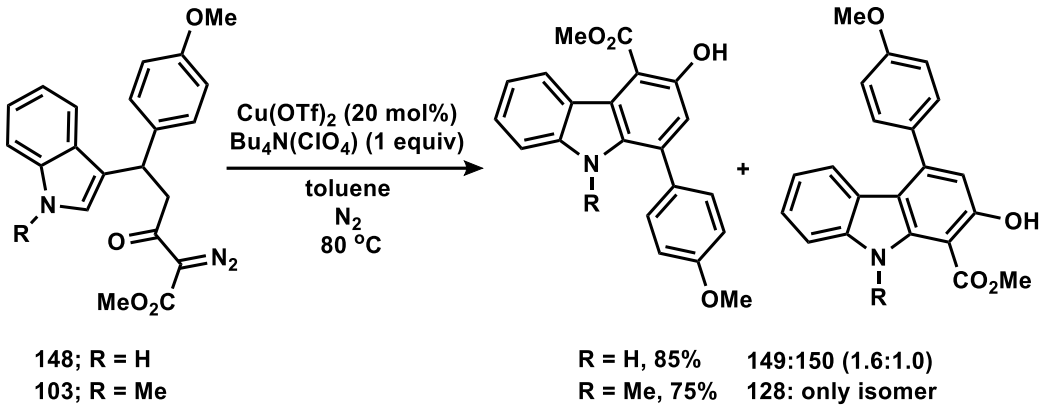

Scheme 3.22: Comparison of substrate **148** and **103** in the selectivity of annulation.

3.7 Expansion of Substrate Scope

Following our successful achievement over the selectivity of formation of the rearranged carbazole isomers, we proceeded to expand our substrate scope. In these experiments the indolyl α-diazocarbonyl substrates with substituents at multiple positions, a) benzenoid position b) migratory group c) nitrogen of indole, were subjected to optimized reaction conditions. The aim of these types of experiments was to identify which substitution location had the greatest influence on the selectivity of the annulation reaction (Table 3.5). To achieve this, the positions of the substituents were varied at the benzenoid position and migratory group of the indolyl α-diazocarbonyl substrates, and the results are summarized for various in Table 3.5.

As expected, based on the preliminary results (Scheme 3.19), regardless of the substitution on the benzenoid ring, when the aryl migratory group is substituted with an electron donating group, the selectivity of the annulation strongly favors the rearranged product (Table 3.5, **151**, **152**, **154**, and **158**). Furthermore, it is observed that some substrates containing electron rich aryl migratory groups, like **159**, **164**, and **167**, exhibited lower yields of the rearranged carbazole. Ultimately, we proposed that the reduced yields or selectivity observed in some of these cases can be attributed to competitive reaction pathways, resulting in the formation of undesired products.

Table 3.5: Reaction Substrate Scope

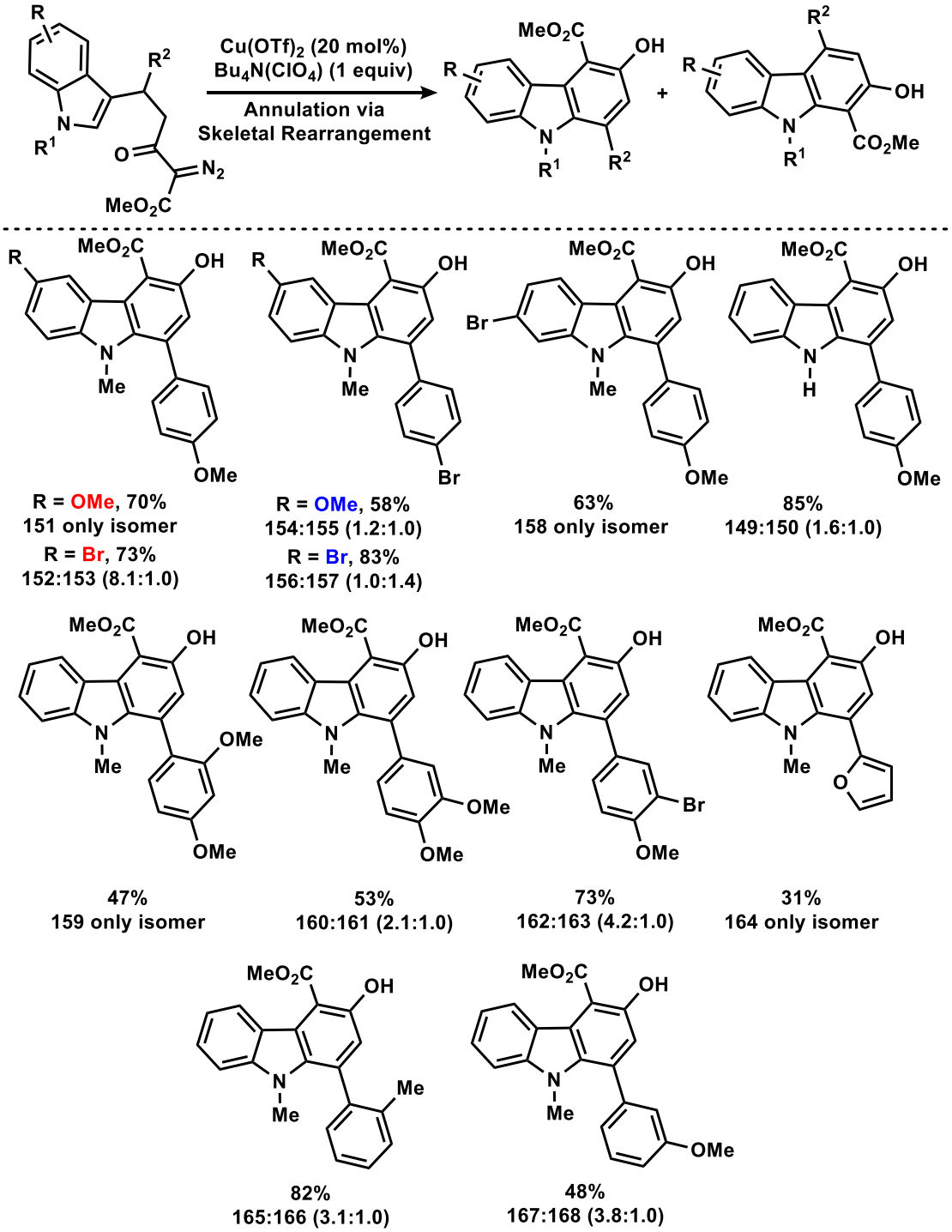

During multiple experiments, when an electron donating group (EDG) was substituted to the aryl migratory group, a complex mixture of unknown compounds was obtained alongside the desired carbazoles. Efforts to separate and analyze these mixtures proved extremely challenging, with one exception: the reaction involving **104**

(Scheme 3.23). Apart from carbazoles **129** and **130**, two naphthalene products (**170** and **171**) were also isolated from this reaction. It appears that the diazo carbon interacts with the aryl ring (path b) instead of the indole (path a), resulting in the formation of the proposed spirocyclic intermediate **169**. Doyle and colleagues also observed a similar outcome, where an indole-substituted dihydronaphthalene was obtained. However, unlike Doyle's work with rhodium, the copper-catalyzed conditions used in this study resulted in the elimination of the indole leading to a mixture of compounds **170** and **171**. Therefore, we concluded that the lower yields observed in **159**, **164**, and **167** (Table 3.5) could be attributed to the competitive reaction of the diazo piece with the aryl ring.

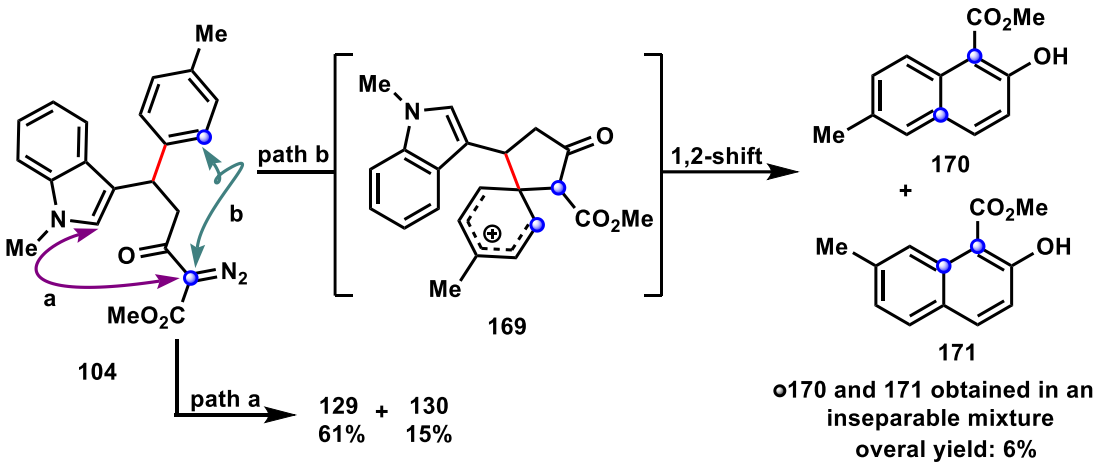

Scheme 3.23: Naphthalene side-product formation via spirocyclic intermediate.

In addition to the generation of naphthalene products, a distinct carbazole isomer (**172**) was detected among the mixtures of side-products in various annulation reactions. By subjecting compound **111** to prolonged heating with $Sc(OTf)_3$ in the presence of air (Scheme 3.24), analytically pure **172** was isolated. This carbazole is believed to originate from a Wolff rearrangement, which is known in the literature.[14] It is worth noting that carbazole **172** was obtained as one of the major products alongside **126** and **127** in the scandium catalyzed reaction, while the copper catalyzed annulation yielded only trace amounts, if any of this product.

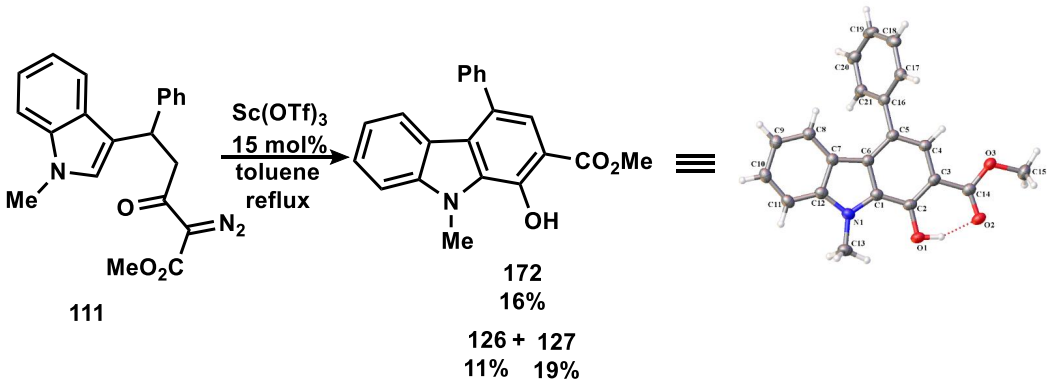

Scheme 3.24: Wolff rearrangement product via scandium catalyzed reaction.

3.8 Conclusion

In conclusion, to control the selectivity of the annulation reaction over the rearranged carbazole product, several contributing factors have been identified. The optimization studies revealed that the appropriate catalyst and ligand system exerted a significant influence. As our investigations progressed, it became evident that, in addition to the catalyst, the electronic properties of different substituents could influence this selectivity. The most profound effect was found to be attributed to the substituent of nitrogen indole, although the electronic properties of the migratory group demonstrated a vital role.

3.9 Experimental

3.9.1 General Procedure

Unless stated otherwise, all reactions were performed in oven- or flame-dried glassware under an atmosphere of dry nitrogen. Dry acetonitrile, dichloromethane, and toluene were obtained by passing these previously degassed solvents through activated alumina columns. *N,N*-dimethylformamide (DMF) was obtained from Sigma Aldrich SureSeal™ bottles. All other reagents were used as received from commercial sources, unless stated otherwise. When indicated, solvents or reagents were degassed by sparging with Argon for 10 minutes in an ultrasound bath at 25 °C. Silicon oil bath was used as the heat source for the reactions performing above room temperature. Reactions were monitored by thin layer chromatography (TLC) on Silicycle Siliaplate™ glass-backed TLC plates (250 μm thickness, 60 Å porosity, F-254 indicator) and visualized by UV irradiation or development with anisaldehyde stain. Volatile solvents were removed under reduced pressure with a rotary evaporator. All flash column chromatography was performed using Silicycle SiliaFlash® F60, 230-400 mesh silica gel (40-63 μm). ^{1}H NMR and ^{13}C NMR spectra were recorded with Bruker AV, spectrometers operating at 300 or 500 MHz for ^{1}H (75, and 125 MHz for ^{13}C) in chloroform-d ($CDC1_3$). Chemical shifts are reported relative to the residual solvent signal (^{1}H NMR: δ = 7.26 ($CDCl_3$), ^{13}C NMR: δ = 77.16 ($CDCl_3$)). NMR data are reported as follows: chemical shift (multiplicity, coupling constants where applicable, number of hydrogens). Splitting is reported with the following symbols: s = singlet, br. s = broad singlet, d = doublet, t = triplet, app t = apparent triplet, dd = doublet of doublets, ddd = doublet of doublet of doublets, dddd = doublet of doublet of doublet of doublets, m = multiplet. Infrared (IR) spectra were recorded on Bruker Alpha and Bruker Tensor 27 FT-IR spectrometers. High resolution mass spectrometry (HRMS) data were obtained using an Agilent 6200 series instrument, employing a TOF mass analyzer. Melting Points (M.P.) were obtained in open glass capillaries on an OptiMelt instrument (a digital apparatus) produced by Stanford Research Systems by scanning temperature ranges from 70 °C to 250 °C at a rate of 10 °C/s.

3.9.2 Synthesis and Characterization of Indolyl *α*-Diazocarbonyls Starting Materials:

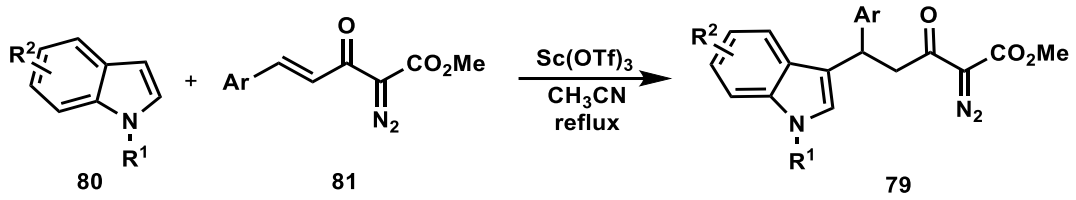

General Experimental Procedure A:

In a round bottom flask equipped with a magnetic stir bar, *N*-substituted indole derivatives (1.1-2 equiv) and diazoacetoacetate enones (1 equiv) were dissolved in CH_3CN (8 mL/mmol of indole). $Sc(OTf)_3$ (0.1-0.2 equiv) was added, and reaction mixture was refluxed until was considered complete as determined by TLC analysis. Then solvent was evaporated under reduced pressure, and the crude residue was purified by silica gel flash column chromatography using a hexanes/EtOAc gradient to give the corresponding indolyl *α*-diazocarbonyl starting materials.

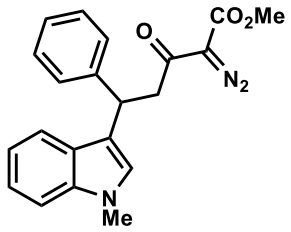

111

Product **111** was prepared following General Experimental Procedure **A**. 1-Methylindole **73** (0.600 g, 4.57 mmol), DAAE **62** (0.955 g, 4.15 mmol), scandium(III) triflate (0.204 g, 0.415 mmol). Product **111** (0.994 g, 2.75 mmol, 66%) was obtained as a cream solid:

***R*f** = 0.32, 20% EtOAc in hexanes;
M.P. = 124-127 ºC
^{1}H NMR (300 MHz, $CDCl_3$) δ = 7.47 (app dt, *J* = 8.0, 1.0 Hz, 1H),7.37 – 7.34 (m, 2H), 7.28 – 7.22 (m, 3H), 7.19 – 7.12 (m, 2H), 7.00 (ddd, *J* = 8.0, 6.9, 1.2 Hz, 1H), 6.91 (br. s, 1H), 4.95 (app t, *J* = 7.5 Hz, 1H), 3.82 (s, 3H), 3.73 (s, 3H), 3.72 (dd, *J* = 16.4, 7.8 Hz, 1H), 3.63 (dd, *J* = 16.4, 7.3 Hz, 1H) ppm;
^{13}C NMR (75 MHz, $CDCl_3$) δ = 191.0, 161.9, 144.3, 137.3, 128.5, 128.0, 127.2, 126.4, 126.35, 121.7, 119.7, 119.0, 117.5, 109.2, 52.3, 46.3, 38.2, 32.9 ppm; (diazo carbon not observed presumably due to overlap)
IR (neat): ν_{max} = 3024, 2953, 2140, 1703, 1651, 1601, 1474, 1328, 1206, 1131, 1022, 750, 700 cm^{-1}.
HRMS (APPI+) calc'd for $C_{21}H_{19}N_3O_3$ $[M^+]$ 361.1426, found 361.1437, calc'd for $C_{21}H_{20}N_3O_3$ $[M+H]^+$ 362.1499, found 362.1532.

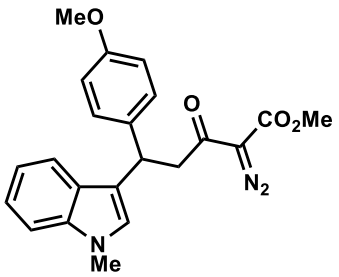

103

Product **103** was prepared following General Experimental Procedure **A**. 1-Methylindole **73** (0.352 g, 2.68 mmol), DAAE **87** (0.349 g, 1.34 mmol), scandium(III) triflate (0.0989 g, 0.201 mmol). Product **103** (0.230 g, 0.588 mmol, 44%) was obtained as an orange foam:

***R*f** = 0.21, 20% EtOAc in hexanes;
^{1}H NMR (300 MHz, $CDCl_3$) δ = 7.46 (app dt, *J* = 7.9, 1.0 Hz, 1H), 7.29 – 7.22 (m, 3H), 7.16 (ddd, *J* = 8.2, 6.9, 1.2 Hz, 1H), 7.00 (ddd, *J* = 8.0, 6.9, 1.2 Hz, 1H), 6.90 (br. s, 1H), 6.81 – 6.76 (m, 2H), 4.90 (apt. t, *J* = 7.5 Hz, 1H), 3.82 (s, 3H), 3.75 (s, 3H), 3.73 (s, 3H), 3.64 (dd, *J* = 17.5, 7.6 Hz, 1H), 3.59 (dd, *J* = 16.2, 7.1 Hz, 1H) ppm;
^{13}C NMR (75 MHz, $CDCl_3$) δ = 191.1, 161.9, 158.0, 137.3, 136.4, 128.9, 127.1, 126.3, 121.7, 119.7, 118.9, 117.9, 113.8, 109.2, 76.4, 55.3, 52.3, 46.4, 37.5, 32.8 ppm;
IR (neat): ν_{max} = 3026, 2951, 2132, 1712, 1649, 1601, 1475, 1307, 1204, 1126, 1042, 790, 743 cm^{-1}.
HRMS (APPI+) calc'd for $C_{22}H_{21}N_3O_4$ [M^+] 391.1532, found 391.1549, calc'd for $C_{22}H_{22}N_3O_4$ [M+H]$^+$ 392.1605, found 392.1616.

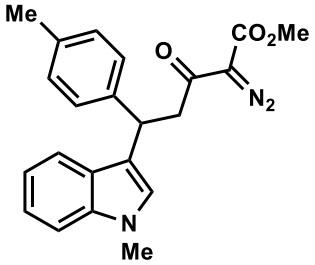

104

Product **104** was prepared following General Experimental Procedure **A**. 1-Methylindole **73** (0.352 g, 2.68 mmol), DAAE **88** (0.327 g, 1.34 mmol), scandium(III) triflate (0.099 g, 0.20 mmol). Product **104** (0.188 mg, 0.501 mmol, 37%) was obtained as a yellow solid:

***R*f** = 0.52, 30% EtOAc in hexanes;
M.P. = 98-100 ºC
^{1}H NMR (300 MHz, $CDCl_3$) δ = 7.48 (app dt, *J* = 7.9, 1.0 Hz, 1H), 7.27 – 7.22 (m, 3H), 7.16 (ddd, *J* = 8.2, 6.9, 1.1 Hz, 1H), 7.08 – 7.03 (m, 2H), 7.01 (ddd, *J* = 8.0, 6.9, 1.2 Hz, 1H), 6.90 (br. s, 1H), 4.92 (app t, *J* = 7.6 Hz, 1H), 3.82 (s, 3H), 3.72 (s, 3H), 3.71 (dd, *J* = 16.2, 8.1 Hz, 1H), 3.61 (dd, *J* = 16.5, 7.2 Hz, 1H), 2.27 (s, 3H) ppm;
^{13}C NMR (75 MHz, $CDCl_3$) δ = 191.1, 161.9, 141.3, 137.3, 135.8, 129.2, 127.8, 127.2, 126.3, 121.7, 119.7, 118.9, 117.8, 109.2, 76.5, 52.3, 46.4, 37.8, 32.8, 21.2 ppm;
IR (neat): ν_{max} = 2900, 2139, 1707, 1655, 1430, 1313, 1207, 1135, 841, 768, 721 cm^{-1}.
HRMS (APPI+) calc'd for $C_{22}H_{21}N_3O_3$ [M^+] 375.1583, found 375.1594.

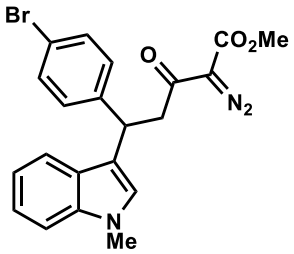

105

Product **105** was prepared following General Experimental Procedure **A**. 1-Methylindole **73** (0.220 g, 1.68 mmol), DAAE **89** (0.473 g, 1.53 mmol), scandium(III) triflate (0.0753 g, 0.153 mmol). Product **105** (0.415 g, 0.943 mmol, 62%) was obtained as a beige solid:

***R*f** = 0.41, 30% EtOAc in hexanes;
M.P. = 129-132 °C
^{1}H NMR (300 MHz, $CDCl_3$) δ = 7.41 (app dt, *J* = 7.9, 1.0 Hz, 1H), 7.37 – 7.34 (m, 2H), 7.27 – 7.22 (m, 3H), 7.20 – 7.15 (m, 1H), 7.01 (ddd, *J* = 8.0, 6.9, 1.1 Hz, 1H), 6.91 (s, 1H), 4.91 (apt. t, *J* = 7.5 Hz, 1H), 3.83 (s, 3H), 3.74 (s, 3H), 3.72 (dd, *J* = 16.5, 8.1 Hz, 1H), 3.58 (dd, *J* = 16.5, 6.9 Hz, 1H) ppm;
^{13}C NMR (75 MHz, $CDCl_3$) δ = 190.7, 161.9, 143.5, 137.4, 131.5, 129.8, 127.0, 126.4, 121.9, 120.1, 119.5, 119.1, 117.0, 109.3, 76.5, 52.3, 46.0, 37.7, 32.9 ppm;
IR (neat): ν_{max} = 2922, 2135, 1715, 1652, 1402, 1320, 1205, 1130, 1074, 996, 797, 739 cm^{-1}.
HRMS (APPI+) calc'd for $C_{21}H_{18}{}^{79}BrN_3O_3$ [M^+] 439.0532, found 439.0549.

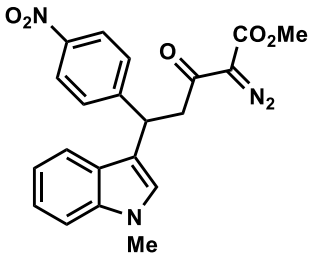

106

Product **106** was prepared following General Experimental Procedure **A**. 1-Methylindole **73** (0.103 g, 0.785 mmol), DAAE **102** (0.197 g, 0.714 mmol), scandium(III) triflate (0.035 g, 0.072 mmol). Product **106** (0.260 g, 0.640 mmol, 89%) was obtained as an orange color solid:

***R*f** = 0.27, 30% EtOAc in hexanes;
M.P. = 153-158 °C
^{1}H NMR (300 MHz, $CDCl_3$) δ = 8.12 – 8.07 (m, 2H), 7.54 – 7.50 (m, 2H), 7.37 (app dt, *J* = 8.0, 1.0 Hz, 1H), 7.27 (apt. dt, *J* = 8.3, 1.0 Hz, 1H), 7.19 (ddd, *J* = 8.2, 7.0, 1.1 Hz, 1H), 7.02 (ddd, *J* = 8.0, 6.9, 1.1 Hz, 1H), 6.97 (br. s, 1H), 5.05 (app t, *J* = 7.5 Hz, 1H), 3.84 (s, 3H), 3.76 (dd, *J* = 16.7, 8.2 Hz, 1H), 3.76 (s, 3H), 3.64 (dd, *J* = 16.7, 6.8 Hz, 1H) ppm;
^{13}C NMR (75 MHz, $CDCl_3$) δ = 190.2, 161.9, 152.3, 146.6, 137.4, 128.9, 126.8, 126.4, 123.8, 122.2, 119.4, 119.2, 116.0, 109.5, 76.5, 52.4, 45.8, 38.1, 32.9 ppm;
IR (neat): ν_{max} = 3039, 2950, 2130, 1713, 1655, 1601, 1514, 1375, 1265, 1127, 737, 701 cm^{-1}.
HRMS (APPI+) calc'd for $C_{21}H_{18}N_4O_5$ [M^+] 406.1277, found 406.1274.

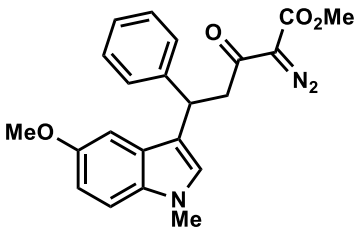

96

Product **96** was prepared following General Experimental Procedure **A**. 5-Methoxy-1-methylindole **90** (0.161 g, 0.999 mmol), DAAE **62** (0.192 g, 0.833 mmol), scandium(III) triflate (0.041 g, 0.083 mmol). Product **96** (0.129 g, 0.330 mmol, 40%) was obtained as a dark yellow foam:

R_f = 0.28, 20% EtOAc in hexanes;
^{1}H NMR (300 MHz, $CDCl_3$) δ = 7.36 (dd, *J* = 8.1, 1.3 Hz, 2H), 7.28 – 7.23 (m, 2H), 7.18 – 7.11 (m, 2H), 6.91 (d, *J* = 2.3 Hz, 1H), 6.87 (s, 1H), 6.82 (dd, *J* = 8.8, 2.5 Hz, 1H), 4.89 (app t, *J* = 7.6 Hz, 1H), 3.82 (s, 3H), 3.76 (s, 3H), 3.71 – 3.59 (m, 2H), 3.69 (s, 3H) ppm; (multiplet signal starting at 3.71 ppm overlaps with methyl singlet signal at 3.69 ppm)
^{13}C NMR (75 MHz, $CDCl_3$) δ = 191.1, 161.9, 153.7, 144.2, 132.8, 128.5, 128.0, 127.5, 127.0, 126.4, 117.0, 111.9, 110.0, 101.7, 56.0, 52.3, 46.2, 38.3, 33.0 ppm; (diazo carbon not observed presumably due to overlap)
IR (neat): ν_{max} = 2921, 2133, 1714, 1650, 1576, 1489, 1306, 1209, 1158, 1047, 793, 744 cm^{-1}.
HRMS (APPI+) calc'd for $C_{22}H_{21}N_3O_4$ $[M^+]$ 391.1532, found 391.1515, calc'd for $C_{22}H_{22}N_3O_4$ $[M+H]^+$ 392.1605, found 392.1604.

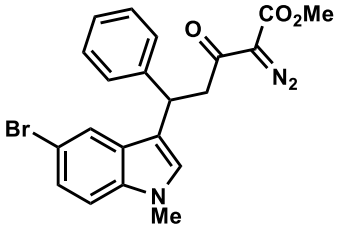

98

Product **98** was prepared following General Experimental Procedure **A**. 5-Bromo-1-methylindole **92** (0.602 g, 2.87 mmol), DAAE **62** (0.332 g, 1.44 mmol), scandium(III) triflate (0.106 g, 0.216 mmol). Product **96** (0.380 g, 0.863 mmol, 60 %) was obtained as an orange foam:

R_f = 0.21, 20% EtOAc in hexanes;
^{1}H NMR (300 MHz, $CDCl_3$) δ = 7.57 (dd, *J* = 1.8, 0.6 Hz, 1H), 7.34 – 7.20 (m, 5H), 7.19 – 7.13 (m, 1H), 7.07 (d, *J* = 8.6 Hz, 1H), 6.91 (br. s, 1H), 4.87 (app t, *J* = 7.5 Hz, 1H), 3.82 (s, 3H), 3.67 (dd, *J* = 16.4, 7.6 Hz, 1H), 3.67 (s, 3H), 3.59 (dd, *J* = 16.4, 7.5 Hz, 1H) ppm;
^{13}C NMR (75 MHz, $CDCl_3$) δ = 190.7, 161.9, 143.8, 136.0, 128.8, 128.6, 127.9, 127.6, 126.5, 124.6, 122.1, 117.2, 112.4, 110.8, 76.4, 52.3, 46.2, 38.0, 33.0 ppm;
IR (neat): ν_{max} = 3059, 2949, 2132, 1711, 1648, 1474, 1307, 1199, 1126, 742, 699 cm^{-1}.
HRMS (APPI+) calc'd for $C_{21}H_{18}{}^{79}BrN_3O_3$ $[M^+]$ 439.0532, found 439.0510, calc'd for $C_{21}H_{19}{}^{81}BrN_3O_3$ $[M+H]^+$ 442.0604, found 442.0611.

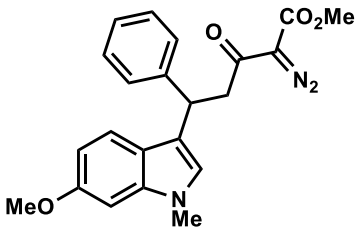

97

Product **97** was prepared following General Experimental Procedure **A**. 6-Methoxy-1-methylindole **91** (0.141 g, 0.875 mmol), DAAE **62** (0.183 g, 0.795 mmol), scandium(III) triflate (0.039 g, 0.080 mmol). Product **97** (0.236 g, 0.603 mmol, 76%) was obtained as a red foam:

***R*f** = 0.25, 20% EtOAc in hexanes;
^{1}H NMR (300 MHz, $CDCl_3$) δ = 7.36 – 7.32 (m, 2H), 7.31 (dd, *J* = 8.3, 0.8 Hz, 1H), 7.29 – 7.21 (m, 2H), 7.17 – 7.11 (m, 1H), 6.80 (d, *J* = 0.9 Hz, 1H), 6.71 – 6.64 (m, 2H), 4.90 (app t, *J* = 7.5 Hz, 1H), 3.83 (s, 3H), 3.82 (s, 3H), 3.66 (s, 3H), 3.68 (dd, *J* = 16.4, 7.6 Hz, 1H), 3.61 (dd, *J* = 16.4, 7.3 Hz, 1H) ppm;
^{13}C NMR (75 MHz, $CDCl_3$) δ = 191.0, 161.9, 156.5, 144.4, 138.1, 128.5, 128.0, 126.4, 125.3, 121.7, 120.3, 117.6, 108.8, 93.0, 76.4, 55.8, 52.3, 46.3, 38.3, 32.8 ppm;
IR (neat): ν_{max} = 3028, 2950, 2125, 1716, 1651, 1622, 1435, 1307, 1220, 1135, 1068, 748, 701 cm^{-1}.
HRMS (APPI+) calc'd for $C_{22}H_{21}N_3O_4$ [M^+] 391.1532, found 391.1520, calc'd for $C_{22}H_{22}N_3O_4$ [M+H]$^+$ 392.1605, found 392.1591.

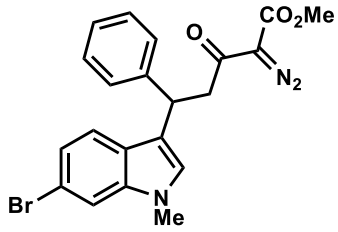

99

Product **99** was prepared following General Experimental Procedure **A**. 6-Bromo-1-methylindole **93** (0.180 g, 0.857 mmol), DAAE **62** (0.179 g, 0.779 mmol), scandium(III) triflate (0.038 g, 0.078 mmol). Product **99** (0.147 g, 0.334 mmol, 43%) was obtained as a pale yellow solid:

***R*f** = 0.41, 30% EtOAc in hexanes;
M.P. = 90-93 °C
^{1}H NMR (300 MHz, $CDCl_3$) δ = 7.39 (d, *J* = 1.4 Hz, 1H), 7.34 – 7.26 (m, 4H), 7.25 – 7.22 (m, 1H), 7.18 – 7.12 (m, 1H), 7.08 (dd, *J* = 8.5, 1.7 Hz, 1H), 6.90 (d, *J* = 0.7 Hz, 1H), 4.90 (app t, *J* = 7.5 Hz, 1H), 3.82 (s, 3H), 3.73 – 3.63 (m, 2H), 3.69 (s, 3H) ppm; (multiplet signal starting at 3.73 ppm overlaps with methyl singlet signal at 3.69 ppm)
^{13}C NMR (75 MHz, $CDCl_3$) δ = 190.8, 161.9, 144.0, 138.2, 128.6, 127.9, 127.0, 126.5, 126.1, 122.2, 121.0, 117.9, 115.6, 112.3, 52.3, 46.2, 38.1, 33.0 ppm; (diazo carbon not observed presumably due to overlap)
IR (neat): ν_{max} = 3029, 2952, 2121, 1724, 1651, 1605, 1438, 1304, 1257, 1207, 1045, 911, 774, 588 cm^{-1}.
HRMS (APPI+) calc'd for $C_{21}H_{18}{}^{79}BrN_3O_3$ [M^+] 439.0532, found 439.0514.

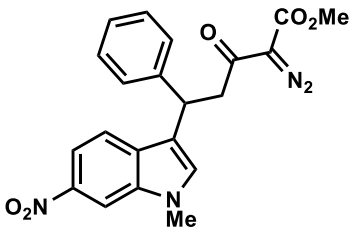

101

Product **101** was prepared following General Experimental Procedure **A**. 6-Nitro-1-methylindole **95** (0.430 g, 2.44 mmol), DAAE **62** (0.281 g, 1.22 mmol), scandium(III) triflate (0.0901 g, 0.183 mmol). Product **101** (0.113 g, 0.278 mmol, 23%) was obtained as an orange solid:

R_f = 0.27, 30% EtOAc in hexanes;
^{1}H NMR (300 MHz, $CDCl_3$) δ = 8.24 (d, *J* = 2.0 Hz, 1H), 7.90 (dd, *J* = 8.8, 2.0 Hz, 1H), 7.48 (d, *J* = 8.8 Hz, 1H), 7.34 – 7.24 (m, 5H), 7.22 – 7.16 (m, 1H), 4.95 (app t, *J* = 7.5 Hz, 1H), 3.85 – 3.66 (m, 2H), 3.85 (s, 6H) ppm;
^{13}C NMR (75 MHz, $CDCl_3$) δ = 190.6, 161.9, 143.5, 143.2, 135.9, 132.1, 131.7, 128.7, 127.8, 126.8, 119.6, 118.9, 114.6, 106.4, 76.5, 52.4, 46.0, 37.9, 33.3 ppm;
IR (neat): ν_{max} = 2953, 2136, 1715, 1651, 1506, 1435, 1334, 1303, 1128, 1048, 734, 701 cm^{-1}.
HRMS (APPI+) calc'd for $C_{21}H_{18}N_4O_5$ [M^+] 406.1277, found 406.1314.

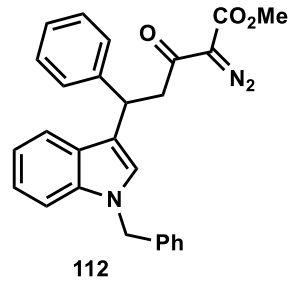

112

Product **112** was prepared following General Experimental Procedure **A**. 1-Benzylindole **109** (0.603 g, 2.91 mmol), DAAE **62** (0.373 g, 1.62 mmol), scandium(III) triflate (0.120 g, 0.243 mmol). Product **112** (0.555 g, 1.27 mmol, 78%) was obtained as a beige solid:

R_f = 0.58, 30% EtOAc in hexanes;
M.P. = 125-128 ºC
^{1}H NMR (300 MHz, $CDCl_3$) δ = 7.47 (app dt, *J* = 7.9, 1.0 Hz, 1H), 7.38 – 7.34 (m, 2H), 7.28 – 7.20 (m, 5H), 7.18 – 7.03 (m, 6H), 6.99 (ddd, *J* = 8.0, 6.9, 1.2 Hz, 1H), 5.26 (s, 2H), 4.97 (app t, *J* = 7.6 Hz, 1H), 3.78 (s, 3H), 3.73 – 3.66 (m, 2H) ppm;
^{13}C NMR (75 MHz, $CDCl_3$) δ = 191.0, 161.9, 144.2, 137.9, 137.1, 128.8, 128.5, 128.1, 127.6, 127.5, 126.7, 126.4, 125.9, 122.0, 119.8, 119.3, 118.2, 109.8, 76.4, 52.3, 50.1, 46.1, 38.5 ppm;
IR (neat): ν_{max} = 3027, 2951, 2134, 1714, 1650, 1602, 1434, 1306, 1194, 1128, 907, 727, 697 cm^{-1}.
HRMS (APPI+) calc'd for $C_{27}H_{23}N_3O_3$ [M^+] 437.1739, found 437.1734.

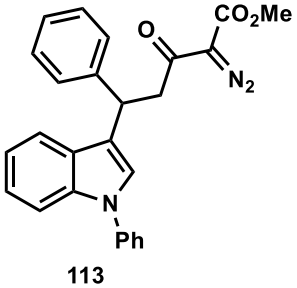

113

Product **113** was prepared following General Experimental Procedure **A**. Indole **110** (0.276 g, 1.43 mmol), DAAE **62** (0.300 g, 1.30 mmol), scandium(III) triflate (0.064 g, 0.13mmol). Product **113** (0.254 g, 0.600 mmol, 46%) was obtained as a white foam:

***R*f** = 0.16, 10% EtOAc in hexanes;
M.P. = 152-154 °C
^{1}H NMR (300 MHz, $CDCl_3$) δ = 7.54 – 7.29 (m, 9H), 7.28 – 7.24 (m, 2H), 7.20 – 7.14 (m, 2H), 7.07 (ddd, *J* = 7.9, 7.1, 1.1 Hz, 1H), 5.02 (app t, *J* = 7.3 Hz, 1H), 3.82 (s, 3H), 3.80 – 7.29 (m, 2H) ppm;
^{13}C NMR (75 MHz, $CDCl_3$) δ = 190.9, 161.9, 143.8, 139.9, 136.4, 129.7, 128.6, 128.3, 128.1, 126.5, 126.3, 125.4, 124.3, 122.7, 120.14, 120.09, 119.9, 110.6, 52.3, 46.1, 38.3 ppm; (diazo carbon not observed presumably due to overlap)
IR (neat): ν_{max} = 3299, 2953, 2138, 1713, 1643, 1592, 1499, 1304, 1213, 1128, 1047, 742, 598 cm^{-1}.
HRMS (APPI+) calc'd for $C_{26}H_{21}N_3O_3$ [M^+] 423.1583, found 423.1590.

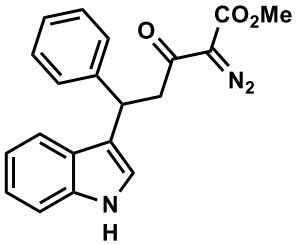

69

Product **69** was prepared following General Experimental Procedure **A**. Indole **1** (0.164 g, 1.40 mmol), DAAE **62** (0.292 g, 1.27 mmol), scandium(III) triflate (0.0625 g, 0.127 mmol). Product **69** (0.284 g, 0.818 mmol, 64%) was obtained as a white solid:

***R*f** = 0.15, 30% EtOAc in hexanes;
M.P. = 152-154 °C
^{1}H NMR (300 MHz, $CDCl_3$) δ = 7.99 (s, 1H), 7.46 (d, *J* = 7.5 Hz, 1H), 7.38 – 7.22 (m, 5H), 7.18 – 7.11 (m, 2H), 7.09 (dd, *J* = 2.5, 0.9 Hz, 1H), 7.01 (ddd, *J* = 8.0, 7.0, 1.1 Hz, 1H), 4.97 (app t, *J* = 7.5 Hz, 1H), 3.82 (s, 3H), 3.70 (d, *J* = 1.2 Hz, 1H), 3.67 (d, *J* = 1.2 Hz, 1H) ppm;
^{13}C NMR (75 MHz, $CDCl_3$) δ = 191.1, 161.9, 144.1, 136.6, 128.5, 128.0, 126.8, 126.4, 122.2, 121.6, 119.6, 119.5, 119.0, 111.2, 52.3, 46.1, 38.3 ppm; (diazo carbon not observed presumably due to overlap)
IR (neat): ν_{max} = 3402, 2952, 2136, 1714, 1636, 1420, 1349, 1263, 1198, 1053, 736, 699, 665 cm^{-1}.
HRMS (APPI+) calc'd for $C_{20}H_{17}N_3O_3$ [M^+] 347.1270, found 347.1264.

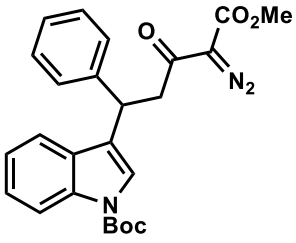

114

Product **114** was prepared by the following procedure: To a stirred solution of indolyl *α*-diazocarbonyls **69** (0.179 g, 0.515 mmol) and DMAP (0.006 g, 0.005 mmol) in THF was added di-*t*-butyl decarbonate (Boc_2O) (0.124 g, 0.567 mmol). The reaction mixture was stirred at room temperature until completion, monitoring by thin layer chromatography, solvent was evaporated under reduced pressure and after purification by column chromatography (EtOAC/Hexanes) **114** (0.213 g, 0.476 mmol, 92%) was obtained as a white solid:

***R*f** = 0.40, 30% EtOAc in hexanes;
M.P. = 131-134 °C

^{1}H NMR (300 MHz, $CDCl_3$) δ = 8.05 (d, *J* = 8.3 Hz, 1H), 7.51 (br. s, 1H), 7.38 – 7.33 (m, 4H), 7.28 – 7.22 (m, 2H), 7.19 – 7.13 (m, 1H), 7.11 (ddd, *J* = 8.1, 7.2, 1.0 Hz, 1H), 4.88 (app t, *J* = 7.4 Hz, 1H), 3.82 (s, 3H), 3.71 (dd, *J* = 16.7, 7.3 Hz, 1H), 3.62 (dd, *J* = 16.7, 7.6 Hz, 1H), 1.67 (s, 9H) ppm;
^{13}C NMR (75 MHz, $CDCl_3$) δ = 190.6, 161.8, 150.0, 142.8, 135.7, 129.9, 128.6, 128.1, 126.8, 124.5, 123.4, 122.6, 122.5, 119.8, 115.3, 83.7, 76.5, 52.4, 45.6, 38.0, 28.4 ppm;
IR (neat): ν_{max} = 2975, 2143, 1730, 1705, 1648, 1454, 1307, 1246, 1201, 1051, 726, 657 cm^{-1}.
HRMS (APPI+) calc'd for $C_{25}H_{25}N_3O_5$ [M^+] 447.1794, found 447.1792.

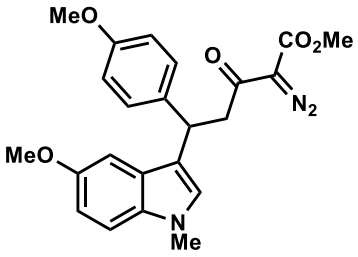

116

Product **116** was prepared following General Experimental Procedure **A**. 5-Methoxy-1-methylindole **90** (0.500 g, 3.10 mmol), DAAE **87** (0.403 g, 1.55 mmol), scandium(III) triflate (0.115 g, 0.233 mmol). Product **116** (0.215 g, 0.510 mmol, 33%) was obtained as a yellow foam:

***R*$_f$** = 0.31, 30% EtOAc in hexanes;
^{1}H NMR (300 MHz, $CDCl_3$) δ = 7.29 – 7.24 (m, 2H), 7.12 (d, *J* = 8.8 Hz, 1H), 6.91 (d, *J* = 2.3 Hz, 1H), 6.85 (s, 1H), 6.85 – 6.77 (m, 3H), 4.84 (app t, *J* = 7.6 Hz, 1H), 3.82 (s, 3H), 3.77 (s, 3H), 3.75 (s, 3H), 3.69 (s, 3H), 3.67 (dd, *J* = 16.2, 8.1 Hz, 1H), 3.59 (dd, *J* = 16.2, 7.1 Hz, 1H) ppm;
^{13}C NMR (75 MHz, $CDCl_3$) δ = 191.2, 161.9, 158.1, 153.7, 136.4, 132.8, 128.9, 127.4, 126.9, 117.4, 113.9, 111.8, 110.0, 101.7, 76.4, 56.0, 55.3, 52.3, 46.3, 37.6, 33.0 ppm;
IR (neat): ν_{max} = 2996, 2950, 2133, 1712, 1650, 1611, 1488, 1302, 1208, 1127, 1033, 792, 727 cm^{-1}.
HRMS (APPI+) calc'd for $C_{23}H_{23}N_3O_5$ [M^+] 421.1638, found 421.1666.

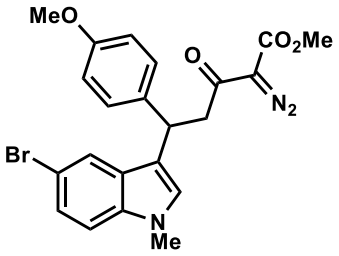

118

Product **118** was prepared following General Experimental Procedure **A**. 5-Bromo-1-methylindole **92** (0.418 g, 1.99 mmol), DAAE **87** (0.260 g, 1.00 mmol), scandium(III) triflate (0.074 g, 0.15 mmol). Product **118** (0.250 g, 0.532 mmol, 53%) was obtained as a yellow foam:

***R*$_f$** = 0.20, 30% EtOAc in hexanes;
^{1}H NMR (300 MHz, $CDCl_3$) δ = 7.57 (d, *J* = 1.9 Hz, 1H), 7.26 – 7.22 (m, 3H), 7.09 (d, *J* = 8.7 Hz, 1H), 6.90 (s, 1H), 6.83 – 6.78 (m, 2H), 4.82 (app t, *J* = 7.6 Hz, 1H), 3.83 (s, 3H), 3.76 (s, 3H), 3.70 (s, 3H), 3.66 – 3.51 (m, 2H) ppm;
^{13}C NMR (75 MHz, $CDCl_3$) δ = 190.9, 161.9, 158.2, 136.0, 135.9, 128.8, 128.8, 127.5, 124.6, 122.1, 117.5, 114.0, 112.4, 110.8, 76.5, 55.3, 52.4, 46.4, 37.3, 33.0 ppm;
IR (neat): ν_{max} = 2951, 2134, 1714, 1651, 1609, 1509, 1475, 1310, 1243, 1175, 1077, 828, 792 cm^{-1}.

HRMS (APPI+) calc'd for $C_{22}H_{20}{}^{79}BrN_3O_4$ [M^+] 469.0637, found 469.0631.

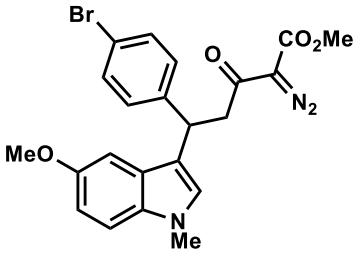

117

Product **117** was prepared following General Experimental Procedure **A**. 5-Methoxy-1-methylindole **90** (0.128 g, 0.794 mmol), DAAE **89** (0.223 g, 0.722 mmol), scandium(III) triflate (0.035 g, 0.072 mmol). Product **117** (0.131 g, 0.279 mmol, 39%) was obtained as a yellow solid:

R_f = 0.30, 30% EtOAc in hexanes;
M.P. = 81-83 ºC
^{1}H NMR (300 MHz, $CDCl_3$) δ = 7.39 – 7.35 (m, 2H), 7.26 – 7.21 (m, 2H), 7.14 (dd, *J* = 8.1, 1.3 Hz, 1H), 6.87 – 6.82 (m, 3H), 4.85 (app t, *J* = 7.5 Hz, 1H), 3.83 (s, 3H), 3.77 (s, 3H), 3.70 (s, 3H), 3.67 (dd, *J* = 16.5, 8.1 Hz, 1H), 3.58 (dd, *J* = 16.5, 7.0 Hz, 1H) ppm;
^{13}C NMR (75 MHz, $CDCl_3$) δ = 190.8, 161.9, 153.8, 143.3, 132.8, 131.5, 129.8, 127.2, 127.0, 120.1, 116.4, 112.0, 110.1, 101.5, 76.5, 56.0, 52.4, 45.9, 37.7, 33.1 ppm;
IR (neat): ν_{max} = 2949, 2135, 1717, 1643, 1489, 1368, 1219, 1137, 1010, 776, 696 cm^{-1}.
HRMS (APPI+) calc'd for $C_{22}H_{20}{}^{79}BrN_3O_4$ [M^+] 469.0637, found 469.0639.

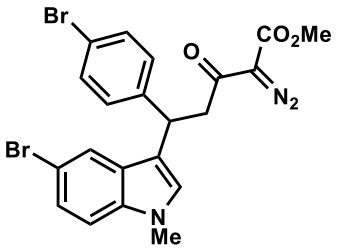

115

Product **115** was prepared following General Experimental Procedure **A**. 5-Bromo-1-methylindole **92** (0.403 g, 1.92 mmol), DAAE **89** (0.297 g, 0.960 mmol), scandium(III) triflate (0.047 g, 0.096 mmol). Product **115** (0.243 g, 0.468 mmol, 49%) was obtained as a yellow solid:

R_f = 0.18, 20% EtOAc in hexanes;
M.P. = 85-88 ºC
^{1}H NMR (300 MHz, $CDCl_3$) δ = 7.53 (d, *J* = 1.9 Hz, 1H), 7.40 – 7.35 (m, 2H), 7.25 – 7.19 (m, 3H), 7.10 (d, *J* = 8.7 Hz, 1H), 6.91 (s, 1H), 4.83 (apt. t, *J* = 7.5 Hz, 1H), 3.84 (s, 3H), 3.70 (s, 3H), 3.63 (dd, *J* = 16.4, 8 Hz, 1H), 3.55 (dd, *J* = 16.4, 7.2 Hz, 1H) ppm;
^{13}C NMR (75 MHz, $CDCl_3$) δ = 190.5, 161.9, 143.0, 136.1, 131.7, 129.7, 128.6, 127.6, 124.8, 121.9, 120.4, 116.6, 112.6, 110.9, 76.5, 52.4, 46.0, 37.5, 33.1 ppm;
IR (neat): ν_{max} = 2950, 2135, 1711, 1649, 1475, 1310, 1251, 1199, 1127, 1008, 790, 728 cm^{-1}.
HRMS (APPI+) calc'd for $C_{21}H_{17}{}^{79}Br_2N_3O_3$ [M^+] 516.9637, found 516.9603.

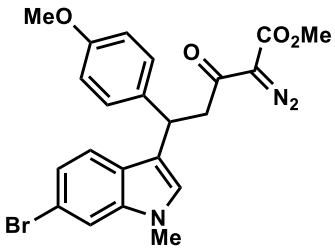

119

Product **119** was prepared following General Experimental Procedure **A**. 6-Bromo-1-methylindole **93** (0.602 g, 2.87 mmol), DAAE **87** (0.497 g, 1.91 mmol), scandium(III) triflate (0.141 g, 0.287 mmol). Product **119** (0.253 g, 0.538 mmol, 28%) was obtained as a yellow foam.

***R*f** = 0.28, 30% EtOAc in hexanes;
^{1}H NMR (300 MHz, $CDCl_3$) δ = 7.39 (d, *J* = 1.7 Hz, 1H), 7.28 (d, *J* = 8.5 Hz, 1H), 7.24 – 7.22 (m, 2H), 7.08 (dd, *J* = 8.5, 1.7 Hz, 1H), 6.88 (s, 1H), 6.81 – 6.76 (m, 2H), 4.85 (app t, *J* = 7.5 Hz, 1H), 3.82 (s, 3H), 3.75 (s, 3H), 3.68 (s, 3H), 3.66 – 3.56 (m, 2H) ppm;
^{13}C NMR (75 MHz, $CDCl_3$) δ = 190.9, 161.9, 158.1, 138.2, 136.1, 128.9, 126.8, 126.0, 122.2, 121.0, 118.2, 115.5, 113.9, 112.3, 76.4, 55.3, 52.3, 46.3, 37.3, 32.9 ppm;
IR (neat): ν_{max} = 2952, 2135, 1713, 1654, 1541, 1435, 1303, 1245, 1129, 1036, 910, 827, 727 cm^{-1}.
HRMS (APPI+) calc'd for $C_{22}H_{20}{}^{79}BrN_3O_4$ [M^+] 469.0637, found 469.0619.

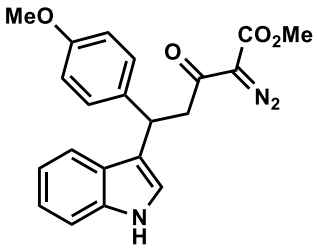

151

Product **148** was prepared following General Experimental Procedure **A**. Indole **1** (0.540 g, 4.61 mmol), DAAE **87** (0.604 g, 2.31 mmol), scandium(III) triflate (0.114 g, 0.231 mmol). Product **148** (0.195 g, 0.517 mmol, 22%) was obtained as a cream color solid:

***R*f** = 0.3, 30% EtOAc in hexanes;
M.P. = 135-138 ºC
^{1}H NMR (300 MHz, $CDCl_3$) δ = 8.03 (s, 1H), 7.44 (d, *J* = 7.9 Hz, 1H), 7.28 – 7.23 (m, 3H), 7.11 (ddd, *J* = 8.2, 7.0, 1.2 Hz, 1H), 7.02 – 7.00 (m, 2H), 6.80 – 6.73 (m, 2H), 4.90 (app t, *J* = 7.5 Hz, 1H), 3.80 (s, 3H), 3.72 (s, 3H), 3.74 – 3.56 (m, 2H) ppm; (multiplet signal starting at 3.74 ppm overlaps with methyl signal at 3.72 ppm)
^{13}C NMR (75 MHz, $CDCl_3$) δ = 191.2, 161.9, 158.0, 136.6, 136.3, 128.9, 126.7, 122.1, 121.5, 119.6, 119.4, 119.2, 113.8, 111.2, 76.5, 55.3, 52.3, 46.3, 37.6 ppm;
IR (neat): ν_{max} = 3378, 3011, 2136, 1707, 1641, 1509, 1435, 1335, 1282, 1133, 1048, 736 cm^{-1}.
HRMS (APPI+) calc'd for $C_{21}H_{19}N_3O_4$ [M^+] 377.1376, found 377.1372.

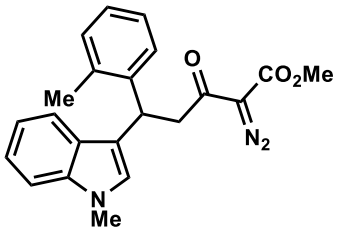

125

Product **125** was prepared following General Experimental Procedure **A**. 1-Methylindole **1** (0.400 g, 3.05 mmol), DAAE (0.413 g, 1.69 mmol), scandium(III) triflate (0.125 g, 0.254 mmol). Product **125** (0.158 g, 0.421 mmol, 25%) was obtained as a yellow solid:

R_f = 0.31, 30% EtOAc in hexanes;
M.P. = 141-144 °C
^{1}H NMR (300 MHz, $CDCl_3$) δ = 7.53 (d, *J* = 7.9 Hz, 1H), 7.32 (dd, *J* = 7.6, 2.0 Hz, 1H), 7.23 – 7.11 (m, 5H), 7.04 (ddd, *J* = 8.0, 6.8, 1.2 Hz, 1H), 6.67 (s, 1H), 5.19 (apt. t, *J* = 7.5 Hz, 1H), 3.81 (s, 3H), 3.72 – 3.64 (m, 2H), 3.69 (s, 3H), 2.42 (s, 3H) ppm; (multiplet signal starting at 3.72 ppm overlaps with methyl singlet signal at 3.69 ppm)
^{13}C NMR (75 MHz, $CDCl_3$) δ = 191.1, 161.9, 142.1, 137.3, 136.2, 130.7, 127.2, 127.1, 126.7, 126.2, 126.1, 121.7, 119.4, 118.9, 117.5, 109.3, 76.4, 52.3, 45.8, 33.6, 32.8, 19.9 ppm;
IR (neat): ν_{max} = 2953, 2142, 1718, 1649, 1458, 1306, 1199, 1154, 1077, 804, 740 cm^{-1}.
HRMS (APPI+) calc'd for $C_{22}H_{21}N_3O_3$ [M^+] 375.1583, found 375.1597.

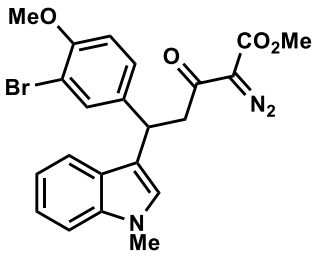

120

Product **120** was prepared following General Experimental Procedure **A**. 1-Methylindole **1** (0.451 g, 3.44 mmol), DAAE (0.583 g, 1.72 mmol), scandium(III) triflate (0.127 g, 0.258 mmol). Product **120** (0.707 g, 1.50 mmol, 87%) was obtained as a yellow foam:

R_f = 0.29, 30% EtOAc in hexanes;
^{1}H NMR (300 MHz, $CDCl_3$) δ = 7.51 (d, *J* = 2.2 Hz, 1H), 7.44 (app dt, *J* = 7.9, 1.0 Hz, 1H), 7.29 – 7.23 (m, 2H), 7.17 (ddd, *J* = 8.2, 6.8, 1.2 Hz, 1H), 7.01 (ddd, *J* = 8.0, 6.9, 1.1 Hz, 1H), 6.92 (br. s, 1H), 6.77 (d, *J* = 8.5 Hz, 1H), 4.87 (app t, *J* = 7.5 Hz, 1H), 3.82 (s, 3H), 3.81 (s, 3H), 3.76 – 3.64 (m, 1H), 3.72 (s, 3H), 3.57 (dd, *J* = 16.4, 6.9 Hz, 1H); (multiplet signal starting at 3.76 ppm overlaps with methyl singlet signal at 3.72 ppm)
^{13}C NMR (75 MHz, $CDCl_3$) δ = 190.7, 161.8, 154.3, 138.1, 137.3, 132.6, 128.1, 126.9, 126.2, 121.8, 119.5, 119.0, 117.1, 111.8, 111.6, 109.3, 76.4, 56.3, 52.3, 46.1, 37.2, 32.8;
IR (neat): ν_{max} = 2951, 2134, 1715, 1647, 1491, 1435, 1308, 1205, 1131, 1050, 814, 737 cm^{-1}.
HRMS (APPI+) calc'd for $C_{22}H_{20}{}^{79}BrN_3O_4$ [M^+] 469.0637, found 469.0631.

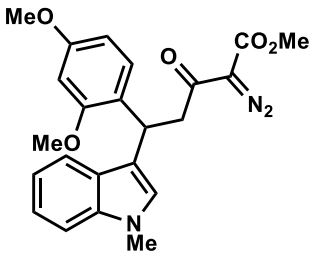

122

Product **122** was prepared following General Experimental Procedure **A**. 1-Methylindole **1** (0.503 g, 3.83 mmol), DAAE (0.557 g, 1.92 mmol), scandium(III) triflate (0.142 g, 0.288 mmol). Product **122** (0.169 g, 0.401 mmol, 21%) was obtained as a yellow foam:

R_f = 0.25, 30% EtOAc in hexanes;

^{1}H NMR (300 MHz, $CDCl_3$) δ = 7.53 (app dt, *J* = 8.0, 1.0 Hz, 1H), 7.23 (d, *J* = 10.4 Hz, 1H), 7.15 (ddd, *J* = 8.2, 6.8, 1.2 Hz, 1H), 7.07 (d, *J* = 8.4 Hz, 1H), 7.01 (ddd, *J* = 8.0, 6.8, 1.2 Hz, 1H), 6.86 (s, 1H), 6.44 (d, *J* = 2.5 Hz, 1H), 6.34 (dd, *J* = 8.4, 2.5 Hz, 1H), 5.29 (app *J* = 7.5 Hz, 1H), 3.83 (s, 3H), 3.82 (s, 3H), 3.75 – 3.69 (m, 1H), 3.74 (s, 3H), 3.71 (s, 3H), 3.51 (dd, *J* = 16.6, 7.3 Hz, 1H) ppm; (multiplet signal starting at 3.75 ppm overlaps with methyl singlet signals at 3.74 and 3.71 ppm)

^{13}C NMR (75 MHz, $CDCl_3$) δ = 191.3, 162.0, 159.2, 157.7, 137.3, 129.0, 127.4, 126.5, 125.0, 121.5, 119.9, 118.7, 117.7, 109.1, 104.2, 98.7, 76.2, 55.6, 55.4, 52.2, 45.3, 32.8, 30.7 ppm;

IR (neat): ν_{max} = 2924, 2133, 1715, 1652, 1585, 1465, 1292, 1205, 1033, 736 cm^{-1}.

HRMS (APPI+) calc'd for $C_{23}H_{23}N_3O_5$ [M^+] 421.1638, found 421.1663.

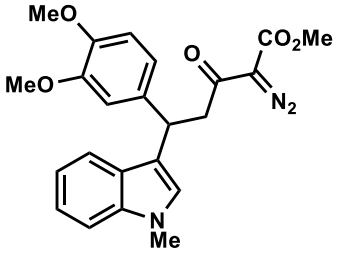

123

Product **123** was prepared following General Experimental Procedure **A**. 1-Methylindole **1** (0.480 g, 3.66 mmol), DAAE (0.708 g, 2.44 mmol), scandium(III) triflate (0.180 g, 0.366 mmol). Product **123** (0.178 g, 0.422 mmol, 17%) was obtained as a yellow foam:

R_f = 0.23, 30% EtOAc in hexanes;

^{1}H NMR (300 MHz, $CDCl_3$) δ = 7.65 (app dt, *J* = 7.9, 1.0 Hz, 1H), 7.22 (d, *J* = 8.2 Hz, 1H), 7.16 (ddd, *J* = 8.1, 6.7, 1.2 Hz, 1H), 7.03 (ddd, *J* = 8.0, 6.8, 1.3 Hz, 1H), 6.97 – 6.88 (m, 2H), 6.86 (s, 1H), 6.74 (dd, *J* = 7.6, 2.0 Hz, 1H), 5.38 (t, *J* = 7.6 Hz, 1H), 3.84 (s, 3H), 3.83 (s, 3H), 3.83 (s, 3H), 3.76 – 3.67 (m, 1H), 3.70 (s, 3H), 3.61 (dd, *J* = 16.9, 7.8 Hz, 1H) ppm;

^{13}C NMR (75 MHz, $CDCl_3$) δ = 190.9, 162.0, 152.9, 146.7, 137.9, 137.2, 127.3, 126.5, 123.8, 121.6, 120.4, 119.8, 118.9, 117.7, 110.4, 109.1, 76.3, 60.8, 55.8, 52.3, 45.6, 32.8, 31.2 ppm;

IR (neat): ν_{max} = 2952, 2135, 1723, 1661, 1584, 1474, 1308, 1270, 1167, 1024, 704 cm^{-1}.

HRMS (APPI+) calc'd for $C_{23}H_{23}N_3O_5$ [M^+] 421.1638, found 421.1634.

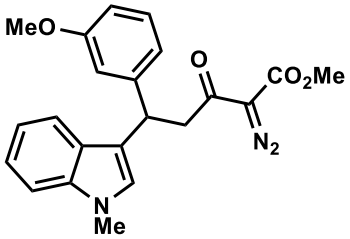

124

Product **124** was prepared following General Experimental Procedure **A**. 1-Methylindole **1** (0.497 g, 3.79 mmol), DAAE (0.760 g, 2.92 mmol), scandium(III) triflate (0.172 g, 0.350 mmol). Product **124** (0.193 g, 0.493 mmol, 17%) was obtained as a yellow oil:

R_f = 0.27, 20% EtOAc in hexanes;

^{1}H NMR (300 MHz, $CDCl_3$) δ = 7.50 (app dt, *J* = 7.9, 1.0 Hz, 1H), 7.23 – 7.13 (m, 3H), 7.04 – 6.99 (m, 1H), 6.98 – 6.91 (m, 2H), 6.90 (s, 1H), 6.69 (dd, *J* = 8.1, 1.9 Hz, 1H), 4.93 (app t, *J* = 7.5 Hz, 1H), 3.81 (s, 3H), 3.76 – 3.68 (m, 1H), 3.74 (s, 3H), 3.70 (s, 3H), 3.61 (dd, *J* = 16.5, 7.2 Hz, 1H) ppm; (multiplet signal starting at 3.76 ppm overlaps with methyl signal at 3.74 ppm)

^{13}C NMR (75 MHz, $CDCl_3$) δ = 190.9, 161.9, 159.7, 146.0, 137.3, 129.4, 127.1, 126.4, 121.7, 120.4, 119.6, 118.9, 117.4, 114.0, 111.4, 109.2, 76.4, 55.2, 52.3, 46.1, 38.2, 32.8 ppm;

IR (neat): ν_{max} = 2952, 2134, 1715, 1651, 1598, 1434, 1306, 1129, 1043, 780, 736 cm^{-1}.

HRMS (APPI+) calc'd for $C_{22}H_{21}N_3O_4$ [M^+] 391.1532, found 391.1536.

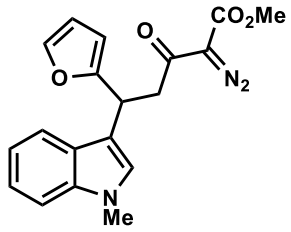

121

Product **121** was prepared following General Experimental Procedure **A**. 1-Methylindole **1** (0.552 g, 4.21 mmol), DAAE (0.579 g, 2.63 mmol), scandium(III) triflate (0.194 g, 0.395 mmol). Product **121** (0.209 g, 0.594 mmol, 23%) was obtained as a thick yellow oil:

R_f = 0.45, 20% EtOAc in hexanes;

^{1}H NMR (300 MHz, $CDCl_3$) δ = 7.59 (d, *J* = 8.0 Hz, 1H), 7.31 – 7.24 (m, 2H), 7.19 (ddd, *J* = 8.2, 6.8, 1.2 Hz, 1H), 7.06 (ddd, *J* = 8.0, 6.8, 1.2 Hz, 1H), 6.96 (s, 1H), 6.25 (dd, *J* = 3.2, 1.9 Hz, 1H), 6.07 (d, *J* = 3.2 Hz, 1H), 5.03 (apt. t, *J* = 7.3 Hz, 1H), 3.80 (s, 3H), 3.73 – 3.70 (m, 1H), 3.71 (s, 3H), 3.61 (dd, *J* = 16.9, 7.2 Hz, 1H) ppm; (multiplet signal starting at 3.73 ppm overlaps with methyl singlet signal at 3.71 ppm)

^{13}C NMR (75 MHz, $CDCl_3$) δ = 190.5, 161.8, 157.0, 141.3, 137.2, 127.0, 126.8, 121.7, 119.6, 119.1, 114.8, 110.2, 109.4, 105.5, 52.3, 44.5, 32.8, 31.9 ppm; (diazo carbon not observed presumably due to overlap)

IR (neat): ν_{max} = 3052, 2952, 2135, 1716, 1653, 1505, 1472, 1309, 1209, 1130, 1012, 910, 732 cm^{-1}.

HRMS (APPI-) calc'd for $C_{19}H_{17}N_3O_4$ [M^-] 351.1219, found 351.1203.

3.9.3 Synthesis and Characterization of Functionalized Carbazoles:

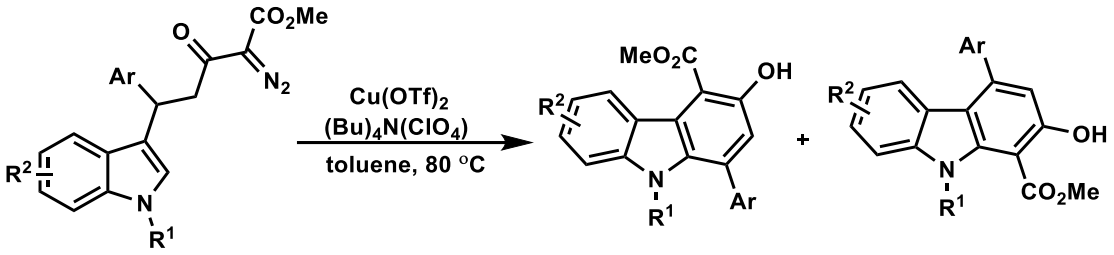

General Experimental Procedure B:

To a flame-dried reaction vial charged with $Cu(OTf)_2$ (0.2 equiv) and $(Bu)_4N(ClO_4)$ (1.0 equiv) was added dried and degassed toluene (18 mL/mmol of $(Bu)_4N(ClO_4)$) and stirred at 80 ˚C for 5 min. The indolyl α-diazocarbonyls **79** (1.0 equiv) was dissolved in dried degassed toluene (12 mL/mmol of indolyl α-diazocarbonyl) and added to catalyst & additive solution dropwise over 15 min. The reaction was stirred at 80 °C under nitrogen until complete consumption of starting material was observed, as determined by TLC analysis. The reaction mixture was then cooled to room temperature, diluted with water and extracted three times with EtOAc. The combined organic phases were washed once with brine, dried over anhydrous $MgSO_4$, and concentrated in *vacuo*. The resulting residue was purified by silica gel flash column chromatography using a hexanes/EtOAc gradient to afford corresponding carbazoles.

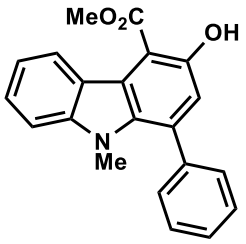

126

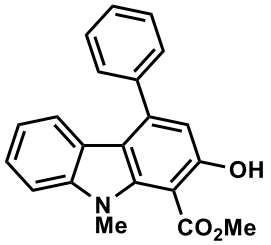

127

Product **126** and **127** were prepared following General Experimental Procedure **B**. Diazo-indole **111** (0.080 g, 0.22 mmol), copper(II) triflate (0.016 g, 0.044 mmol), tetrabutylammonium perchlorate (0.075 g, 0.22 mmol). Product **126** (0.046 g, 0.14 mmol, 64%) was obtained as a yellow solid and product **127** (0.019 g, 0.057 mmol, 26%) was obtained as a cream solid:

Compound **126**:

R_f = 0.60, 20% EtOAc in hexanes;

M.P. = 105-107 °C

^{1}H NMR (300 MHz, $CDCl_3$) δ = 10.74 (s, 1H), 8.45 (d, *J* = 8.3 Hz, 1H), 7.50 – 7.43 (m, 6H), 7.34 (d, *J* = 8.2 Hz, 1H), 7.21 (ddd, *J* = 8.2, 7.0, 1.2 Hz, 1H), 7.02 (s, 1H), 4.19 (s, 3H), 3.30 (s, 3H) ppm;

^{13}C NMR (75 MHz, $CDCl_3$) δ = 171.4, 156.2, 143.5, 139.5, 134.0, 133.6, 129.4, 128.3, 128.1, 126.4, 124.9, 121.7, 121.3, 119.0, 118.8, 109.4, 105.3, 52.1, 33.5 ppm;

IR (neat): ν_{max} = 3043, 2945, 1651, 1607, 1481, 1314, 1206, 1028, 909, 726, 697 cm^{-1}.

HRMS (APPI+) calc'd for $C_{21}H_{17}NO_3$ [M^+] 331.1208, found 331.1182, calc'd for $C_{21}H_{18}NO_3$ [M+H]$^+$ 332.1281, found 332.1255.

Compound **127**:

***R*f** = 0.33, 20% EtOAc in hexanes;

M.P. = 88-91 °C

^{1}H NMR (300 MHz, $CDCl_3$) δ = 10.48 (s, 1H), 7.55 – 7.50 (m, 5H), 7.38 – 7.34 (m, 2H), 7.20 (app dt, *J* = 7.9, 1.0 Hz, 1H), 6.97 (ddd, *J* = 8.1, 6.6, 1.6 Hz, 1H), 6.76 (s, 1H), 4.09 (s, 3H), 3.79 (s, 3H) ppm;

^{13}C NMR (75 MHz, $CDCl_3$) δ = 170.0, 160.5, 144.8, 143.2, 141.9, 140.1, 128.8, 128.7, 128.4, 124.9, 123.0, 121.2, 120.2, 115.7, 111.0, 109.5, 97.4, 52.2, 35.8 ppm;

IR (neat): ν_{max} = 3053, 2947, 1657, 1560, 1465, 1254, 1194, 1097, 728, 699 cm^{-1}.

HRMS (APPI+) calc'd for $C_{21}H_{17}NO_3$ [M^+] 331.1208, found 331.1185, calc'd for $C_{21}H_{18}NO_3$ [M+H]$^+$ 332.1281, found 332.1257.

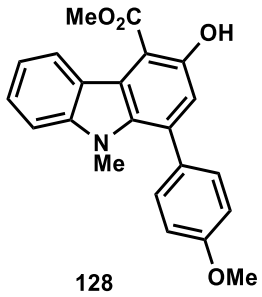

128

Product **128** was prepared following General Experimental Procedure **B**. Diazo-indole **103** (0.079 g, 0.20 mmol), copper(II) triflate (0.014 g, 0.040 mmol), tetrabutylammonium perchlorate (0.068 g, 0.20 mmol). Product **128** (0.053 g, 0.15 mmol, 75%) was obtained as a yellow solid:

Compound **128**:

***R*f** = 0.36, 20% EtOAc in hexanes;

M.P. = 138-140 °C

^{1}H NMR (300 MHz, $CDCl_3$) δ = 10.78 (s, 1H), 8.43 (d, *J* = 8.2 Hz, 1H), 7.46 (ddd, *J* = 8.2, 7.0, 1.1 Hz, 1H), 7.40 – 7.35 (m, 2H), 7.32 (d, *J* = 8.2 Hz, 1H), 7.19 (ddd, *J* = 8.2, 7.0, 1.1 Hz, 1H), 7.02 – 6.97 (m, 3H), 4.16 (s, 3H), 3.88 (s, 3H), 3.31 (s, 3H) ppm;

^{13}C NMR (75 MHz, $CDCl_3$) δ = 171.5, 159.6, 156.3, 143.6, 133.9, 131.7, 130.5, 126.3, 124.9, 121.8, 121.3, 119.0, 118.8, 113.8, 109.4, 105.0, 55.5, 52.1, 33.5 ppm; (one aromatic carbon is not observed presumably due to overlap)

IR (neat): ν_{max} = 2922, 2851, 1649, 1610, 1442, 1296, 1207, 1027, 814, 741, 731 cm^{-1}.

HRMS (APPI+) calc'd for $C_{22}H_{19}NO_4$ [M^+] 361.1314, found 361.1307.

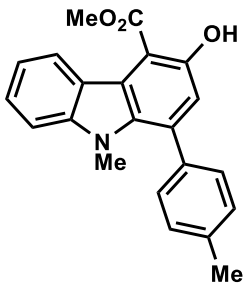

129

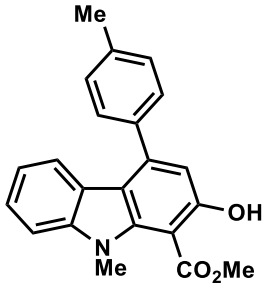

130

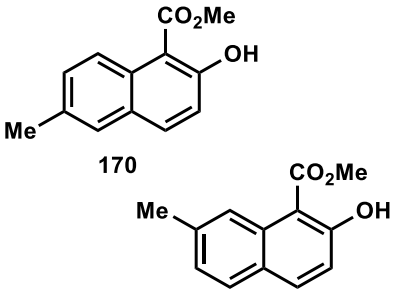

170 171

Product **129**, **130**, and **170, 171** were prepared following General Experimental Procedure **B**. Diazo-indole **104** (0.104 g, 0.280 mmol), copper(II) triflate (0.020 g, 0.056 mmol), tetrabutylammonium perchlorate (0.096 g, 0.28 mmol). Product **129** (0.058 g, 0.17 mmol, 61%) was obtained as a yellow solid. Product **130** (0.014 g, 0.041 mmol, 15%) was obtained as a light brown solid and products **170, 171** (0.006 g, 0.017 mmol, 6%) were obtained as an inseparable mixture (2:1) as a colorless oil:

Compound **129**:

***R*f** = 0.55, 20% EtOAc in hexanes;

M.P. = 147-150 ºC

^{1}H NMR (300 MHz, $CDCl_3$) δ = 10.77 (s, 1H), 8.45 (ddd, *J* = 8.3, 1.2, 0.7 Hz, 1H), 7.47 (ddd, *J* = 8.2, 7.0, 1.2 Hz, 1H), 7.37 – 7.26 (m, 5H), 7.21 (ddd, *J* = 8.2, 6.9, 1.2 Hz, 1H), 7.00 (s, 1H), 4.18 (s, 3H), 3.32 (s, 3H), 2.46 (s, 3H) ppm;

^{13}C NMR (75 MHz, $CDCl_3$) δ = 171.5, 156.3, 143.6, 138.0, 136.5, 134.2, 133.8, 129.2, 129.0, 126.3, 124.9, 121.8, 121.3, 119.0, 118.8, 109.4, 105.1, 52.1, 33.5, 21.5 ppm;

IR (neat): ν_{max} = 3016, 2945, 1648, 1611, 1485, 1441, 1319, 1203, 1081, 915, 820, 740, 729 cm^{-1}.

HRMS (APPI+) calc'd for $C_{22}H_{19}NO_3$ [M^+] 345.1365, found 345.1351.

Compound **130**:

***R*f** = 0.35, 20% EtOAc in hexanes;

M.P. = 98-101 ºC

^{1}H NMR (300 MHz, $CDCl_3$) δ = 10.48 (s, 1H), 7.48 – 7.44 (m, 2H), 7.40 – 7.27 (m, 5H), 6.99 (ddd, *J* = 8.1, 6.4, 1.7 Hz, 1H), 6.75 (s, 1H), 4.08 (s, 3H), 3.78 (s, 3H), 2.49 (s, 3H) ppm;

^{13}C NMR (75 MHz, $CDCl_3$) δ = 170.0, 160.5, 145.0, 143.2, 141.9, 138.2, 137.1, 129.3, 128.7, 124.8, 123.1, 121.3, 120.1, 115.7, 111.0, 109.5, 97.2, 52.1, 35.8, 21.5 ppm;

IR (neat): ν_{max} =2952, 2918, 1670, 1558, 1469, 1395, 1258, 1192, 1097, 796, 685 cm^{-1}.

HRMS (APPI+) calc'd for $C_{22}H_{19}NO_3$ [M^+] 345.1365, found 345.1357.

Compound **170**:

***R*f** = 0.70, 20% EtOAc in hexanes;

^{1}H NMR (300 MHz, $CDCl_3$) δ = 12.18 (s, 1H), 8.63 (d, *J* = 8.9 Hz, 1H), 7.82 (d, *J* = 9.0 Hz, 1H), 7.53 (s, 1H), 7.39 (dd, *J* = 8.9, 2.0 Hz, 1H), 7.14 (d, *J* = 9.0 Hz, 1H), 4.10 (s, 3H), 2.47 (s, 3H) ppm;

^{13}C NMR (75 MHz, $CDCl_3$) δ = 163.9, 136.5, 133.3, 130.7, 129.8, 129.1, 129.0, 128.5, 125.3, 119.4, 104.7, 29.9, 21.1 ppm;

Compound **171**:

^{1}H NMR (300 MHz, $CDCl_3$) δ = 12.23 (s, 1H), 8.52 (d, *J* = 0.9 Hz, 1H), 7.85 (d, *J* = 9.0 Hz, 1H), 7.65 (d, *J* = 8.1 Hz, 1H), 7.21 (dd, *J* = 8.4, 1.4 Hz, 1H), 7.09 (d, *J* = 9.0 Hz, 1H), 4.12 (s, 3H), 2.54 (s, 2H) ppm;
^{13}C NMR (75 MHz, $CDCl_3$) δ = 173.0, 164.6, 138.6, 136.8, 132.1, 129.1, 127.0, 125.8, 124.9, 118.4, 104.4, 52.5, 22.7 ppm;
IR (neat) (mixture of 15a/b): ν_{max} = 3007, 2952, 2920, 2852, 2361, 2337, 1724, 1647, 1580, 1514, 1439, 1332, 1217, 1051, 1166, 1051, 828, 777, 701 cm^{-1}.
HRMS (mixture of 15a/b) (APPI+) calc'd for $C_{13}H_{12}O_3$ [M^+] 216.0786, found 216.0789.

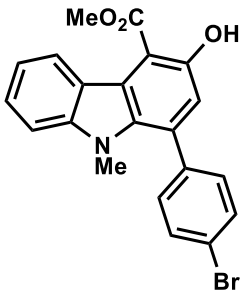

131

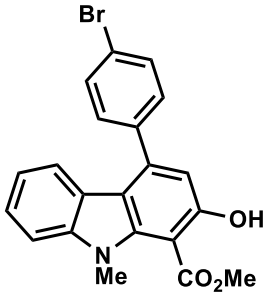

132

Product **131** and **132** were prepared following General Experimental Procedure **B**. Diazo-indole **105** (0.079 g, 0.18 mmol), copper(II) triflate (0.013 g, 0.036 mmol), tetrabutylammonium perchlorate (0.062 g, 0.18 mmol). Product **131** (0.039 g, 0.095 mmol, 53%) was obtained as a yellow solid and product **132** (0.025 g, 0.061 mmol, 34%) was obtained as a cream solid:
Compound **131**:
***R*$_f$** = 0.63, 20% EtOAc in hexanes;
M.P. = 179-181 °C
^{1}H NMR (300 MHz, $CDCl_3$) δ = 10.71 (s, 1H), 8.43 (app dt, *J* = 8.3, 0.9 Hz, 1H), 7.63 – 7.59 (m, 2H), 7.48 (ddd, *J* = 8.2, 7.0, 1.0 Hz, 1H), 7.36 – 7.32 (m, 3H), 7.21 (ddd, *J* = 8.2, 7.1, 1.0 Hz, 1H), 6.97 (s, 1H), 4.17 (s, 3H), 3.31 (s, 3H) ppm;
^{13}C NMR (75 MHz, $CDCl_3$) δ = 171.3, 156.2, 143.6, 138.5, 133.5, 132.4, 131.6, 131.0, 126.6, 125.0, 122.5, 121.7, 121.7, 119.2, 118.6, 109.5, 105.7, 52.2, 33.7 ppm;
IR (neat): ν_{max} = 3146, 2924, 1647, 1611, 1482, 1319, 1207, 1012, 825, 731 cm^{-1}.
HRMS (APPI+) calc'd for $C_{21}H_{16}{}^{79}BrNO_3$ [M^+] 409.0314, found 409.0286.
Compound **132**:
***R*$_f$** = 0.45, 20% EtOAc in hexanes;
M.P. = 145-147 °C
^{1}H NMR (300 MHz, $CDCl_3$) δ = 10.44 (s, 1H), 7.67 – 7.63 (m, 2H), 7.45 – 7.40 (m, 2H), 7.38 – 7.33 (m, 2H), 7.22 (app dt, *J* = 8.0, 1.0 Hz, 1H), 7.01 (ddd, *J* = 8.1, 6.1, 2.1 Hz, 1H), 6.71 (s, 1H), 4.08 (s, 3H), 3.78 (s, 3H) ppm;
^{13}C NMR (75 MHz, $CDCl_3$) δ = 169.9, 160.4, 143.3, 143.2, 141.9, 139.0, 131.9, 130.6, 125.1, 122.7, 122.6, 121.1, 120.3, 115.4, 110.8, 109.7, 97.7, 52.2, 35.8 ppm;
IR (neat): ν_{max} = 2949, 2920, 1655, 1573, 1469, 1390, 1202, 1101, 829, 731 cm^{-1}.
HRMS (APPI-) calc'd for $C_{21}H_{16}{}^{79}BrNO_3$ [M^-] 409.0313, found 409.0350.

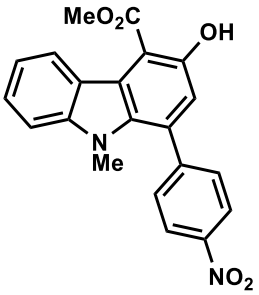

133

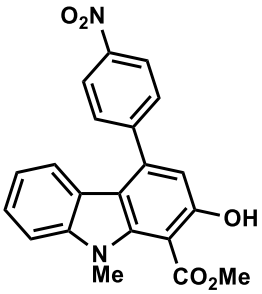

134

Product **133** and **134** were prepared following General Experimental Procedure **B**. Diazo-indole **106** (0.089 g, 0.22 mmol), copper(II) triflate (0.016 g, 0.044 mmol), tetrabutylammonium perchlorate (0.075 g, 0.22 mmol). Product **133** (0.014 g, 0.037 mmol, 17%) was obtained as a yellow solid and product **134** (0.023 g, 0.061 mmol, 28%) was obtained as a yellow solid:

Compound **133**:

R_f = 0.43, 20% EtOAc in hexanes;

M.P. = 196-199 °C

^{1}H NMR (300 MHz, $CDCl_3$) δ = 10.69 (s, 1H), 8.45 (app dt, *J* = 8.3, 0.9 Hz, 1H), 8.38 – 8.34 (m, 2H), 7.69 – 7.65 (m, 2H), 7.51 (ddd, *J* = 8.2, 7.0, 1.2 Hz, 1H), 7.36 (app dt, *J* = 8.3, 0.9 Hz, 1H), 7.24 (ddd, *J* = 8.2, 7.0, 1.1 Hz, 1H), 7.00 (s, 1H), 4.20 (s, 3H), 3.31 (s, 3H) ppm;

^{13}C NMR (75 MHz, $CDCl_3$) δ = 171.1, 156.0, 147.7, 146.3, 143.7, 133.3, 130.8, 130.3, 127.0, 125.0, 123.7, 122.1, 121.7, 119.5, 118.4, 109.6, 106.5, 52.4, 34.1 ppm;

IR (neat): ν_{max} = 2919, 2850, 1663, 1588, 1466, 1318, 1203, 1100, 859, 709 cm^{-1}.

HRMS (APPI+) calc'd for $C_{21}H_{16}N_2O_5$ [M^+] 376.1059, found 376.1047.

Compound **134**:

R_f = 0.31, 30% EtOAc in hexanes;

M.P. = 172-175 °C

^{1}H NMR (300 MHz, $CDCl_3$) δ = 10.44 (s, 1H), 8.40 – 8.36 (m, 2H), 7.75 – 7.70 (m, 2H), 7.44 – 7.35 (m, 2H), 7.10 (app dt, *J* = 8.0, 1.0 Hz, 1H), 7.00 (ddd, *J* = 8.0, 6.3, 1.8 Hz, 1H), 6.73 (s, 1H), 4.10 (s, 3H), 3.80 (s, 3H) ppm;

^{13}C NMR (75 MHz, $CDCl_3$) δ = 169.7, 160.3, 148.0, 146.8, 143.3, 141.9, 141.7, 130.0, 125.4, 124.0, 122.3, 120.7, 120.5, 115.1, 110.7, 109.9, 98.4, 52.4, 35.8 ppm;

IR (neat): ν_{max} = 2920, 2850, 1654, 1560, 1465, 1342, 1200, 1096, 912, 750 cm^{-1}.

HRMS (APPI+) calc'd for $C_{21}H_{16}N_2O_5$ [M^+] 376.1059, found 376.1056.

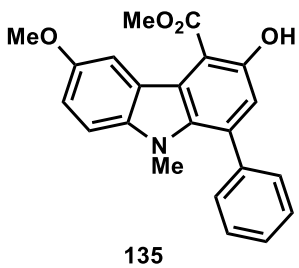

135

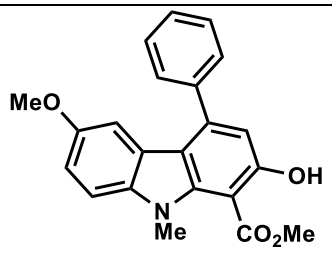

136

Product **135** and **136** were prepared following General Experimental Procedure **B**. Diazo-indole **96** (0.080 g, 0.20 mmol), copper(II) triflate (0.014 g, 0.040 mmol), tetrabutylammonium perchlorate (0.068 g, 0.20 mmol). Product **135** (0.040 g, 0.11 mmol, 55%) was obtained as a yellow solid and product **136** (0.023 g, 0.064 mmol, 32%) was obtained as a yellow solid:

Compound **135**:

***R*f** = 0.41, 20% EtOAc in hexanes;

M.P. = 164-166 °C

^{1}H NMR (300 MHz, $CDCl_3$) δ = 10.76 (s, 1H), 7.98 (d, *J* = 2.5 Hz, 1H), 7.50 – 7.42 (m, 5H), 7.24 (d, *J* = 9.2 Hz, 1H), 7.14 (dd, *J* = 9.0, 2.5 Hz, 1H), 6.99 (s, 1H), 4.19 (s, 3H), 3.93 (s, 3H), 3.25 (s, 3H) ppm;

^{13}C NMR (75 MHz, $CDCl_3$) δ = 171.3, 156.3, 153.1, 139.5, 139.0, 134.3, 134.2, 129.4, 128.4, 128.1, 121.9, 121.0, 118.8, 116.2, 110.0, 107.6, 105.1, 56.1, 52.1, 33.6 ppm;

IR (neat): ν_{max} = 2918, 2850, 1649, 1567, 1488, 1445, 1262, 1149, 800, 720 cm^{-1}.

HRMS (APPI+) calc'd for $C_{22}H_{19}NO_4$ $[M^+]$ 361.1314, found 361.1301, calc'd for $C_{22}H_{20}NO_4$ $[M+H]^+$ 362.1387, found 362.1377.

Compound **136**:

***R*f** = 0.29, 30% EtOAc in hexanes;

M.P. = 118-120 °C

^{1}H NMR (300 MHz, $CDCl_3$) δ = 10.52 (s, 1H), 7.57 – 7.48 (m, 5H), 7.26 (d, *J* = 8.8 Hz, 1H), 6.96 (dd, *J* = 8.8, 2.5 Hz, 1H), 6.74 (s, 1H), 6.64 (d, *J* = 2.5 Hz, 1H), 4.08 (s, 3H), 3.75 (s, 3H), 3.56 (s, 3H) ppm;

^{13}C NMR (75 MHz, $CDCl_3$) δ = 170.0, 160.7, 154.1, 144.9, 142.3, 140.0, 138.2, 128.9, 128.6, 128.4, 123.5, 115.6, 113.6, 110.5, 110.1, 104.5, 97.4, 55.7, 52.1, 35.9 ppm;

IR (neat): ν_{max} = 2917, 2824, 1659, 1561, 1430, 1292, 1174, 1097, 799, 731 cm^{-1}.

HRMS (APPI+) calc'd for $C_{22}H_{19}NO_4$ $[M^+]$ 361.1314, found 361.1334, calc'd for $C_{22}H_{20}NO_4$ $[M+H]^+$ 362.1387, found 362.1406.

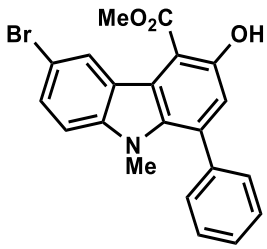

137

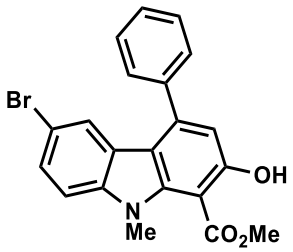

138

Product **137** and **138** were prepared following General Experimental Procedure **B**. Diazo-indole **98** (0.098 g, 0.22 mmol), copper(II) triflate (0.016 g, 0.044 mmol), tetrabutylammonium perchlorate (0.075 g, 0.22 mmol). Product **137** (0.047 g, 0.11 mmol, 50%) was obtained as a yellow solid and product **137** (0.030 g, 0.073 mmol, 33%) was obtained as a cream solid:

Compound **137**:

***R*f** = 0.51, 20% EtOAc in hexanes;

M.P. = 162-165 °C

^{1}H NMR (300 MHz, $CDCl_3$) δ = 10.86 (s, 1H), 8.62 (d, *J* = 1.8 Hz, 1H), 7.54 (dd, *J* = 8.8, 2.0 Hz, 1H), 7.50 – 7.43 (m, 5H), 7.21 (d, *J* = 8.8 Hz, 1H), 7.04 (s, 1H), 4.20 (s, 3H), 3.27 (s, 3H) ppm;
^{13}C NMR (75 MHz, $CDCl_3$) δ = 171.1, 156.8, 142.0, 139.1, 134.3, 133.9, 129.4, 128.9, 128.4, 128.3, 127.9, 123.3, 120.2, 119.7, 111.9, 110.8, 105.2, 52.1, 33.6 ppm;
IR (neat): ν_{max} = 2952, 2926, 1654, 1588, 1441, 1388, 1211, 1166, 1033, 779 cm^{-1}.
HRMS (APPI+) calc'd for $C_{21}H_{16}{}^{79}BrNO_3$ [M^+] 409.0314, found 409.0308.
Compound **138**:
***R*$_f$** = 0.30, 20% EtOAc in hexanes;
M.P. = 173-175 °C
^{1}H NMR (300 MHz, $CDCl_3$) δ = 10.49 (s, 1H), 7.54 – 7.51 (m, 5H), 7.42 (dd, *J* = 8.6, 2.0 Hz, 1H), 7.29 (dd, *J* = 2.0, 0.5 Hz, 1H), 7.26 – 7.23 (m, 1H), 6.78 (s, 1H), 4.09 (s, 3H), 3.76 (s, 3H) ppm;
^{13}C NMR (75 MHz, $CDCl_3$) δ = 169.7, 161.0, 145.0, 142.2, 141.8, 139.4, 128.8, 128.7, 128.6, 127.5, 124.7, 123.8, 114.7, 113.2, 111.5, 110.9, 97.5, 52.3, 35.9 ppm;
IR (neat): ν_{max} = 3058, 2950, 1659, 1557, 1439, 1388, 1249, 1068, 864, 773 cm^{-1}.
HRMS (APPI+) calc'd for $C_{21}H_{16}{}^{79}BrNO_3$ [M^+] 409.0314, found 409.0299.

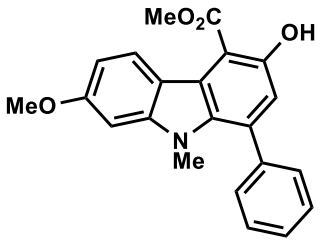

139

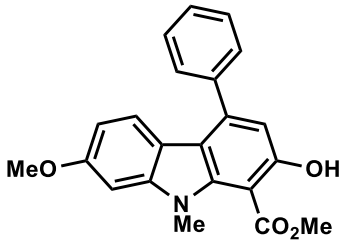

140

Product **139** and **140** were prepared following General Experimental Procedure **B**. Diazo-indole **97** (0.080 g, 0.20 mmol), copper(II) triflate (0.014 g, 0.040 mmol), tetrabutylammonium perchlorate (0.068 g, 0.20 mmol). Product **139** (0.037 g, 0.10 mmol, 50%) was obtained as a yellow solid and product **140** (0.025 g, 0.069 mmol, 35%) was obtained as a cream solid:
Compound **139**:
***R*$_f$** = 0.44, 30% EtOAc in hexanes;
M.P. = 159-162 °C
^{1}H NMR (300 MHz, $CDCl_3$) δ = 10.80 (s, 1H), 8.34 (d, *J* = 9.1 Hz, 1H), 7.48 – 7.42 (m, 5H), 6.92 (s, 1H), 6.83 (dd, *J* = 9.1, 2.4 Hz, 1H), 6.72 (d, *J* = 2.4 Hz, 1H), 4.16 (s, 3H), 3.92 (s, 3H), 3.23 (s, 3H) ppm;
^{13}C NMR (75 MHz, $CDCl_3$) δ = 171.5, 159.4, 156.4, 145.3, 139.6, 133.7, 133.6, 129.4, 128.3, 128.1, 126.1, 122.0, 117.3, 115.9, 108.3, 104.7, 92.6, 55.7, 52.1, 33.6 ppm;
IR (neat): ν_{max} = 2921, 2850, 1653, 1614, 1443, 1257, 1163, 1032, 776, 704 cm^{-1}.
HRMS (APPI+) calc'd for $C_{22}H_{19}NO_4$ [M^+] 361.1314, found 361.1298.
Compound **140**:
***R*$_f$** = 0.29, 30% EtOAc in hexanes;
M.P. = 134-137 °C

^{1}H NMR (300 MHz, $CDCl_3$) δ = 10.31 (s, 1H), 7.57 – 7.47 (m, 5H), 7.08 (d, *J* = 8.7 Hz, 1H), 6.85 (d, *J* = 2.2 Hz, 1H), 6.74 (s, 1H), 6.59 (dd, *J* = 8.7, 2.3 Hz, 1H), 4.08 (s, 3H), 3.87 (s, 3H), 3.73 (s, 3H) ppm;
^{13}C NMR (75 MHz, $CDCl_3$) δ = 169.9, 159.5, 158.4, 144.6, 143.7, 141.9, 140.2, 128.8, 128.6, 128.3, 121.9, 116.8, 115.8, 110.7, 108.1, 97.6, 94.5, 55.8, 52.1, 35.9 ppm;
IR (neat): ν_{max} = 2921, 2851, 1655, 1560, 1473, 1288, 1201, 1100, 848, 773, 703 cm^{-1}.
HRMS (APPI+) calc'd for $C_{22}H_{19}NO_4$ [M^+] 361.1314, found 361.1316.

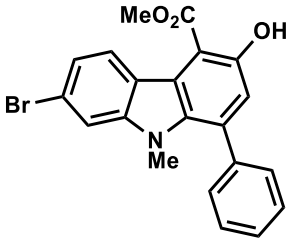

141

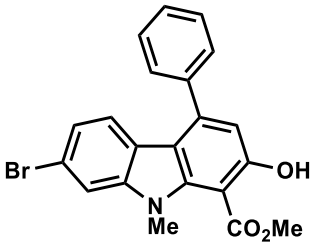

142

Product **141** and **142** were prepared following General Experimental Procedure **B**. Diazo-indole **99** (0.094 g, 0.21 mmol), copper(II) triflate (0.015 g, 0.042 mmol), tetrabutylammonium perchlorate (0.072 g, 0.21 mmol). Product **141** (0.037 g, 0.090 mmol, 43%) was obtained as a yellow solid and product **142** (0.033 g, 0.080 mmol, 38%) was obtained as a brown solid:
Compound **141**:
***R*$_f$** = 0.50, 20% EtOAc in hexanes;
M.P. = 152-155 ºC
^{1}H NMR (300 MHz, $CDCl_3$) δ = 10.79 (s, 1H), 8.29 (d, *J* = 8.9 Hz, 1H), 7.50 – 7.41 (m, 6H), 7.28 (dd, *J* = 8.9, 1.9 Hz, 1H), 7.02 (s, 1H), 4.16 (s, 3H), 3.24 (s, 3H) ppm;
^{13}C NMR (75 MHz, $CDCl_3$) δ = 171.1, 156.7, 144.3, 139.1, 134.2, 133.6, 129.3, 128.4, 128.3, 126.3, 122.2, 121.0, 120.7, 120.3, 119.4, 112.3, 105.2, 52.2, 33.6 ppm;
IR (neat): ν_{max} = 2921, 2851, 1651, 1600, 1439, 1313, 1210, 933, 775, 705 cm^{-1}.
HRMS (APPI+) calc'd for $C_{21}H_{16}{}^{79}BrNO_3$ [M^+] 409.0314, found 409.0287.
Compound **142**:
***R*$_f$** = 0.33, 20% EtOAc in hexanes;
M.P. = 117-120 ºC
^{1}H NMR (300 MHz, $CDCl_3$) δ = 10.45 (s, 1H), 7.53 – 7.48 (m, 6H), 7.06 (dd, *J* = 8.5, 1.6 Hz, 1H), 7.01 (d, *J* = 8.1 Hz, 1H), 6.76 (s, 1H), 4.08 (s, 3H), 3.74 (s, 3H) ppm;
^{13}C NMR (75 MHz, $CDCl_3$) δ = 169.7, 160.8, 144.7, 144.0, 142.0, 139.7, 128.8, 128.7, 128.5, 123.3, 122.3, 121.9, 118.3, 115.1, 112.7, 111.5, 97.6, 52.3, 35.9 ppm;
IR (neat): ν_{max} = 2958, 2922, 1698, 1651, 1475, 1264, 1204, 1013, 957, 730, 698 cm^{-1}.
HRMS (APPI+) calc'd for $C_{21}H_{16}{}^{79}BrNO_3$ [M^+] 409.0314, found 409.0330.

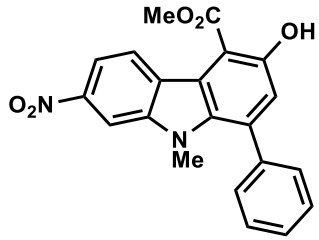

143

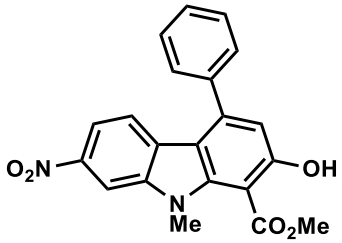

144

Product **143** and **144** were prepared following General Experimental Procedure **B**. Diazo-indole **101** (0.084 g, 0.21 mmol), copper(II) triflate (0.015 g, 0.042 mmol), tetrabutylammonium perchlorate (0.072 g, 0.21 mmol). Product **143** (0.043 g, 0.11 mmol, 52%) was obtained as a yellow solid and product **144** (0.018 g, 0.048 mmol, 23%) was obtained as a yellow solid:

Compound **143**:

R_f = 0.58, 30% EtOAc in hexanes;

M.P. = 206-208 °C

^{1}H NMR (300 MHz, $CDCl_3$) δ = 10.89 (s, 1H), 8.56 (d, *J* = 9.1 Hz, 1H), 8.26 (d, *J* = 2.1 Hz, 1H), 8.05 (dd, *J* = 9.1, 2.2 Hz, 1H), 7.54 – 7.44 (m, 5H), 7.14 (s, 1H), 4.20 (s, 3H), 3.38 (s, 3H);

^{13}C NMR (75 MHz, $CDCl_3$) δ = 170.7, 157.3, 145.6, 142.0, 138.5, 135.9, 134.7, 129.3, 128.7, 128.6, 126.3, 125.3, 121.7, 119.9, 113.6, 105.5, 105.4, 52.5, 33.8;

IR (neat): ν_{max} = 3152, 2923, 1653, 1503, 1436, 1318, 1249, 1106, 871, 799, 701 cm^{-1}.

HRMS (APPI+) calc'd for $C_{21}H_{16}N_2O_5$ [M^+] 376.1059, found 376.1057.

Compound **144**:

R_f = 0.42, 30% EtOAc in hexanes;

M.P. = 166-169 °C

^{1}H NMR (300 MHz, $CDCl_3$) δ = 10.71 (s, 1H), 8.32 (d, *J* = 2.1 Hz, 1H), 7.87 (dd, *J* = 8.8, 2.1 Hz, 1H), 7.58 – 7.49 (m, 5H), 7.21 (d, *J* = 8.8 Hz, 1H), 6.84 (s, 1H), 4.12 (s, 3H), 3.88 (s, 3H);

^{13}C NMR (75 MHz, $CDCl_3$) δ = 169.5, 162.4, 145.9, 144.8, 144.2, 142.0, 139.1, 128.9, 128.6, 128.2, 120.9, 115.6, 114.5, 112.7, 105.7, 97.7, 52.5, 36.1; (one aromatic carbon is not observed presumably due to overlap)

IR (neat): ν_{max} = 2956, 2920, 1698, 1506, 1438, 1330, 1274, 1108, 800, 780, 710 cm^{-1}.

HRMS (APPI+) calc'd for $C_{21}H_{16}N_2O_5$ [M^+] 376.1059, found 376.1076.

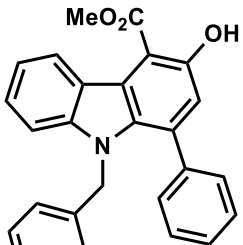

145

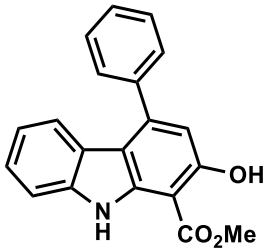

70

Product **145** and **70** were prepared following General Experimental Procedure **B**. Diazo-indole **112** (0.099 g, 0.23 mmol), copper(II) triflate (0.017 g, 0.046 mmol), tetrabutylammonium perchlorate (0.079 g, 0.23 mmol). Product **145** (0.057 g,

0.140 mmol, 61%) was obtained as a yellow solid and product **70** (0.010 g, 0.032 mmol, 14%) was obtained as white solid:

Compound **145**:

***R*f** = 0.48, 20% EtOAc in hexanes;

M.P. = 121-124 °C

^{1}H NMR (300 MHz, $CDCl_3$) δ = 10.72 (s, 1H), 8.48 (d, *J* = 7.7 Hz, 1H), 7.42 – 7.36 (m, 1H), 7.35 – 7.29 (m, 1H), 7.25 – 7.14 (m, 6H), 7.12 – 7.04 (m, 3H), 6.93 (s, 1H), 6.47 (d, *J* = 6.5 Hz, 2H), 5.06 (s, 2H), 4.20 (s, 3H) ppm;

^{13}C NMR (75 MHz, $CDCl_3$) δ = 171.4, 156.3, 143.2, 138.8, 137.5, 134.3, 132.8, 129.0, 128.3, 128.1, 128.0, 126.9, 126.6, 125.6, 124.9, 122.0, 121.8, 119.4, 119.2, 110.1, 105.5, 52.2, 48.2 ppm;

IR (neat): ν_{max} = 3025, 2947, 1657, 1561, 1438, 1314, 1202, 1030, 912, 707 cm^{-1}.

HRMS (APPI+) calc'd for $C_{27}H_{21}NO_3$ [M^+] 407.1521, found 407.1515.

Compound **70**:

***R*f** = 0.39, 30% EtOAc in hexanes;

M.P. = 100-103 °C

^{1}H NMR (300 MHz, $CDCl_3$) δ = 11.02 (s, 1H), 9.39 (s, 1H), 7.60 – 7.48 (m, 5H), 7.43 (app dt, *J* = 7.4, 1.1 Hz, 1H), 7.31 – 7.24 (m, 2H), 6.97 (ddd, *J* = 8.0, 7.3, 1.0 Hz, 1H), 6.74 (s, 1H), 4.15 (s, 3H) ppm;

^{13}C NMR (75 MHz, $CDCl_3$) δ = 170.5, 161.3, 145.6, 140.0, 139.6, 139.1, 128.8, 128.6, 128.4, 124.7, 122.8, 121.4, 120.0, 114.3, 111.0, 110.7, 95.5, 52.7 ppm;

IR (neat): ν_{max} = 3469, 3058, 2918, 1664, 1541, 1444, 1371, 1199, 1138, 779, 734 cm^{-1}.

HRMS (APPI+) calc'd for $C_{20}H_{15}NO_3$ [M^+] 317.1052, found 317.1047.

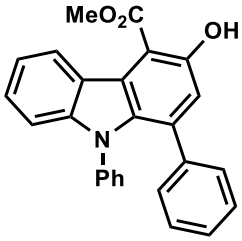

146

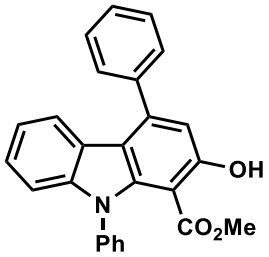

147

Product **146** and **147** were prepared following General Experimental Procedure **B**. Diazo-indole **113** (0.085 g, 0.20 mmol), copper(II) triflate (0.014 g, 0.039 mmol), tetrabutylammonium perchlorate (0.068 g, 0.20 mmol). Product **146** and **147** (0.052 g, 0.13 mmol, 65%) were obtained as a 1.0:1.7 mixture respectively, as a light-yellow foam. *Note:* isomers **146** and **147** were separated by preparative TLC (5% EtOAc in hexanes, developed three times sequentially) for characterization.

Compound **146**:

***R*f** = 0.28, 10% EtOAc in hexanes;

^{1}H NMR (300 MHz, $CDCl_3$) δ = 10.76 (s, 1H), 8.49 (d, *J* = 8.7 Hz, 1H), 7.36 (ddd, *J* = 8.3, 7.0, 1.3 Hz, 1H), 7.28 – 7.17 (m, 3H), 7.09 – 6.94 (m, 10H), 4.23 (s, 3H) ppm;

^{13}C NMR (75 MHz, $CDCl_3$) δ = 171.4, 156.8, 143.8, 138.3, 138.0, 134.8, 133.0, 129.1, 128.8, 128.5, 127.5, 127.2, 127.0, 126.6, 124.7, 122.3, 122.0, 119.9, 119.2, 110.8, 105.3, 52.3 ppm;

IR (neat): ν_{max} = 3056, 2952, 1728, 1661, 1594, 1438, 1357, 1264, 1202, 1148, 1097, 755, 698 cm^{-1}.
HRMS (APPI+) calc'd for $C_{26}H_{19}NO_3$ [M^+] 393.1365, found 393.1365.
Compound **147**:
R_f = 0.25, 10% EtOAc in hexanes;
^{1}H NMR (300 MHz, $CDCl_3$) δ = 10.34 (s, 1H), 7.63 – 7.52 (m, 7H), 7.44 – 7.38 (m, 3H), 7.25 – 7.19 (m, 2H), 6.99 (ddd, *J* = 8.0, 7.1, 1.2 Hz, 1H), 6.84 (s, 1H), 3.14 (s, 3H) ppm;
^{13}C NMR (75 MHz, $CDCl_3$) δ = 169.5, 160.1, 144.6, 142.7, 141.7, 140.5, 140.1, 130.0, 128.8, 128.7, 128.4, 127.3, 125.9, 124.9, 123.3, 121.3, 120.9, 116.5, 112.0, 110.5, 98.3, 51.4 ppm;
IR (neat): ν_{max} = 3057, 2951, 1663, 1592, 1564, 1445, 1398, 1266, 1196, 1129, 767, 700 cm^{-1}.
HRMS (APPI+) calc'd for $C_{26}H_{19}NO_3$ [M^+] 393.1365, found 393.1354.

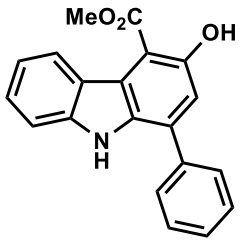

71

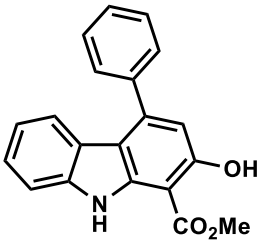

70

Product **71** and **70** were prepared following General Experimental Procedure **B**. Diazo-indole **69** (0.081 g, 0.23 mmol), copper(II) triflate (0.017 g, 0.046 mmol), tetrabutylammonium perchlorate (0.079 g, 0.23 mmol). Product **71** (0.017 g, 0.054 mmol, 23%) was obtained as a thick yellow oil and product **70** (0.047 g, 0.15 mmol, 65%) was obtained as white solid:
Compound **71**:
R_f = 0.58, 30% EtOAc in hexanes;
^{1}H NMR (300 MHz, $CDCl_3$) δ = 11.16 (s, 1H), 8.48 (d, *J* = 8.4 Hz, 1H), 8.31 (s, 1H), 7.67 – 7.53 (m, 4H), 7.52 – 7.46 (m, 1H), 7.42 – 7.37 (m, 2H), 7.21 (ddd, *J* = 8.3, 5.7, 2.5 Hz, 1H), 7.13 (s, 1H), 4.19 (s, 3H) ppm;
^{13}C NMR (75 MHz, $CDCl_3$) δ = 171.7, 158.1, 140.7, 137.6, 133.1, 131.9, 129.5, 128.8, 128.5, 126.4, 125.2, 122.7, 120.6, 119.4, 116.3, 111.1, 105.0, 52.1 ppm;
IR (neat): ν_{max} = 3362, 2923, 2851, 1699, 1647, 1437, 1389, 1245, 1194, 1026, 842, 704 cm^{-1}.
HRMS (APPI+) calc'd for $C_{20}H_{15}NO_3$ [M^+] 317.1052, found 317.1041.
Compound **70**:
Spectral data matched is reported before.

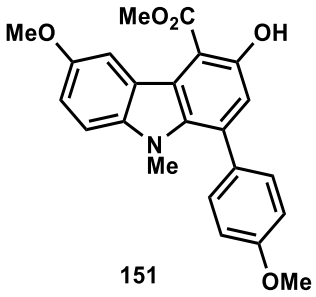

151

Product **151** was prepared following General Experimental Procedure **B**. Diazo-indole **116** (0.099 g, 0.23 mmol), copper(II) triflate (0.017 g, 0.046 mmol), tetrabutylammonium perchlorate (0.079 g, 0.23 mmol). Product **151** (0.063 g, 0.16 mmol, 70%) was obtained as a yellow solid.

Compound **151**:

***R*f** = 0.41, 30% EtOAc in hexanes;

M.P. = 198-200 °C

^{1}H NMR (300 MHz, $CDCl_3$) δ = 10.78 (s, 1H), 7.98 (d, *J* = 2.5 Hz, 1H), 7.41 – 7.35 (m, 2H), 7.25 (d, *J* = 8.9 Hz, 1H), 7.14 (dd, *J* = 9.0, 2.5 Hz, 1H), 7.04 – 6.99 (m, 2H), 6.97 (s, 1H), 4.19 (s, 3H), 3.93 (s, 3H), 3.89 (s, 3H), 3.30 (s, 3H) ppm;

^{13}C NMR (75 MHz, $CDCl_3$) δ = 171.4, 159.6, 156.3, 153.0, 139.1, 134.6, 134.1, 131.7, 130.5, 121.9, 120.9, 118.8, 116.2, 113.8, 110.0, 107.5, 104.8, 56.1, 55.5, 52.1, 33.6 ppm;

IR (neat): ν_{max} = 3157, 2941, 1669, 1608, 1483, 1320, 1279, 1028, 826, 803 cm^{-1}.

HRMS (APPI+) calc'd for $C_{23}H_{21}NO_5$ [M^+] 391.1420, found 391.1416, calc'd for $C_{23}H_{22}NO_5$ [M+H]$^+$ 492.1492, found 392.1485.

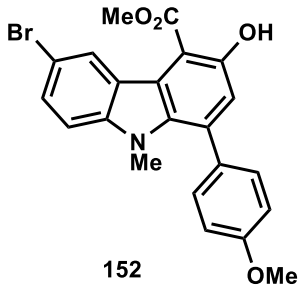

152

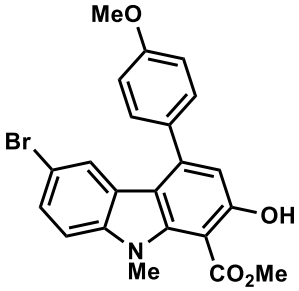

153

Product **152** and **153** were prepared following General Experimental Procedure **B**. Diazo-indole **118** (0.095 g, 0.20 mmol), copper(II) triflate (0.014 g, 0.040 mmol), tetrabutylammonium perchlorate (0.068 g, 0.20 mmol). Product **152** (0.058 g, 0.13 mmol, 65%) was obtained as a yellow solid and product **153** (0.0070 g, 0.016 mmol, 8%) was obtained as thick brown oil:

Compound **152**:

***R*f** = 0.60, 20% EtOAc in hexanes;

M.P. = 170-172 °C

^{1}H NMR (300 MHz, $CDCl_3$) δ = 10.89 (s, 1H), 8.61 (d, *J* = 2.0 Hz, 1H), 7.53 (dd, *J* = 8.8, 2.0 Hz, 1H), 7.38 – 7.35 (m, 2H), 7.21 (d, *J* = 8.8 Hz, 1H), 7.03 – 6.98 (m, 3H), 4.19 (s, 3H), 3.90 (s, 3H), 3.31 (s, 3H) ppm;

^{13}C NMR (75 MHz, $CDCl_3$) δ = 171.1, 159.7, 156.8, 142.0, 134.2, 134.1, 131.2, 130.4, 128.8, 127.8, 123.3, 120.1, 119.8, 113.8, 111.8, 110.8, 104.8, 55.5, 52.1, 33.6 ppm;

IR (neat): ν_{max} = 2951, 2919, 1653, 1607, 1469, 1386, 1209, 1065, 925, 879, 740 cm^{-1}.
HRMS (APPI+) calc'd for $C_{22}H_{18}{}^{79}BrNO_4$ [M^+] 439.0419, found 439.0417.
Compound **153**:
***R*f** = 0.55, 20% EtOAc in hexanes;
^{1}H NMR (300 MHz, $CDCl_3$) δ = 10.52 (s, 1H), 7.51 – 7.41 (m, 4H), 7.25 (d, *J* = 8.6 Hz, 1H), 7.10 – 7.05 (m, 2H), 6.75 (s, 1H), 4.08 (s, 3H), 3.93 (s, 3H), 3.76 (s, 3H) ppm;
^{13}C NMR (75 MHz, $CDCl_3$) δ = 169.8, 161.1, 160.1, 145.0, 142.3, 141.8, 131.7, 130.0, 127.4, 124.9, 123.8, 114.7, 114.2, 113.2, 111.6, 110.9, 97.2, 55.6, 52.3, 36.0 ppm;
IR (neat): ν_{max} = 2952, 2919, 1699, 1607, 1481, 1457, 1388, 1199, 1068, 796 cm^{-1}.
HRMS (APPI+) calc'd for $C_{22}H_{18}{}^{79}BrNO_4$ [M^+] 439.0419, found 439.0399.

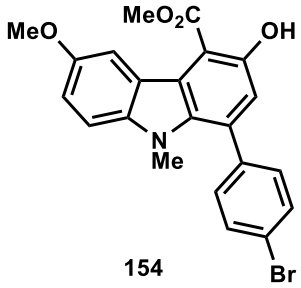

154

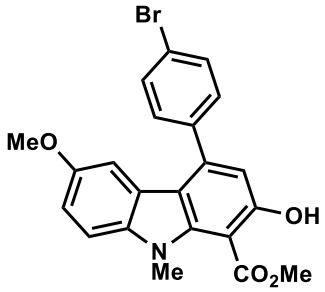

155

Product **154** and **155** were prepared following General Experimental Procedure **B**. Diazo-indole **117** (0.068 g, 0.14 mmol), copper(II) triflate (0.010 g, 0.028 mmol), tetrabutylammonium perchlorate (0.048 g, 0.14 mmol). Product **154** (0.020 g, 0.045 mmol, 32%) was obtained as a yellow solid and product **155** (0.016 g, 0.036 mmol, 26%) was obtained as thick yellow oil:
Compound **154**:
***R*f** = 0.47, 30% EtOAc in hexanes;
M.P. = 192-195 °C
^{1}H NMR (300 MHz, $CDCl_3$) δ = 10.73 (s, 1H), 7.97 (d, *J* = 2.4 Hz, 1H), 7.64 – 7.59 (m, 2H), 7.37 – 7.33 (m, 2H), 7.26 (d, *J* = 8.9 Hz, 1H), 7.16 (dd, *J* = 9.0, 2.5 Hz, 1H), 6.96 (s, 1H), 4.20 (s, 3H), 3.93 (s, 3H), 3.29 (s, 3H) ppm;
^{13}C NMR (75 MHz, $CDCl_3$) δ = 171.2, 156.1, 153.2, 139.1, 138.4, 134.1, 132.6, 131.6, 131.0, 122.4, 121.8, 121.2, 118.6, 116.4, 110.1, 107.5, 105.4, 56.1, 52.2, 33.9 ppm;
IR (neat): ν_{max} = 2949, 2920, 1646, 1574, 1481, 1333, 1205, 1102, 1038, 865, 787, 730 cm^{-1}.
HRMS (APPI+) calc'd for $C_{22}H_{18}{}^{79}BrNO_4$ [M^+] 439.0419, found 439.0401.
Compound **155**:
***R*f** = 0.35, 30% EtOAc in hexanes;
^{1}H NMR (300 MHz, $CDCl_3$) δ = 10.52 (s, 1H), 7.68 – 7.64 (m, 2H), 7.46 – 7.41 (m, 2H), 7.28 (d, *J* = 8.9 Hz, 1H), 6.98 (dd, *J* = 8.8, 2.5 Hz, 1H), 6.69 (s, 1H), 6.68 (d, *J* = 2.3 Hz, 1H), 4.08 (s, 3H), 3.75 (s, 3H), 3.63 (s, 3H) ppm;
^{13}C NMR (75 MHz, $CDCl_3$) δ = 169.9, 160.6, 154.2, 143.3, 142.4, 138.8, 138.2, 131.8, 130.6, 123.2, 122.6, 115.3, 113.4, 110.4, 110.2, 104.7, 97.6, 55.8, 52.2, 36.0 ppm;
IR (neat): ν_{max} = 2924, 2852, 1654, 1477, 1388, 1259, 1172, 1008, 826, 796, 726 cm^{-1}.
HRMS (APPI+) calc'd for $C_{22}H_{18}{}^{79}BrNO_4$ [M^+] 439.0419, found 439.0404.

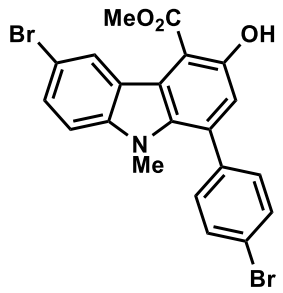

156

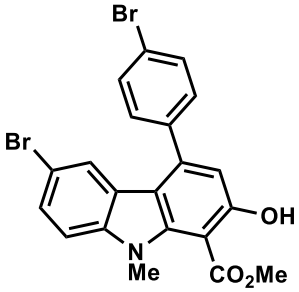

157

Product **156** and **157** were prepared following General Experimental Procedure **B**. Diazo-indole **115** (0.10 g, 0.19 mmol), copper(II) triflate (0.014 g, 0.038 mmol), tetrabutylammonium perchlorate (0.065 g, 0.19 mmol). Product **156** (0.033 g, 0.067 mmol, 35%) was obtained as a yellow solid and product **157** (0.045 g, 0.092 mmol, 48%) was obtained as a brown solid:

Compound **156**:

***R*f** = 0.55, 20% EtOAc in hexanes;

M.P. = 200-203 °C

^{1}H NMR (300 MHz, $CDCl_3$) δ = 10.83 (s, 1H), 8.60 (d, *J* = 1.9 Hz, 1H), 7.64 – 7.60 (m, 2H), 7.54 (dd, *J* = 8.8, 2.0 Hz, 1H), 7.35 – 7.31 (m, 2H), 7.20 (d, *J* = 8.8 Hz, 1H), 6.99 (s, 1H), 4.18 (s, 3H), 3.29 (s, 3H) ppm;

^{13}C NMR (75 MHz, $CDCl_3$) δ = 170.9, 156.7, 142.0, 138.0, 133.7, 132.7, 131.7, 131.0, 129.1, 127.9, 123.3, 122.7, 120.5, 119.6, 112.0, 110.8, 105.5, 52.9, 33.8 ppm;

IR (neat): ν_{max} = 2920, 2850, 1698, 1655, 1470, 1280, 1166, 1013, 925, 828, 731 cm^{-1}.

HRMS (APPI+) calc'd for $C_{21}H_{15}{}^{79}Br_2NO_3$ [M^+] 486.9419, found 486.9426.

Compound **157**:

***R*f** = 0.28, 20% EtOAc in hexanes;

M.P. = 214-216 °C

^{1}H NMR (300 MHz, $CDCl_3$) δ = 10.47 (s, 1H), 7.69 – 7.64 (m, 2H), 7.44 – 7.37 (m, 3H), 7.34 (d, *J* = 1.6 Hz, 1H), 7.23 (d, *J* = 8.6 Hz, 1H), 6.71 (s, 1H), 4.08 (s, 3H), 3.74 (s, 3H) ppm;

^{13}C NMR (75 MHz, $CDCl_3$) δ = 169.6, 161.0, 143.5, 142.2, 141.8, 138.3, 132.0, 130.4, 127.7, 124.4, 123.6, 123.0, 114.3, 113.3, 111.5, 111.1, 97.7, 52.3, 35.9 ppm;

IR (neat): ν_{max} = 2920, 2850, 1654, 1576, 1436, 1286, 1202, 1068, 830, 797 cm^{-1}.

HRMS (APPI+) calc'd for $C_{21}H_{15}{}^{79}Br_2NO_3$ [M^+] 486.9419, found 486.9414.

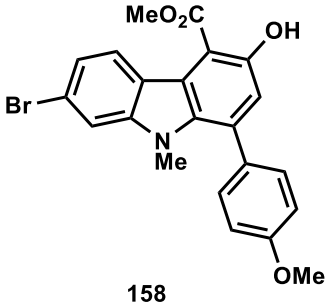

158

Product **158** was prepared following General Experimental Procedure **B**. Diazo-indole **119** (0.091 g, 0.19 mmol), copper(II) triflate (0.014 g, 0.038 mmol),

tetrabutylammonium perchlorate (0.065 g, 0.19 mmol). Product **158** (0.053 g, 0.12 mmol, 63%) was obtained as a yellow solid:

Compound **158**:

***R*f** = 0.56, 20% EtOAc in hexanes;

M.P. = 129-132 ºC

^{1}H NMR (300 MHz, $CDCl_3$) δ = 10.83 (s, 1H), 8.29 (d, *J* = 8.9 Hz, 1H), 7.47 (d, *J* = 1.8 Hz, 1H), 7.38 – 7.33 (m, 2H), 7.28 (dd, *J* = 8.9, 1.9 Hz, 1H), 7.03 – 6.98 (m, 3H), 4.15 (s, 3H), 3.89 (s, 3H), 3.28 (s, 3H) ppm;

^{13}C NMR (75 MHz, $CDCl_3$) δ = 171.2, 159.7, 156.8, 144.3, 134.1, 133.9, 131.3, 130.4, 126.2, 122.2, 120.9, 120.7, 120.2, 119.4, 113.9, 112.4, 104.9, 55.5, 52.2, 33.6 ppm;

IR (neat): ν_{max} = 2949, 2926, 1650, 1602, 1438, 1312, 1245, 1067, 915, 787 cm^{-1}.

HRMS (APPI+) calc'd for $C_{22}H_{18}Br^{79}NO_4$ [M^+] 439.0419, found 439.0431.

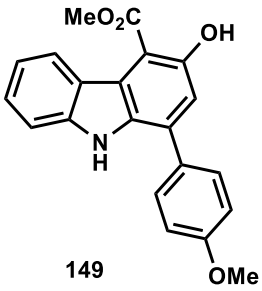

149

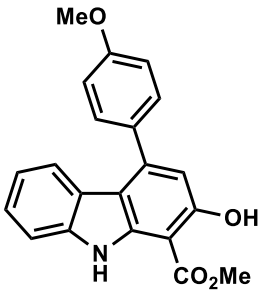

159

Product **149** and **150** were prepared following General Experimental Procedure **B**. Diazo-indole **148** (0.081 g, 0.21 mmol), copper(II) triflate (0.015 g, 0.042 mmol), tetrabutylammonium perchlorate (0.072 g, 0.21 mmol). Product **149** (0.037 g, 0.11 mmol, 52%) was obtained as a yellow solid and product **150** (0.024 g, 0.069 mmol, 33%) was obtained as cream solid:

Compound **149**:

***R*f** = 0.50, 20% EtOAc in hexanes;

M.P. = 158-160 ºC

^{1}H NMR (300 MHz, $CDCl_3$) δ = 11.18 (s, 1H), 8.48 (d, *J* = 8.7 Hz, 1H), 8.31 (s, 1H), 7.62 – 7.57 (m, 2H), 7.42 – 7.38 (m, 2H), 7.21 (ddd, *J* = 8.3, 5.2, 3.0 Hz, 1H), 7.11-7.06 (m, 3H), 4.19 (s, 3H), 3.89 (s, 3H) ppm;

^{13}C NMR (75 MHz, $CDCl_3$) δ = 171.8, 160.1, 158.2, 140.7, 132.9, 132.0, 129.8, 129.7, 126.3, 125.3, 122.8, 120.5, 119.4, 116.1, 115.0, 111.1, 104.6, 55.6, 52.1 ppm;

IR (neat): ν_{max} = 3422, 3339, 2953, 1740, 1659, 1506, 1438, 1317, 1250, 1182, 1034, 832, 728 cm^{-1}.

HRMS (APPI+) calc'd for $C_{21}H_{17}NO_4$ [M^+] 347.1158, found 347.1155.

Compound **150**:

***R*f** = 0.45, 20% EtOAc in hexanes;

M.P. = 142-145 ºC

^{1}H NMR (300 MHz, $CDCl_3$) δ = 11.00 (s, 1H), 9.42 (s, 1H), 7.57 – 7.52 (m, 2H), 7.47 – 7.41 (m, 2H), 7.30 (ddd, *J* = 8.2, 7.2, 1.2 Hz, 1H), 7.10 – 7.04 (m, 2H), 7.00 (ddd, *J* = 8.1, 7.2, 1.1 Hz, 1H), 6.73 (s, 1H), 4.18 (s, 3H), 3.93 (s, 3H) ppm;

^{13}C NMR (75 MHz, $CDCl_3$) δ = 170.5, 161.3, 159.9, 145.5, 139.7, 139.1, 132.3, 130.1, 124.7, 122.9, 121.5, 115.0, 114.4, 114.0, 111.0, 110.7, 95.2, 55.5, 52.7 ppm;

IR (neat): ν_{max} = 3438, 2924, 2853, 1662, 1588, 1441, 1272, 1244, 1024, 831, 731 cm^{-1}.
HRMS (APPI+) calc'd for $C_{21}H_{17}NO_4$ [M^+] 347.1158, found 347.1167.

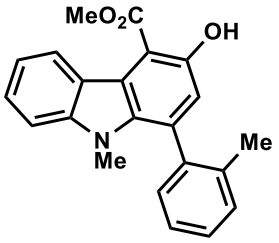

165

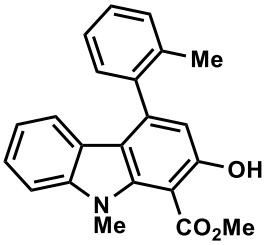

166

Product **165** and **166** were prepared following General Experimental Procedure **B**. Diazo-indole **125** (0.079 g, 0.21 mmol), copper(II) triflate (0.015 g, 0.042 mmol), tetrabutylammonium perchlorate (0.072 g, 0.21 mmol). Product **165** (0.045 g, 0.13 mmol, 62%) was obtained as a yellow solid and product **166** (0.014 g, 0.041 mmol, 20%) was obtained as thick brown oil:

Compound **165**:

***R*f** = 0.62, 20% EtOAc in hexanes;

M.P. = 143-146 °C

^{1}H NMR (300 MHz, $CDCl_3$) δ = 10.79 (s, 1H), 8.47 (dd, *J* = 8.4 Hz, 1H), 7.47 (ddd, *J* = 8.2, 7.0, 1.2 Hz, 1H), 7.40 – 7.28 (m, 5H), 7.21 (ddd, *J* = 8.2, 6.9, 1.1 Hz, 1H), 6.94 (s, 1H), 4.19 (s, 3H), 3.22 (s, 3H), 2.07 (s, 3H) ppm;

^{13}C NMR (75 MHz, $CDCl_3$) δ = 171.5, 156.3, 143.1, 138.9, 136.7, 133.4, 133.4, 130.0, 129.8, 128.5, 126.3, 125.8, 124.9, 121.6, 120.8, 118.9, 118.4, 109.2, 105.4, 52.1, 31.5, 20.2 ppm;

IR (neat): ν_{max} = 3052, 2924, 1652, 1589, 1470, 1386, 1192, 1100, 931, 746, 728 cm^{-1}.

HRMS (APPI+) calc'd for $C_{22}H_{19}NO_3$ [M^+] 345.1365, found 345.1370.

Compound **166**:

***R*f** = 0.50, 20% EtOAc in hexanes;

^{1}H NMR (300 MHz, $CDCl_3$) δ = 10.52 (s, 1H), 7.45 – 7.39 (m, 1H), 7.38 – 7.25 (m, 5H), 6.71 (s, 1H), 6.69 (d, *J* = 7.6 Hz, 1H), 6.94 (ddd, *J* = 8.1, 6.7, 1.5 Hz, 1H), 4.09 (s, 3H), 3.80 (s, 3H), 2.09 (s, 3H) ppm;

^{13}C NMR (75 MHz, $CDCl_3$) δ = 170.0, 160.6, 144.2, 143.0, 141.4, 139.6, 136.0, 130.2, 128.7, 128.4, 126.2, 124.8, 123.2, 120.6, 120.5, 116.2, 110.5, 109.4, 97.5, 52.2, 35.8, 19.8 ppm;

IR (neat): ν_{max} = 3054, 2949, 1719, 1660, 1593, 1467, 1395, 1254, 1098, 913, 749 cm^{-1}.

HRMS (APPI+) calc'd for $C_{22}H_{19}NO_3$ [M^+] 345.1365, found 345.1352.

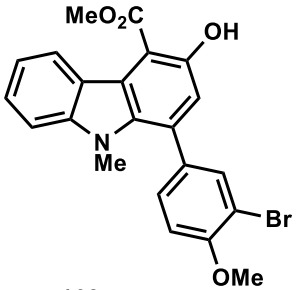

162

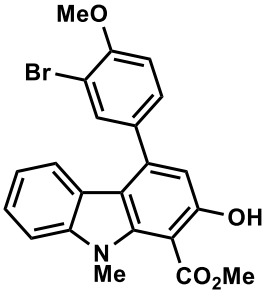

163

Product **162** and **163** were prepared following General Experimental Procedure **B**. Diazo-indole **120** (0.082 g, 0.17 mmol), copper(II) triflate (0.012 g, 0.034 mmol), tetrabutylammonium perchlorate (0.058 g, 0.17 mmol). Product **162** (0.046 g, 0.10 mmol, 59%) was obtained as a yellow solid and product **163** (0.010 g, 0.023 mmol, 14%) was obtained as cream color solid:

Compound **162**:

R_f = 0.48, 30% EtOAc in hexanes;

M.P. = 198-201 °C

^{1}H NMR (300 MHz, $CDCl_3$) δ = 10.75 (s, 1H), 8.44 (ddd, *J* = 8.3, 1.2, 0.7 Hz, 1H), 7.68 (d, *J* = 2.2 Hz, 1H), 7.49 (ddd, *J* = 8.2, 7.0, 1.2 Hz, 1H), 7.41 – 7.34 (m, 2H), 7.22 (ddd, *J* = 8.2, 7.0, 1.2 Hz, 1H), 7.01 (d, *J* = 8.5 Hz, 1H), 6.98 (s, 1H), 4.19 (s, 3H), 3.99 (s, 3H), 3.36 (s, 3H) ppm;

^{13}C NMR (75 MHz, $CDCl_3$) δ = 171.3, 156.2, 155.9, 143.6, 134.1, 133.6, 133.0, 132.0, 129.4, 126.5, 124.9, 121.7, 121.6, 119.1, 118.8, 111.58, 111.56, 109.5, 105.5, 56.5, 52.2, 33.7 ppm;

IR (neat): ν_{max} = 2949, 2921, 1652, 1558, 1489, 1318, 1252, 1082, 871, 728 cm^{-1}.

HRMS (APPI+) calc'd for $C_{22}H_{18}{}^{79}BrNO_4$ [M^+] 439.0419, found 439.0425.

Compound **163**:

R_f = 0.33, 30% EtOAc in hexanes;

M.P. = 223-225 °C

^{1}H NMR (300 MHz, $CDCl_3$) δ = 10.45 (s, 1H), 7.78 (d, *J* = 2.1 Hz, 1H), 7.49 (dd, *J* = 8.4, 2.1 Hz, 1H), 7.41 – 7.34 (m, 2H), 7.31 (d, *J* = 7.9 Hz, 1H), 7.06 – 7.00 (m, 2H), 6.72 (s, 1H), 4.09 (s, 3H), 4.02 (s, 3H), 3.78 (s, 3H) ppm;

^{13}C NMR (75 MHz, $CDCl_3$) δ = 169.9, 160.4, 156.1, 143.2, 142.9, 141.9, 133.72, 133.68, 129.1, 125.0, 122.8, 121.1, 120.3, 115.6, 111.9, 111.8, 111.0, 109.6, 97.5, 56.5, 52.2, 35.9 ppm;

IR (neat): ν_{max} = 2917, 2848, 1669, 1557, 1488, 1437, 1389, 1256, 1196, 1013, 798, 737 cm^{-1}.

HRMS (APPI+) calc'd for $C_{22}H_{18}{}^{79}BrNO_4$ [M^+] 439.0419, found 439.0421.

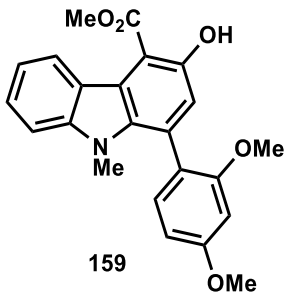

159

Product **159** was prepared following General Experimental Procedure **B**. Diazo-indole **122** (0.081 g, 0.19 mmol), copper(II) triflate (0.014 g, 0.038 mmol), tetrabutylammonium perchlorate (0.065 g, 0.19 mmol). Product **159** (0.035 g, 0.089 mmol, 47%) was obtained as a yellow solid:

Compound **159**:

R_f = 0.47, 20% EtOAc in hexanes;

M.P. = 169-171 °C
^{1}H NMR (300 MHz, $CDCl_3$) δ = 10.76 (s, 1H), 8.44 (apt. dt, *J* = 8.3, 0.9 Hz, 2H),7.45 (ddd, *J* = 8.2, 6.9, 1.2 Hz, 1H), 7.32 (d, *J* = 8.2 Hz, 1H), 7.23 (d, *J* = 8.1 Hz, 1H), 7.18 (ddd, *J* = 8.2, 7.0, 1.2 Hz, 1H), 6.95 (s, 1H), 6.60 (dd, *J* = 8.2, 2.4 Hz, 1H), 6.56 (d, *J* = 2.3 Hz, 1H), 4.17 (s, 3H), 3.89 (s, 3H), 3.68 (s, 3H), 3.36 (s, 3H) ppm;
^{13}C NMR (75 MHz, $CDCl_3$) δ = 171.6, 161.4, 158.1, 156.2, 142.8, 134.2, 131.5, 130.5, 126.0, 124.9, 121.5, 121.1, 120.4, 119.5, 118.6, 109.0, 105.2, 104.3, 98.5, 55.6, 55.5, 52.0, 31.3 ppm;
IR (neat): ν_{max} = 2947, 2920, 1699, 1654, 1488, 1439, 1241, 1194, 906, 769 cm^{-1}.
HRMS (APPI+) calc'd for $C_{23}H_{21}NO_5$ [M^+] 391.1420, found 391.1407.

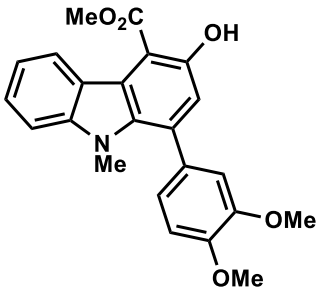

160

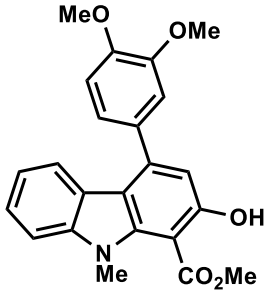

161

Product **160** and **161** were prepared following General Experimental Procedure **B**. Diazo-indole **123** (0.10 g, 0.24 mmol), copper(II) triflate (0.017 g, 0.048 mmol), tetrabutylammonium perchlorate (0.082 g, 0.24 mmol). Product **160** (0.034 g, 0.087 mmol, 36%) was obtained as a yellow solid and product **161** (0.016 g, 0.041 mmol, 17%) was obtained as yellow solid:
Compound **160**:
***R*$_f$** = 0.53, 20% EtOAc in hexanes;
M.P. = 159-161 °C
^{1}H NMR (300 MHz, $CDCl_3$) δ = 10.77 (s, 1H), 8.45 (d, *J* = 8.6 Hz, 1H), 7.46 (ddd, *J* = 8.2, 6.9, 1.3 Hz, 1H), 7.32 (d, *J* = 8.2 Hz, 1H), 7.22 – 7.13 (m, 2H), 7.03 (dd, *J* = 8.3, 1.6 Hz, 1H), 7.01 (s, 1H), 6.95 (dd, *J* = 7.5, 1.6 Hz, 1H), 4.19 (s, 3H), 3.94 (s, 3H), 3.52 (s, 3H), 3.37 (s, 3H) ppm;
^{13}C NMR (75 MHz, $CDCl_3$) δ = 171.6, 155.9, 152.9, 146.8, 143.0, 134.1, 133.8, 130.0, 126.2, 124.8, 124.1, 123.0, 121.4, 120.7, 118.8, 118.7, 112.6, 109.2, 105.5, 60.7, 56.0, 52.1, 31.5 ppm;
IR (neat): ν_{max} = 2957, 2930, 1660, 1608, 1442, 1388, 1260, 1075, 998, 724 cm^{-1}.
HRMS (APPI-) calc'd for $C_{23}H_{21}NO_5$ [M^-] 391.1420, found 391.1416.
Compound **161**:
***R*$_f$** = 0.35, 20% EtOAc in hexanes;
M.P. = 118-121 °C
^{1}H NMR (300 MHz, $CDCl_3$) δ = 10.48 (s, 1H), 7.37 – 7.29 (m, 2H), 7.17 (d, *J* = 7.9 Hz, 1H), 7.08 (dd, *J* = 8.2, 1.6 Hz, 1H), 6.96 (dd, *J* = 5.7, 1.4 Hz, 2H), 6.91 (dd, *J* = 7.6, 1.6 Hz, 1H), 6.78 (s, 1H), 4.08 (s, 3H), 3.97 (s, 3H), 3.78 (s, 3H), 3.54 (s, 3H) ppm;

^{13}C NMR (75 MHz, $CDCl_3$) δ = 170.1, 160.2, 153.2, 146.7, 143.1, 141.5, 140.8, 134.3, 124.7, 124.3, 123.1, 122.4, 121.1, 120.4, 116.5, 112.6, 111.0, 109.4, 97.6, 61.2, 56.1, 52.2, 35.8 ppm;
IR (neat): ν_{max} = 2958, 2920, 1699, 1560, 1465, 1306, 1260, 1080, 793, 731 cm^{-1}.
HRMS (APPI-) calc'd for $C_{23}H_{21}NO_5$ [M^-] 391.1420, found 391.1424.

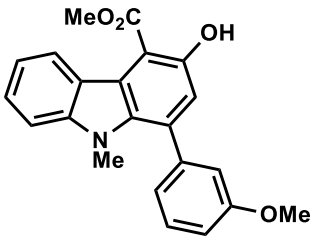

167

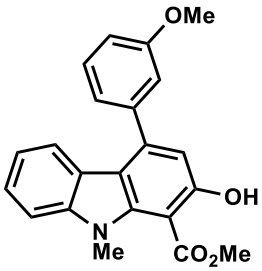

168

Product **167** and **168** were prepared following General Experimental Procedure **B**. Diazo-indole **124** (0.092 g, 0.24 mmol), copper(II) triflate (0.017 g, 0.048 mmol), tetrabutylammonium perchlorate (0.082 g, 0.24 mmol). Product **167** (0.033 g, 0.091 mmol, 38%) was obtained as a yellow solid and product **168** (0.0090 g, 0.025 mmol, 10%) was obtained as thick yellow oil:
Compound **167**:
R_f = 0.67, 20% EtOAc in hexanes;
M.P. = 123-125 °C
^{1}H NMR (300 MHz, $CDCl_3$) δ = 10.76 (s, 1H), 8.45 (d, *J* = 8.3 Hz, 1H), 7.48 (ddd, *J* = 8.2, 6.9, 1.2 Hz, 1H), 7.42 – 7.34 (m, 2H), 7.21 (ddd, *J* = 8.2, 6.9, 1.1 Hz, 1H), 7.0 – 6.98 (m, 4H), 4.19 (s, 3H), 3.86 (s, 3H), 3.35 (s, 3H) ppm;
^{13}C NMR (75 MHz, $CDCl_3$) δ = 171.4, 159.5, 156.2, 143.5, 140.8, 133.8, 133.6, 129.4, 126.4, 124.9, 122.0, 121.7, 121.3, 119.0, 118.6, 114.9, 113.9, 109.4, 105.4, 55.5, 52.2, 33.4 ppm;
IR (neat): ν_{max} = 3000, 2947, 1699, 1576, 1444, 1317, 1198, 1048, 780, 728 cm^{-1}.
HRMS (APPI-) calc'd for $C_{22}H_{19}NO_4$ [M^-] 361.1314, found 361.1321.
Compound **168**:
R_f = 0.40, 20% EtOAc in hexanes;
^{1}H NMR (300 MHz, $CDCl_3$) δ = 10.47 (s, 1H), 7.46 – 7.28 (m, 4H), 7.15 (d, *J* = 7.6 Hz, 1H), 7.10 – 7.03 (m, 2H), 7.00 (ddd, *J* = 8.1, 6.7, 1.9 Hz, 1H), 6.77 (s, 1H), 4.09 (s, 3H), 3.84 (s, 3H), 3.79 (s, 3H) ppm;
^{13}C NMR (75 MHz, $CDCl_3$) δ = 170.0, 160.4, 159.8, 144.6, 143.2, 141.9, 141.4, 129.7, 124.9, 122.9, 121.4, 121.2, 120.2, 115.6, 114.4, 113.9, 110.8, 109.5, 97.4, 55.5, 52.2, 35.9 ppm;
IR (neat): ν_{max} = 3294, 2950, 1705, 1659, 1558, 1467, 1346, 1239, 1067, 731 cm^{-1}.
HRMS (APPI-) calc'd for $C_{22}H_{19}NO_4$ [M^-] 361.1314, found 361.1299.

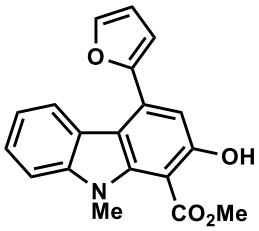

164

Product **164** was prepared following General Experimental Procedure **B**. Diazo-indole **121** (0.082 g, 0.23 mmol), copper(II) triflate (0.017 g, 0.046 mmol), tetrabutylammonium perchlorate (0.079 g, 0.23 mmol). Product **164** (0.023 g, 0.072 mmol, 31%) was obtained as an orange solid:

Compound **164**:

***R*f** = 0.65, 20% EtOAc in hexanes;

M.P. = 94-96 ºC

^{1}H NMR (300 MHz, $CDCl_3$) δ = 10.68 (s, 1H), 8.40 (apt. dt, *J* = 8.3, 1.0 Hz, 1H),7.61 (d, *J* = 0.9 Hz, 1H), 7.48 (ddd, *J* = 8.2, 6.9, 1.2 Hz, 1H), 7.38 (d, *J* = 8.2 Hz, 1H), 7.20 (ddd, *J* = 8.2, 6.9, 1.2 Hz, 1H), 7.16 (s, 1H), 6.62 – 6.58 (m, 2H), 4.17 (s, 3H), 3.47 (s, 3H) ppm;

^{13}C NMR (75 MHz, $CDCl_3$) δ = 171.2, 155.9, 151.1, 143.6, 142.8, 133.8, 126.6, 124.9, 122.2, 121.8, 121.6, 119.1, 118.5, 111.9, 110.4, 109.5, 106.6, 52.2, 31.9 ppm;

IR (neat): ν_{max} = 2953, 2924, 1653, 1541, 1441, 1374, 1257, 1081, 829, 738 cm^{-1}.

HRMS (APPI-) calc'd for $C_{19}H_{15}NO_4$ [M^-] 321.1001, found 321.1006.

3.10 References

1. Snyder, H. R.; Macdonald, J. A. *J. Am. Chem. Soc.* **1955**, *77*, 1257-1259.
2. Noland; W. E.; Hartmann; P. J. *J. Am. Chem. Soc.* **1954**, *76*, 3227-3228.
3. Dujardin, G.; Poirer, J. M. *Bull. Soc. Chim. Fr.* **1994**, *131*, 900-909.
4. Harrington, P. E.; Kerr, M. A. **1996**, *Synlett*, 1047-1048.
5. a) Yadav, J. S.; Abraham, S.; Reddy, B. V. S.; Sabitha, G. Synthesis **2001**, 2165-2169. b) Bandini, M.; Cozzi, P. G.; Giacomini, M.; Melchiorre, P.; Selva, S.; Umani-Ronchi, A. *J. Org. Chem.* **2002**, *67*, 3700-3704. c) Nayak, S. Synth. Commun. **2006,** *36*, 1307-1315. d) Xu, R.; Ding, J. C.; Chen. X. A.; Liu, M. C.; Wu, H. Y. *Chin. Chem. Lett.* **2009**, *20*, 676-679. e) Metz, T. L.; Evans, J.; Stanley, L. M. *Org. Lett.* **2017**, *19*, 3442-3445.
6. a) Lim, S.; Sim, K.; Abdullah, Z.; Hiraku, O.; Hayashi, M.; Komiyama, K.; Lam, T. S. *J. Nat. Prod.* **2007**, *70*, 1380-1383. b) Jones, S. B.; Simmons, B.; Mastracchio, A.; MacMillan, D. W. C. Nature **2011**, *475*, 183-188. c) Dethe, D. H.; Erande, R. D.; Ranjan, A. *J. Org. Chem*., **2013**, *78*, 10106-10120. d) Singh, T. P.; Singh, O. M. *Mini Rev. Med. Chem*. **2018**, *18*, 9-25.
7. a) Jackson, A. H.; Nadoo B.; Smith, P. *Tetrahedron* **1968***, 24,* 6119-6129. b) Jackson, A. H.; Smith, P. *J. Chem. Soc., Chem. Commun.* **1967**, *24*, 264-266.
8. James, M. J.; Cuthbertson, J. D.; O'Brien, P.; Taylor, R. J. K.; Unsworth, W. P. *Angew. Chem. Int. Ed.* **2015**, *54*, 7640-7643.
9. Liddon, T. R.; James, M. J.; Clarke, A. K.; O'Brien, P.; Taylor, R. J. K.; Unsworth, W. P. *Chem. Eur. J.* **2016**, *22*, 8777-8780.
10. Zhuo, C. X.; Wu, Q. F.; Zhao, Q.; Xu, Q. L.; You, S. L. *J. Am. Chem. Soc*. **2013**, *135*, 8169-8172.
11. Graebe, C.; Glazer, C. *Ber. Dtsch. Chem. Ges.* **1872**, *5*, 968-969.
12. a) Głuszynska, A. *Eur. J. Med. Chem*. **2015**, *94*, 405-426. b) Wex, B.; Kaafarani, B. R. *J. Mater. Chem. C* **2017**, *5*, 8622-8653. c) Caruso, A.; Ceramella, J.; Iacopetta, D.; Saturnino, C.; Mauro, M. V.; Bruno, R.; Aquaro, S.; Sinicropi, M. S. *Molecules* **2019**, *24*, 1912-1936. d) Zenlov, R. G.; Ektova, L. V.; Vlasova, O. A.; Belistkiy, G. A.; Yakubovskaya, M. G.; Kirsanov, K. I. *Chem. Heterocycl. Compd*, **2020**, *56*, 644-658. e) Verma, N.; Awasthi, S.; Jain, V. *Asian J. Res. Chem.* **2022**, *15*, 163-165. f) Wang, G.; Sun, S.; Guo, H. *Eur. J. Med. Chem.* **2022**,

229,113999. d) Ketavath, R.; Naik, K. P. K.; Ghugal, S. G.; Katturi, N. K.; Swetha, T.; Soma, V. R.; Murali, B. *J. Mater. Chem. C* **2020**, *8*, 16188−16197.

13. a) Park, I. K.; Suh, S. E.; Lim, B. Y.; Cho, C. G. *Org. Lett.* **2009**, *11*, 5454-5456. b) Robinson, R. *Chem. Rev.* **1969**, *69*, 227-250. c) Preston, R. W. G.; Tucker, S. H.; Cameron, J. M. L. *J. Chem. Soc.* **1942**, 500-504. d) Iddon, B.; MethCohn, O.; Scriven, E.; Suschitzky, H.; Gallagher, P. *Angew. Chem.* **1979**, *91*, 900-917. Majgier-Baranowska, H.; Williams, J. D.; Li, B.; Peet, N. P. *Tetrahedron Lett.* **2012**, *53*, 4785-4788.
14. James, M. J.; O'Brien, P.; Taylor, R. J. K.; Unsworth, W. P. *Angew. Chem. Int. Ed*. **2016**, *55*, 9671-9675.
15. Sakthivel, S.; Balamurugan, R. *J. Org. Chem.* **2018**, *83*, 12171-12183.
16. Shanahan, C. S.; Truong, P.; Mason, S. M.; Leszczynski, J. S.; Doyle, M. P. *Org. Lett.* **2013**, *15*, 3642-3645.
17. X-ray crystal structural elucidation was completed by Dr. J-B. Lin, C-CART, CREAIT Network, Memorial University of Newfoundland.
18. a) Wagner, G. *J. Russ. Phys. Chem. Soc.* **1899**, *31*, 680-684. b) Meerwein, H. *Justus Liebigs Ann. Chem.* **1914**, *405*, 129-175.
19. Regitz, M.; Menz, F.; Liedhegener, A. *Justus Liebigs Ann. Chem.* **1970**, *739*, 174-184.
20. a) Bartoli, G.; Bartolacci, M.; Bosco, M.; Foglia, G.; Giuliani, A.; Marcantoni, E.; Sambri, L.; Torregiani, L. *J. Org. Chem.* **2003**, *68*, 4594-4597. b) Firouzabadi, H.; Iranpoor, N.; Nowrouzi, F. *Chem. Commun*. **2005**, 789-791. c) Ji, X.; Tong, H.; Yuan, Y. *Synth. Commun.* **2011**, *41*, 372-379.
21. Appel, R.; Mayr, H. *J. Am. Chem. Soc.* **2011**, *133*, 8240-8251.
22. (a) Vorobyeva, D. V.; Osipov, S. N. *Synthesis* **2018**, *50*, 227-240. (d) Ciszewski, L. W.; Durka, J.; Gryko, D. *Org. Lett.* **2019**, *21*, 7028-7032.

3.11 Selected ^{1}H and ^{13}C NMR spectral data

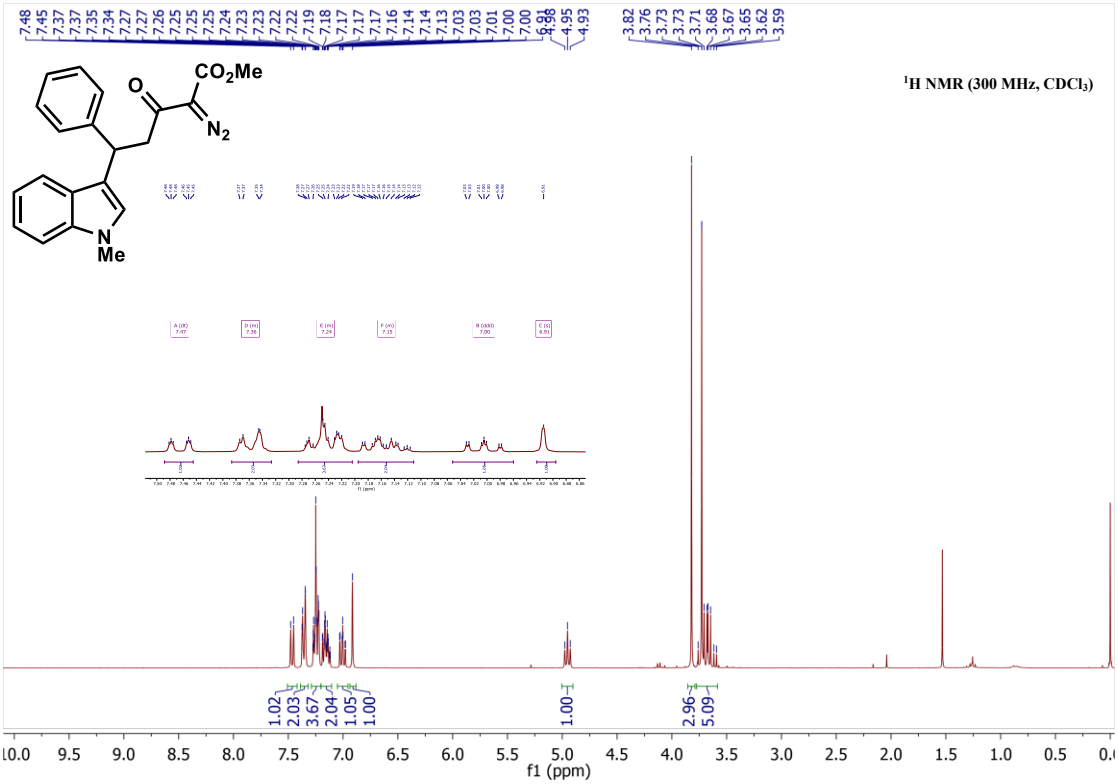

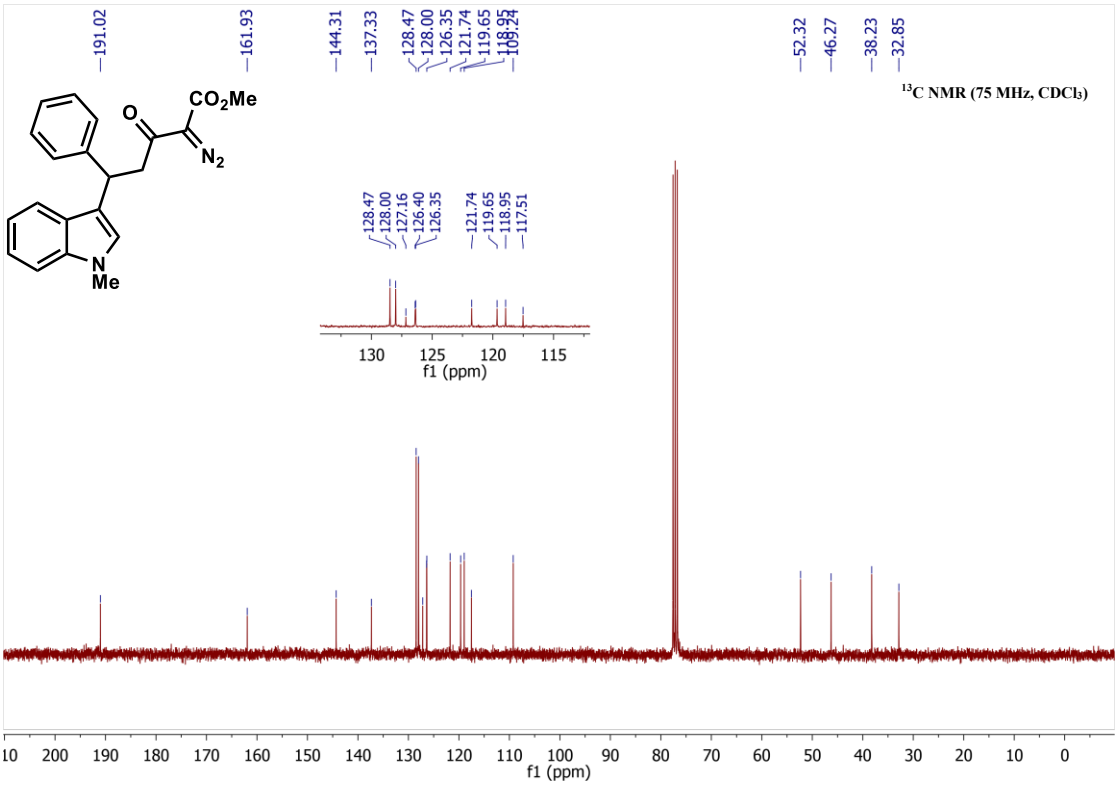

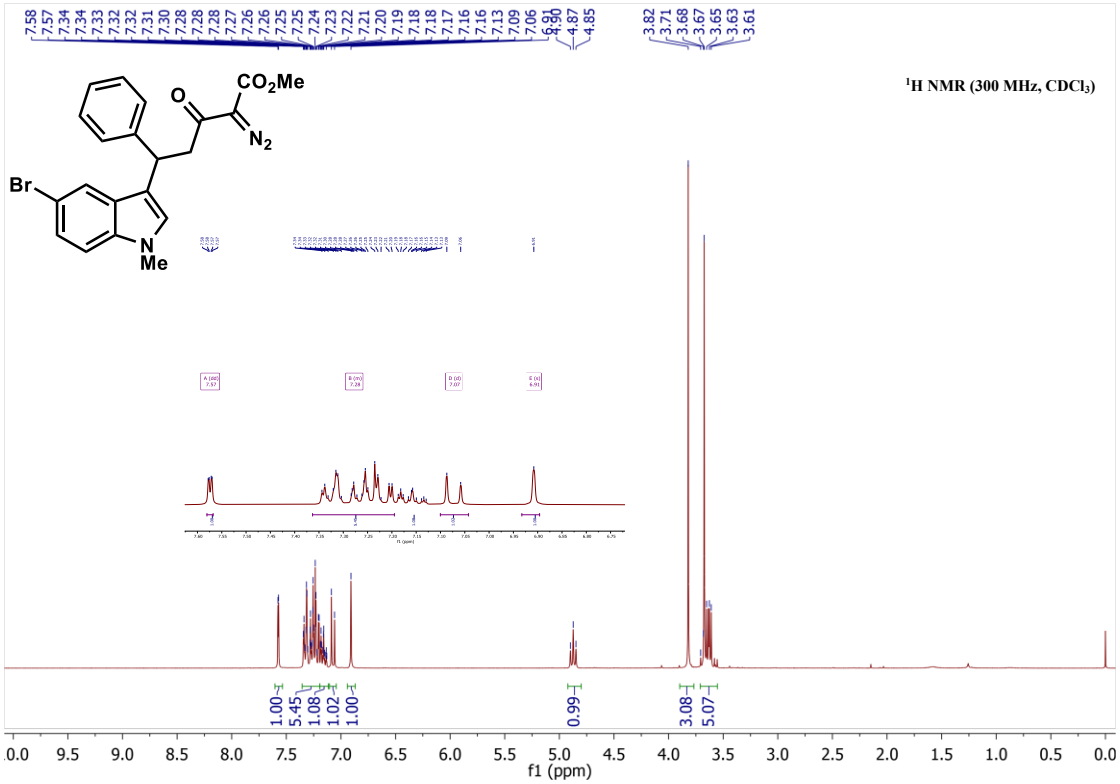
^{1}H NMR (300 MHz, CDCl$_3$)
CO$_2$Me
O
N$_2$
Br
N
Me
7.58 7.57 7.34 7.34 7.33 7.32 7.32 7.31 7.30 7.28 7.28 7.27 7.26 7.26 7.25 7.25 7.24 7.23 7.22 7.21 7.20 7.19 7.18 7.18 7.17 7.16 7.16 7.13 7.09 7.06 6.90 6.90 4.87 4.85
3.82 3.71 3.68 3.67 3.65 3.63 3.61
1.00 5.45 1.08 1.02 1.00 0.99 3.08 5.07
f1 (ppm)

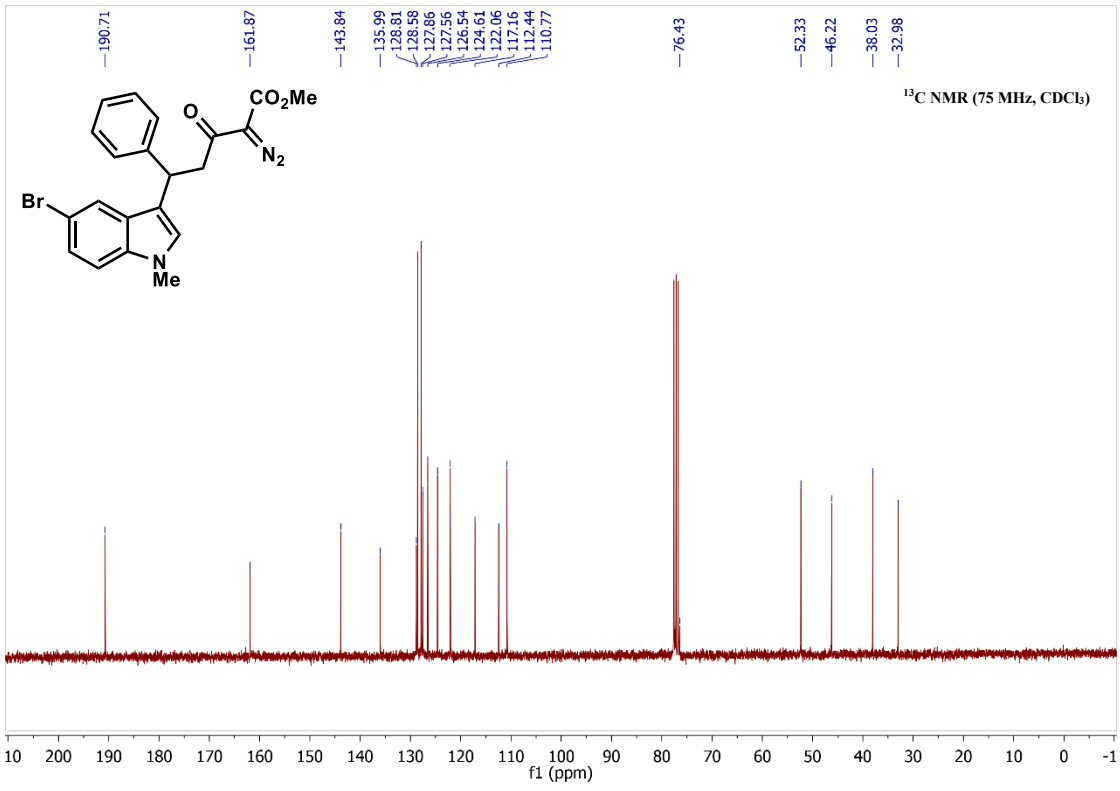
^{13}C NMR (75 MHz, CDCl$_3$)
CO$_2$Me
O
N$_2$
Br
N
Me
190.71 161.87 143.84 135.99 128.81 128.58 127.86 127.56 126.54 124.61 122.06 117.16 112.44 110.77
76.43
52.33 46.22 38.03 32.98
f1 (ppm)

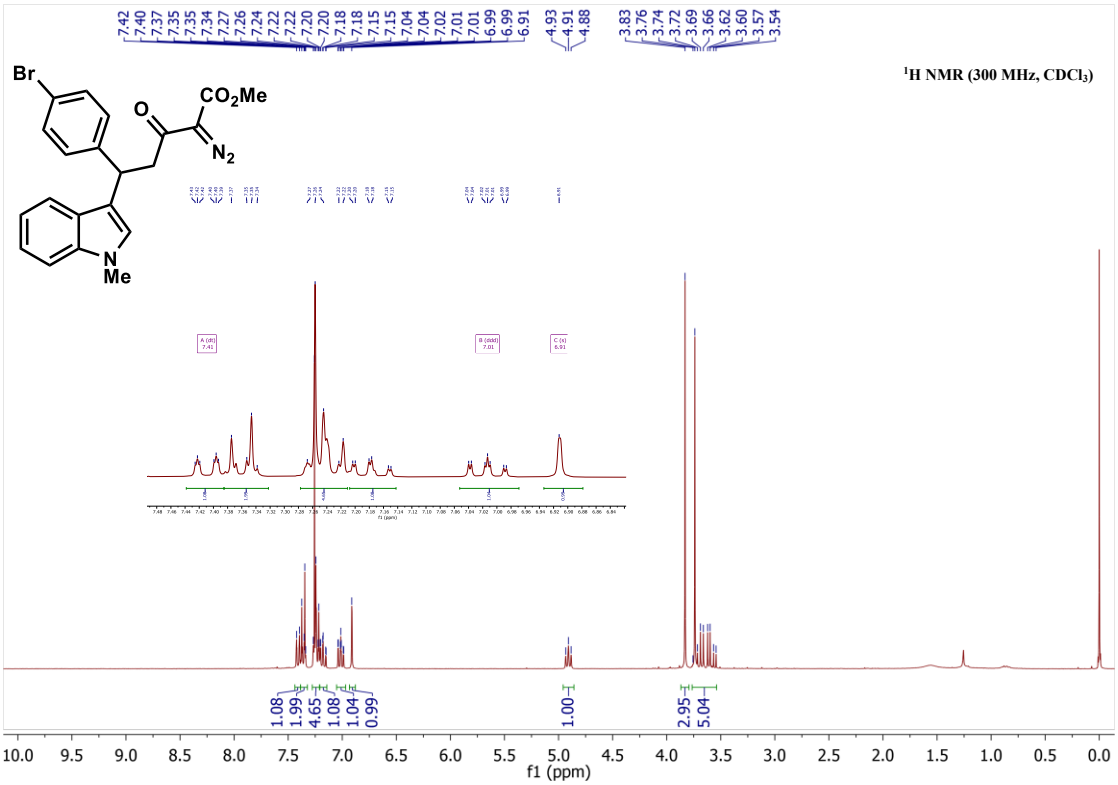
^{1}H NMR (300 MHz, CDCl$_3$)
Br
CO$_2$Me
O
N$_2$
N
Me
7.42 7.40 7.37 7.35 7.35 7.34 7.27 7.26 7.24 7.22 7.22 7.20 7.20 7.18 7.18 7.15 7.15 7.04 7.04 7.02 7.01 7.01 6.99 6.99 6.91
4.93 4.91 4.88
3.83 3.76 3.74 3.72 3.69 3.66 3.62 3.60 3.57 3.54
1.08 1.99 4.65 1.08 1.04 0.99 1.00 2.95 5.04
f1 (ppm)

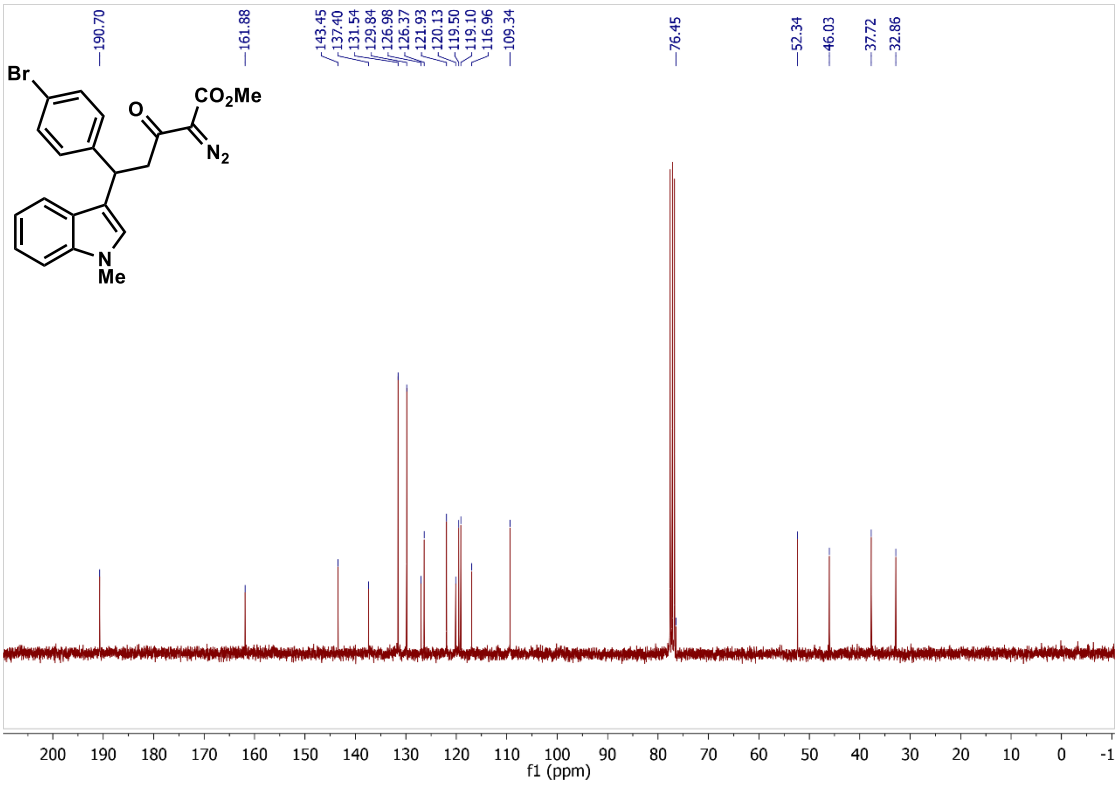
Br
CO$_2$Me
O
N$_2$
N
Me
190.70 161.88 143.45 137.40 131.54 129.84 126.98 126.37 121.93 120.13 119.50 119.10 116.96 109.34 76.45 52.34 46.03 37.72 32.86
f1 (ppm)

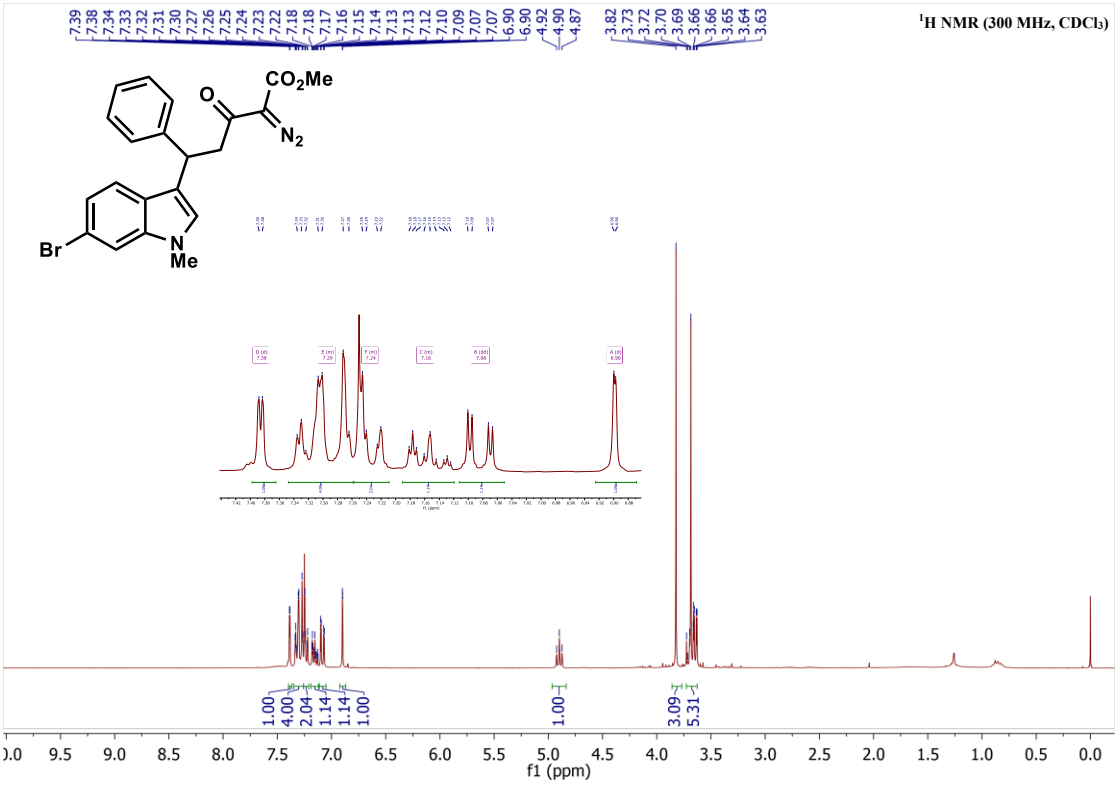
^{1}H NMR (300 MHz, CDCl$_3$)
7.39 7.38 7.34 7.33 7.32 7.31 7.30 7.27 7.26 7.25 7.24 7.23 7.22 7.18 7.18 7.17 7.16 7.15 7.14 7.13 7.13 7.12 7.10 7.09 7.07 7.07 6.90 6.90 4.92 4.90 4.87
3.82 3.73 3.72 3.70 3.69 3.66 3.66 3.65 3.64 3.63
CO2Me
O
N2
Br
N
Me
1.00 4.00 2.04 1.14 1.14 1.00 1.00 3.09 5.31
f1 (ppm)

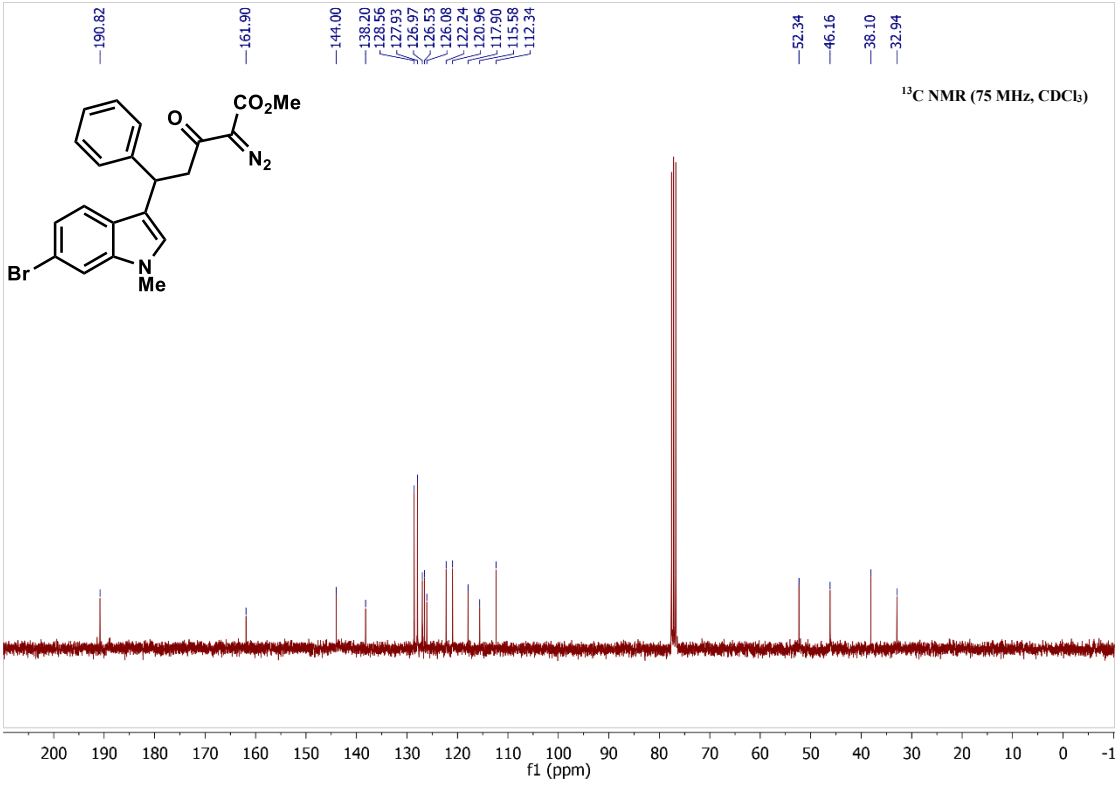
^{13}C NMR (75 MHz, CDCl$_3$)
190.82 161.90 144.00 138.20 128.56 127.93 126.97 126.53 126.08 122.24 120.96 117.90 115.58 112.34
52.34 46.16 38.10 32.94
CO2Me
O
N2
Br
N
Me
f1 (ppm)

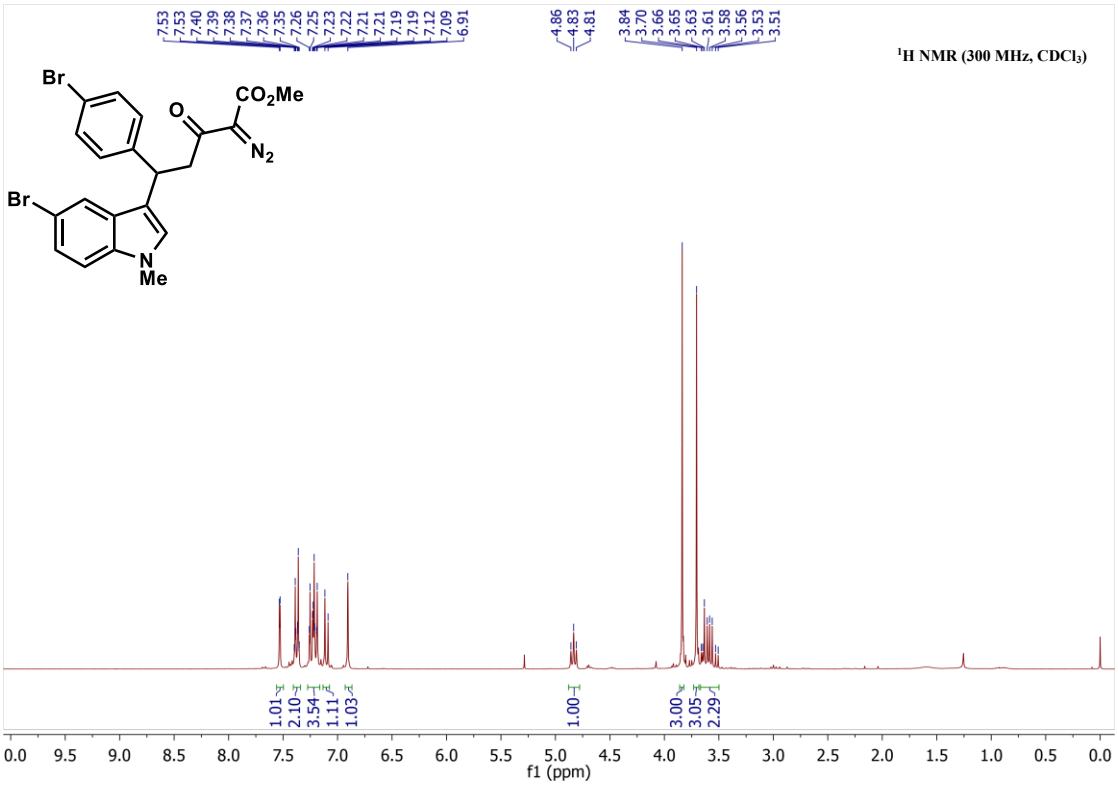
^{1}H NMR (300 MHz, CDCl$_3$)
Br
O
CO$_2$Me
N$_2$
Br
N
Me
7.53
7.53
7.40
7.39
7.38
7.37
7.36
7.35
7.26
7.25
7.23
7.22
7.21
7.21
7.19
7.19
7.12
7.09
6.91
4.86
4.83
4.81
3.84
3.70
3.66
3.65
3.63
3.61
3.58
3.56
3.53
3.51
1.01
2.10
3.54
1.11
1.03
1.00
3.00
3.05
2.29
0.0 9.5 9.0 8.5 8.0 7.5 7.0 6.5 6.0 5.5 5.0 4.5 4.0 3.5 3.0 2.5 2.0 1.5 1.0 0.5 0.0
f1 (ppm)

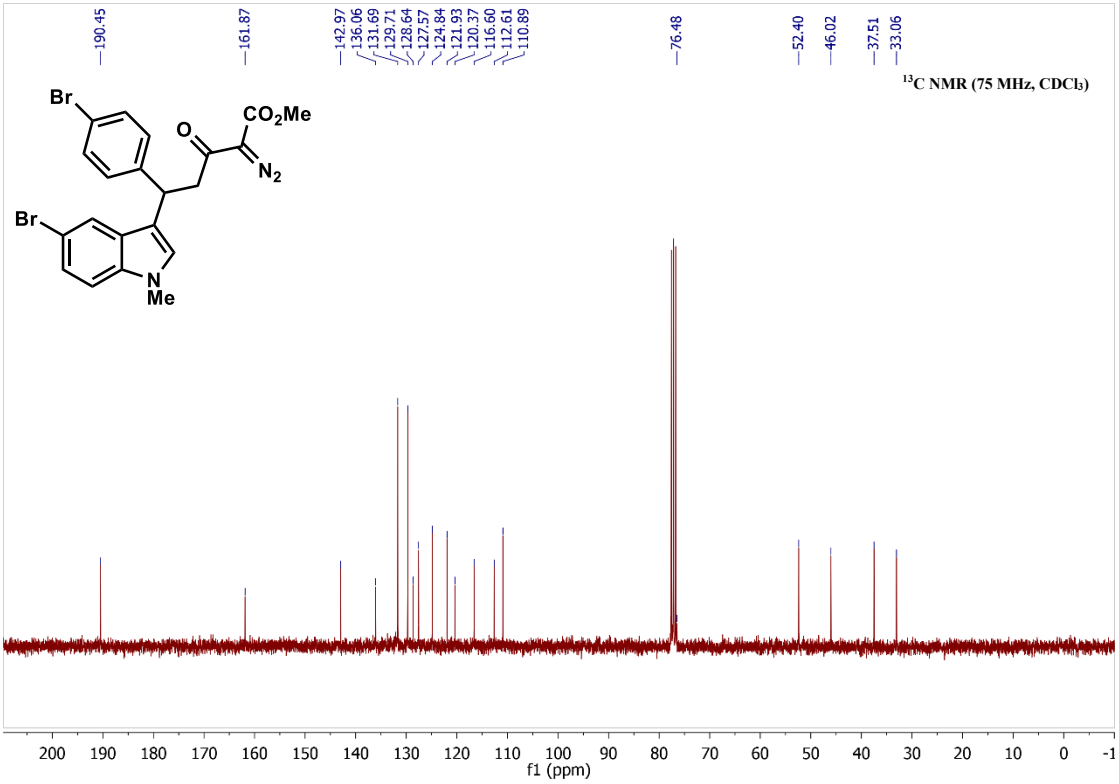
^{13}C NMR (75 MHz, CDCl$_3$)
Br
O
CO$_2$Me
N$_2$
Br
N
Me
190.45
161.87
142.97
136.06
131.69
129.71
128.64
127.57
124.84
121.93
120.37
116.60
112.61
110.89
76.48
52.40
46.02
37.51
33.06
200 190 180 170 160 150 140 130 120 110 100 90 80 70 60 50 40 30 20 10 0 -1
f1 (ppm)

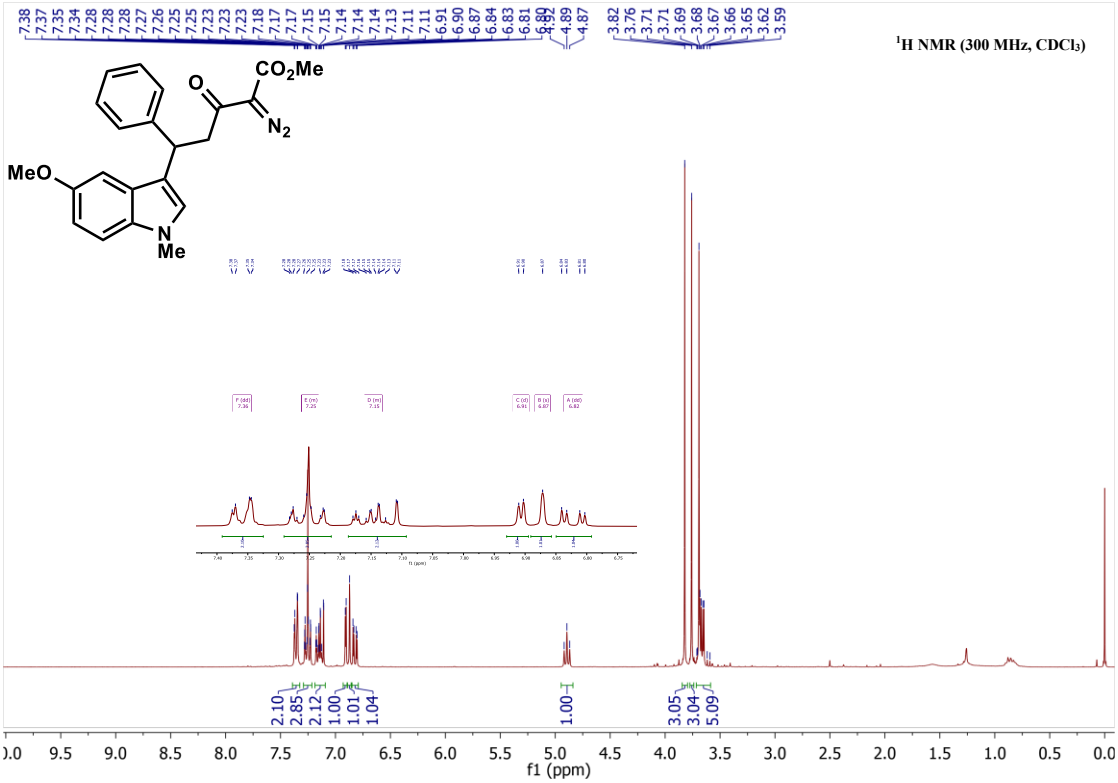
^{1}H NMR (300 MHz, CDCl$_3$)
CO$_2$Me
O
N$_2$
MeO
N
Me
7.38 7.37 7.35 7.34 7.28 7.28 7.28 7.27 7.26 7.25 7.25 7.23 7.23 7.23 7.18 7.17 7.17 7.15 7.15 7.14 7.14 7.14 7.13 7.11 7.11 6.91 6.90 6.87 6.84 6.83 6.81 6.80 4.92 4.89 4.87
3.82 3.76 3.71 3.71 3.69 3.68 3.67 3.66 3.65 3.62 3.59
2.10 2.85 2.12 1.00 1.01 1.04 1.00 3.05 3.04 5.09
f1 (ppm)

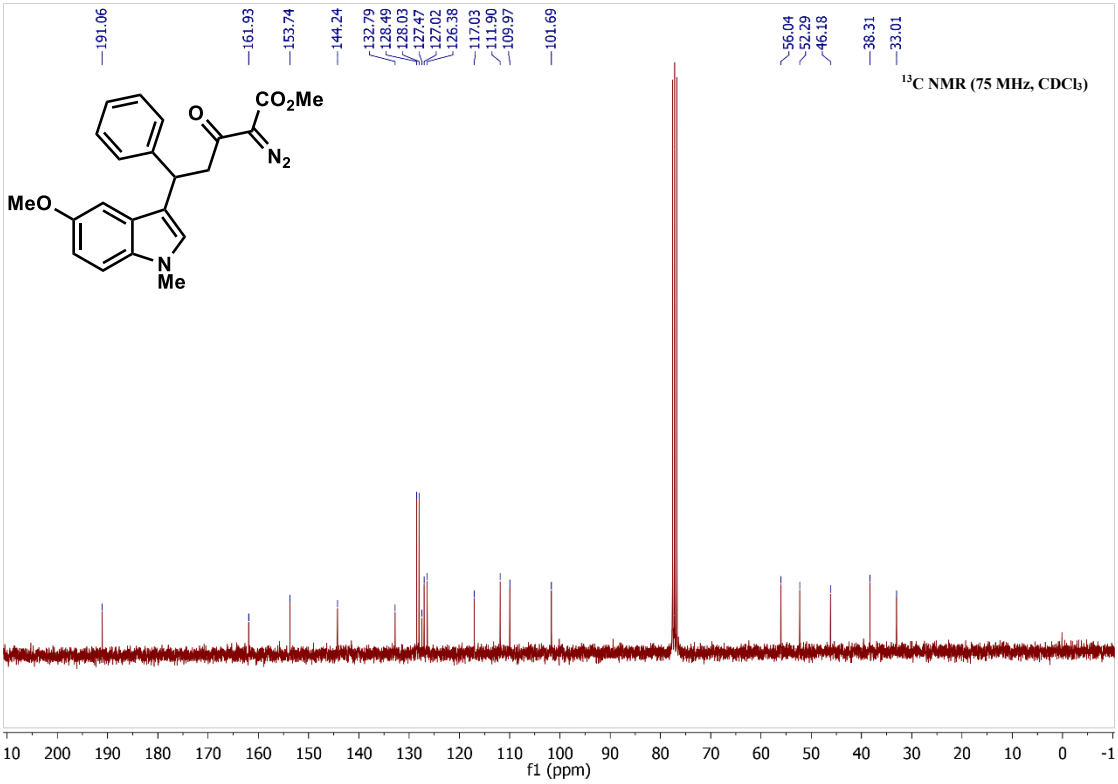
^{13}C NMR (75 MHz, CDCl$_3$)
CO$_2$Me
O
N$_2$
MeO
N
Me
191.06 161.93 153.74 144.24 132.79 128.49 128.03 127.47 127.02 126.38 117.03 111.90 109.97 101.69 56.04 52.29 46.18 38.31 33.01
f1 (ppm)

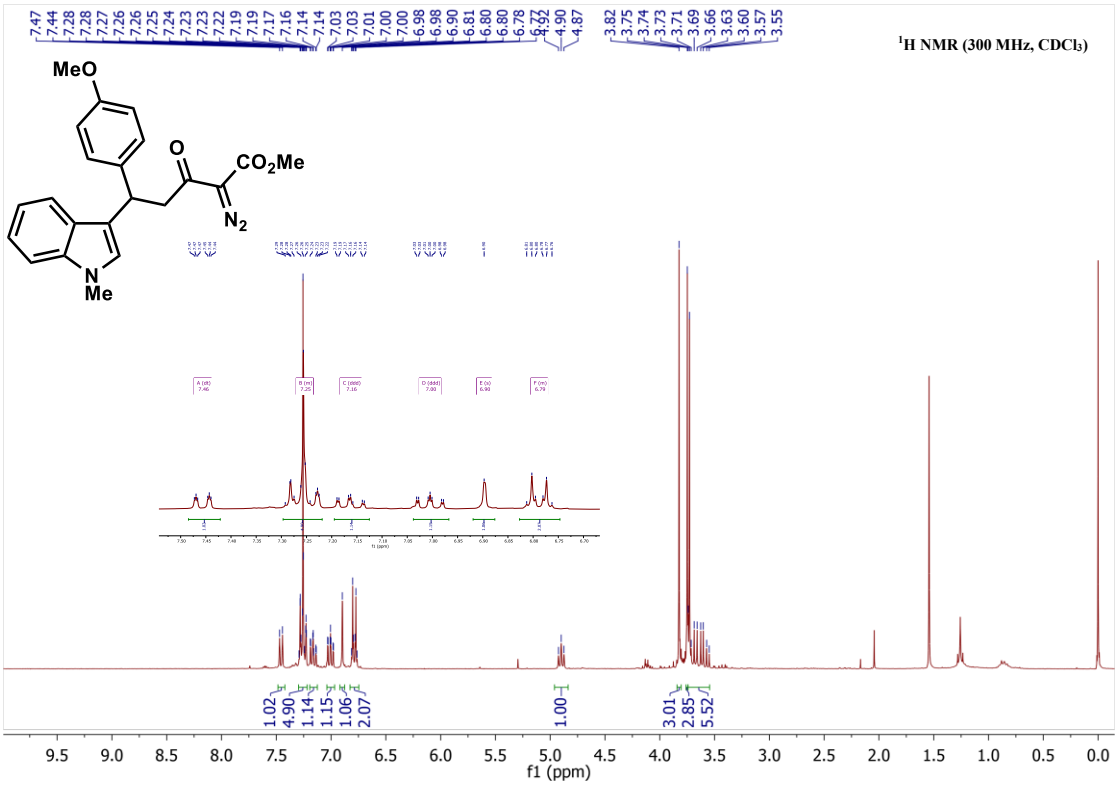
^{1}H NMR (300 MHz, CDCl$_3$)
MeO
O
CO$_2$Me
N$_2$
N
Me
7.47 7.44 7.28 7.28 7.27 7.26 7.26 7.25 7.24 7.23 7.23 7.22 7.19 7.17 7.16 7.14 7.14 7.03 7.03 7.01 7.00 7.00 6.98 6.98 6.90 6.81 6.80 6.78 6.77 4.92 4.90 4.87 3.82 3.75 3.74 3.73 3.71 3.69 3.66 3.63 3.60 3.57 3.55
1.02 4.90 1.14 1.15 1.06 2.07 1.00 3.01 2.85 5.52
9.5 9.0 8.5 8.0 7.5 7.0 6.5 6.0 5.5 5.0 4.5 4.0 3.5 3.0 2.5 2.0 1.5 1.0 0.5 0.0
f1 (ppm)

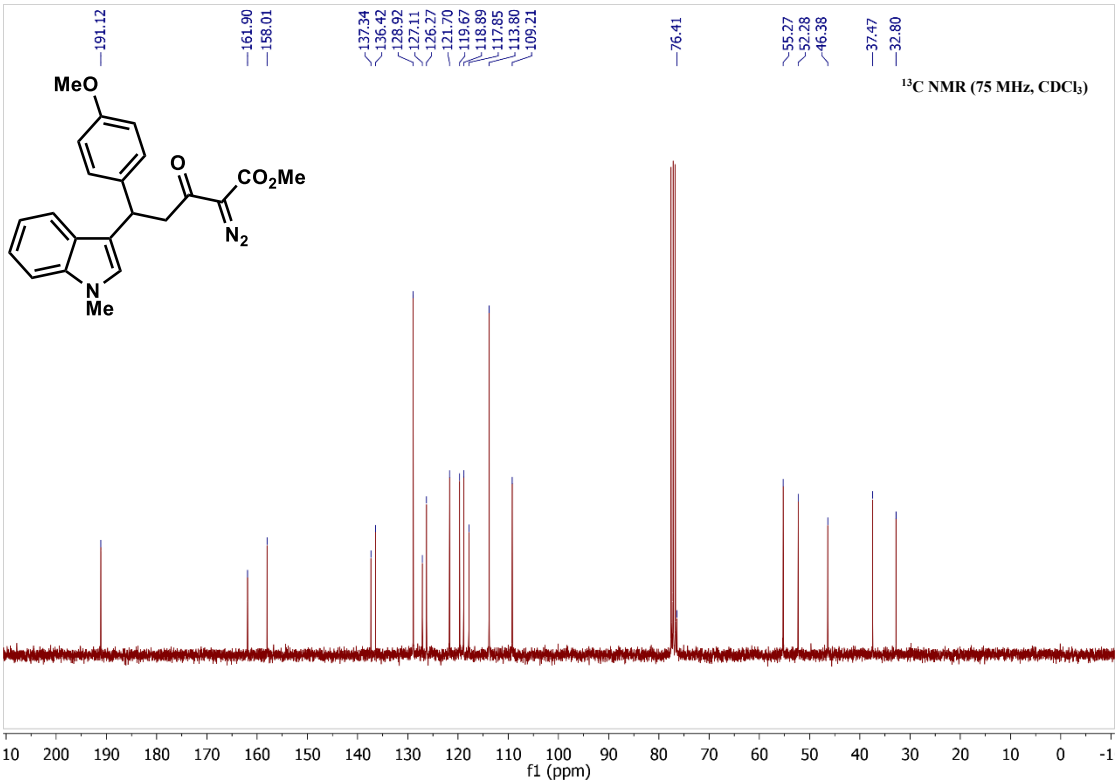
^{13}C NMR (75 MHz, CDCl$_3$)
MeO
O
CO$_2$Me
N$_2$
N
Me
191.12 161.90 158.01 137.34 136.42 128.92 127.11 126.27 121.70 119.67 118.89 117.85 113.80 109.21 76.41 55.27 52.28 46.38 37.47 32.80
10 200 190 180 170 160 150 140 130 120 110 100 90 80 70 60 50 40 30 20 10 0 -1
f1 (ppm)

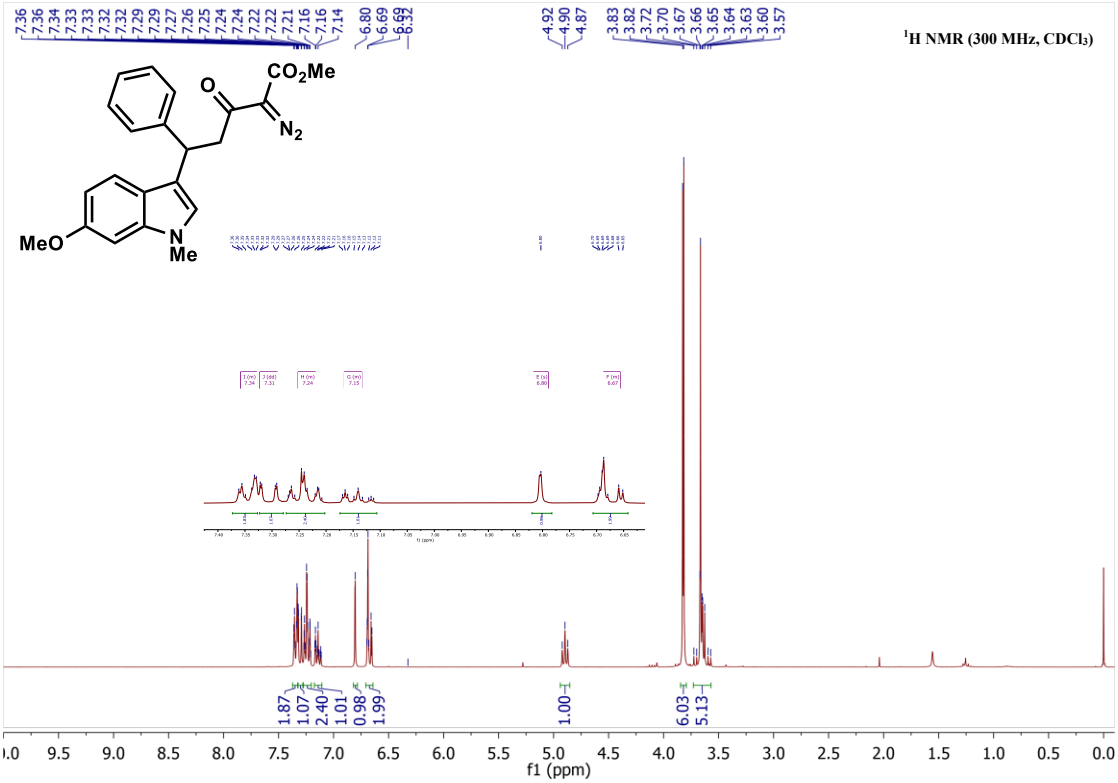
^{1}H NMR (300 MHz, CDCl$_3$)
CO$_2$Me
O
N$_2$
MeO
N
Me
7.36 7.36 7.34 7.33 7.32 7.32 7.29 7.29 7.27 7.26 7.25 7.24 7.24 7.22 7.22 7.21 7.16 7.16 7.14 6.80 6.69 6.69 6.32
4.92 4.90 4.87
3.83 3.82 3.72 3.70 3.67 3.66 3.65 3.64 3.63 3.60 3.57
1.87 1.07 2.40 1.01 0.98 1.99 1.00 6.03 5.13
f1 (ppm)

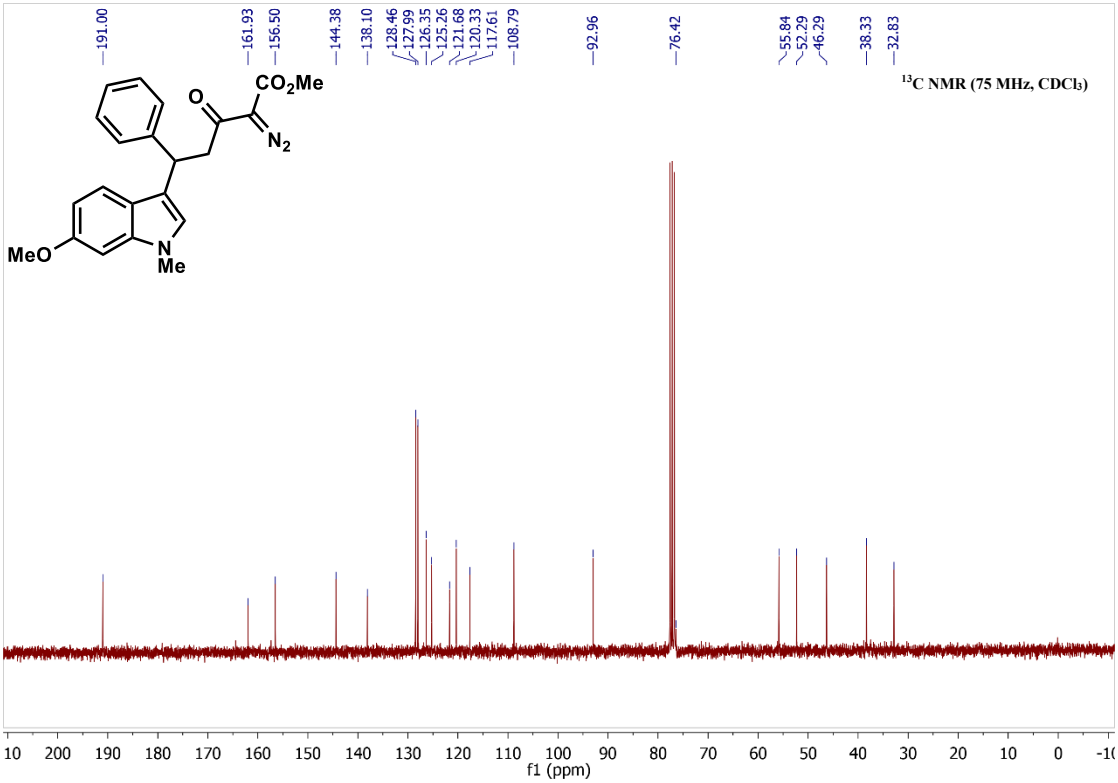
^{13}C NMR (75 MHz, CDCl$_3$)
CO$_2$Me
O
N$_2$
MeO
N
Me
191.00
161.93 156.50 144.38 138.10 128.46 127.99 126.35 125.26 121.68 120.33 117.61 108.79
92.96 76.42
55.84 52.29 46.29 38.33 32.83
f1 (ppm)

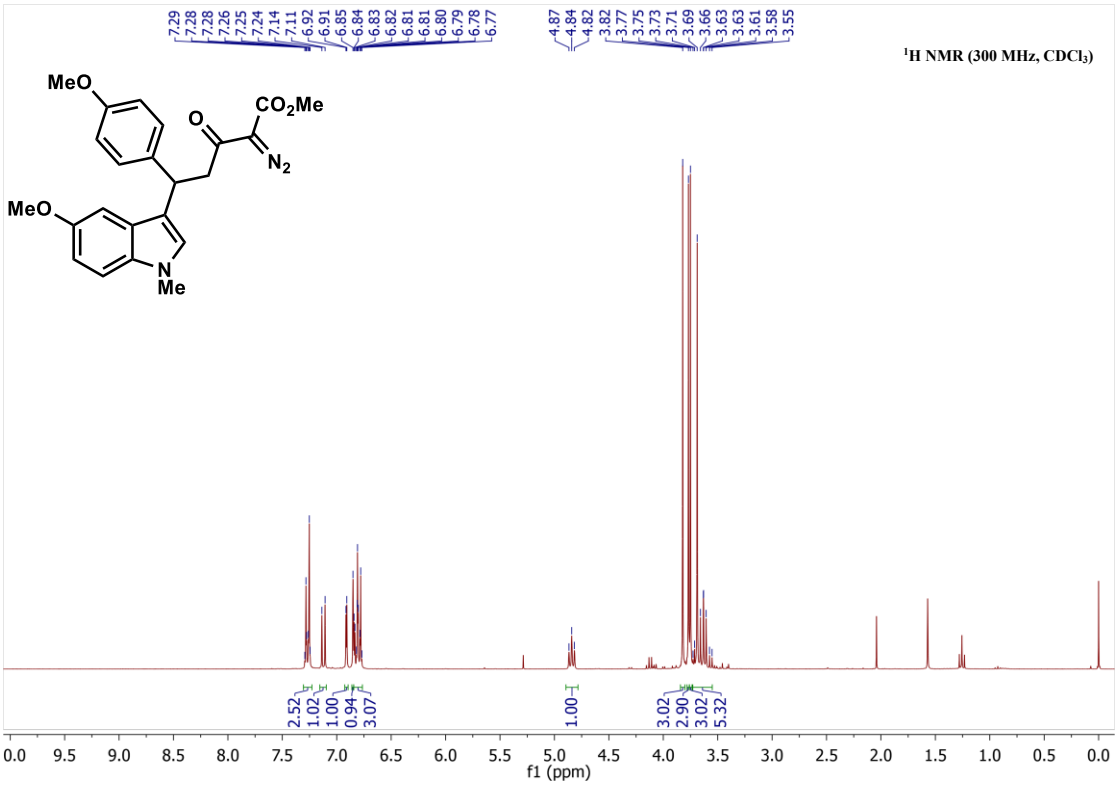
^{1}H NMR (300 MHz, CDCl$_3$)
MeO
CO$_2$Me
O
N$_2$
MeO
N
Me
7.29 7.28 7.28 7.26 7.25 7.24 7.14 7.11 6.92 6.91 6.85 6.84 6.83 6.82 6.81 6.81 6.80 6.79 6.78 6.77
4.87 4.84 4.82 3.82 3.77 3.75 3.73 3.71 3.69 3.66 3.63 3.63 3.61 3.58 3.55
2.52 1.02 1.00 0.94 3.07 1.00 3.02 2.90 3.02 5.32
0.0 9.5 9.0 8.5 8.0 7.5 7.0 6.5 6.0 5.5 5.0 4.5 4.0 3.5 3.0 2.5 2.0 1.5 1.0 0.5 0.0
f1 (ppm)

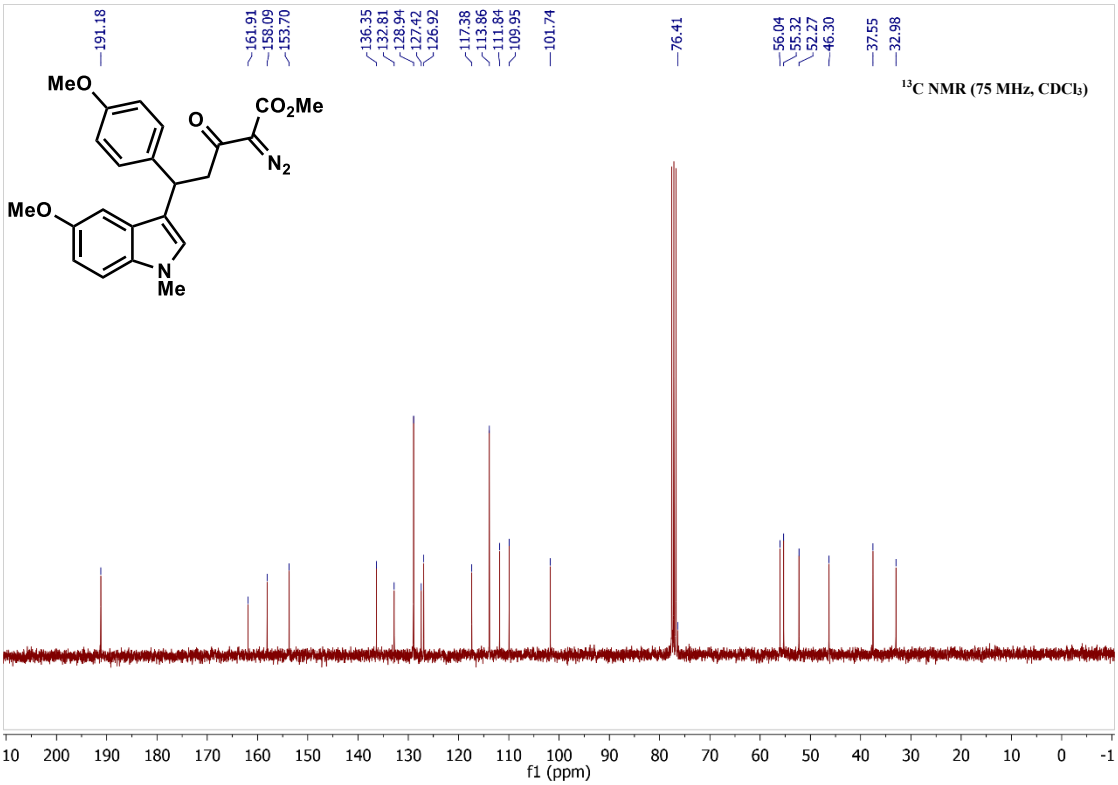
^{13}C NMR (75 MHz, CDCl$_3$)
MeO
CO$_2$Me
O
N$_2$
MeO
N
Me
191.18
161.91 158.09 153.70
136.35 132.81 128.94 127.42 126.92
117.38 113.86 111.84 109.95
101.74
76.41
56.04 55.32 52.27 46.30
37.55 32.98
10 200 190 180 170 160 150 140 130 120 110 100 90 80 70 60 50 40 30 20 10 0 -1
f1 (ppm)

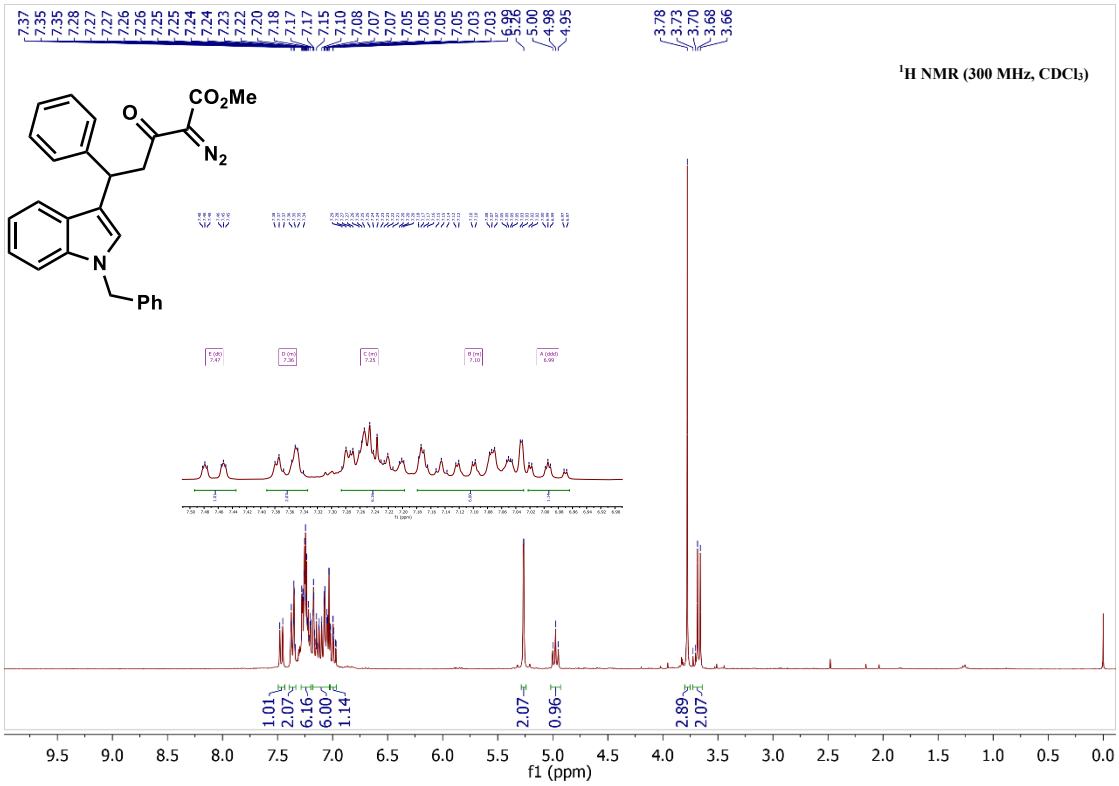
^{1}H NMR (300 MHz, CDCl$_3$)
CO2Me
O
N2
N
Ph
f1 (ppm)

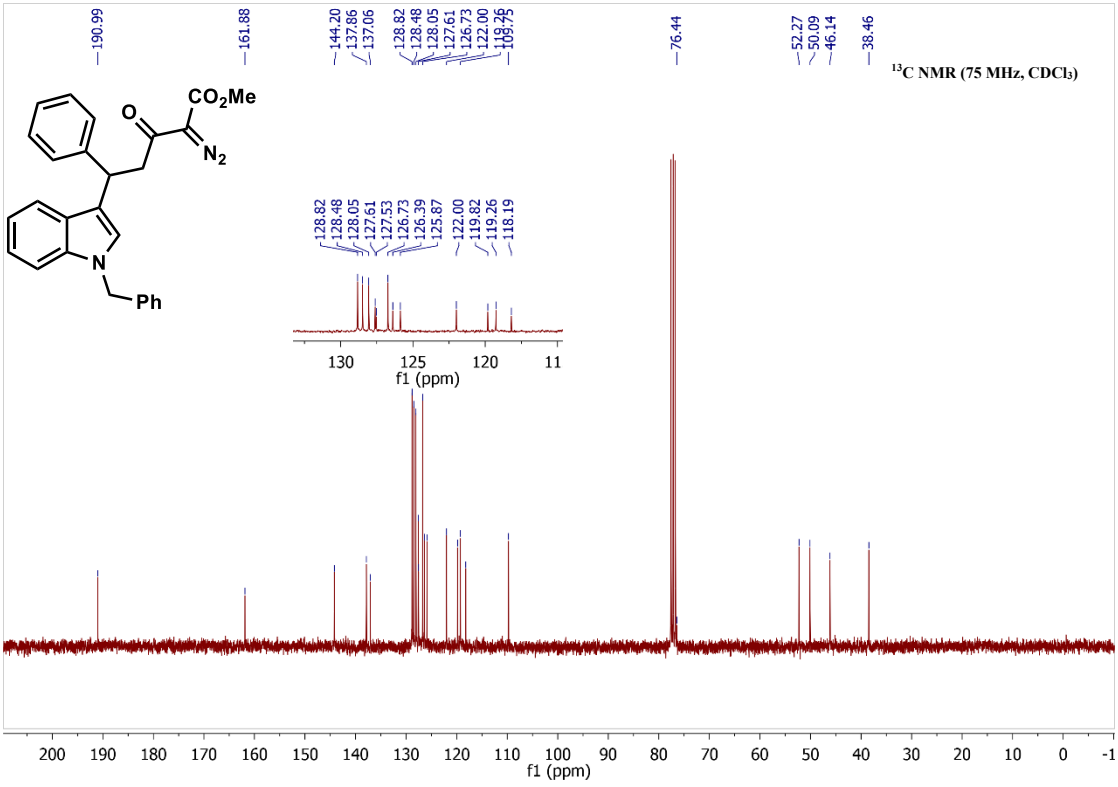
^{13}C NMR (75 MHz, CDCl$_3$)
CO2Me
O
N2
N
Ph
f1 (ppm)

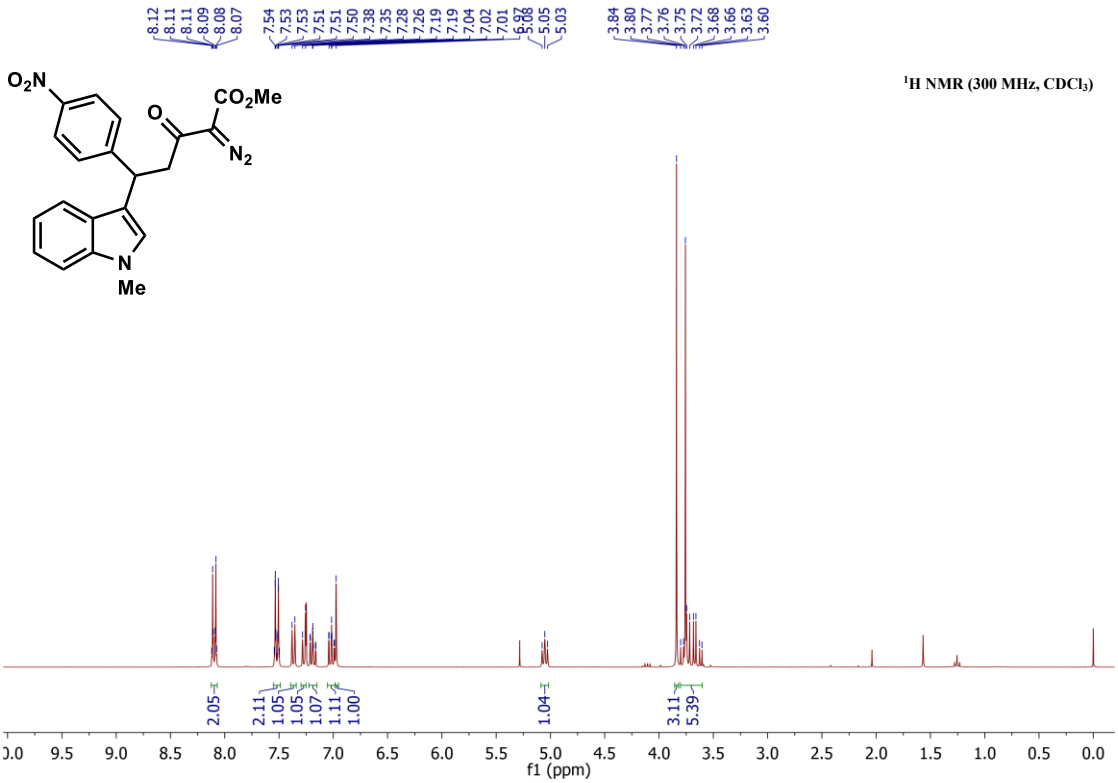

^{1}H NMR (300 MHz, $CDCl_3$)

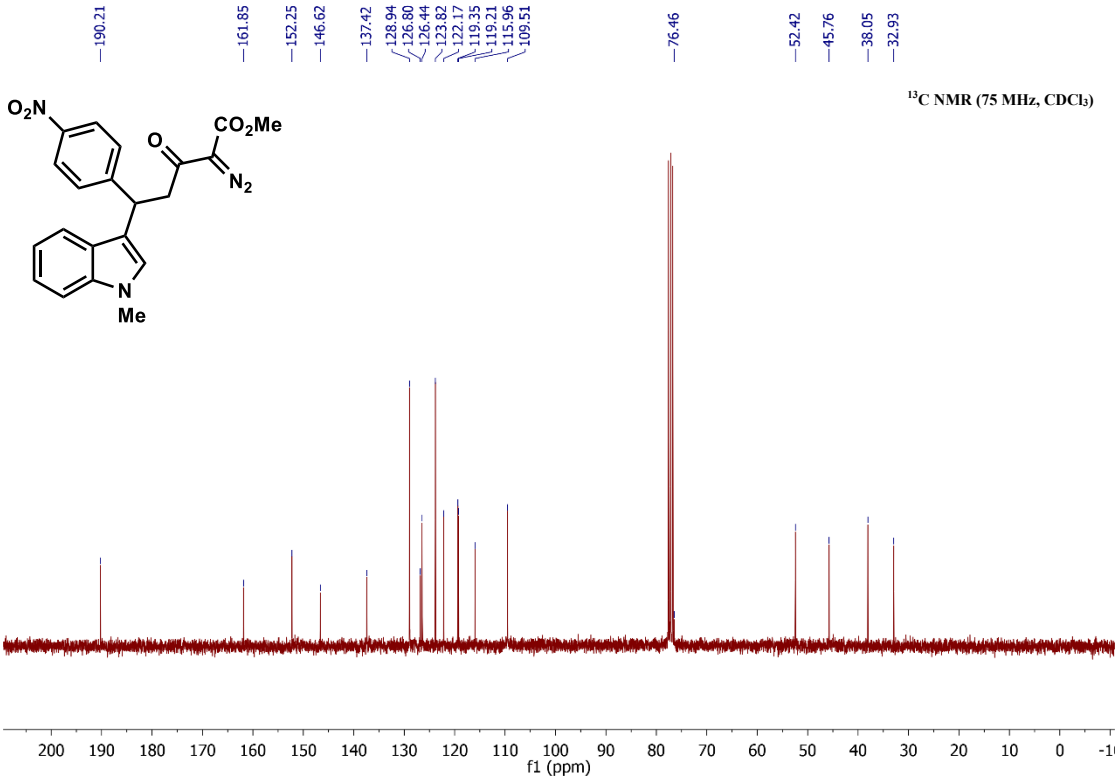

^{13}C NMR (75 MHz, $CDCl_3$)

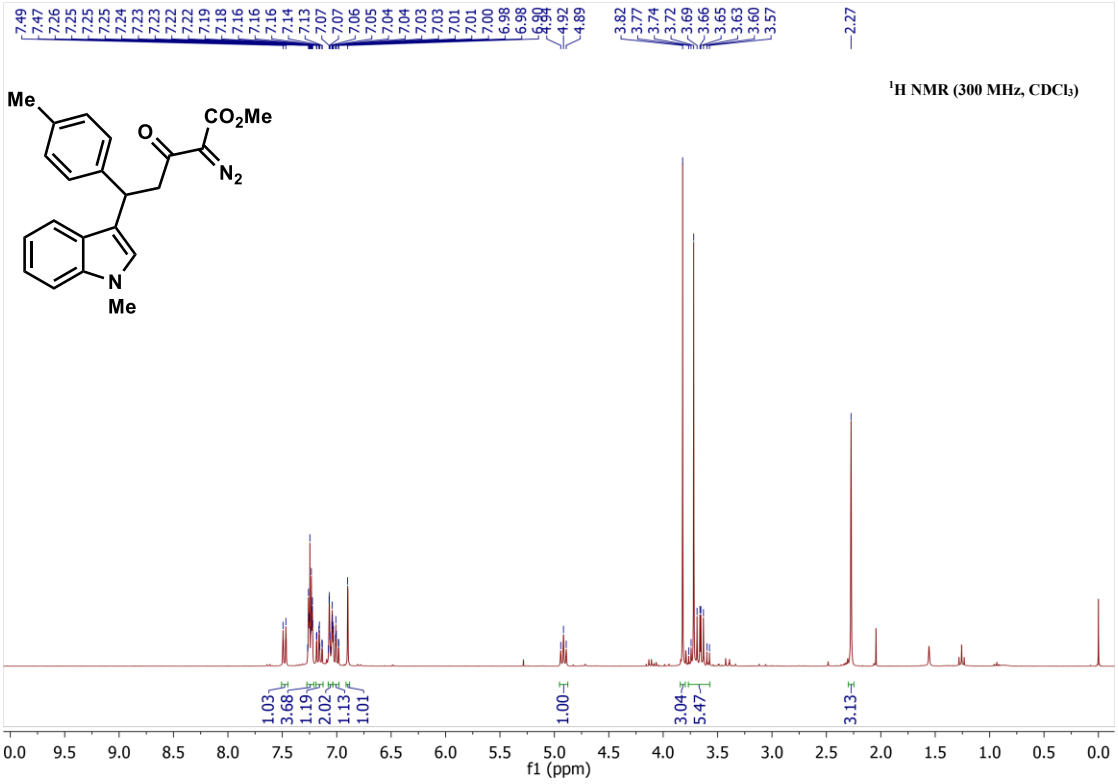
7.49
7.47
7.26
7.25
7.25
7.25
7.24
7.23
7.22
7.22
7.19
7.18
7.16
7.16
7.16
7.14
7.13
7.07
7.07
7.06
7.05
7.04
7.04
7.03
7.03
7.01
7.01
7.00
6.98
6.98
6.90
4.94
4.92
4.89
3.82
3.77
3.74
3.72
3.69
3.66
3.65
3.63
3.60
3.57
2.27
Me
O
CO2Me
N2
N
Me
1H NMR (300 MHz, CDCl3)
1.03
3.68
1.19
2.02
1.13
1.01
1.00
3.04
5.47
3.13
0.0 9.5 9.0 8.5 8.0 7.5 7.0 6.5 6.0 5.5 5.0 4.5 4.0 3.5 3.0 2.5 2.0 1.5 1.0 0.5 0.0
f1 (ppm)

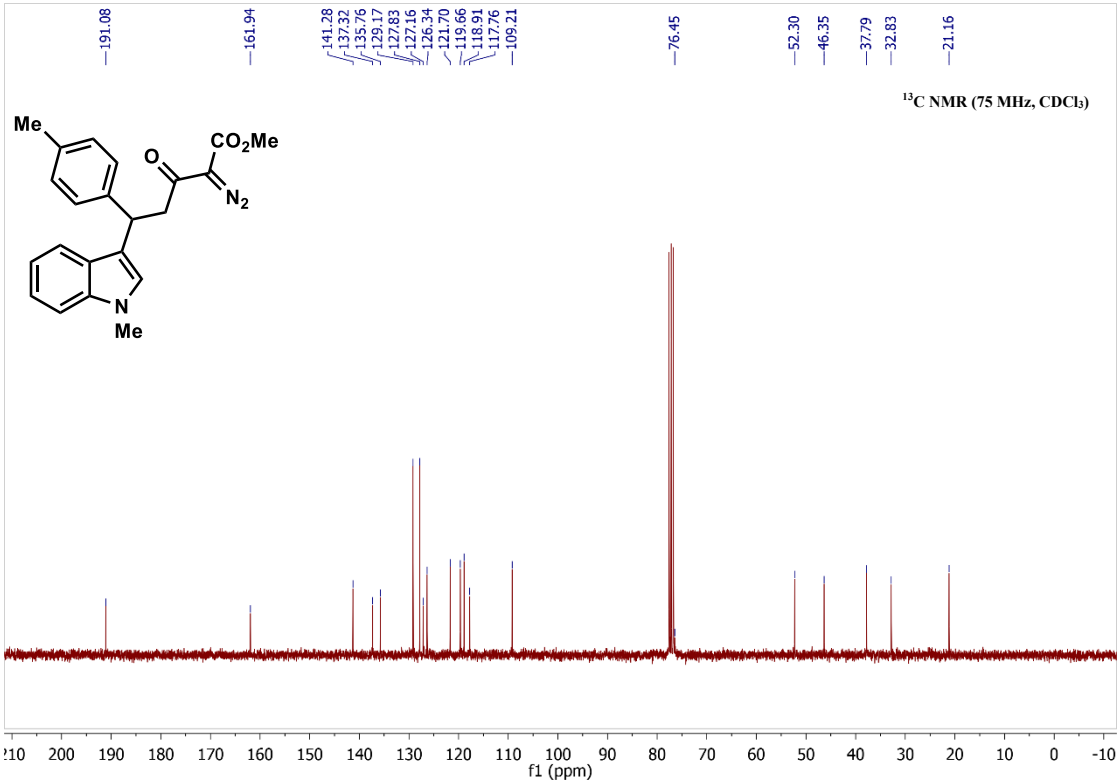
191.08
161.94
141.28
137.32
135.76
129.17
127.83
127.16
126.34
121.70
119.66
118.91
117.76
109.21
76.45
52.30
46.35
37.79
32.83
21.16
Me
O
CO2Me
N2
N
Me
13C NMR (75 MHz, CDCl3)
210 200 190 180 170 160 150 140 130 120 110 100 90 80 70 60 50 40 30 20 10 0 -10
f1 (ppm)

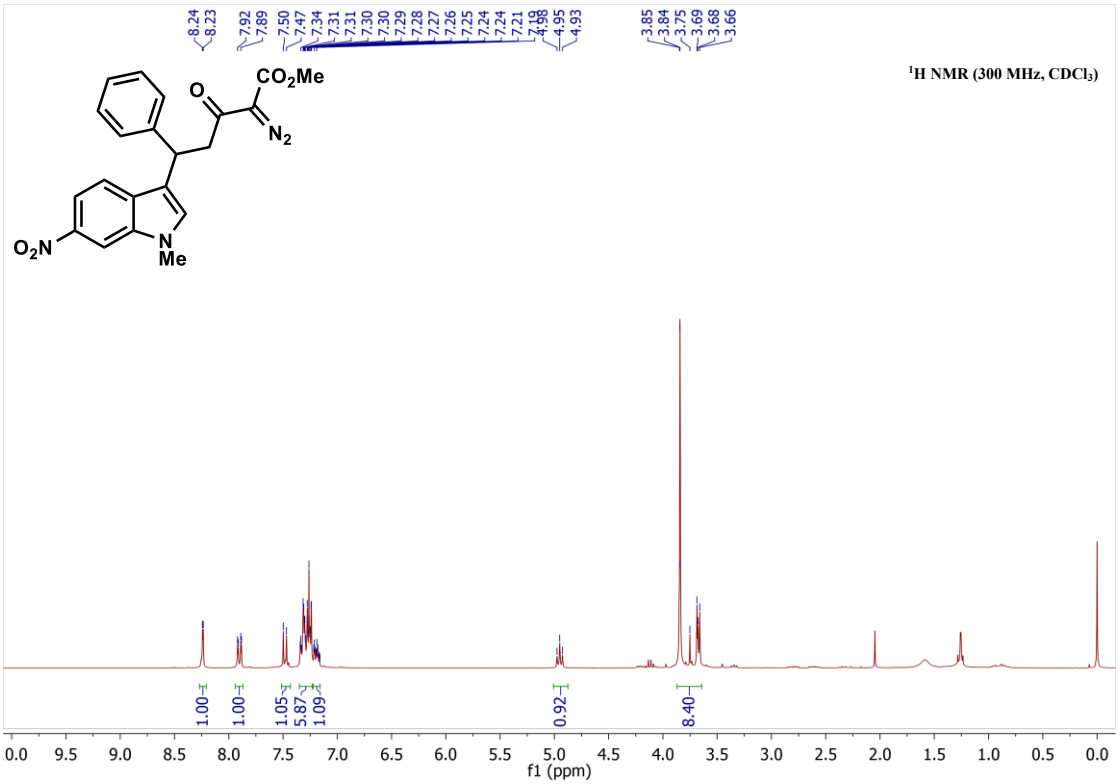
^{1}H NMR (300 MHz, CDCl$_3$)
CO$_2$Me
O
N$_2$
O$_2$N
N
Me
f1 (ppm)

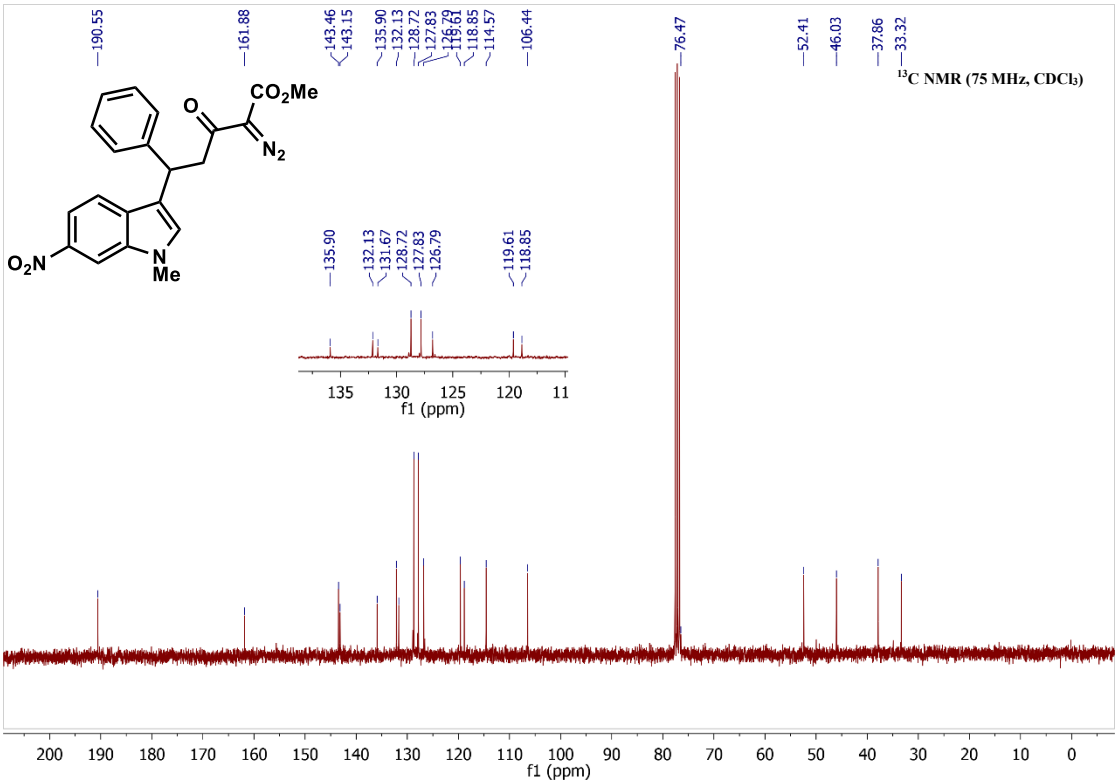
^{13}C NMR (75 MHz, CDCl$_3$)
CO$_2$Me
O
N$_2$
O$_2$N
N
Me
f1 (ppm)

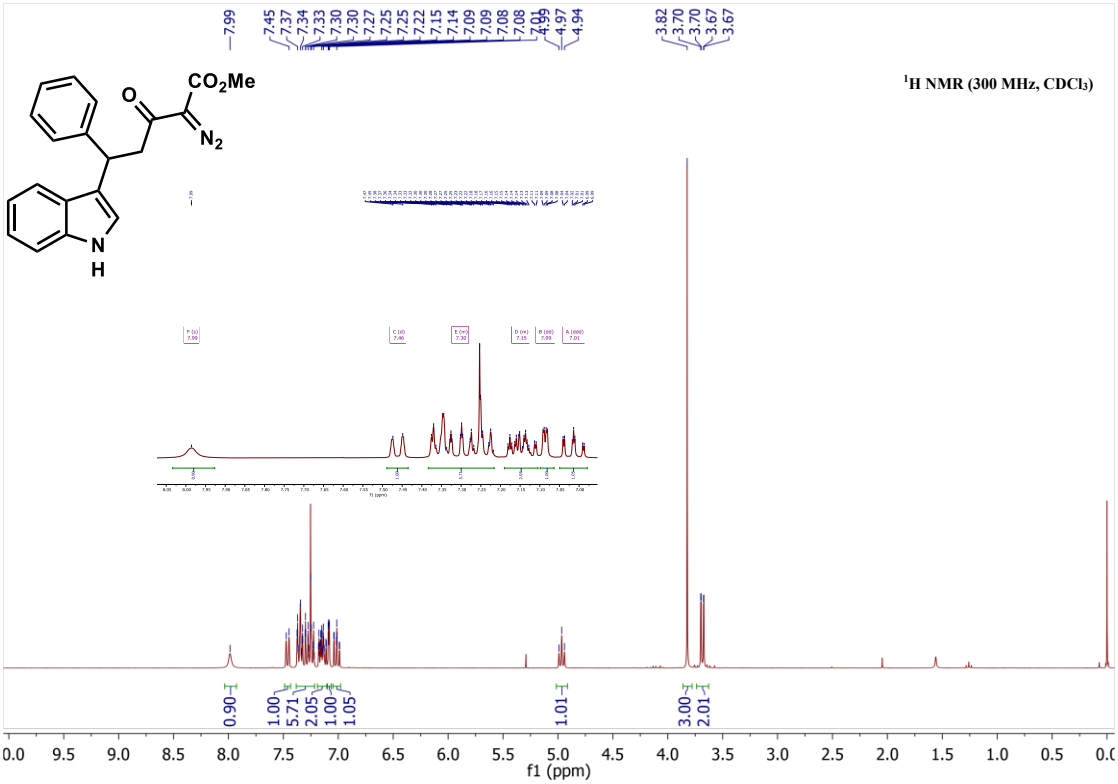
7.99
7.45
7.37
7.34
7.33
7.30
7.30
7.27
7.25
7.25
7.22
7.15
7.14
7.09
7.09
7.08
7.08
7.01
4.99
4.97
4.94
3.82
3.70
3.70
3.67
3.67
CO2Me
O
N2
N
H
1H NMR (300 MHz, CDCl3)
0.90
1.00
5.71
2.05
1.00
1.05
1.01
3.00
2.01
f1 (ppm)

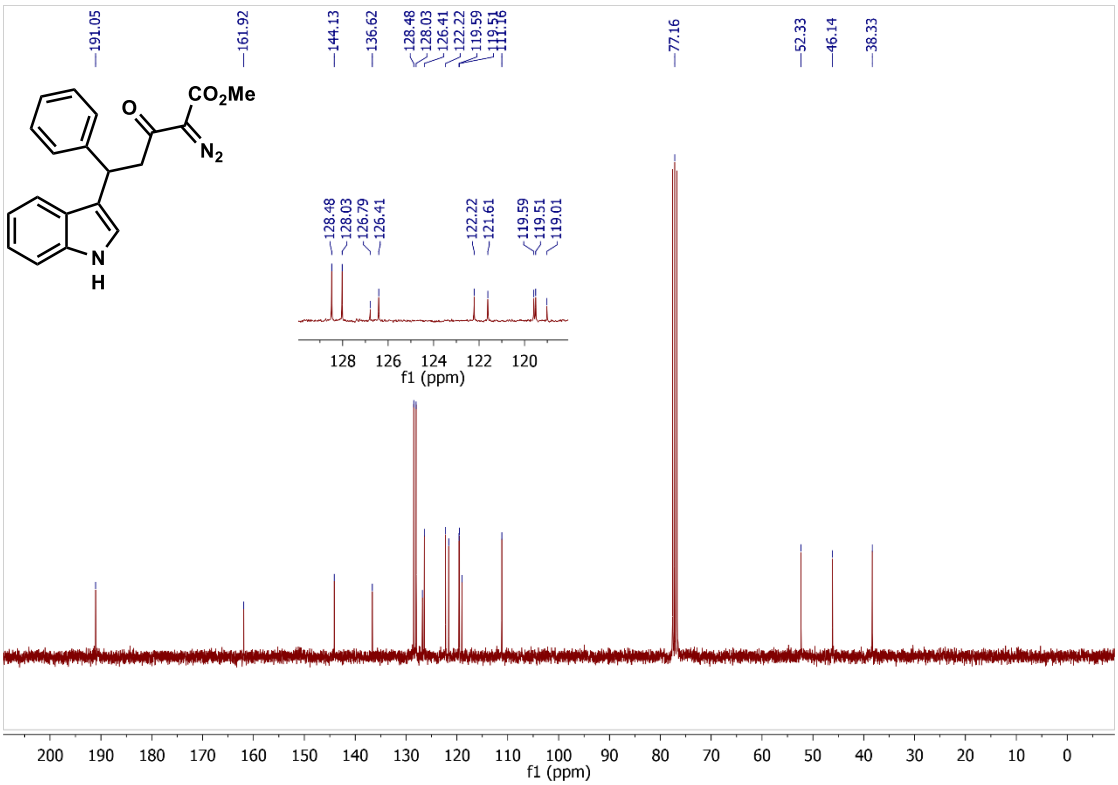
191.05
161.92
144.13
136.62
128.48
128.03
126.41
122.22
119.59
119.51
111.16
77.16
52.33
46.14
38.33
CO2Me
O
N2
N
H
128.48
128.03
126.79
126.41
122.22
121.61
119.59
119.51
119.01
f1 (ppm)
f1 (ppm)

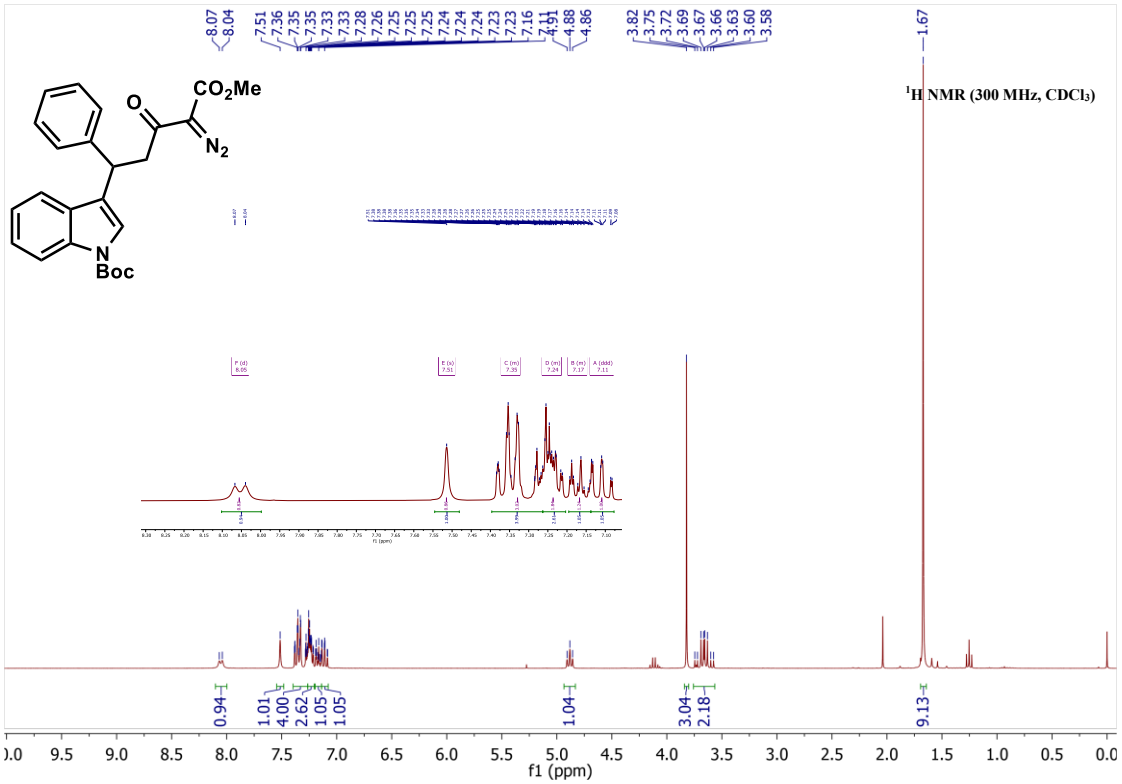
^{1}H NMR (300 MHz, CDCl$_3$)
CO$_2$Me
O
N$_2$
N
Boc
f1 (ppm)

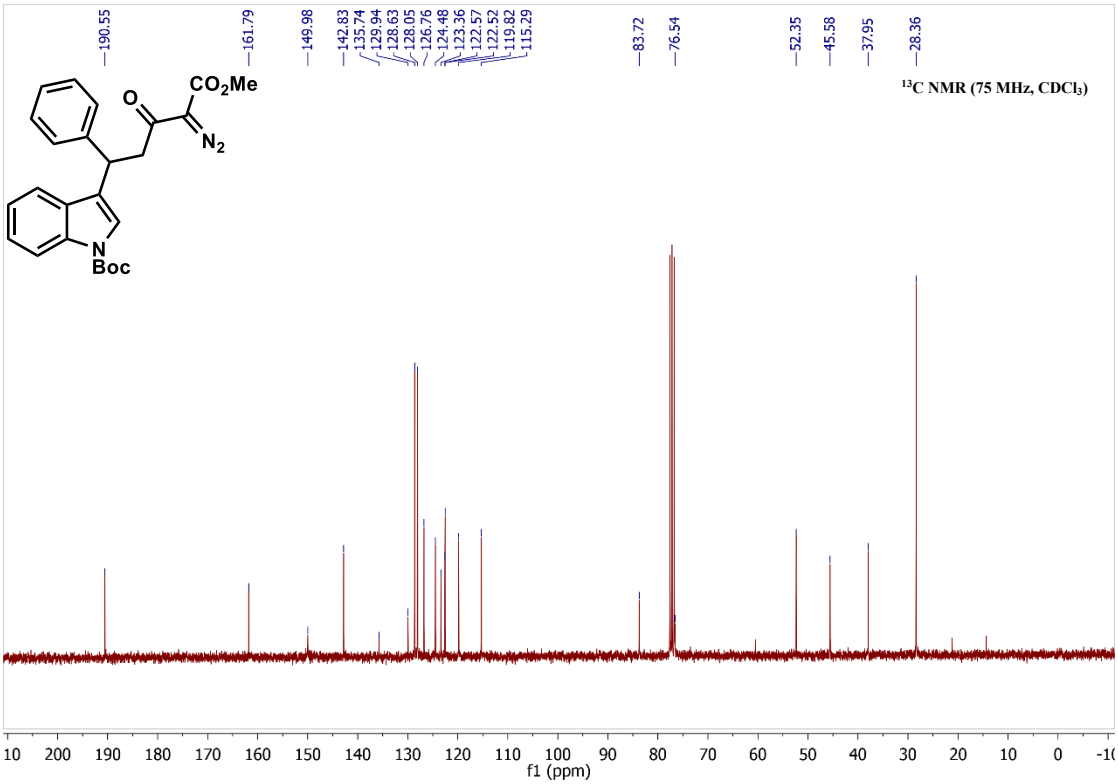
^{13}C NMR (75 MHz, CDCl$_3$)
CO$_2$Me
O
N$_2$
N
Boc
f1 (ppm)

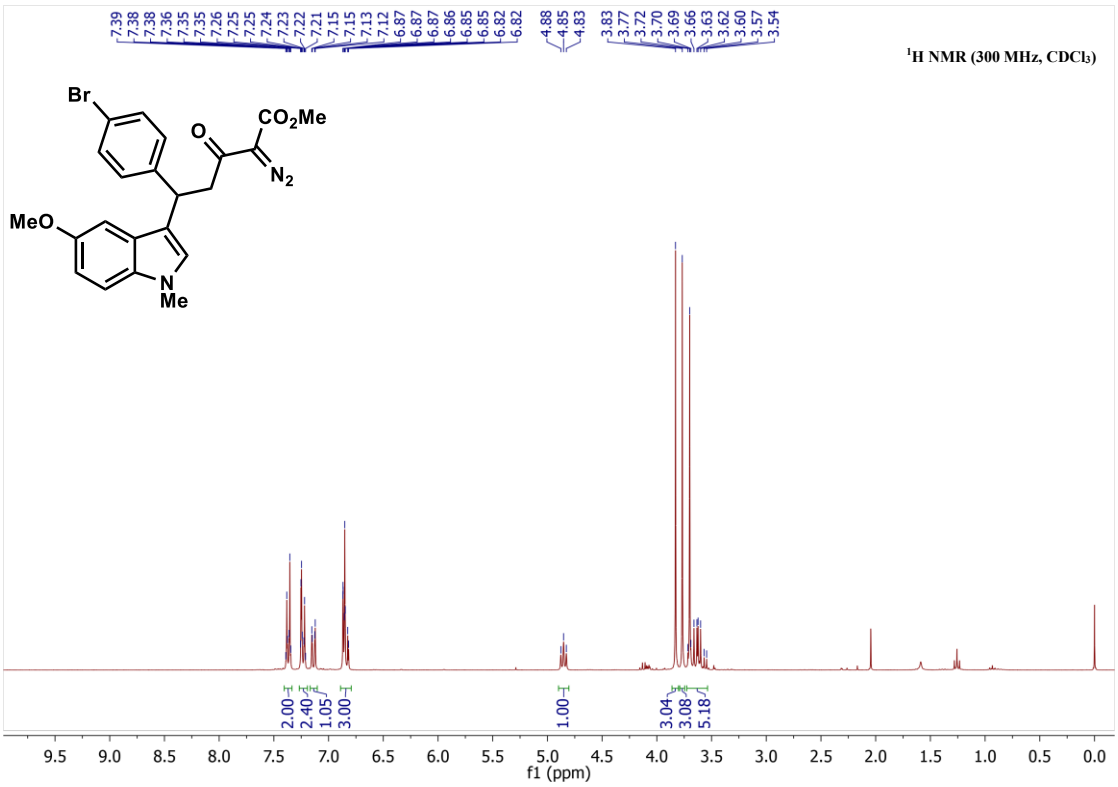
^{1}H NMR (300 MHz, CDCl$_3$)
Br
CO$_2$Me
O
N$_2$
MeO
N
Me
f1 (ppm)

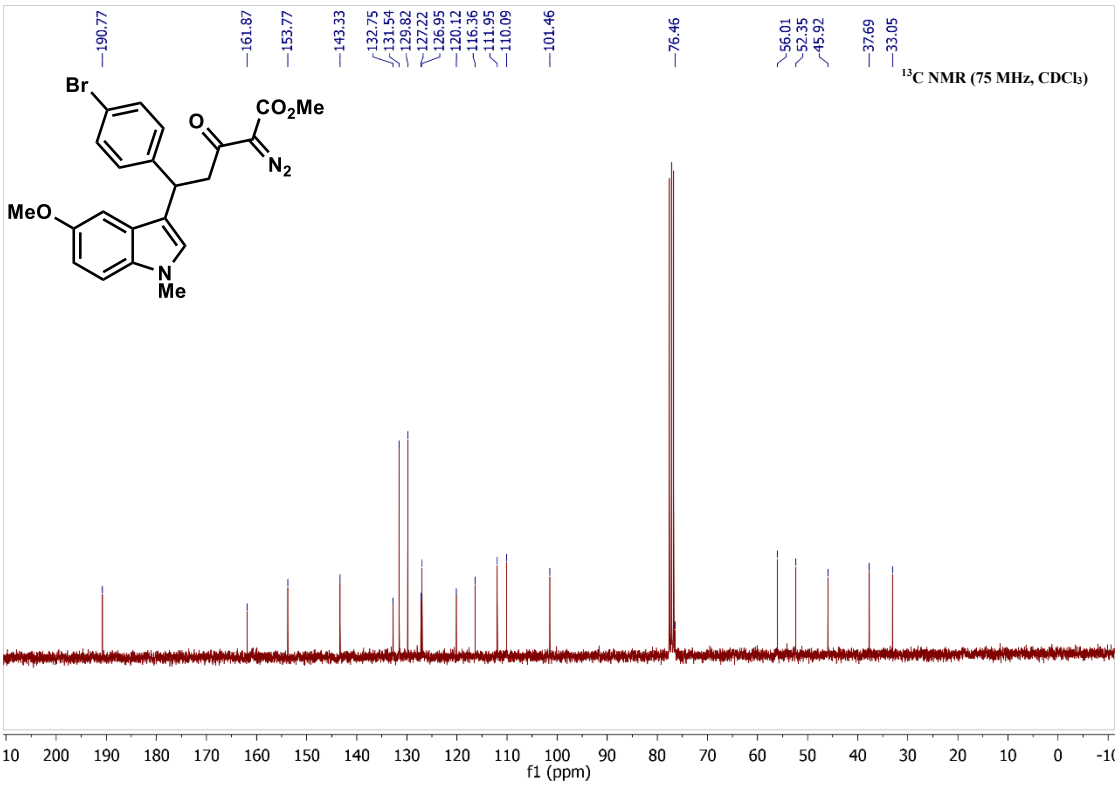
^{13}C NMR (75 MHz, CDCl$_3$)
Br
CO$_2$Me
O
N$_2$
MeO
N
Me
f1 (ppm)

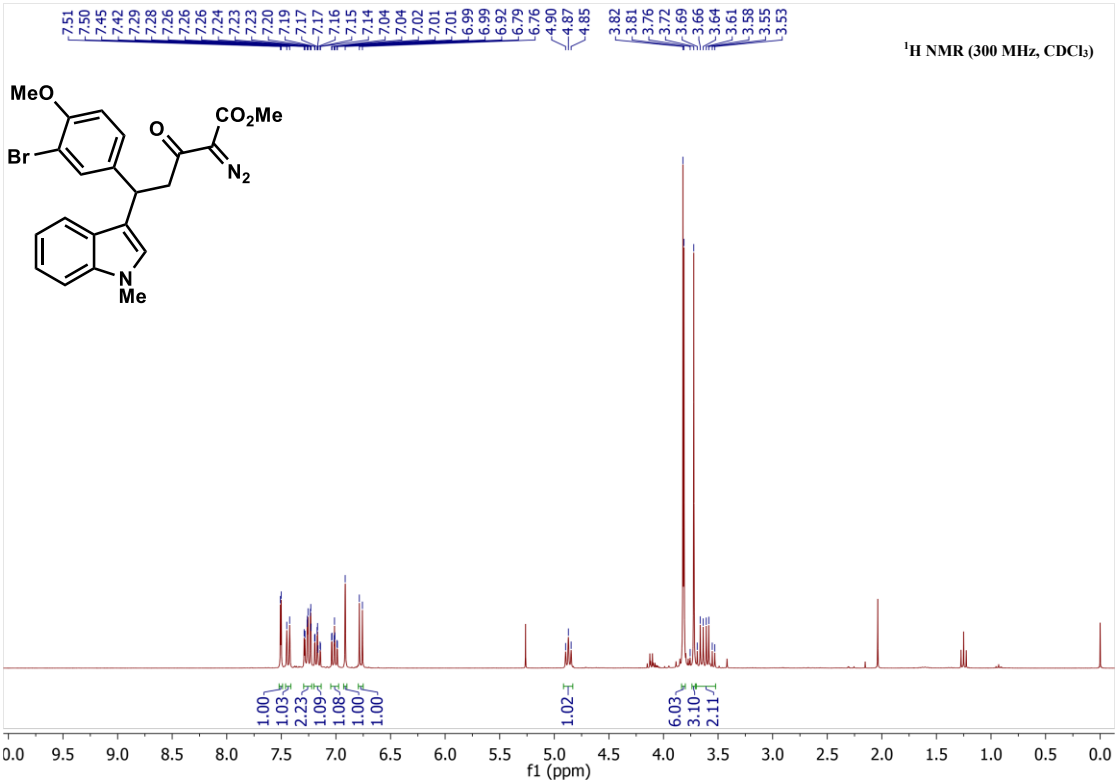
^{1}H NMR (300 MHz, CDCl$_3$)
MeO
Br
O
CO$_2$Me
N$_2$
N
Me
7.51 7.50 7.45 7.42 7.29 7.28 7.26 7.26 7.26 7.24 7.23 7.23 7.20 7.19 7.17 7.17 7.16 7.15 7.14 7.04 7.04 7.02 7.01 7.01 6.99 6.99 6.92 6.79 6.76 4.90 4.87 4.85 3.82 3.81 3.76 3.72 3.69 3.66 3.64 3.61 3.58 3.55 3.53
1.00 1.03 2.23 1.09 1.08 1.00 1.00 1.02 6.03 3.10 2.11
f1 (ppm)

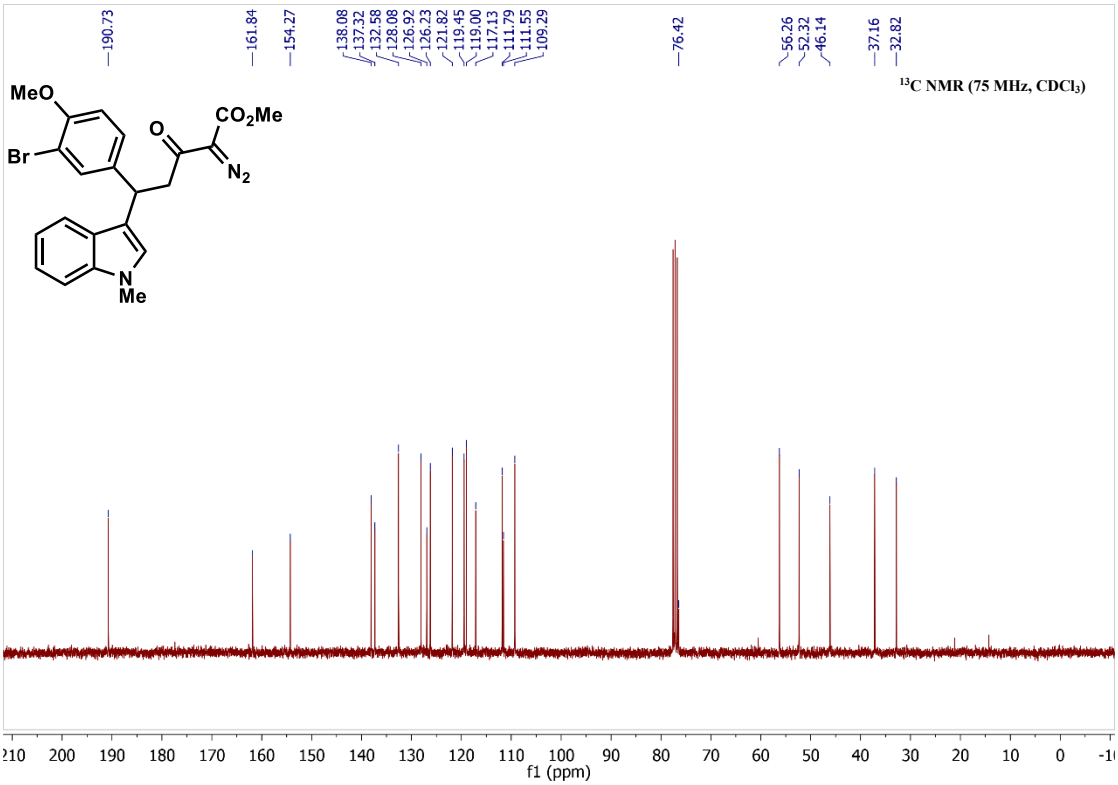
^{13}C NMR (75 MHz, CDCl$_3$)
MeO
Br
O
CO$_2$Me
N$_2$
N
Me
190.73 161.84 154.27 138.08 137.32 132.58 128.08 126.92 126.23 121.82 119.45 119.00 117.13 111.79 111.55 109.29 76.42 56.26 52.32 46.14 37.16 32.82
f1 (ppm)

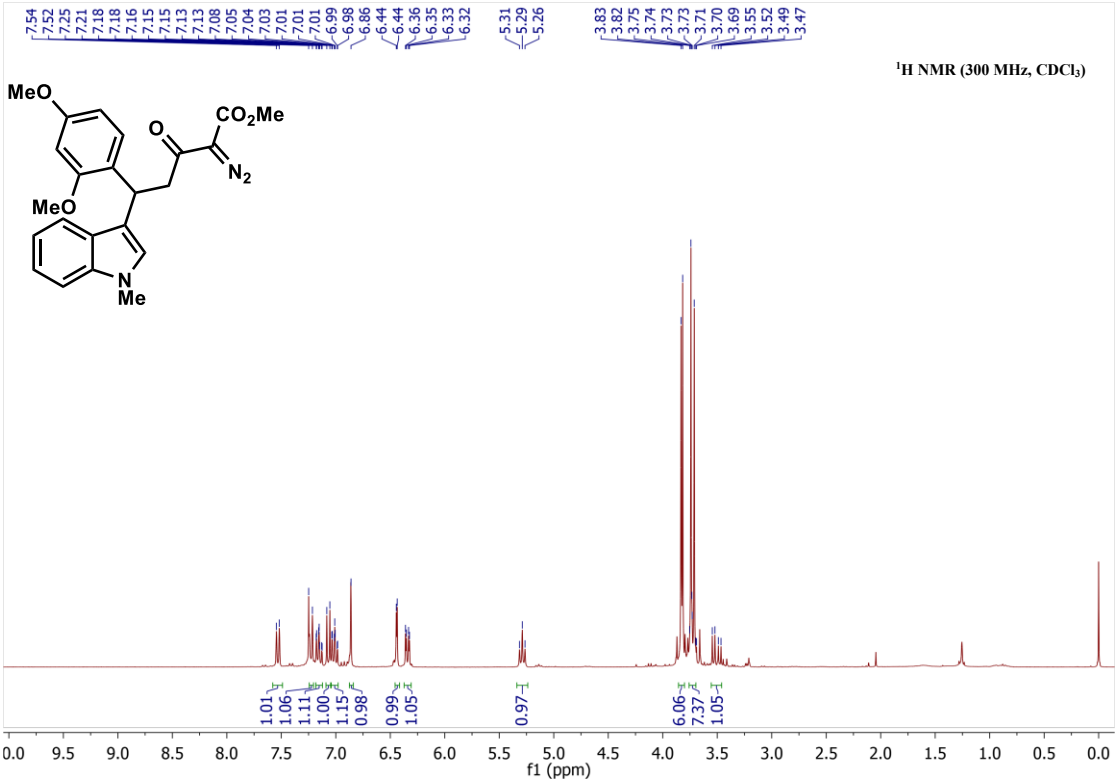
7.54
7.52
7.25
7.21
7.18
7.18
7.16
7.15
7.15
7.13
7.13
7.08
7.05
7.04
7.03
7.01
7.01
7.01
6.99
6.98
6.86
6.44
6.36
6.35
6.33
6.32
5.31
5.29
5.26
3.83
3.82
3.75
3.74
3.73
3.73
3.71
3.70
3.69
3.55
3.52
3.49
3.47
^{1}H NMR (300 MHz, CDCl$_3$)
MeO
CO$_2$Me
O
N$_2$
MeO
N
Me
1.01
1.06
1.11
1.00
1.15
0.98
0.99
1.05
0.97
6.06
7.37
1.05
f1 (ppm)

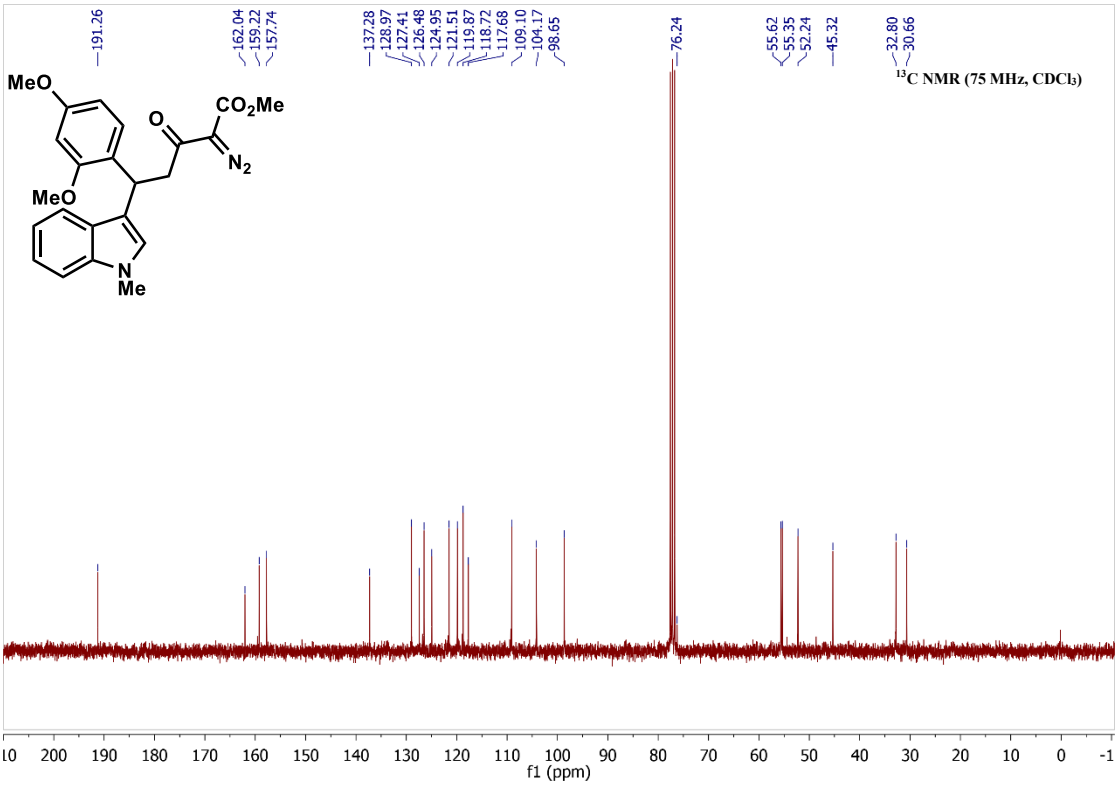
191.26
162.04
159.22
157.74
137.28
128.97
127.41
126.48
124.95
121.51
119.87
118.72
117.68
109.10
104.17
98.65
76.24
55.62
55.35
52.24
45.32
32.80
30.66
^{13}C NMR (75 MHz, CDCl$_3$)
MeO
CO$_2$Me
O
N$_2$
MeO
N
Me
f1 (ppm)

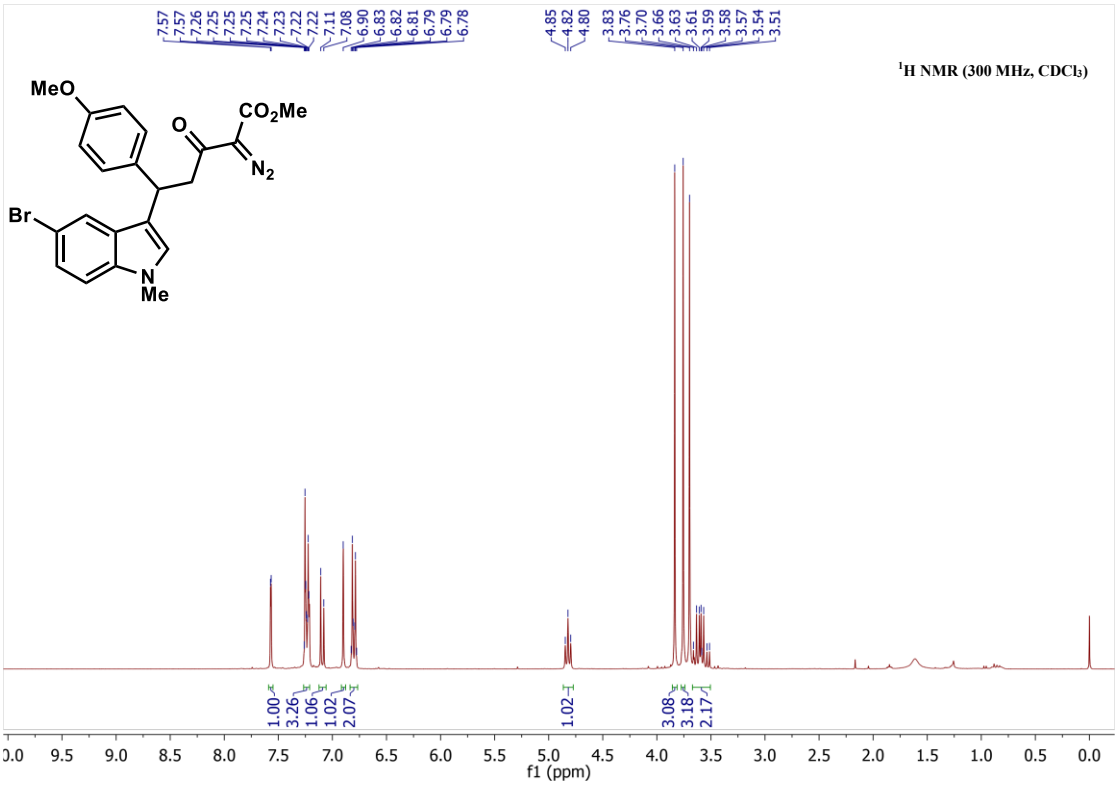
^{1}H NMR (300 MHz, CDCl$_3$)
MeO
O
CO$_2$Me
N$_2$
Br
N
Me
f1 (ppm)

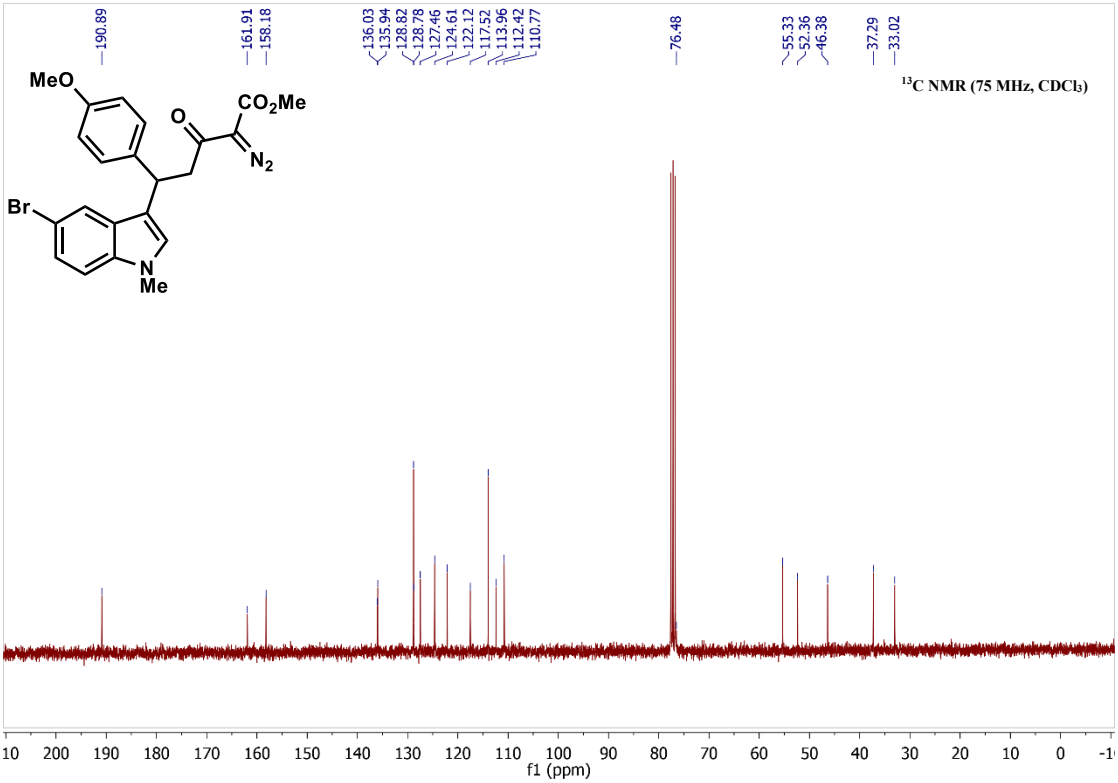
^{13}C NMR (75 MHz, CDCl$_3$)
MeO
O
CO$_2$Me
N$_2$
Br
N
Me
f1 (ppm)

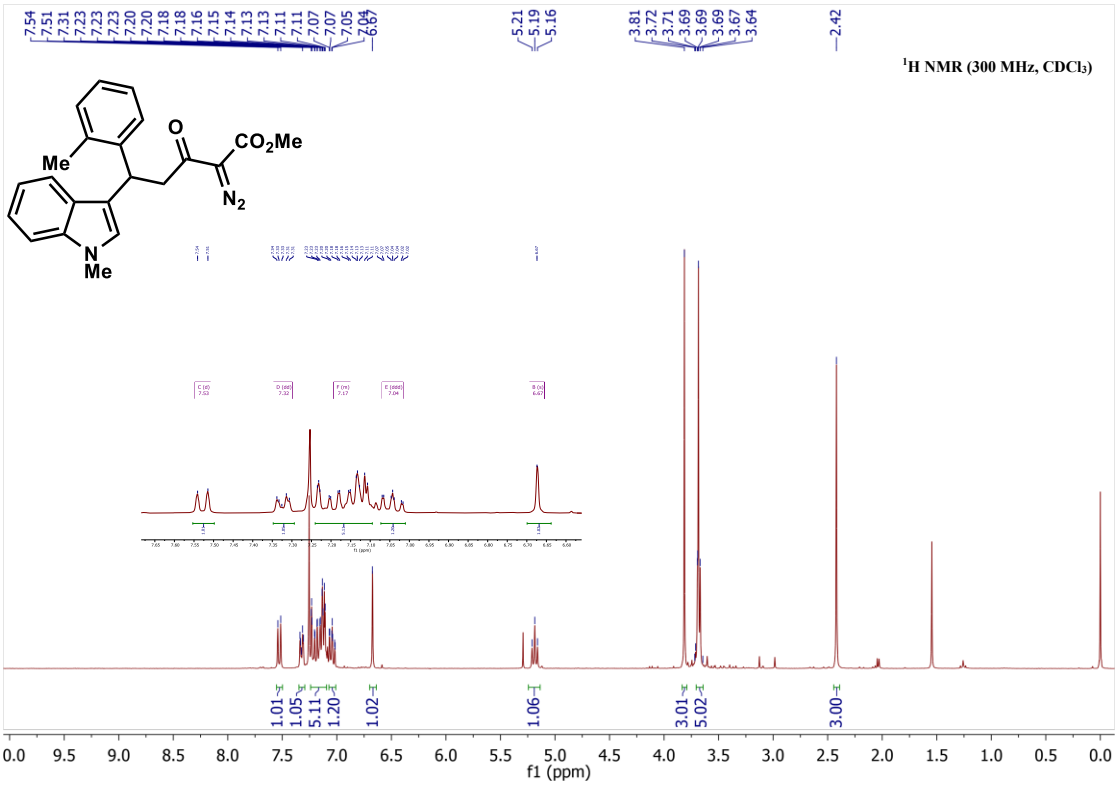
7.54
7.51
7.31
7.23
7.23
7.23
7.20
7.18
7.18
7.16
7.15
7.14
7.13
7.13
7.11
7.11
7.07
7.07
7.05
7.04
6.67
5.21
5.19
5.16
3.81
3.72
3.71
3.69
3.69
3.69
3.67
3.64
2.42
^{1}H NMR (300 MHz, CDCl$_3$)
Me
O
CO$_2$Me
N$_2$
N
Me
1.01
1.05
5.11
1.20
1.02
1.06
3.01
5.02
3.00
0.0 9.5 9.0 8.5 8.0 7.5 7.0 6.5 6.0 5.5 5.0 4.5 4.0 3.5 3.0 2.5 2.0 1.5 1.0 0.5 0.0
f1 (ppm)

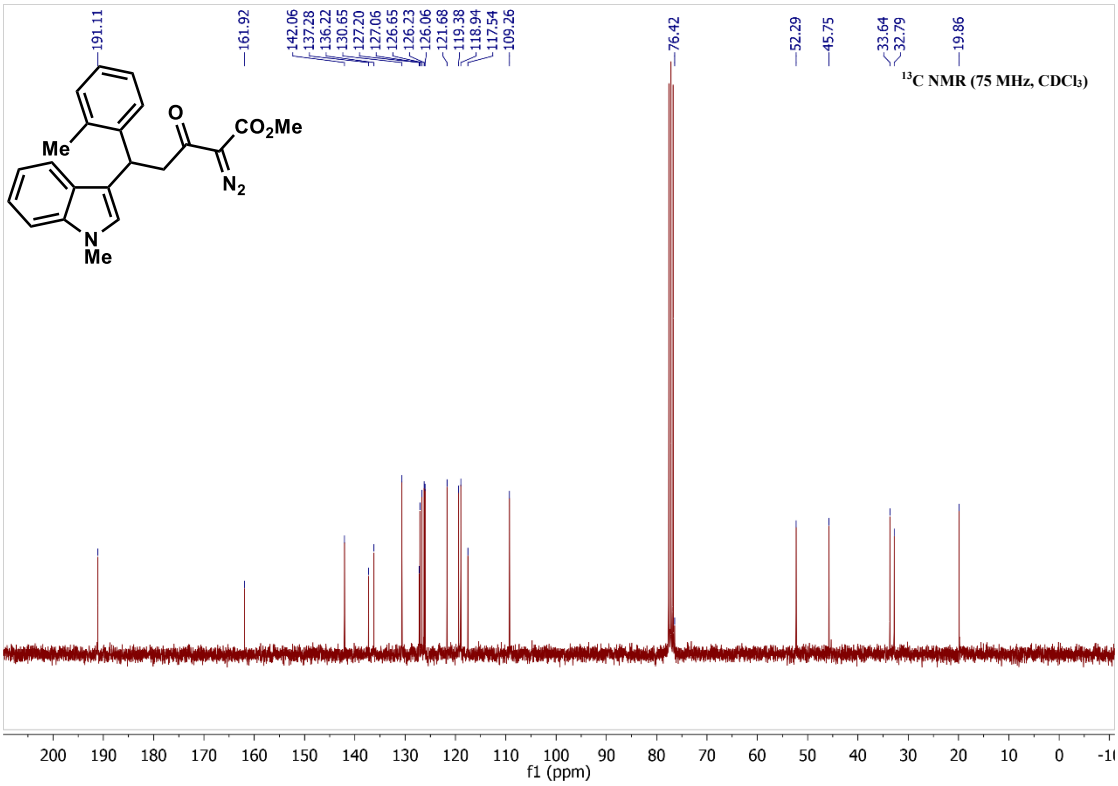
191.11
161.92
142.06
137.28
136.22
130.65
127.20
127.06
126.65
126.23
126.06
121.68
119.38
118.94
117.54
109.26
76.42
52.29
45.75
33.64
32.79
19.86
^{13}C NMR (75 MHz, CDCl$_3$)
Me
O
CO$_2$Me
N$_2$
N
Me
200 190 180 170 160 150 140 130 120 110 100 90 80 70 60 50 40 30 20 10 0
f1 (ppm)

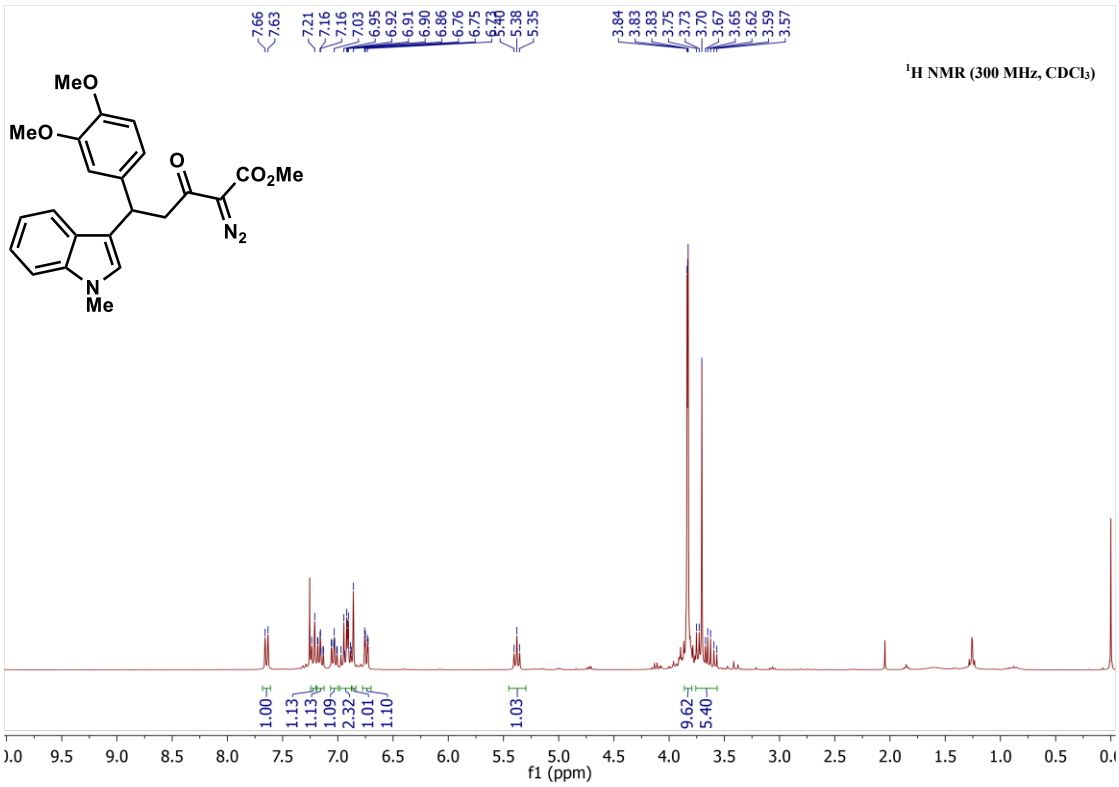
^{1}H NMR (300 MHz, CDCl$_3$)
MeO
MeO
O
CO$_2$Me
N$_2$
N
Me
7.66
7.63
7.21
7.16
7.16
7.03
6.95
6.92
6.91
6.90
6.86
6.76
6.75
5.38
5.35
3.84
3.83
3.83
3.75
3.73
3.70
3.67
3.65
3.62
3.59
3.57
1.00
1.13
1.13
1.09
2.32
1.01
1.10
1.03
9.62
5.40
f1 (ppm)

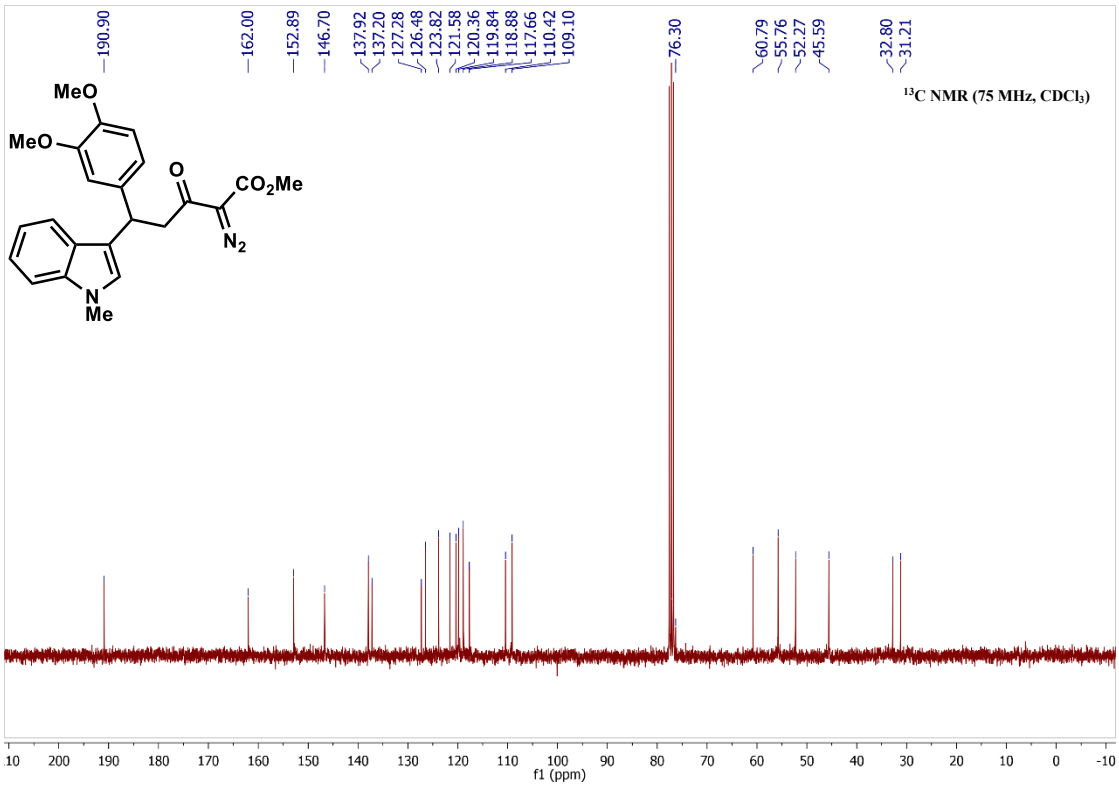
^{13}C NMR (75 MHz, CDCl$_3$)
MeO
MeO
O
CO$_2$Me
N$_2$
N
Me
190.90
162.00
152.89
146.70
137.92
137.20
127.28
126.48
123.82
121.58
120.36
119.84
118.88
117.66
110.42
109.10
76.30
60.79
55.76
52.27
45.59
32.80
31.21
f1 (ppm)

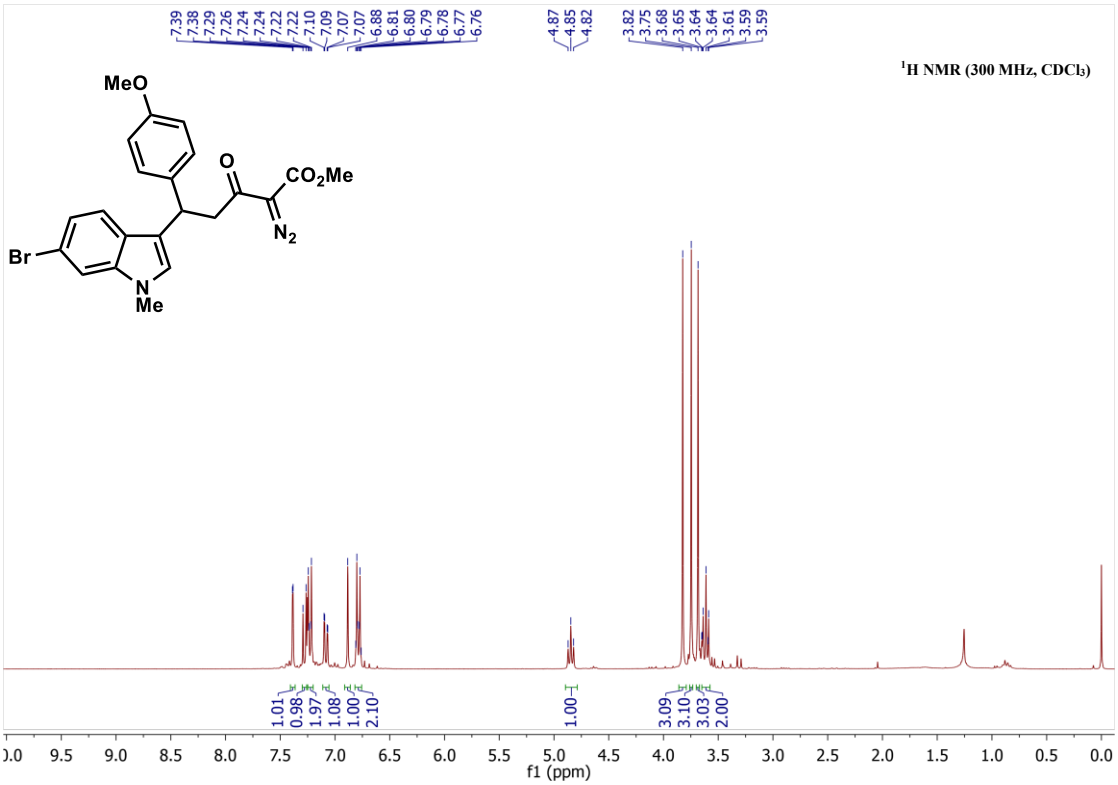
7.39
7.38
7.29
7.26
7.24
7.24
7.22
7.22
7.10
7.09
7.07
7.07
6.88
6.81
6.80
6.79
6.78
6.77
6.76
4.87
4.85
4.82
3.82
3.75
3.68
3.65
3.64
3.64
3.61
3.59
3.59
^{1}H NMR (300 MHz, CDCl$_3$)
MeO
O
CO$_2$Me
N$_2$
Br
N
Me
1.01
0.98
1.97
1.08
1.00
2.10
1.00
3.09
3.10
3.03
2.00
f1 (ppm)

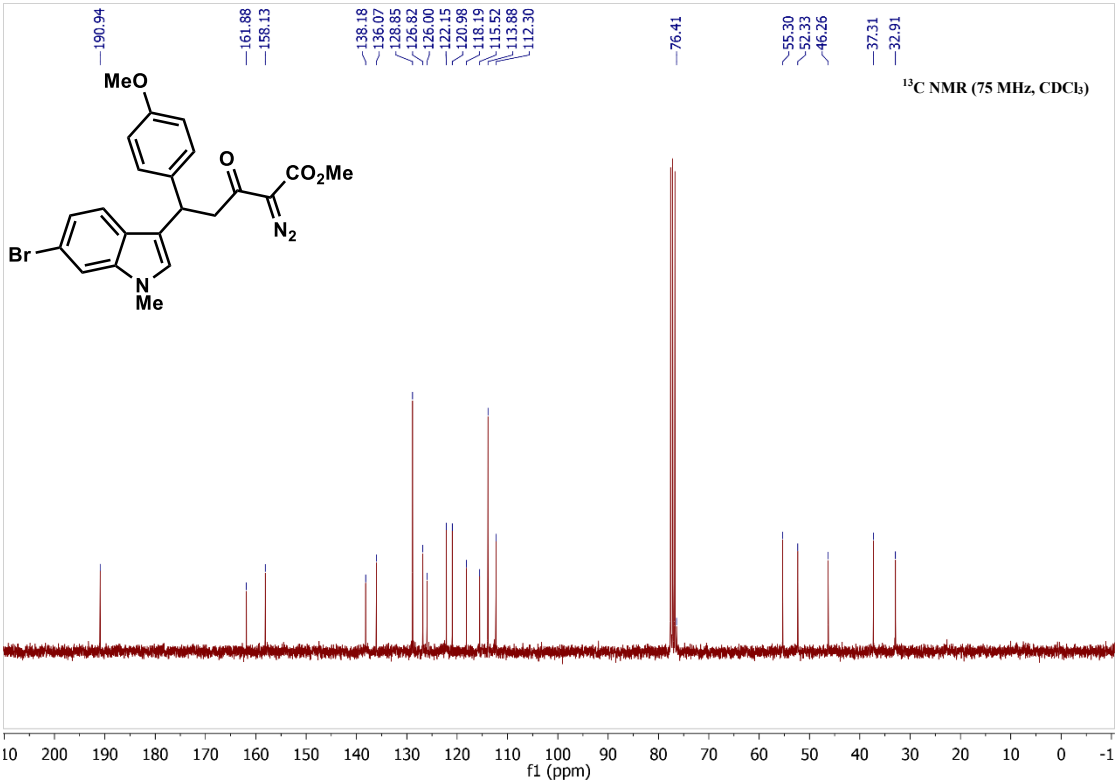
190.94
161.88
158.13
138.18
136.07
128.85
126.82
126.00
122.15
120.98
118.19
115.52
113.88
112.30
76.41
55.30
52.33
46.26
37.31
32.91
^{13}C NMR (75 MHz, CDCl$_3$)
MeO
O
CO$_2$Me
N$_2$
Br
N
Me
f1 (ppm)

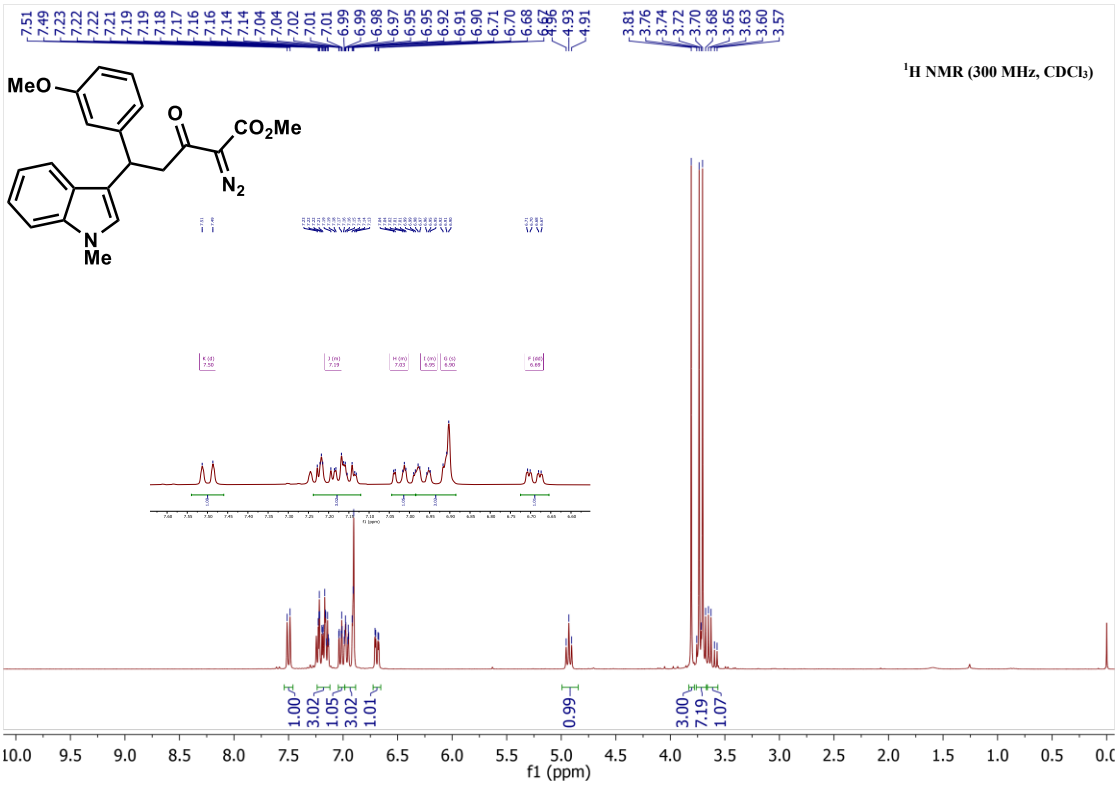
7.51 7.49 7.23 7.22 7.22 7.21 7.19 7.19 7.18 7.17 7.16 7.16 7.14 7.14 7.04 7.04 7.02 7.01 7.01 6.99 6.99 6.98 6.97 6.95 6.95 6.92 6.91 6.90 6.71 6.70 6.68 4.93 4.91 3.81 3.76 3.74 3.72 3.70 3.68 3.65 3.63 3.60 3.57
^{1}H NMR (300 MHz, CDCl$_3$)
MeO
O
CO$_2$Me
N$_2$
N
Me
1.00 3.02 1.05 3.02 1.01 0.99 3.00 7.19 1.07
10.0 9.5 9.0 8.5 8.0 7.5 7.0 6.5 6.0 5.5 5.0 4.5 4.0 3.5 3.0 2.5 2.0 1.5 1.0 0.5 0.0
f1 (ppm)

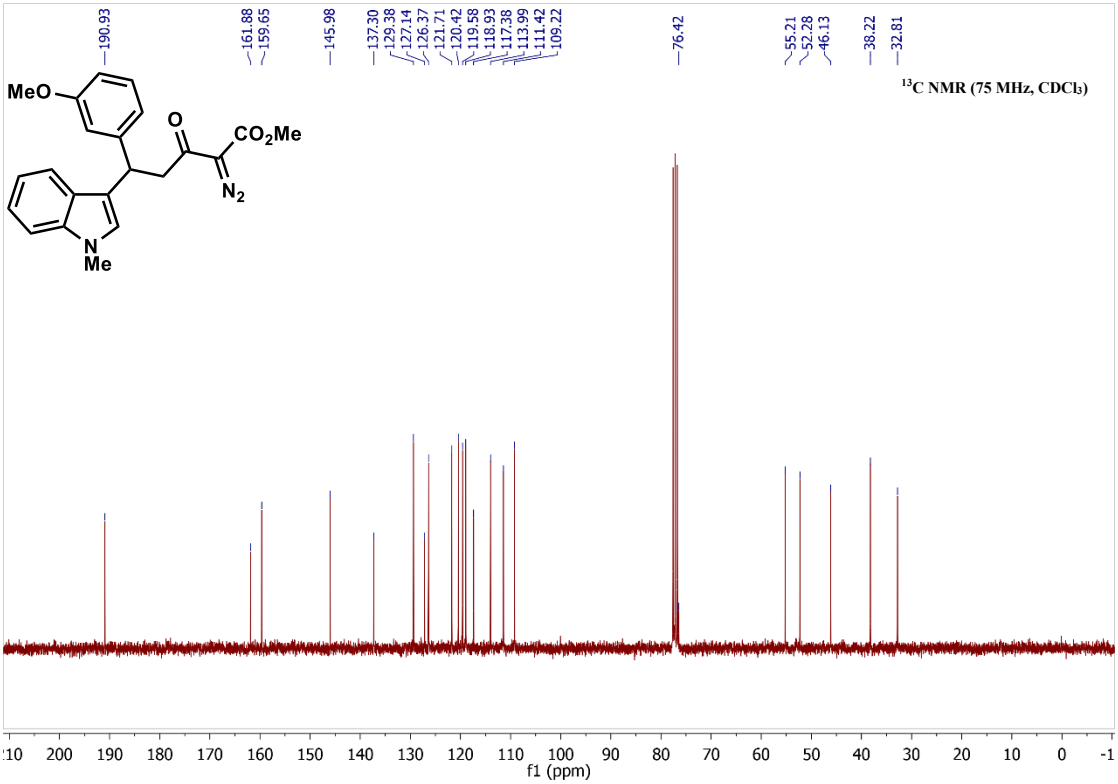
190.93 161.88 159.65 145.98 137.30 129.38 127.14 126.37 121.71 120.42 119.58 118.93 117.38 113.99 111.42 109.22 76.42 55.21 52.28 46.13 38.22 32.81
^{13}C NMR (75 MHz, CDCl$_3$)
MeO
O
CO$_2$Me
N$_2$
N
Me
210 200 190 180 170 160 150 140 130 120 110 100 90 80 70 60 50 40 30 20 10 0 -10
f1 (ppm)

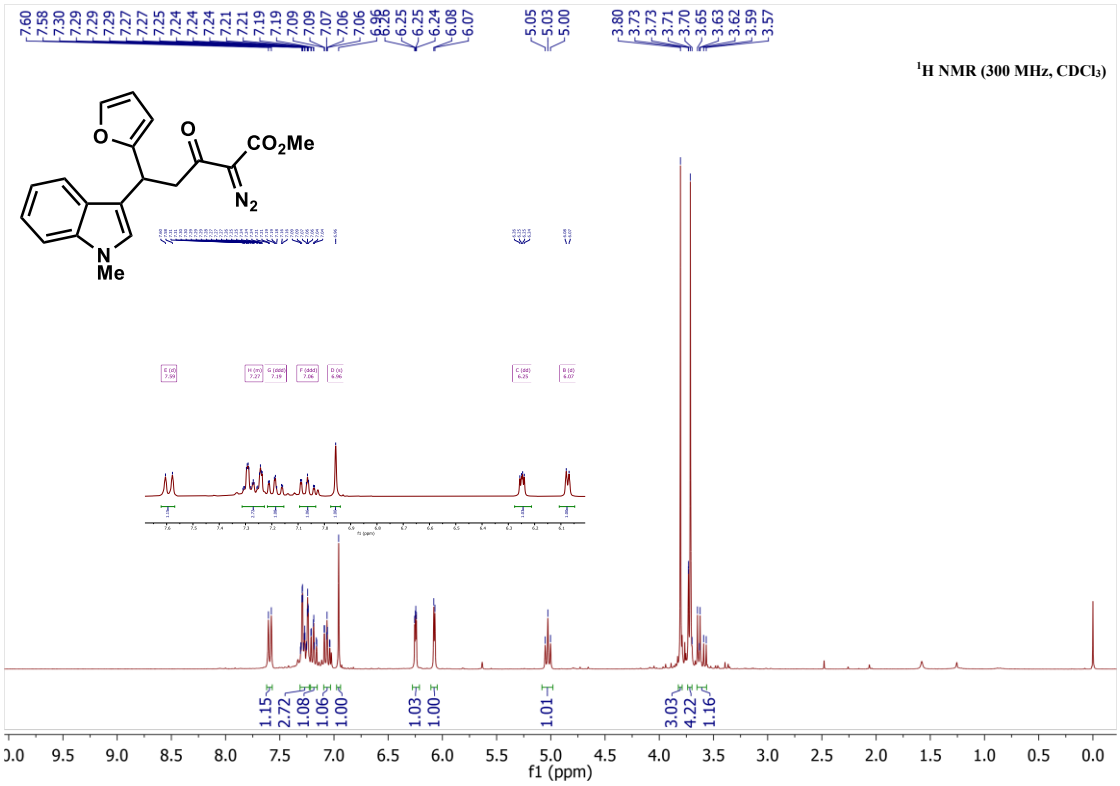
7.60 7.58 7.30 7.29 7.29 7.29 7.27 7.27 7.25 7.24 7.24 7.24 7.21 7.21 7.19 7.19 7.09 7.09 7.07 7.06 7.06 6.26 6.25 6.25 6.24 6.08 6.07
5.05 5.03 5.00
3.80 3.73 3.73 3.71 3.70 3.65 3.63 3.62 3.59 3.57
^{1}H NMR (300 MHz, CDCl$_3$)
O
O
CO$_2$Me
N$_2$
N
Me
1.15 2.72 1.08 1.06 1.00 1.03 1.00 1.01 3.03 4.22 1.16
f1 (ppm)

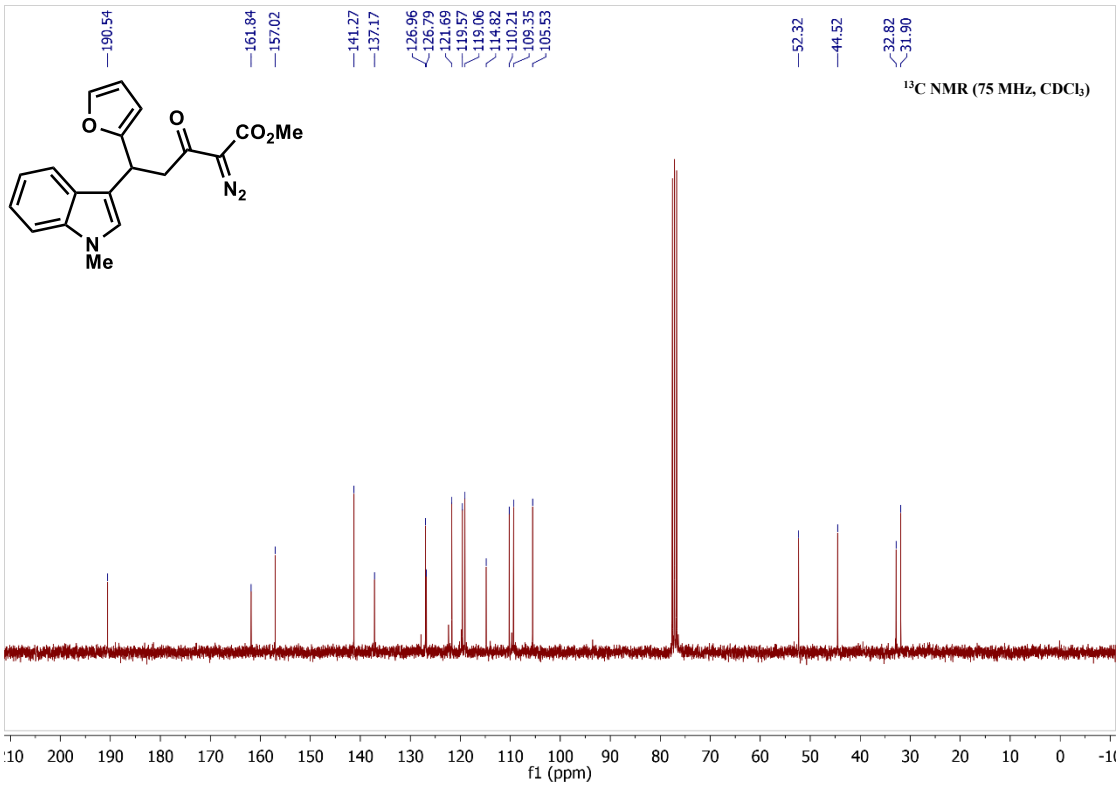
190.54
161.84 157.02
141.27 137.17
126.96 126.79 121.69 119.57 119.06 114.82 110.21 109.35 105.53
52.32 44.52 32.82 31.90
^{13}C NMR (75 MHz, CDCl$_3$)
O
O
CO$_2$Me
N$_2$
N
Me
f1 (ppm)

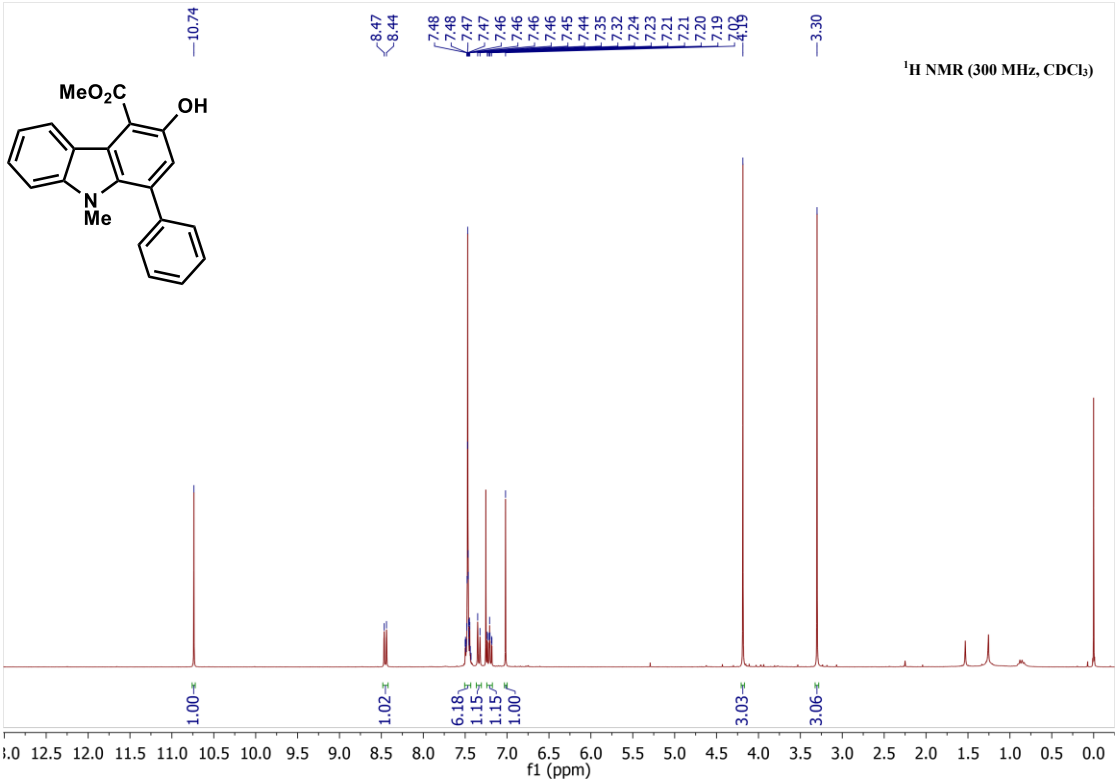
^{1}H NMR (300 MHz, CDCl$_3$)
MeO$_2$C
OH
N
Me
10.74
8.47
8.44
7.48
7.48
7.47
7.47
7.46
7.46
7.46
7.46
7.45
7.44
7.35
7.32
7.24
7.23
7.21
7.21
7.20
7.19
7.02
4.19
3.30
1.00
1.02
6.18
1.15
1.15
1.00
3.03
3.06
f1 (ppm)

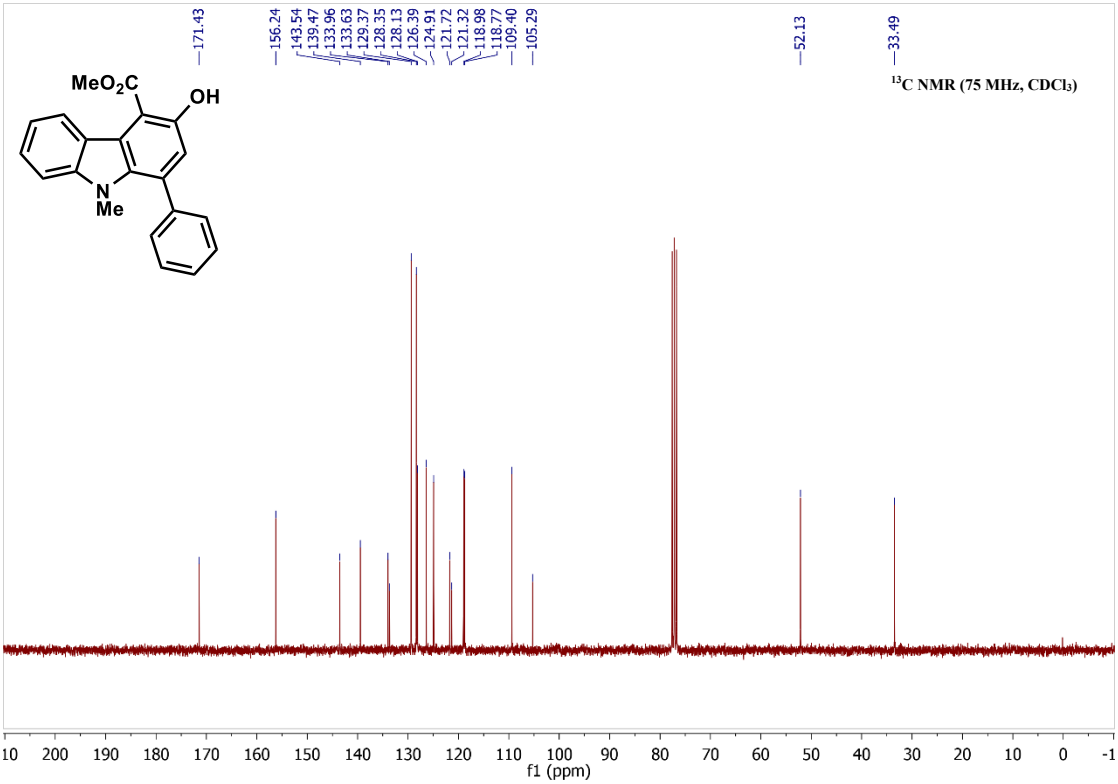
^{13}C NMR (75 MHz, CDCl$_3$)
MeO$_2$C
OH
N
Me
171.43
156.24
143.54
139.47
133.96
133.63
129.37
128.35
128.13
126.39
124.91
121.72
121.32
118.98
118.77
109.40
105.29
52.13
33.49
f1 (ppm)

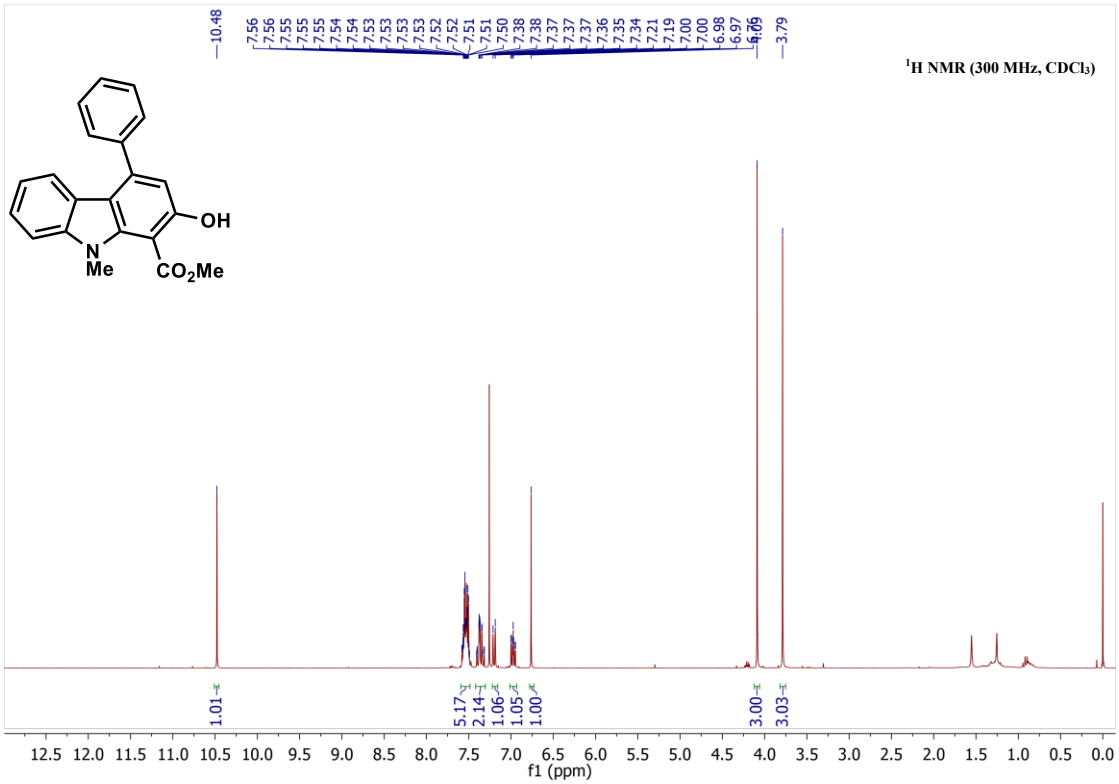
^{1}H NMR (300 MHz, CDCl$_3$)
OH
N
Me
CO$_2$Me
f1 (ppm)

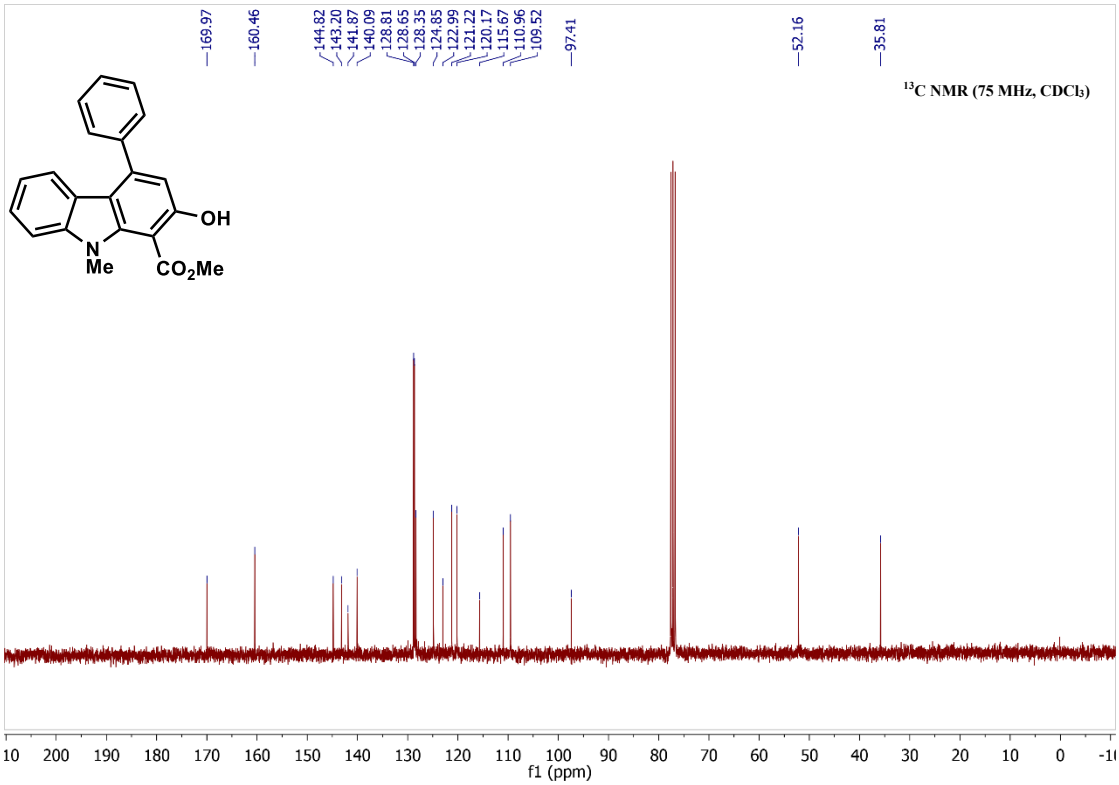
^{13}C NMR (75 MHz, CDCl$_3$)
OH
N
Me
CO$_2$Me
f1 (ppm)

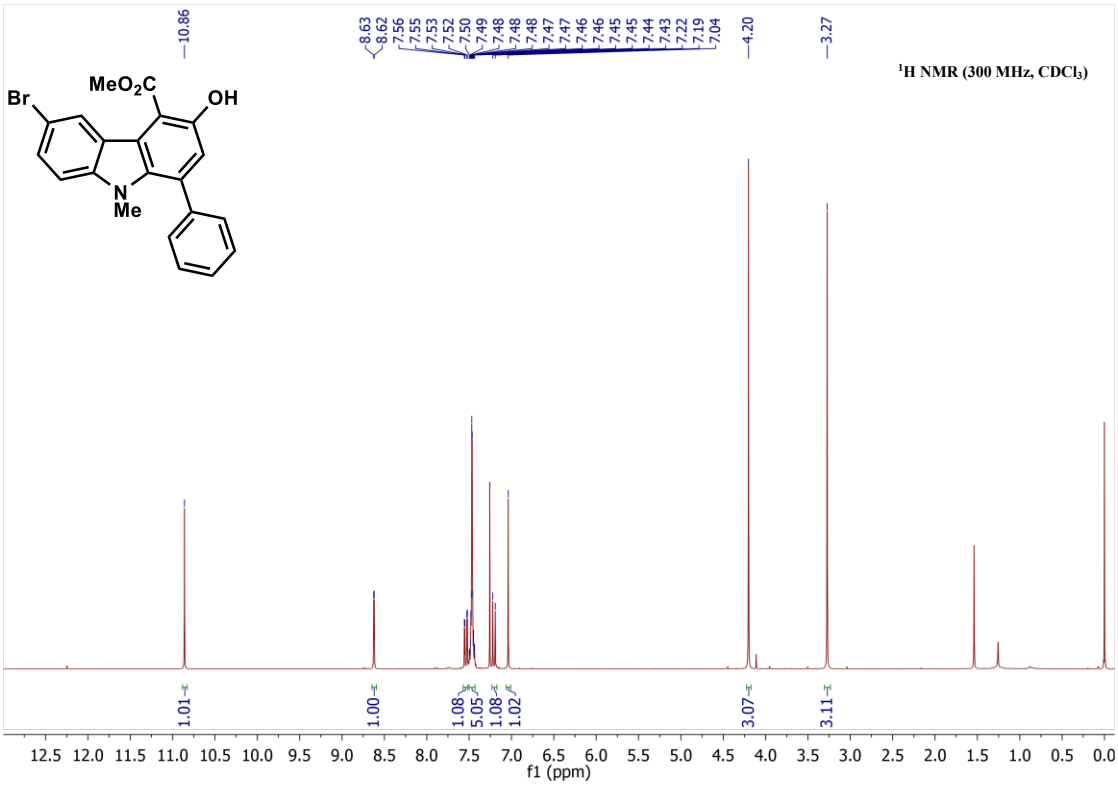
^{1}H NMR (300 MHz, CDCl$_3$)
Br
MeO$_2$C
OH
N
Me
f1 (ppm)

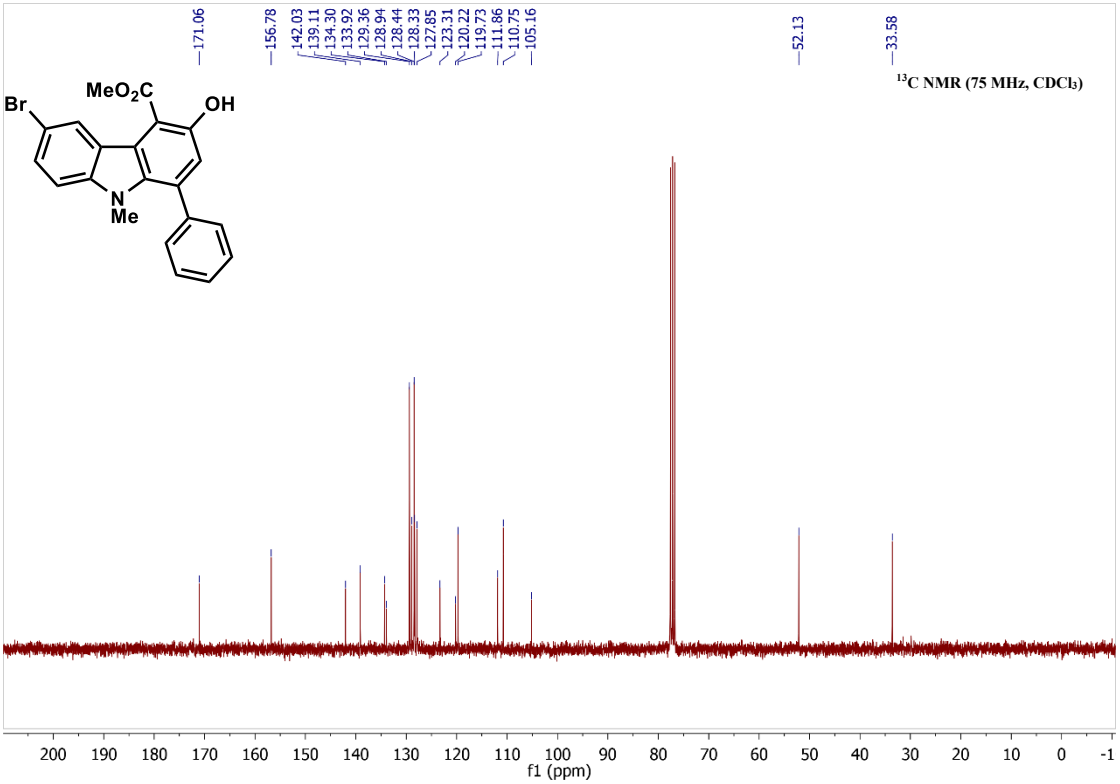
^{13}C NMR (75 MHz, CDCl$_3$)
Br
MeO$_2$C
OH
N
Me
f1 (ppm)

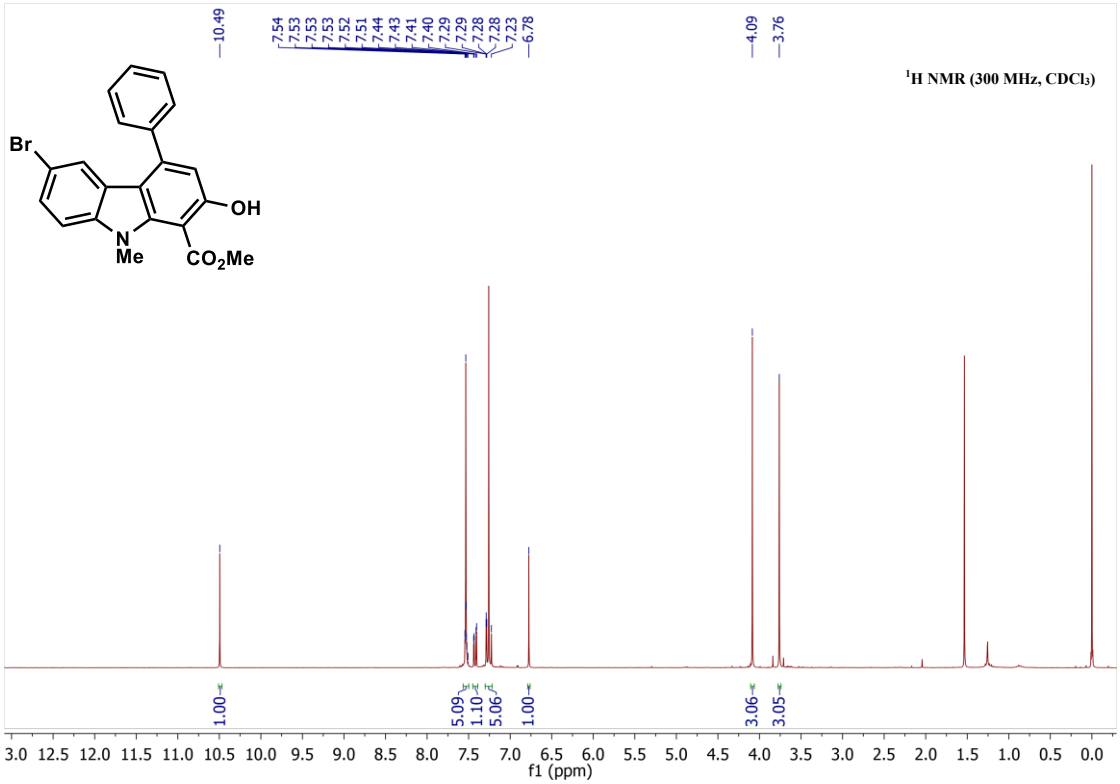
10.49
7.54
7.53
7.53
7.53
7.52
7.51
7.44
7.43
7.41
7.40
7.29
7.29
7.28
7.28
7.23
6.78
4.09
3.76
^{1}H NMR (300 MHz, CDCl$_3$)
Br
OH
N
Me
CO$_2$Me
1.00
5.09
1.10
5.06
1.00
3.06
3.05
f1 (ppm)

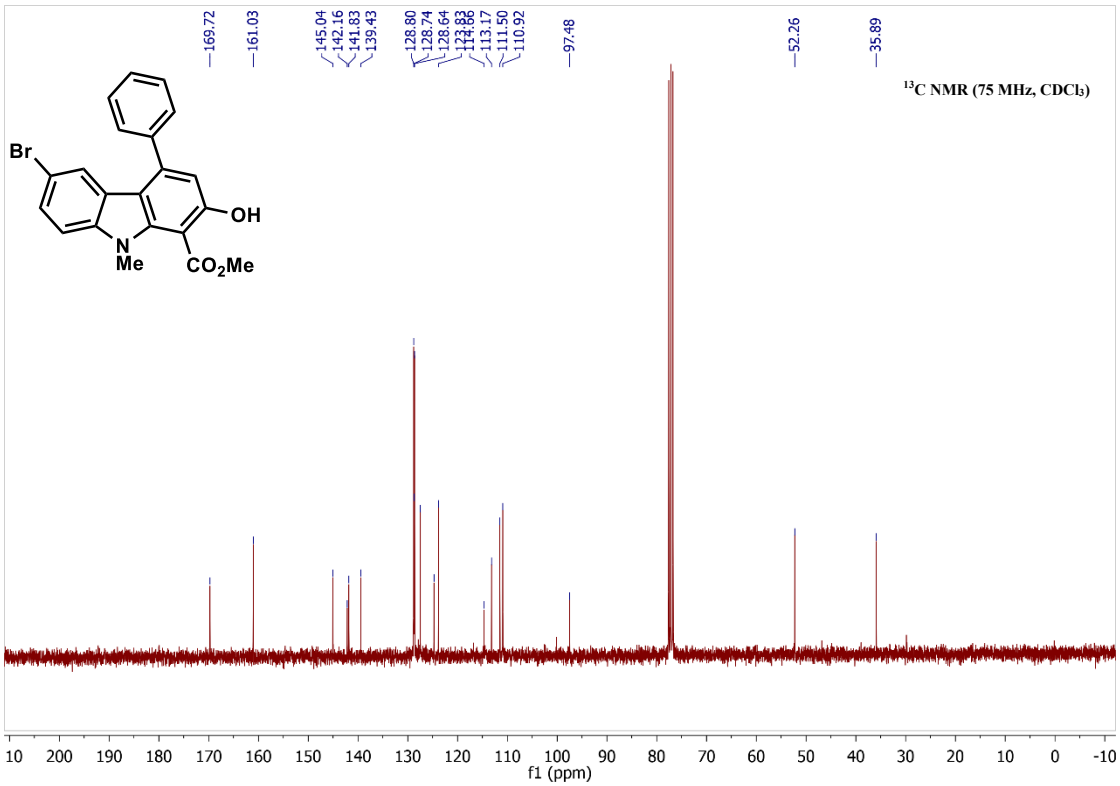
169.72
161.03
145.04
142.16
141.83
139.43
128.80
128.74
128.64
113.17
111.50
110.92
97.48
52.26
35.89
^{13}C NMR (75 MHz, CDCl$_3$)
Br
OH
N
Me
CO$_2$Me
f1 (ppm)

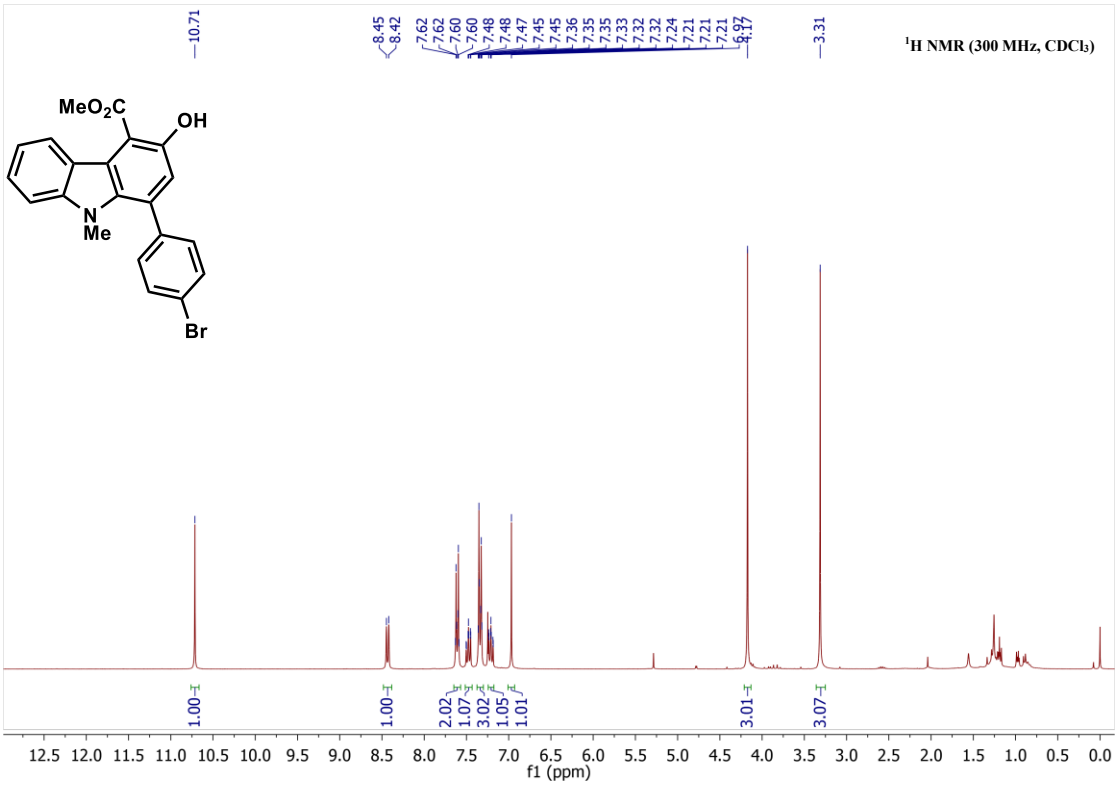
^{1}H NMR (300 MHz, CDCl$_3$)
MeO$_2$C
OH
N
Me
Br
10.71
8.45
8.42
7.62
7.62
7.60
7.60
7.48
7.47
7.45
7.45
7.36
7.35
7.33
7.32
7.32
7.24
7.21
7.21
7.21
6.97
6.97
3.31
1.00
1.00
2.02
1.07
3.02
1.05
1.01
3.01
3.07
f1 (ppm)

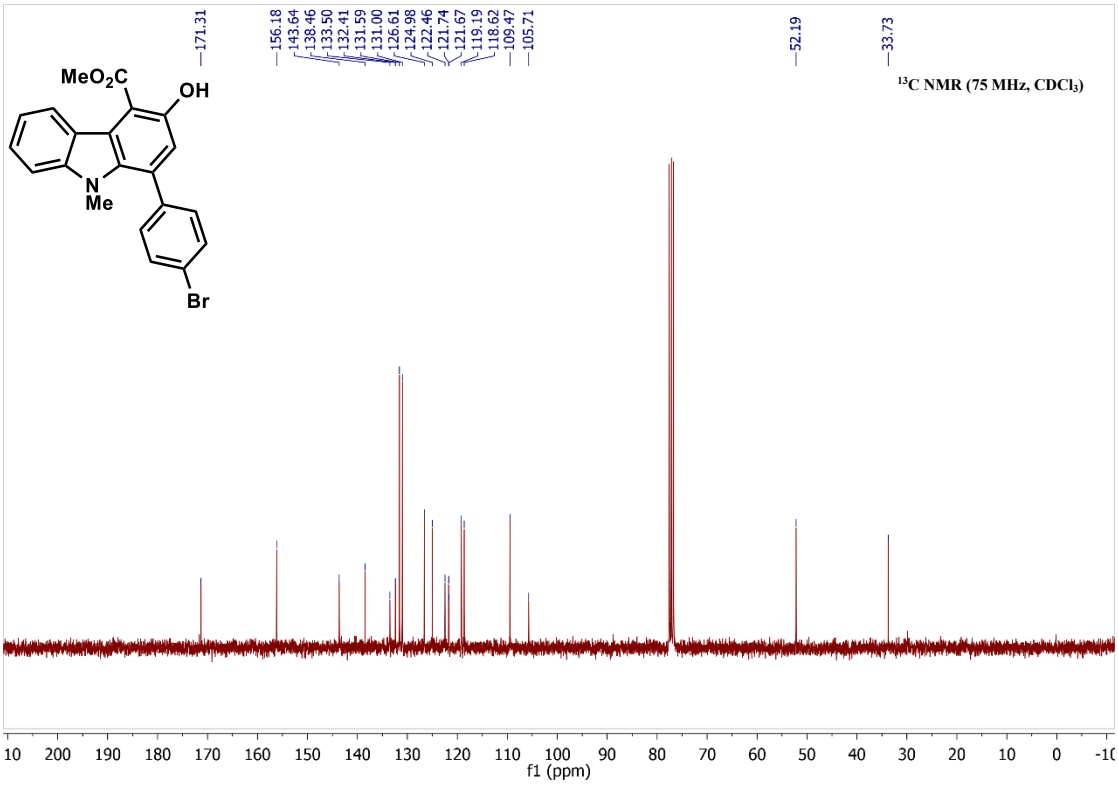
^{13}C NMR (75 MHz, CDCl$_3$)
MeO$_2$C
OH
N
Me
Br
171.31
156.18
143.64
138.46
133.50
132.41
131.59
131.00
126.61
124.98
122.46
121.74
121.67
119.19
118.62
109.47
105.71
52.19
33.73
f1 (ppm)

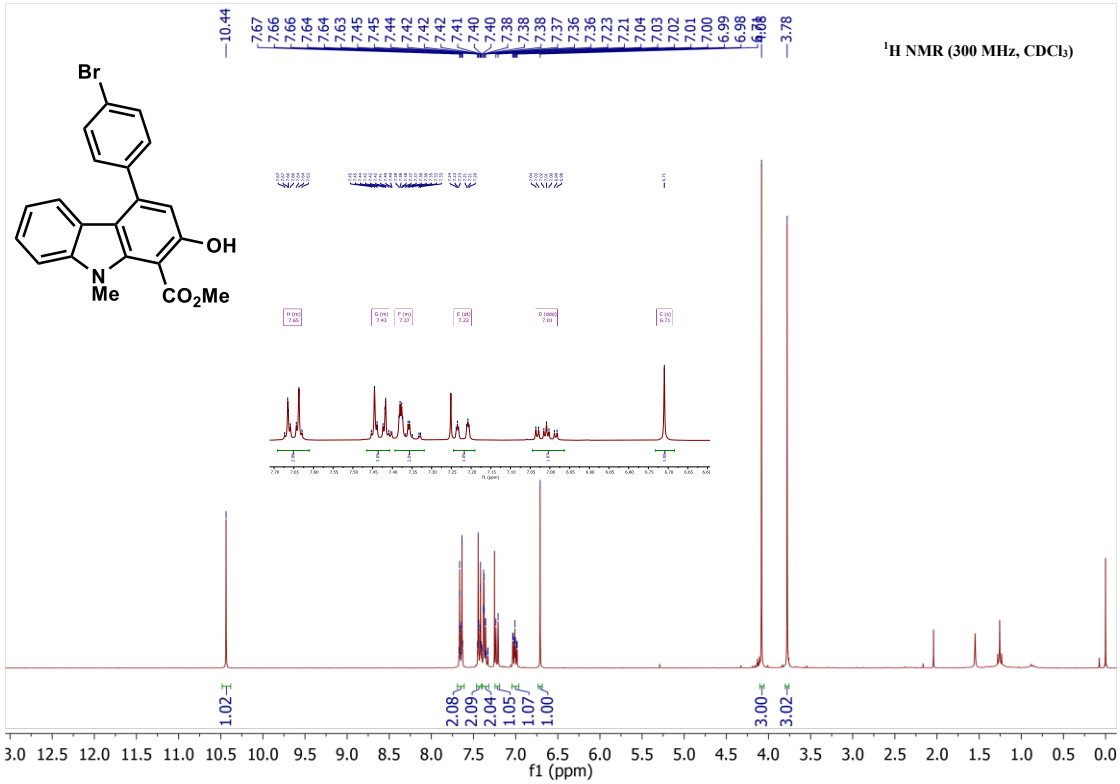
^{1}H NMR (300 MHz, CDCl$_3$)
Br
OH
N
Me
CO$_2$Me
10.44
7.67
7.66
7.66
7.64
7.64
7.63
7.45
7.45
7.44
7.42
7.42
7.42
7.41
7.40
7.40
7.38
7.38
7.38
7.37
7.36
7.36
7.23
7.21
7.04
7.03
7.02
7.01
7.00
6.99
6.98
3.78
1.02
2.08
2.09
2.04
1.05
1.07
1.00
3.00
3.02
f1 (ppm)

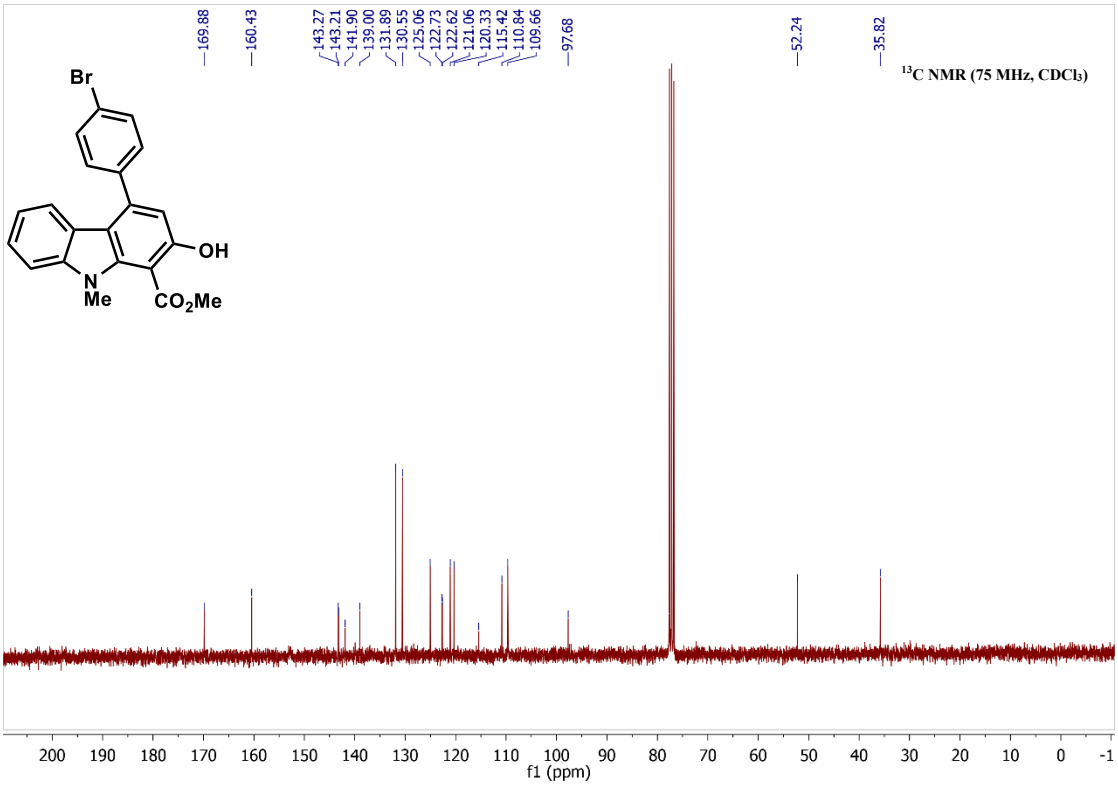
^{13}C NMR (75 MHz, CDCl$_3$)
Br
OH
N
Me
CO$_2$Me
169.88
160.43
143.27
143.21
141.90
139.00
131.89
130.55
125.06
122.73
122.62
121.06
120.33
115.42
110.84
109.66
97.68
52.24
35.82
f1 (ppm)

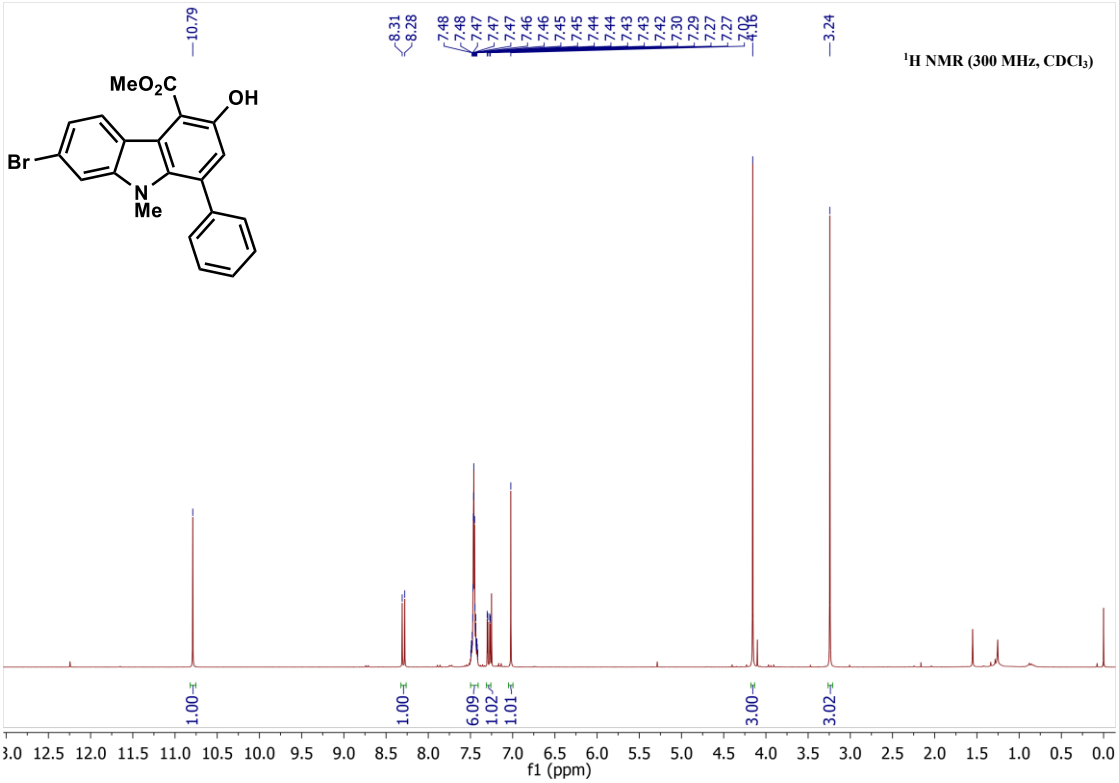
^{1}H NMR (300 MHz, CDCl$_3$)
MeO$_2$C
OH
Br
N
Me
10.79
8.31
8.28
7.48
7.47
7.46
7.45
7.44
7.43
7.42
7.30
7.29
7.27
4.16
3.24
1.00
1.00
6.09
1.02
1.01
3.00
3.02
f1 (ppm)

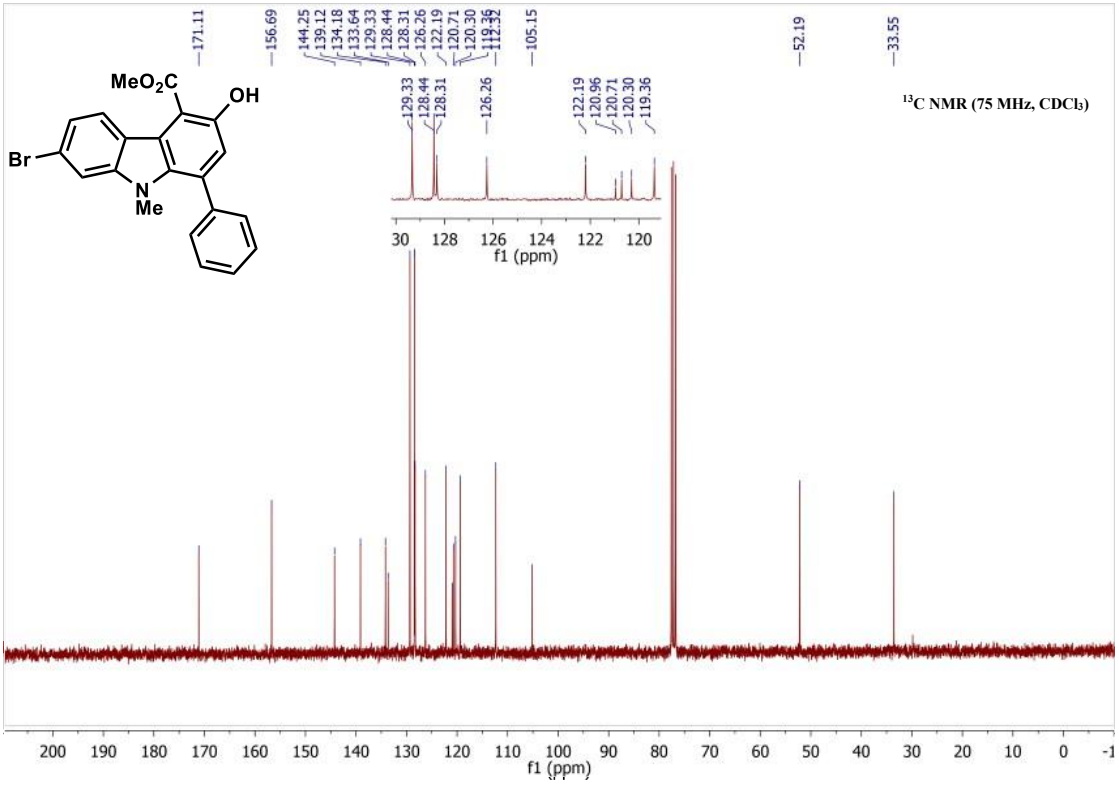
^{13}C NMR (75 MHz, CDCl$_3$)
MeO$_2$C
OH
Br
N
Me
171.11
156.69
144.25
139.12
134.18
133.64
129.33
128.44
128.31
126.26
122.19
120.71
120.30
119.36
105.15
52.19
33.55
f1 (ppm)

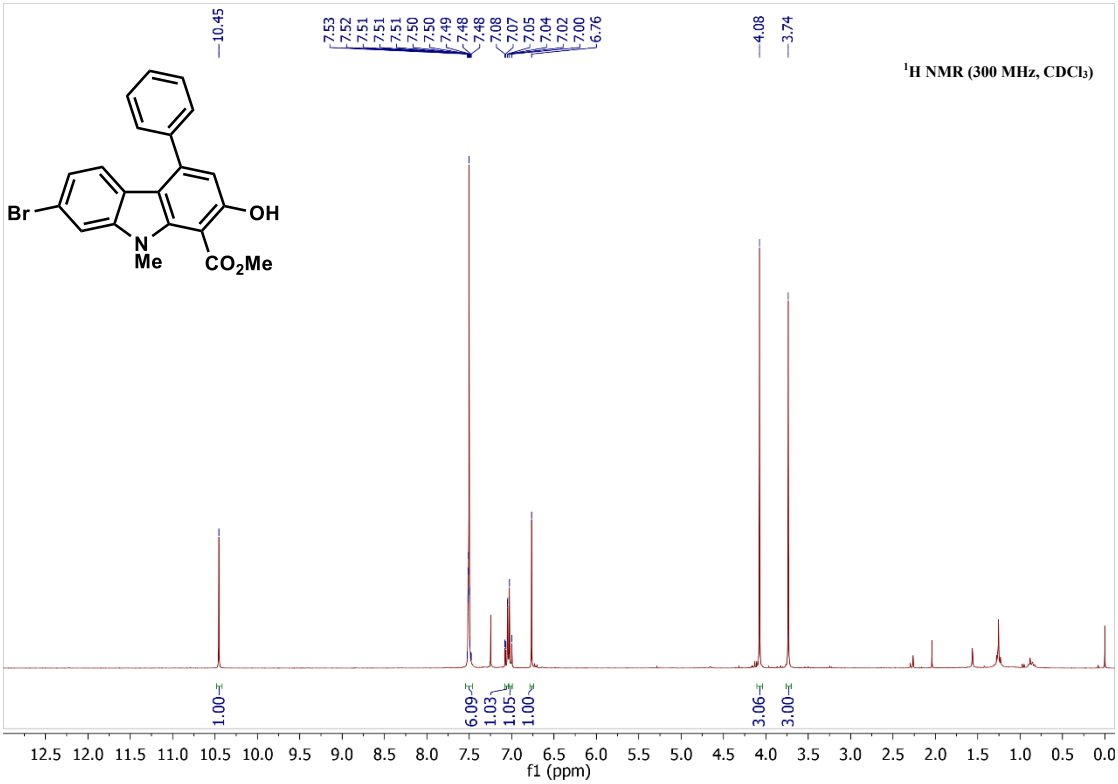
10.45
7.53
7.52
7.51
7.51
7.51
7.50
7.50
7.49
7.48
7.48
7.08
7.07
7.05
7.04
7.02
7.00
6.76
4.08
3.74
1H NMR (300 MHz, CDCl3)
Br
OH
N
Me
CO2Me
1.00
6.09
1.03
1.05
1.00
3.06
3.00
12.5 12.0 11.5 11.0 10.5 10.0 9.5 9.0 8.5 8.0 7.5 7.0 6.5 6.0 5.5 5.0 4.5 4.0 3.5 3.0 2.5 2.0 1.5 1.0 0.5 0.0
f1 (ppm)

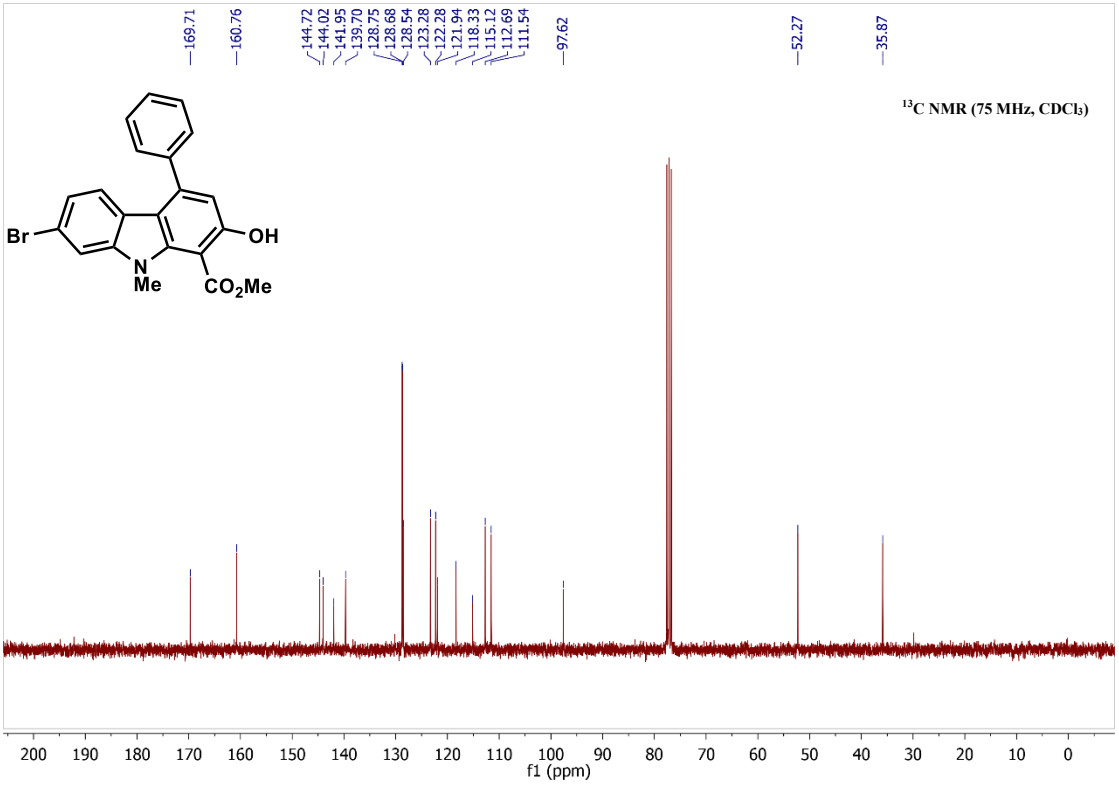
169.71
160.76
144.72
144.02
141.95
139.70
128.75
128.68
128.54
123.28
122.28
121.94
118.33
115.12
112.69
111.54
97.62
52.27
35.87
13C NMR (75 MHz, CDCl3)
Br
OH
N
Me
CO2Me
200 190 180 170 160 150 140 130 120 110 100 90 80 70 60 50 40 30 20 10 0
f1 (ppm)

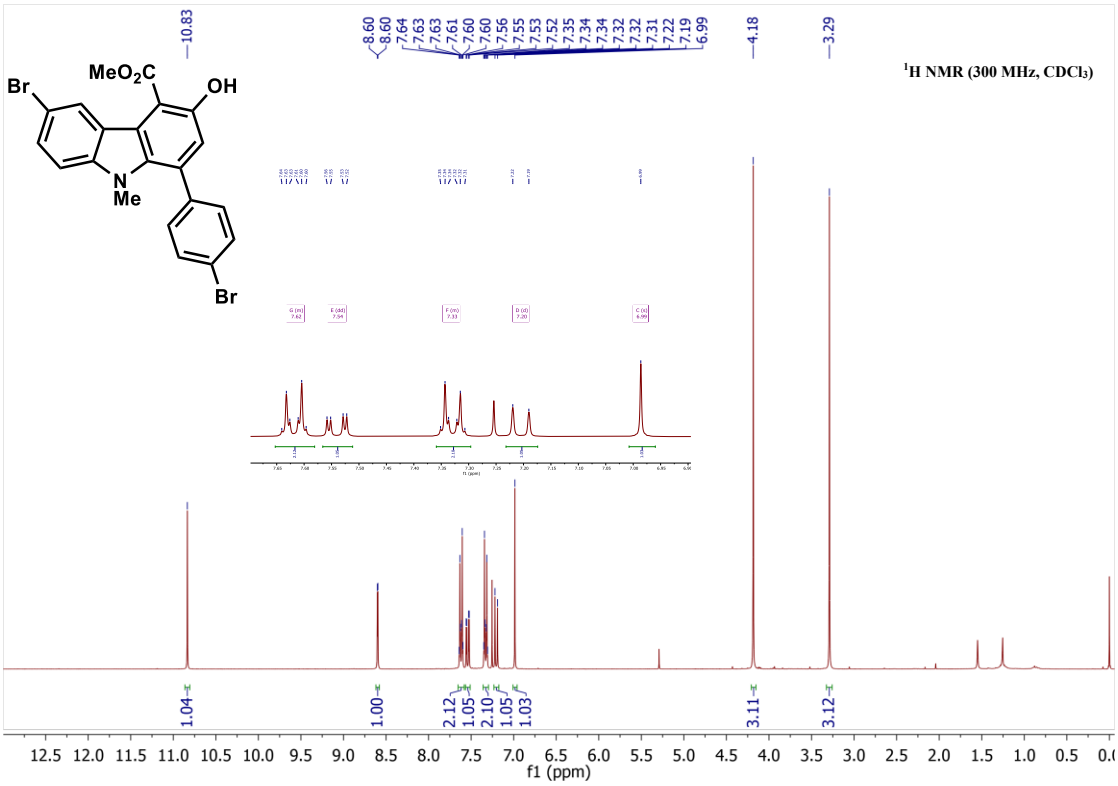
^{1}H NMR (300 MHz, CDCl$_3$)
MeO$_2$C
OH
Br
N
Me
Br
10.83
8.60
8.60
7.64
7.63
7.63
7.61
7.60
7.60
7.56
7.55
7.53
7.52
7.35
7.34
7.34
7.32
7.32
7.31
7.22
7.19
6.99
4.18
3.29
1.04
1.00
2.12
1.05
2.10
1.05
1.03
3.11
3.12
f1 (ppm)

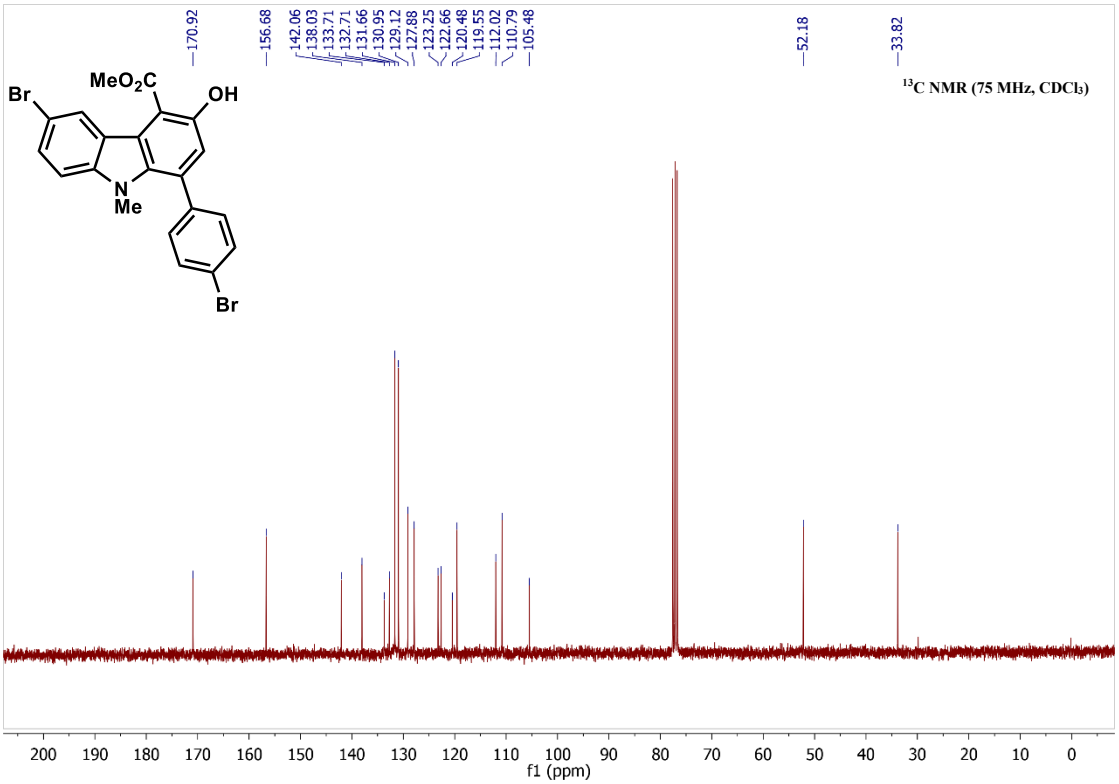
^{13}C NMR (75 MHz, CDCl$_3$)
MeO$_2$C
OH
Br
N
Me
Br
170.92
156.68
142.06
138.03
133.71
132.71
131.66
130.95
129.12
127.88
123.25
122.66
120.48
119.55
112.02
110.79
105.48
52.18
33.82
f1 (ppm)

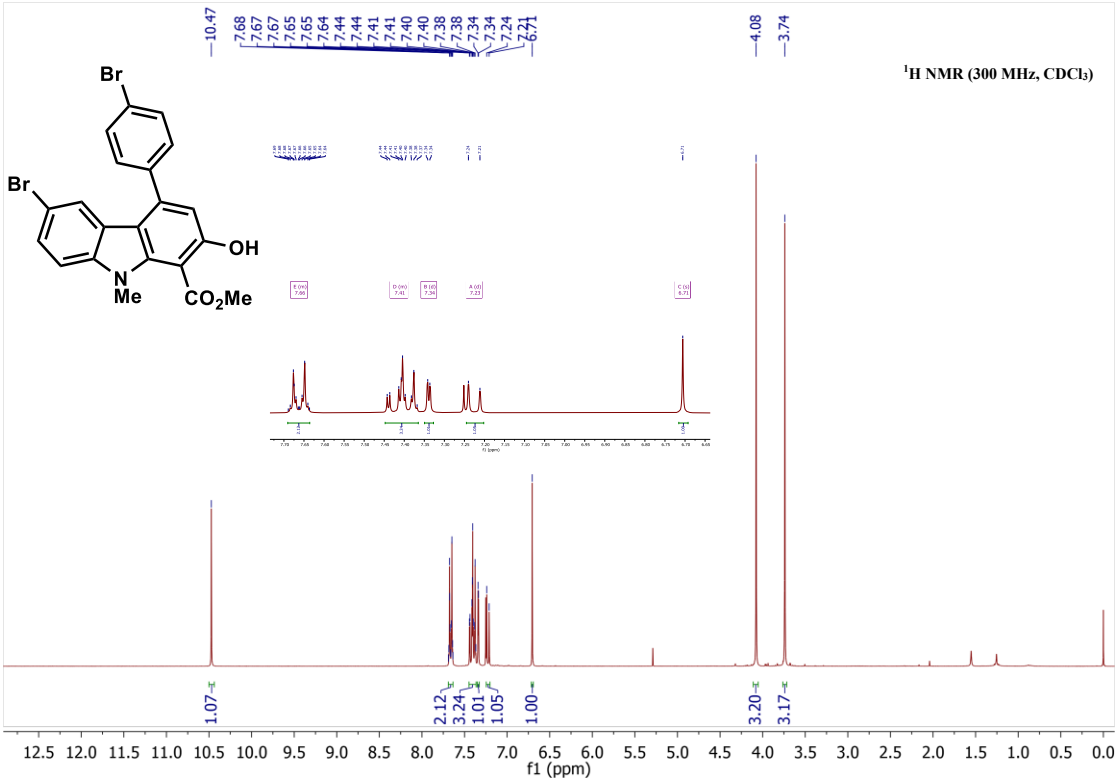
10.47
7.68
7.67
7.67
7.65
7.65
7.64
7.44
7.44
7.41
7.41
7.40
7.40
7.38
7.38
7.34
7.34
7.24
7.21
6.71
4.08
3.74
Br
Br
OH
N
Me
CO2Me
1H NMR (300 MHz, CDCl3)
1.07
2.12
3.24
1.01
1.05
1.00
3.20
3.17
12.5 12.0 11.5 11.0 10.5 10.0 9.5 9.0 8.5 8.0 7.5 7.0 6.5 6.0 5.5 5.0 4.5 4.0 3.5 3.0 2.5 2.0 1.5 1.0 0.5 0.0
f1 (ppm)

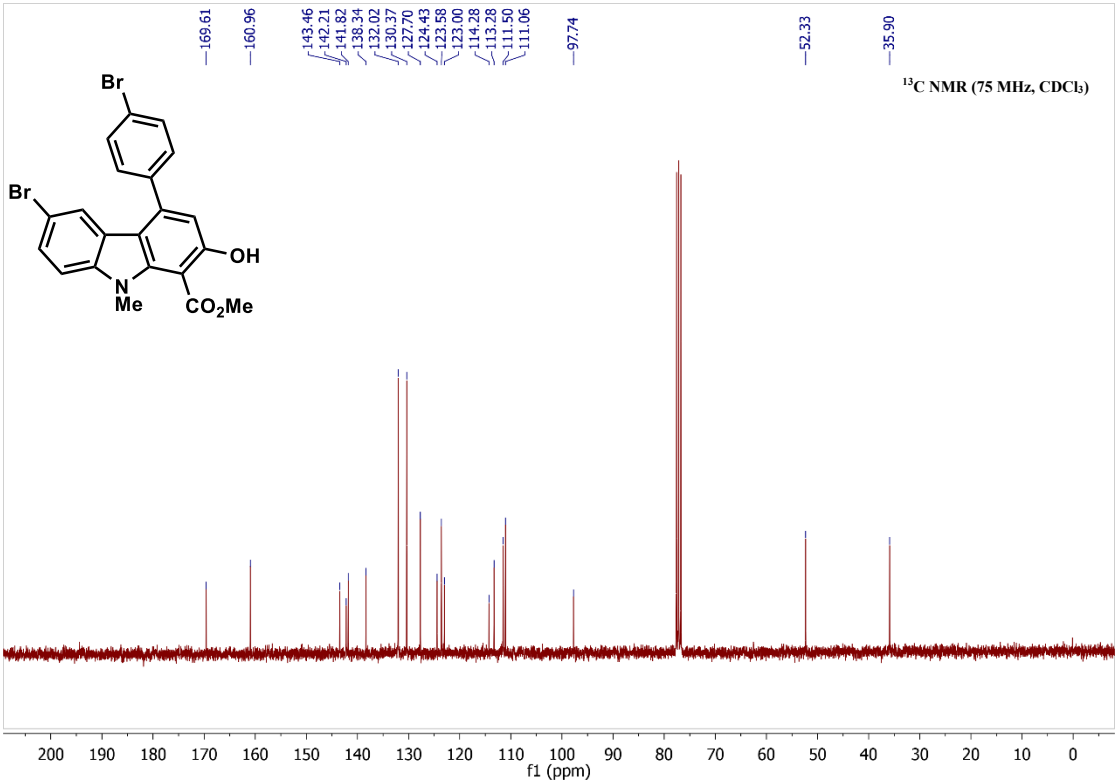
169.61
160.96
143.46
142.21
141.82
138.34
132.02
130.37
127.70
124.43
123.58
123.00
114.28
113.28
111.50
111.06
97.74
52.33
35.90
Br
Br
OH
N
Me
CO2Me
13C NMR (75 MHz, CDCl3)
200 190 180 170 160 150 140 130 120 110 100 90 80 70 60 50 40 30 20 10 0
f1 (ppm)

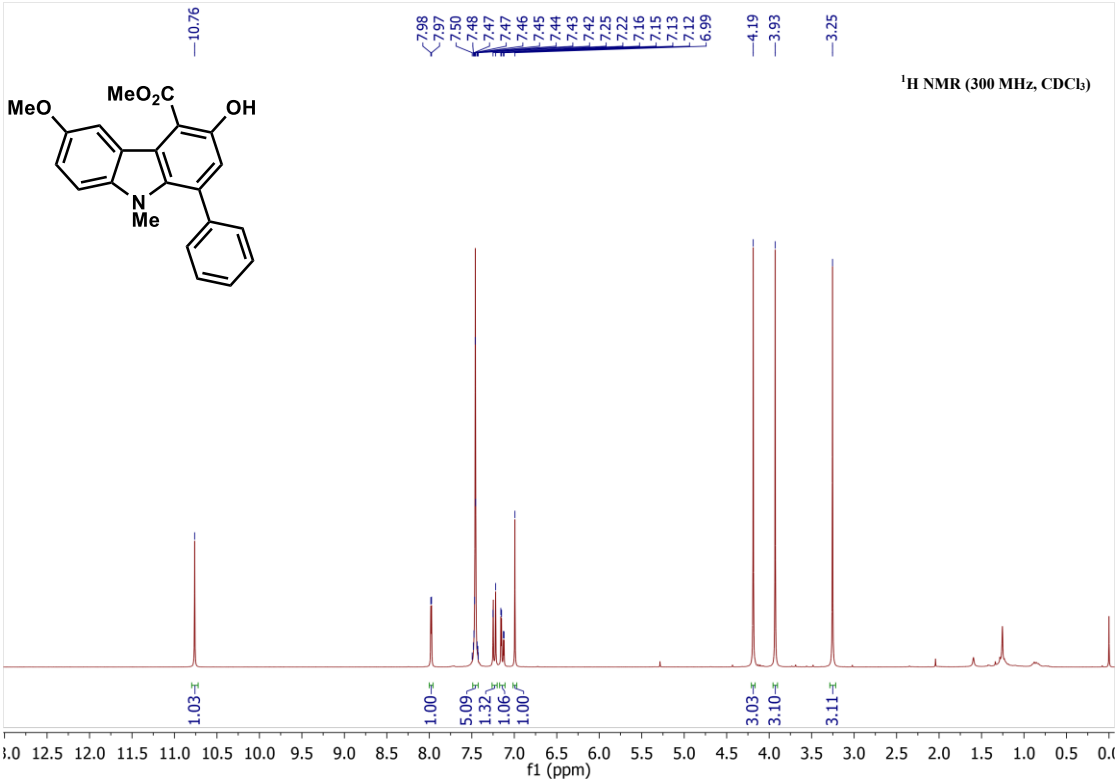
MeO
MeO2C
OH
N
Me
1H NMR (300 MHz, CDCl3)
10.76
7.98
7.97
7.50
7.48
7.47
7.47
7.46
7.45
7.44
7.43
7.42
7.25
7.22
7.16
7.15
7.13
7.12
6.99
4.19
3.93
3.25
1.03
1.00
5.09
1.32
1.06
1.00
3.03
3.10
3.11
f1 (ppm)

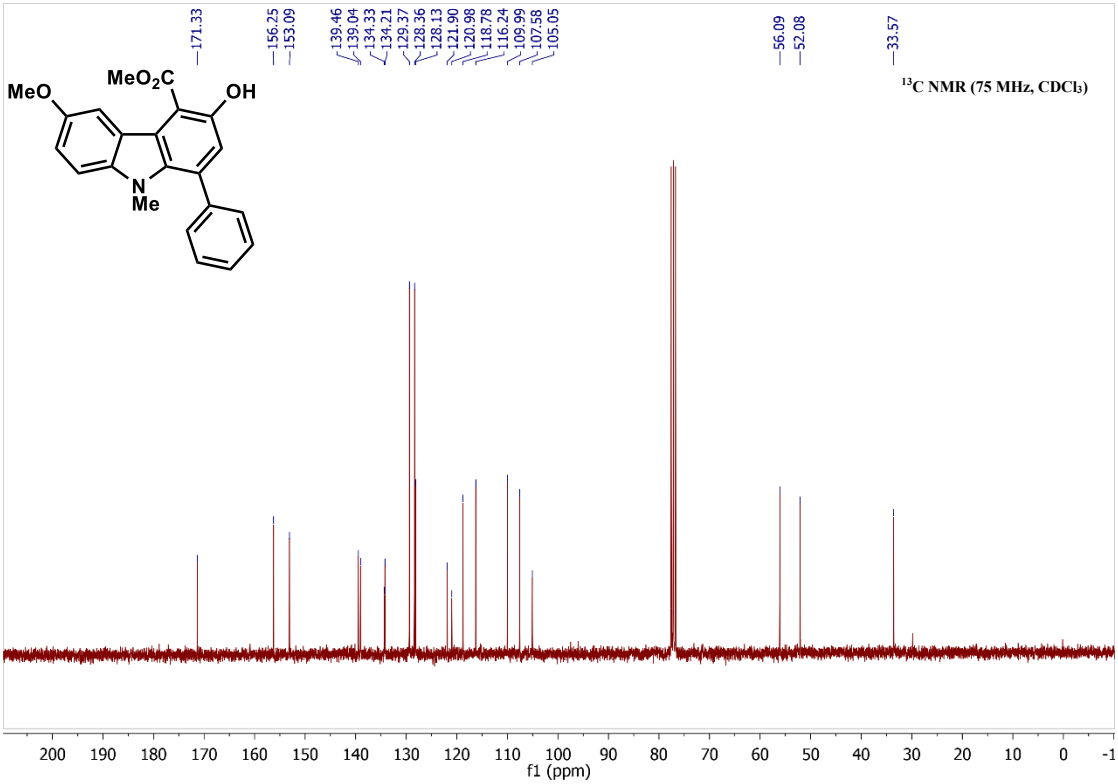
MeO
MeO2C
OH
N
Me
13C NMR (75 MHz, CDCl3)
171.33
156.25
153.09
139.46
139.04
134.33
134.21
129.37
128.36
128.13
121.90
120.98
118.78
116.24
109.99
107.58
105.05
56.09
52.08
33.57
f1 (ppm)

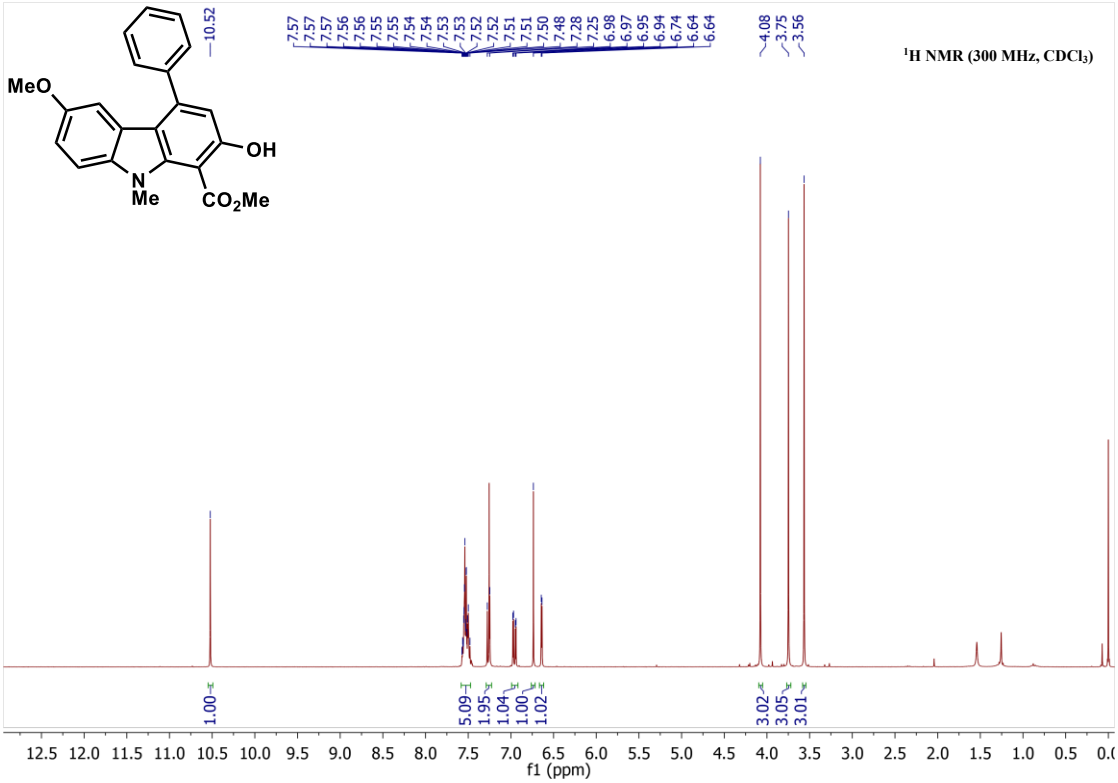
MeO
OH
N
Me
CO2Me
10.52
7.57
7.57
7.57
7.56
7.56
7.55
7.55
7.54
7.54
7.53
7.53
7.52
7.52
7.51
7.51
7.50
7.48
7.28
7.25
6.98
6.97
6.95
6.94
6.74
6.64
6.64
4.08
3.75
3.56
1H NMR (300 MHz, CDCl3)
1.00
5.09
1.95
1.04
1.00
1.02
3.02
3.05
3.01
f1 (ppm)

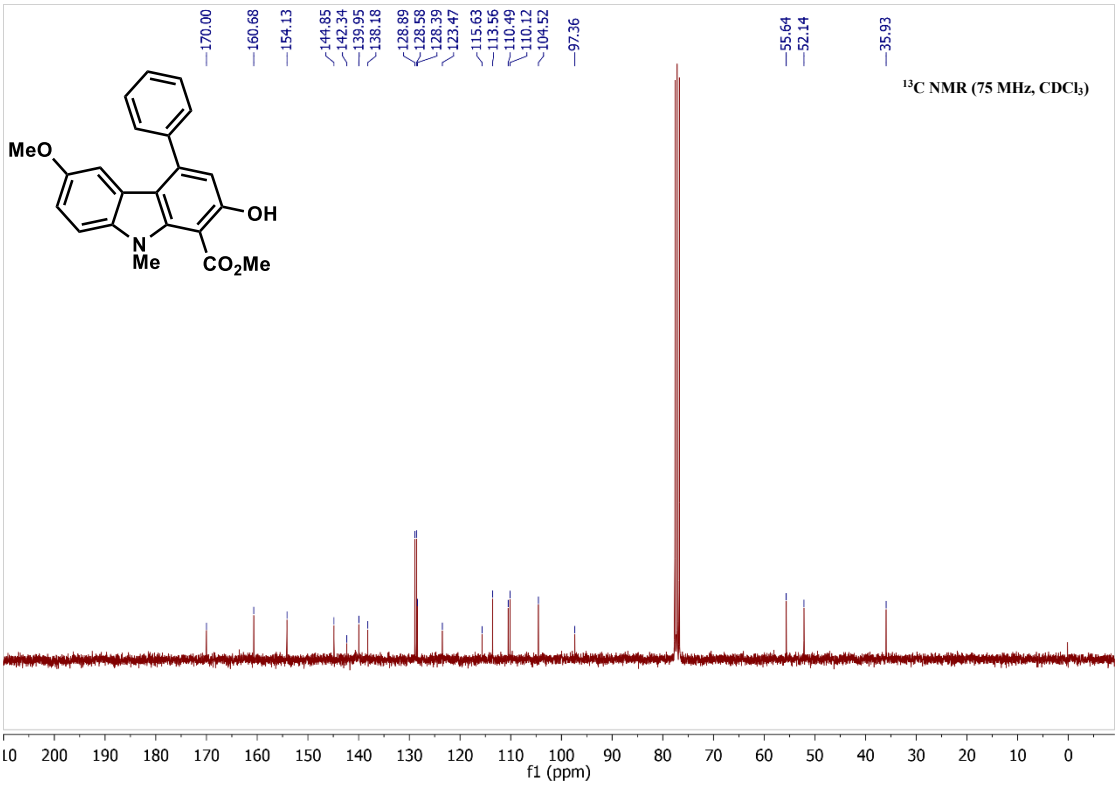
MeO
OH
N
Me
CO2Me
170.00
160.68
154.13
144.85
142.34
139.95
138.18
128.89
128.58
128.39
123.47
115.63
113.56
110.49
110.12
104.52
97.36
55.64
52.14
35.93
13C NMR (75 MHz, CDCl3)
f1 (ppm)

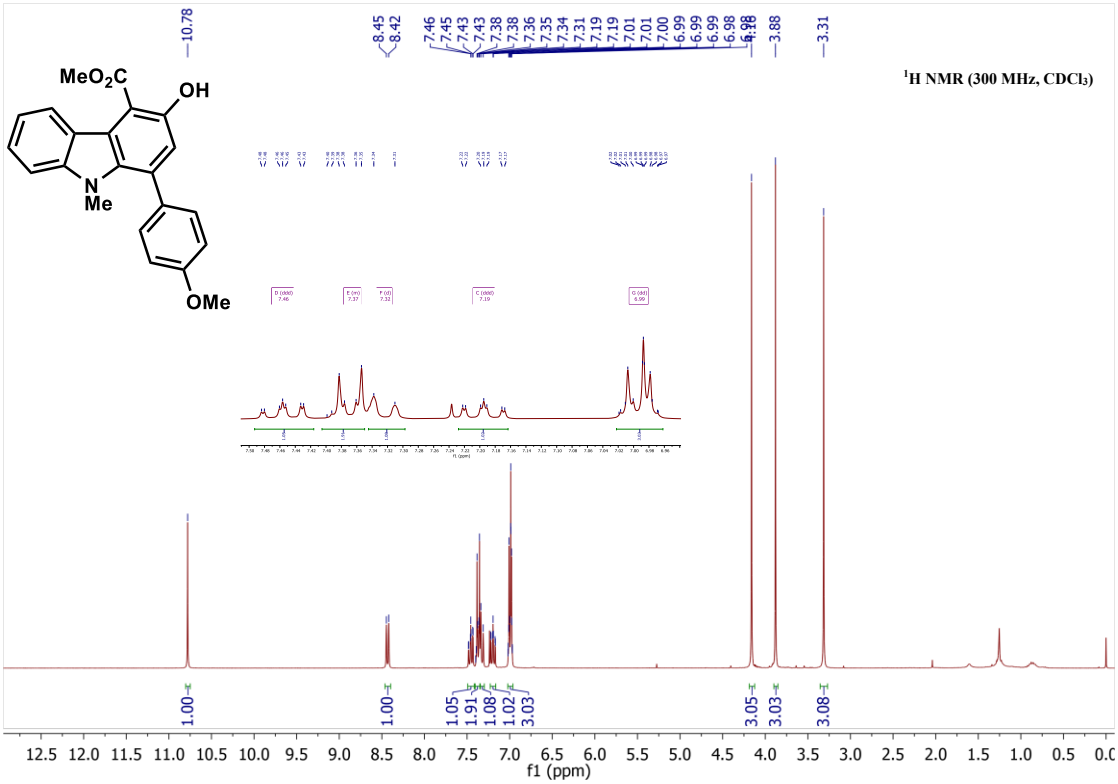
MeO2C
OH
N
Me
OMe
1H NMR (300 MHz, CDCl3)
10.78
8.45
8.42
7.46
7.45
7.43
7.43
7.38
7.38
7.36
7.35
7.34
7.31
7.19
7.19
7.01
7.01
7.00
6.99
6.99
6.98
6.98
3.88
3.31
1.00
1.00
1.05
1.91
1.08
1.02
3.03
3.05
3.03
3.08
f1 (ppm)

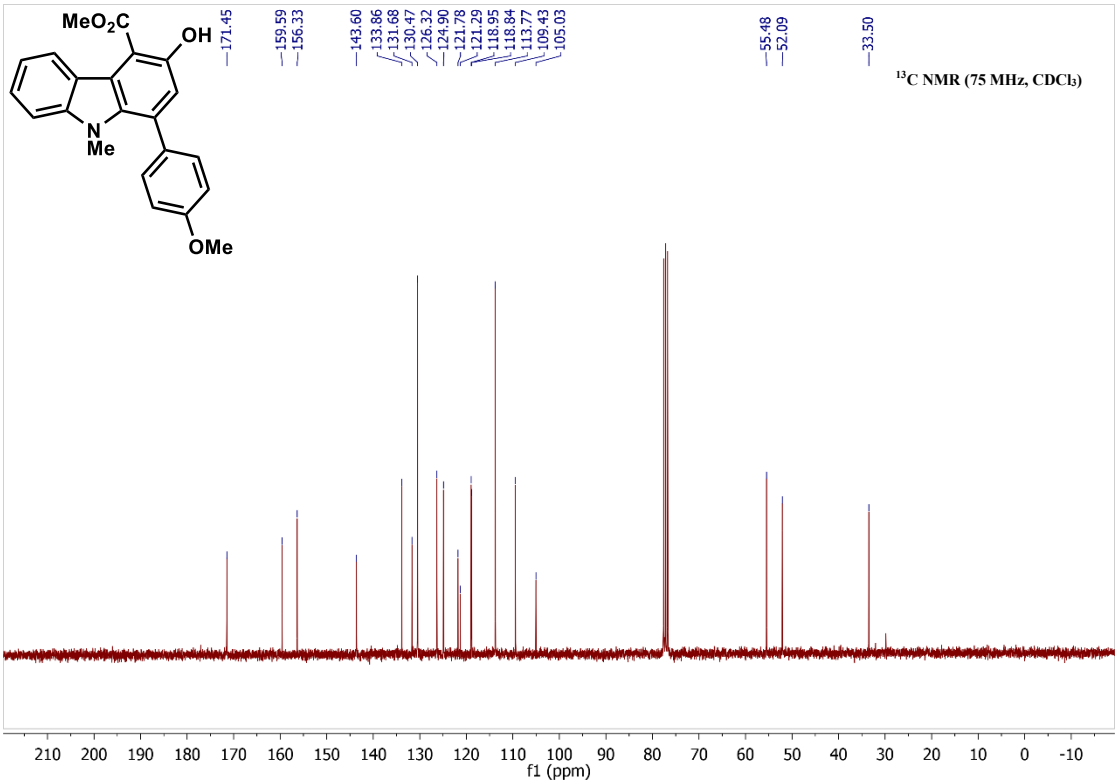
MeO2C
OH
N
Me
OMe
13C NMR (75 MHz, CDCl3)
171.45
159.59
156.33
143.60
133.86
131.68
130.47
126.32
124.90
121.78
121.29
118.95
118.84
113.77
109.43
105.03
55.48
52.09
33.50
f1 (ppm)

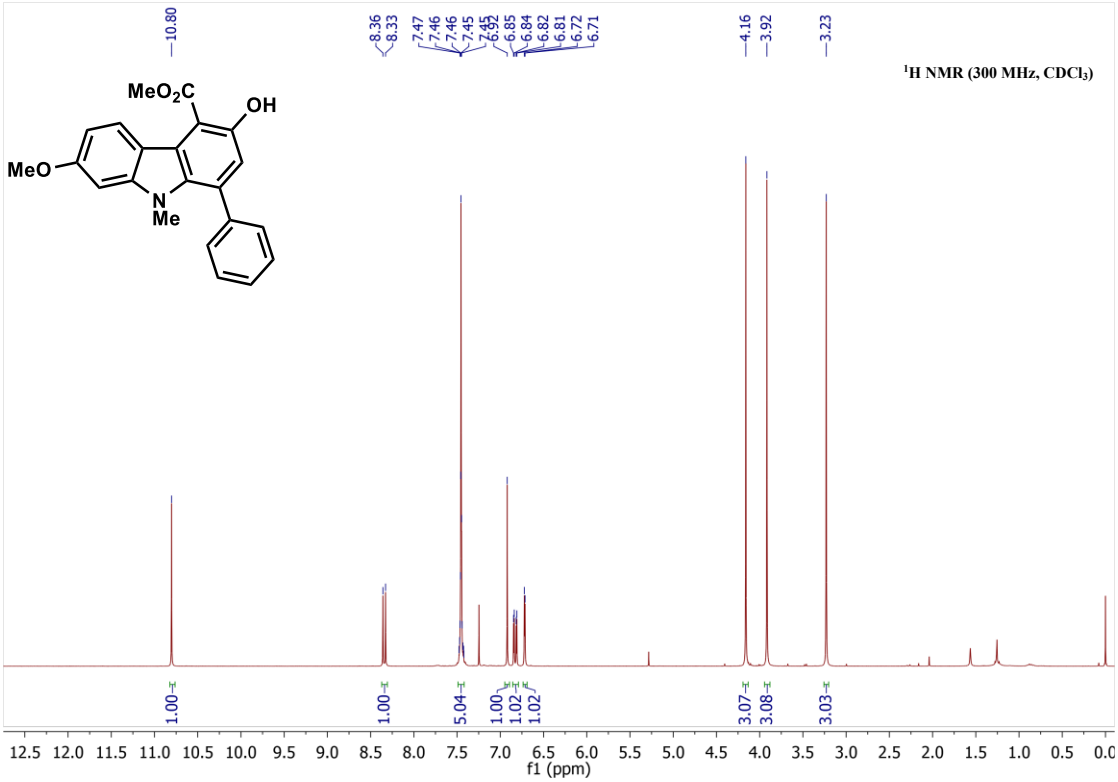
^{1}H NMR (300 MHz, CDCl$_3$)
MeO$_2$C
OH
MeO
N
Me
10.80
8.36
8.33
7.47
7.46
7.46
7.45
7.45
6.92
6.85
6.84
6.82
6.81
6.72
6.71
4.16
3.92
3.23
1.00
1.00
5.04
1.00
1.02
1.02
3.07
3.08
3.03
f1 (ppm)

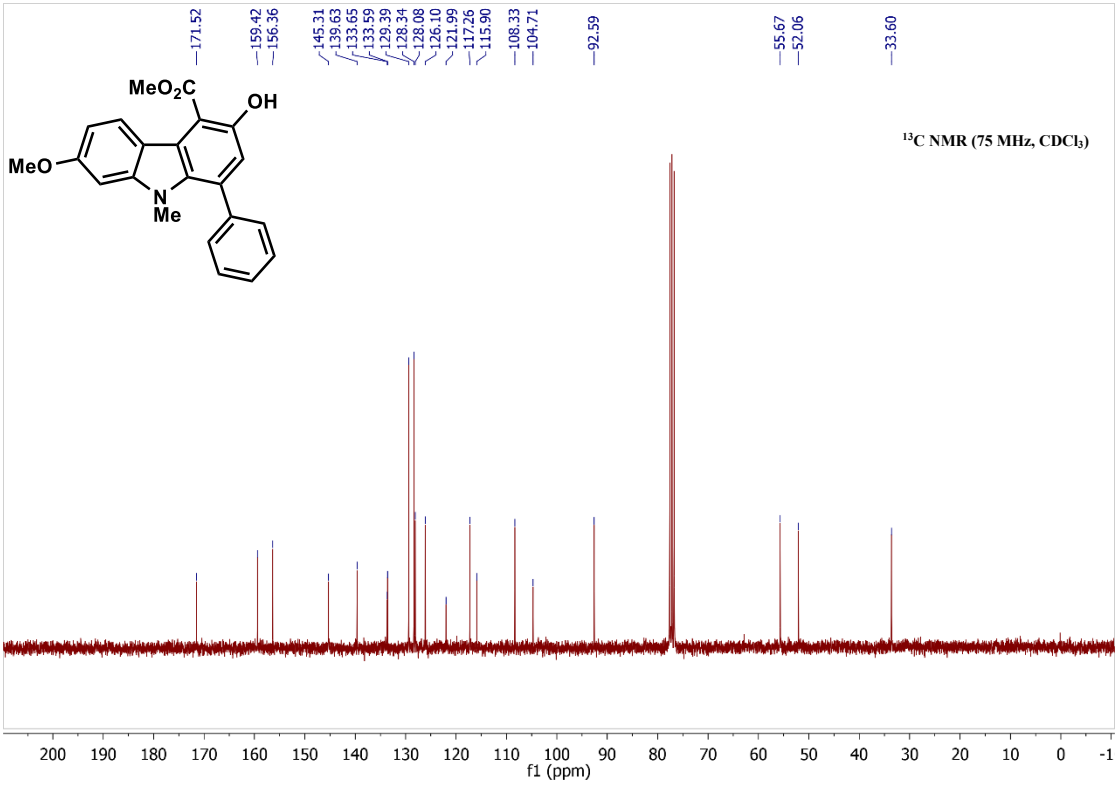
^{13}C NMR (75 MHz, CDCl$_3$)
MeO$_2$C
OH
MeO
N
Me
171.52
159.42
156.36
145.31
139.63
133.65
133.59
129.39
128.34
128.08
126.10
121.99
117.26
115.90
108.33
104.71
92.59
55.67
52.06
33.60
f1 (ppm)

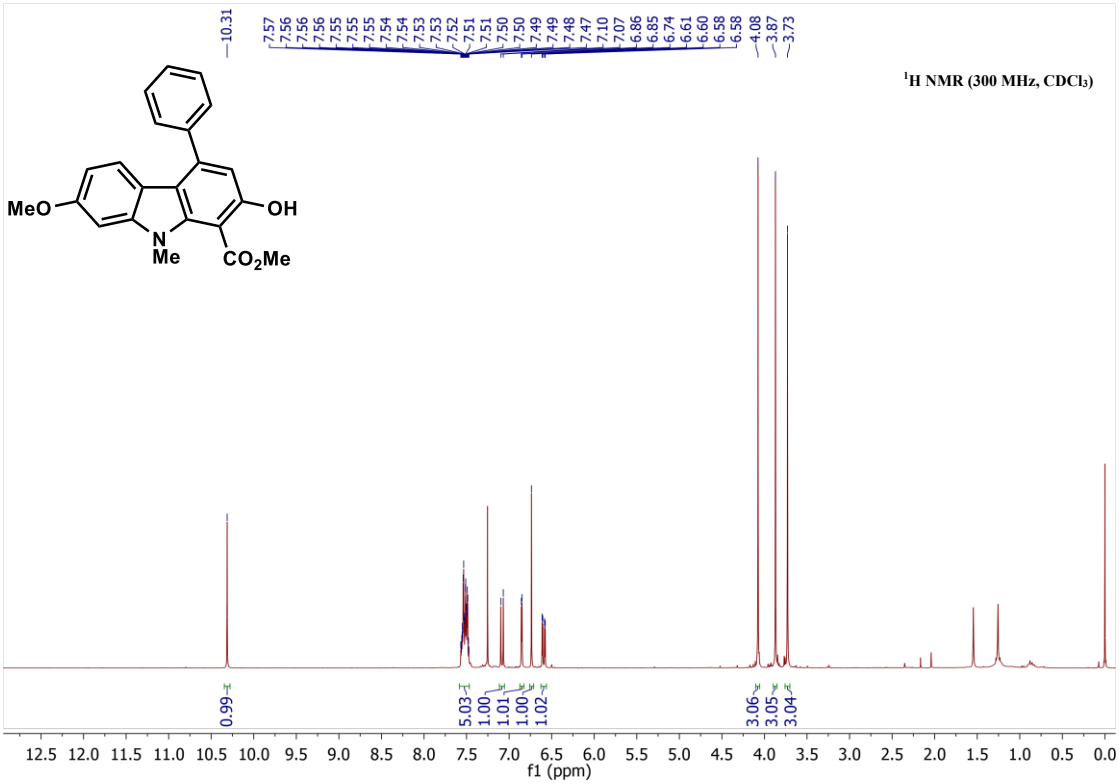
^{1}H NMR (300 MHz, CDCl$_3$)
MeO
OH
N
Me
CO$_2$Me
f1 (ppm)

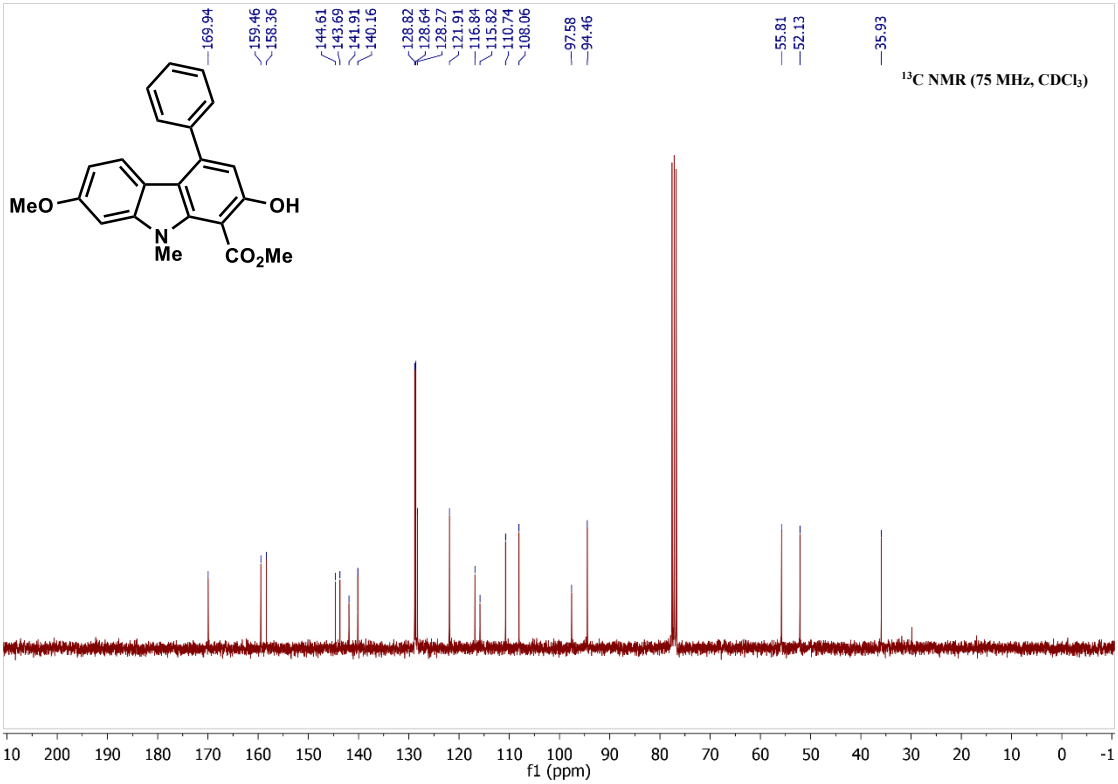
^{13}C NMR (75 MHz, CDCl$_3$)
MeO
OH
N
Me
CO$_2$Me
f1 (ppm)

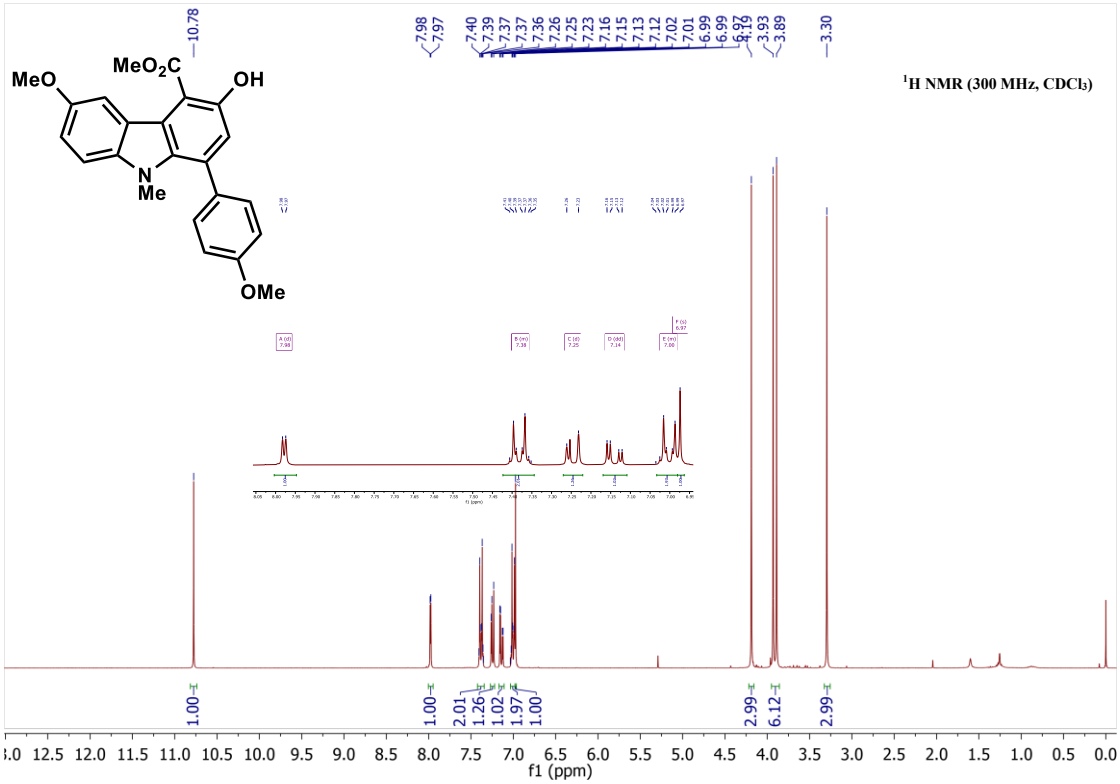
MeO
MeO2C
OH
N
Me
OMe
10.78
7.98
7.97
7.40
7.39
7.37
7.37
7.36
7.26
7.25
7.23
7.16
7.15
7.13
7.12
7.02
7.01
6.99
6.99
3.93
3.89
3.30
1H NMR (300 MHz, CDCl3)
1.00
1.00
2.01
1.26
1.02
1.97
1.00
2.99
6.12
2.99
f1 (ppm)

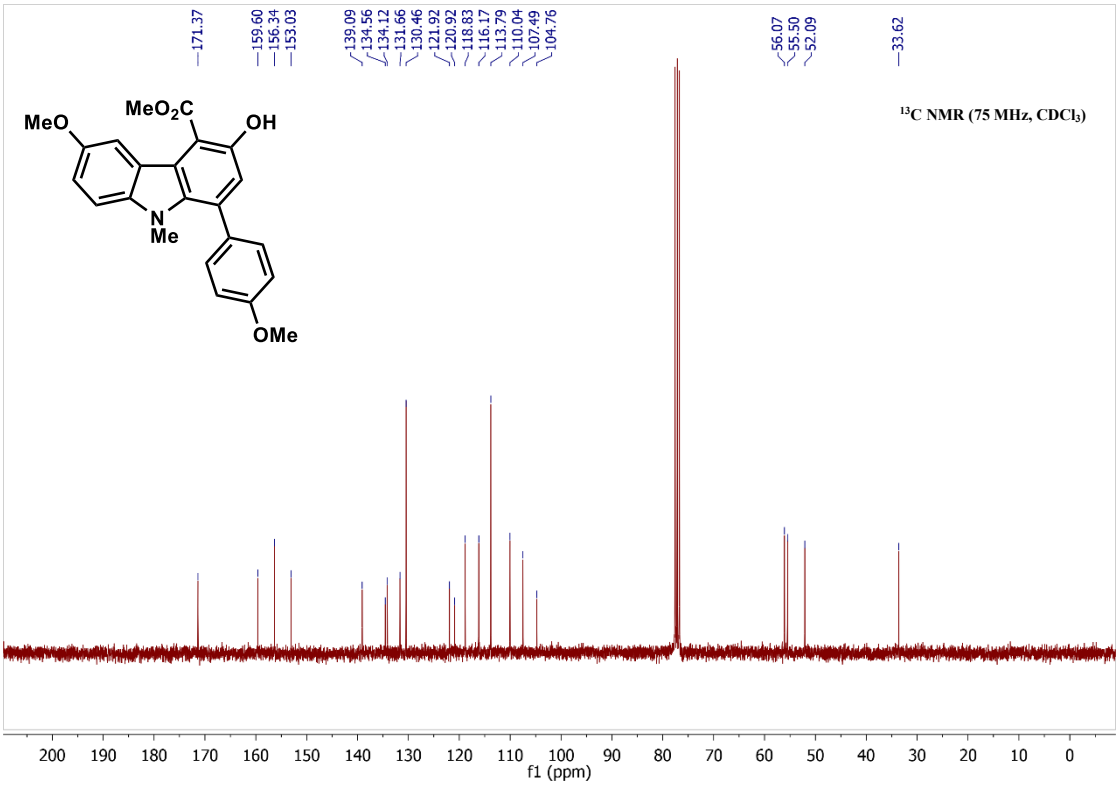
MeO
MeO2C
OH
N
Me
OMe
171.37
159.60
156.34
153.03
139.09
134.56
134.12
131.66
130.46
121.92
120.92
118.83
116.17
113.79
110.04
107.49
104.76
56.07
55.50
52.09
33.62
13C NMR (75 MHz, CDCl3)
f1 (ppm)

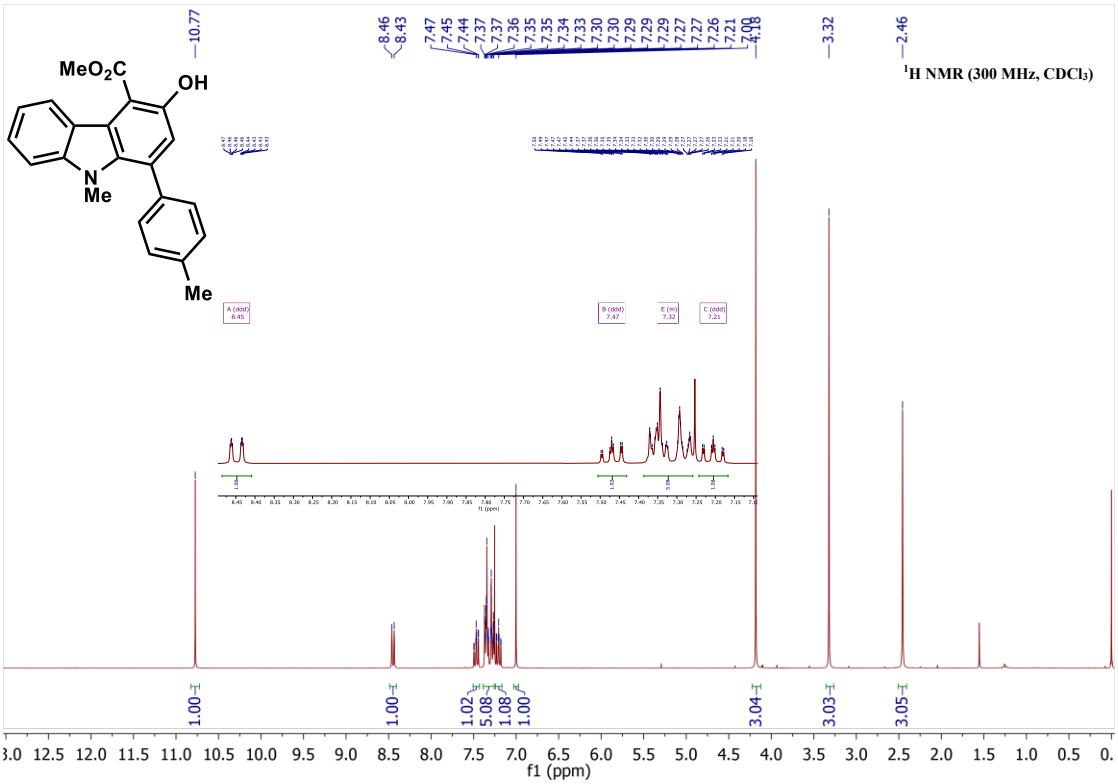
MeO2C
OH
N
Me
Me
10.77
8.46
8.43
7.47
7.45
7.44
7.37
7.37
7.36
7.35
7.35
7.34
7.33
7.30
7.30
7.29
7.29
7.29
7.27
7.27
7.26
7.21
7.00
4.18
3.32
2.46
1H NMR (300 MHz, CDCl3)
1.00
1.00
1.02
5.08
1.08
1.00
3.04
3.03
3.05
f1 (ppm)

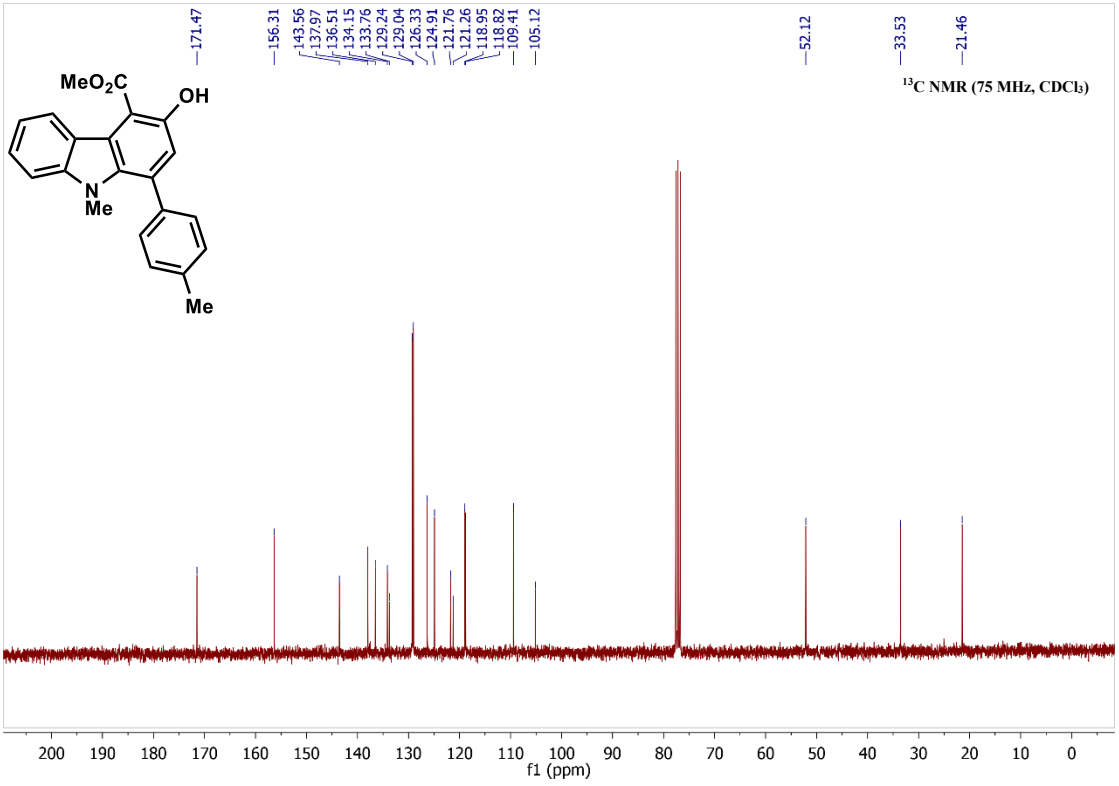
MeO2C
OH
N
Me
Me
171.47
156.31
143.56
137.97
136.51
134.15
133.76
129.24
129.04
126.33
124.91
121.76
121.26
118.95
118.82
109.41
105.12
52.12
33.53
21.46
13C NMR (75 MHz, CDCl3)
f1 (ppm)

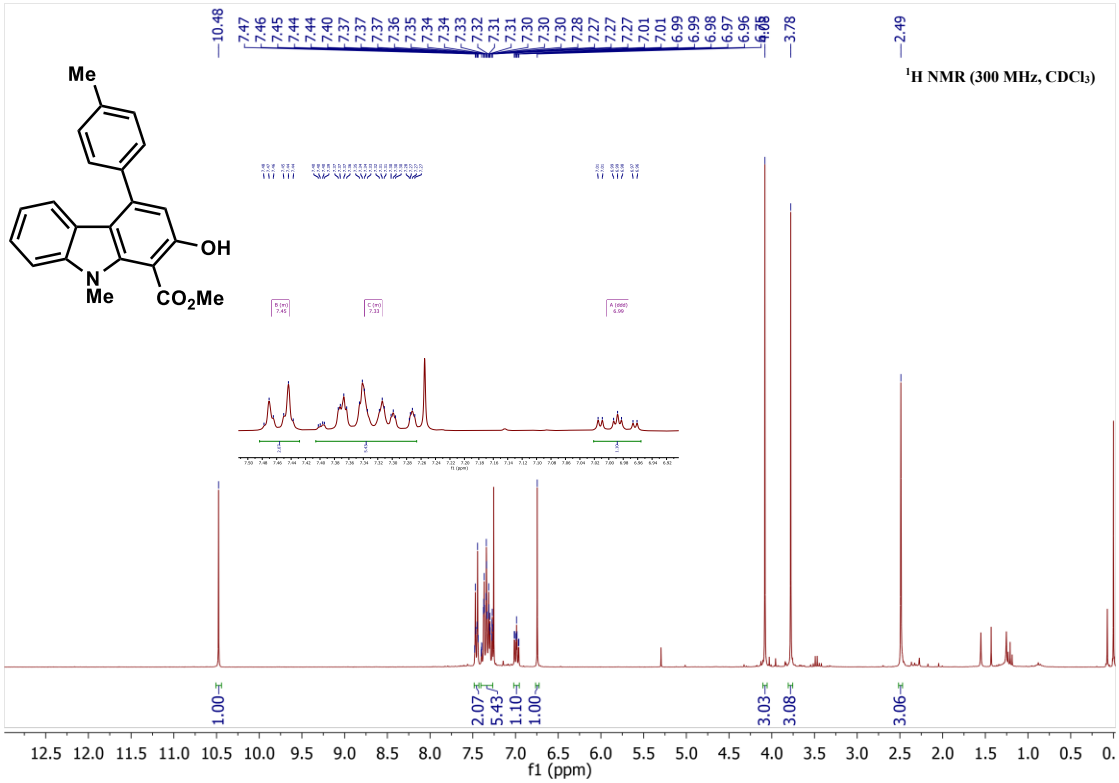
Me
OH
N
Me
CO2Me
10.48
7.47
7.46
7.45
7.44
7.40
7.37
7.37
7.37
7.36
7.35
7.34
7.34
7.33
7.32
7.31
7.31
7.30
7.30
7.30
7.28
7.27
7.27
7.27
7.01
7.01
6.99
6.99
6.98
6.97
6.96
3.78
2.49
1H NMR (300 MHz, CDCl3)
1.00
2.07
5.43
1.10
1.00
3.03
3.08
3.06
12.5 12.0 11.5 11.0 10.5 10.0 9.5 9.0 8.5 8.0 7.5 7.0 6.5 6.0 5.5 5.0 4.5 4.0 3.5 3.0 2.5 2.0 1.5 1.0 0.5 0.
f1 (ppm)

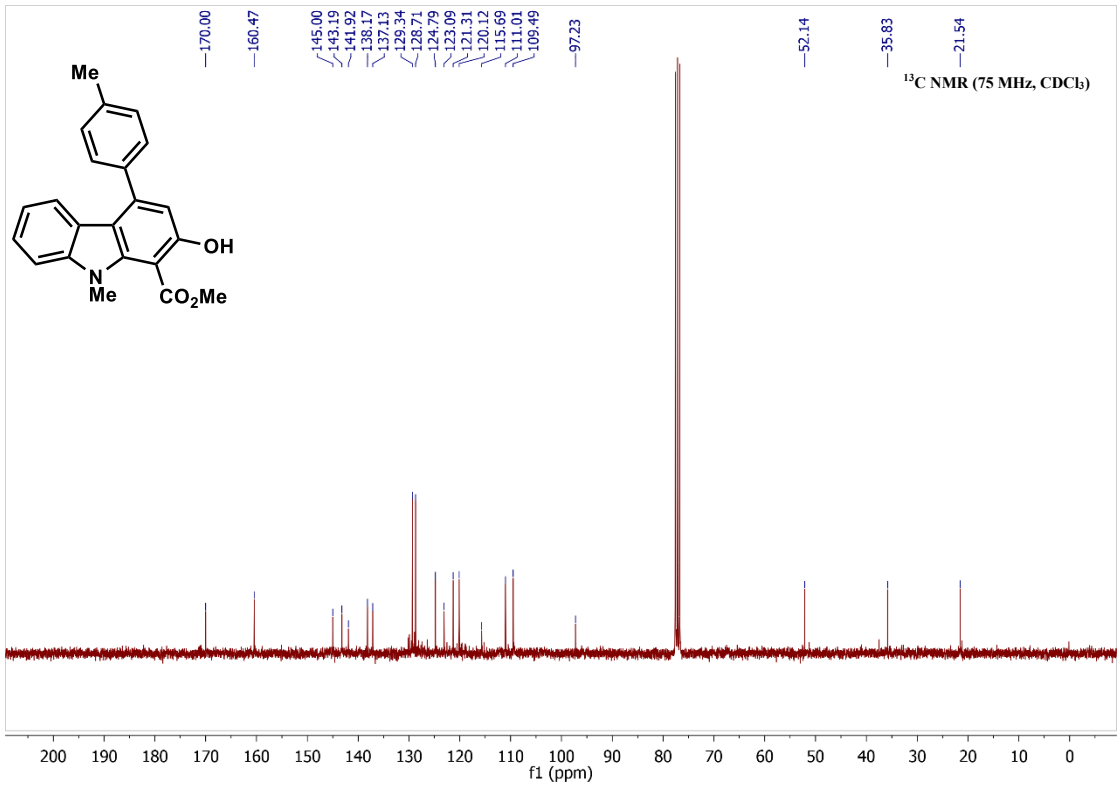
Me
OH
N
Me
CO2Me
170.00
160.47
145.00
143.19
141.92
138.17
137.13
129.34
128.71
124.79
123.09
121.31
120.12
115.69
111.01
109.49
97.23
52.14
35.83
21.54
13C NMR (75 MHz, CDCl3)
200 190 180 170 160 150 140 130 120 110 100 90 80 70 60 50 40 30 20 10 0
f1 (ppm)

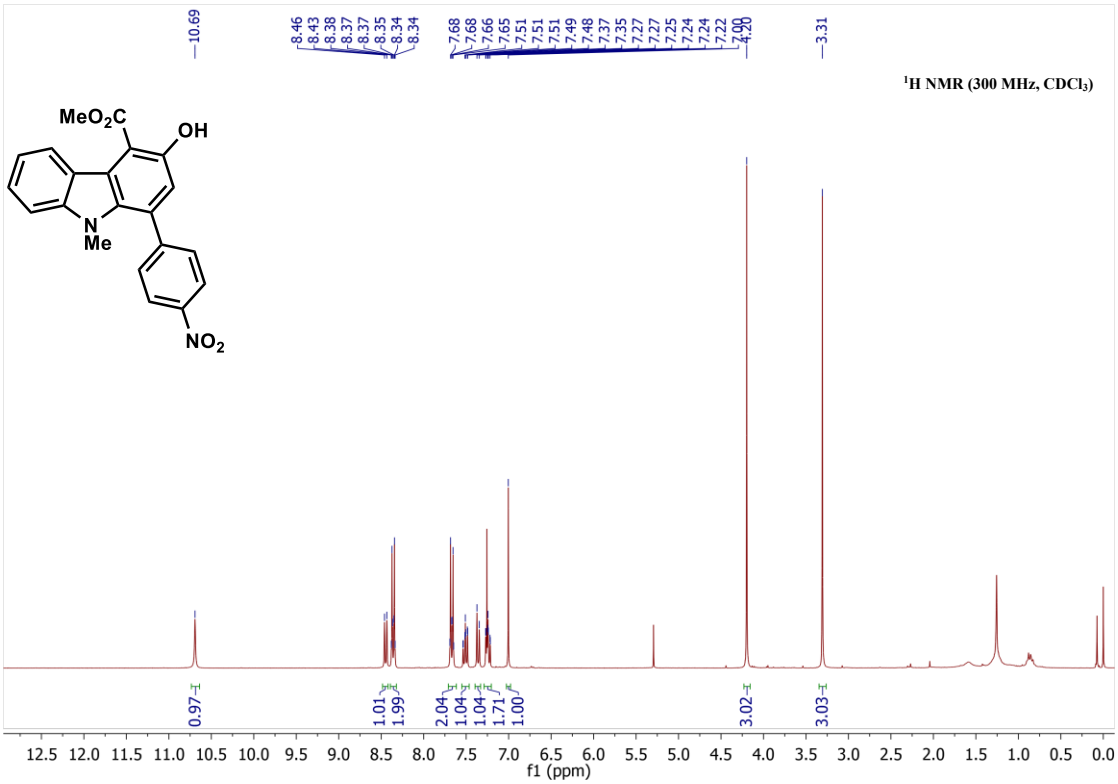
^{1}H NMR (300 MHz, CDCl$_3$)
MeO$_2$C
OH
N
Me
NO$_2$
10.69
8.46
8.43
8.38
8.37
8.37
8.35
8.34
8.34
7.68
7.68
7.66
7.65
7.51
7.51
7.51
7.49
7.48
7.37
7.35
7.27
7.27
7.25
7.24
7.24
7.22
7.00
4.20
3.31
0.97
1.01
1.99
2.04
1.04
1.04
1.71
1.00
3.02
3.03
f1 (ppm)

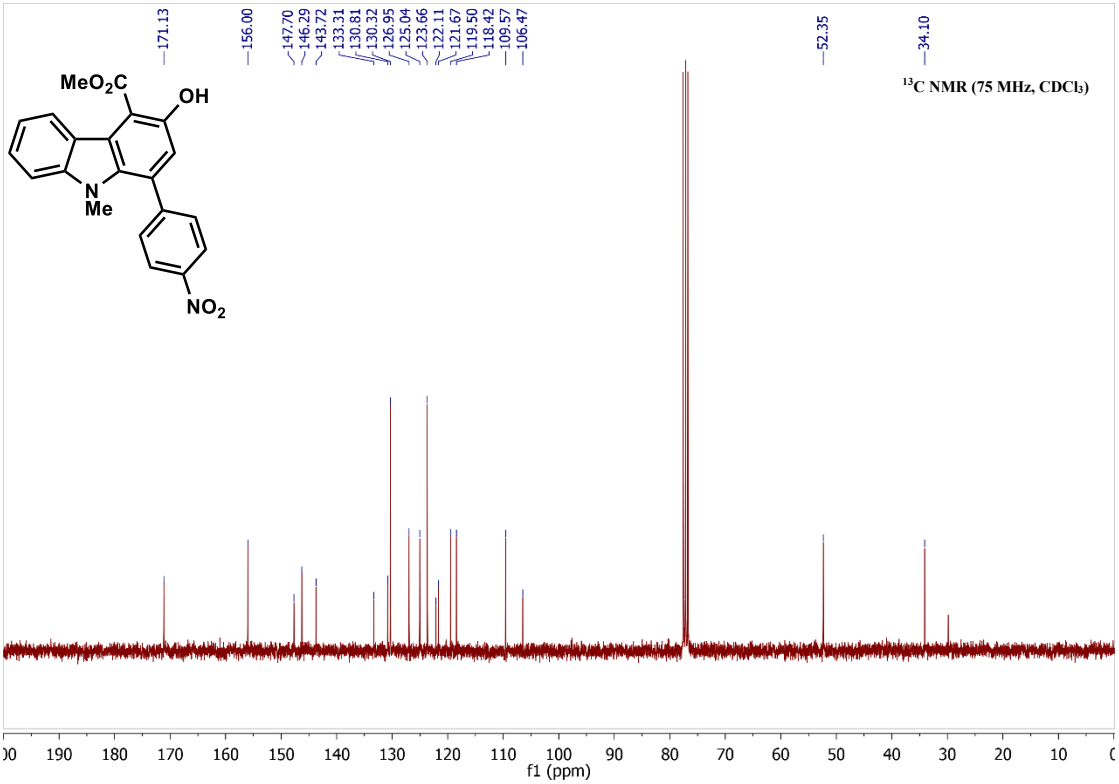
^{13}C NMR (75 MHz, CDCl$_3$)
MeO$_2$C
OH
N
Me
NO$_2$
171.13
156.00
147.70
146.29
143.72
133.31
130.81
130.32
126.95
125.04
123.66
122.11
121.67
119.50
118.42
109.57
106.47
52.35
34.10
f1 (ppm)

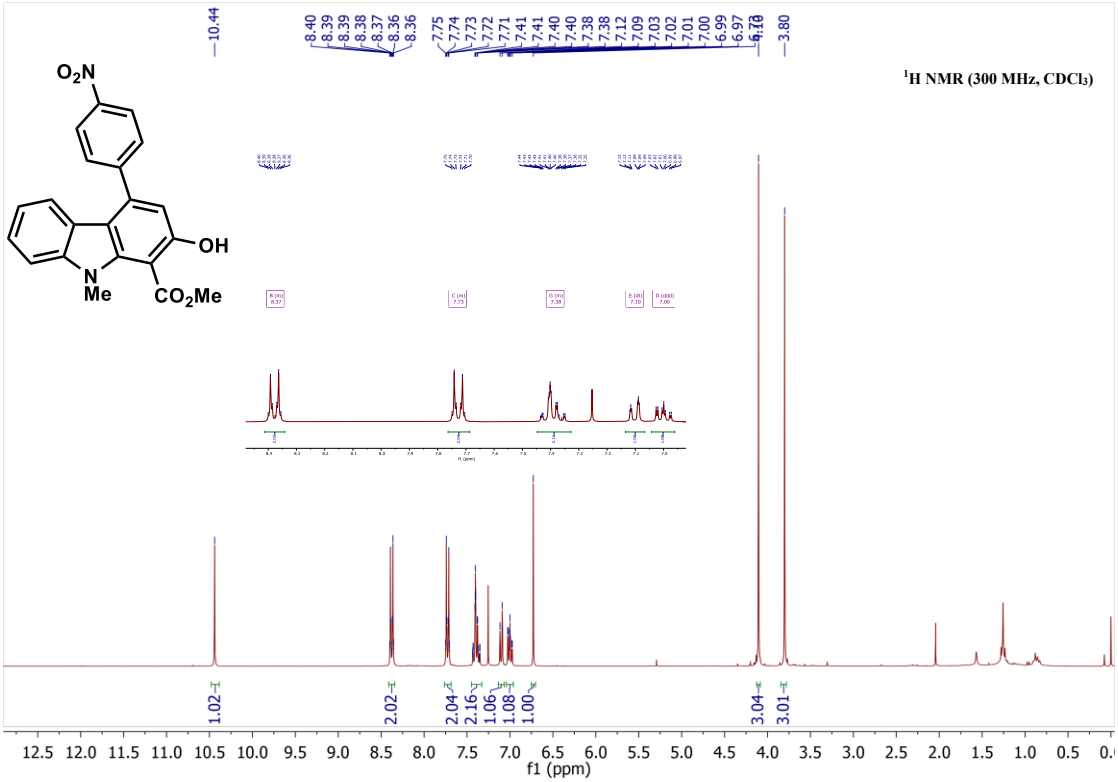
^{1}H NMR (300 MHz, CDCl$_3$)
O2N
OH
N
Me
CO2Me
10.44
8.40 8.39 8.39 8.38 8.37 8.36 8.36
7.75 7.74 7.73 7.72 7.71 7.41 7.41 7.40 7.40 7.38 7.38 7.12 7.09 7.03 7.02 7.01 7.00 6.99 6.97
3.80
1.02 2.02 2.04 2.16 1.06 1.08 1.00 3.04 3.01
f1 (ppm)

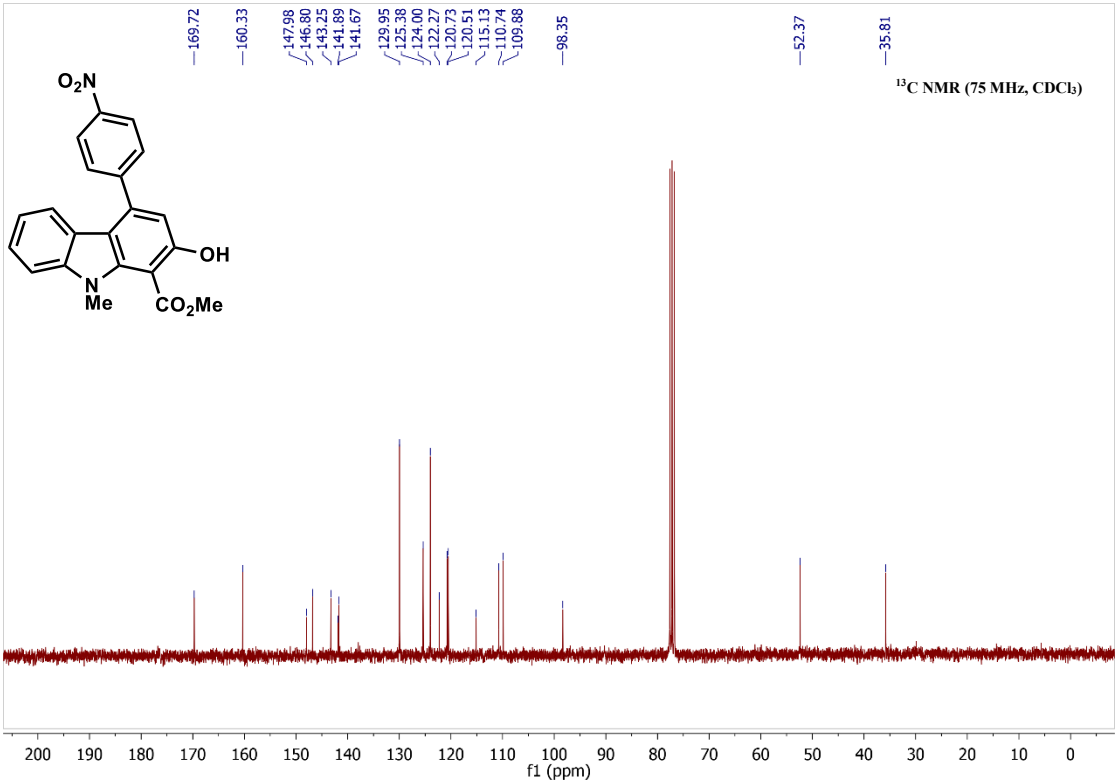
^{13}C NMR (75 MHz, CDCl$_3$)
O2N
OH
N
Me
CO2Me
169.72 160.33 147.98 146.80 143.25 141.89 141.67 129.95 125.38 124.00 122.27 120.73 120.51 115.13 110.74 109.88 98.35 52.37 35.81
f1 (ppm)

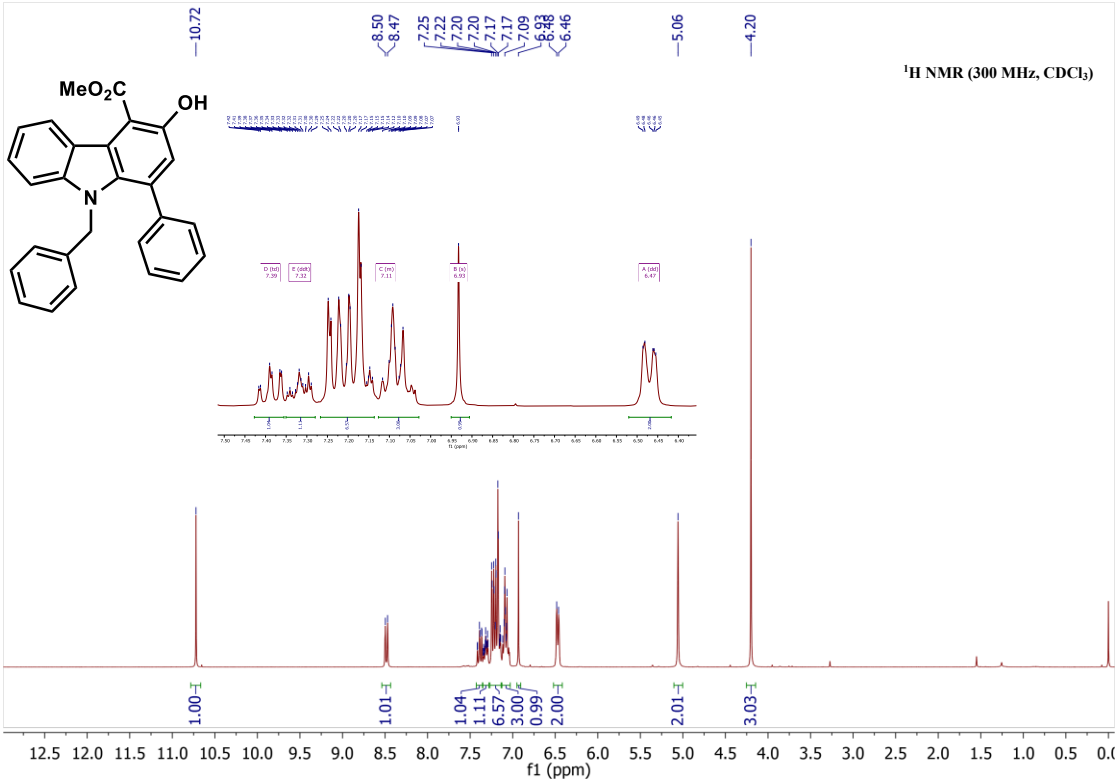
^{1}H NMR (300 MHz, CDCl$_3$)
MeO2C
OH
N
10.72
8.50
8.47
7.25
7.22
7.20
7.20
7.17
7.17
7.09
6.93
6.48
6.46
5.06
4.20
1.00
1.01
1.04
1.11
6.57
3.00
0.99
2.00
2.01
3.03
f1 (ppm)

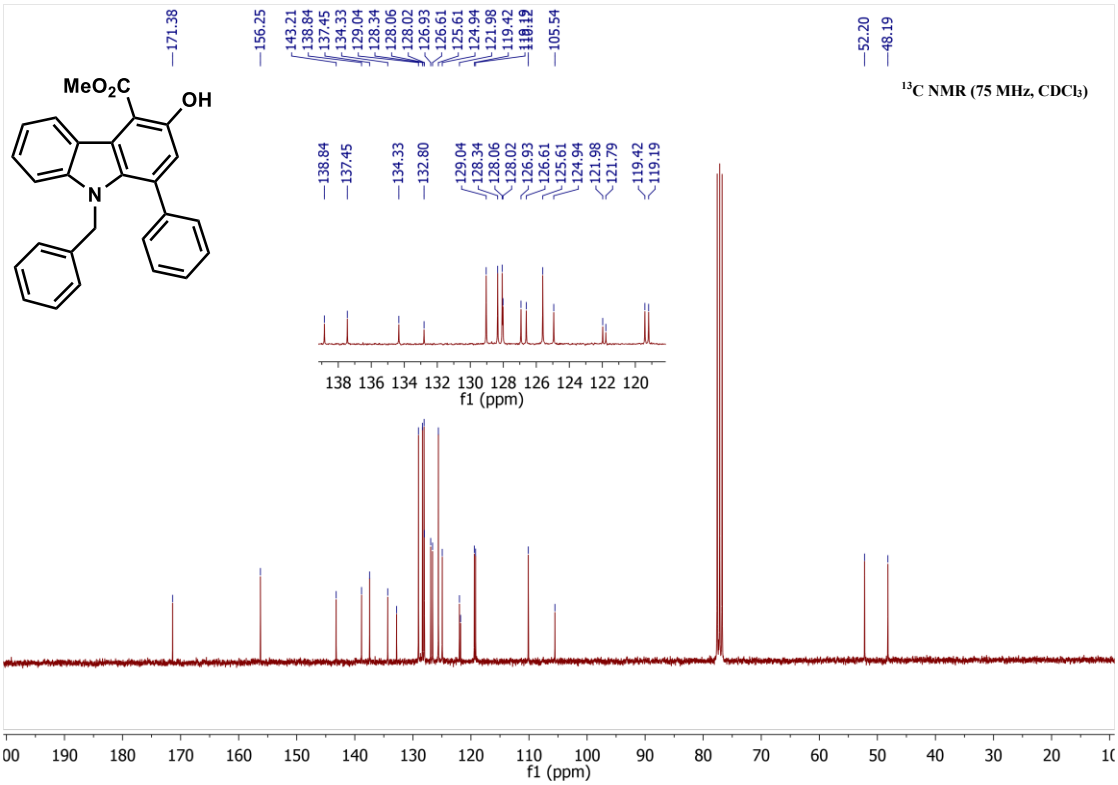
^{13}C NMR (75 MHz, CDCl$_3$)
MeO2C
OH
N
171.38
156.25
143.21
138.84
137.45
134.33
129.04
128.34
128.06
128.02
126.93
126.61
125.61
124.94
121.98
119.42
105.54
52.20
48.19
f1 (ppm)

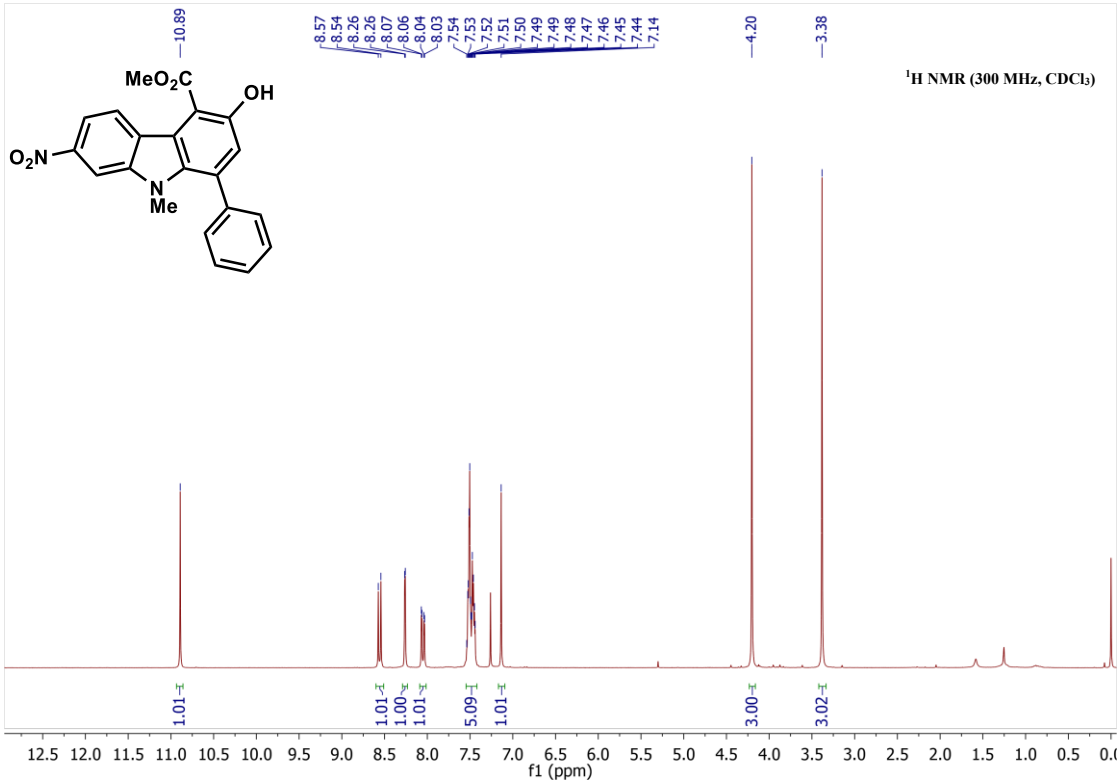
^{1}H NMR (300 MHz, CDCl$_3$)
MeO$_2$C
OH
O$_2$N
N
Me
10.89
8.57
8.54
8.26
8.26
8.07
8.06
8.04
8.03
7.54
7.53
7.52
7.51
7.50
7.49
7.49
7.48
7.47
7.46
7.45
7.44
7.14
4.20
3.38
1.01
1.01
1.00
1.01
5.09
1.01
3.00
3.02
f1 (ppm)

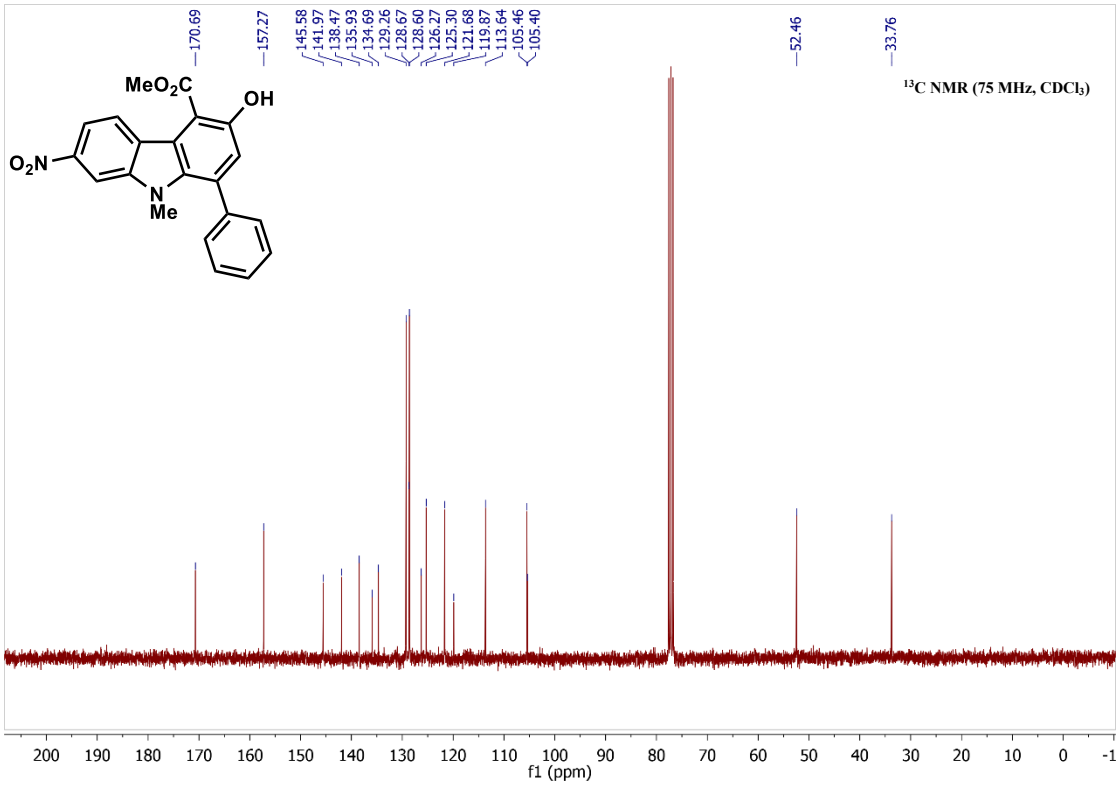
^{13}C NMR (75 MHz, CDCl$_3$)
MeO$_2$C
OH
O$_2$N
N
Me
170.69
157.27
145.58
141.97
138.47
135.93
134.69
129.26
128.67
128.60
126.27
125.30
121.68
119.87
113.64
105.46
105.40
52.46
33.76
f1 (ppm)

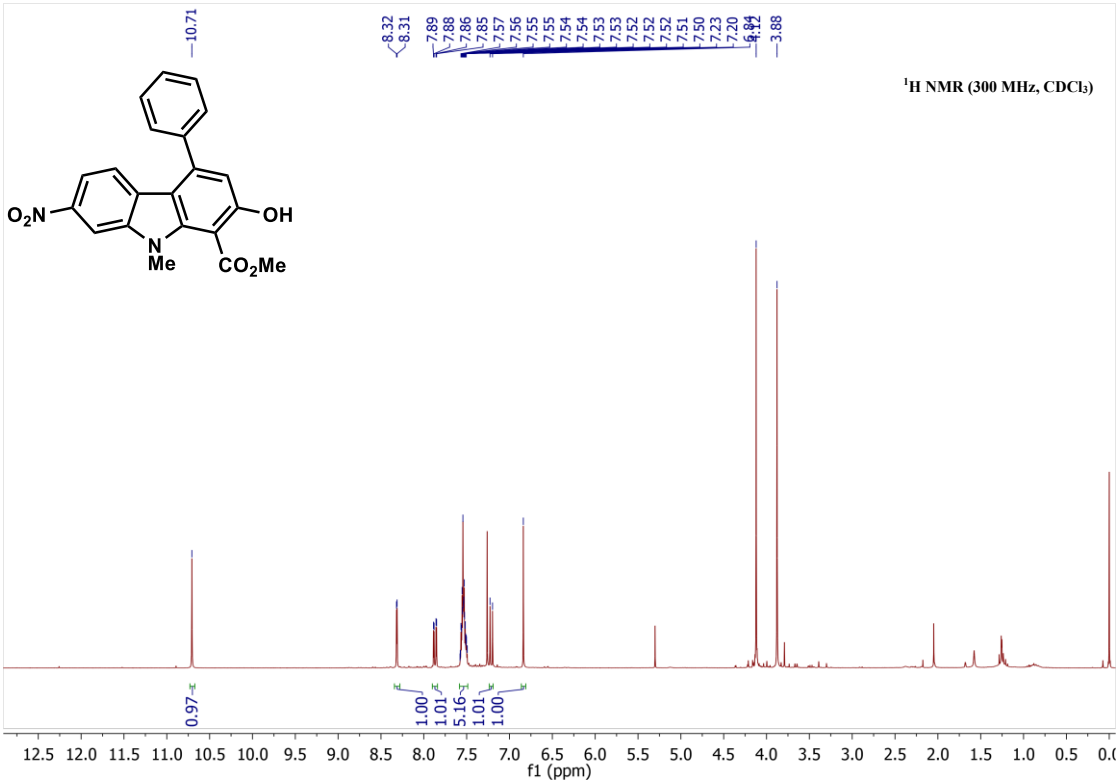
^{1}H NMR (300 MHz, CDCl$_3$)
10.71
8.32
8.31
7.89
7.88
7.86
7.85
7.57
7.56
7.55
7.55
7.54
7.54
7.53
7.53
7.52
7.52
7.52
7.51
7.50
7.23
7.20
6.84
6.82
3.88
O2N
OH
N
Me
CO2Me
0.97
1.00
1.01
5.16
1.01
1.00
f1 (ppm)

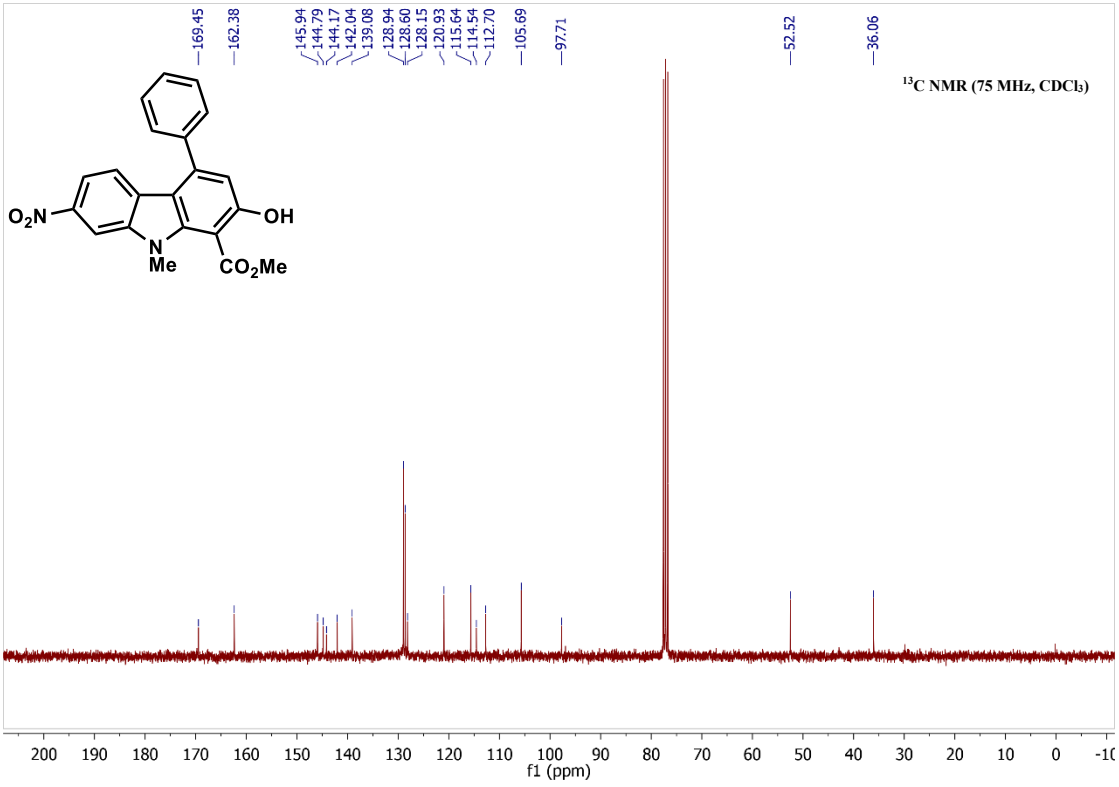
^{13}C NMR (75 MHz, CDCl$_3$)
169.45
162.38
145.94
144.79
144.17
142.04
139.08
128.94
128.60
128.15
120.93
115.64
114.54
112.70
105.69
97.71
52.52
36.06
O2N
OH
N
Me
CO2Me
f1 (ppm)

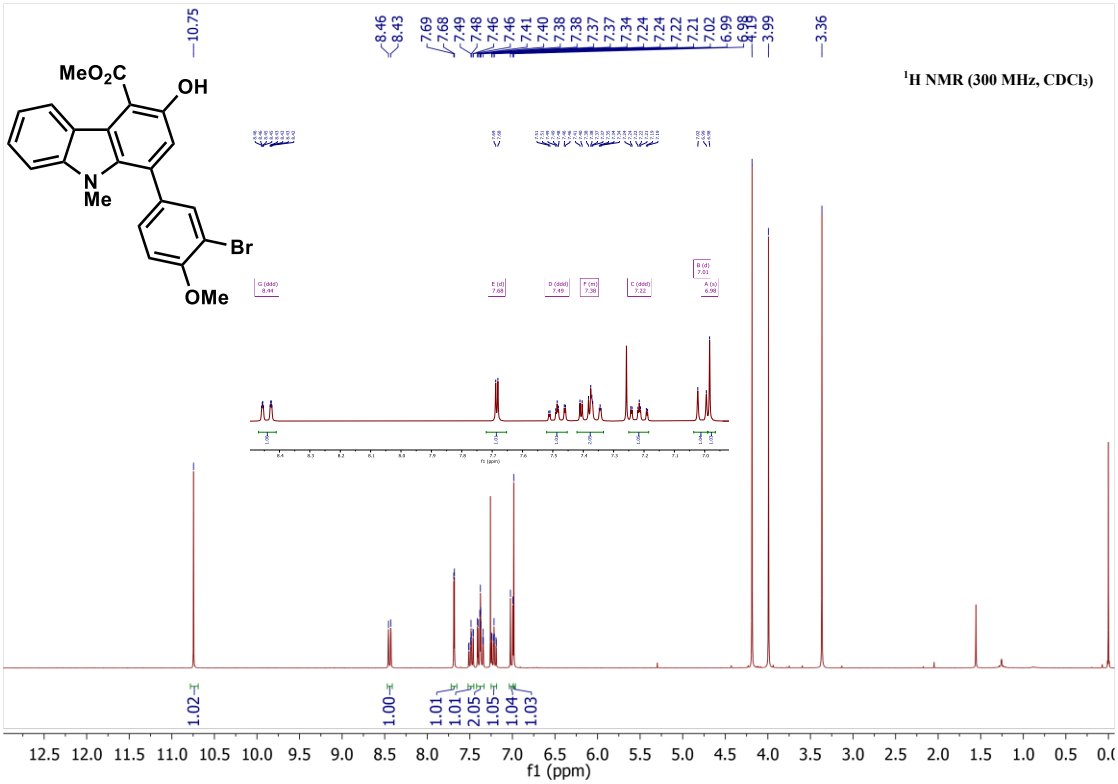
^{1}H NMR (300 MHz, CDCl$_3$)
MeO$_2$C
OH
N
Me
Br
OMe
10.75
8.46
8.43
7.69
7.68
7.49
7.48
7.46
7.46
7.41
7.40
7.38
7.38
7.37
7.37
7.34
7.24
7.24
7.22
7.21
7.02
6.99
6.98
4.19
3.99
3.36
1.02
1.00
1.01
1.01
2.05
1.05
1.04
1.03
f1 (ppm)

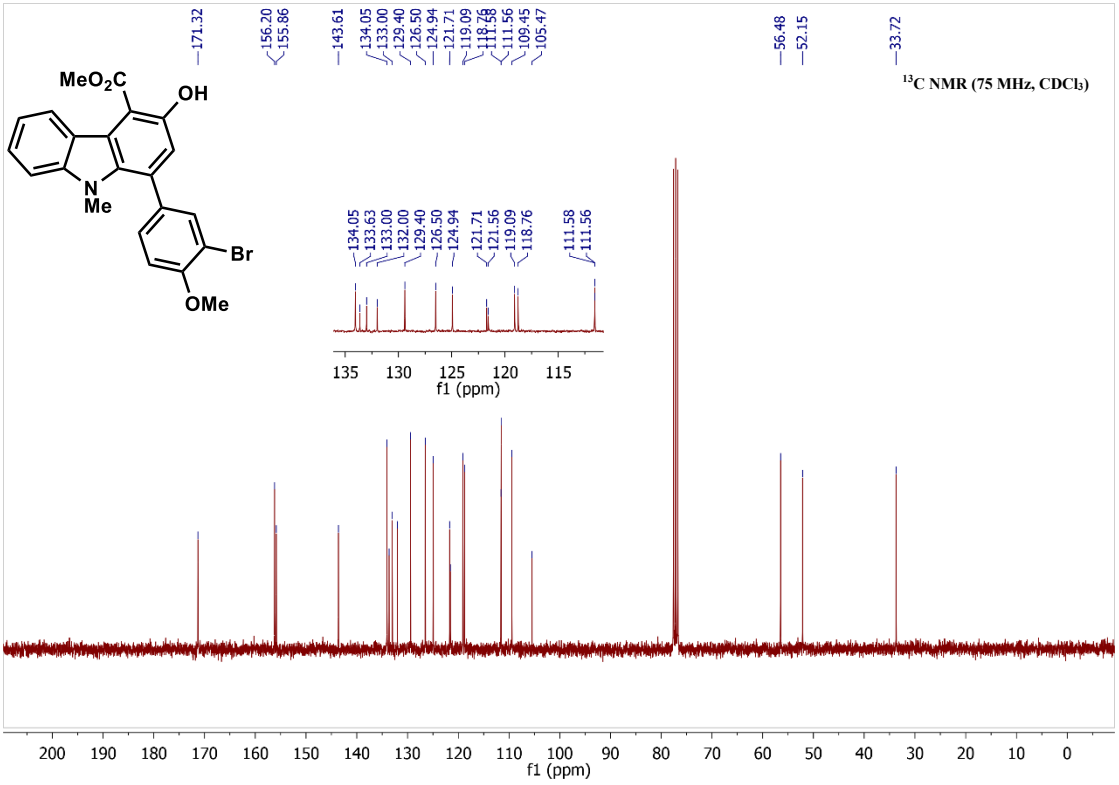
^{13}C NMR (75 MHz, CDCl$_3$)
MeO$_2$C
OH
N
Me
Br
OMe
171.32
156.20
155.86
143.61
134.05
133.00
129.40
126.50
124.94
121.71
119.09
118.76
111.58
111.56
109.45
105.47
56.48
52.15
33.72
134.05
133.63
133.00
132.00
129.40
126.50
124.94
121.71
121.56
119.09
118.76
111.58
111.56
f1 (ppm)

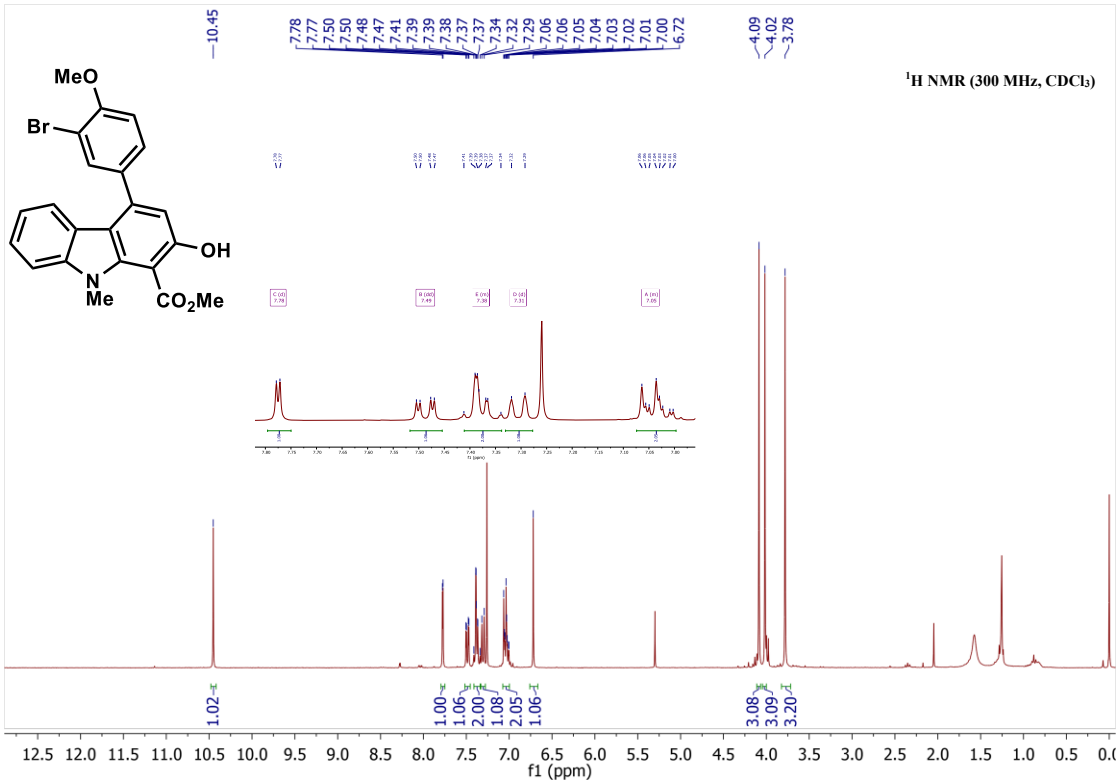
MeO
Br
OH
N
Me
CO2Me
1H NMR (300 MHz, CDCl3)
f1 (ppm)

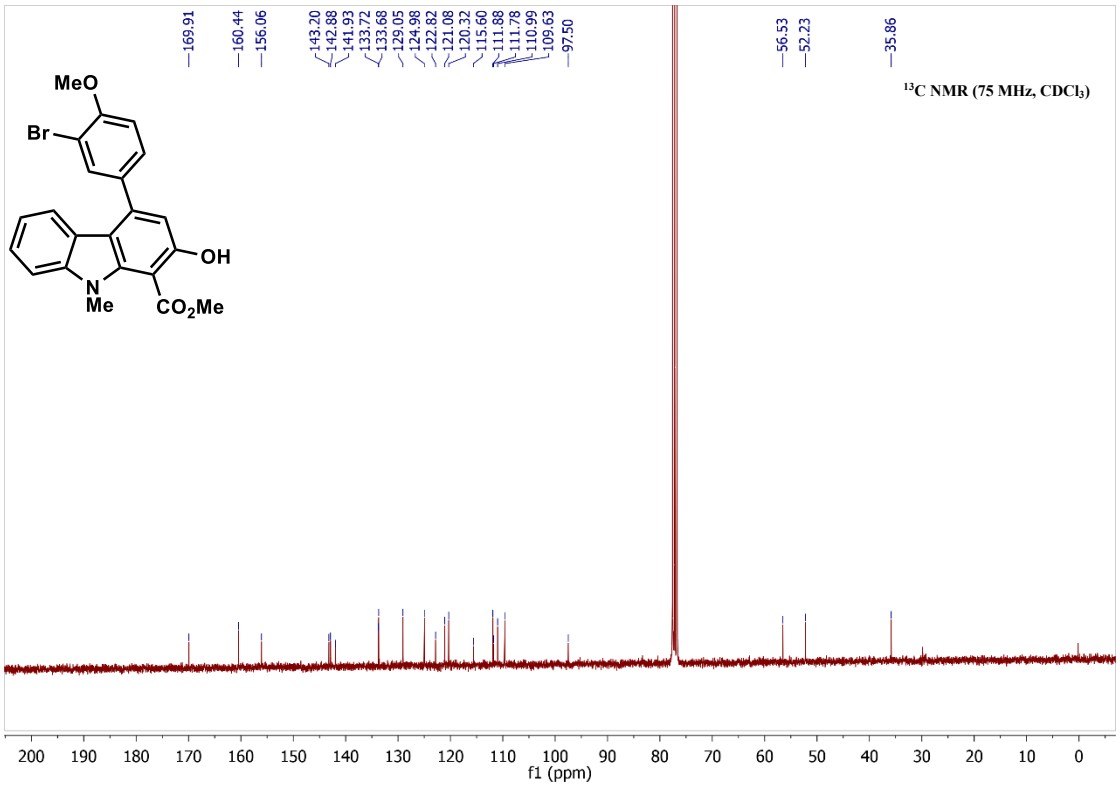
MeO
Br
OH
N
Me
CO2Me
13C NMR (75 MHz, CDCl3)
f1 (ppm)

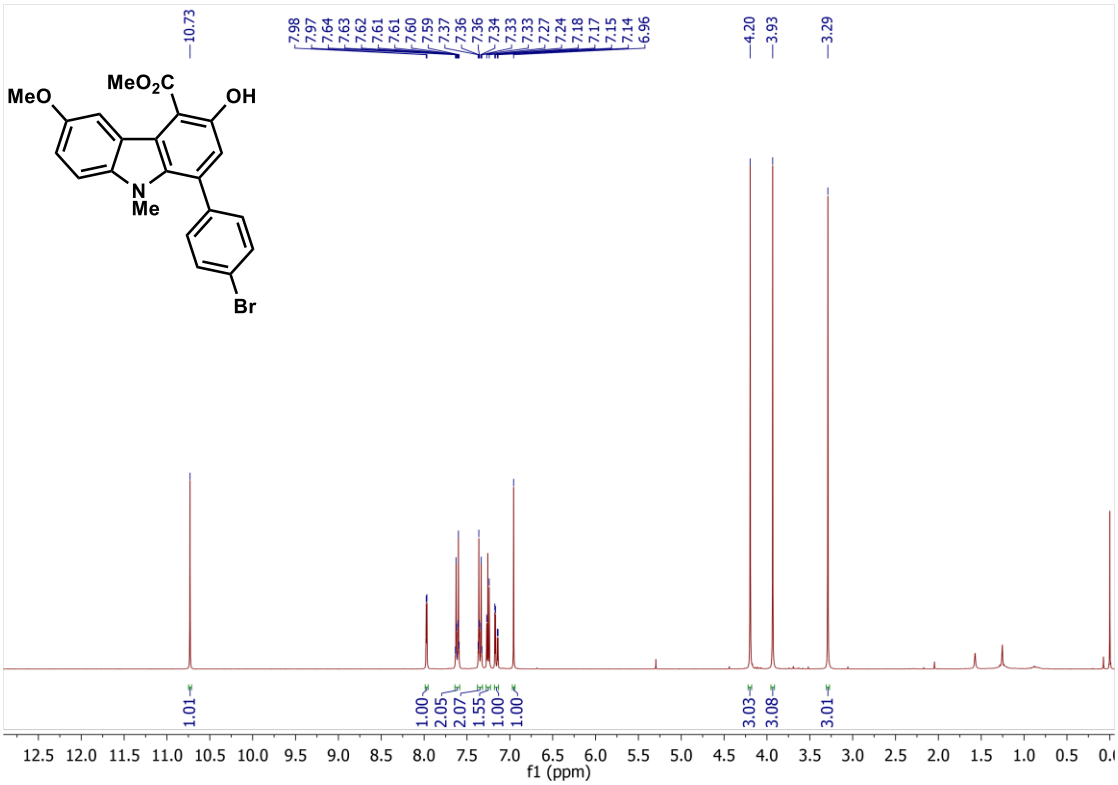
MeO
MeO2C
OH
N
Me
Br
10.73
7.98
7.97
7.64
7.63
7.62
7.61
7.61
7.60
7.59
7.37
7.36
7.36
7.34
7.33
7.33
7.27
7.24
7.18
7.17
7.15
7.14
6.96
4.20
3.93
3.29
1.01
1.00
2.05
2.07
1.55
1.00
1.00
3.03
3.08
3.01
f1 (ppm)

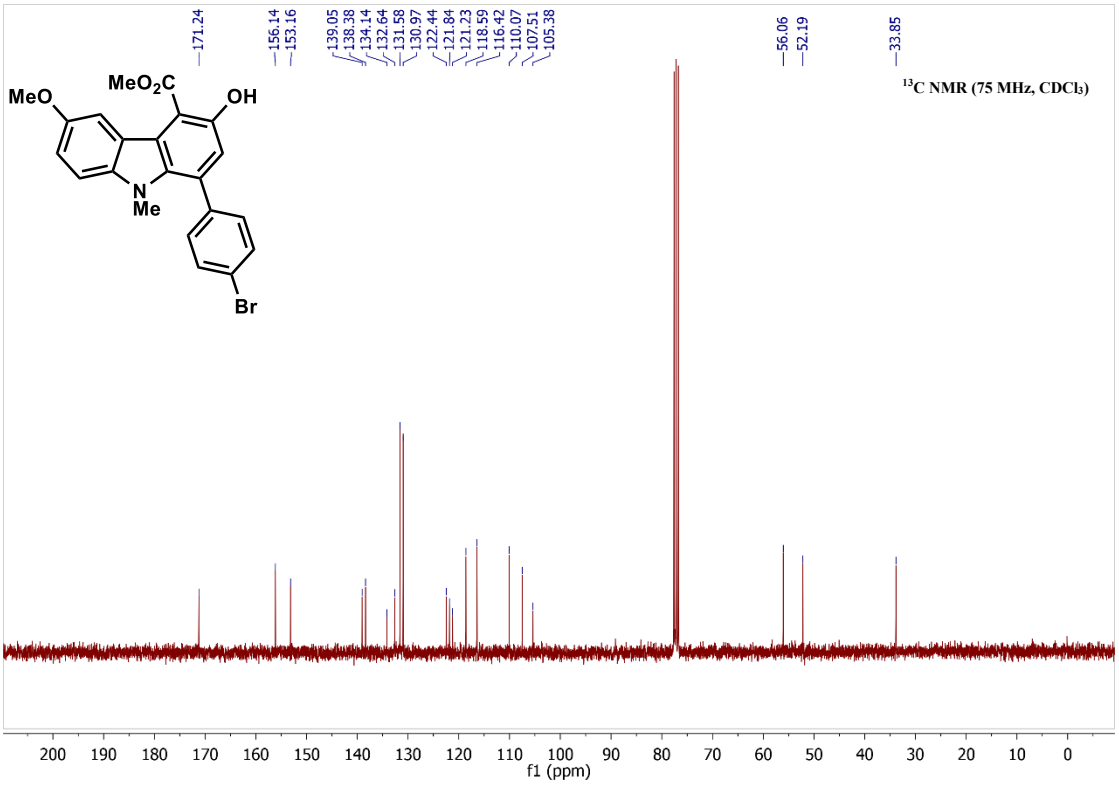
MeO
MeO2C
OH
N
Me
Br
171.24
156.14
153.16
139.05
138.38
134.14
132.64
131.58
130.97
122.44
121.84
121.23
118.59
116.42
110.07
107.51
105.38
56.06
52.19
33.85
13C NMR (75 MHz, CDCl3)
f1 (ppm)

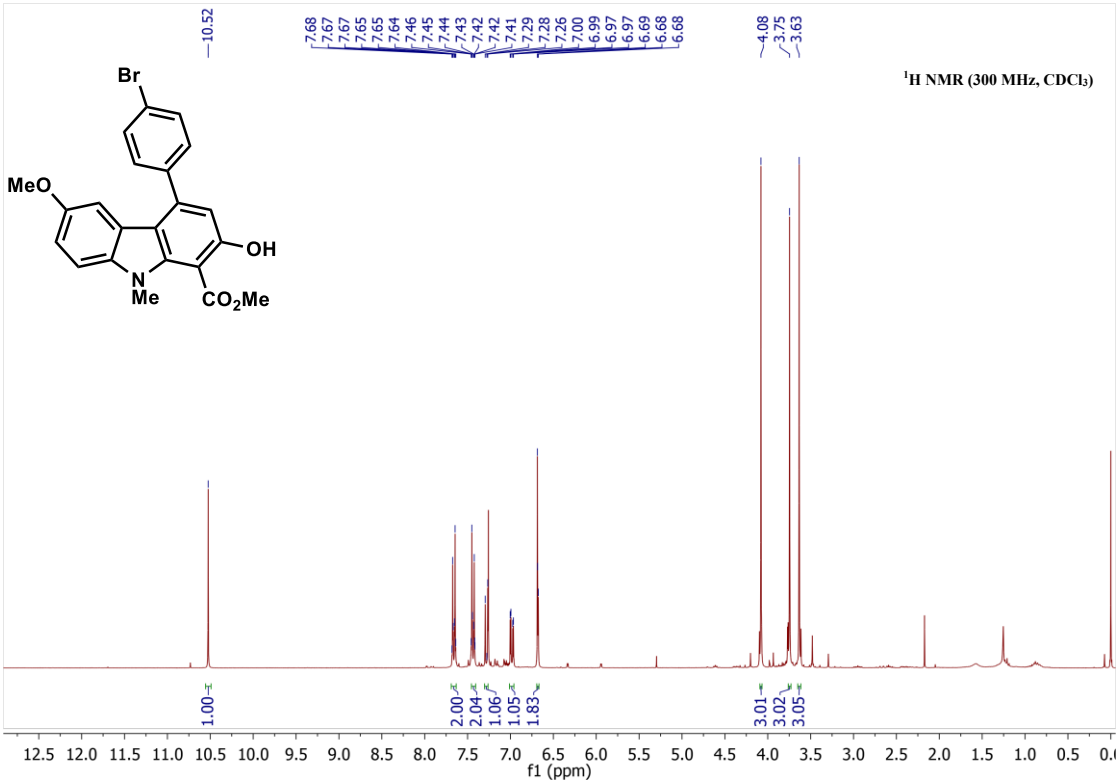
Br
MeO
OH
N
Me
CO2Me
1H NMR (300 MHz, CDCl3)
10.52
7.68
7.67
7.67
7.65
7.65
7.64
7.46
7.45
7.44
7.43
7.42
7.42
7.41
7.29
7.28
7.26
7.00
6.99
6.97
6.97
6.69
6.68
6.68
4.08
3.75
3.63
1.00
2.00
2.04
1.06
1.05
1.83
3.01
3.02
3.05
f1 (ppm)

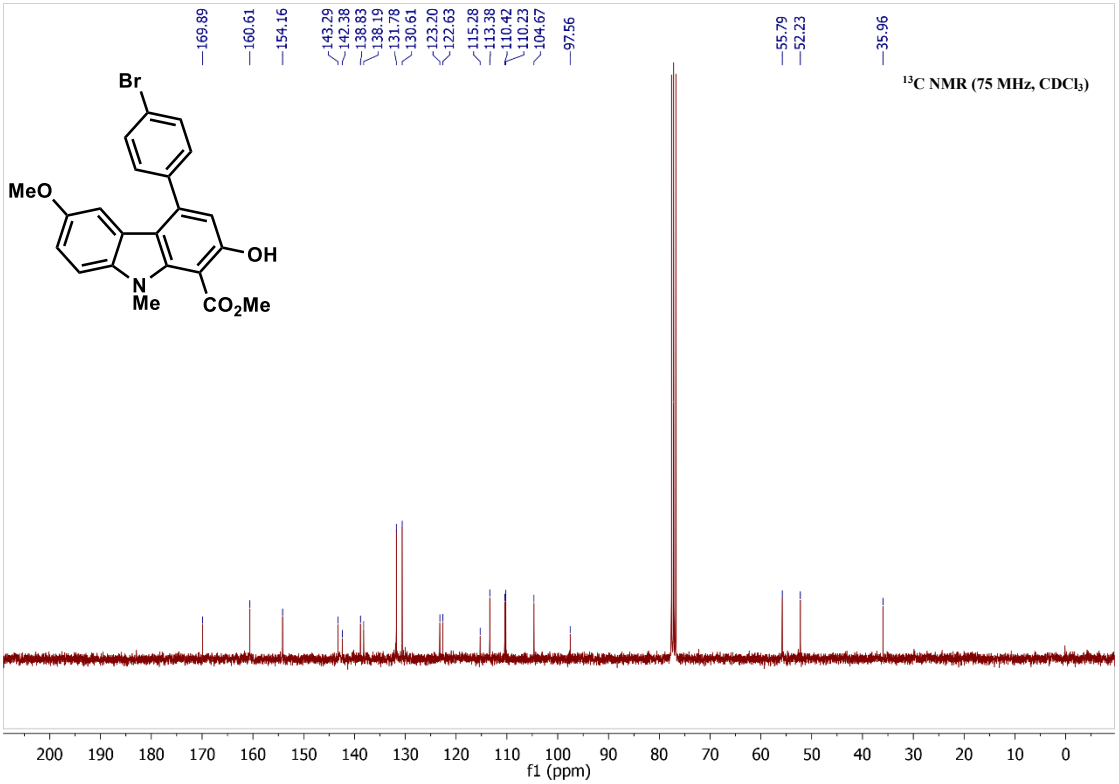
Br
MeO
OH
N
Me
CO2Me
13C NMR (75 MHz, CDCl3)
169.89
160.61
154.16
143.29
142.38
138.83
138.19
131.78
130.61
123.20
122.63
115.28
113.38
110.42
110.23
104.67
97.56
55.79
52.23
35.96
f1 (ppm)

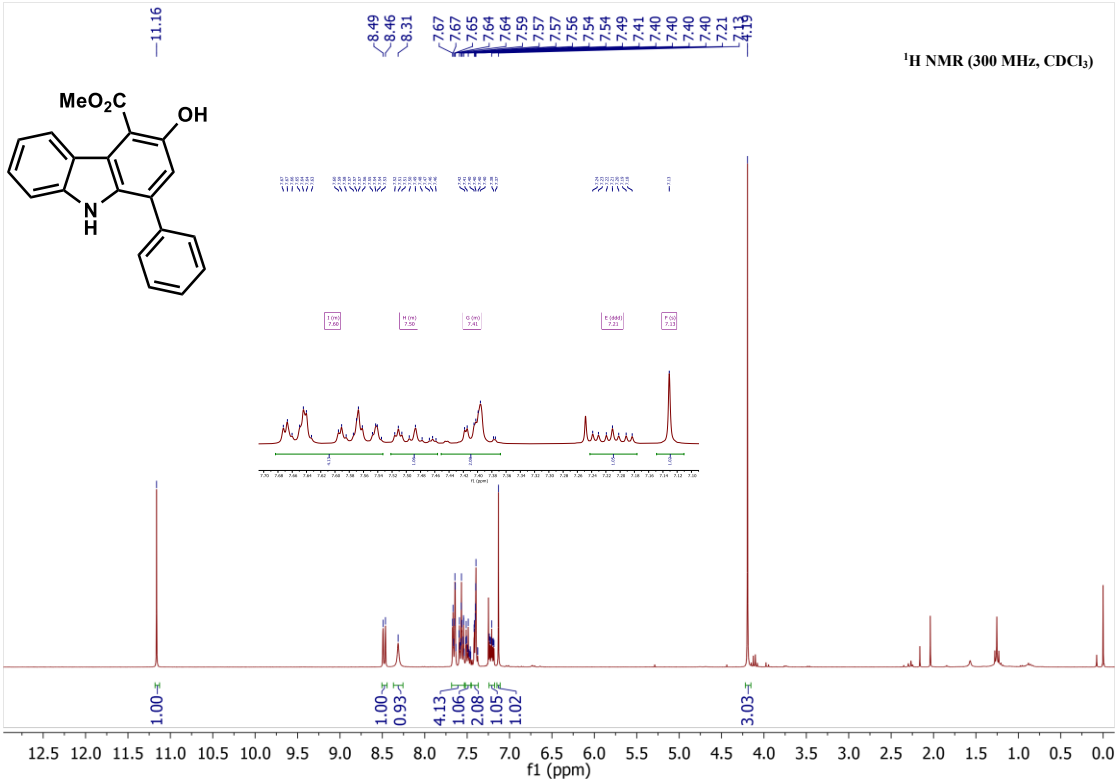
^{1}H NMR (300 MHz, CDCl$_3$)
MeO$_2$C
OH
N
H
11.16
8.49
8.46
8.31
7.67
7.65
7.64
7.59
7.57
7.56
7.54
7.49
7.41
7.40
7.21
4.13
1.00
1.00
0.93
4.13
1.06
2.08
1.05
1.02
3.03
f1 (ppm)

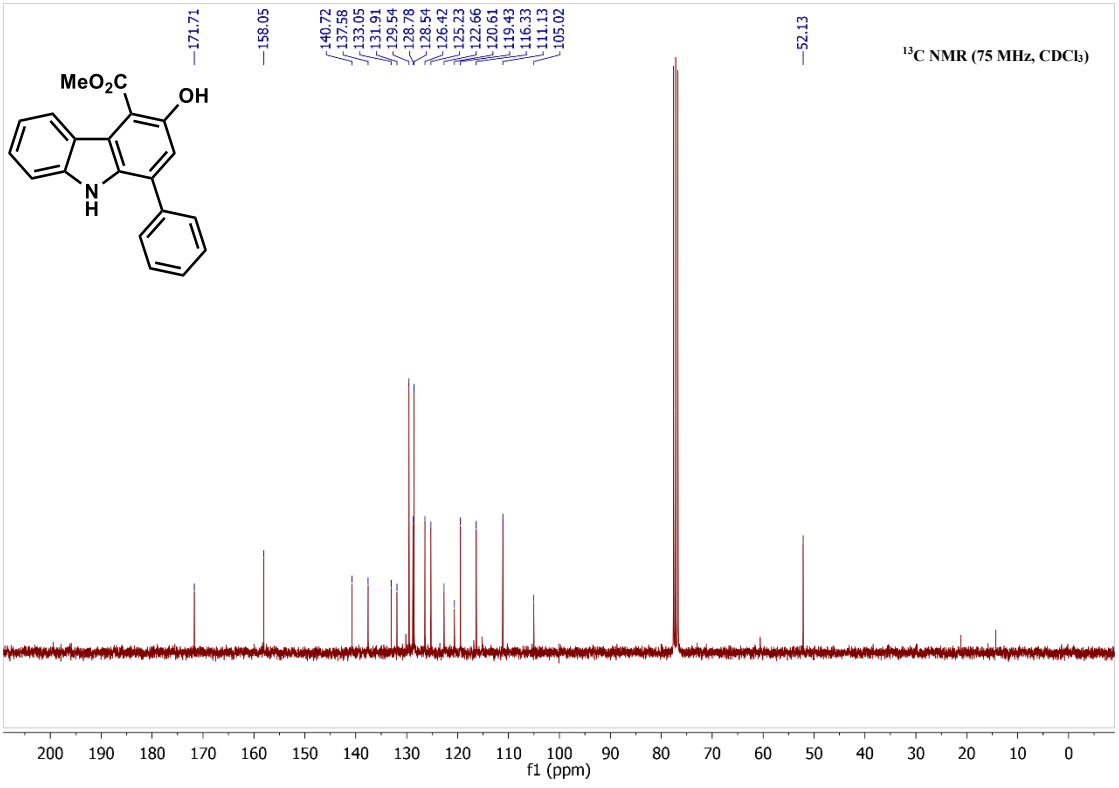
^{13}C NMR (75 MHz, CDCl$_3$)
MeO$_2$C
OH
N
H
171.71
158.05
140.72
137.58
133.05
131.91
129.54
128.78
128.54
126.42
125.23
122.66
120.61
119.43
116.33
111.13
105.02
52.13
f1 (ppm)

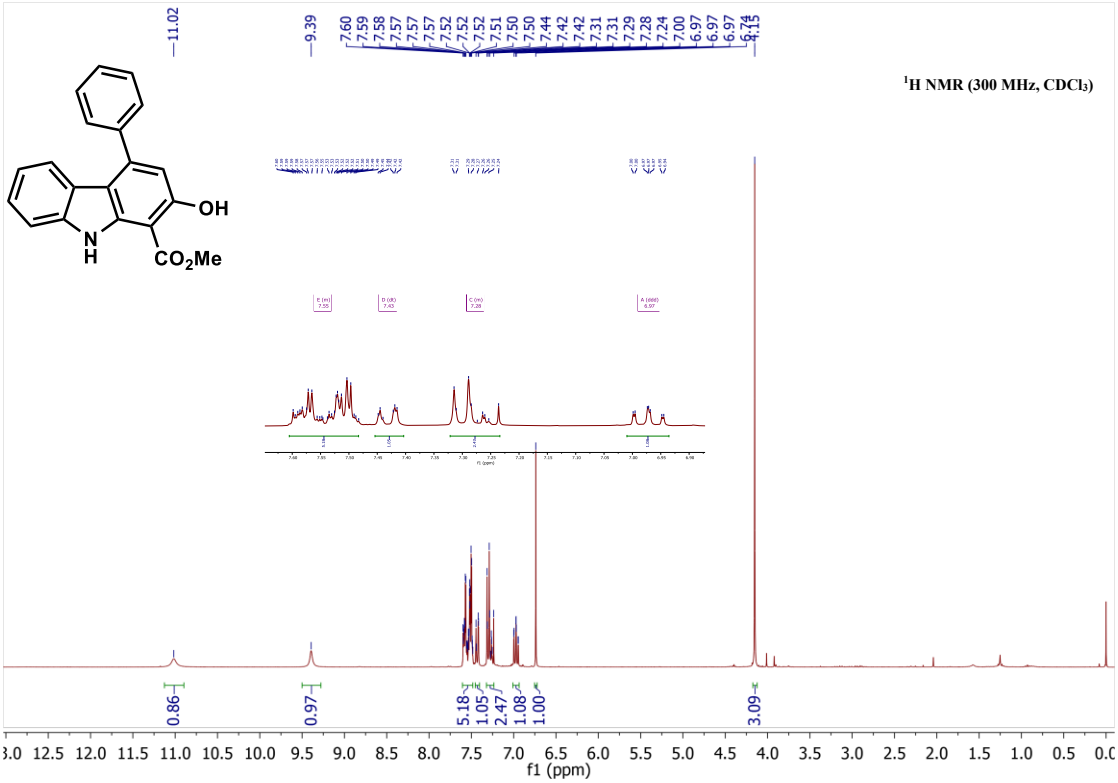
^{1}H NMR (300 MHz, CDCl$_3$)
OH
N
H
CO$_2$Me
11.02
9.39
7.60
7.59
7.58
7.57
7.57
7.57
7.52
7.52
7.52
7.51
7.50
7.50
7.44
7.42
7.42
7.31
7.31
7.29
7.28
7.24
7.00
6.97
6.97
6.97
6.74
6.73
4.15
0.86
0.97
5.18
1.05
2.47
1.08
1.00
3.09
f1 (ppm)

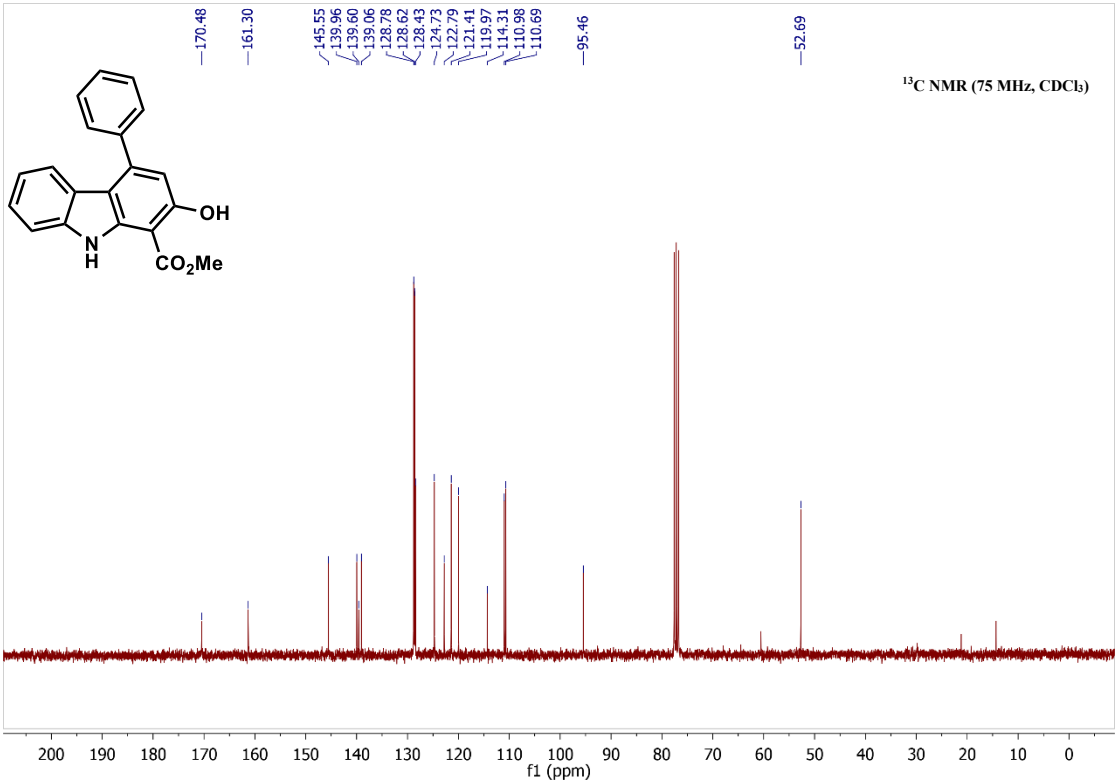
^{13}C NMR (75 MHz, CDCl$_3$)
OH
N
H
CO$_2$Me
170.48
161.30
145.55
139.96
139.60
139.06
128.78
128.62
128.43
124.73
122.79
121.41
119.97
114.31
110.98
110.69
95.46
52.69
f1 (ppm)

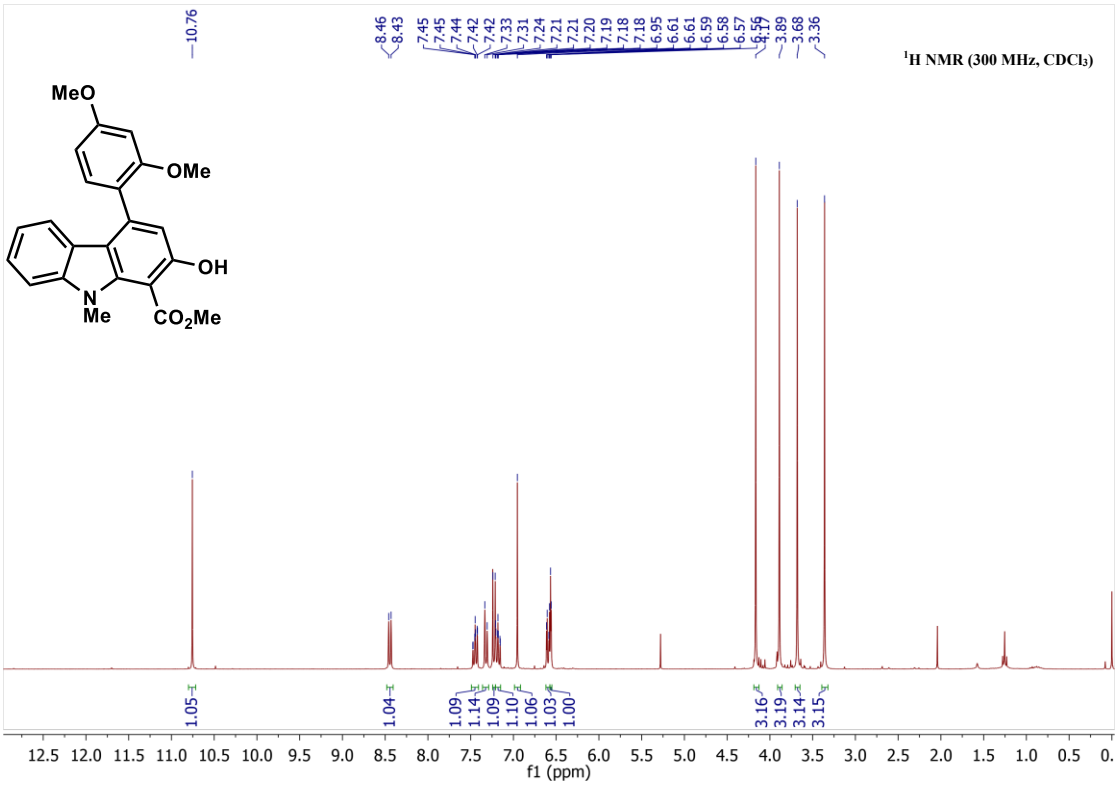
^{1}H NMR (300 MHz, CDCl$_3$)
MeO
OMe
OH
N
Me
CO$_2$Me
f1 (ppm)

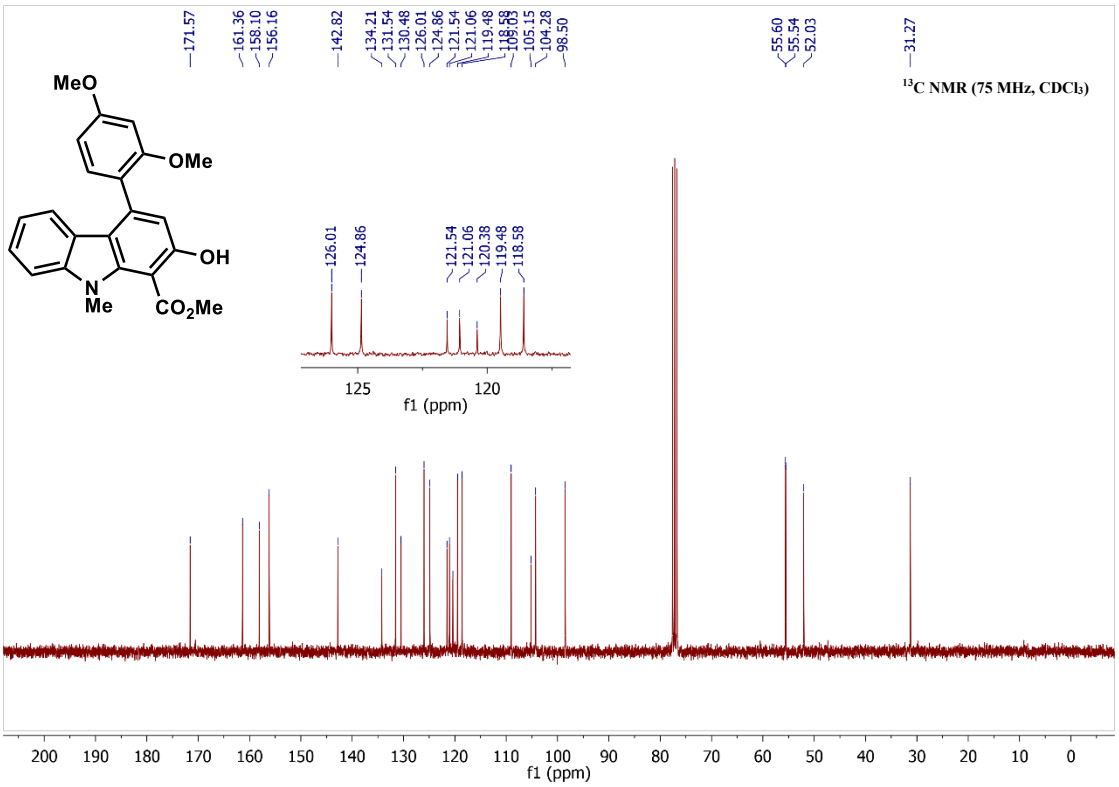
^{13}C NMR (75 MHz, CDCl$_3$)
MeO
OMe
OH
N
Me
CO$_2$Me
f1 (ppm)

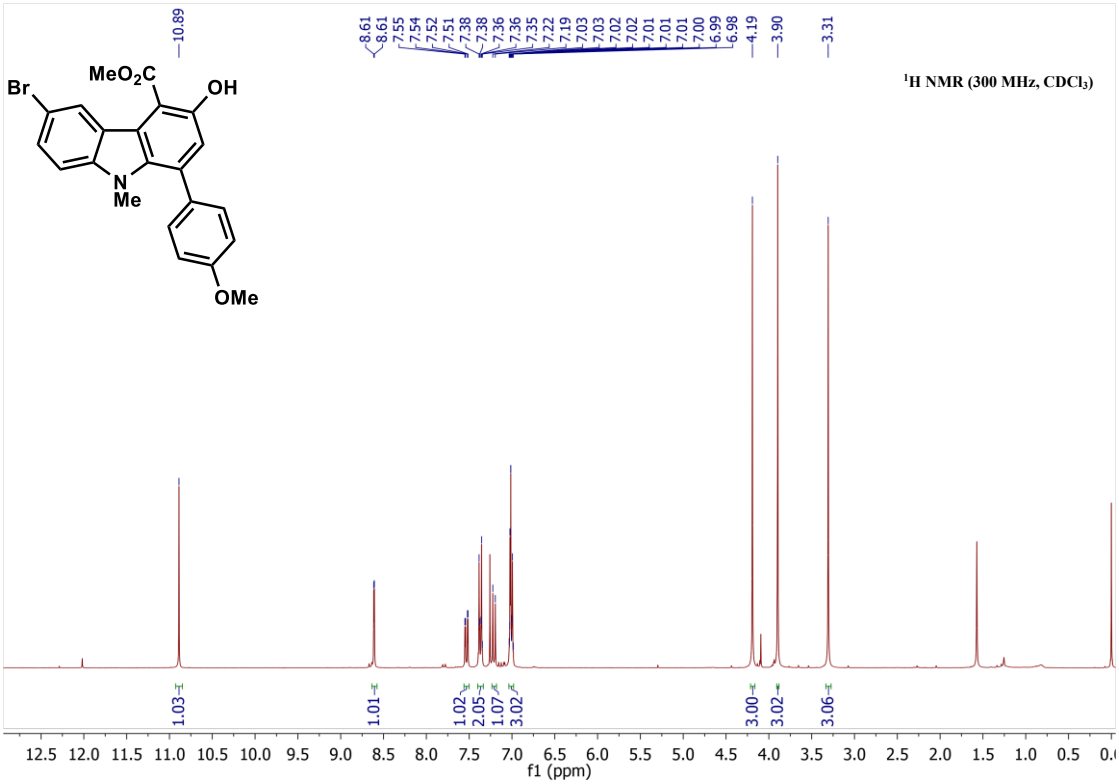
Br
MeO2C
OH
N
Me
OMe
1H NMR (300 MHz, CDCl3)
10.89
8.61
8.61
7.55
7.54
7.52
7.51
7.38
7.38
7.36
7.36
7.35
7.22
7.19
7.03
7.03
7.02
7.02
7.01
7.01
7.01
7.00
6.99
6.98
4.19
3.90
3.31
1.03
1.01
1.02
2.05
1.07
3.02
3.00
3.02
3.06
f1 (ppm)

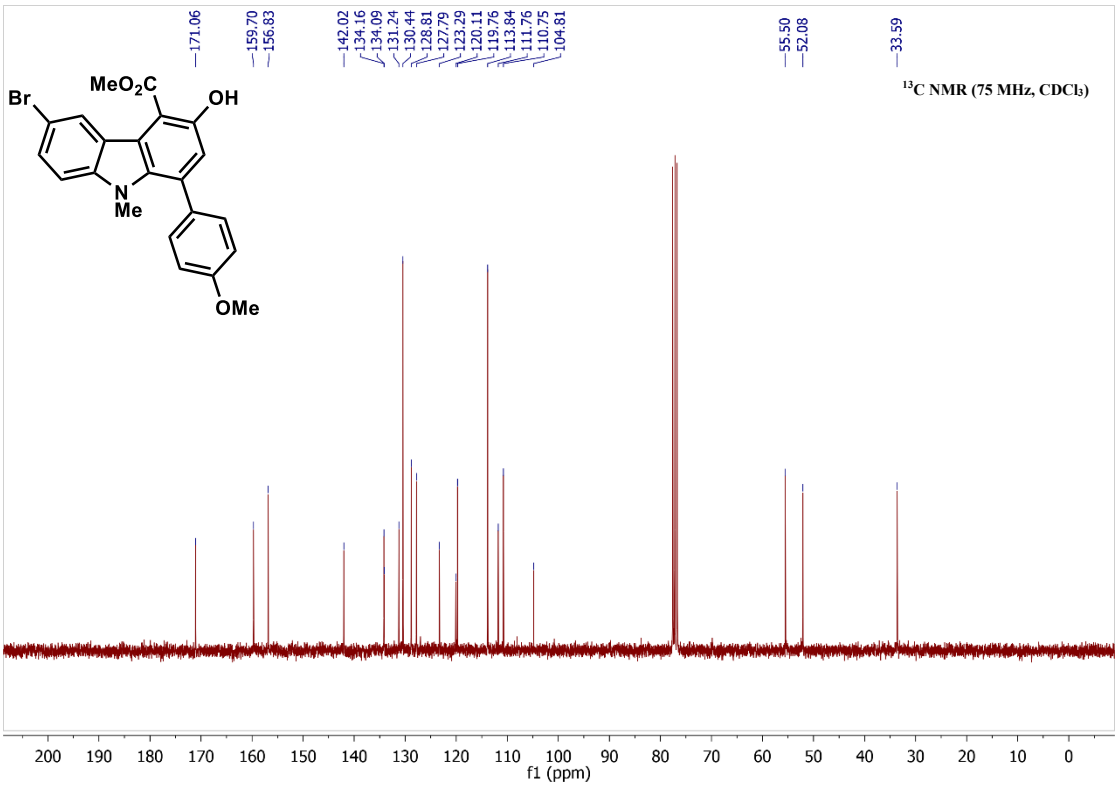
Br
MeO2C
OH
N
Me
OMe
13C NMR (75 MHz, CDCl3)
171.06
159.70
156.83
142.02
134.16
134.09
131.24
130.44
128.81
127.79
123.29
120.11
119.76
113.84
111.76
110.75
104.81
55.50
52.08
33.59
f1 (ppm)

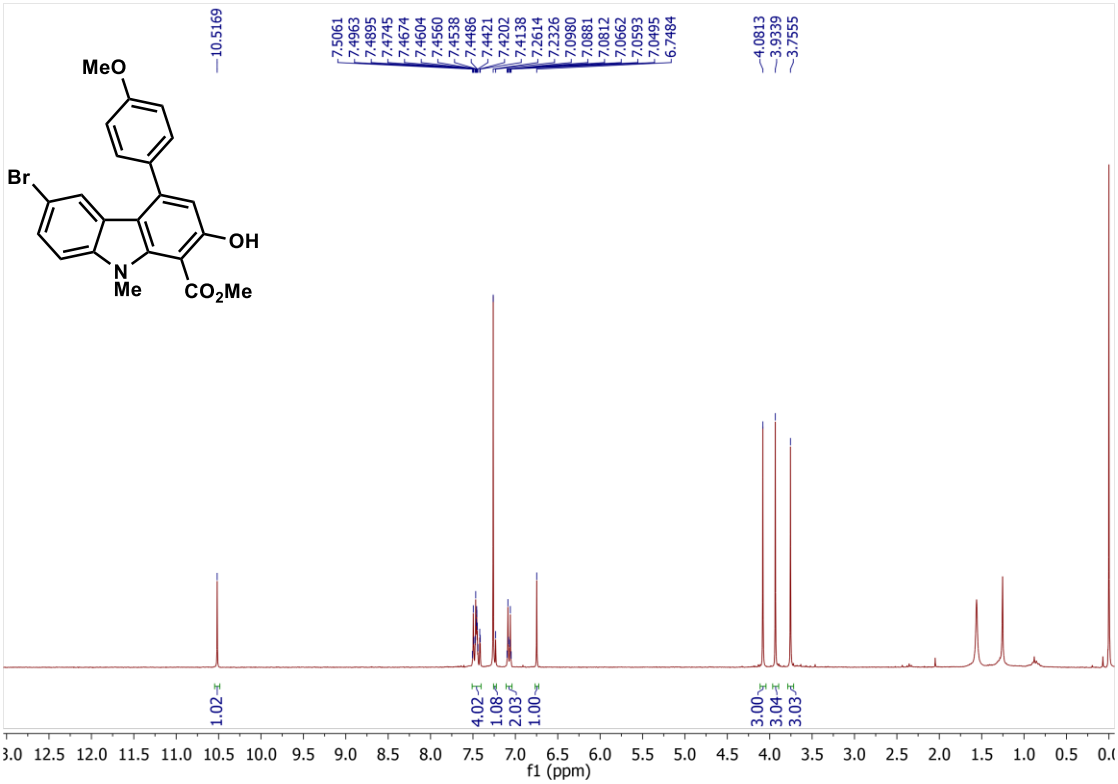
MeO
Br
OH
N
Me
CO2Me
10.5169
7.5061
7.4963
7.4895
7.4745
7.4674
7.4604
7.4560
7.4538
7.4486
7.4421
7.4202
7.4138
7.2614
7.2326
7.0980
7.0881
7.0812
7.0662
7.0593
7.0495
6.7484
4.0813
3.9339
3.7555
1.02
4.02
1.08
2.03
1.00
3.00
3.04
3.03
f1 (ppm)

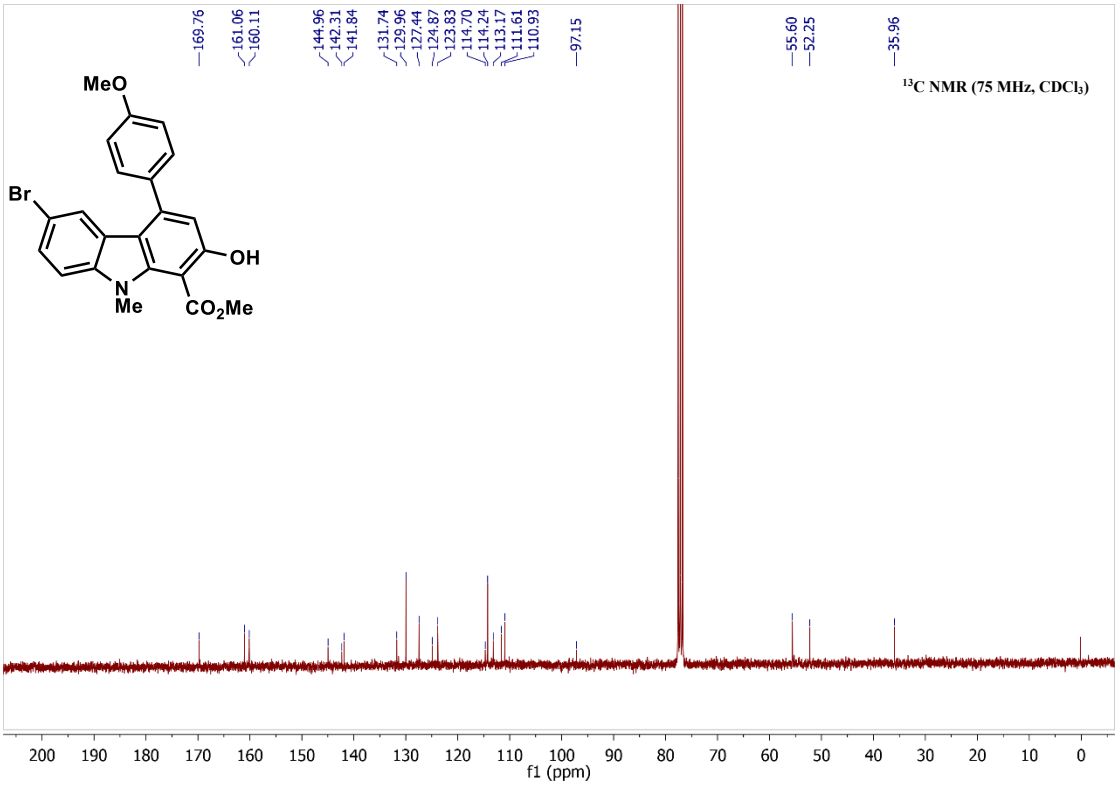
MeO
Br
OH
N
Me
CO2Me
169.76
161.06
160.11
144.96
142.31
141.84
131.74
129.96
127.44
124.87
123.83
114.70
114.24
113.17
111.61
110.93
97.15
55.60
52.25
35.96
13C NMR (75 MHz, CDCl3)
f1 (ppm)

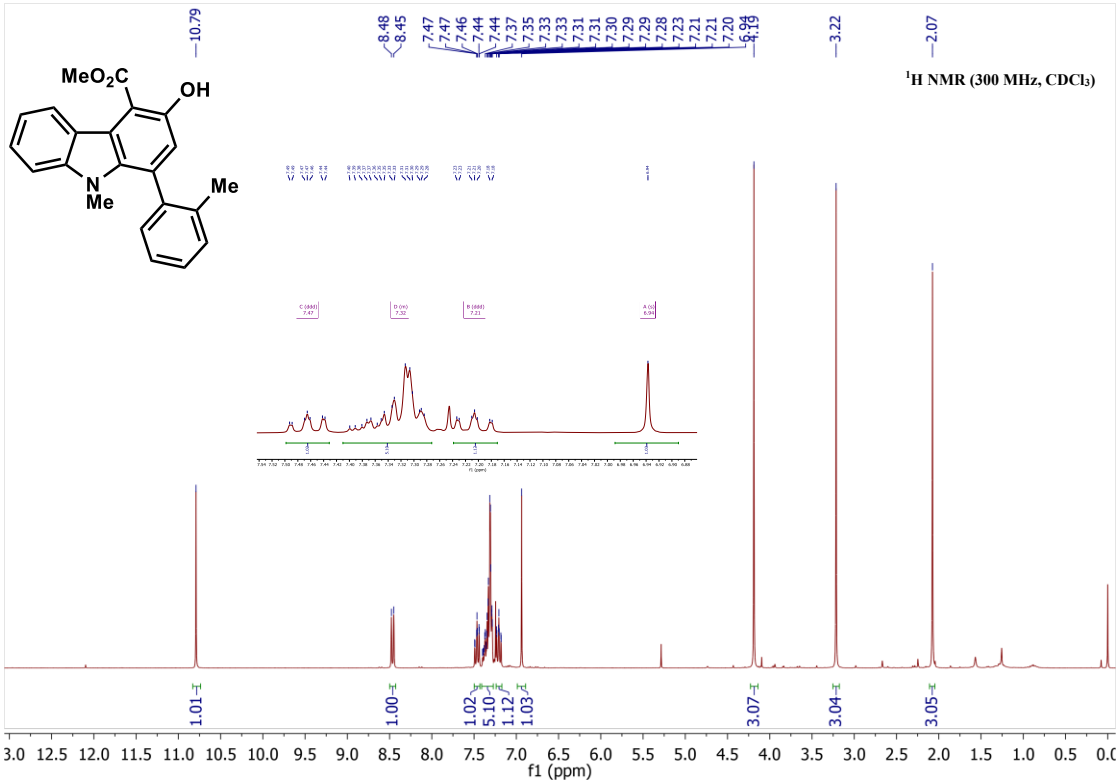
^{1}H NMR (300 MHz, CDCl$_3$)
MeO2C
OH
N
Me
Me
10.79
8.48
8.45
7.47
7.47
7.46
7.44
7.44
7.37
7.35
7.33
7.33
7.31
7.31
7.30
7.29
7.29
7.28
7.23
7.21
7.21
7.20
6.98
6.97
4.19
3.22
2.07
1.01
1.00
1.02
5.10
1.12
1.03
3.07
3.04
3.05
f1 (ppm)

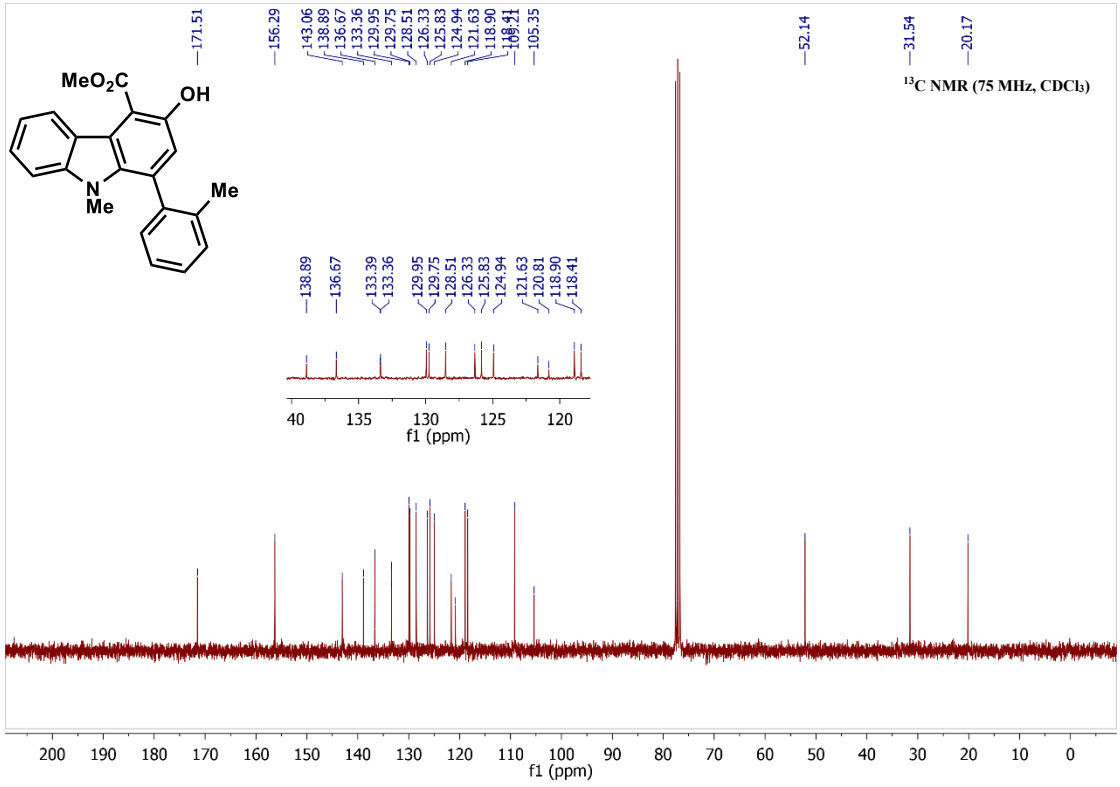
^{13}C NMR (75 MHz, CDCl$_3$)
MeO2C
OH
N
Me
Me
171.51
156.29
143.06
138.89
136.67
133.36
129.95
129.75
128.51
126.33
125.83
124.94
121.63
118.90
105.35
52.14
31.54
20.17
f1 (ppm)

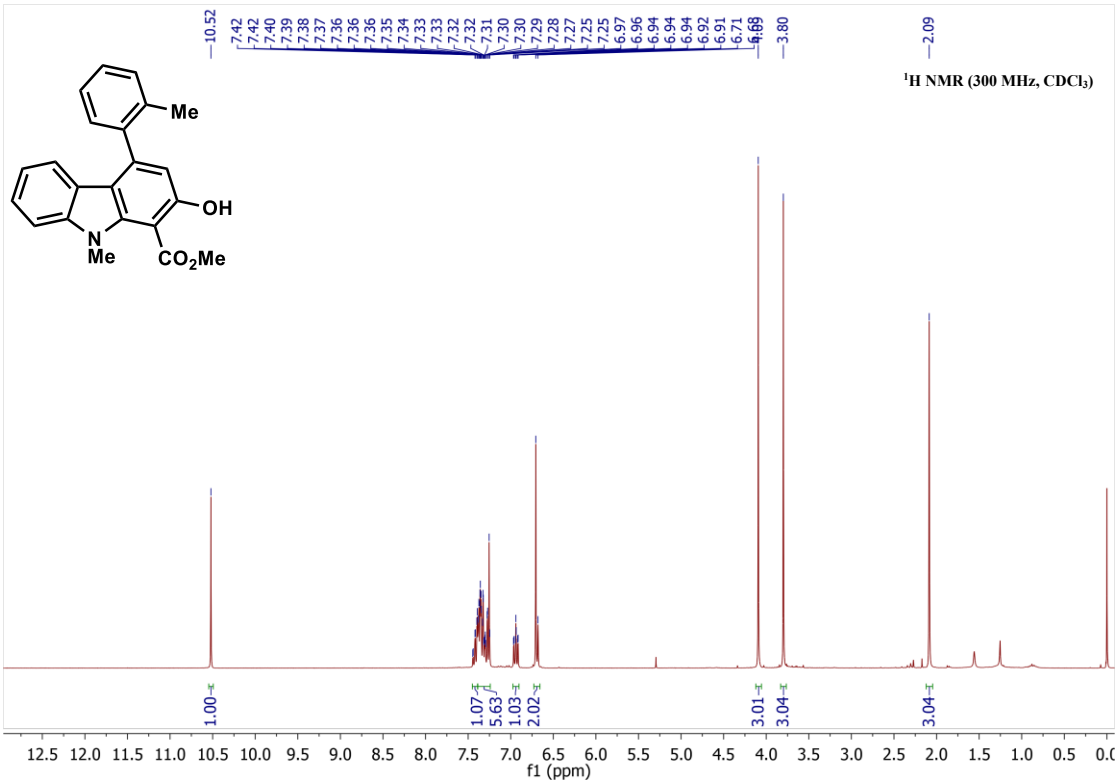
Me
OH
N
Me
CO2Me
1H NMR (300 MHz, CDCl3)
f1 (ppm)

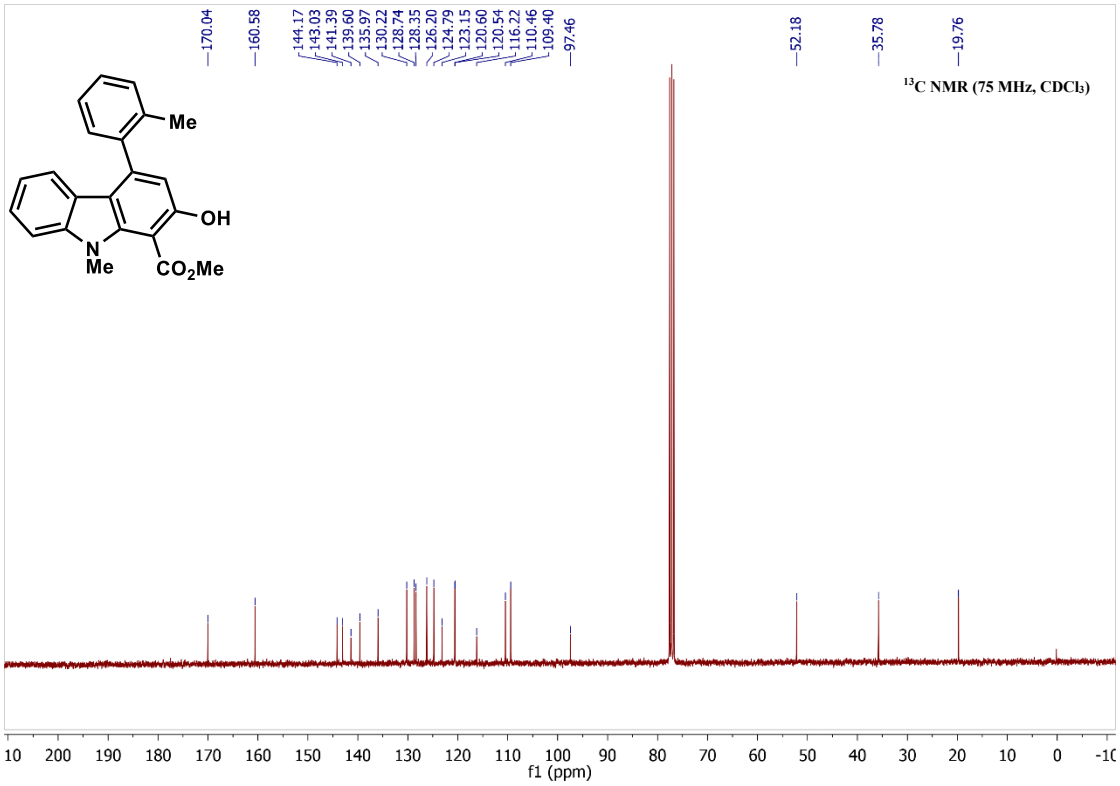
Me
OH
N
Me
CO2Me
13C NMR (75 MHz, CDCl3)
f1 (ppm)

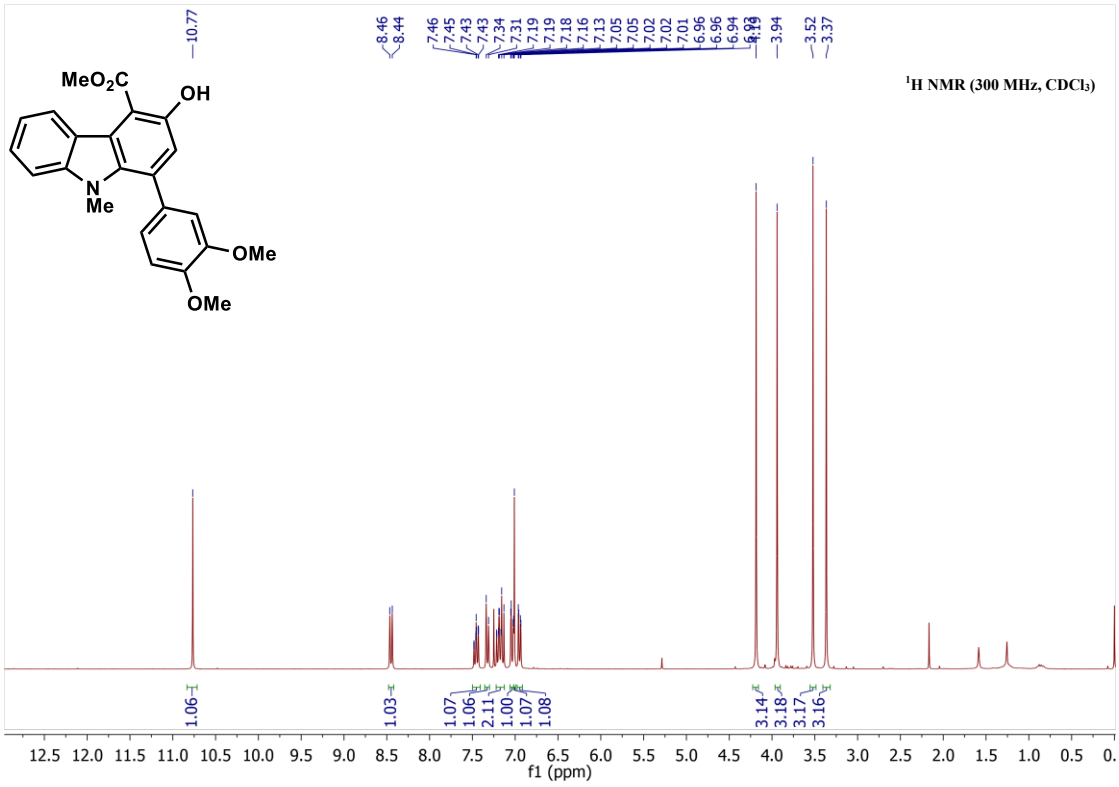
MeO2C
OH
N
Me
OMe
OMe
10.77
8.46
8.44
7.46
7.45
7.43
7.43
7.34
7.31
7.19
7.19
7.18
7.16
7.13
7.05
7.05
7.02
7.02
7.01
6.96
6.96
6.94
3.94
3.52
3.37
1H NMR (300 MHz, CDCl3)
1.06
1.03
1.07
1.06
2.11
1.00
1.07
1.08
3.14
3.18
3.17
3.16
12.5 12.0 11.5 11.0 10.5 10.0 9.5 9.0 8.5 8.0 7.5 7.0 6.5 6.0 5.5 5.0 4.5 4.0 3.5 3.0 2.5 2.0 1.5 1.0 0.5 0.
f1 (ppm)

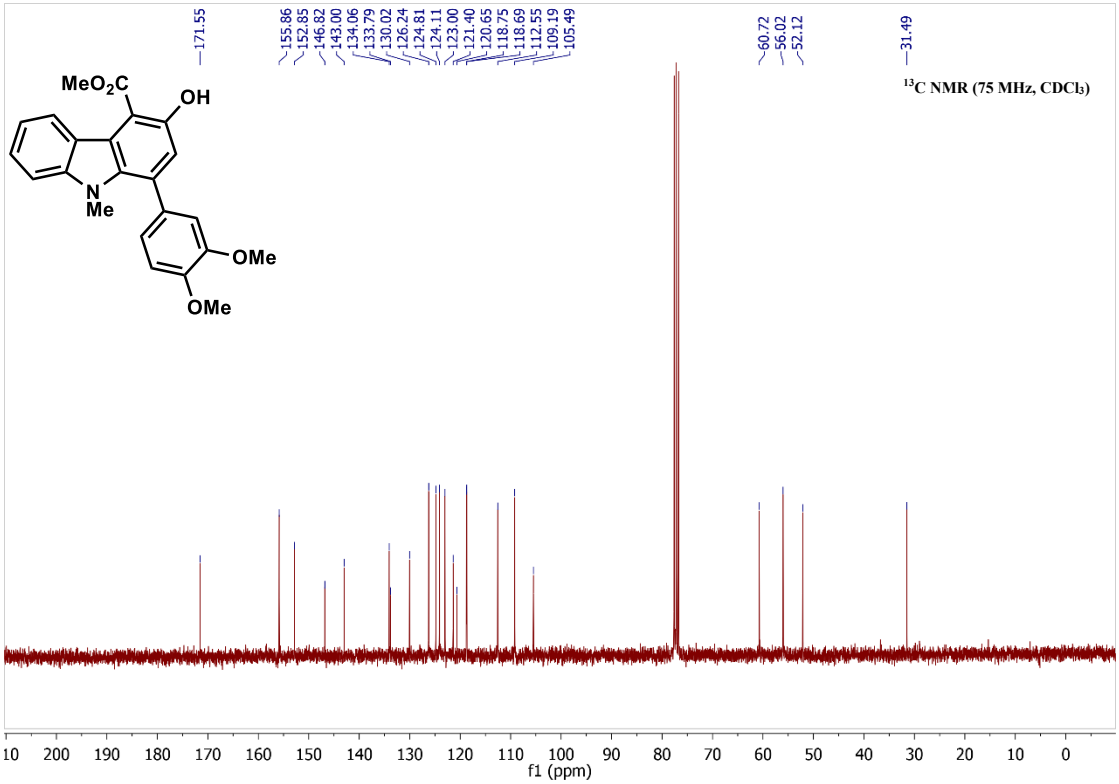
MeO2C
OH
N
Me
OMe
OMe
171.55
155.86
152.85
146.82
143.00
134.06
133.79
130.02
126.24
124.81
124.11
123.00
121.40
120.65
118.75
118.69
112.55
109.19
105.49
60.72
56.02
52.12
31.49
13C NMR (75 MHz, CDCl3)
10 200 190 180 170 160 150 140 130 120 110 100 90 80 70 60 50 40 30 20 10 0
f1 (ppm)

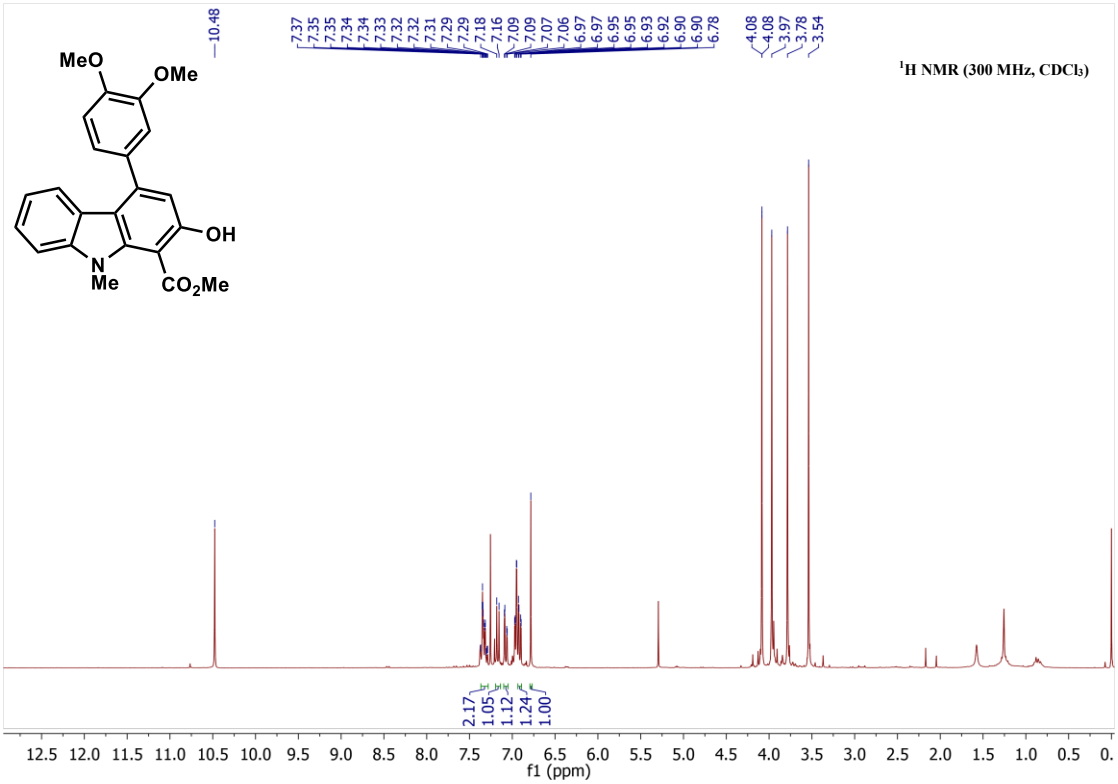
MeO
OMe
OH
N
Me
CO2Me
10.48
7.37
7.35
7.35
7.34
7.34
7.33
7.32
7.32
7.31
7.29
7.29
7.18
7.16
7.09
7.09
7.07
7.06
6.97
6.97
6.95
6.95
6.93
6.92
6.90
6.90
6.78
4.08
4.08
3.97
3.78
3.54
1H NMR (300 MHz, CDCl3)
2.17
1.05
1.12
1.24
1.00
12.5 12.0 11.5 11.0 10.5 10.0 9.5 9.0 8.5 8.0 7.5 7.0 6.5 6.0 5.5 5.0 4.5 4.0 3.5 3.0 2.5 2.0 1.5 1.0 0.5 0.
f1 (ppm)

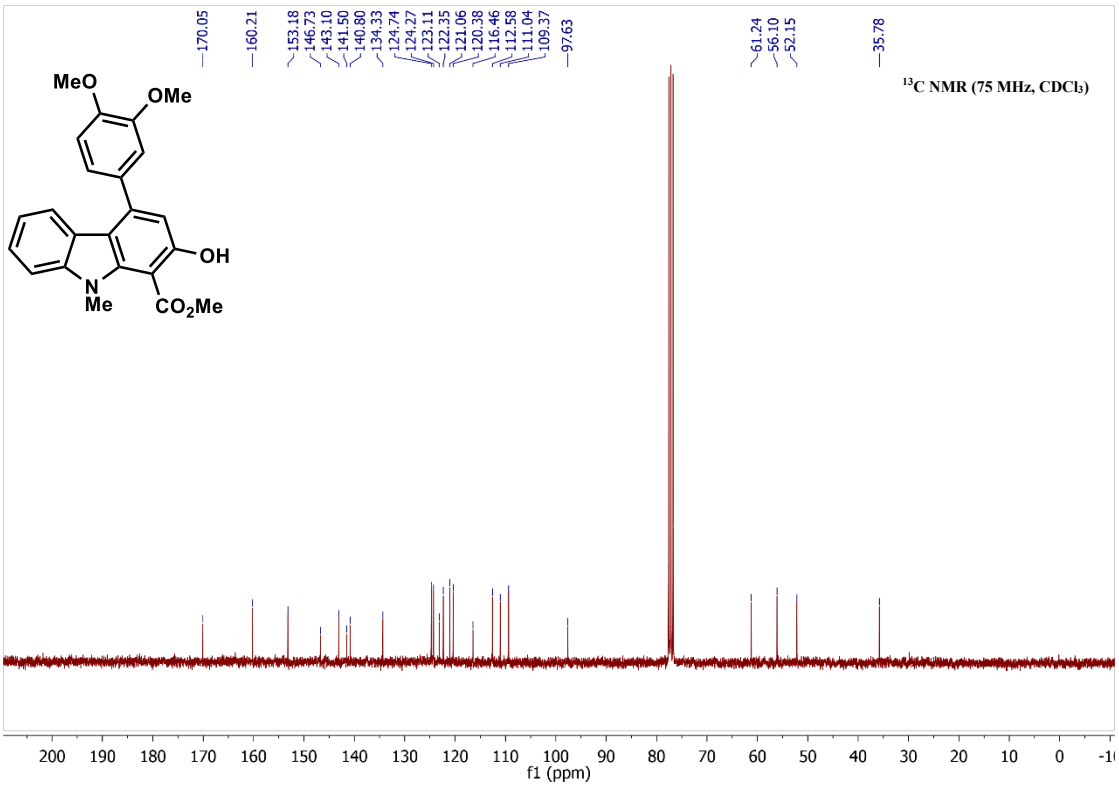
MeO
OMe
OH
N
Me
CO2Me
170.05
160.21
153.18
146.73
143.10
141.50
140.80
134.33
124.74
124.27
123.11
122.35
121.06
120.38
116.46
112.58
111.04
109.37
97.63
61.24
56.10
52.15
35.78
13C NMR (75 MHz, CDCl3)
200 190 180 170 160 150 140 130 120 110 100 90 80 70 60 50 40 30 20 10 0
f1 (ppm)

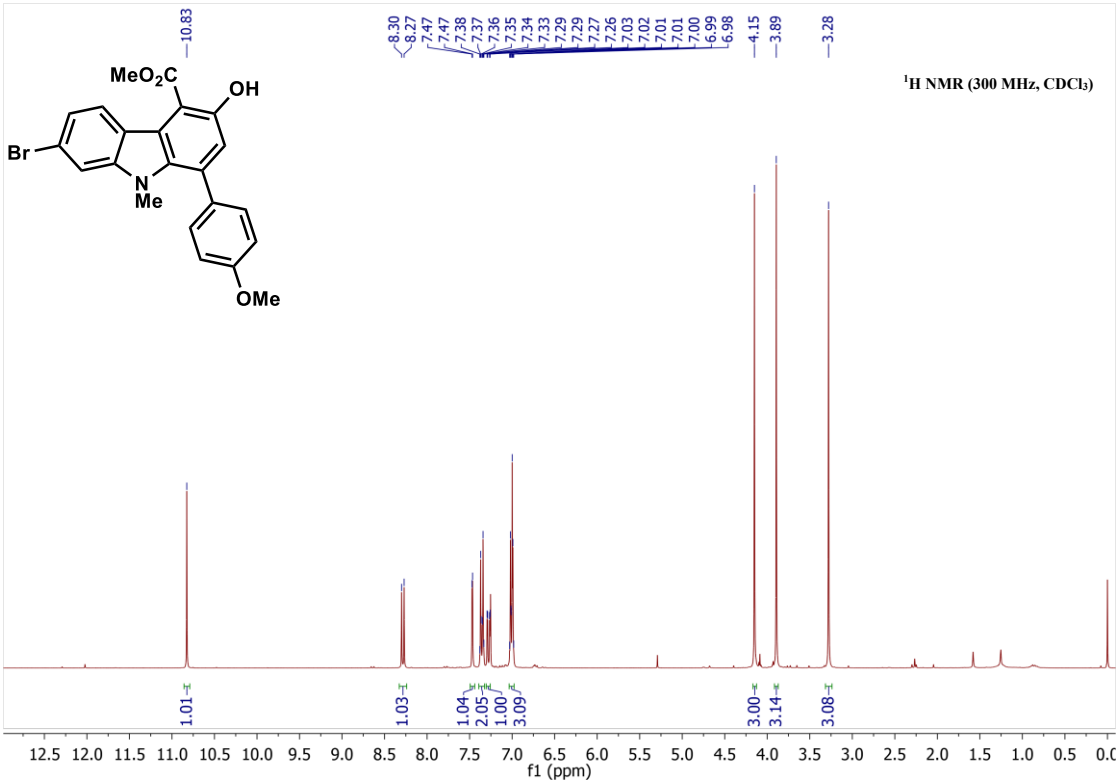
^{1}H NMR (300 MHz, CDCl$_3$)
MeO$_2$C
OH
Br
N
Me
OMe
10.83
8.30
8.27
7.47
7.47
7.38
7.37
7.36
7.35
7.34
7.33
7.29
7.29
7.27
7.26
7.03
7.02
7.01
7.01
7.00
6.99
6.98
4.15
3.89
3.28
1.01
1.03
1.04
2.05
1.00
3.09
3.00
3.14
3.08
f1 (ppm)

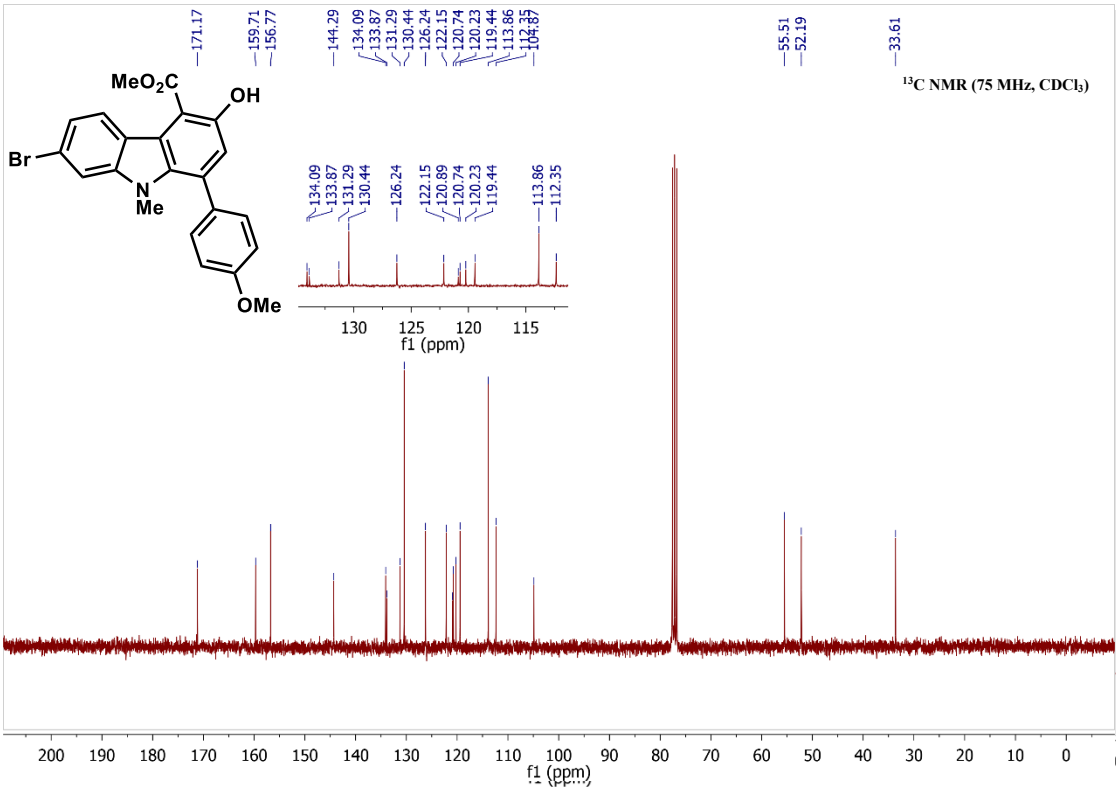
^{13}C NMR (75 MHz, CDCl$_3$)
MeO$_2$C
OH
Br
N
Me
OMe
171.17
159.71
156.77
144.29
134.09
133.87
131.29
130.44
126.24
122.15
120.74
120.23
119.44
113.86
112.35
104.87
55.51
52.19
33.61
f1 (ppm)

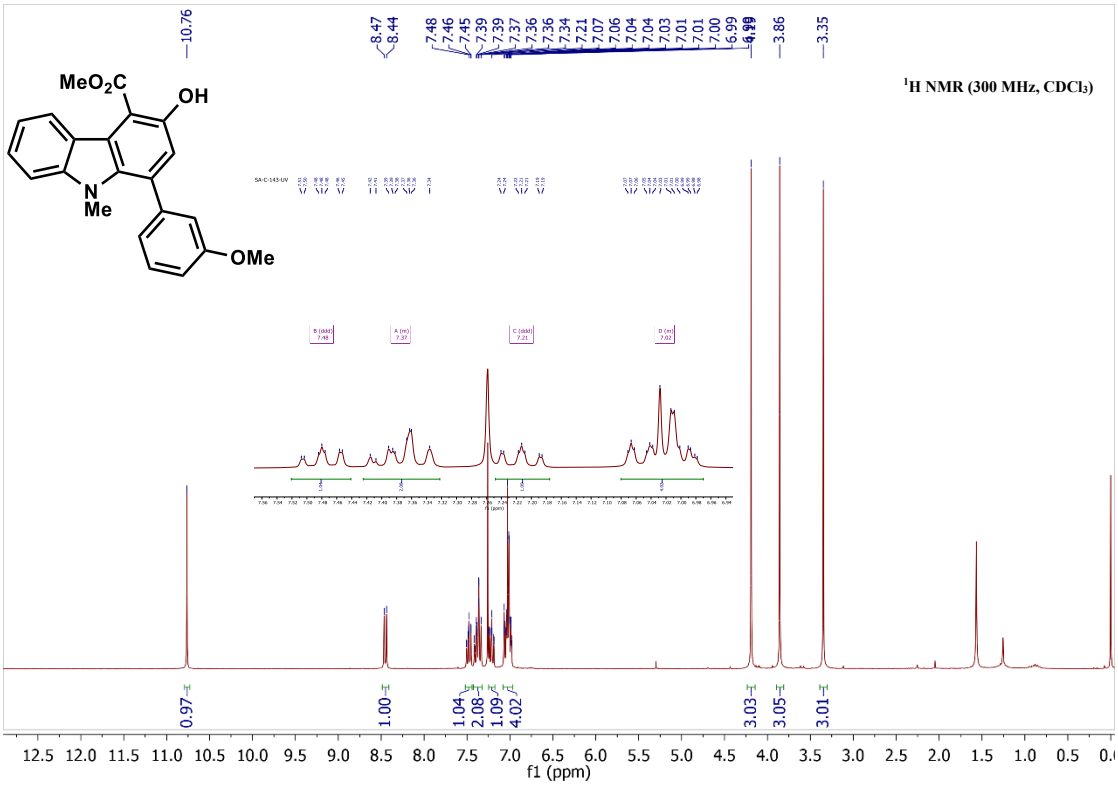
MeO2C
OH
N
Me
OMe
10.76
8.47
8.44
7.48
7.46
7.45
7.39
7.39
7.37
7.36
7.36
7.34
7.21
7.07
7.06
7.04
7.04
7.03
7.01
7.01
7.00
6.99
3.86
3.35
1H NMR (300 MHz, CDCl3)
0.97
1.00
1.04
2.08
1.09
4.02
3.03
3.05
3.01
f1 (ppm)

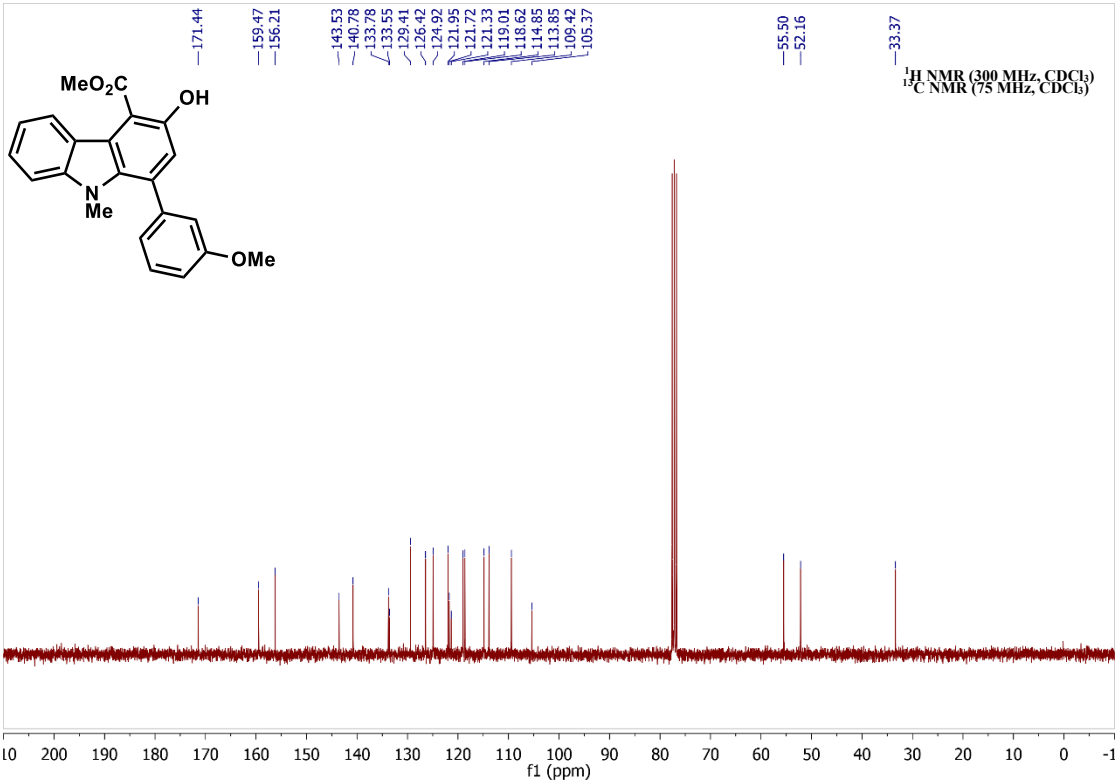
MeO2C
OH
N
Me
OMe
171.44
159.47
156.21
143.53
140.78
133.78
133.55
129.41
126.42
124.92
121.95
121.72
121.33
119.01
118.62
114.85
113.85
109.42
105.37
55.50
52.16
33.37
1H NMR (300 MHz, CDCl3)
13C NMR (75 MHz, CDCl3)
f1 (ppm)

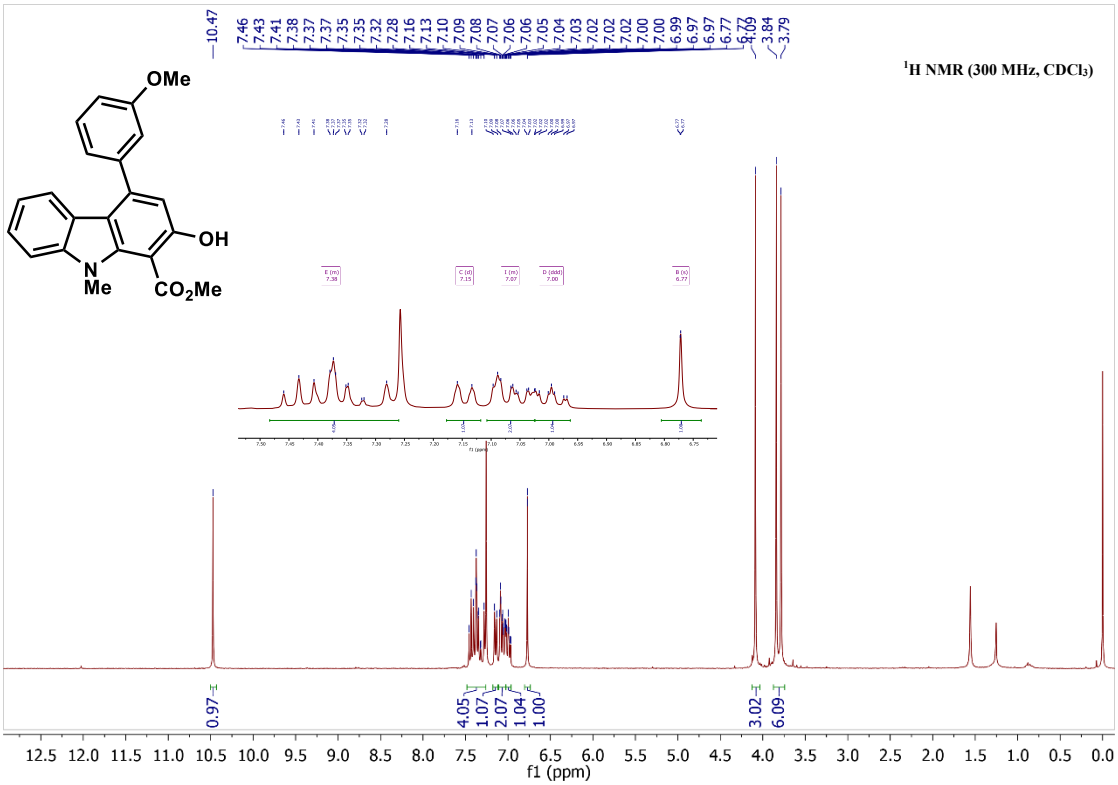
^{1}H NMR (300 MHz, CDCl$_3$)
OMe
OH
N
Me
CO$_2$Me
10.47
7.46
7.43
7.41
7.38
7.37
7.37
7.35
7.35
7.32
7.28
7.16
7.13
7.10
7.09
7.08
7.07
7.06
7.06
7.05
7.04
7.03
7.02
7.02
7.02
7.00
7.00
6.99
6.97
6.97
6.77
6.77
4.09
3.84
3.79
0.97
4.05
1.07
2.07
1.04
1.00
3.02
6.09
f1 (ppm)

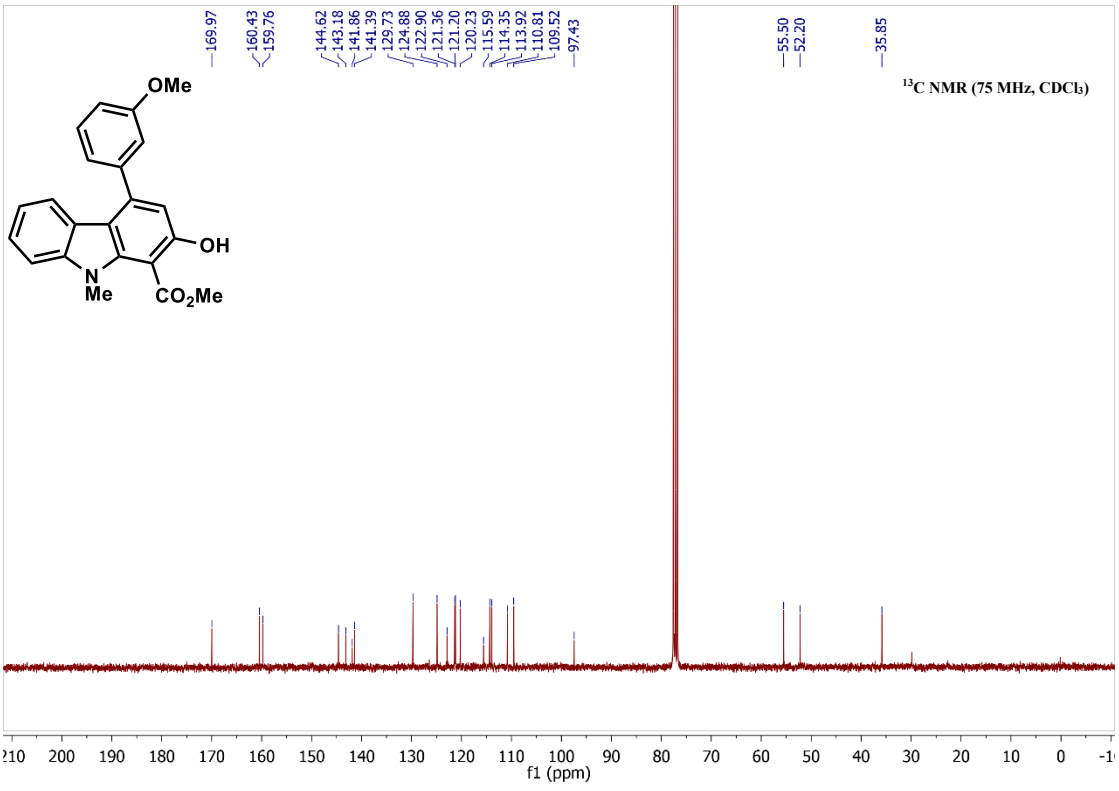
^{13}C NMR (75 MHz, CDCl$_3$)
OMe
OH
N
Me
CO$_2$Me
169.97
160.43
159.76
144.62
143.18
141.86
141.39
129.73
124.88
122.90
121.36
121.20
120.23
115.59
114.35
113.92
110.81
109.52
97.43
55.50
52.20
35.85
f1 (ppm)

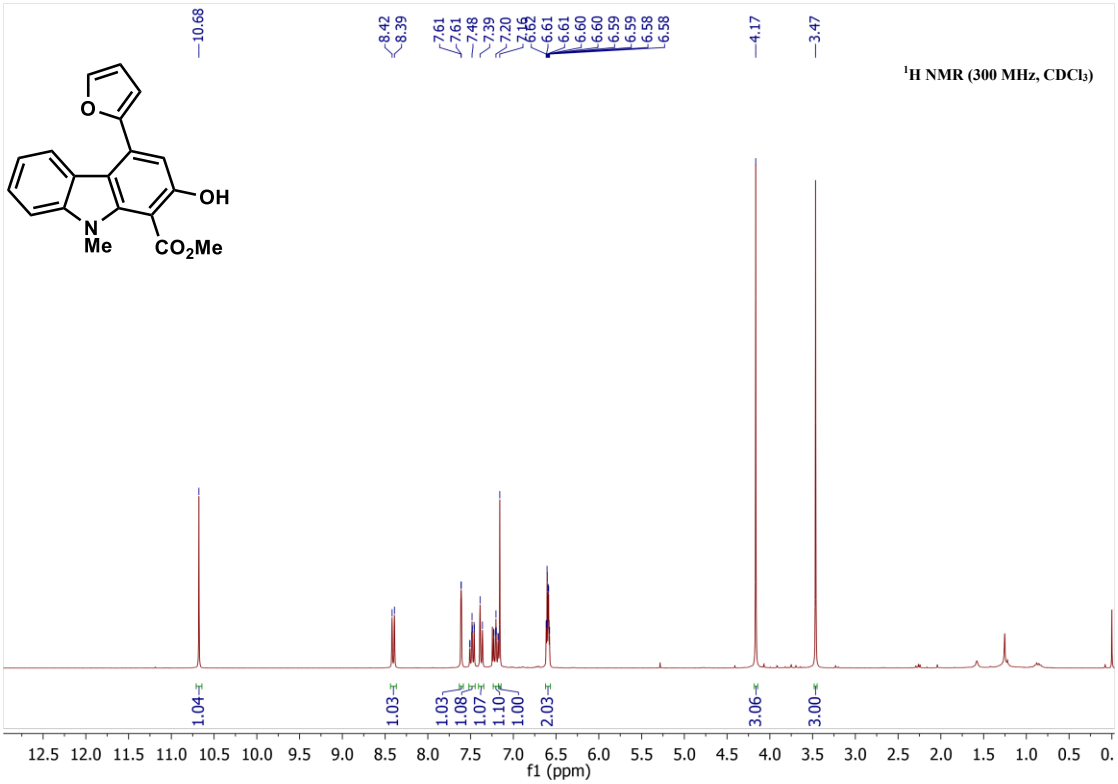
10.68
8.42
8.39
7.61
7.61
7.48
7.39
7.20
7.16
6.62
6.61
6.61
6.60
6.60
6.59
6.59
6.58
6.58
4.17
3.47
1H NMR (300 MHz, CDCl3)
O
OH
N
Me
CO2Me
1.04
1.03
1.03
1.08
1.07
1.10
1.00
2.03
3.06
3.00
12.5 12.0 11.5 11.0 10.5 10.0 9.5 9.0 8.5 8.0 7.5 7.0 6.5 6.0 5.5 5.0 4.5 4.0 3.5 3.0 2.5 2.0 1.5 1.0 0.5 0.
f1 (ppm)

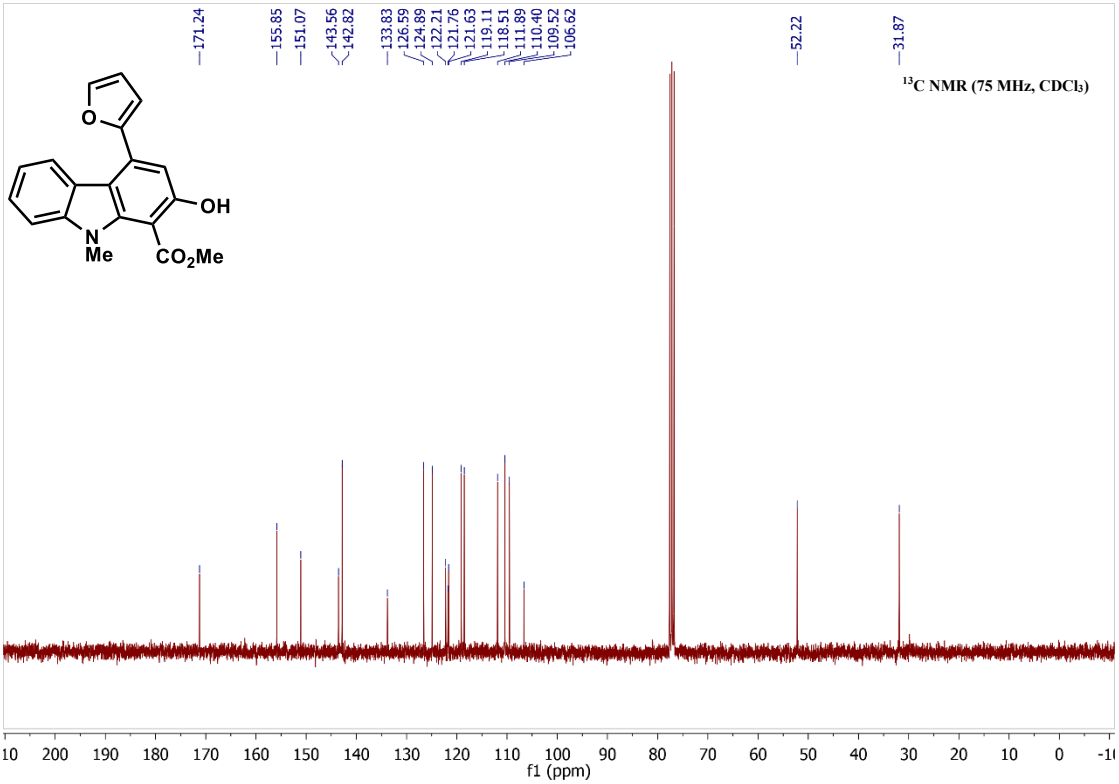
171.24
155.85
151.07
143.56
142.82
133.83
126.59
124.89
122.21
121.76
121.63
119.11
118.51
111.89
110.40
109.52
106.62
52.22
31.87
13C NMR (75 MHz, CDCl3)
O
OH
N
Me
CO2Me
10 200 190 180 170 160 150 140 130 120 110 100 90 80 70 60 50 40 30 20 10 0 -10
f1 (ppm)

3.12 X-ray Crystallographic Analysis of 126

Experimental details

Single-crystal X-ray diffraction data was collected at 100(2) K on a XtaLAB Synergy-S, Dualflex, HyPix-6000HE diffractometer using Cu-K radiation (λ = 1.5406 Å). Crystal was mounted on nylon CryoLoops with Paraton-N. The data collection and reduction were processed within *CrysAlisPro* (Rigaku OD, 2019). A multi-scan absorption correction was applied to the collected reflections. Using Olex^2 [1], the structure was solved with the ShelXT [2] structure solution program using Intrinsic Phasing and refined with the ShelXL [3] refinement package using Least Squares minimisation. All non-hydrogen atoms were refined anisotropically. The hydroxyl hydrogen atom was located in difference Fourier maps and refined by using the HTAB command. The organic hydrogen atoms were generated geometrically.

1. Dolomanov, O.V., Bourhis, L.J., Gildea, R.J, Howard, J.A.K. & Puschmann, H. (2009), *J. Appl. Cryst*. 42, 339-341.
2. Sheldrick, G.M. (2015). *Acta Cryst*. A71, 3-8.
3. Sheldrick, G.M. (2015). *Acta Cryst*. C71, 3-8.

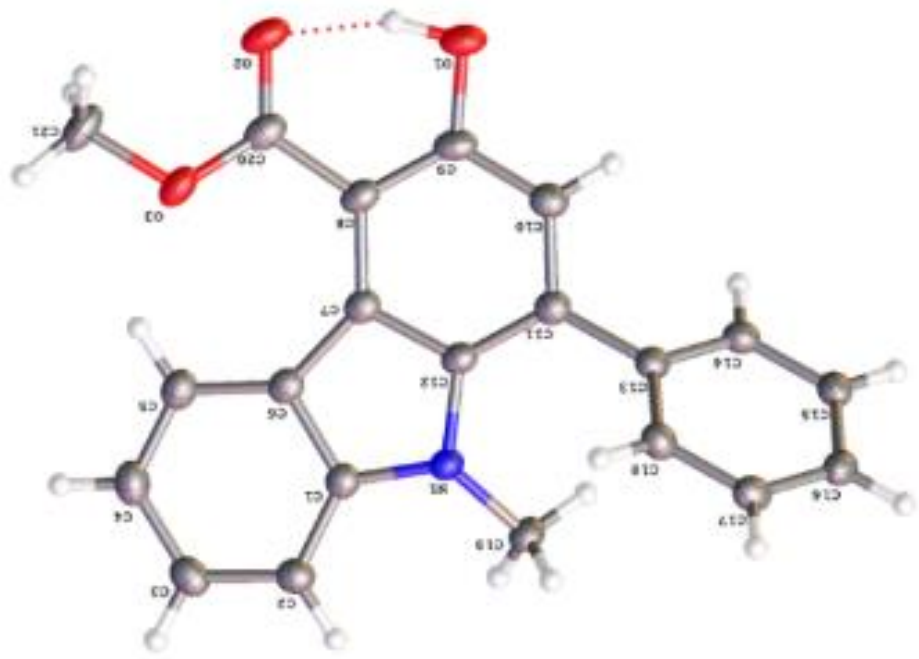

Figure **3.3**: X-ray crystal structure of **126** (non-hydrogen atoms are represented by displacement ellipsoids at the 50% probability level)

Table 3.6: Crystal data and structure refinement for **126**

Empirical formula	$C_{21}H_{17}NO_3$
Formula weight	331.36
Temperature/K	100(2)
Crystal system	monoclinic
Space group	*C*2/*c*
a/Å	7.05741(6)
b/Å	19.83846(19)
c/Å	23.04368(20)
α/°	90
β/°	95.9321(8)
γ/°	90
Volume/Å^3	3209.03(5)
Z	8
ρ_{calc}g/cm^3	1.372
μ/mm^{-1}	0.744
F(000)	1392.0
Crystal size/mm^3	0.2 × 0.2 × 0.1
Radiation	CuK$_\alpha$ (λ = 1.54184)
2Θ range for data collection/°	7.714 to 154.736
Index ranges	$-8 \leq h \leq 8$, $-24 \leq k \leq 22$, $-27 \leq l \leq 29$
Reflections collected	28380
Independent reflections	3391 [R_{int} = 0.0589, R_{sigma} = 0.0219]
Data/restraints/parameters	3391/0/233
Goodness-of-fit on F^2	1.074
Final R indexes [I>=2σ (I)]	R_1 = 0.0375, wR_2 = 0.1114
Final R indexes [all data]	R_1 = 0.0511, wR_2 = 0.1265
Largest diff. peak/hole / e Å^{-3}	0.36/-0.38

Table 3.7: Fractional Atomic Coordinates ($\times 10^4$) and Equivalent Isotropic Displacement Parameters ($Å^2 \times 10^3$). U_{eq} is defined as 1/3 of of the trace of the orthogonalised U_{IJ} tensor

Atom	***x***	***y***	***z***	**U(eq)**
O1	7591.3(13)	4580.5(5)	1884.2(4)	30.4(2)
O2	7648.0(14)	5757.1(5)	1431.7(4)	32.1(2)
O3	8182.0(13)	6637.9(5)	2029.4(4)	27.9(2)
N1	6871.4(14)	5807.9(5)	3995.6(4)	20.6(2)
C1	6791.8(16)	6482.0(6)	3851.0(5)	20.8(3)
C2	6563.0(17)	7023.2(6)	4227.3(5)	24.4(3)
C3	6473.3(18)	7665.8(7)	3994.0(6)	27.1(3)
C4	6596.2(18)	7766.4(6)	3396.2(6)	27.9(3)
C5	6849.4(17)	7230.1(6)	3028.6(5)	24.8(3)
C6	6985.8(16)	6567.5(6)	3248.5(5)	21.1(3)
C7	7230.5(15)	5891.6(6)	3014.8(5)	20.5(3)
C8	7457.1(16)	5607.2(6)	2454.4(5)	22.3(3)
C9	7463.6(17)	4903.5(7)	2399.5(5)	24.0(3)
C10	7427.0(17)	4484.1(6)	2887.3(5)	24.3(3)
C11	7324.0(16)	4743.4(6)	3439.8(5)	21.6(3)
C12	7141.6(16)	5445.2(6)	3490.5(5)	20.0(3)
C13	7465.1(17)	4275.6(6)	3946.5(5)	21.6(3)
C14	6169.2(17)	3746.9(6)	3967.5(5)	23.3(3)
C15	6297.0(18)	3310.8(6)	4441.5(5)	24.6(3)
C16	7709.2(19)	3401.0(6)	4902.4(5)	25.4(3)
C17	9013.2(18)	3924.5(6)	4883.8(5)	25.8(3)
C18	8904.9(18)	4357.1(6)	4408.0(5)	24.4(3)
C19	6015.4(18)	5552.4(6)	4503.2(5)	23.7(3)
C20	7746.7(16)	5999.0(7)	1926.6(5)	24.7(3)
C21	8376.2(19)	7057.1(8)	1526.6(6)	32.6(3)

Table 3.8: Selected Bond Distances (Å)

Atom	Atom	Length/Å	Atom	Atom	Length/Å
O1	C9	1.3603(14)	C7	C8	1.4333(16)
O2	C20	1.2326(16)	C7	C12	1.4158(16)
O3	C20	1.3197(17)	C8	C9	1.4020(18)
O3	C21	1.4442(14)	C8	C20	1.4752(16)
N1	C1	1.3779(15)	C9	C10	1.4008(18)
N1	C12	1.3982(14)	C10	C11	1.3822(17)
N1	C19	1.4615(15)	C11	C12	1.4042(17)
C1	C2	1.3999(17)	C11	C13	1.4867(16)
C1	C6	1.4192(16)	C13	C14	1.3958(17)
C2	C3	1.3824(18)	C13	C18	1.4021(17)
C3	C4	1.4033(19)	C14	C15	1.3891(17)
C4	C5	1.3831(18)	C15	C16	1.3908(18)
C5	C6	1.4085(17)	C16	C17	1.3912(18)
C6	C7	1.4618(17)	C17	C18	1.3883(17)

Table 3.9: Selected Bond Angles

Atom	Atom	Atom	Angle/°	Atom	Atom	Atom	Angle/°
C20	O3	C21	116.65(10)	O1	C9	C10	115.40(12)
C1	N1	C12	107.69(9)	C10	C9	C8	121.24(11)
C1	N1	C19	121.35(10)	C11	C10	C9	121.69(12)
C12	N1	C19	126.22(10)	C10	C11	C12	117.36(11)
N1	C1	C2	126.80(11)	C10	C11	C13	119.06(11)
N1	C1	C6	110.30(10)	C12	C11	C13	123.56(11)
C2	C1	C6	122.91(11)	N1	C12	C7	110.08(10)
C3	C2	C1	118.03(11)	N1	C12	C11	126.95(11)
C2	C3	C4	120.53(12)	C11	C12	C7	122.97(11)
C5	C4	C3	121.11(12)	C14	C13	C11	120.35(11)

C4	C5	C6	120.39(11)	C14	C13	C18	119.11(11)
C1	C6	C7	106.13(10)	C18	C13	C11	120.54(11)
C5	C6	C1	116.97(11)	C15	C14	C13	120.38(11)
C5	C6	C7	136.86(11)	C14	C15	C16	120.23(12)
C8	C7	C6	136.18(11)	C15	C16	C17	119.79(11)
C12	C7	C6	105.79(10)	C18	C17	C16	120.21(11)
C12	C7	C8	118.00(11)	C17	C18	C13	120.27(11)
C7	C8	C20	124.98(12)	O2	C20	O3	122.00(11)
C9	C8	C7	118.36(11)	O2	C20	C8	123.92(12)
C9	C8	C20	116.64(11)	O3	C20	C8	114.05(10)
O1	C9	C8	123.29(11)				

Table 3.10. Hydrogen Bonds

D	**H**	**A**	**d(D-H)/Å**	**d(H-A)/Å**	**d(D-A)/Å**	**D-H-A/°**
O1	H1	O2	0.94(2)	1.67(2)	2.5585(15)	158(2)

3.13 X-ray Crystallographic Analysis of 172

Experimental details

Single-crystal X-ray diffraction data was collected at 100(2) K on a XtaLAB Synergy-S, Dualflex, HyPix-6000HE diffractometer using Cu-*K* radiation (λ = 1.5406 Å). Crystal was mounted on nylon CryoLoops with Paraton-N. The data collection and reduction were processed within *CrysAlisPro* (Rigaku OD, 2019). A multi-scan absorption correction was applied to the collected reflections. Using Olex^2 [1], the structure was solved with the ShelXT [2] structure solution program using Intrinsic Phasing and refined with the ShelXL [3] refinement package using Least Squares minimisation. All non-hydrogen atoms were refined anisotropically. The hydroxyl hydrogen atoms were located in difference Fourier maps and refined by using the HTAB command. All other organic hydrogen atoms were generated geometrically. For detailed information about the crystallographic analysis with 2081554 CCDC number refer to: [https://www.ccdc.cam.ac.uk/structures/search?pid=ccdc:2081554&id=doi:10.1021/acs.orglett.1c01965]

1. Dolomanov, O.V., Bourhis, L.J., Gildea, R.J, Howard, J.A.K. & Puschmann, H. (2009), *J. Appl. Cryst*. 42, 339-341.
2. Sheldrick, G.M. (2015). *Acta Cryst*. A71, 3-8.
3. Sheldrick, G.M. (2015). *Acta Cryst*. C71, 3-8.

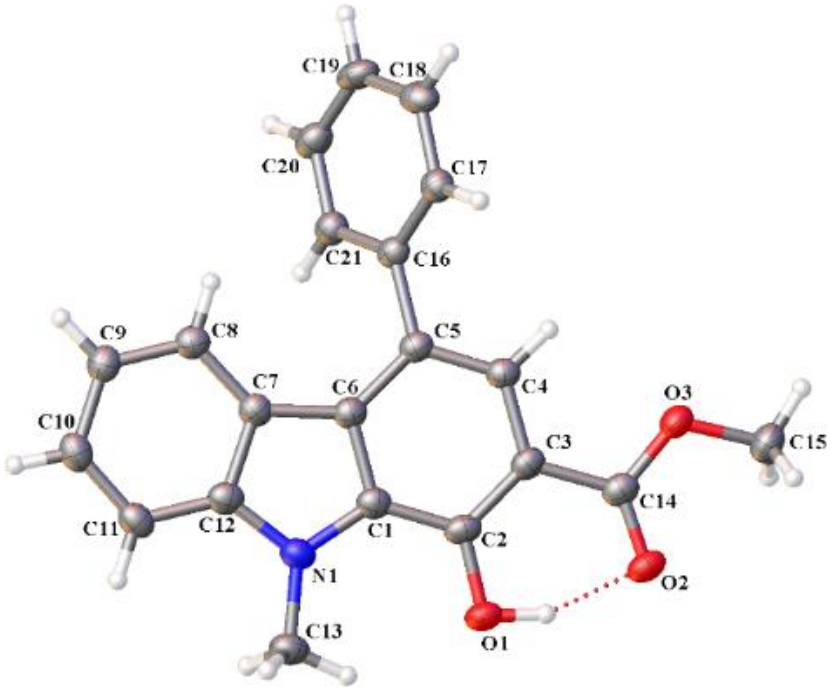

Figure 3.4: X-ray crystal structure of **172** (non-hydrogen atoms are represented by displacement ellipsoids at the 50% probability level)

Table 3.10: Crystal data and structure refinement for **172**

Empirical formula	$C_{21}H_{17}NO_3$
Formula weight	331.36
Temperature/K	100(2)
Crystal system	monoclinic
Space group	$P2_1/c$
a/Å	8.36270(10)
b/Å	17.8643(4)
c/Å	21.5532(4)
β/°	96.119(2)
Volume/Å^3	3201.57(10)
Z	8
ρ_{calc}g/cm^3	1.375
μ/mm^{-1}	0.746
F(000)	1392.0
Crystal size/mm^3	0.266 × 0.062 × 0.025
Radiation	Cu $K\alpha$ (λ = 1.54184)
2θ range for data collection/°	6.442 to 154.808
Index ranges	$-10 \leq h \leq 10$, $-20 \leq k \leq 22$, $-27 \leq l \leq 24$
Reflections collected	39512
Independent reflections	6675 [R_{int} = 0.0693, R_{sigma} = 0.0425]
Data/restraints/parameters	6675/0/463
Goodness-of-fit on F^2	1.027
Final R indexes [I>=2σ (I)]	R_1 = 0.0543, wR_2 = 0.1495
Final R indexes [all data]	R_1 = 0.0718, wR_2 = 0.1638
Largest diff. peak/hole / e Å^{-3}	0.31/-0.26

Table 3.11: Fractional Atomic Coordinates ($\times 10^4$) and Equivalent Isotropic Displacement Parameters ($Å^2 \times 10^3$). U_{eq} is defined as 1/3 of the trace of the orthogonalised U_{IJ} tensor.

Atom	*x*	*y*	*z*	U(eq)
O1	3216.3(16)	6594.0(8)	4748.1(6)	32.0(3)
O2	3190.1(15)	5152.7(8)	4694.6(5)	32.3(3)
O3	4196.0(15)	4590.5(7)	3890.8(5)	30.1(3)
N1	4150.4(18)	7977.5(9)	4114.1(7)	28.4(3)
C1	4345(2)	7244.3(10)	3928.2(7)	26.5(4)
C2	3947(2)	6574.0(11)	4214.5(7)	27.4(4)
C3	4321(2)	5901.5(10)	3933.0(7)	26.2(4)
C4	5019.2(19)	5901.8(10)	3360.2(7)	25.3(4)
C5	5352.8(19)	6553.3(10)	3062.9(7)	25.0(4)
C6	5060.9(19)	7238.4(10)	3361.1(7)	24.9(4)
C7	5344.5(19)	8008.4(10)	3212.6(8)	25.6(4)
C8	6051(2)	8376.8(10)	2733.4(8)	27.1(4)
C9	6111(2)	9148.3(10)	2730.7(8)	28.9(4)
C10	5495(2)	9568.4(11)	3201.5(8)	30.8(4)
C11	4816(2)	9225.4(11)	3685.4(8)	29.7(4)
C12	4751(2)	8444.5(11)	3685.4(8)	28.2(4)
C13	3415(2)	8255.1(12)	4649.8(8)	33.7(4)
C14	3856(2)	5197.2(11)	4212.8(8)	28.1(4)
C15	3624(2)	3886.0(11)	4107.5(9)	35.6(4)
C16	5839(2)	6520.0(10)	2417.9(7)	25.0(4)
C17	7080(2)	6051.1(10)	2268.7(8)	27.6(4)
C18	7445(2)	5989.9(11)	1658.0(9)	33.0(4)
C19	6576(2)	6393.4(12)	1186.2(8)	35.8(4)
C20	5338(2)	6860.8(12)	1327.6(8)	33.2(4)
C21	4964(2)	6922.5(10)	1937.5(8)	28.4(4)

Atom	*x*	*y*	*z*	U(eq)
O4	-1686.5(16)	8110.6(9)	4762.8(6)	34.7(3)
O5	-1782.8(16)	9548.4(8)	4713.9(5)	34.0(3)
O6	-894.1(15)	10132.7(7)	3896.5(6)	31.2(3)
N2	-772.6(18)	6742.0(9)	4109.9(7)	29.0(3)
C22	-619(2)	7480.0(10)	3922.5(7)	26.3(4)
C23	-1023(2)	8144.1(11)	4215.5(8)	27.6(4)
C24	-704(2)	8824.4(10)	3927.6(8)	26.0(4)
C25	-51(2)	8831.8(10)	3346.7(8)	25.3(4)
C26	296.5(19)	8180.5(10)	3046.0(7)	24.4(3)
C27	60.4(19)	7494.1(10)	3348.3(7)	25.1(4)
C28	379.7(19)	6721.9(10)	3197.0(8)	25.6(4)
C29	1080(2)	6365.5(10)	2714.2(8)	26.4(4)
C30	1178(2)	5596.2(11)	2710.6(8)	29.2(4)
C31	589(2)	5165.0(11)	3183.9(8)	30.2(4)
C32	-86(2)	5501.2(11)	3673.3(8)	30.2(4)
C33	-173(2)	6283.5(10)	3676.8(8)	26.7(4)
C34	-1473(2)	6458.7(12)	4652.1(8)	34.7(4)
C35	-1175(2)	9520.5(11)	4219.0(8)	28.5(4)
C36	-1444(2)	10830.1(11)	4138.3(9)	36.4(4)
C37	765.4(19)	8212.9(10)	2398.8(8)	24.8(3)
C38	2021(2)	8670.2(10)	2247.4(8)	27.2(4)
C39	2402(2)	8713.6(11)	1636.3(8)	32.0(4)
C40	1544(2)	8301.3(11)	1169.0(8)	32.5(4)
C41	274(2)	7849.3(11)	1311.6(8)	31.0(4)
C42	-109(2)	7808.8(10)	1919.4(8)	26.6(4)

Table 3.12: Selected Bond Distances (Å)

Atom	Atom	Length/Å	Atom	Atom	Length/Å
O1	C2	1.359(2)	O4	C23	1.358(2)
O2	C14	1.232(2)	O5	C35	1.231(2)
O3	C14	1.334(2)	O6	C35	1.330(2)
O3	C15	1.442(2)	O6	C36	1.444(2)
N1	C1	1.384(2)	N2	C22	1.389(2)
N1	C12	1.379(2)	N2	C33	1.376(2)
N1	C13	1.452(2)	N2	C34	1.453(2)
C1	C2	1.403(3)	C22	C23	1.402(3)
C1	C6	1.417(2)	C22	C27	1.416(2)
C2	C3	1.396(3)	C23	C24	1.403(3)
C3	C4	1.421(2)	C24	C25	1.418(2)
C3	C14	1.465(2)	C24	C35	1.466(2)
C4	C5	1.372(2)	C25	C26	1.378(2)
C5	C6	1.416(2)	C26	C27	1.412(2)
C5	C16	1.491(2)	C26	C37	1.490(2)
C6	C7	1.438(2)	C27	C28	1.449(3)
C7	C8	1.407(2)	C28	C29	1.400(2)
C7	C12	1.414(2)	C28	C33	1.413(2)
C8	C9	1.379(3)	C29	C30	1.377(3)
C9	C10	1.403(3)	C30	C31	1.409(3)
C10	C11	1.383(3)	C31	C32	1.385(3)
C11	C12	1.396(3)	C32	C33	1.399(3)
C16	C17	1.397(2)	C37	C38	1.396(2)
C16	C21	1.401(2)	C37	C42	1.401(2)
C17	C18	1.387(2)	C38	C39	1.390(2)
C18	C19	1.387(3)	C39	C40	1.385(3)

Atom	Atom	Length/Å	Atom	Atom	Length/Å
C19	C20	1.389(3)	C40	C41	1.394(3)
C20	C21	1.388(2)	C41	C42	1.383(2)

Table 3.13: Selected Bond Angles

Atom	Atom	Atom	Angle/°	Atom	Atom	Atom	Angle/°
C14	O3	C15	116.38(14)	C35	O6	C36	116.11(14)
C1	N1	C13	128.76(16)	C22	N2	C34	128.49(16)
C12	N1	C1	108.42(14)	C33	N2	C22	108.42(14)
C12	N1	C13	122.80(16)	C33	N2	C34	123.07(16)
N1	C1	C2	129.74(16)	N2	C22	C23	129.64(16)
N1	C1	C6	109.28(15)	N2	C22	C27	109.22(15)
C2	C1	C6	120.99(16)	C23	C22	C27	121.13(16)
O1	C2	C1	119.92(16)	O4	C23	C22	119.64(16)
O1	C2	C3	122.15(16)	O4	C23	C24	122.49(17)
C3	C2	C1	117.92(16)	C22	C23	C24	117.87(15)
C2	C3	C4	120.61(16)	C23	C24	C25	120.51(16)
C2	C3	C14	118.57(15)	C23	C24	C35	118.22(16)
C4	C3	C14	120.62(16)	C25	C24	C35	121.11(16)
C5	C4	C3	121.94(16)	C26	C25	C24	121.85(16)
C4	C5	C6	117.91(15)	C25	C26	C27	117.99(15)
C4	C5	C16	119.42(16)	C25	C26	C37	119.82(16)
C6	C5	C16	122.36(15)	C27	C26	C37	121.97(15)
C1	C6	C7	106.25(15)	C22	C27	C28	106.29(15)
C5	C6	C1	120.47(16)	C26	C27	C22	120.50(16)
C5	C6	C7	133.28(15)	C26	C27	C28	133.21(15)
C8	C7	C6	134.68(16)	C29	C28	C27	134.57(16)
C8	C7	C12	118.58(17)	C29	C28	C33	119.14(17)
C12	C7	C6	106.73(15)	C33	C28	C27	106.29(15)

Atom	Atom	Atom	Angle/°	Atom	Atom	Atom	Angle/°
C9	C8	C7	119.27(16)	C30	C29	C28	119.19(16)
C8	C9	C10	121.00(17)	C29	C30	C31	121.08(17)
C11	C10	C9	121.34(18)	C32	C31	C30	121.10(18)
C10	C11	C12	117.52(16)	C31	C32	C33	117.57(16)
N1	C12	C7	109.30(16)	N2	C33	C28	109.74(16)
N1	C12	C11	128.43(16)	N2	C33	C32	128.38(16)
C11	C12	C7	122.26(16)	C32	C33	C28	121.88(16)
O2	C14	O3	121.78(17)	O5	C35	O6	122.13(17)
O2	C14	C3	124.45(17)	O5	C35	C24	124.09(17)
O3	C14	C3	113.76(14)	O6	C35	C24	113.78(15)
C17	C16	C5	121.43(15)	C38	C37	C26	121.40(15)
C17	C16	C21	118.66(16)	C38	C37	C42	118.40(15)
C21	C16	C5	119.74(16)	C42	C37	C26	120.11(15)
C18	C17	C16	120.64(17)	C39	C38	C37	120.54(17)
C17	C18	C19	120.25(18)	C40	C39	C38	120.42(17)
C18	C19	C20	119.73(16)	C39	C40	C41	119.70(16)
C21	C20	C19	120.26(18)	C42	C41	C40	119.86(17)
C20	C21	C16	120.45(17)	C41	C42	C37	121.07(17)

Table 3.14: Selected Torsion Angles

A	B	C	D	Angle/°	A	B	C	D	Angle/°
O1	C2	C3	C4	177.16(15)	O4	C23	C24	C25	-178.22(15)
O1	C2	C3	C14	2.2(2)	O4	C23	C24	C35	-2.8(2)
N1	C1	C2	O1	2.0(3)	N2	C22	C23	O4	-0.8(3)
N1	C1	C2	C3	-178.15(16)	N2	C22	C23	C24	178.57(16)
N1	C1	C6	C5	-178.42(14)	N2	C22	C27	C26	178.00(14)
N1	C1	C6	C7	1.60(18)	N2	C22	C27	C28	-2.04(18)
C1	N1	C12	C7	0.06(19)	C22	N2	C33	C28	-0.16(19)

A	B	C	D	Angle/°	A	B	C	D	Angle/°
C1	N1	C12	C11	-179.63(16)	C22	N2	C33	C32	-179.77(16)
C1	C2	C3	C4	-2.7(2)	C22	C23	C24	C25	2.4(2)
C1	C2	C3	C14	-177.65(15)	C22	C23	C24	C35	177.86(15)
C1	C6	C7	C8	177.76(18)	C22	C27	C28	C29	-177.38(18)
C1	C6	C7	C12	-1.52(18)	C22	C27	C28	C33	1.90(18)
C2	C1	C6	C5	1.6(2)	C23	C22	C27	C26	-2.2(3)
C2	C1	C6	C7	-178.40(15)	C23	C22	C27	C28	177.79(15)
C2	C3	C4	C5	0.0(3)	C23	C24	C25	C26	-0.2(3)
C2	C3	C14	O2	-2.2(3)	C23	C24	C35	O5	2.7(3)
C2	C3	C14	O3	176.80(14)	C23	C24	C35	O6	-176.90(14)
C3	C4	C5	C6	3.4(2)	C24	C25	C26	C27	-3.2(2)
C3	C4	C5	C16	-170.33(15)	C24	C25	C26	C37	171.57(15)
C4	C3	C14	O2	-177.12(16)	C25	C24	C35	O5	178.14(16)
C4	C3	C14	O3	1.8(2)	C25	C24	C35	O6	-1.5(2)
C4	C5	C6	C1	-4.2(2)	C25	C26	C27	C22	4.3(2)
C4	C5	C6	C7	175.82(16)	C25	C26	C27	C28	-175.63(17)
C4	C5	C16	C17	-51.3(2)	C25	C26	C37	C38	53.4(2)
C4	C5	C16	C21	123.81(18)	C25	C26	C37	C42	-123.39(18)
C5	C6	C7	C8	-2.2(3)	C26	C27	C28	C29	2.6(3)
C5	C6	C7	C12	178.50(17)	C26	C27	C28	C33	-178.15(17)
C5	C16	C17	C18	175.68(16)	C26	C37	C38	C39	-177.62(16)
C5	C16	C21	C20	-175.95(16)	C26	C37	C42	C41	177.96(16)
C6	C1	C2	O1	-177.99(15)	C27	C22	C23	O4	179.38(15)
C6	C1	C2	C3	1.9(2)	C27	C22	C23	C24	-1.2(2)
C6	C5	C16	C17	135.25(18)	C27	C26	C37	C38	-132.10(18)
C6	C5	C16	C21	-49.6(2)	C27	C26	C37	C42	51.1(2)
C6	C7	C8	C9	179.33(17)	C27	C28	C29	C30	-179.22(17)

A	B	C	D	Angle/°	A	B	C	D	Angle/°
C6	C7	C12	N1	0.93(18)	C27	C28	C33	N2	-1.10(18)
C6	C7	C12	C11	-179.36(15)	C27	C28	C33	C32	178.55(15)
C7	C8	C9	C10	0.7(2)	C28	C29	C30	C31	-0.1(2)
C8	C7	C12	N1	-178.49(14)	C29	C28	C33	N2	178.31(15)
C8	C7	C12	C11	1.2(2)	C29	C28	C33	C32	-2.0(2)
C8	C9	C10	C11	0.3(3)	C29	C30	C31	C32	-1.0(3)
C9	C10	C11	C12	-0.6(2)	C30	C31	C32	C33	0.6(2)
C10	C11	C12	N1	179.46(17)	C31	C32	C33	N2	-179.46(16)
C10	C11	C12	C7	-0.2(2)	C31	C32	C33	C28	1.0(2)
C12	N1	C1	C2	178.94(17)	C33	N2	C22	C23	-178.41(17)
C12	N1	C1	C6	-1.06(19)	C33	N2	C22	C27	1.40(19)
C12	C7	C8	C9	-1.5(2)	C33	C28	C29	C30	1.6(2)
C13	N1	C1	C2	-2.7(3)	C34	N2	C22	C23	3.3(3)
C13	N1	C1	C6	177.30(16)	C34	N2	C22	C27	-176.92(16)
C13	N1	C12	C7	-178.41(15)	C34	N2	C33	C28	178.28(15)
C13	N1	C12	C11	1.9(3)	C34	N2	C33	C32	-1.3(3)
C14	C3	C4	C5	174.91(15)	C35	C24	C25	C26	-175.52(15)
C15	O3	C14	O2	5.0(2)	C36	O6	C35	O5	-4.0(2)
C15	O3	C14	C3	-174.02(14)	C36	O6	C35	C24	175.59(14)
C16	C5	C6	C1	169.35(15)	C37	C26	C27	C22	-170.30(15)
C16	C5	C6	C7	-10.7(3)	C37	C26	C27	C28	9.8(3)
C16	C17	C18	C19	-0.2(3)	C37	C38	C39	C40	-0.3(3)
C17	C16	C21	C20	-0.7(3)	C38	C37	C42	C41	1.1(3)
C17	C18	C19	C20	0.1(3)	C38	C39	C40	C41	1.0(3)
C18	C19	C20	C21	-0.3(3)	C39	C40	C41	C42	-0.7(3)
C19	C20	C21	C16	0.6(3)	C40	C41	C42	C37	-0.3(3)
C21	C16	C17	C18	0.5(3)	C42	C37	C38	C39	-0.8(3)

Table 3.15: Hydrogen Bonds

D	H	A	d(D-H)/Å	d(H-A)/Å	d(D-A)/Å	D-H-A/°
O1	H1	O2	0.95(3)	1.68(3)	2.577(2)	156(2)
O4	H4A	O5	0.93(3)	1.69(3)	2.572(2)	158(3)

References:

1) C. S. Shanahan, P. Truong, S. M. Mason, J. S. Leszcynski, M. P. Doyle, *Org. Lett.*, **2013**, *15*, 3642-3645

Chapter 4: Exploiting Diazo-Enones in Natural Products Synthesis in Hauser-Kraus Annulation

4.1 Introduction and Overview

As described in Chapters 2 and 3, owing to their multifunctional nature, *α,β*-unsaturated diazoketones have been amenable to tandem or sequential bond forming transformations to generate molecular complexity in short order. By utilizing this multifunctional character, we successfully developed a method to construct substituted carbazoles from **1** and **2** through a two-step Michael addition/annulation rearranged sequence that formed one new C–C bond in each step of the sequence (Scheme 4.1A, see Chapter 3 for details). Encouraged by these results, we envisioned that diazo-enones **5** could be further leveraged to form several bonds, in potentially as little as one step, while constructing complex fused ring systems (Scheme 4.1B). Of particular interest would be the exploitation of **5** in the synthesis of complex bioactive natural products, a topic that forms the foundation of this chapter of the thesis.

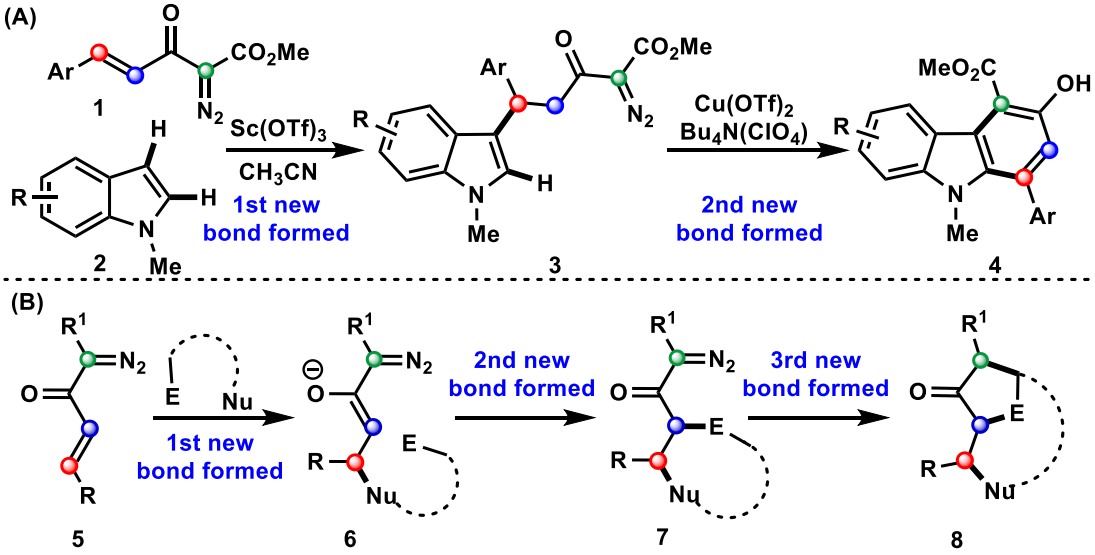

Scheme 4.1: (A) Rearranged carbazole construction via two C–C bond formation sequences exploiting diazo-enones. **(B)** Fused ring system construction by several bond formation utilizing functionalized diazo-enones.

4.1.1 Utilization of Diazo-Enones in Natural Product Synthesis

In the field of synthetic chemistry, diazo-enones have been demonstrated to be useful starting materials in the construction of scaffolds that are present in nature. In

2014, the Burtoloso group developed a three-step synthetic method involving *α,β*-unsaturated diazoketones to produce the natural product preussin and some of its analogues (Scheme 4.2).[1] The alkaloid preussin demonstrates potent antifungal, antiviral, and antibacterial properties, while also triggering apoptosis in multiple human cancer cell lines.[2] The long alkyl chain of the natural product was installed through the preparation of diazo-enone **11**, which was synthesized from decanal (**10**) and the olefination reagent diethyl 3-diazo-2-oxopropylphosphonate **9** via Horner-Wadsworth-Emmons Reaction. Next, the diazo-enone **11** was subjected to a reaction with methylbenzylamine (**12**), which furnished intermediate **13** via aza-Michael addition reaction. Treatment of **13** with $Cu(acac)_2$ provided ylide intermediate **14**, via an intramolecular cyclization, which then underwent a 1,2-Stevens rearrangement.[3] This transformation leads to the formation of the thermodynamically more stable 2,5-*cis*-pyrrolidinone **15** in a yield of 57%. Finally, preussin (**16**) was delivered in 80% yield upon reduction of **15** with L-selectride as the reducing agent. An overall 40% yield was reported for this multi-step synthesis, in which the diazo-enone **11** was manipulated as the main building block.

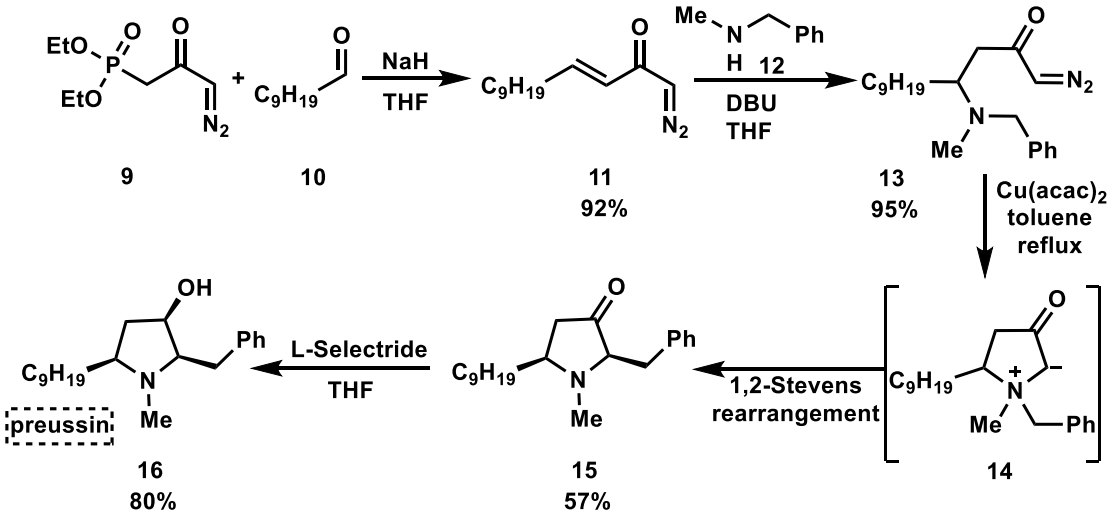

Scheme 4.2: Synthesis of preussin from diazo-enone **11**.

In a subsequent study, Burtoloso and co-workers investigated the synthesis of barmumycin by employing another "acceptor" type diazo-enone **17**.[4] The total synthesis of the natural product barmumycin (**24**) was accomplished in three steps from pyrrolidinone **19** (Scheme 4.3). Diazo-enone **17** and amine **18** were subjected to a copper catalyst to form **19** in a 50% yield via a one-pot Michael addition/N–H insertion

sequence. The transformation was followed by the installation of the exocyclic double bond via Julia-Kocienski olefination[5] employing 5-ethylsulfonyl-1-phenyltetrazole **20** in the presence of LDA. Next, the removal of both the PMB (*para*-methoxybenzyl) and TBS (*t*-butyldimethylsilyl) protecting groups was carried out using 1-chloroethyl chloroformate (ACE-Cl).[6] This process yielded crude alcohol **22**, which was used in crude in the subsequent step. The final step involved coupling of the free amine with vanillic acid **23** to furnish barmumycin in overall 27% overall yield from **21**. As showcased in the last two examples (Scheme 4.2 and 4.3), utilization of diazo-enones substrates to construct complex molecules can be a valuable synthetic strategy in the synthesis of natural products along with their unnatural analogs.

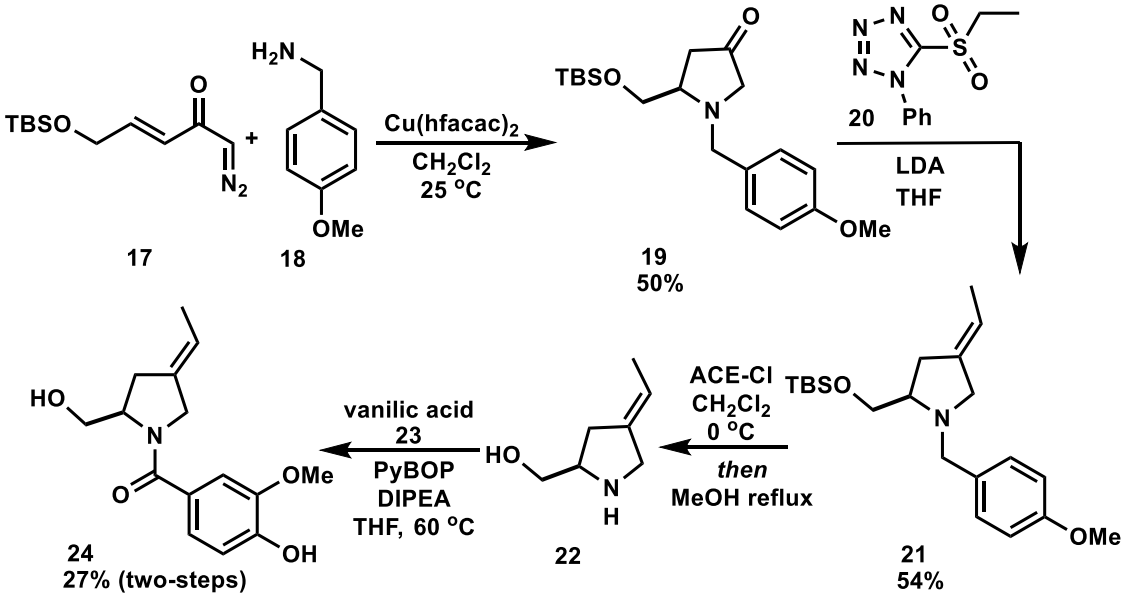

Scheme 4.3: Three-step barmumycin synthesis.

4.2 Hauser-Kraus Annulation

4.2.1 Introduction

Polycyclic aromatic compounds have been known to display a range of important physical and biological properties[7] and, as such, the synthesis of these types of compounds has been of ongoing interest to the organic chemist. Annulation reactions play a crucial role in synthesizing polycyclic compounds, and researchers have developed many annulation methodologies to accomplish the synthesis of these systems.[8] The Hauser-Kraus (H-K) annulation is a well-known reaction that entails a

benzannulation of an appropriate substrate to generate fused ring systems. For the first time in 1978, Hauser et al. described the synthesis of substituted naphthalenes **28** by employing 3-(phenylsulfonyl)phthalide (**25**) in a reaction with *α,β*-unsaturated carbonyl compounds **27** under basic conditions (Scheme 4.4).[9a] At about the same time as Hauser, Kraus and co-workers reported the synthesis of **28** in a similar reaction of 3-cyanophthalide (**26**) with enone substrates **27** in slightly higher yields when compared to the reactions performed by Hauser.[9b] After these findings, researchers have exploited this annulation reaction of phthalides with a variety of Michael acceptors, including acrylates, *α,β*-unsaturated carbonyl compounds, acrylonitriles, vinyl sulfones, vinyl phosphonates, imines, allene carboxylates, and dienones or dienamine to generate various functionalized dihydroxynapthalenes.[10]

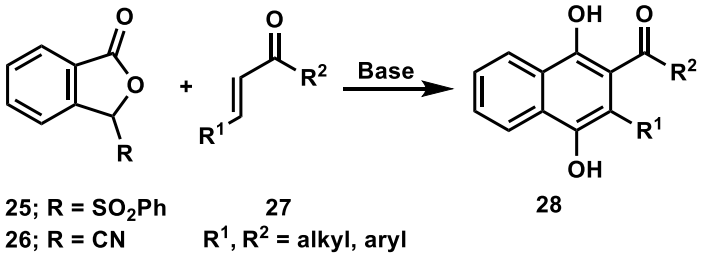

Scheme 4.4: Classical Hauser-Kraus annulation reaction.

4.2.2 Mechanism of the Hauser-Kraus Annulation

Mechanistically, a Hauser-Kraus annulation can proceed through either a stepwise or concerted pathway, both of which involve a base-mediated process (Scheme 4.5).[10] The stepwise mechanism (path a) commences with the deprotonation of phthalide **26**, which then initiates a 1,4-addition reaction with **27** to generate the Michael adduct intermediate **30**. Next, **30** can undergo a Dieckmann-type condensation involving the lactone carbonyl group, leading to the formation of a naphthoquinone intermediate **31** upon loss of $^{-}$CN, which undergoes a tautomerization and yields the final product known as the Hauser-Kraus product **28** (path a, Scheme 4.5). Alternatively, the H-K annulation can proceed via a [4+2]-cycloaddition mechanism initiated by the deprotonation of **26**, following a Diels-Alder type reaction with enone **27** leading to the formation of a bridged cyclic intermediate **32**. A subsequent ring opening of **32**, followed by tautomerization of **31**, furnishes product **28** (path b, Scheme 4.5).

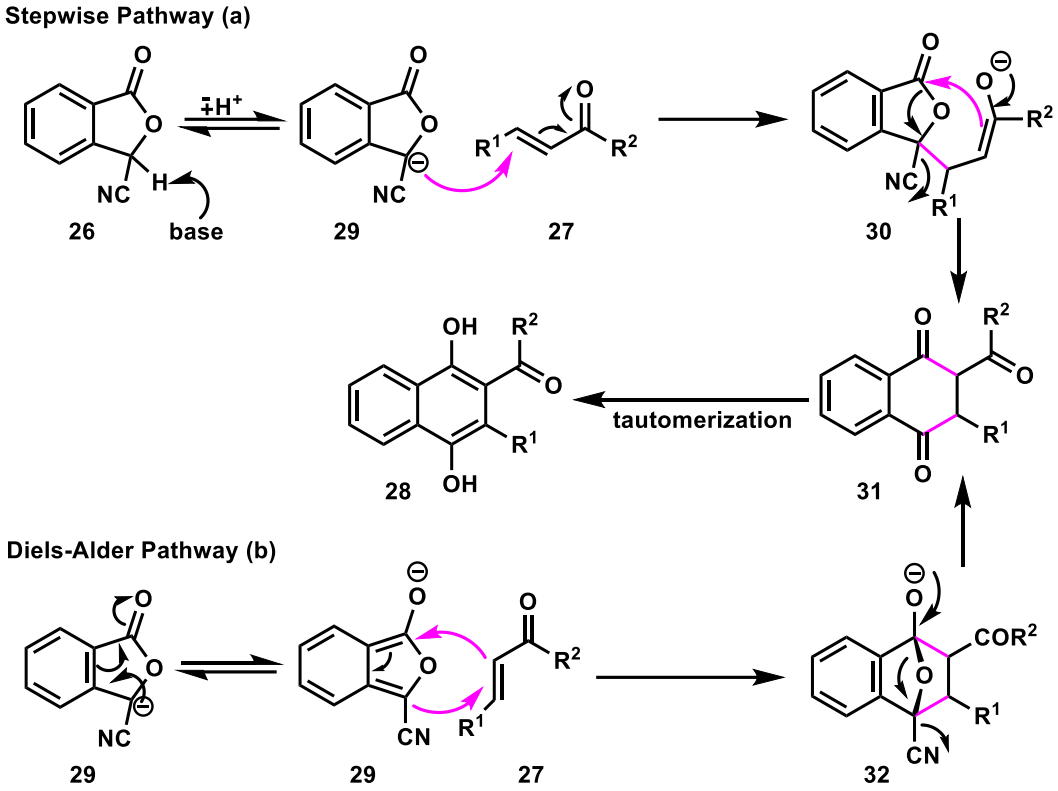

Scheme 4.5: Mechanism of Hauser-Kraus annulation.

4.2.3 Recent Advances of Hauser-Kraus Annulation in Natural Product Synthesis

Several natural products and pharmaceuticals contain complex fused-aromatic ring systems, and the Hauser-Kraus annulation has proven to be a valuable tool for their synthesis.[11] For example, parvinaphthol B (**37**), a natural product extracted from the roots of *Pentas parvifolia*, which has revealed cytotoxic properties against cell lines associated with breast cancer, has recently been synthesized by Ahn and Han through a H-K annulation pathway (Scheme 4.6).[12] In order to obtain cyano phthalide **35**, a three-step synthetic approach was employed, commencing from piperonylic acid (**33**). The carboxylic acid **33** was subjected to a sequential treatment with oxalyl chloride and the corresponding diethylamine to obtain an amide. Next, directed *ortho*-lithiation of this amide was achieved by treatment with *t*-BuLi in the presence of tetramethylethylenediamine, leading to the formation of aldehyde **34** upon quenching the corresponding lithiate with DMF. Aldehyde **34** was subjected to a reaction with KCN and TMSCN (trimethylsilyl cyanide) to form the cyanophthalide **35** in 94% yield. LiHMDS (lithium hexamethyldisilazide) was utilized as base to promote the H-K

annulation of phthalide **35** and methyl acrylate. The product of the annulation (dihydroxynaphthoate) underwent a methylation reaction to afford dimethoxynaphthoate **36**. The final step of the synthesis involved the addition of boron trichloride (BCl_3) to a solution of **36** in CH_2Cl_2 at room temperature, which delivered parvinaphthol B in 71%.

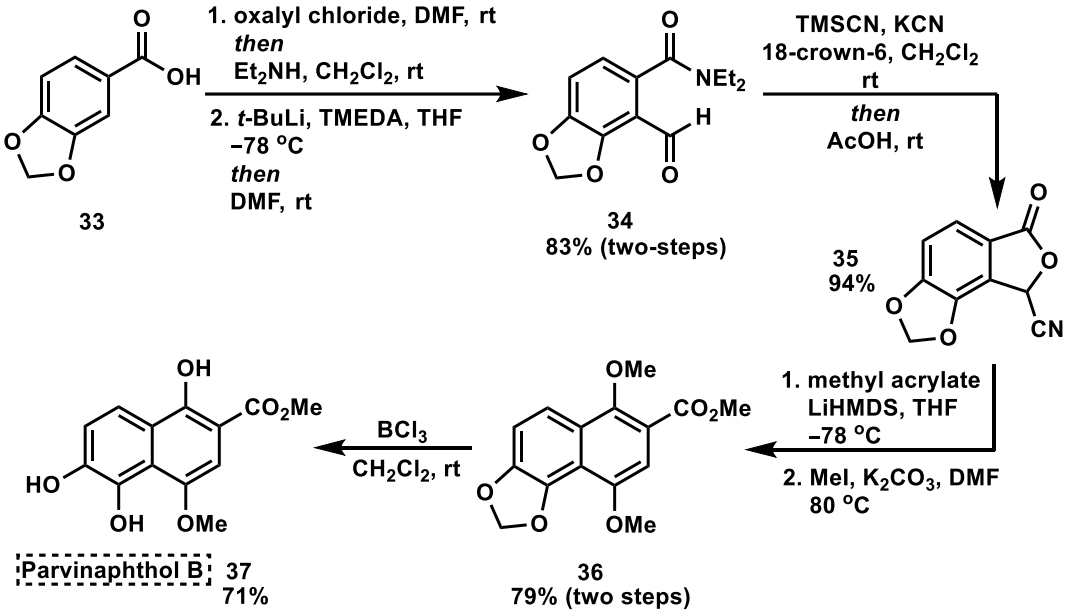

Scheme 4.6: Synthetic pathway for parvinaphthol B.

In a recent report by the Kraus group, naphthacemycin A9 was synthesized in nine-steps by a sequence featuring a Diels-Alder reaction of a hindered arylbutadiene and a Hauser-Kraus annulation reaction (Scheme 4.7).[13] Preparation of the 3-cyanophthalide precursor **42** involved several steps and started from aldehyde **38**. An aldol reaction was conducted with **38** and acetone, followed by silyl enol ether formation that delivered diene **39**. Diene **39** was subjected to a Diels-Alder reaction with alkyne **40**, resulting in the formation of a dihydrobiphenyl intermediate. Upon reacting this intermediate with DDQ and then tetrabutylammonium fluoride (TBAF), the following hydrolysis yielded the formylbiphenylcarboxylate (**41**) in 63% yield. After methylation of the hydroxy group, the phthalide **42** was delivered under KCN and TMSCN conditions. After obtaining **42**, the Hauser-Kraus annulation was carried out using lithium *t*-butoxide (LiO*t*-Bu) and enone **43**, resulting in the formation of a 1,4-dihydroxy tetracyclic compound. Finally, a subsequent debenzylation and oxidation led to the formation of the final product **44**. As shown through these two recent

examples (Scheme 4.6 and 4.7), the efficiency and versatility of the Hauser-Kraus annulation to construct densely functionalized naphthalene ring systems has become a powerfull strategy in the synthesis of polycyclic aromatic natural product scaffolds.

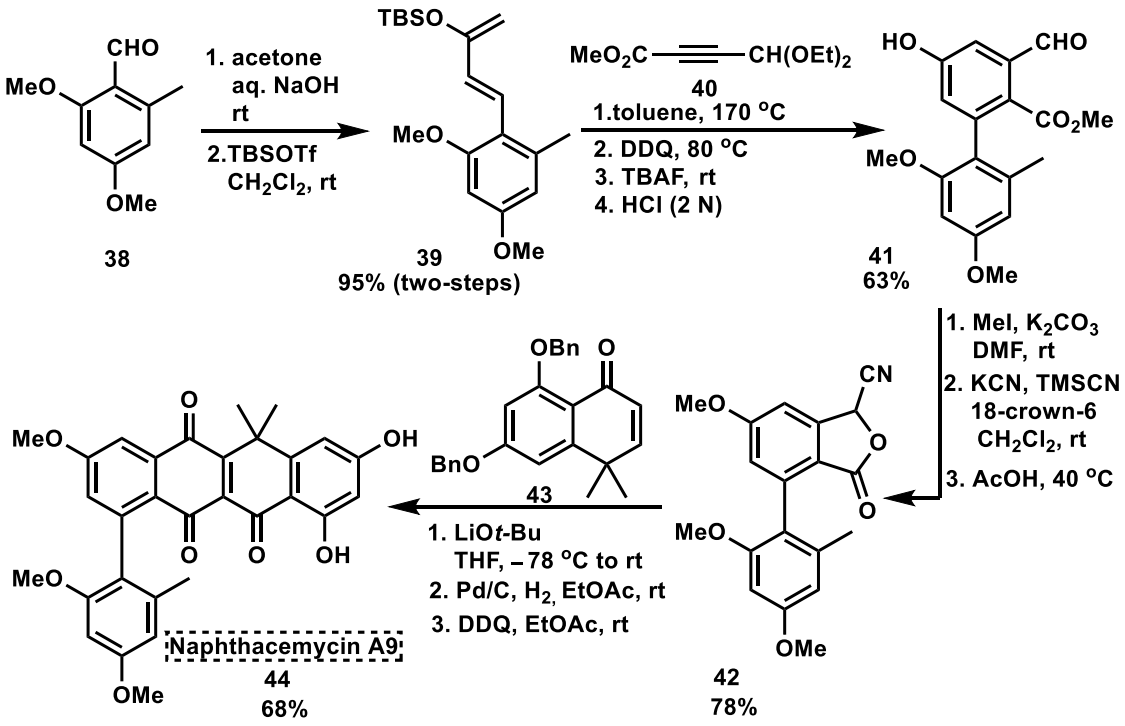

Scheme 4.7: Total synthesis of naphthacemycin A9.

4.3 Project Objectives

Naphthofurans, which are aromatic compounds containing a furan ring fused to a naphthalene moiety, hold a significant position within the area of organic chemistry.[14] These heterocyclic motifs are prevalent in natural products and bioactive agents, which offer valuable pharmaceutical properties.[15] Furomollugin and radermachol, compounds **45** and **46** respectively in Figure 4.1, are notable examples of biologically active scaffolds belonging to the dihydronaphtho[1,2-*b*]furan natural product compounds. Furomollugin, obtained from rubia cordifolia, demonstrates antioxidant and antibacterial activities, along with significant potential as an anticancer agent.[16] Radermachol is a bright red pigment, was first isolated from radermachera xylocarpa K, which is used as traditional medicine. Due to their potential pharmaceutical importance and unique structural connectivity, there is ongoing interest in developing synthetic strategies for constructing these naphthofuran scaffolds.[17]

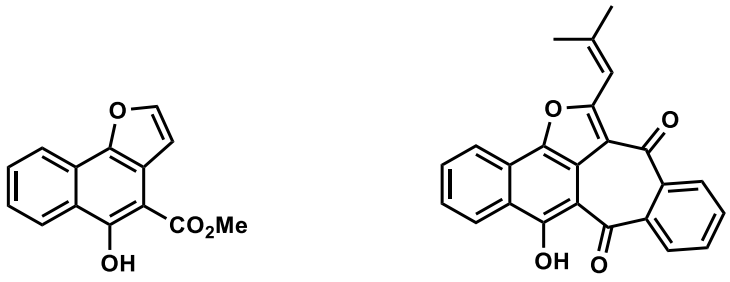

Figure 4.1: Structure of furomollugin and fadermachol.

As previously illustrated in Scheme 4.4, the Hauser-Kraus (H-K) annulation is recognized as a versatile chemical reaction capable of yielding naphthalene hydroquinones. We envisioned that accessing naphthofuran scaffolds could be achievable in a sequence involving a H-K reaction to form the 1,4-dihydroxynaphthalene moiety from which a subsequent O–H insertion could deliver the furanone containing scaffold. Firstly, the *α,β*–unsaturated diazo compounds could facilitate the H-K annulation by engaging in a reaction with the phthalide anion of **50** and the alkene functional group of **51** to generate the dihydronaphthalene (**49**). Secondly, the diazo functional group would play a pivotal role in the subsequent O–H insertion step (**48**, Scheme 4.8). By developing this novel adaptation of the H-K reaction, I would not only be able to showcase the utility of diazo-enones in reaction sequences that form three new bonds in quick succession, but this methodology could also allow access to various naphthofuran natural products, including furomollugin.

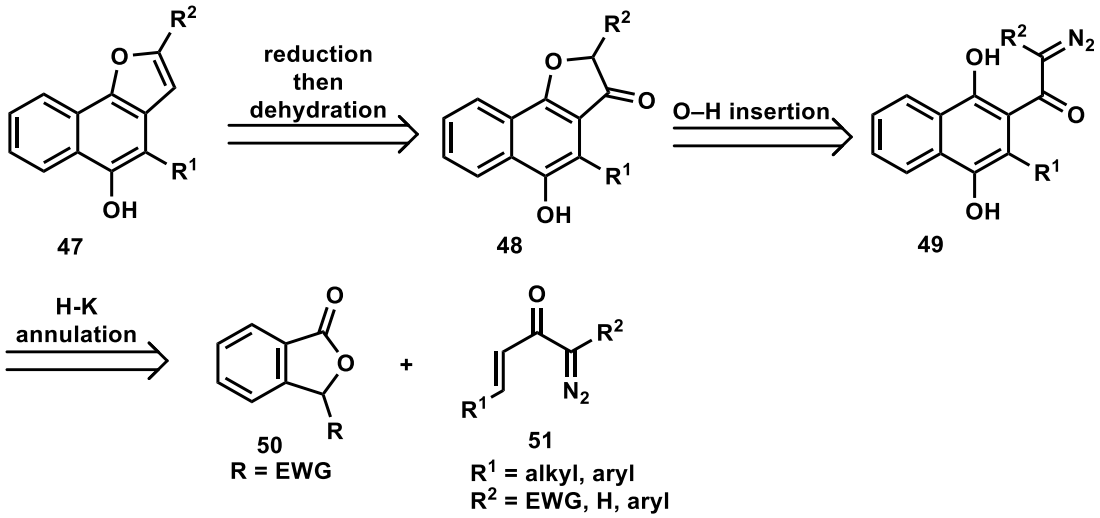

Scheme 4.8: Proposed retrosynthetic pathway for naphthofuran scaffolds.

4.4 Result and Discussion

4.4.1 Initial Investigation to Proceed Hauser-Kraus Reaction

To achieve our synthetic goals toward the synthesis of functionalized naphthofurans, we first needed to assess the compatibility of diazo-enones to the basic Hauser-Kraus reaction conditions. To complete this task, we needed access to properly functionalized starting materials (e.g., **50** and **51**, Scheme 4.8). With readily available access to diazo-enones (see Chapter 3, Section 3.15) our preliminary objective became the synthesis of the phthalide coupling partner. To construct the 3-cyanophthalide substrate, a two-step process was utilized based on known literature procedures, starting from 2-carboxybenzaldehyde (**52**) (Scheme 4.9).[18] The process entailed addition of cyanide to the aldehyde moiety, followed by a DCC-mediated coupling of the resulting secondary alcohol to deliver the lactone ring. This sequence resulted in the formation of compound **26** with an overall yield of 86%.

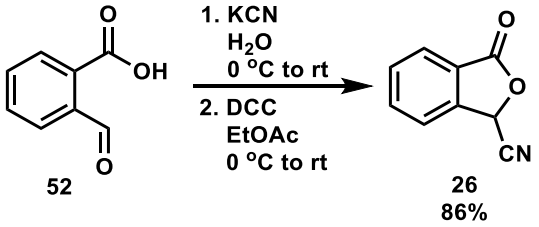

Scheme 4.9: Preparation of 3-cyanophthalide substrate **26**.

The H-K annulation, as an anionic cyclization, has been promoted using several different bases.[19] With starting materials in hand, our objective was to identify a compatible base that could effectively facilitate the annulation between the phthalide **26** and enone **53** without destroying the diazo functional group (Scheme 4.10A). Unfortunately, despite exploring various traditional bases, the targeted naphthalene compound **55** was never observed. In several cases, particularly when employing LiHMDS as the base, the major product isolated from these experiments was the Michael adduct **54**, in yields as high as 60%. (Note: The initial optimization studies were carried out by my colleague, Kirklind Lockyer). In order to complete the annulation step of the H-K reaction, Michael addition product **54** was resubjected to various bases in hopes of generating the enolate required to promote the Dieckmann-type ring closure (Scheme 4.10B). Unfortunately, while starting material

was consumed, these reactions were unsuccessful, leading only to trace quantities of diazo-enone **53**, formed via a retro-Michael addition, along with decomposition.

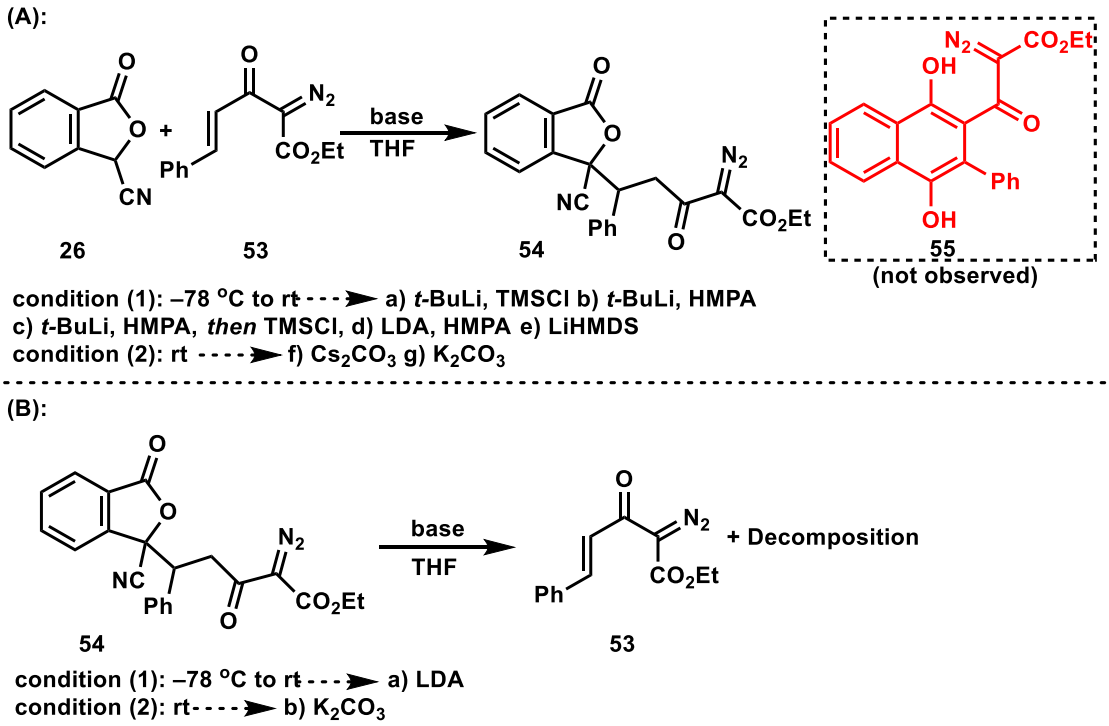

Scheme 4.10: (A) Reaction of **26** and **53** under basic conditions. **(B)** Base-catalyzed control experiments for **54**.

Although various amide (e.g., LDA) and carbanion (e.g., *t*-BuLi) bases have been employed to facilitate this class of annulation reaction, the use of alkoxy bases (e.g., LiO*t*-Bu) have widely been recognized to promote the Hauser-Kraus reaction.[20] Subjecting 3-cyanophthalide **26** and diazo-enone **53** to a base mediated reaction with LiO*t*-Bu provided Michael adduct **54** in 30% yield (Scheme 4.11). Interestingly, in addition to the generation of **54**, reaction under these conditions also delivered a trace amount (~5%) of the furanone product **56**. This result held significant value as it not only demonstrated the feasibility of conducting the Hauser-Kraus annulation with diazo-enones to generate two new C–C bonds, but also showed that a C–O bond could be formed via a formal diazo O–H insertion in a one-pot reaction without the use of a transition metal catalyst.

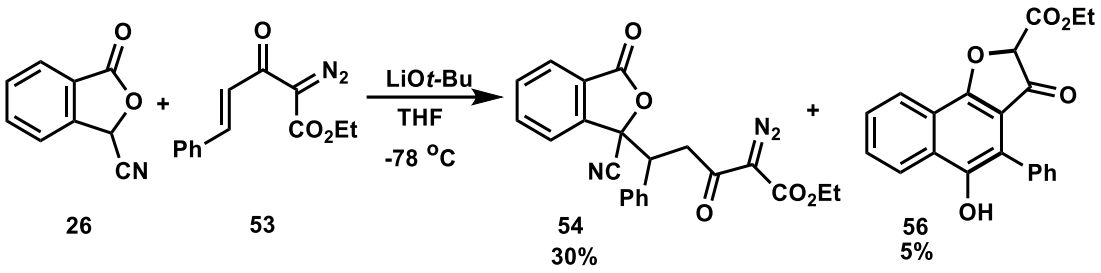

Scheme 4.11: Naphthofuran formation via LiO*t*-Bu catalyzed reaction.

While the formation of **54** and **56** (Scheme 4.11) under these reaction conditions was a significant finding, the rather high amount of decomposition observed in this reaction (based on TLC and mass balance of isolated products) was surprising, given the fact that both starting materials were completely consumed during the course of the reaction. In order to elucidate what was occurring in the reaction, we performed a control experiment. Subjecting diazo-enone **53** in THF to LiO*t*-Bu at –78 °C resulted in complete consumption of **53** within 5 min (TLC analysis), leading to a large amount of decomposition and trace quantities of cinnamic acid **57** (Scheme 4.12). Based on this observation, we hypothesized that the existence of α-diazoester moiety on the enone could be serving as a leaving group (i.e., loss of ethyl diazoacetate) in hydrolysis or other nucleophilic acyl substitution type reactions. This finding inspired us to perform the Hauser-Kraus annulation reactions employing acceptor type diazo-enones. The rationale behind this approach was to replace the diazoester group with diazomethane, considering that diazomethane, as a leaving group, might not exhibit the same reactivity as ethyl diazoacetate.

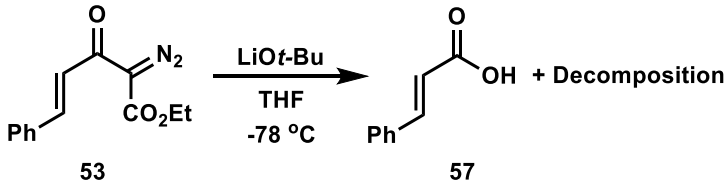

Scheme 4.12: Control experiment for **53**.

To explore this hypothesis, the required known diazo-enone **61**, was synthesized following a modified Danheiser strategy (Note: information about the Danheiser method can be found in Chapter 2) (Scheme 4.13A).[21] The approach consists of a two-step synthetic pathway, initiated with enolization of methyl-enone **58** using LiHMDS, followed by a subsequent Claisen condensation with ethyl trifluoroacetate **59**

to provide intermediate **60**. After performing a diazo transfer reaction using mesyl azide (MsN_3), with in situ elimination of trifluoro ketone group, diazo compound **61** was successfully formed with a yield of 92%. Due to the successful formation of naphthofuranone **56** (Scheme 4.11) using LiO*t*-Bu, we proceeded with carrying out the annulation reaction via the treatment of 3-cyanophthalide and diazo-enone **61** with LiO*t*-Bu (Scheme 4.13B). The preliminary results showed a promising outcome with a yield of 32% for the formation of **62** when the reaction was quenched and work-up was performed using a saturated aqueous solution of ammonium chloride (NH_4Cl). Encouraged by these initial findings, we proceeded with further optimization experiments to improve yield of the annulation product **62**.

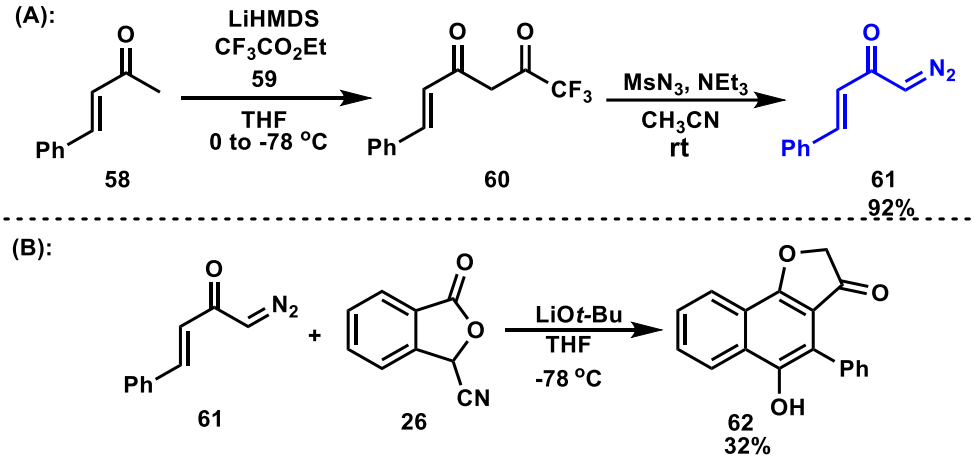

Scheme 4.13: (A) Modified Danheiser reaction to synthesize diazo-enone **61**. **(B)** Hauser-Kraus annulation employing LiO*t*-Bu as base.

4.4.2 Optimization of the Hauser-Kraus Reaction

The optimization investigations were conducted with the aim of improving the yield of naphthofuranone **62** (Table 4.1). Initially, we explored the impact of other leaving groups, such as sulfonyl (**25**) and sulfide (**63**) on the phthalide coupling partner. Through exploiting phthalide **25,** the desired product **62** was observed, but the yield of formation was very low (less than 5%) (entry 1). When the 3-(phenylthio)phthalide substrate **63** was utilized in a reaction with diazo-enone **61**, no reaction occurred, and starting materials were recovered (entry 2). Next, we switched back to the cyano substituted phthalide (**26**) and varying the temperature of the reaction was explored (entries 3 and 4). When the reaction was conducted at –78 °C and quenched at

this temperature with an aqueous NH_4Cl solution and slowly warmed up to room temperature, immediately following the consumption of starting material as determined by TLC analysis, then a 32% isolated yield of **62** was obtained (entry 3). Interestingly, if the reaction was allowed to warm to room temperature over a 3 h period after the consumption of starting material and then quenched with an aqueous NH4Cl solution, a noticeable decrease in yield was observed, potentially indicating the instability of the product to the basic conditions warmer temperatures (entry 4). In fact, reactions conducted at 0 °C and room temperature resulted in no product formation and only complex unknown mixtures of material. Next, we explored the use of other acids to quench the reaction to determine if this variable had any impact on the yield of product **62**. When acetic acid was added at –78 °C to quench the reaction and the solution was warmed to room temperature, only decomposition of **62** was observed (entry 5). Next, we tried addition of aqueous HCl solution (2 N) and warming the solution to room temperature, after completion of the reaction. Remarkably, using this procedure the yield of formation naphthofuranone **62** was successfully enhanced to 40% (entry 6). During the optimization the starting materials were fully consumed, and formation of no other side- product was observed. Due to time limitations, we were unable to complete additional optimization studies. However, the achieved 40% overall yield in a reaction that formed three new bonds without requiring a transition metal catalyst was promising for us to initiate exploring the application of this reaction in the total synthesis of natural products.

Table 4.1: Optimization of Formation Naphthofuranone **62**

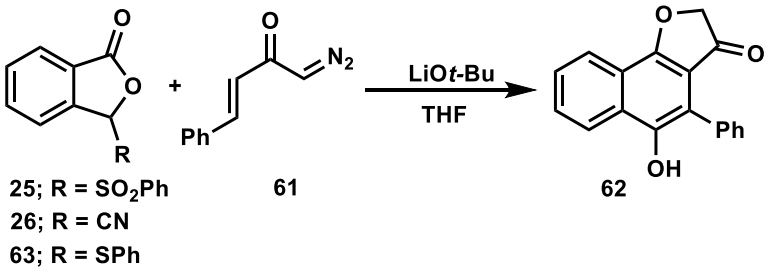

Entry[a]	R	Reaction Temperature	Work-up[b]	Result
1	SO_2Ph	–78 °C	NH_4Cl Solution	Trace Product
2	SPh	–78 °C	-	No Reaction
3	CN	–78 °C	NH_4Cl Solution	32%
4	CN	–78 °C to rt	-	Product Decomposed
5	CN	–78 °C to rt	CH_3CO_2H	Product Decomposed
6	CN	–78 °C	HCl Solution	40%

[a] (2 equiv) Phathalide, (1 equiv) **61**, and (1.8 equiv) LiO*t*-Bu. [b] The proton source used to quench the reaction was introduced at –78 °C, and the resulting solution was slowly warmed to room temperature over 3 hours, except for entries 4 and 5, where the proton source was added at room temperature.

4.4.3 Total Synthesis of Furomollugin via Hauser-Kraus Annulation

As previously stated, the primary goal of our project was to synthesize naphthofuranone containing natural products such as furomollugin **45**. To achieve this goal, enone **70** was required as the diazo-enone to carry out the Hauser-Kruas annulation (Scheme 4.14). To generate diazo-enone **70**, we initially prepared enone **68** through a three-step synthetic process (Scheme 4.14A). Commencing from the methylation of tartaric acid **64**, followed by an Malaprade oxidative cleavage using periodic acid **65**, the methyl glyoxylate **66** was obtained in 73% yield.[22] The required enone **68** was successfully synthesized through a Wittig reaction by exploiting the triphenyl phosphonium ylide **67**, in 44% yield. Finally, by employing the Danheiser method (Note: for more details, refer to Chapter 2) the diazo-enone **70** was delivered, with a yield of 34%.

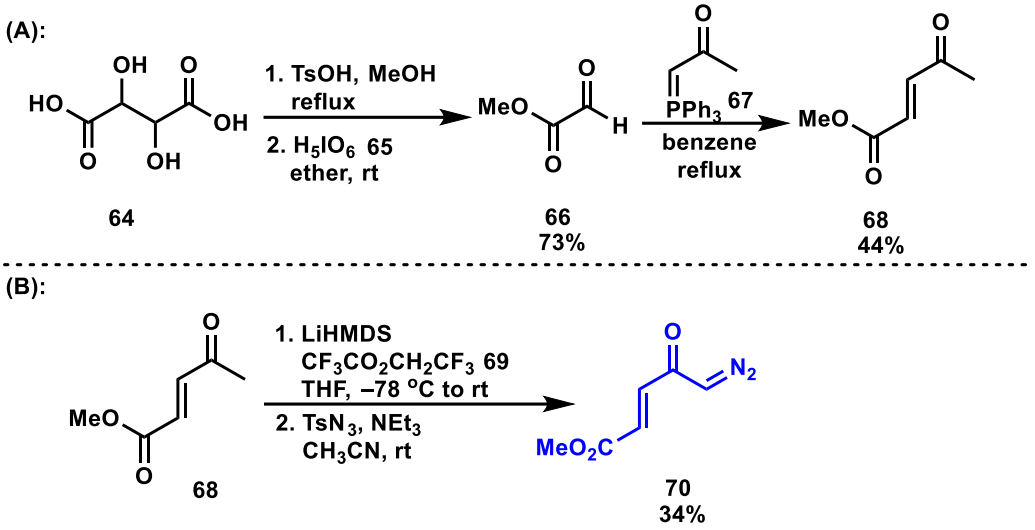

Scheme 4.14: (A) Three-step synthetic pathway for enone **68**. **(B)** Danheiser reaction to synthesize diazo-enone **70**.

Subsequently, we proceeded by employing the optimized H-K reaction conditions, involving the utilization of LiO*t*-Bu, which yielded a satisfactory 40% production of naphthofuranone **62** (Table 1.4). Remarkably, through subjecting diazo-enone **70** to a reaction with cyano phthalide **26** in the presence of LiO*t*-Bu the naphthofuranone **71** was successfully obtained in 27% yield. To achieve the targeted naphtho[1,2-*b*]furan **45**, furomollugin, **71** was reduced using sodium borohydride ($NaBH_4$). Interestingly, the use of $NaBH_4$ not only facilitated the reduction reaction, but also upon subsequent dehydration, delivered furomollugin in a 33% yield.

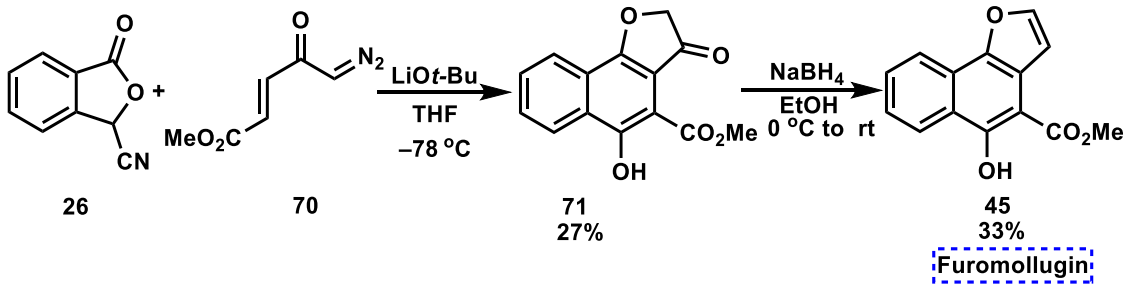

Scheme 4.15: Hauser-Kraus annulation to synthesize furomollugin (**45**).

Following the successful achievement of the furomollugin synthesis, we employed optimized conditions for the Hauser-Kraus annulation to construct another natural product, 5-hydroxy-4-methylnaphtho[1,2-*b*]furan-3-one (**74**, Scheme 4.16).[23] The initial step entailed the construction of the needed diazo-enone **72** via the modified

Danheiser strategy. Through utilizing enone **72** in a two-step synthetic fashion, enone activation/diazo transfer, the targeted diazo-enone **73** was formed in a yield of 41%. Next, the Hauser-Kraus annulation was carried out and efficiently provided the naphthofuranone **74** in a 36% isolated yield (Scheme 4.16).

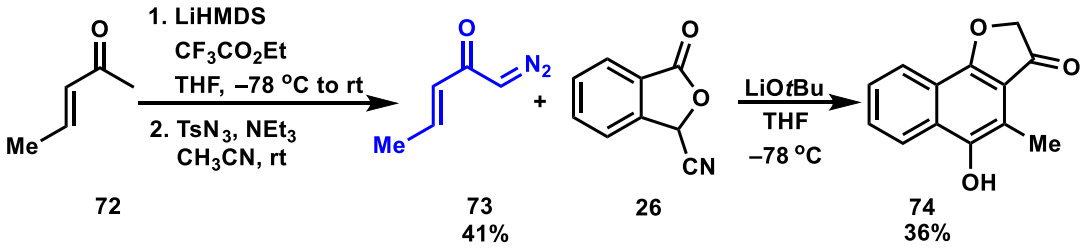

Scheme 4.16: Synthesize of 5-hydroxy-4-methylnaphtho[1,2-*b*]furan-3-one **73**.

4.5 Conclusion

In conclusion, the utility of diazo-enones was showcased in the synthesis of complex natural products by construction of multiple bonds in a one-pot reaction. Through optimization studies, several influential factors were identified in the formation of naphthofuranone derivatives via the Hauser-Kraus annulation/O–H insertion process. First, the optimization studies showed the importance of the type of nucleophilic phthalide, with cyanophthalide proving to be the most efficacious in comparison with sulfonylphthalide and thiophthalide. Secondly, while the choice of the base was revealed as the most effective factor, the investigations have indicated that, alongside the base, the appropriate work-up condition (basic or acidic work-up, as well as the temperature) could clearly affect the yield of the desired naphthofuranone products. While the conditions were effective in facilitating the Hauser-Kraus annulation/O–H process for various alkyl and aryl groups attached to the diazo-enone, it is worth noting that the type of the substituent also influence on the reaction yield.

4.6 Experimental

4.6.1 General Procedure

Unless stated otherwise, all reactions were performed in oven- or flame-dried glassware under an atmosphere of dry nitrogen. Dry tetrahydrofuran, dichloromethane, acetonitrile, and toluene were obtained by passing these previously degassed solvents through activated alumina columns. All other reagents were used as received from commercial sources, unless stated otherwise. When indicated, solvents or reagents were degassed by sparging with Argon for 10 minutes in an ultrasound bath at 25 °C. Silicon oil bath was used as the heat source for the reactions performing above room temperature. Reactions were monitored by thin layer chromatography (TLC) on Silicycle Siliaplate™ glass-backed TLC plates (250 μm thickness, 60 Å porosity, F-254 indicator) and visualized by UV irradiation or development with anisaldehyde stain. Volatile solvents were removed under reduced pressure with a rotary evaporator. All flash column chromatography was performed using Silicycle SiliaFlash® F60, 230-400 mesh silica gel (40-63 μm). ^{1}H NMR and ^{13}C NMR spectra were recorded with Bruker AV, spectrometers operating at 300 or 500 MHz for ^{1}H (75, and 125 MHz for ^{13}C) in chloroform-d ($CDCl_3$). Chemical shifts are reported relative to the residual solvent signal (^{1}H NMR: δ = 7.26 ($CDCl_3$), ^{13}C NMR: δ = 77.16 ($CDCl_3$)). NMR data are reported as follows: chemical shift (multiplicity, coupling constants where applicable, number of hydrogens). Splitting is reported with the following symbols; s = singlet, bs = broad singlet, d = doublet, t = triplet, appt = apparent triplet, dd = doublet of doublets, ddd = doublet of doublet of doublets, dddd = doublet of doublet of doublet of doublets, m = multiplet. Infrared (IR) spectra were recorded on Bruker Alpha or Bruker Tensor 27 FT-IR spectrometers. High resolution mass spectrometry (HRMS) data were obtained using an Agilent 6200 series instrument, employing a TOF mass analyzer.

4.6.2 Synthesis and Characterization of Cyanophthalide 26

To a solution of 2-carboxybenzaldehyde **52** (4.00 g, 26.6 mmol) and potassium cyanide (KCN) (2.60 g, 39.9 mmol) in H_2O (27 mL) was slowly added 37% HCl solution (8ml) at 0 °C over 1 h and the resulting solution was stirred for 40 min at 0 °C. The reaction mixture was extracted with EtOAc (3 x 80 mL), and the organic layers were washed with brine. The organic phase was cooled down to 0 °C and treated with DCC (6.87 g, 33.3 mmol). The generated precipitate was warmed up to room temperature and stirred for 16 h. The resulting suspension was filtered through sintered glass funnel and the filtrate concentrated under reduced pressure. The obtained solid was crystallized in EtOH/hexane to deliver product **26** (3.65 g) in 83% yield.

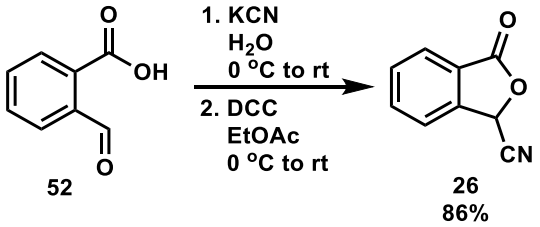

R_f = 0.33, 20% EtOAc in hexanes;
^{1}H NMR (300 MHz, $CDCl_3$) δ = 8.04 – 7.98 (m, 1H), 7.90 – 7.83 (m, 1H), 7.76 – 7.68 (m, 2H), 6.10 (s, 1H).

4.6.3 Synthesis and Characterization of Diazo-Enone Starting Materials

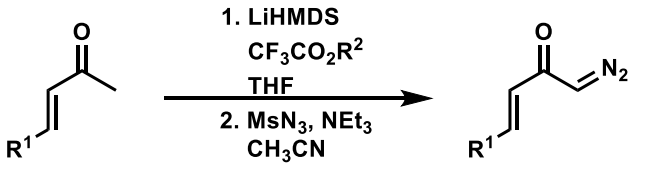

R^1 = phenyl, 58
CO_2Me, 68
Me, 72
R^2 = Et, CH_2CF_3

R^1 = phenyl, 61
CO_2Me, 70
Me, 73

General Experimental Procedure A:

A flame-dried round bottom flask equipped with a magnetic stir bar, was charged with a 0.4 M solution of 1,1,1,3,3,3-hexamethyldisilazane (HMDS) (1.1 equiv) in THF and then cooled at 0 °C in an ice-water bath while *n*-butyllithium solution (2.25 M in hexane, 1.1 eqiuv) was added rapidly dropwise, under nitrogen. After 10 min, the resulting solution was cooled at –78 °C in a dry ice-acetone bath, while a

0.4 M solution of enone (1.0 equiv) in THF was added dropwise over 15 min. The reaction mixture was stirred at –78 °C for 30 min, and then 2,2,2-trifluoroethyl trifluoroacetate or ethyl trifluoroacetate (1.2 equiv) was added rapidly by syringe in one portion. After 15 min, the reaction mixture was poured into a separatory funnel containing a 5% aqueous HC1 solution and Et_2O. The aqueous phase was extracted with Et_2O two more times, and the combined organic phases were then washed with saturated NaCl solution and concentrated at reduced pressure. The crude product was dissolved in CH_3CN (0.25 M, 1.0 equiv), then water (1 equiv), and NEt_3 (1.4 equiv) were added. A 0.4 M solution of methanesulfonyl azide (1.5 equiv) in CH_3CN was added dropwise over 20 min. The resulting solution was stirred at room temperature overnight and then concentrated to a volume of 10 mL. The residue was diluted with Et_2O and washed with three portions of 10% aqueous NaOH solution, washed with saturated NaCl solution, dried over $MgSO_4$, filtered, and concentrated in *vacuo*. The resulting residue was purified by silica gel flash column chromatography using a hexanes/EtOAc gradient to afford corresponding diazo-enones (**61**, **70**, and **73**).

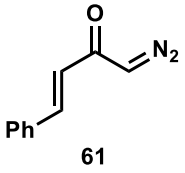

61

Product **61** was prepared following General Experimental Procedure **A**. HMDS (3.15 mL, 15.1 mmol), enone **58** (2.00 g, 13.7 mmol), *n*-BuLi (6.70 mL, 15.1 mmol), ethyl trifluoroacetate (1.96 ml, 16.4 mmol). Product **61** (2.17 g, 12.6 mmol, 92%) was obtained as a yellow color solid:

R_f = 0.35, 20% EtOAc in hexanes;
^{1}H NMR (300 MHz, $CDCl_3$) δ = 7.60 (d, *J* = 15.8 Hz, 1H), 7.56 – 7.52 (m, 2H), 7.41 – 7.35 (m, 3H), 6.60 (d, *J* = 15.8 Hz, 1H), 5.45 (s, 1H);
^{13}C NMR (75 MHz, $CDCl_3$) δ = 184.4, 140.8, 134.6, 130.4, 129.0, 128.4, 56.3 ppm; (Note: one aromatic carbon is not observed presumably due to overlap)
IR (neat): ν_{max} = 3078, 2092, 1647, 1591, 1361, 110, 987, 755, 513 cm^{-1};
HRMS (APPI+) calc'd for $C_{10}H_8N_2O$ [M^+] 172.0637, found 172.0684.

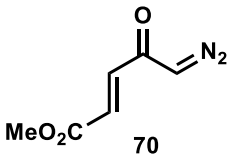

70

Product **70** was prepared following General Experimental Procedure **A**. HMDS (0.864 mL, 4.13 mmol), enone **68** (0.480 g, 3.75 mmol), *n*-BuLi (1.83 mL, 4.13 mmol), trifluoroethyl trifluoroacetate (0.605 mL, 4.50 mmol). Product **70** (0.120 g, 0.779 mmol, 34%) was obtained as a yellow solid: (Note: the reported yield is based on the mass of crude product from the first step)

R_f = 0.20, 20% EtOAc in hexanes;
^{1}H NMR (300 MHz, $CDCl_3$) δ = 6.98 (d, *J* = 15.6 Hz, 1H), 6.76 (d, *J* = 15.5 Hz, 1H), 5.52 (s, 1H), 3.81 (s, 3H);
^{13}C NMR (75 MHz, $CDCl_3$) δ = 182.5, 166.0, 138.4, 129.1, 58.1, 52.5 ppm;
IR (neat): ν_{max} = 3097, 2955, 2103, 1709, 1604, 1443, 1361, 1292, 992, 756, 523 cm^{-1};

HRMS (APPI+) calc'd for $C_6H_6N_2O_3$ [M^+] 154.0378, found 154.0386.

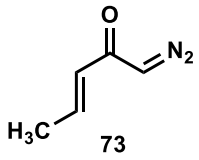

73

Product **73** was prepared following General Experimental Procedure **A**. HMDS (1.78 mL, 6.53 mmol), enone **72** (0.581 mL, 5.94 mmol), *n*-BuLi (2.61 mL, 6.53 mmol), ethyl trifluoroacetate (0.957 mL, 7.13 mmol). Product **73** (0.100 g, 0.910 mmol, 41%) was obtained as a thick oil: (Note: the reported yield is based on the mass of crude product from the first step)

R_f = 0.30, 20% EtOAc in hexanes;
^{1}H NMR (300 MHz, $CDCl_3$) δ = 6.82 (dq, *J* = 15.3, 6.9 Hz, 1H), 6.09 – 5.97 (m, 1H), 5.33 (s, 1H), 1.89 (dd, *J* = 6.9, 1.7 Hz, 3H);
^{13}C NMR (75 MHz, $CDCl_3$) δ = 184.8, 140.4, 128.9, 55.0, 18.1 ppm;
IR (neat): ν_{max} = 3287, 2916, 2097, 1654, 1598, 1357, 1148, 964, 504 cm^{-1};
HRMS (APPI+) calc'd for $C_5H_6N_2O$ [M^+] 110.0480, found 110.0496.

4.6.4 Synthesis and Characterization of Naphthofuranones

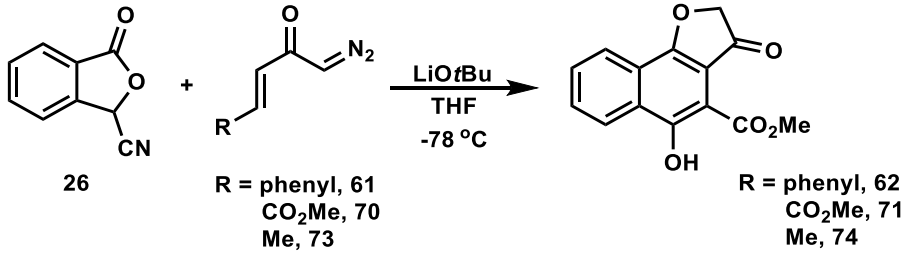

26 R = phenyl, 61; CO_2Me, 70; Me, 73 R = phenyl, 62; CO_2Me, 71; Me, 74

General Experimental Procedure B:

To a flame-dried round bottom flask equipped with a magnetic stir bar charged with cyano phthalide (2.0 equiv) and diazo-enone (1.0 equiv), was added THF at –78 °C under N_2 (0.06 M solution). Then, LiO*t*-Bu (1.8 equiv) was added to the reaction flask, and the resulting solution was stirred for 1 h at –78 °C. After completion of the reaction, 2 N HCl aqueous solution was poured into the reaction flask and slowly warmed up to room temperature while stirring. The resulting solution was diluted with water and extracted three times with EtOAc. The combined organic phases were dried over anhydrous $MgSO_4$ and concentrated *in vacuo*. The resulting residue was purified with silica gel flash column chromatography using a hexanes/EtOAc gradient to afford corresponding naphthofuranones.

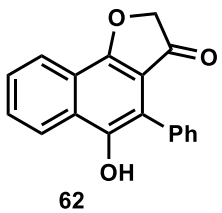

62

Product **62** was prepared following General Experimental Procedure **A**. cyanophthalide **26** (0.185 g, 1.16 mmol), diazo-enone **61** (0.100 g, 0.581 mmol), LiO*t*-Bu (1.04 mL, 1.04 mmol). Product **62** (0.064 g, 0.232 mmol, 40%) was obtained as a yellow solid:

R_f = 0.50, 20% EtOAc in hexanes;
^{1}H NMR (300 MHz, $CDCl_3$) δ = 8.32 (ddd, *J* = 8.4, 1.2, 0.7 Hz, 1H), 8.25 (ddd, *J* = 8.2, 1.4, 0.7 Hz, 1H), 7.77 (ddd, *J* = 8.4, 7.0, 1.4 Hz, 1H), 7.66 (ddd, *J* = 8.2, 7.0, 1.2 Hz, 1H), 7.60 – 7.43 (m, 5H), 5.63 (s, 1H), 4.77 (s, 2H);
^{13}C NMR (75 MHz, $CDCl_3$) δ = 198.4, 170.0, 143.4, 131.7, 130.7, 130.3, 129.8, 129.4, 128.9, 127.4, 123.8, 122.2, 121.8, 114.4, 113.3, 75.7 ppm;
IR (neat): ν_{max} = 3215, 1675, 1624, 1497, 1376, 1136, 764, 692 cm^{-1};
HRMS (APPI+) calc'd for $C_{18}H_{12}O_3$ [M^+] 276.0786, found 276.0806.

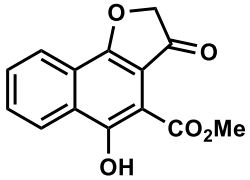

71

Product **71** was prepared following General Experimental Procedure **A**. cyano phthalide **26** (0.180 g, 1.14 mmol), diazo-enone **70** (0.0880 g, 0.571 mmol), LiO*t*-Bu (1.03 mL, 1.03 mmol). Product **71** (0.040 g, 0.155 mmol, 27%) was obtained as a pale-yellow color solid.

R_f = 0.45, 20% EtOAc in hexanes;
^{1}H NMR (300 MHz, $CDCl_3$) δ = 12.27 (s, 1H), 8.53 – 8.43 (m, 1H), 8.25 – 8.17 (m, 1H), 7.87 – 7.73 (m, 2H), 4.80 (s, 2H), 4.06 (s, 3H).

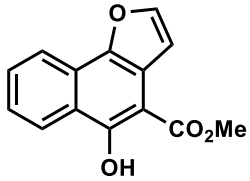

45

Product **45** was prepared using the following experimental procedure: To a suspension of **71** (0.30 g, 0.116 mmol) in EtOH was added $NaBH_4$ (0.048 g, 1.28 mmol) at 0 °C. Reaction mixture stirred at 0 °C for 30 min, and saturated NH_4Cl solution was poured to the reaction flask. To the resulting solution was added water and the resulting mixture extracted with DCM three times. The combined organic phases were dried over anhydrous $MgSO_4$ and concentrated *in vacuo*. The resulting residue was purified with silica gel flash column chromatography using hexanes/EtOAc product **45** (9.10 mg, 0.0376 mmol, 32%) was obtained as a yellow solid.

R_f = 0.55, 20% EtOAc in hexanes;
^{1}H NMR (300 MHz, $CDCl_3$) δ = 12.28 (s, 1H), 8.47 (ddd, *J* = 8.4, 1.3, 0.7 Hz, 1H), 8.20 (apt. dt, *J* = 8.2, 1.0 Hz, 1H), 7.75 – 7.69 (m, 2H), 7.53 (ddd, *J* = 8.3, 7.0, 1.3 Hz, 1H), 7.20 (d, *J* = 2.0 Hz, 1H), 4.09 (s, 3H);
^{13}C NMR (75 MHz, $CDCl_3$) δ = 172.2, 159.5, 144.6, 144.5, 130.3, 125.3, 125.1, 125.1, 123.10, 120.0, 119.8, 109.4, 99.4, 52.4 ppm;
IR (neat): ν_{max} = 2953, 1656, 1638, 1443, 1343, 1239, 1167, 767, 696 cm^{-1};
HRMS (APPI+) calc'd for $C_{14}H_{10}O_4$ [M^+] 242.0579, found 242.0601.

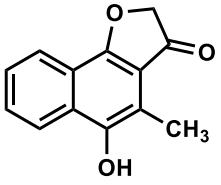

74

Product **74** was prepared following General Experimental Procedure **A**. Cyanophthalide **26** (0.245 g, 1.54 mmol), diazo-enone **73** (0.085 g, 0.772 mmol), LiO*t*-Bu (1.39 mL, 1.39 mmol). Product **74** (0.0600 g, 0.280 mmol, 36%) was obtained as a pale-yellow solid.

R_f = 0.40, 20% EtOAc in hexanes;
^{1}H NMR (300 MHz, $CDCl_3$) δ = 8.22 – 8.15 (m, 2H), 7.73 (ddd, *J* = 8.5, 6.9, 1.4 Hz, 1H), 7.57 (ddd, *J* = 8.1, 7.0, 1.2 Hz, 1H), 4.92 (s, 1H), 4.77 (s, 2H), 2.63 (s, 3H);

IR (neat): ν_{max} = 3382, 2921, 1778, 1654, 1464, 1399, 1257, 1019, 759, 685 cm^{-1};
HRMS (APPI+) calc'd for $C_{13}H_{10}O_3$ [M^+] 214.0630, found 214.0711.

4.7 References

1. Rosset, I. G.; Dias, R. M. P.; Pinho, V. D.; Burtoloso, A. C. B. *J. Org. Chem.* **2014**, *79*, 6748-6753.
2. Fukuda, T.; Sudoh, Y.; Tsuchiya, Y.; Okuda, T.; Igarashi, Y. *J. Nat. Prod.* **2014**, *77*, 813-817.
3. Vanecko, J. A.; Wan, H.; West, F. G. *Tetrahedron* **2006**, *62*, 1043-1062.
4. Dias, R. M. P.; Momo, P. B.; Burtoloso A. C. B. *Tetrahedron* **2017**, *73*, 3720-3729.
5. Sakaine, G.; Leitis, Z.; Ločmele, R.; Smits, G. *Eur. J. Org. Chem.* 2023, *26*, e202201217.
6. Yang, B. V.; O'Rourke, D.; Li, J. *Synlett* **1993**, *1993*,195-196.
7. Feng, X.; Pisula, W.; Müllen, K. *Pure Appl. Chem.* **2009**, *81*, 2203-2224.
8. (a) Jung, M. E. *Tetrahedron* **1976**, *32*, 3-31. (b) Duarah, G.; Kaishap, P. P.; Begum, T.; Gogoi, S. *Adv. Synth. Catal.* **2019**, *361*, 654-672.
9. (a) Hauser, F. M.; Rhee, R. P. *J. Org. Chem.* **1978**, *43*, 178-180. (b) Kraus, G. A.; Sugimoto, H. *Tetrahedron Lett.* **1978**, *19*, 2263-2266.
10. (a) Mal, D.; Pahari, P. *Chem. Rev.* **2007**, *107*, 1892-1918. (b) Mal, D. Anionic Annulations in Organic Synthesis: A Versatile and Prolific Class of Ring-Forming Reactions; *Elsevier: Amsterdam,* **2019**, *63*.
11. Sankara, C. S.; Gaikwad, S. P.; Namboothiri, I. N. N. *Synlett*, **2023**, *34*, A-Q.
12. Ahn, S.; Han, Y. T. *Tetrahedron Lett.* **2017**, *58*, 4779-4780.
13. Wang, S.; Kraus, G. A. *J. Org. Chem.* **2018**, *83*, 15549-15552.
14. Abdelwahab, A. H. F.; Fekry, S. A. H. *Eur. J. Chem.* **2021**, *12*, 340-359.
15. a) Sastry, M. N. V.; Claessens, S.; Habonimana, P.; de Kimpe, N. *J. Org. Chem.* **2010**, *75*, 2274-2280. c) Lumb, J. P.; Trauner, D. *J. Am. Chem. Soc.* **2005**, *127*, 2870−2871. c) Lim, C. J.; Choi, J. Y.; Lee, B. H.; Oh, K.-S.; Yi, K. Y. *Chem. Pharm. Bull.* **2013**, *61*, 1239-1247. d) Mishra, K.; Basavegowda, N.; Lee, Y. R. *Catal. Sci. Technol.* **2015**, *5*, 2612-2621.
16. Xia, L.; Idhayadhulla, A.; Lee, Y. R.; Kim, S. H.; Wee, Y. J. *Med. Chem. Res.* **2014**, *23*, 3528-3538.
17. a) Kraus, G. A.; Dong, P. *Nat. Prod. Commun.* **2015**, *10*, 1025-1026. b) Buccini, M.; Piggott M. *J. Org. Lett.* **2014**, *16*, 2490-2493. c) Samineni, R.; Srihari, P.; Mehta, G.

Org. Lett. **2016**, *18*, 2832-2835.

18. Crawley, M. L.; Hein, K. J.; Markgraf J. H. *J. Chem. Research* **2003**, 470-47.
19. a) Schünemann, K.; Furkert, D. P.; Choi, E.; Connelly, S.; Fraser, J. D.; Sperry, J.; Brimble, M. A. *Org. Biomol. Chem.* **2014**, *12*, 905-912. b) Hassan, N. P. S.; Naysmith, B. J.; Sperry, J.; Brimble M. A. *Tetrahedron* **2015**, *71*, 7137-7143. c) Kitamura, K.; Kanagawa, H.; Ozakai, C.; Nishimura, T.; Tokuda, H.; Tsunoda, T.; Kaku, H. *Synthesis* **2021**, *53*, 1629-1635. d) Basu, P.; Satam, N.; Pati, S.; Suresh, A.; Namboothiri, I. N. N. *J. Org. Chem.* **2023**, *88*, 4038-4051.
20. a) Kitamura, K.; Kanagawa, H.; Ozakai, C.; Nishimura, T.; Tokuda, H.; Tsunoda, T.; Kaku, H. *Synthesis* **2021**, *53*, 1629-1635. b) Mal, D.; Ghosh, K.; Chakraborty, S. *Synthesis* **2015**, *47*, 2473-2484.
21. Danheiser, R. L.; Miller, R. F.; Brisbois, R. G.; Park, S. Z. *J. Org. Chem.* **1990**, *55*, 1959-1964.
22. Kolodziejczyk, A.; Blaziak, M.; Podgorniak, K., Jezierska, A.; Blaziak, K. *Phys. Chem. Chem. Phys.* **2023**, *25*, 21448-21455.
23. Arfana, M.; Shaabana, K. A.; Schüfflerb, A; Laatsch, *Nat. Prod. Commun.* **2012**, *7*, 1199-1202.

4.8 Selected ^{1}H and ^{13}C NMR Spectral Data

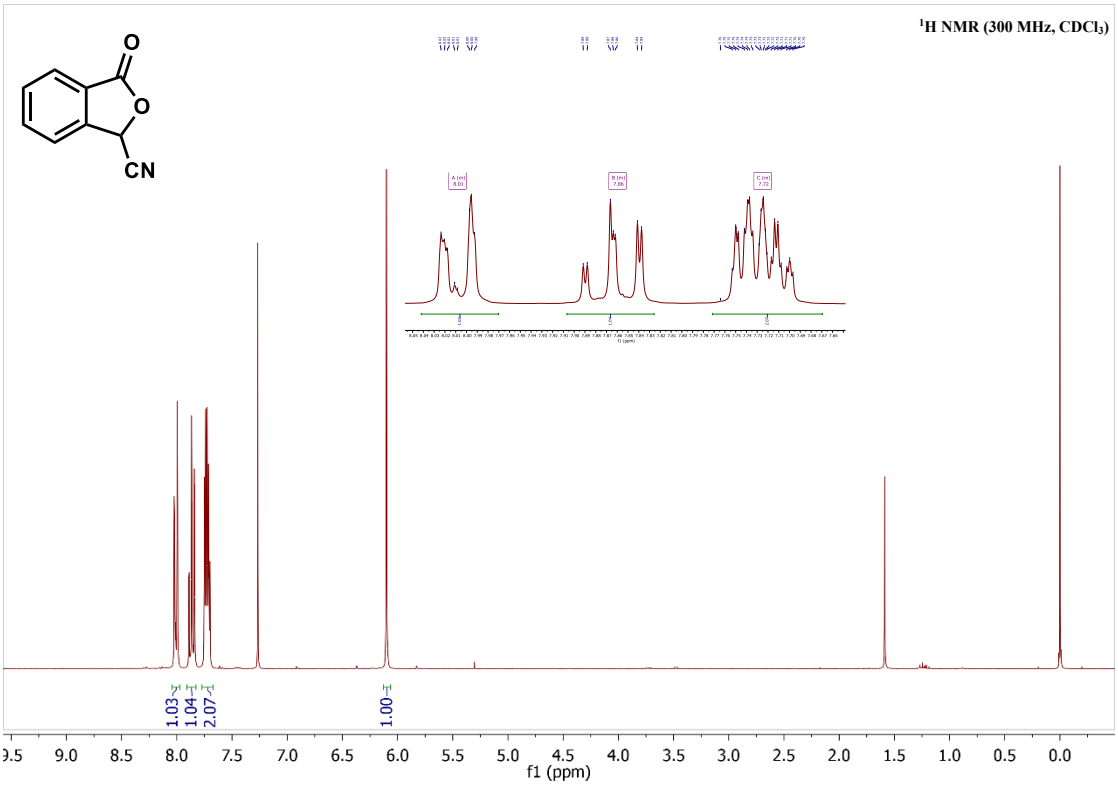

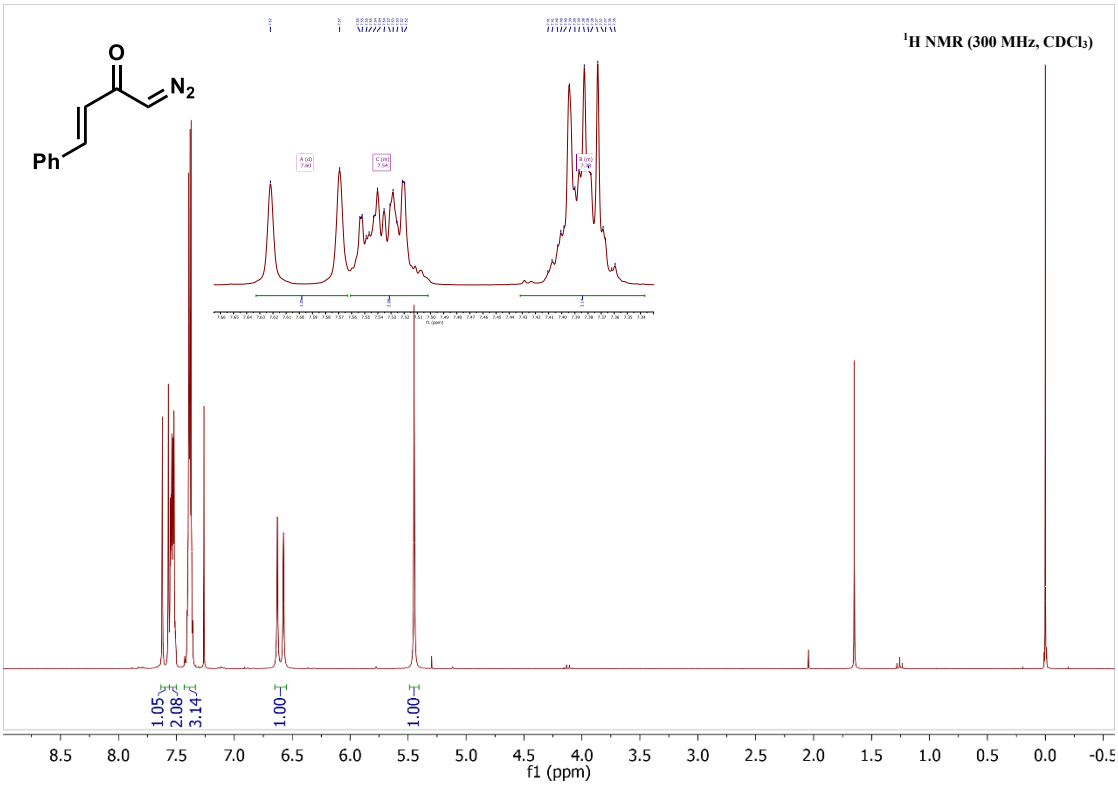
^{1}H NMR (300 MHz, CDCl$_3$)
O
N$_2$
Ph
1.05
2.08
3.14
1.00
1.00
8.5 8.0 7.5 7.0 6.5 6.0 5.5 5.0 4.5 4.0 3.5 3.0 2.5 2.0 1.5 1.0 0.5 0.0 -0.5
f1 (ppm)

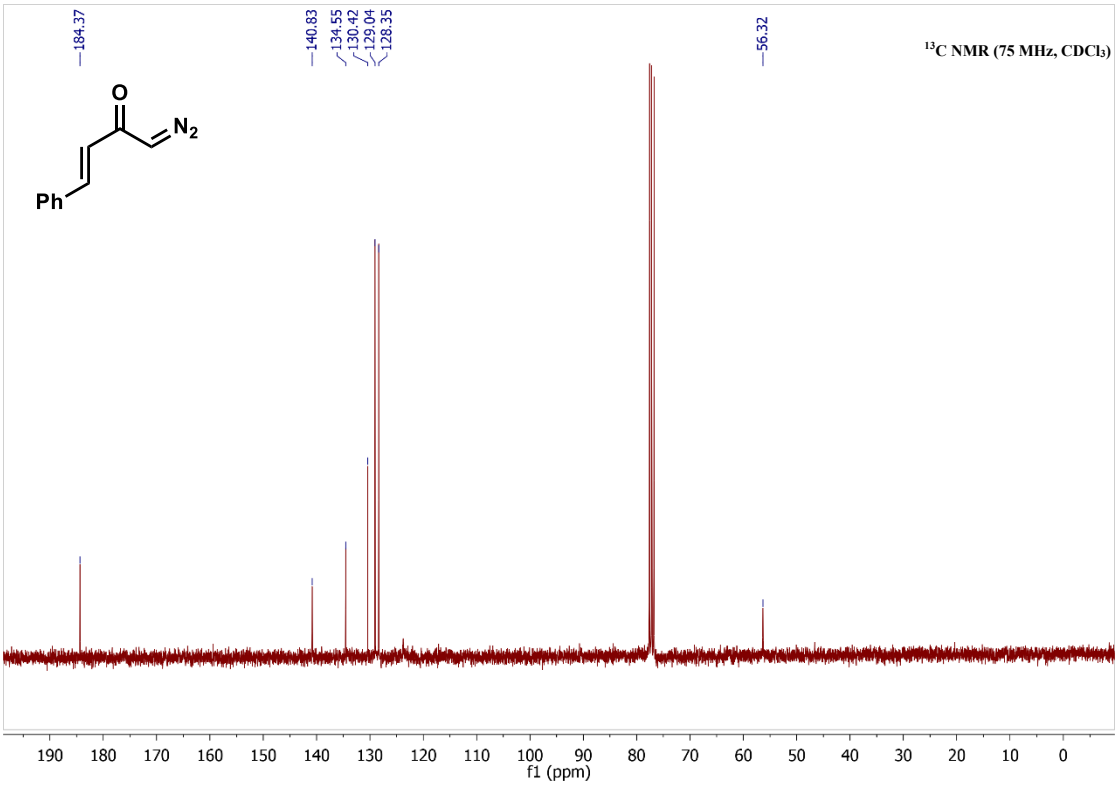
184.37
140.83
134.55
130.42
129.04
128.35
56.32
^{13}C NMR (75 MHz, CDCl$_3$)
O
N$_2$
Ph
190 180 170 160 150 140 130 120 110 100 90 80 70 60 50 40 30 20 10 0
f1 (ppm)

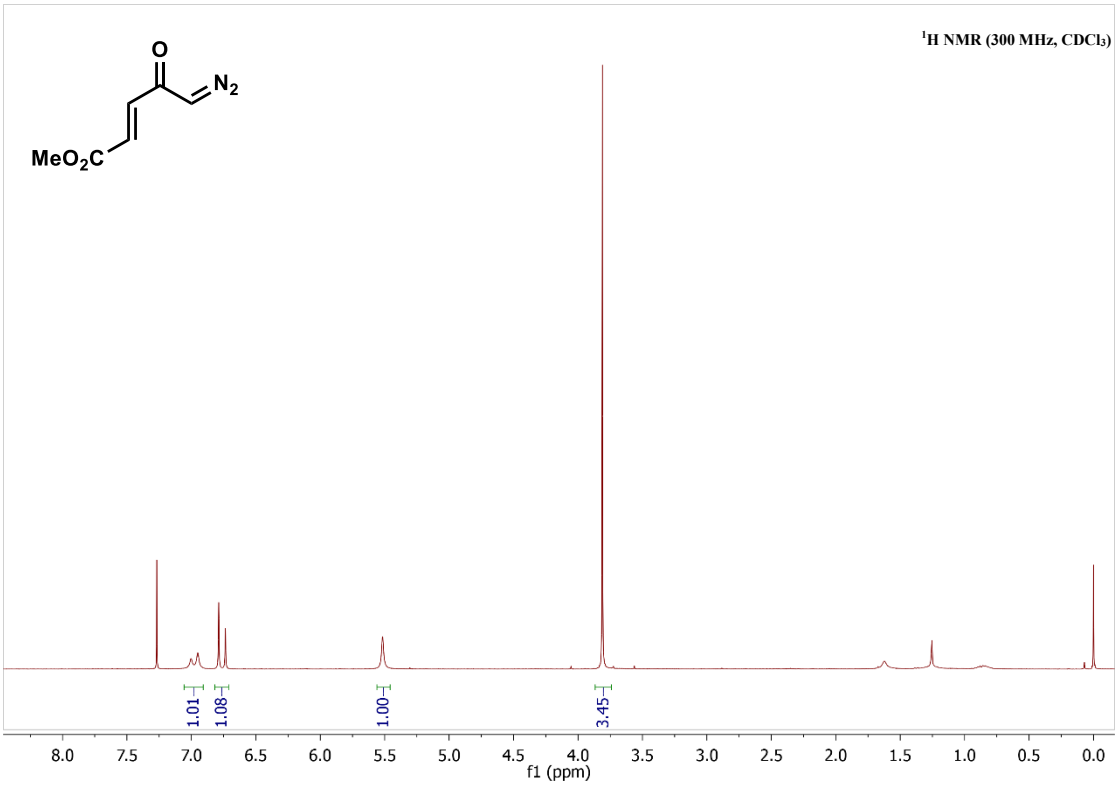
^{1}H NMR (300 MHz, CDCl$_3$)
O
N$_2$
MeO$_2$C
1.01
1.08
1.00
3.45
8.0 7.5 7.0 6.5 6.0 5.5 5.0 4.5 4.0 3.5 3.0 2.5 2.0 1.5 1.0 0.5 0.0
f1 (ppm)

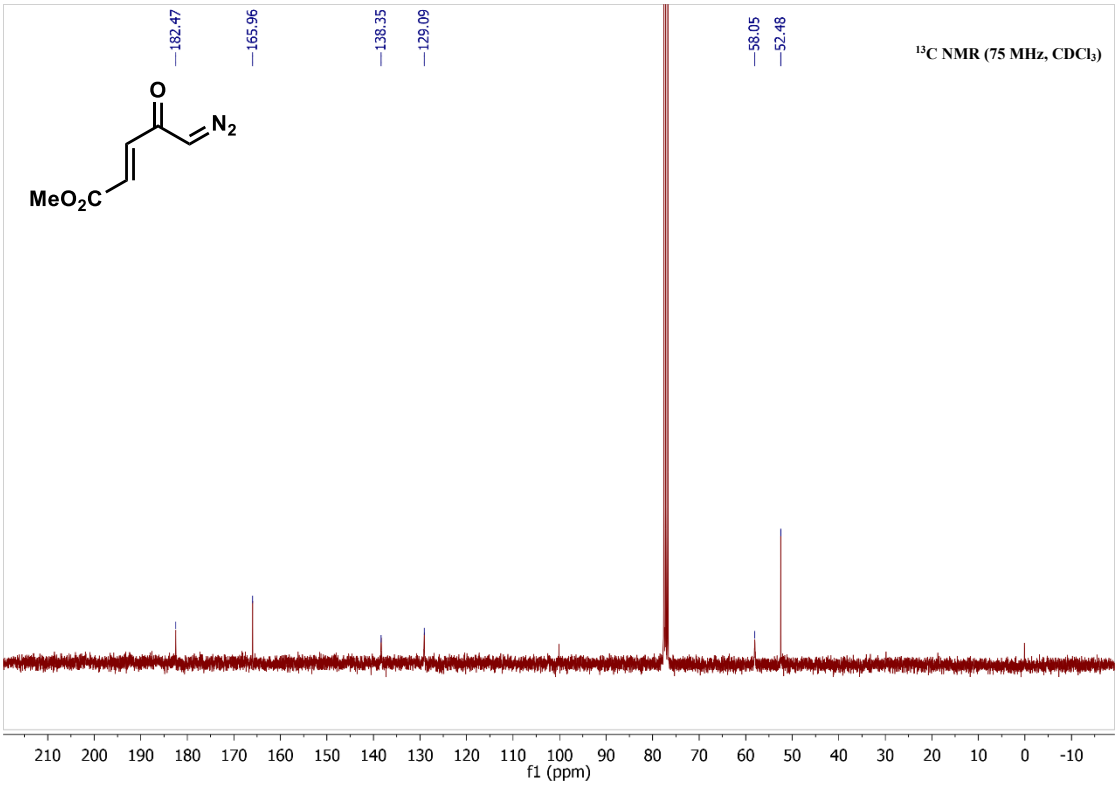
182.47
165.96
138.35
129.09
58.05
52.48
^{13}C NMR (75 MHz, CDCl$_3$)
O
N$_2$
MeO$_2$C
210 200 190 180 170 160 150 140 130 120 110 100 90 80 70 60 50 40 30 20 10 0 -10
f1 (ppm)

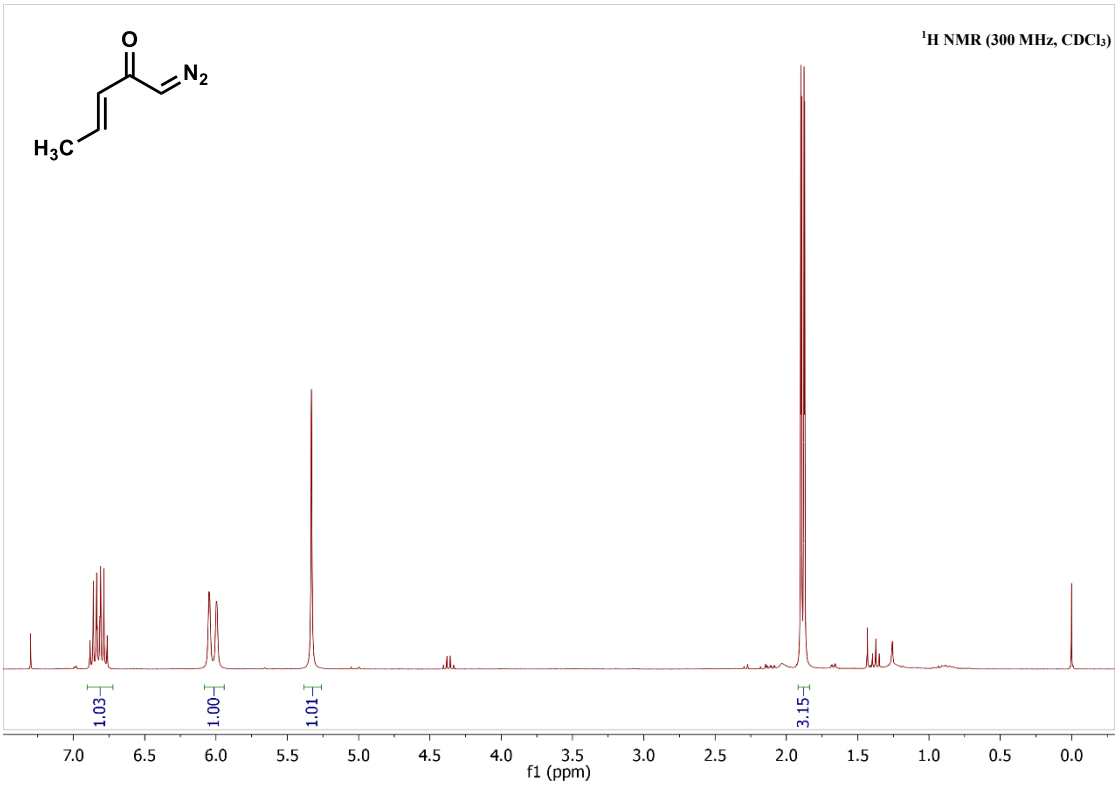
^{1}H NMR (300 MHz, CDCl$_3$)
O
N$_2$
H$_3$C
1.03
1.00
1.01
3.15
7.0 6.5 6.0 5.5 5.0 4.5 4.0 3.5 3.0 2.5 2.0 1.5 1.0 0.5 0.0
f1 (ppm)

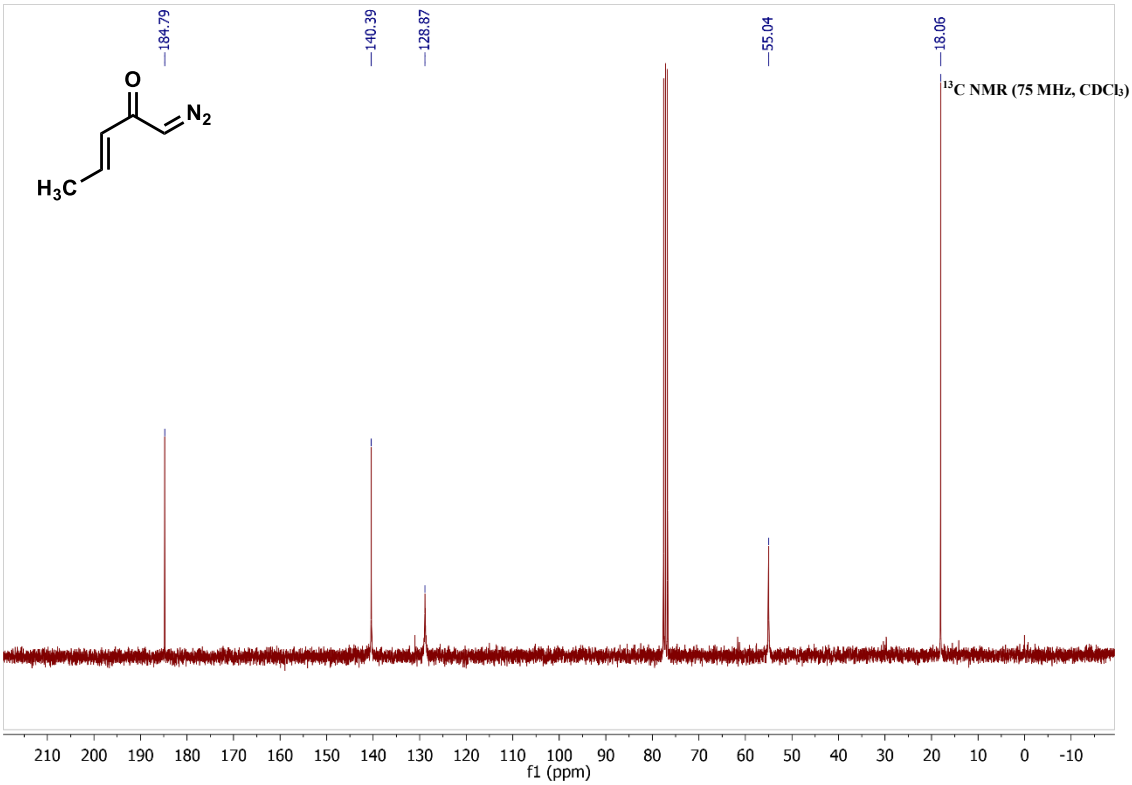
184.79
140.39
128.87
55.04
18.06
^{13}C NMR (75 MHz, CDCl$_3$)
O
N$_2$
H$_3$C
210 200 190 180 170 160 150 140 130 120 110 100 90 80 70 60 50 40 30 20 10 0 -10
f1 (ppm)

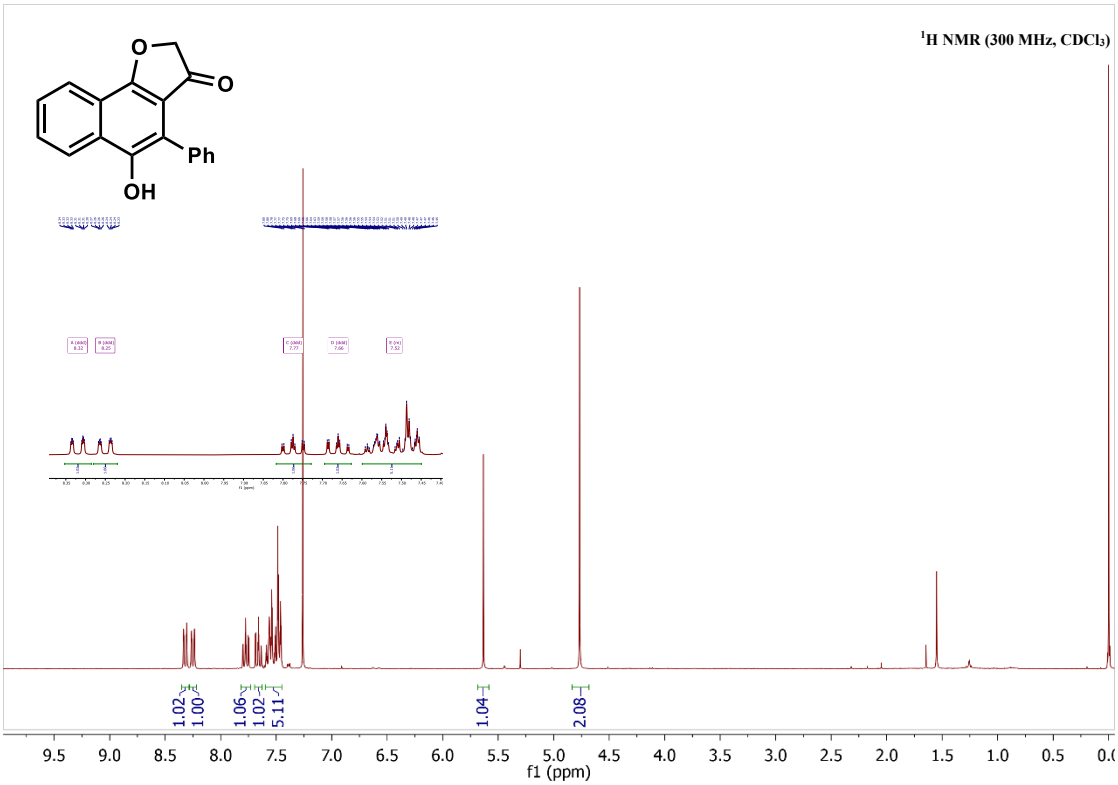
^{1}H NMR (300 MHz, CDCl$_3$)
O
O
Ph
OH
1.02
1.00
1.06
1.02
5.11
1.04
2.08
9.5 9.0 8.5 8.0 7.5 7.0 6.5 6.0 5.5 5.0 4.5 4.0 3.5 3.0 2.5 2.0 1.5 1.0 0.5
f1 (ppm)

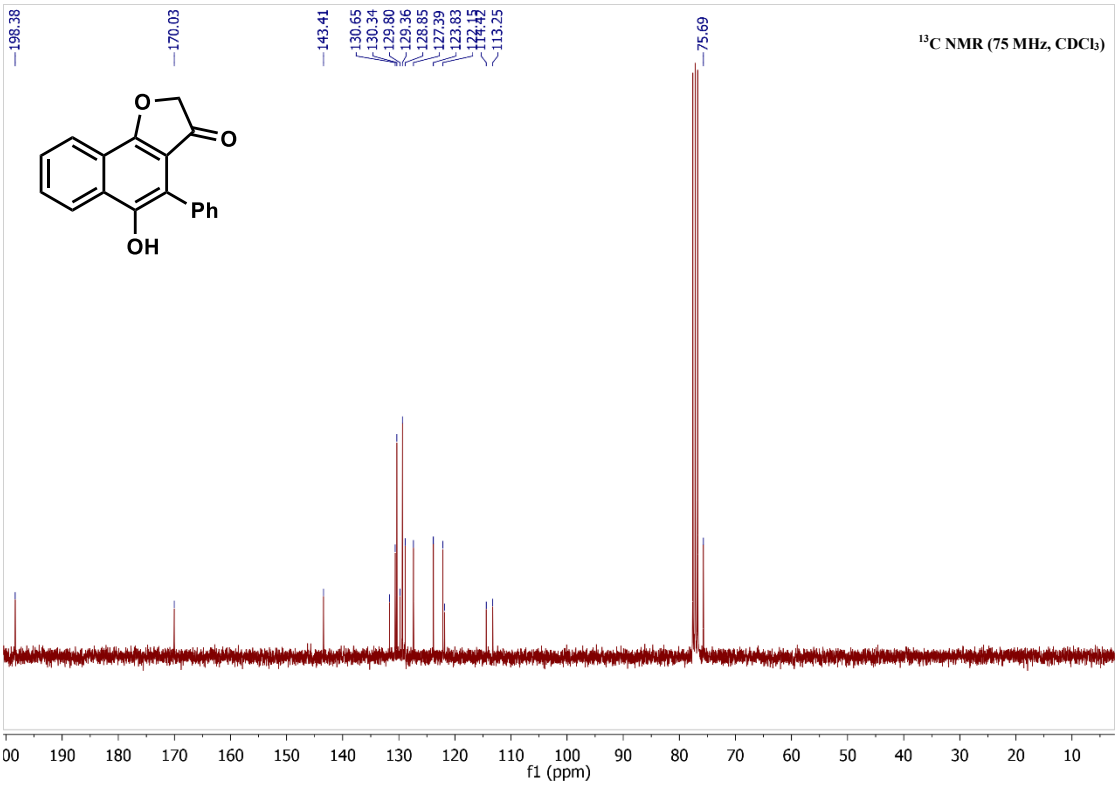
198.38
170.03
143.41
130.65
130.34
129.80
129.36
128.85
127.39
123.83
113.25
75.69
^{13}C NMR (75 MHz, CDCl$_3$)
O
O
Ph
OH
190 180 170 160 150 140 130 120 110 100 90 80 70 60 50 40 30 20 10
f1 (ppm)

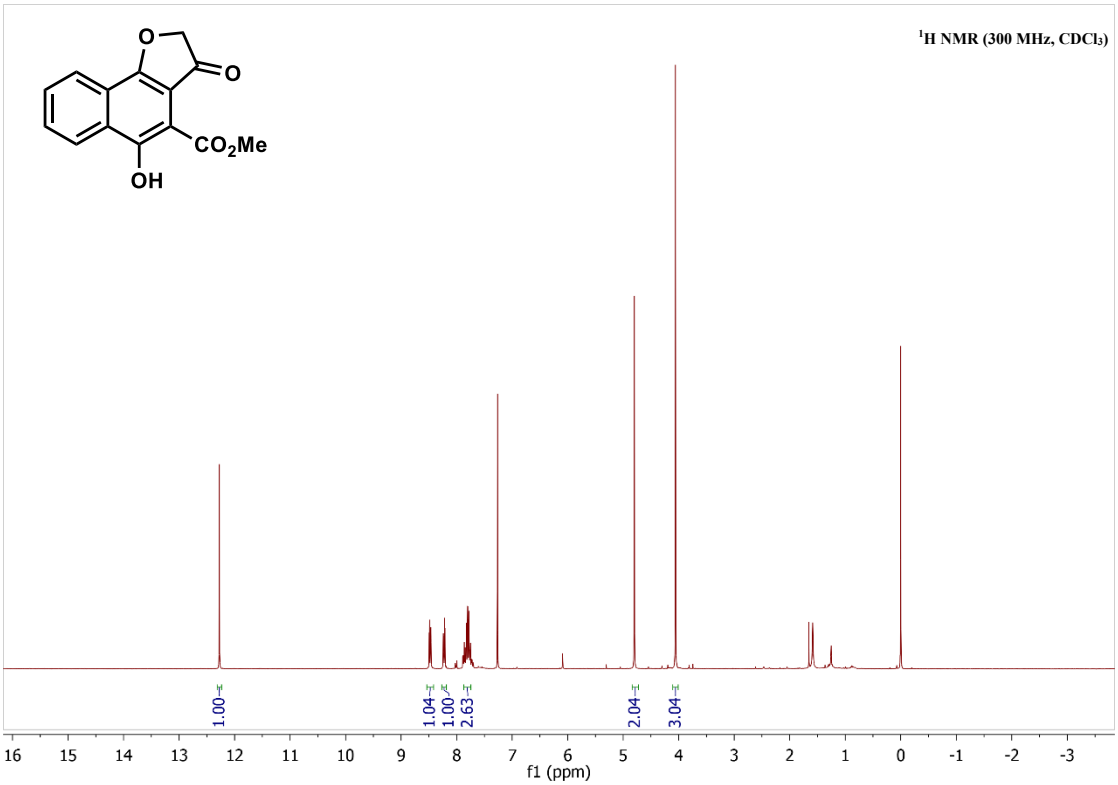
^{1}H NMR (300 MHz, CDCl$_3$)
O
O
CO$_2$Me
OH
1.00
1.04
1.00
2.63
2.04
3.04
16 15 14 13 12 11 10 9 8 7 6 5 4 3 2 1 0 -1 -2 -3
f1 (ppm)

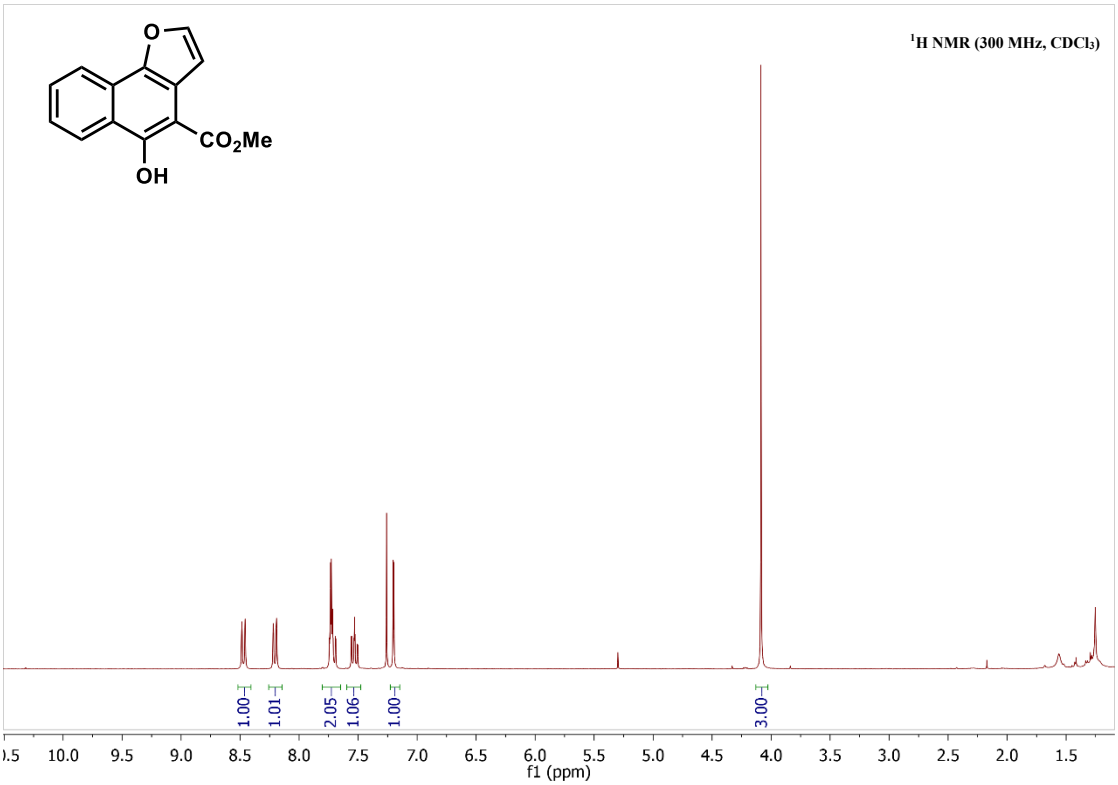
^{1}H NMR (300 MHz, CDCl$_3$)
O
CO$_2$Me
OH
1.00
1.01
2.05
1.06
1.00
3.00
10.0 9.5 9.0 8.5 8.0 7.5 7.0 6.5 6.0 5.5 5.0 4.5 4.0 3.5 3.0 2.5 2.0 1.5
f1 (ppm)

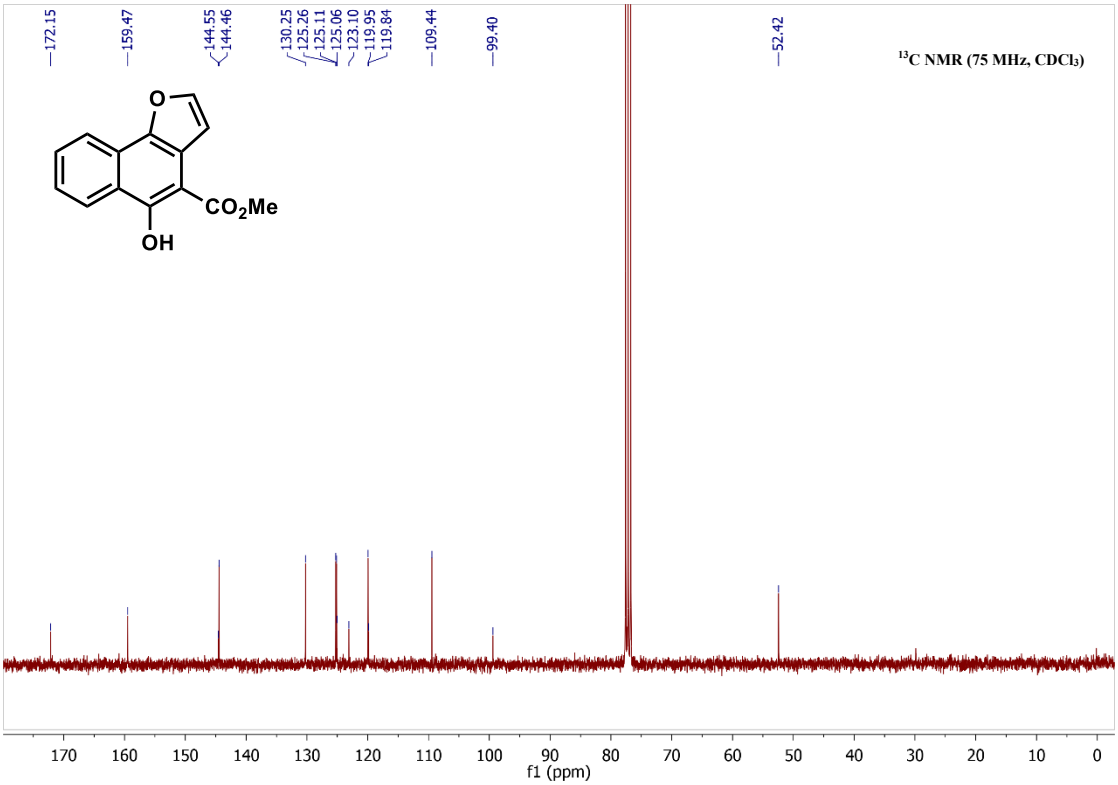
172.15
159.47
144.55
144.46
130.25
125.26
125.11
125.06
123.10
119.95
119.84
109.44
99.40
52.42
^{13}C NMR (75 MHz, CDCl$_3$)
O
CO$_2$Me
OH
170 160 150 140 130 120 110 100 90 80 70 60 50 40 30 20 10 0
f1 (ppm)

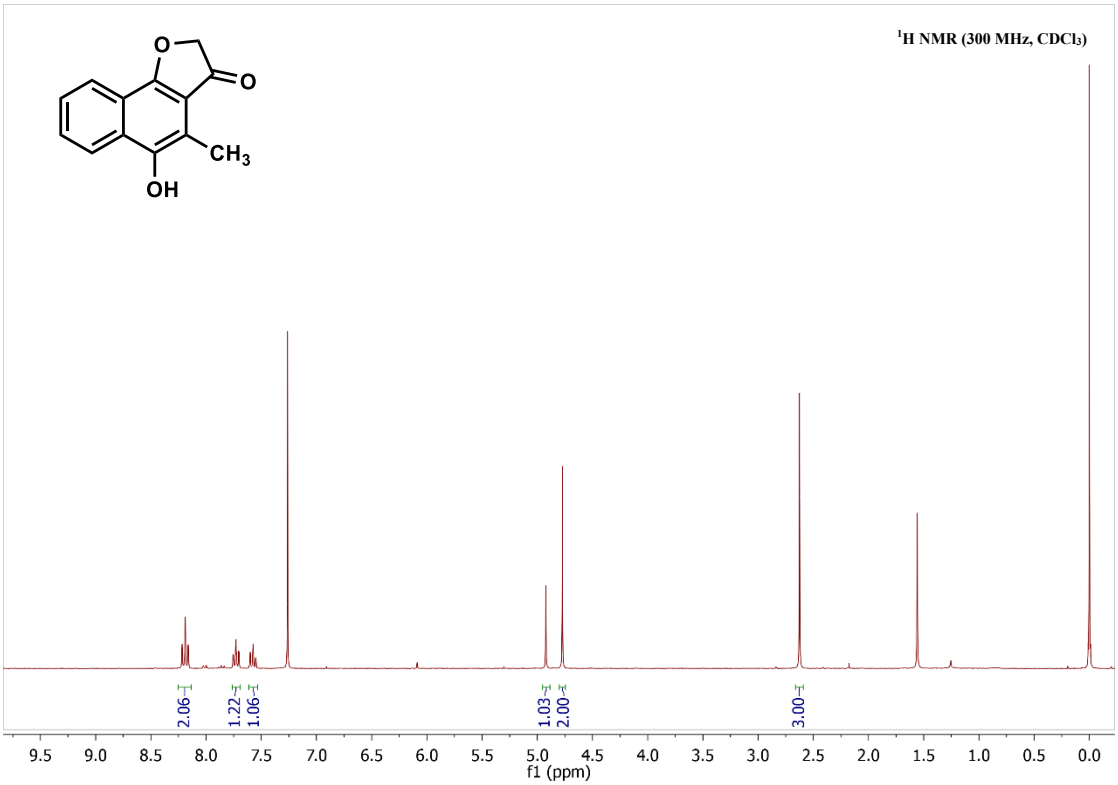
^{1}H NMR (300 MHz, CDCl$_3$)
O
O
CH$_3$
OH
2.06
1.22
1.06
1.03
2.00
3.00
9.5 9.0 8.5 8.0 7.5 7.0 6.5 6.0 5.5 5.0 4.5 4.0 3.5 3.0 2.5 2.0 1.5 1.0 0.5 0.0
f1 (ppm)

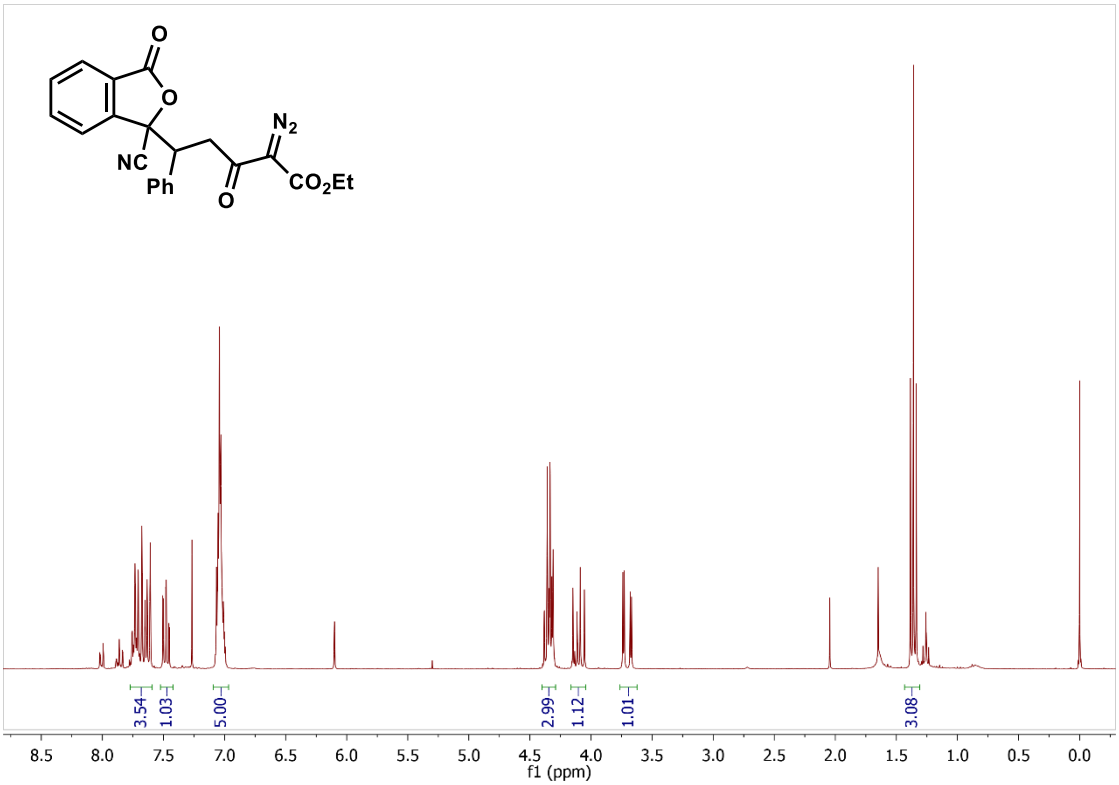
O
O
NC
Ph
O
N2
CO2Et
3.54
1.03
5.00
2.99
1.12
1.01
3.08
8.5
8.0
7.5
7.0
6.5
6.0
5.5
5.0
4.5
4.0
3.5
3.0
2.5
2.0
1.5
1.0
0.5
0.0
f1 (ppm)

Chapter 5: Summary and Future Work

5.1 Chapter 1

5.1.1 Summary

In Chapter 1 of this thesis, we explored a facile methodology for synthesis of pyrroloindoles utilizing a dual catalyst system (Rh/Zn) via a tandem C−H functionalization/Conia-ene annulation between *N*-propargylindoles and α-diazomalonates. The reactions involve the C–H functionalization step of *N*-propargyl indole substrates employing α-diazocarbonyls (**2**) catalyzed by rhodium(II). This catalytic process leads to the generation of rhodium carbenoid intermediates, facilitating the desired transformations. Upon a zinc(II) catalyzed Conia-ene cyclization, the pyrroloindole frameworks are obtained, which are valuable structural motifs in numerous bioactive compounds. The reaction conditions are tolerant of various functional groups on the indole starting material and are amenable to the construction of larger ring systems, including pyridoindoles and azepinoindoles, in good overall yields.

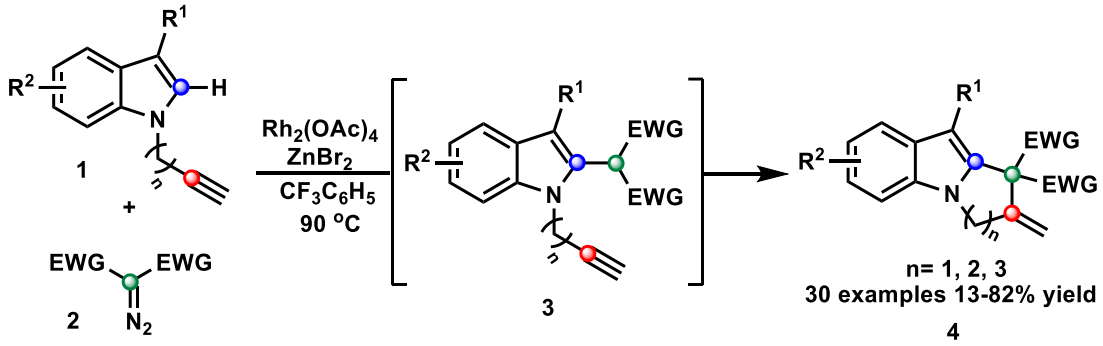

Scheme 5.1: Dual catalyst system for construction of pyrroloindole frameworks.

5.1.2 Future Work

To further expand the current reaction manifold involving C–H insertion/Conia-ene annulation, potential future investigations could involve varying the indole substrates. These substrates would feature the alkyne moiety tethered to different positions of the pyrrole ring, such as C3 or C4, allowing for exploration of new reactivity and selectivity patterns (**5**/**8**, Scheme 5.2A/5.2B). By this strategy, fused indoles could be achieved, the scaffolds of which are found in numerous natural

products and drug molecules. The presented approach is applicable to reactions involving various heterocycles, such as pyrrole, furan, and thiophene, enabling the construction of bicyclic scaffolds following a comparable pattern (**11**, Scheme 5.2C).

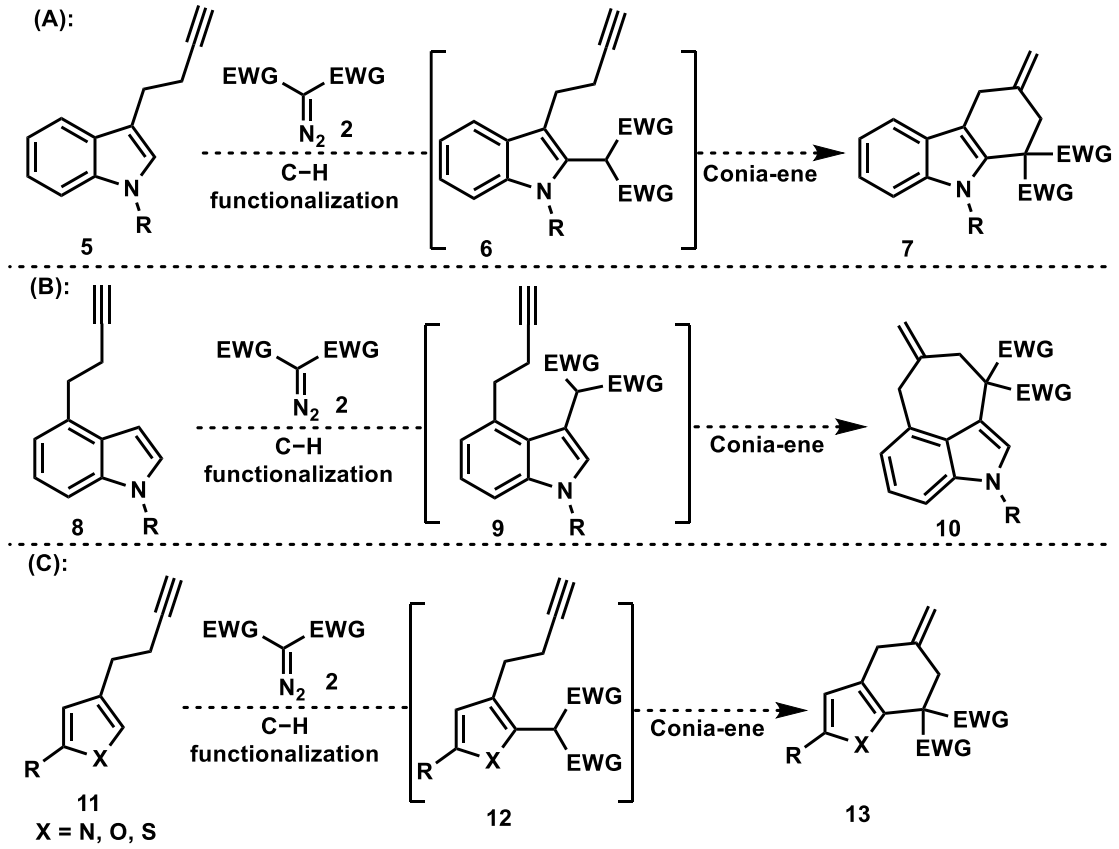

Scheme 5.2: Potential utility of C–H insertion/Conia-ene annulation in construction of fused-heterocyclic compounds.

5.2 Chapter 3

5.2.1 Summary

In Chapter 3 our investigations focused on the conversion of indolyl α-diazocarbonyl compounds to into multi-functionalized carbazoles through a rearrangement pathway (Scheme 5.3). We achieved this goal by utilizing a $Cu(OTf)_2$ catalyst in the presence of $Bu_4N(ClO_4)$ as additive to control the selectivity of the reaction to favor the rearrangement pathway. Construction of carbazoles via a rearrangement pathway has not been mentioned in the literature by utilizing similar indolyl α-diazocarbonyls, as previously reported by the Doyle[1] and Unsworth[2] research groups.

A variety of important factors have been observed that contribute to the selectivity of the reaction, including catalyst, migratory group substitution, and indole nitrogen substitution. The substituent on the indole nitrogen was found to exert the most significant influence on the selectivity of the reaction. At the same time, the electronic properties of the migratory group played a crucial role in determining the selectivity of the reaction. The current method provides access to a myriad of highly decorated carbazoles, in good to excellent yields, with serviceable to exceptional annulation selectivity.

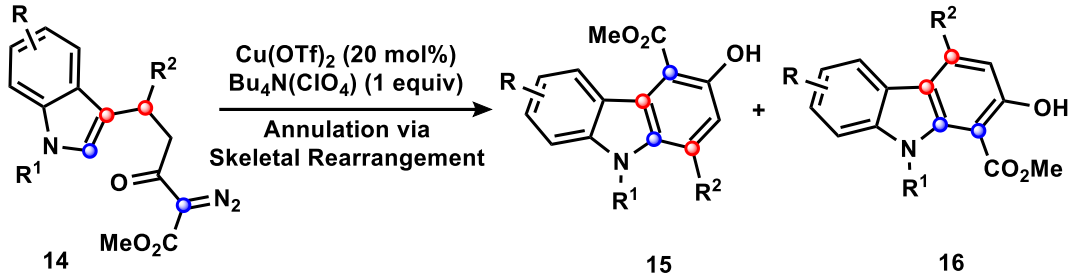

Scheme 5.3: Copper-catalyzed carbazole construction via rearrangement pathway.

5.2.2 Future Work

It is feasible to construct carbazoles by extending this method through utilization of acceptor/donor type diazo-enone substrates. The enone substrates can undergo Michael addition reactions with indoles to generate indolyl α-diazocarbonyl compounds (**17**). The objective is to use standard conditions in the presence of **17** and assess whether the reaction yields a mixture of carbazoles through both the rearranged pathway and direct insertion (**18** and **19**, Scheme 5.4). This approach effectively expands the range of accessible multi-functionalized carbazole compounds, incorporating diverse functional groups.

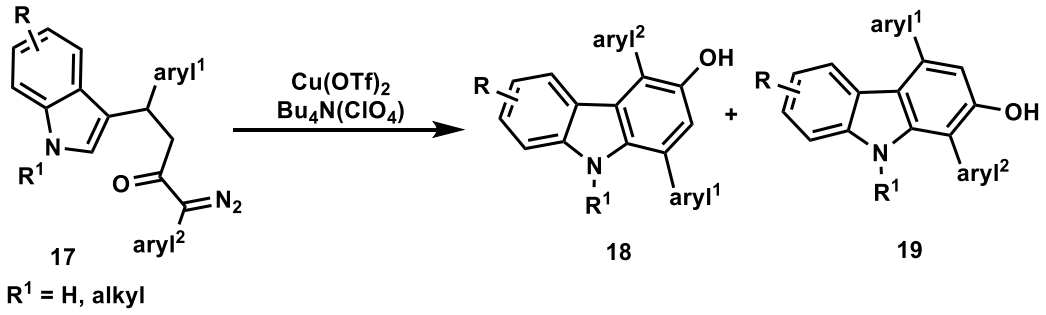

Scheme 5.4: Exploiting acceptor/donor diazo-enones in construction of carbazoles.

As described in Chapter 3, the use of standard conditions revealed that substrates with more electron rich migratory groups exhibited more selectivity in formation of the carbazole via the rearranged pathway. This synthetic strategy enables the possibility of an intermolecular process to access compounds with different bond connections compared to starting materials. Through the reaction of diazo compounds with C3-substituted indoles containing electron rich groups (**20**), such as *p*-methoxyphenyl, the indolenine intermediate **21** can be generated. Under standard conditions, this intermediate **21** can undergo a 1,2-migration to yield 2,3-disubstituted indoles **22** via rearrangement.

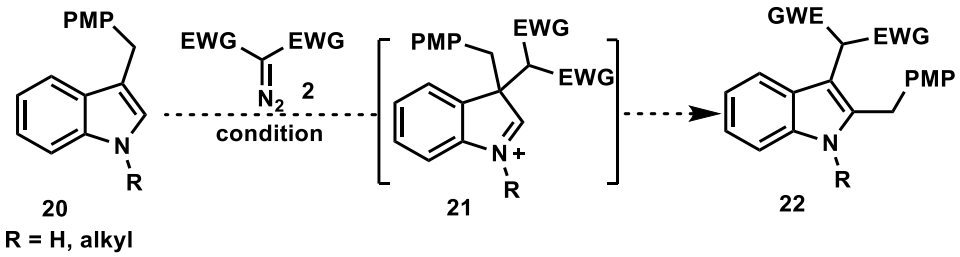

Scheme 5.5: 2,3-substituted indole construction via rearrangement.

5.3 Chapter 4

5.3.1 Summary

In Chapter 4, a novel application of the Hauser-Kraus annulation is described for synthesizing naphthofuranone derivatives, utilizing “acceptor” type diazo-enones (Scheme 5.6). The approach encompasses a Hauser-Kraus reaction, followed by O–H insertion, resulting in the formation of furanone moieties. This method effectively facilitated the formation of three new bonds in a one-pot reaction without the need for a transition metal catalyst compared to other methods.[3] The optimization studies revealed the importance of nucleophilic phthalide in facilitating the reaction. Additionally, the choice of base, along with the work-up conditions, showed a significant effect on the yield of the desired products (**27**). We successfully applied this methodology in the synthesis of naturally occurring naphthofuran scaffolds, such as compounds **28** and **29**.

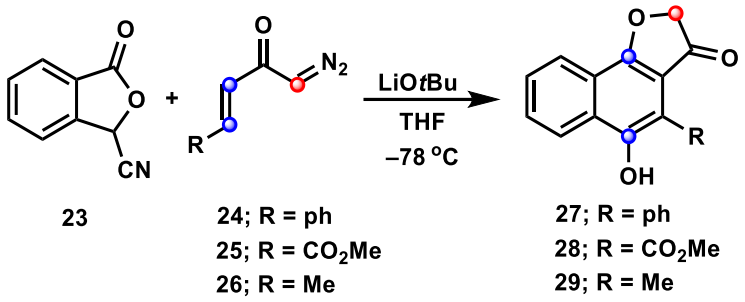

Scheme 5.6: Hauser-Kraus annulation/O–H insertion reaction for the synthesis of naphthofuran scaffolds.

5.3.2 Future Works

As described, functionalized naphthofurans are important building blocks in organic synthesis and medicinal chemistry. To expand the substrate scope of the described H-K annulation/ O–H insertion reaction (Scheme 5.7), future research efforts might involve the exploitation of other types of diazo-enones, such as "acceptor/donor" substrates, in the context of this study. To achieve this goal, first step would be synthesizing diazo-enones which are accessible via a coupling reaction (Scheme 5.8). By incorporating diverse *α,β*-unsaturated enones into the H-K annulation/O-H insertion process, a diverse library of naphthofurans could be generated.

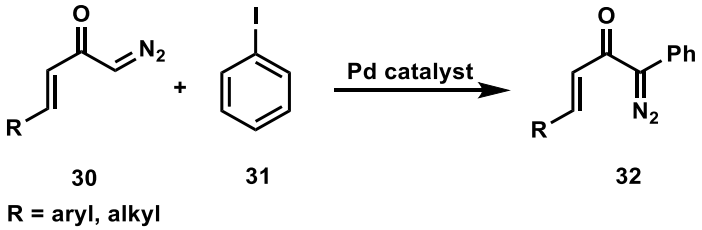

Scheme 5.7: Synthesize of "acceptor/donor" diazo-enones.

5.4 References

1. Shanahan, C. S.; Truong, P.; Mason, S. M.; Leszczynski, J. S.; Doyle, M. P. *Org. Lett.* **2013**, *15*, 3642-3645.

2. Liddon, T. R.; James, M. J.; Clarke, A. K.; O'Brien, P.; Taylor, R. J. K.; Unsworth, W. P. *Chem. Eur. J.* **2016**, *22*, 8777-8780.

3. Kraus, G. A.; Dong, P. *Nat. Prod. Commun.* **2015**, *10*, 1025-1026. b) Buccini, M.; Piggott M. *J. Org. Lett.* **2014**, *16*, 2490-2493.